UNIVERSITY OF SOUTHAMPTON

FACULTY OF MEDICINE

Centre for Human Development, Stem Cells and Regeneration

Mechanisms regulating stem cell self-renewal

Sophie Alice Arthur

Thesis for the degree of Doctor of Philosophy

September 2018

Supervisors: Dr Franchesca Houghton & Dr Jeremy Blaydes

‘Everything will be alright in the end.

If it is not okay, then it is not the end’

UNIVERSITY OF SOUTHAMPTON

ABSTRACT

FACULTY OF MEDICINE

Centre for Human Development, Stem Cells and Regeneration

Thesis for the degree of Doctor of Philosophy

MECHANISMS REGULATING STEM CELL SELF-RENEWAL

Sophie Arthur

Human embryonic stem cells (hESCs) hold potential in the field of tissue engineering to treat a wide range of diseases, given their capacity for both limitless self-renewal and differentiation to any somatic cell type. However, under standard culture conditions, hESCs have a tendency to spontaneously differentiate. Thus, research is required to understand the mechanisms that regulate stem cell self-renewal and the impact on hESC culture. Human embryonal teratocarcinoma cells (hECCs), the malignant counterparts of hESCs, are also pluripotent, proliferate by self-renewal, and provide a convenient alternative model to study the regulation of pluripotency. Accumulating evidence suggests that glycolysis and hypoxia, through the hypoxia inducible factor HIF-2α, are key regulators of hESC self-renewal, but how changes in metabolism affect gene expression is poorly understood. The aim of this study was to determine how glycolysis affected the epigenetic and metabolic regulation of hESC self-renewal maintenance under hypoxia.

Chromatin immunoprecipitation (ChIP) analysis showed that HIF-2α directly binds to a HRE site in the proximal promoters of the metabolic sensors CtBPs, which link the metabolic state of the cell to changes in gene expression. HIF-2α was also demonstrated to regulate the expression of the chromatin modifiers JMJDs in hESCs under hypoxia, except for *JMJD2c*. *JMJD2c* expression peaked within the first 48 hours of exposure to hypoxia and thus was regulated instead by HIF-1α. Inhibiting glycolysis with the addition of glycolytic inhibitors revealed a consequential decrease in JMJD, CtBP and pluripotency marker expression, but intriguingly also HIF-2α, in hESCs maintained under hypoxia by inducing a more heterochromatic state in the proximal promoters of key genes. ChIP analysis revealed that JMJD2a plays a role in hESC self-renewal by inducing a more euchromatic and accessible state around the HREs in the proximal promoters of OCT4, SOX2 and NANOG by removing H3K9me3 histone modifications. CtBPs were also demonstrated to have a role in hESC self-renewal by acting as a transcriptional coactivator. Furthermore, the mechanisms regulating hESC self-renewal were compared to those in the malignant counterparts, hECCs. All mechanisms analysed were similar between the two cell types, except that pluripotency marker expression was not regulated by environmental oxygen in hECCs. Both HIF-1α and HIF-2α were expressed in hECCs maintained at 20% oxygen, and HIF-α subunit accumulation was caused by high levels of nitric oxide preventing HIF degradation by PHDs.

The data presented in this thesis has identified several mechanisms that enhance self-renewal including hypoxia, metabolic sensors, epigenetics, nitric oxide and most importantly glycolysis. Together, these data have uncovered a potential insight into how hESCs first adapt to hypoxia, but also mechanisms into how that cell identity is maintained and enhanced under long-term hypoxia. However, crucially, glycolysis appears to not be just a feature of pluripotency, but is intrinsic to the acquisition and maintenance of self-renewal.

Table of Contents

Figure legends

Table legends

Declaration of Authorship

I, Sophie Arthur declare that this thesis entitled:

'Mechanisms regulating stem cell self-renewal'

and the work presented in it are my own and has been generated by me as the result of my own original research.

I confirm that:

1. This work was done wholly or mainly while in candidature for a research degree at this University;
2. Where any part of this thesis has previously been submitted for a degree or any other qualification at this University or any other institution, this has been clearly stated;
3. Where I have consulted the published work of others, this is always clearly attributed;
4. Where I have quoted from the work of others, the source is always given. With the exception of such quotations, this thesis is entirely my own work;
5. I have acknowledged all main sources of help;
6. Where the thesis is based on work done by myself jointly with others, I have made clear exactly what was done by others and what I have contributed myself;
7. Either none of this work has been published before submission, or parts of this work have been published as:

Publications:

Sophie A. Arthur, Jeremy P. Blaydes and Franchesca D. Houghton. (2019). 'Glycolysis regulates human embryonic stem cell self-renewal under hypoxia via HIF-2α and the glycolytic sensors CtBPs', Stem Cell Reports, 12, DOI: 10.1016/j.stemcr.2019.02.005

Abstracts:

Sophie A. Arthur, Jeremy P. Blaydes and Franchesca D. Houghton, 'Human embryonic stem cells utilise the CtBP family of glycolytic sensors to regulate pluripotency', Southampton Medical and Health Research Conference, Southampton General Hospital, 14th-15th June 2017.

Sophie A. Arthur, Jeremy P. Blaydes and Franchesca D. Houghton, 'Glycolysis regulates human embryonic stem cell pluripotency under hypoxia through HIF-2α and the glycolytic sensors CtBPs', Southampton Medical and Health Research Conference, Southampton General Hospital, 6th-7th June 2018.

Signed:

Date:

Acknowledgements

Firstly, I would like to express a big thank you to my supervisor Dr. Franchesca Houghton for all the support, advice and guidance through these years of my PhD which continuously stimulated my interest and motivated my research all the time. I will always remember the exciting discussions we had over my results and the stories you shared with me that have made me the resilient scientist I am today. You have, somehow, managed to keep me motivated through all the Western blotting issues I've experienced, whilst making me the 'Queen of Western blotting' by helping me troubleshoot what feels like every possible issue I could have had and your enthusiasm for the results I've generated has always given me a huge confidence boost and the belief that I am doing the right thing!

I extend that thank you to my other supervisor Dr. Jeremy Blaydes for your input and guidance through my research so far. You constantly remind me to think of the bigger picture and consider how my research will mean something to the wider audience, whilst bringing a different perspective to ideas and ensuring I don't get too carried away with one possibility.

I have to thank Kate Parry, David Christensen, Sophia Sander, May de Andres Gonzalez, Tilman Sanchez-Elsner and Matt Darley for their help in teaching me all the techniques and analysis I have used so far and providing me with all the necessary training for me to be able to produce the data which I truly enjoy generating. I wish to extend that thanks to the rest of the JPB research group for any additional help and advice you have all given me.

I want to thank all past and present members of the Houghton lab; Franchesca, Kate, David, Sophia, Lauren, Ada and Irina, who make my time in the lab and as a part of this lab group so much more enjoyable and full of probably too much cake! I also want to extend that thanks to all the MRes and medical students that joined our lab group; Jack, Nairn, Denise, Jay and Matt. I absolutely loved teaching you all whilst you also taught me a lot too about myself, my confidence in teaching and the techniques and helped me realise my love for educating – I just hope I returned the favour and you all learnt something useful from me.

I also have to thank all those that gave me the support and advice outside of the lab too. To all my fellow scientists and science communicators in The STEM Squad and The Sci Community for all their support and words of advice as well as becoming such great friends over my PhD years. I have to give a huge shout out to the Cresselly Ladies. You girls mean so much to me and give me such FOMO being so far from home, especially in the summer! But I don't think I would have

made it through these years without our Whatsapp group – even sometimes coming out of the lab to 100s of messages. There would rarely be a day where you girls couldn't put a smile on my face. So, thank you for all the laughs and your friendship. Let's go Doves!

I would like to thank my family for all their advice, understanding and patience throughout these years, and for asking questions about all that I do even though you weren't that interested. You all always say how proud you are of what I've achieved but hopefully I can continue to do that and inspire many more people around me too.

Finally, I have to thank my amazing fiancé Dale. I definitely could not have finished this without you, and I'm sorry for not listening to you about working too much, but I'm afraid I'm just a workaholic. Thank you for listening to me when I needed to moan about lab life or celebrate good results even though you weren't really that interested. I am so grateful that you followed me down to Southampton and supported me endlessly throughout these last few years including all the trips out where I made you get me some chocolate and ice cream to make my day better. Now this chapter is nearly over in our lives, I simply can't wait to finally be able to focus my attention on wedding and planning the perfect day for both of us. 28th September is going to be a date that means so much to me for the rest of my life. Not only will it be the date I handed in my PhD thesis, but the date that I get to marry the love of my life. I truly cannot thank you enough, but thank you for understanding my decisions and always being at my side.

Abbreviations

2-DG	2-deoxyglucose; glycolysis inhibitor
3-BrP	3-bromopyruvate; glycolysis inhibitor
Acetyl-coA	Acetyl-coenzyme A
AFP	Alpha fetoprotein
ARNT	Aryl hydrocarbon nuclear translocator
ATP	Adenosine triphosphate
bFGF	Basic fibroblast growth factor
bHLH	Basic helix-loop-helix
BMP4	Bone morphogenic protein 4
BSA	Bovine serum albumin
CDH1	E-cadherin/cadherin-1
cDNA	Complementary deoxyribonucleic acid
ChIP	Chromatin immunoprecipitation assay
CM	MEF-conditioned media
CpG	C-phosphate-G
CR3	Conserved region 3
CtBP	C-terminal binding protein
CtBP1/2 siRNA	One single siRNA that targets both CtBP isoforms
CtBP1+2 siRNA	Two individual siRNAs, one that targets CtBP1 and one that targets CtBP2, transfected simultaneously in the same transfection mix to silence both CtBP isoforms
CXCR4	C-X-C chemokine receptor 4
D2-HDH	NAD-dependent D2-hydroxy acid dehydrogenase
DAF-FM DA	4-amino-5-methylamino-2',7'-difluorofluorescein diacetate
DAPI	4',6-diamidino-2-phenylindole

DMEM	Dulbecco's modified eagle medium
DMSO	Dimethyl sulfoxide
DNase	Deoxyribonuclease
DNMT3A, B, 1	DNA methyltransferases A, B, 1
dNTP	Deoxyribonucleotide triphosphate
DTT	Dithiothreitol
EDTA	Ethylenediaminetetracetic acid
eNOS	Endothelial NOS; *NOS3*
EPAS1	Endothelial PAS domain 1
EpiSC	Epiblast stem cell
ESC	Embryonic stem cell
ETC	Electron transport chain
FAM	Fluorescein amidite
FBS	Fetal bovine serum
FGF	Fibroblast growth factor
FIH	Factor inhibiting HIF
FITC	Fluorescein isothiocyanate
FOXC1	Forkhead Box C1
GATA4	GATA binding protein 4
GCT	Germ cell tumour
gDNA	Genomic DNA
GLUT1/3/4/6	Glucose transporter 1/3/4/6
GSK3	Glycogen synthase kinase 3
H3K27me2/3	Histone 3 bi/tri-methylated at Lysine 27 residue
H3K36 me2/3	Histone 3 bi/tri-methylated at Lysine 36 residue

H3K4me2/3	Histone 3 bi/tri-methylated at Lysine 4 residue
H3K9me2/3	Histone 3 bi/tri-methylated at Lysine 9 residue
HAT	Histone acetyltransferases
HDAC	Histone deacetylases
HDM	Histone demethylases
hECC	Human embryonal carcinoma cell
hESC	Human embryonic stem cell
HIF	Hypoxia-inducible factor
HIF-1, 2, 3α	Hypoxia inducible factor 1, 2, 3 alpha subunit
HK2	Hexokinase 2
HMG	High mobility group
HMT	Histone methyltransferase
HPC	Human Polycomb protein 2
HRE	Hypoxia response element
HRP	Horse-radish peroxidase
Hues-7	Human embryonic stem cell line
ICC	Immunocytochemistry
ICM	Inner cell mass (of the blastocyst)
IgG	Immunoglobulin G
IgM	Immunoglobulin M
iNOS	Inducible NOS; *NOS2*
IPAS	Inhibitory PAS domain protein
iPSCs	Induced pluripotent stem cells
JMJD	Lysine-specific demethylase; Jumonji-C (JmjC)-domain containing histone demethylase
KDM	Lysine demthylase

KDR	Kinase insert domain receptor
LDHA	Lactate dehydrogenase A
LIF	Leukaemia inhibitory factor
LIN28B	LIN-28 homolog B
L-NAME	N(G)-Nitro-L-arginine methyl ester
LSD1	Lysine-specific histone demethylase 1
MEF	Mouse embryonic fibroblast
mESC	Mouse embryonic stem cell
MMLV	Moloney murine leukaemia virus
mRNA	Messenger RNA
MTOB	4-methylthio-2-oxobutyric acid; CtBP inhibitor
NAD^+	Oxidised nicotinamide adenine dinucleotide
NADH	Reduced nicotinamide adenine dinucleotide
NANOG	Tir nan Og, land of the ever-young; homeobox-containing transcription factor
NF-κB	Nuclear factor κB
NLS	Nuclear localisation signal
nNOS	Neuronal NOS; *NOS1*
NO	Nitric oxide
NODAL	Nodal growth differentiation factor
NOS	Nitric oxide synthase
ns	Not significant
NT2	NTERA-2; human embryonal testicular teratocarcinoma cell line
NuRD	Nucleosome remodelling deacetylase
OCT4	POU class 5 homeobox 1 transcription factor
ODD	Oxygen dependent degradation domain

OXPHOS	Oxidative phosphorylation
P/CAF	P300/CBP-associated factor
P300/CBP	E1A binding protein 300/cAMP response element Binding Protein
PAK1	P21-activated kinase 1
PAS	Period circadian protein (Per), aryl hydrocarbon receptor nuclear translocator protein (Arnt); single-minded protein (Sim)
PAX6	Paired box protein 6
PBS	Phosphate buffered saline
PBS-T	Phosphate buffered saline with 0.1% Tween
PcG	Polycomb group proteins
PDH	Pyruvate dehydrogenase
PDK	Pyruvate dehydrogenase kinase
PFA	Paraformaldehyde
PHD	Prolyl-4-hydroxylase proteins
PI3K	Phosphoinositide 3-kinase
PIC	Protease inhibitor cocktail
PKM	Pyruvate kinase enzyme
PMSF	Phenylmethylsulphonyl fluoride; serine protease inhibitor
POU5F1	POU class 5 homeobox 1 transcription factor
PRC2	Polycomb repressive complex 2
qPCR	Quantitative polymerase chain reaction
RIPA	Radio immuno-precipitation assay
ROS	Reactive oxygen species
RT	Reverse transcriptase
RT-qPCR	Reverse transcription qPCR
SALL4	Sal-like protein 4

SAM	S-adenosylmethionine
SD	Standard deviation
SDS	Sodium dodecyl sulphate
SEM	Standard error of the mean
SetDB	Histone-lysine N-methyltransferase
Shef3	Human embryonic stem cell line
siRNA	Small interfering RNA
SOX2	Sex-determining region Y (SRY)-box containing gene 2
SSEA-1, 3, 4	Stage-specific embryonic antigen-1, 3, 4
STAT3	Signal transducer and activator of transcription 3
TAE	Tris-acetate-EDTA
TBS	Tris-buffered saline
TBS-T	Tris-buffered saline with 0.1% Tween
TCA cycle	Tricarboxylic acid cycle
TEMED	Tetramethylethylenediamine
TF	DNA-binding transcription factor
TLN1	Talin-1
TRA-1-60/-1-81	Keratin sulphate antigen-1-60/-1-81
Trx	Trithorax group protein
UBC	Ubiquitin C
VHL	Von Hippel-Lindau protein
xeno	Non-human

Mechanisms regulating stem cell self-renewal

Chapter 1
Introduction

Chapter 1: Introduction

Human embryonic stem cells (hESCs) offer a potential cell source for research, drug screening and regenerative medicine applications due to their unique ability to self-renew and differentiate into all somatic cell types. Promising clinical trials have already begun and are ongoing for the treatment of, for example, spinal cord injuries, Parkinson's disease, type I diabetes, heart disease and age-related macular degeneration, where differentiated hESCs are transplanted into patients (Keirstead et al., 2005; Schwartz et al., 2012; Menasche et al., 2015; Schulz, 2015; Schwartz et al., 2015; Barker et al., 2017; Menasche et al., 2018). These treatments all require hESCs to be cultured in a highly pluripotent state on a larger scale, in order for them to be efficiently and reproducibly directly differentiated down a specific lineage. This highlights the need for research to enhance our knowledge of the mechanisms which regulate pluripotency and hESC maintenance and thus, preventing spontaneous differentiation.

Current knowledge of the biology, particularly the transcriptional regulatory network, behind pluripotency maintenance and self-renewal of hESCs is poorly understood, but is fundamental to comprehend human development and to realise the therapeutic potential of these cells for regenerative therapies. Understanding pluripotency maintenance and its regulation will allow the improvement of hESC culture conditions. In turn, this will improve resources for hESC researchers and by directing differentiation of hESCs down specific lineages more efficiently can provide disease models and cells for use in regenerative medicine.

1.1 Human embryonic stem cells

1.1.1 Derivation of hESCs

hESCs are derived from the inner cell mass (ICM) of the blastocyst; the final stage of preimplantation embryo development (Evans and Kaufman, 1981; Martin, 1981; Thomson et al., 1998; Reubinoff et al., 2000). Embryos used to generate hESCs are obtained with informed consent from couples undergoing *in vitro* fertilisation treatment. Donated embryos are cultured *in vitro* until the blastocyst stage, and it is at this stage that hESC lines are derived through two different primary methods; immunosurgery or blastocyst outgrowth (Figure 1.1). Immunosurgery involves isolating the cells of the ICM from the trophectoderm, which would otherwise develop into the extra-embryonic tissues. Firstly, the zona pellucida; the glycoprotein coat of the blastocyst is dissolved with acid tyrodes (Chen and Melton, 2007) or digested with a pronase enzyme (Reubinoff et al.,

2000). This is followed by complement lysis, where polyclonal anti-human serum antibodies allow for the selective lysis of trophectoderm cells (Chen and Melton, 2007). The lysed cells are removed with mechanical disaggregation to reveal an isolated ICM for culture of hESCs (Reubinoff et al., 2000). Blastocyst outgrowth, on the other hand, does not require the removal of the zona pellucida or trophectoderm; instead cells from the ICM grow out following blastocyst hatching, where they can be isolated and cultured as hESCs (Reubinoff et al., 2000). Studies have shown that hESC lines can, also, be derived through clonal expansion of a single cell, mechanical or laser dissection, or through epiblast microdissection. (Brook and Gardner, 1997; Amit et al., 2000; Tanaka et al., 2006; Strom et al., 2007; Turetsky et al., 2008; Meng et al., 2010a). Subsequently, the isolated ICM is cultured on feeder layers, followed by its dissociation and re-plating on new feeder layers to propagate established pluripotent hESC lines. Additionally, hESCs cell lines maintain their potential to differentiate into all three germ layers *in vitro*; endoderm, mesoderm and ectoderm, even after prolonged culture. hESCs, much like their mouse counterparts, can form benign tumours, called teratomas, after injection into immunodeficient mice; another defining trait of hESCs. These teratomas, also, consist of cells from all three germ layers (Thomson et al., 1998).

1.1.2 hESC culture

After derivation, hESCs are co-cultured and maintained on feeder layers, with irradiated mouse embryonic fibroblasts (MEFs) being the most common, whilst maintaining a pluripotent state and karyotypic and phenotypic stability (Thomson et al., 1998; Reubinoff et al., 2000; Amit et al., 2003). Furthermore, new hESC lines have been derived more recently and propagated using a human foreskin fibroblast (HFF) cell line, where the HFF feeder maintained undifferentiated hESC growth in xeno-free culture for more than 80 passages (Aguilar-Gallardo et al., 2010; Rajala et al., 2010). Additionally, it was found that hESCs could be maintained on a feeder-free matrix called Matrigel. This comprises of a matrix secreted by Engelberth-Holm-Swarm mouse sarcoma cells, made up mostly of laminin, collagen IV and heparin sulphate proteoglycan, with a MEF-conditioned medium (CM) (Kleinman et al., 1982; Bissell et al., 1987; Xu et al., 2001). hESCs cultured on Matrigel generate more colonies that are less compact than those cultured on MEF feeder layers, but they are still karyotypically stable and can differentiate to form cells of the three developmental germ layers *in vitro* (Xu et al., 2001). However, in spite of this progress, several disadvantages still persist. Standard culture of

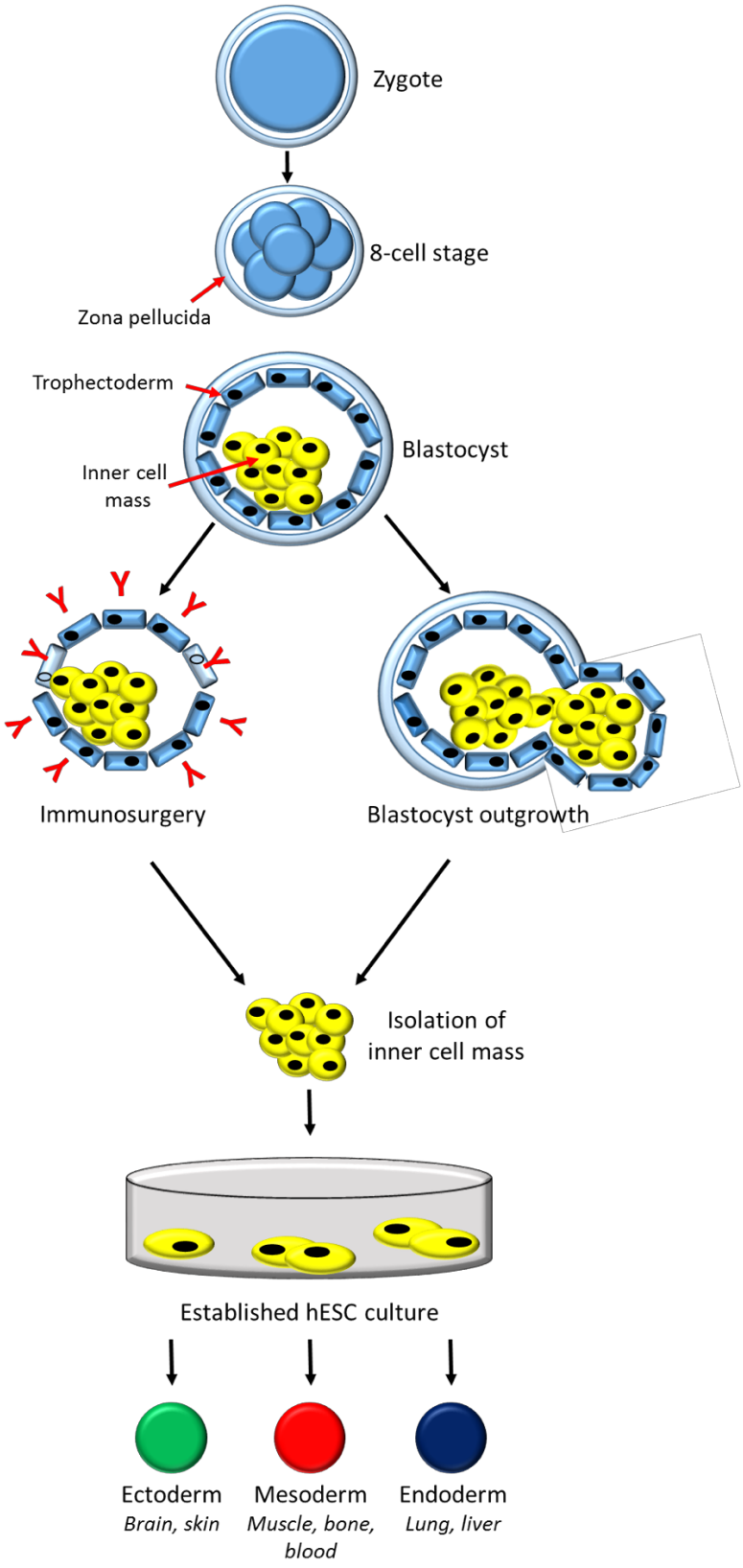

Figure 1.1. Derivation of human embryonic stem cells.
hESCs are derived from the inner cell mass (ICM) of the blastocyst. There are primarily two main methods of derivation; immunosurgery or blastocyst outgrowth. Both lead to established culture of hESCs where the addition of specific growth factors leads to the differentiation of cells of the three developmental germ layers.

hESCs on MEFs, and in media supplemented with fetal bovine serum (FBS), exposes cells to potential transfer of non-human pathogens. Therefore, it is necessary to use xeno-free conditions throughout hESC derivation and long-term culture if they are to be of therapeutic use, which is ultimately rendering the majority of current hESC lines unsuitable for clinical purposes. Furthermore, the potential problem of xeno-contamination still persists in a feeder-free system, such as the Matrigel matrix (Amit et al., 2004; Desai et al., 2015).

Development of xeno-free culture models has already begun, where the potential of a variety of human cell types to act as feeder layers and support hESC self-renewal have been evaluated, such as human embryonic fibroblasts, umbilical cord, fetal foreskin, fetal muscle and skin, bone marrow and placental cells (Richards et al., 2002; Amit et al., 2003; Genbacev et al., 2005; Cho et al., 2010; Meng et al., 2010b; Rajala et al., 2010). However, the development of a serum-free and feeder-free system using fibronectin-coated or vitronectin-coated cell culture plates has demonstrated a potential solution to this problem (Braam et al., 2008; Baxter et al., 2009), where hESCs were cultured over several passages whilst maintaining their undifferentiated phenotype in a defined culture medium (Amit et al., 2004).

1.1.3 Potency

Potency is defined as a measure of the differentiation potential of stem cells, where the greater a cell's potency, the more cell types it can differentiate into. There are four main types of potency; totipotent, pluripotent, multipotent and unipotent, from greatest potential to least potential. Only the zygote is totipotent, as it can create an entire organism by generating cells of both embryonic and extra-embryonic lineages (Mitalipov and Wolf, 2009). Pluripotent cells, such as ESCs, have the ability to produce cells of the three germ layers; ectoderm, mesoderm and endoderm, but not the extra-embryonic structures. Multipotent stem cells are more restricted. Bone marrow derived mesenchymal stem cells are an example of multipotent cells, as they have the capability to differentiate into all bone, fat and cartilage cell types, but limited to those within their specific lineage. Finally, unipotent cells, such as adult muscle stem cells, have the least developmental potential and can only produce one cell type, but they do possess the ability to self-renew which distinguishes them from non-stem cells, such as progenitor cells.

hESCs are defined as pluripotent cells and their differentiation capacity can be demonstrated *in vivo* by injecting hESCs into SCID mice. They maintain their pluripotent state after transplantation and develop into teratomas, containing derivatives of all three embryonic germ cell layers, as previously mentioned (Thomson et al., 1998; Reubinoff et al., 2000).

However, there appears to be two distinct stages of pluripotency; naïve and primed. From the blastocyst, there are two key lineages; the ICM and the trophectoderm. The ICM develops into the epiblast, which is functionally and molecularly distinct from blastomeres and ICM cells; and the hypoblast, another extra-embryonic layer surrounding the pluripotent epiblast. Additionally, the surrounding trophectoderm makes up the extra-embryonic tissues, like the placenta (Gardner, 1998; Kurimoto et al., 2006; Kaji et al., 2007). Shortly following implantation, the epiblast transforms into a cup-shaped epithelium and becomes primed for lineage specification and poised to respond to stimuli from extra-embryonic tissues.

The naïve and primed pluripotent states can be preserved in mESC culture by blocking lineage commitment with the addition of specific factors, termed two inhibitor (2i)/leukaemia inhibitory factor (LIF) conditions (Hanna et al., 2010b) and fibroblast growth factor (FGF) supplementation respectively (Joo et al., 2014). Ground state naïve pluripotency is established in the epiblast of the mature mouse blastocyst, which is captured *in vitro* in the form of mESCs (Evans and Kaufman, 1981; Martin, 1981; Thomson et al., 1998) with the addition of LIF with 2i culture conditions by adding MEK, an Erk-inhibiting signalling kinase, and glycogen synthase kinase 3 (GSK3) inhibitors (Ying et al., 2008). The cooperation of a transcription factor complex containing OCT4, SOX2, NANOG and KLF4 keeps mESCs in a naïve pluripotent state. KLF4 is the first of these transcription factors to be removed from the complex and relocalise to the cytoplasm at the initiation of differentiation (Dhaliwal et al., 2018). Post-implantation epiblast stem cells (EpiSCs) are the *in vitro* counterpart of the primed epiblast, and hence represent primed pluripotent stem cells (Hanna et al., 2009; Nichols and Smith, 2009), which can be stabilised *in vitro* by exogenous supplementation of bFGF and Activin/Nodal pathways that maintains their self-renewal in culture (Tesar et al., 2007; Buecker et al., 2014; Joo et al., 2014).

However, in recent years, it has been reported that hESCs which are blastocyst-derived, share more features with murine EpiSCs; a primed pluripotent stem cell derived from post-implantation epiblasts (Brons et al., 2007; Tesar et al., 2007; Rossant, 2008; Nichols and Smith, 2009). Therefore, cells in the naïve stage encompass the ICM of preimplantation embryos and the *in vitro* equivalents such as mouse ESCs, whereas the primed stage includes post-implantation epiblast-derived cells and their *in vitro* equivalents, such as mouse EpiSCs and hESCs.

However, realising that murine EpiSCs are developmentally equivalent to hESCs proposed the question: can naïve hESCs be established? The standard 2i/LIF culture conditions associated with naïve pluripotent cell culture were not sufficient to maintain human cells, unlike murine cells (Hanna et al., 2010a; Theunissen et al., 2014; Manor et al., 2015). It has been shown subsequently that naïve hESCs can be generated using two different methods without the reliance on transgenes for stable culture. The first method is by pre-culture of primed hESC lines in a histone deacetylase inhibitor consisting of sodium butyrate and suberoylanilide hydroxamic acid prior to standard naïve culture in 2i conditions termed 'reverse toggling' (Ware et al., 2014). The second method uses direct derivation from an eight-cell human embryo in 2i culture conditions with the addition of FGF2 (Gafni et al., 2013; Ware et al., 2014). These naïve hESC lines appear to be more analogous to mouse ESCs (Hanna et al., 2010a; Ware et al., 2014; Warrier et al., 2016). However, none of the current conditions for expanding human naïve pluripotent stem cells generate cells identical to murine naïve ESCs or the human ICM (Gafni et al., 2013).

Highly pluripotent cell populations would need to be maintained efficiently to be able to yield large quantities of cells for use in a clinical setting and directed differentiation through a specific lineage. Generating and maintaining a human naïve pluripotent stem cell line that resembles the ICM may not be possible currently, but the derivation of these cell lines without genetic manipulation represents a step in the right direction (Ware et al., 2014). It is not yet clearly understood how hESCs maintain their pluripotent state, therefore an understanding of the core transcriptional network and epigenetic characteristics of human naïve pluripotency may provide insights into whether this goal is achievable and whether human naïve pluripotent stem cells could be used as a gold standard starting material for personalised medicine.

1.1.4 hESC characteristics

Apart from being pluripotent cells, and therefore having the capability to generate cells from the three germ layers, hESCs have a variety of other distinguishable characteristics including (Evans and Kaufman, 1981; Martin, 1981; Thomson et al., 1998; Reubinoff et al., 2000; Sathananthan et al., 2002; Becker et al., 2006):

- Derived from ICM of the blastocyst
- Ability to self-renew indefinitely
- High telomerase expression and activity
- Shortened G1 cell cycle phase, and therefore rapid cell division
- High nuclear to cytoplasmic ratio
- A stable diploid karyotype
- Immature mitochondria
- Express characteristic surface markers and transcription factors

hESCs are defined by their capacity to indefinitely self-renew and proliferate in an undifferentiated state by dividing symmetrically to produce progeny cells with equivalent proliferative and developmental potential as the parent cell (Avery et al., 2006). This infinite self-renewal coupled with the high telomerase activity that hESCs possess; an enzyme that preserves the length of telomeres on the ends of chromosomes which is important in replicative lifespan, strongly correlates with cell immortality (Harley, 1991; Harley et al., 1992; Thomson et al., 1998). This self-renewal is supported by a shortened G1 phase in the cell cycle, to allow rapid cell division compared to somatic cells (Becker et al., 2006). This abbreviated cell cycle time appears to be a universal characteristic of mammalian ESCs in culture (Savatier et al., 1994; Stead et al., 2002; Becker et al., 2006; Fluckiger et al., 2006), however the physiological relevance of these unique cell cycle kinetics is yet to be determined experimentally (Kapinas et al., 2013). However, it is proposed that it may be linked to the smaller size of pluripotent cells, compared to their differentiated counterparts, and therefore the absence of regulatory complexity. Furthermore, cells preferentially start to differentiate in G1 phase, so a short G1 phase limits the time that a cell can respond to exogenous differentiation signals and compromise their pluripotent state. This is supported by the fact that hESCs have a naïve transcriptome which is competent enough to regulate their own cell cycle. This simplicity

supports their need to self-propagate and suppress gene expression associated with lineage commitment and differentiation (Becker et al., 2006; Kapinas et al., 2013).

hESCs are described as having immature mitochondria with an elongated and tubular morphology (Sathananthan et al., 2002). There are several studies in a number of hESC lines that report that hESCs have very few mitochondria with poorly developed cristae (Sathananthan et al., 2002; Oh et al., 2005; Cho et al., 2006; St John et al., 2006). With differentiation of hESCs, the resulting cells clearly showed numerous larger mitochondria with distinct cristae (Lonergan et al., 2007) concomitant with the increase in ATP levels produced by a metabolic switch to oxidative phosphorylation (Cho et al., 2006). Hence, this suggests that the immature state of the mitochondria reflects the metabolic demands of hESCs, as they rely on an anaerobic metabolism to produce ATP due to not having the mitochondria to produce large amounts of ATP via oxidative phosphorylation (Brown, 1992).

hESCs can be identified by their characteristic undifferentiated cobblestone morphology which form colonies in culture. hESCs display a high nuclear to cytoplasmic ratio, as well as a stable XX or XY diploid karyotype of 46 chromosomes, even after prolonged culture (Thomson et al., 1998). Additionally, several well-established markers are associated with pluripotent cells and the maintenance of their undifferentiated phenotype, such as transcription factors (TFs) OCT4, SOX2 and NANOG, and surface markers, like stage-specific embryonic antigen (SSEA)-3, SSEA-4, TRA-1-60, TRA-1-81 and alkaline phosphatase (Thomson et al., 1998).

1.2 The pluripotency network

There are a variety of transcription factors and cell-surface markers collectively known as pluripotency markers that characterise ESC identity. Elucidating the molecular mechanisms, particularly the transcriptional regulatory circuit, which regulates pluripotency maintenance and self-renewal of hESCs is fundamental to improving maintenance of an undifferentiated state in hESC culture, in addition to generating induced pluripotent stem cells (iPSCs) and contributing to advances that enable the therapeutic use of hESCs.

1.2.1 Pluripotency markers

hESCs require a co-ordinated network of transcription factors to maintain pluripotency or initiate differentiation down specific lineages. Central to these processes are the proteins OCT4, SOX2 and NANOG; collectively termed the 'core pluripotency factors' in hESCs. These core pluripotency factors are central to the transcriptional hierarchy that specifies ESC identity in early development and are essential for pluripotency maintenance and self-renewal of hESCs in culture because of their unique expression patterns (Nichols et al., 1998; Avilion et al., 2003; Chambers et al., 2003; Mitsui et al., 2003; Boyer et al., 2005; Loh et al., 2006).

Octamer-binding protein 4 (OCT4), also known as POU5F1 or OCT3/4, is a member of the POU gene family and encoded by the human gene *POU5F1 (POU domain class 5 transcription factor 1)*. OCT4 is essential for generating pluripotent cells in the embryo and propagating undifferentiated cells *in vitro* (Boyer et al., 2005), as *OCT4*-deficient embryos cannot form an ICM *in vivo* or ESC colonies *in vitro*, despite being able to survive to the morula stage (Nichols et al., 1998). OCT4 expression levels need to be carefully regulated to maintain hESC pluripotency since a 50% increase or decrease in expression can lead to ESC differentiation into primitive endoderm and mesoderm, or trophectoderm respectively (Niwa et al., 2000). The human *POU51F* gene consists of five exons and is located on chromosome 6 in the region of the major histocompatibility complex and can generate three mRNA isoforms through alternative splicing – OCT4A, OCT4B and OCT4B1 (Takeda et al., 1992; Atlasi et al., 2008). OCT4A and OCT4B1 orchestrate gene transcription in the nucleus supporting self-renewal and pluripotency maintenance in ESCs and embryonal carcinoma cells, whereas OCT4B is localised in the cytoplasm in various non-pluripotent cell types and cannot sustain self-renewal and pluripotency (Cauffman et al., 2006; Lee et al., 2006a; Atlasi et al., 2008; Papamichos et

al., 2009). OCT4 is a member of the Octamer class of transcription factors which recognise the 8 base pair (bp) consensus motif 5'-ATGCAAAT-3' in the promoter or enhancer DNA sequence of their target genes (Parslow et al., 1984; Petryniak et al., 1990; Herr and Cleary, 1995). The POU (Pit-Oct-Unc) domain is a bipartite DNA-binding domain present in all POU TFs, including OCT4, that directly bind this motif. It comprises of two sub-domains; a lower affinity POU-specific domain and a higher affinity POU-homeodomain connected by a flexible linker (Sturm and Herr, 1988; Klemm and Pabo, 1996). The flexibility of this linker region allows each sub-domain to interact with the DNA-binding site independently of the other, whilst the linker itself tracks along the minor groove. Each domain positions itself either side of the DNA helix, where the POU-specific domain contacts the ATGC subsite of the consensus motif, and the POU-homeodomain binds the more highly conserved AAAT site in the major groove (Phillips and Luisi, 2000). The POU domain is flanked by two regulatory regions; an N-terminal and a C-terminal transactivation domain that can activate expression. Recent reports have demonstrated that all isoforms share identical POU DNA-binding and C-terminal domains, but they differ in their N-terminal region (Cauffman et al., 2006; Lee et al., 2006a). The N-terminal domain of OCT4B is reported to have an inhibitory effect on its DNA-binding domain, and consequently cannot stimulate transcription from OCT4-dependent promoters (Atlasi et al., 2008).

SOX2 is a member of the *Sox* (SRY-related high mobility group (HMG) box) gene family, located on chromosome 3 (Stevanovic et al., 1994), which encode transcription factors containing a single highly conserved HMG DNA-binding domain. SOX2 expression is widely distributed throughout the developing embryo, including the ICM, epiblast and trophectoderm, but later is restricted to the ICM (Avilion et al., 2003). *SOX2*-deficient embryos cannot survive past the implantation stage as they fail to form a pluripotent ICM, and SOX2 knockdown leads to dedifferentiation to the trophectodermal lineage, therefore emphasises its necessity in ESC self-renewal and pluripotency (Wood and Episkopou, 1999; Avilion et al., 2003; Ivanova et al., 2006; Masui, 2009). This phenotype is similar to the one observed in OCT4 knockdowns, as SOX2 and OCT4 often act as a heterodimer to regulate transcription of key genes, such as *FGF4* (Yuan et al., 1995; Ambrosetti et al., 2000), *NANOG* (Kuroda et al., 2005) and each other (Tomioka et al., 2002; Okumura-Nakanishi et al., 2005). As a target gene of OCT4, SOX2 contains an octamer-binding motif to facilitate the interaction between its HMG domain and the low affinity POU-

specific domain of OCT4 (Ambrosetti et al., 1997; Ambrosetti et al., 2000) and SOX2 interacts with DNA in the minor groove by binding to the consensus sequence 5'-(A/T)(A/T)CAAAG-3' (Bowles et al., 2000). SOX2 cooperates with many other TFs to perform essential developmental functions, where the interaction with the DNA-binding domain of the TF was in direct contact with the C-terminal region of the HMG domain of SOX2. Mutagenesis studies revealed that it was the C-terminal tail region of the third helix of the HMG domain that was essential for TF binding and recruitment (Wissmuller et al., 2006), whereas the flanking sequences of the HMG domain indicate the target specificity as all HMG-containing proteins all recognise the same consensus motif (Wegner, 2010). Therefore, HMG proteins have three core functions; DNA-binding, DNA-bending and protein-interacting ability (Wissmuller et al., 2006).

NANOG is a highly conserved homeodomain-containing TF (Chambers et al., 2003) that works cooperatively with OCT4 and SOX2 to establish ESC identity and alleviates the requirement of LIF, which is normally required for ESC maintenance *in vitro* (Mitsui et al., 2003). NANOG maps to chromosome 12 (Kim et al., 2005b), and is expressed heterogeneously in ES cells, where cells expressing the TF are associated with self-renewal, but cells with no NANOG expression are prone to differentiation into cells of extra-embryonic endodermal lineages (Chambers et al., 2007). This is supported when *NANOG*-null embryos cause early embryonic lethality (Mitsui et al., 2003), whereas constitutive expression supports ESC self-renewal (Chambers et al., 2003) and feeder-free propagation for multiple passages in hESCs (Darr et al., 2006). NANOG binds DNA through its single homeodomain, however the consensus DNA sequence recognised by NANOG is a matter of some controversy within the literature. A core recognition sequence of 5'-TAAT-3' was identified (Mitsui et al., 2003), and later extended to 5'-TAAT(G/T)(G/T)-3' through detailed DNA-binding analysis of the purified homeodomain alone (Jauch et al., 2008), however a global localisation study identified the sequence to be 5'-CATT-3' (Loh et al., 2006). NANOG comprises of three functional domains; a serine-rich N-terminal domain, a central homeodomain and a C-terminal domain. The homeodomain is formed by three α-helices, where helix α3 is the so-called 'recognition helix'. Helix α3 binds the DNA by inserting into the major groove and forming an extensive DNA contact interface. Residues 1-10 of the homeodomain are often referred to as the N-terminal arm and also contribute to DNA binding through

interactions with the minor groove of the DNA (Gehring et al., 1994; Billeter, 1996; Jauch et al., 2008).

Interestingly, NANOG is remarkably dispensable for the establishment and maintenance of pluripotency as previous studies have derived *Nanog*$^{-/-}$ ESCs and *Nanog*$^{-/-}$ iPSCs (Takahashi and Yamanaka, 2006; Chambers et al., 2007; Carter et al., 2014; Schwarz et al., 2014). However, this emphasises that our knowledge about the underlying mechanisms of pluripotency maintenance is lacking.

In addition to OCT4, SOX2 and NANOG, there are key surface markers associated with undifferentiated hESCs. Trafalgar antigens (TRA), such as TRA-1-60 and TRA-1-81 are sialylated keratin sulphate proteoglycans expressed on the surface of hESCs (Pera et al., 2000). Likewise, hESCs express stage-specific embryonic antigens (SSEA), such as SSEA-3 and SSEA-4, on their cell surface (Henderson et al., 2002) that are globoseries glycolipids, whereas expression of SSEA-1 is an indicator of early differentiation (Reubinoff et al., 2000; Boyer et al., 2005). The differentiation of hESCs is characterised by the loss of all these molecular markers typical of the undifferentiated state.

1.2.2 Control and regulation of the pluripotent state

The basis of pluripotency resides in a conserved transcriptional regulatory network coupled with networks of protein-protein interactions between TFs and epigenetic regulators (Wang et al., 2006a; Kim et al., 2008), which combine to repress developmental genes and activate expression of pluripotency-associated factors in hESCs. However, an understanding of the transcriptional regulatory circuitry that is responsible for maintenance of hESC pluripotency and self-renewal is crucial to understanding human development and realising the therapeutic potential of these cells, but currently TF expression dynamics and regulatory mechanisms regulating hESC pluripotency is poorly understood.

As previously described, a decrease in *OCT4* expression leads to differentiation of ESCs into trophectoderm, deletion of *SOX2* results in a similar phenotype and the loss of *NANOG* expression results in the formation of extra-embryonic endodermal lineages (Nichols et al., 1998; Mitsui et al., 2003; Masui et al., 2007). It is because of these observations and the interactions between these TFs that they are considered necessary to establish and sustain ESC identity. The core pluripotency network comprises of these core factors (Niwa et al., 2000; Loh et al., 2006; Kim et al., 2008; Chambers and

Tomlinson, 2009; van den Berg et al., 2010; Young, 2011; Yeo and Ng, 2013) and extends to additional TFs, epigenetic regulators and signalling pathways (Niwa et al., 1998; Chen et al., 2008b; Ying et al., 2008; Hall et al., 2009; Ho et al., 2009; Niwa et al., 2009; ten Berge et al., 2011; Ding et al., 2012; Festuccia et al., 2012; Martello et al., 2012; Huang et al., 2015).

1.2.2.1 Core pluripotency network

Genome-wide localisation studies have revealed that the core pluripotency TFs act together through an auto-regulatory network and cross-regulatory interactions in hESCs, including roles in regulating the expression of each other (Figure 1.2) (Boyer et al., 2005). Additionally, they have been found to act through direct binding to multiple active and silent genome loci to regulate the expression of overlapping downstream target genes (Boyer et al., 2005; Loh et al., 2006), where approximately 50% of promoter regions bound by OCT4 are also bound by SOX2, and more than 90% of those motifs bound by both OCT4 and SOX2 are also bound by NANOG. Therefore, in hESCs, there are at least 353 genes where their promoter regions are occupied by all three core pluripotency factors, where these binding sites are within close proximity of each other (Boyer et al., 2005). These target genes frequently encode for transcription factors, many of which are homeodomain proteins that are important developmentally (Boyer et al., 2005). For example, OCT4 and SOX2 can form heterodimers, as previously mentioned, and these heterodimers have been shown to bind to regulatory motifs in the *Nanog* promoter (Kuroda et al., 2005; Rodda et al., 2005; Petruzzelli et al., 2014). Therefore, these data re-emphasise that OCT4, SOX2 and NANOG function together to regulate a significant proportion of target genes in hESCs. Large chromatin immunoprecipitation studies have more recently demonstrated that the co-localisation of OCT4, SOX2 and NANOG extends to additional TFs associated with pluripotency, such as Kruppel-like factor 4 (Klf4), Estrogen receptor-related β (Essrb) and T-cell factor 3 (Tcf3) (Chen et al., 2008b; Cole et al., 2008; Kim et al., 2008). One study, in particular, looked at the binding site of nine pluripotency-associated TFs in mouse ESCs, including OCT4, SOX2, NANOG and Klf4, to reveal that this extended network of pluripotency TFs act in a combinatorial manner, as a significant proportion of promoters were found to be bound by at least four of the nine TFs examined. Additionally, they observed that promoters bound by multiple TFs were associated with genes that were actively expressed in ESCs and repressed upon the initiation of differentiation, whereas promoters bound by a single TF were connected

to genes that were repressed in ESCs, but subsequently expressed after differentiation. These observations suggest a direct involvement of these factors in promoting self-renewal by activating the expression of the target genes, including the core pluripotency factors themselves, whilst simultaneously inhibiting the expression of genes associated with differentiation.

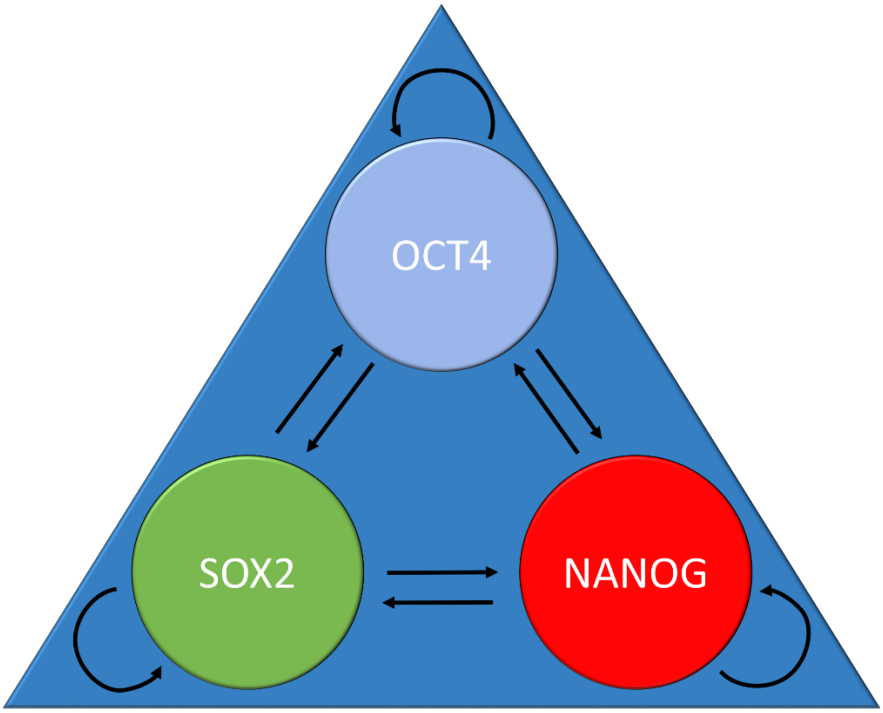

Figure 1.2. A simplified model of the auto-feedback loop within the core pluripotency network.
OCT4, SOX2 and NANOG are central to the pluripotency network and the maintenance of ESC identity. These core pluripotency factors each upregulate their own expression and the expression of both the other transcription factors within the core network. Adapted from (Chan et al., 2011).

It is possible that the pluripotency factors serve as weak activators of gene expression, and that the multi-factor binding increases their activator function (Kim et al., 2008). OCT4, SOX2 and NANOG, also, occupy regulatory regions of repressed genes that encode lineage-specific regulators, and so the repression of these genes is essential for hESC pluripotency maintenance (Boyer et al., 2005; Lee et al., 2006b; Pasini et al., 2008; Bilodeau et al., 2009). The loss of this repression leads to a rapid increase in the

expression of these lineage specifying genes, indicating that these genes are poised for activation in response to developmental cues.

This interconnected regulatory feedback loop between OCT4, SOX2 and NANOG generates a bistable state in hESCs, where they reside in a positive feedback-controlled gene expression programme when these core factors are expressed at appropriate levels, or they enter into a differentiation gene expression programme when any of the three factors are functionally unavailable (Boyer et al., 2005; Loh et al., 2006). This model of pluripotency regulation (Figure 1.2), likely explains both the tendency of hESCs to spontaneously differentiate, as a slight imbalance in the expression of any of the core factors would lead to hESC differentiation, and the ability to initiate a pluripotency gene expression programme during reprogramming by forced expression of reprogramming factors (Jaenisch and Young, 2008).

Post-translational modifications are well-documented to have broad effects on protein stability, activity and subcellular localisation, and have been reported as a regulatory mechanism for OCT4, SOX2 and NANOG. OCT4 and SOX2 are both SUMOylated (Tsuruzoe et al., 2006; Wei et al., 2007), which increases the stability and DNA-binding ability of OCT4, but decreases the ability of SOX2 to bind DNA. All three of these transcription factors have been reported to be phosphorylated (Yates and Chambers, 2005; Swaney et al., 2009; Fang et al., 2014), but the functional consequences of these modifications are not fully understood.

A more recent study investigated the post-translational regulation of SOX2, which highlighted a switch between methylation and phosphorylation of the SOX2 protein. Mono-methylation of SOX2 at K119 inhibited SOX2 transcriptional activation and induced its ubiquitination, and therefore degradation. Conversely, phosphorylating SOX2 at T118 resulted in increased stability of the SOX2 protein (Fang et al., 2014). This emphasises the importance of post-translational modifications in determining cell identity, particularly hESC maintenance. Additionally, SOX2 can become acetylated at a key lysine residue in its nuclear export signal. Blocking this acetylation retains SOX2 in the nucleus and sustains expression of its target genes under hyper-acetylation (Baltus et al., 2009). Together, these studies suggest that post-translational modifications may be critical for regulating the activity of the core pluripotency factors and balancing the levels of these factors to maintain a pluripotent state.

1.2.2.2 Signalling to the core pluripotency network

Cells sense and respond to stimuli in their microenvironment through signal transduction pathways, which can deliver information to the genome in the form of activated transcription factors or cofactors. For ESCs, maintenance of their pluripotent state relies on the inhibition of developmental cues that initiate differentiation and the continued expression of pluripotency markers (Silva and Smith, 2008; Pera and Tam, 2010).

Mouse ESCs depend on LIF and bone morphogenic protein (BMP) signalling pathways to maintain their pluripotency. However, despite *in vitro* and *in vivo* studies establishing that the core pluripotency factors OCT4, SOX2 and NANOG are responsible for pluripotency in both species, hESCs rely on different extrinsic signals to maintain their pluripotent state. The key signalling pathways involved in hESC maintenance are relatively well known and include the WNT/β-catenin, Activin/Nodal and FGF/ERK signalling pathways, where the TFs associated with these signalling pathways often co-occupy enhancers bound by OCT4, SOX2 and NANOG (Chen et al., 2008a; Chen et al., 2008b; Cole et al., 2008; Tam et al., 2008). The WNT signalling pathway is initiated by the binding of the WNT protein to the Frizzled receptor. This leads to the inhibition of glycogen-synthase kinase 3 (GSK3), which allows the translocation of β-catenin into the nucleus. The β-catenin can then act as a coactivator, when bound with transcription factor T-cell factor 3 (Tcf3), to activate *OCT4*, *SOX2* and *NANOG* gene expression. Therefore, this demonstrates that an active WNT signalling pathway is associated with the maintenance of a pluripotent state in hESCs (Sato et al., 2004). Activin/Nodal signalling and its downstream effectors, SMAD2/3, is essential for maintaining a pluripotent state, inhibiting neuroectoderm specification and driving mesoendoderm differentiation. An Activin-SMAD2/3 complex can achieve each of these functions by interacting with tissue-specific regulators to direct SMAD2/3 to transcriptional regulatory regions. SMAD2/3 directly interacts and controls the activity of the *NANOG* gene in hESCs, as inhibiting this signalling pathway resulted in a loss of NANOG expression (Vallier et al., 2009). A later study revealed a role for Activin/Nodal signalling in pluripotency maintenance by changing the epigenetic signature in hESCs. SMAD2/3 interacts with NANOG and this binding induces the recruitment of histone methyltransferases onto Activin/Nodal target genes. In particular, this interaction allows the deposition of histone 3 lysine 4 trimethylation (H3K4me3) marks on such target genes resulting in their expression (Bertero et al., 2015), and therefore demonstrating that Activin/Nodal

signalling has a role in orchestrating the cell fate of hESCs. FGF signalling is triggered by the ligand binding to the specific receptor. This interaction induces the auto-phosphorylation of tyrosine residues within the intracellular domain of the FGF receptor, followed by activation of downstream signalling pathways, primarily the RAS-MEK-ERK signalling cascade (Lanner and Rossant, 2010). hESCs differ from mESCs in their culture conditions in that hESCs require fibroblast growth factor 2 (FGF2) to support self-renewal (Tesar et al., 2007). FGF has been documented to cooperate with Activin/Nodal signalling to maintain high levels of NANOG expression in hESCs, whilst simultaneously activating the PI3K/AKT signalling pathway to promote proliferation and hESC survival (Vallier et al., 2005; Greber et al., 2007a; Li et al., 2007; Greber et al., 2010). Furthermore, multiple studies have demonstrated that the inhibition of the FGF signalling pathway resulted in hESC differentiation (Vallier et al., 2005; Yang et al., 2012a) and thus suggests a role for FGF in the activation of downstream signalling cascades which collectively contribute to the maintenance of the pluripotent state.

These extrinsic signalling components have, also, been documented to be regulated by the core pluripotency factors. One particular study performed an OCT4 knockdown in a hESC line which revealed WNT antagonists *DKK1*, *DKK3* and *FRZB* increase upon OCT4 knockdown, and FRAT2, a GSK3-β-interacting positive effector of WNT signalling, is downregulated. Additionally, they observed reduced expression of autocrine factors *FGF2*, *FGF12*, NODAL and its coreceptor upon OCT4 knockdown in hESCs (Babaie et al., 2007).

1.2.2.3 Chromatin regulators in the extended pluripotency network

Various observations have suggested that several crucial epigenetic alterations are performed during mammalian development and ESC differentiation; switching from an open chromatin state, called euchromatin, to a more compact, closed heterochromatic state upon differentiation. These unique chromatin dynamics in ESCs have led to suggestions that the chromatin state holds some of the secrets behind pluripotency maintenance (Boheler, 2009). Multiple TFs that are associated with regulating the pluripotent state have been identified, however how these pluripotency factors and chromatin regulators interact to help maintain the pluripotent state are less well understood. Several links between OCT4 and chromatin modifiers have been documented (Ding et al., 2012), which suggests that ESCs may use specific pathways to modulate the

chromatin landscape and therefore regulate gene expression programmes that are essential for pluripotency maintenance.

Core pluripotency factors and chromatin regulators provide fundamental mechanisms underlying pluripotency, but both, also, demonstrate a degree of cross-talk between each other to maintain a pluripotent state. Firstly, the core pluripotency factors regulate genes that encode epigenetic control factors, where it has been shown that OCT4, SOX2 and NANOG co-regulate chromatin remodelling and histone modifying complexes (Boyer et al., 2005). OCT4, SOX2 and NANOG have, also, been shown to interact with histone modifying enzymes and chromatin remodelling complexes. For example, OCT4 and NANOG bind directly or indirectly with PcG proteins, the histone deacetylase NuRD and the histone demethylase SetDB1 to modulate the expression of genes associated with lineage specification (Wang et al., 2006a; Bilodeau et al., 2009). Amongst the downstream targets of the core pluripotency factors are several genes that encode chromatin modifiers (Boyer et al., 2005). The binding of these pluripotency factors to the promoter regions of such target genes initiates a cascade of downstream effects, so therefore pluripotency factors influence changes in gene expression of hESCs indirectly by regulating the expression of the chromatin regulators. For example, OCT4 enhances the expression of some histone modifiers, such as *Jmjd1a* and *Jmjd2c*. These genes encode histone H3K9 demethylases and so facilitate the prevention of repressive methylation marks at the promoter regions of genes associated with pluripotency maintenance, such as *NANOG* (Loh et al., 2007; Shakya et al., 2015). Jarid2 has been identified as two components of the Polycomb Repressive Complex 2 (PRC2) which mediates histone H3K27 trimethylation (Peng et al., 2009; Landeira et al., 2010; Walker et al., 2010). In addition, *Jarid2* expression has, also, been documented to be enhanced by OCT4 (Kim et al., 2008). Given that OCT4 is directly regulating the expression patterns of chromatin modifiers in ESCs suggests an alternative mechanism and additional layer of regulating a pluripotent state.

To reveal more about chromatin regulators in the expanded pluripotency network, large scale RNA interference-mediated gene knockdowns were used in an attempt to observe any loss in pluripotency. This technique has previously led to the discovery of several important factors in mouse ESCs such as Essrb (Ivanova et al., 2006) and chromatin regulator SetDB1 (Bilodeau et al., 2009). This approach was extended to look for additional important factors in hESCs, where components of the IN080 chromatin

remodelling complex, the mediator and TAF transcriptional regulatory complexes, were identified as important factors (Chia et al., 2010). This highlights that the extended pluripotency network includes chromatin remodelling and modifying factors, DNA methyltransferases and Polycomb group (PcG) proteins, and therefore suggests that the core pluripotency factors may regulate gene expression through the modulation of chromatin states.

Additionally, there is emerging evidence describing that extracellular signals from specific signalling pathways may have a role in coordinating the chromatin state in hESCs (Fagnocchi et al., 2016). A recent study demonstrated that the Activin/Nodal signalling pathway interacted with the core pluripotency factor NANOG in hESCs. This cooperation led to the recruitment of the DPY30-COMPASS histone modifiers to key developmental genes and control the histone H3K4 trimethylation marks on these genes (Bertero et al., 2015).

Cofactors are protein complexes that contribute to the activation or repression of gene expression, as coactivators or corepressors respectively, but they do not possess their own DNA-binding ability. Some cofactors mobilise or modify nucleosomes to exert their effects, and so are also considered as chromatin regulators (Young, 2011). Cofactors are generally expressed in most cell types, however ESCs tend to show reduced levels of certain cofactors and chromatin regulators, such as mediator and cohesin (Fazzio and Panning, 2010; Kagey et al., 2010). Previous studies have shown that mediator physically links OCT4/SOX2/NANOG-bound enhancers to the promoters of active genes in the core pluripotency network by complexing with cohesin to form a loop in the chromosome architecture between the enhancers and core promoters necessary for normal gene activation (Kagey et al., 2010). Additionally, a recent study documented the histone methyltransferase Set1a as a key coactivator of OCT4 and is essential for generating an OCT4 positive ICM. Set1a specifically interacts with OCT4, and is recruited to OCT4 target gene promoters and aids in the transcriptional activation of OCT4 target genes in ESCs (Fang et al., 2016). Alternatively, corepressors, such as Dax1 and Trim28, are implicated in the control of the pluripotent state. Overexpression of Dax1 leads to ESC differentiation, likely due to an inhibitory interaction with OCT4, and loss of Trim28, also, causes ESCs to differentiate into primitive endoderm lineages (Hu et al., 2009; Sun et al., 2009). In summary, ESCs are particularly sensitive to reduced levels of coactivators, potentially as a large proportion of the ESC genome is transcriptionally

active and the coactivators are limiting. Additionally, ESCs are sensitive to the loss of corepressors, which can possibly exert their control by acting on OCT4 directly or through repressive chromatin-modifying activities.

In summary, the core TFs regulate their own expression and that of each other and activate the expression of pluripotency-associated genes, while simultaneously contributing to the repression of lineage-specifying genes via the recruitment of repressive chromatin regulators. Additionally, the core pluripotency factors frequently bind enhancers that are shared with TFs associated in signalling transduction pathways, so they can signal directly to the target genes of the core factors. The discovery of targets that regulate the core pluripotency network, including the additional TFs, chromatin regulators and signalling pathway components, will allow the development of a more comprehensive and detailed network of the transcriptional regulation of hESCs.

Together, these observations suggest how a pluripotent state is maintained by a complex combination of specific signalling pathways and transcription factors that cooperate to establish a unique epigenetic state.

1.3 hESC culture under reduced oxygen tensions

hESCs can be propagated in culture in an undifferentiated, pluripotent state whilst maintaining their self-renewal potential and ability to generate any cell type in the body. However, hESCs are notoriously difficult to maintain in culture due to their propensity to spontaneously differentiate under atmospheric oxygen tensions, an effect likely caused by suboptimal culture conditions (Thomson et al., 1998; Reubinoff et al., 2000).

Standard hESC culture is performed at atmospheric oxygen tensions, also called 'normoxia'. Hypoxia occurs in a variety of physiological settings when the rate of tissue growth exceeds the oxygen availability in the blood supply (Covello et al., 2006). Additionally, a hypoxic environment transpires at the preimplantation stage of development which occurs at a low, 3-5% oxygen tension. As preimplantation embryos are exposed to lower oxygen tensions *in vivo*, these conditions were mimicked *in vitro* and were shown to improve the *in vitro* embryo development of several species, including humans (Dumoulin et al., 1999; Petersen et al., 2005; Kirkegaard et al., 2013). Moreover, gene expression of mouse pre-implantation embryos cultured *in vitro* at 5% oxygen was more similar to the *in vivo* control embryos, than those cultured *in vitro* at 20% oxygen (Rinaudo et al., 2006). When this lower oxygen tension is mimicked through *in vitro* culture of hESCs at 5% oxygen, it has shown there is a reduction in spontaneous differentiation compared with 20% oxygen tensions (Ezashi et al., 2005). Culture of hESCs under hypoxic conditions has demonstrated other benefits such as increased proliferation, increased rate of glycolysis and increased expression of pluripotency markers, such as OCT4, SOX2 and NANOG (Ezashi et al., 2005; Westfall et al., 2008; Forristal et al., 2010; Forristal et al., 2013) with no effects on morphology compared with normoxic conditions. Additionally, low oxygen tension levels have been reported to enhance iPSC generation (Mathieu et al., 2013). This suggests that culturing hESCs at reduced oxygen tensions is advantageous for pluripotency maintenance, and so would be the preferred method for long-term, large scale culture of hESCs for therapeutic benefit.

Previous studies have shown that various hESC lines showed changes in metabolism, epigenetics, transcription, self-renewal capacity and pluripotency in response to changes in environmental oxygen tension (Ezashi et al., 2005; Forsyth et al., 2006; Forsyth et al., 2008; Westfall et al., 2008; Prasad et al., 2009; Forristal et al., 2013; Christensen et al., 2014; Harvey et al., 2014; Petruzzelli et al., 2014). Additionally, a hESC line has now been derived and cultured under low oxygen tensions for the first time (Lengner et al.,

2010). These cells demonstrated a more immature state, decreased differentiation and prevented X chromosome inactivation. However, despite these fundamental findings, much controversy still remains over the benefit of hESC culture and *in vitro* embryo culture under reduced oxygen tensions (Lengner et al., 2010; Gomes Sobrinho et al., 2011).

1.3.1 Hypoxia-inducible factors

Hypoxia-inducible factors (HIFs) are transcription factors that mediate cellular responses to reduced oxygen concentrations (Kaluz et al., 2008) by regulating the expression of more than 200 genes involved in cell metabolism, particularly glycolysis, angiogenesis, survival, and cell motility amongst others (Semenza, 2000a; Smith et al., 2008) (Chen et al., 2001; Hu et al., 2003). Additionally, HIFs have been shown to directly upregulate the expression of the core pluripotency factors; OCT4, SOX2 and NANOG (Covello et al., 2006; Petruzzelli et al., 2014).

HIFs were discovered through the identification of a minimal hypoxic response element (HRE) in the 3' enhancer of the erythropoietin gene (Semenza and Wang, 1992). HIFs act as heterodimers composed of an α (HIFα) and a β (HIF-1β) subunit. Each heterodimer is made up of the constitutively expressed HIF-1β subunit, also known as aryl hydrocarbon nuclear translocator (ARNT), and one of the three oxygen-regulated α subunits (HIF-1α, HIF-2α or HIF-3α) which are phosphorylation-dependent proteins that bind in the major groove of the DNA under hypoxic conditions (Wang and Semenza, 1993a, 1995; Keith et al., 2001). Both HIF-α and HIF-β subunits belong to the basic helix-loop-helix (bHLH)-Per/Arnt/Sim (PAS) domain family of transcription factors, which are comprised of several conserved domain, including the bHLH domain for DNA-binding and two PAS domains for dimerisation and gene targeting (Figure 1.3) (Wang et al., 1995).

All three HIF-α isoforms are greatly conserved in terms of amino acid sequence and they possess similar biochemical properties in the fact that they all bind HIF-1β, coactivators and HREs (Kaluz et al., 2008). HIF-2α, also known as endothelial PAS domain protein 1 (EPAS-1) (Flamme et al., 1997), and HIF-3α, also known as inhibitory PAS domain protein (IPAS) (Gu et al., 1998) were discovered subsequently to HIF-1α, but displayed a more restricted expression pattern compared to the ubiquitous expression of HIF-1α. HIF-1α is known to bind HREs in hypoxia responsive genes in almost every cell type, but

HIF-2α transcripts are enriched in certain cell types, such as endothelial cells, kidney fibroblasts, glial cells, neural crest cell derivatives and interstitial cells of the pancreas amongst others (Tian et al., 1997; Wiesener et al., 2003). Additionally, HIF-2α is detected in many human tumours both associated and not associated with von Hippel Lindau (VHL) disease, including renal clear cell carcinomas and head and neck squamous cell carcinomas (Harris, 2002). Intriguingly, approximately 50% of renal clear cell carcinoma cells isolated from VHL patients expressed HIF-2α, but not HIF-1α. Hence, this suggests that HIF-2α has a critical role not only in normal development, but also in tumour progression (Maxwell et al., 1999). HIF-3α is the least characterised HIFα subunit and is expressed, for example, in the cerebral cortex, hippocampus, thymus, corneal epithelium, type II pneumocytes and cells of the myeloid lineage (Heidbreder et al., 2003; Wang et al., 2005; Heikkila et al., 2011). Additionally, HIF-3α has several splicing variants, some of which have been reported to inhibit HIF-1α and HIF-2α (Makino et al., 2001; Makino et al., 2002; Maynard et al., 2005; Heikkila et al., 2011).

HIF-1α and HIF-2α share an extensive degree of homology, sharing 48% overall amino acid identity (Hu et al., 2003), however they have distinct non-redundant roles. The first indication that HIF-1α and HIF-2α had distinct roles came from mouse models, in which mice with *Hif2-α* deletions displayed distinct phenotypes from *Hif-1α*$^{-/-}$ embryos, where more than half of HIF-2α$^{-/-}$ mutants died in utero as a result of severe vascular defects and mice which reached full term were smaller and displayed cardiac hypertrophy and haematopoiesis (Peng et al., 2000; Compernolle et al., 2002; Scortegagna et al., 2003a; Scortegagna et al., 2003b; Scortegagna et al., 2005). While HIF-1α has been connected with a metabolic switch towards glycolysis and angiogenesis, HIF-2α has been associated with cell migration, cell proliferation, pluripotency through OCT4, SOX2 and NANOG induction and angiogenesis (Elvert et al., 2003; Covello et al., 2006; Petruzzelli et al., 2014).

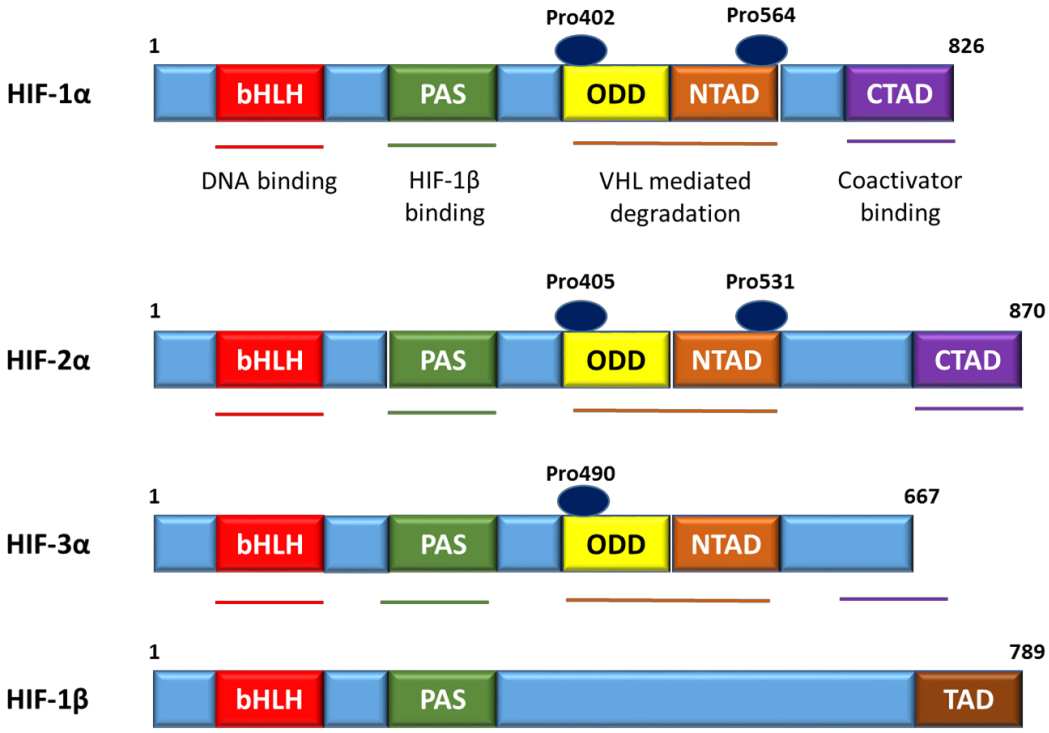

Figure 1.3. Structural domains of the hypoxia-inducible factor (HIF) subunits.
Schematic representation of HIF-1α, HIF-2α, HIF-3α and HIF-1β subunits demonstrating their conserved functional domains. The basic helix-loop-helix (bHLH) and Per/Arnt/Sim (PAS) domains are involved in DNA-binding and heterodimerisation with HIF-1β. The oxygen dependent degradation (ODD) domain is necessary for hydroxylation by prolyl hydroxylases (PHD) and targeting for degradation by VHL proteins. The N-terminal and C-terminal transactivation domains (NTAD and CTAD, respectively) are involved in transcriptional activation. The specific conserved residues to be hydroxylated under normoxic conditions are noted above each isoform. Coloured bars below each protein indicate particular interactions those regions are responsible for within each HIF protein. Adapted from (Rocha, 2007).

1.3.1.1 Regulation of HIFs

HIF regulation is complex, and involves multiple factors which exert different effects both in the stability of the HIF-α subunits and the transcriptional activity of the protein. The primary mechanism of regulation involves HIF-α protein oxygen dependent degradation (Figure 1.4).

Under normoxic oxygen tensions, HIF-α subunits are maintained at low levels of expression as they are hydroxylated by prolyl hydroxylases (PHD), which are dependent upon oxygen and iron as cofactors, on one or two conserved proline residues (Pro402 and Pro564) located within the oxygen-dependent degradation domain of HIF-α subunits in a

Leu-X-X-Leu-Ala-Pro sequence motif. This leads to the inactivation of the HIF-α subunit. Additionally, hydroxylated HIF-α subunits are tagged for recognition by the VHL tumour suppressor protein; an E3 ubiquitin ligase complex comprising of VHL, elongin B, elongin C, Cul2 and Rbx1, and subsequently degraded through the ubiquitin/proteasome complex (Maxwell et al., 1999; Kamura et al., 2000; Bruick and McKnight, 2001). Under normoxia, VHL binds to amino acids 380-417 and 557-571 in HIF-1α and amino acids 383-418 and 517-534 in HIF-2α, while the elongins bind to the C-terminal domains of the HIF-α subunits (Cockman et al., 2000).

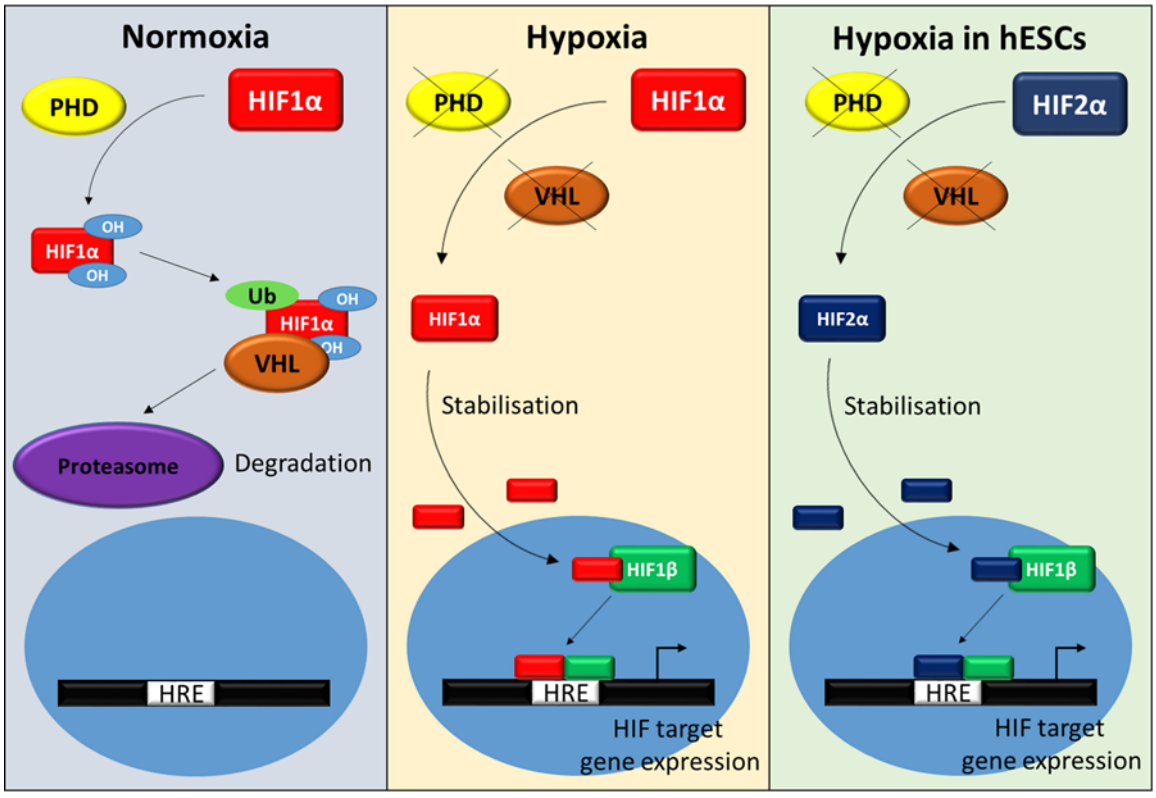

Figure 1.4. Mechanisms of HIF regulation in response to hypoxia.
Under normoxic conditions, HIF1α becomes hydroxylated by prolyl hydroxylases (PHD). The hydroxylated HIF1α subunit is recognised and bound by Von Hippel-Lindau tumour suppressor proteins (VHL) and becomes ubiquitinated by an ubiquitin ligase and targeted for degradation by the proteasome. In contrast, under hypoxia, HIF1α is not hydroxylated and hence, not degraded, but is stabilised and translocates to the nucleus. In the nucleus, it binds the HIF1β subunit, resulting in a complex which can interact with the hypoxia response element (HRE) and initiate the transcription of HIF target genes. Alternatively, HIF2α is the predominant regulator of the hypoxic response in hESCs. Adapted from (De Miguel et al., 2015).

In contrast, hypoxic conditions allow the stabilisation of α subunits, as the PHDs and VHL are inactive due to oxygen deficiency, therefore preventing the hydroxylation of the proline residues and targeting for proteasomal degradation. This leads to the stabilisation and translocation of HIFα subunits from the cytoplasm to the nucleus where they dimerise with HIF-1β to form an active transcriptional complex and enhance the expression of hypoxia-responsive genes (Kallio et al., 1998). All three α subunits bind HREs by recognising a *cis*-acting consensus motif of 5′-(A/G)CGTG-3′ within the proximal promoter or enhancer regions of more than 200 target genes involved in an array of cellular processes (Semenza and Wang, 1992; Wang and Semenza, 1993a, b; Semenza et al., 1994; Semenza, 1996). All these factors bind with the co-activators p300/CREB binding protein (CBP) to complete the fully functional complex at the HRE site, as observed at the glucose transporter 1 (GLUT1) HRE (Rolfs et al., 1997; Wenger, 2000; Chen et al., 2001). However, the dimerisation between the HIF-α and HIF-β subunits and their interaction with the HRE is necessary but not sufficient for the transcriptional activation of hypoxic response genes. HREs also contain binding sites for other TFs to amplify the response, which suggests that HIFs may interact with adjacent proteins and TFs and form multi-protein complexes, where each complex would be different for each hypoxic response gene (Wenger, 2002).

HIF activity can also be regulated through other pathways, such as factor inhibiting HIF1 (FIH-1) which binds HIF-α subunits at its C-terminal transcriptional activation domain (C-TAD). FIH-1 hydroxylates an asparagine residue, which blocks the HIF-α subunit interacting with p300/CBP and impairing HIF transcriptional activity (Mahon et al., 2001; Lando et al., 2002; Webb et al., 2009). Environmental stress also affects HIF-1α expression. Under normoxic conditions HIF-1α expression may also be promoted by Reactive Oxygen Species (ROS), nitric oxide (NO) and heat shock. Mitochondria stimulate the production of ROS under moderate hypoxia, which inhibits PHD, and therefore prevents the degradation of HIFs. The increased ROS production, also, favours HIF stabilisation (Kaelin, 2005; Lum et al., 2007; Majmundar et al., 2010). Moreover, sirtuins, a family of NAD^+ dependent histone deacetylases, have recently been reported to modulate HIF activity. These enzymes represent sensors of the cellular redox state by responding to changes in the NAD^+/NADH ratio. Sirt1 has been reported to bind HIF-1α and HIF-2α and to deacetylate lysine residues located within the proteins, and hence enhance HIF-2α transcriptional activity *in vitro*. With regards to HIF-1α, the

deacetylation caused by Sirt1 decreases its transcriptional activity and Sirt6 modulates glucose levels through HIF-1α inhibition (Dioum et al., 2009; Lim et al., 2010; Zhong et al., 2010).

1.3.1.2 Alternative mechanisms of HIF regulation

There are several alternative mechanisms where HIF-α subunits are regulated under atmospheric oxygen conditions. These mechanisms include cytokines, interleukin-1β, epidermal growth factor, insulin-like growth factor 1 and 2 and platelet-derived growth factor (Zelzer et al., 1998; Feldser et al., 1999; Jung et al., 1999; Stiehl et al., 2002; Gorlach, 2004). Two important mechanisms involved in HIF-α regulation though involve nitric oxide (NO) and reactive oxygen species (ROS).

1.3.1.2.1. Nitric oxide

NO is a free radical and important signalling molecule (Moncada et al., 1991). However, if NO is present in high levels, it can be toxic. NO is synthesised from L-arginine using NO synthases (NOS) of which there are three isoforms; neuronal NOS (nNOS), endothelial NOS (eNOS) and the inducible NOS (iNOS), and each display a specific expression pattern (Ignarro, 1990). NO is important for signal transduction acting in several pathways including the glycogen synthase kinase 3 beta (GSK3β) signalling pathway. NO has been shown to play a crucial role on mESC differentiation by enhancing self-renewal (Tejedo et al., 2010). NO also affects HIF-α activation through concentration dependent mechanisms involving NO metabolites and the availability of oxygen. For example, low NO concentrations have been shown to induce HIF-1α degradation in human embryonic kidney cells. However, high NO levels stabilise HIF-1α in cells maintained under normoxia mimicking the hypoxic response leading to HIF-α accumulation and activity (Mateo et al., 2003). In particular, NO binds with Fe^{2+} which acts to inhibit PHDs and Factor inhibiting HIF (FIH) activity by preventing the hydroxylation of proline residues in HIF-1α that tag the protein for proteasomal degradation (Sandau et al., 2001) (Figure 1.5).

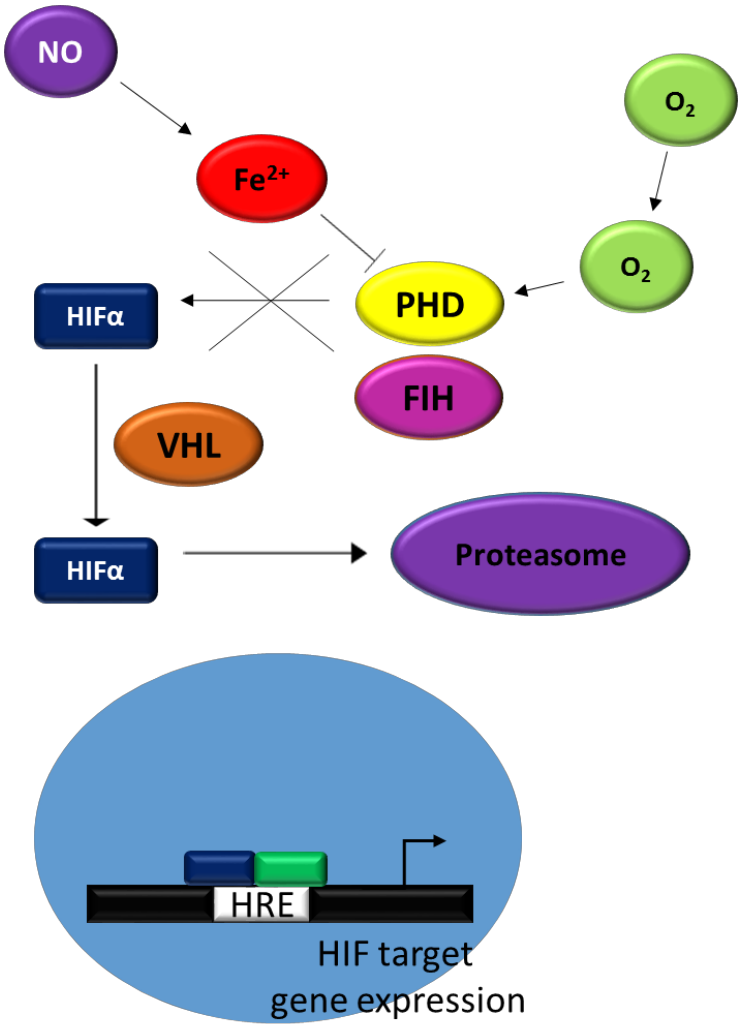

Figure 1.5. Regulation of HIF by NO under normoxia.
NO inhibits PHD and FIH activity by interacting with Fe^{2+} to prevent HIF degradation. As such, HIF-α subunits can accumulate and bind to HREs present in the proximal promoters of target genes, even under normoxia.

1.3.2 Hypoxia, HIFs & pluripotency

There is accumulating data which supports the role of hypoxia in pluripotency, suggesting that environmental oxygen concentration is related to the development and maintenance of pluripotent stem cells. Ezashi *et al*. (2005) were the first to demonstrate that hESCs maintained in a hypoxic environment demonstrated a significant reduction in the percentage of spontaneous differentiation. This study demonstrated that low oxygen concentrations prevented the differentiation of hESCs in culture, and that a hypoxic condition maintained the majority of hESCs within a colony in a pluripotent state. Moreover, the expression of pluripotency-associated genes; OCT4, SOX2 and NANOG, was found to be increased in hESCs cultured under hypoxic conditions, whilst genes associated with differentiation displayed higher levels of expression in hESCs cultured under atmospheric oxygen tensions (Westfall et al., 2008; Forristal et al., 2010; Forristal et al., 2013).

In hESCs, the mechanism of hypoxic regulation differs. hESCs cultured under reduced (2-5%) oxygen tensions only transiently express HIF-1α for approximately 48 hours and so is responsible for the initial adaptive response to hypoxic conditions, whereas HIF-2α is the predominant regulator for the long term hypoxic response in hESCs and moves from being cytoplasmic to nuclear (Forristal et al., 2010). Silencing HIF-2α and HIF-3α, but not HIF-1α, in hESCs cultured under hypoxia, leads to a decrease in the mRNA and protein levels of these genes. In addition, hESCs deficient in HIF-2α fail to proliferate, preventing their maintenance *in vitro* (Forristal et al., 2010). Additionally, HIFs have been subsequently proven to enhance pluripotency-related gene expression. HIF-2α has been reported as a direct regulator of OCT4, SOX2 and NANOG (Covello et al., 2006; Petruzzelli et al., 2014) as well as the glucose transporter GLUT1 (Forristal et al., 2013). Together, these observations indicate that a low oxygen tension is beneficial for the culture and maintenance of hESC pluripotency and self-renewal.

This evidence further supports using a low oxygen tension for the culture of hESCs. However, the mechanisms and regulation of HIFs and how they support pluripotency maintenance under hypoxic conditions still require further investigation.

1.4 Energy metabolism

Energy metabolism provides the fundamental requirements of any cell to support its stage-specific cellular energy needs. However, there is a growing appreciation of metabolic pathways in the regulation of vital cell functions. In this case, the stem cell lifecycle – from acquisition and maintenance of the pluripotent state, to lineage commitment and differentiation – is becoming increasingly more recognised as a metabolism-dependent process.

To meet the energetic demands of a given cell, energy is generated in the form of adenosine-5'-triphosphate (ATP), which can be produced through oxidative phosphorylation or glycolysis. However, these energetic demands are highly likely to vary with cell type. For example, hESCs are rapidly dividing cells, and so will have different energetic demands compared to a larger, differentiated cell (Rafalski et al., 2012). As previously mentioned, hESCs have a shortened G1 cell cycle phase (Becker et al., 2006), and it is within this stage that the majority of biomass accumulation and differentiation occurs. Therefore, the biosynthetic demands during this shortened phase are higher, and so hESCs must reach a suitable balance between ATP production and the biosynthesis of nucleotides, proteins and lipids.

1.4.1 Glycolysis & oxidative phosphorylation

Energy production during early mammalian development is dependent upon several factors including substrate availability, substrate uptake and oxygen tension. All mammalian cells produce ATP through differing proportions of glycolysis and oxidative phosphorylation (OXPHOS), with a balance between the two pathways controlled by various intra- and extracellular factors at different developmental stages and states of cellular activation.

Glycolysis is the enzymatic conversion of glucose into pyruvate generating a net gain of 2 molecules of ATP per glucose molecule (Figure 1.6). Additionally, cells that predominantly depend on glycolysis for ATP production further convert pyruvate into lactate, which is subsequently secreted. In contrast, cells in the presence of oxygen may primarily use OXPHOS for much more efficient ATP production, by metabolising glucose into carbon dioxide through the oxidation of pyruvate generated in glycolysis into acetyl-coenzyme A (acetyl-coA) in the tricarboxylic acid (TCA) cycle. The TCA cycle produces reduced nicotinamide adenine dinucleotide (NADH), which subsequently

drives mitochondrial OXPHOS to generate up to 36 ATPs per molecule of glucose metabolised (Figure 1.6) (Lehninger et al., 1993).

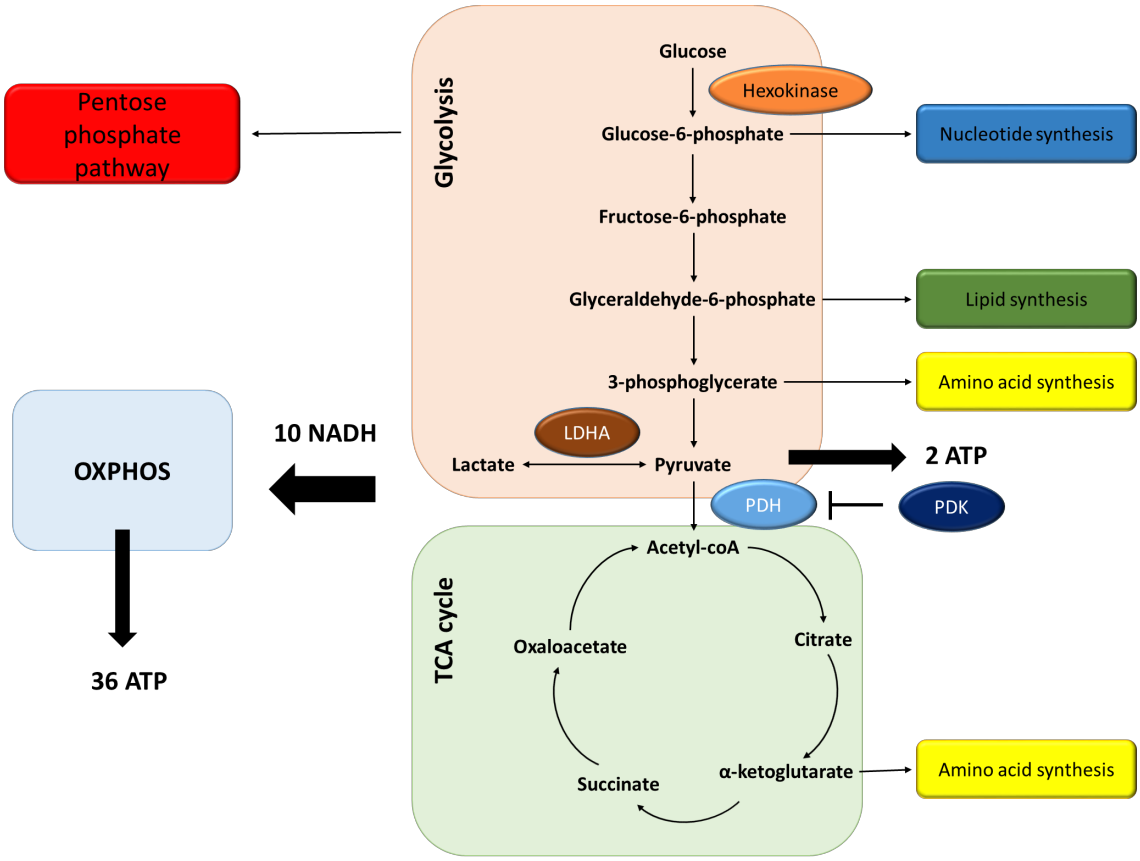

Figure 1.6 Schematic diagram illustrating oxidative and non-oxidative metabolism.
hESCs mostly rely on a glycolytic metabolism for their energy generation. This provides a suitable balance between ATP production and biosynthesis of nucleotides, lipids and proteins, via flux through the pentose phosphate pathway and the use of intermediates in the TCA cycle. Cells undergoing differentiation switch to a metabolism that is more reliant on oxidative phosphorylation, which allows more efficient production of ATP per glucose molecule metabolised. Adapted from (Folmes and Terzic, 2016). OXPHOS, oxidative phosphorylation; TCA, tricarboxylic acid cycle, PDH, pyruvate dehydrogenase; PDK, pyruvate dehydrogenase kinase; LDHA, lactate dehydrogenase A.

During early embryonic development, there is a metabolic shift which sees cells switch from an OXPHOS based metabolism towards a predominantly glycolytic metabolism for

their energetic needs. It is not until implantation of the embryo that the metabolic state shifts back to a reliance on OXPHOS (Leese and Barton, 1984). This is emphasised in studies with mouse blastocysts, where the ICM possesses a completely glycolytic metabolism. In comparison, the differentiated trophectoderm displays higher oxygen consumption and the rate of glucose uptake and lactate production is three to five times lower than cells of the ICM (Hewitson and Leese, 1993; Houghton, 2006). *In vivo* differences in early mammalian embryo energy metabolism might be replicated in their *in vitro* counterparts from different stages of mammalian development, which has been demonstrated in a recent study where naïve hESCs demonstrated increased glycolytic flux compared to primed hESCs and their differentiated counterparts (Gu et al., 2016).

Many stem cells types, including hESCs, produce their energy through anaerobic glycolysis, which is consistent with their origin and their immature mitochondrial phenotype. In fact, hESCs rely heavily on glycolysis for their energy supply, with approximately 50-70% of glucose converted into lactate by the enzyme lactate dehydrogenase A (LDHA; Figure 1.6) (Varum et al., 2011). Interestingly, as these pluripotent cells differentiate, there is a simultaneous switch to an oxidative phosphorylation metabolism, which again mimics their *in vivo* counterparts (Figure 1.7) (Cho et al., 2006; Ramalho-Santos et al., 2009; Prigione and Adjaye, 2010). Additionally, the reverse switch occurs with the generation of iPSCs, as cells show an increased glycolytic flux and reduced OXPHOS after reprogramming (Prigione and Adjaye, 2010; Folmes et al., 2011; Varum et al., 2011). Levels of OXPHOS in hESCs are relatively low, which is supported by the immature mitochondrial phenotype displayed by hESCs, consisting of perinuclear mitochondria with a swollen morphology displaying a lack of inner membrane cristae folds usually observed in differentiated cell types (Sathananthan et al., 2002; Varum et al., 2011). Furthermore, the metabolic switch observed upon differentiation of hESCs is accompanied by the gain of a mature mitochondrial phenotype displaying distinct cristae folds (Cho et al., 2006; St John et al., 2006; Ramalho-Santos et al., 2009).

It has been documented that hESCs maintained at 5% oxygen tension take up significantly more glucose and produce more lactate compared to hESCs cultured at 20% oxygen tension, thus suggesting the rate of flux through glycolysis is greater at 5% oxygen compared to 20% (Forristal et al., 2013). Together, these studies illustrate how a hypoxic environment supports a glycolytic-dependent metabolism to the detriment of OXPHOS

in hESCs (Figure 1.7). Yet, standard culture of hESCs occurs at 20% oxygen tensions and hESCs maintained under these conditions also display an anaerobic glycolytic metabolism.

The first glycolytic reaction after glucose has entered a cell through transporters, such as GLUTs, is the conversion of glucose into glucose-6-phosphate by the enzyme hexokinase (Figure 1.5). Cells that display a high rate of glycolysis, also, express high levels of hexokinase (Bustamante and Pedersen, 1977; Bustamante et al., 1981). Furthermore, the pyruvate dehydrogenase (PDH) complex links glycolysis with the TCA cycle and catalyses the conversion of pyruvate into acetyl-coA and NADH. Phosphorylation of its E1α subunit by one isoform of the four pyruvate dehydrogenase kinases (PDK) inactivates the complex (Figure 1.6). This forces glucose metabolism towards lactate production as the TCA cycle is inaccessible (Holness and Sugden, 2003; Roche and Hiromasa, 2007).

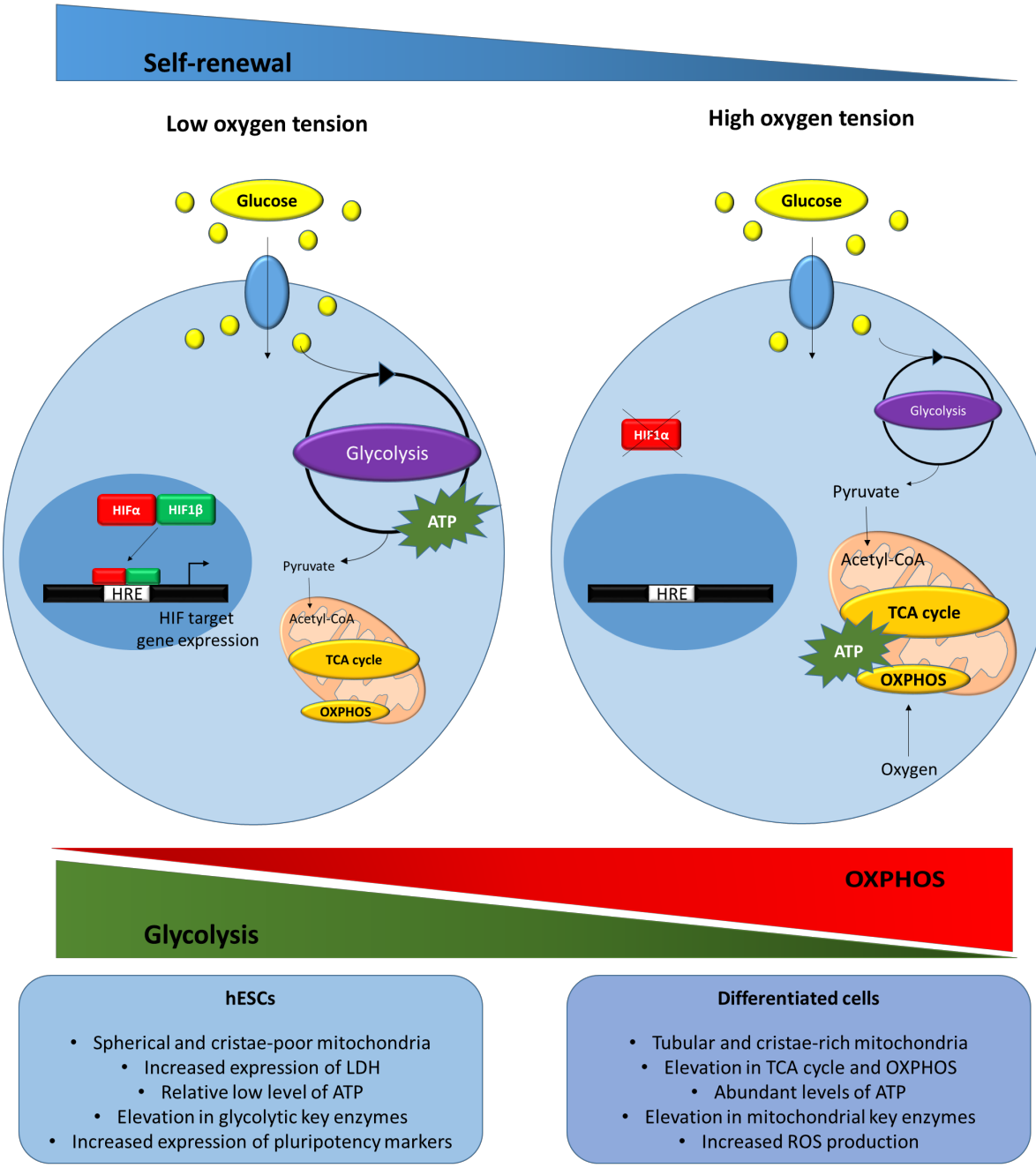

Figure 1.7. Influence of energy metabolism on the hESC pluripotent state.
Many stem cell niches exhibit low oxygen tensions. Stem cells, such as hESCs, generate ATP predominantly through glycolysis, which is independent of oxygen tension. Under low oxygen tensions, HIF-α is stabilised and binds to its partner HIF-1β. The HIF heterodimer binds to the HRE site within the proximal promoter of HIF target genes, such as those involved in glucose metabolism and transport. This leads to an increased rate of glycolytic flux in hESCs, and hence leads to a shift towards a predominantly anaerobic glycolytic metabolism. Conversely, upon differentiation, there is a switch towards a more oxidative metabolism, which is supported with the maturation of mitochondria. Differentiated cells generate ATP primarily through OXPHOS, which requires oxygen due to being the final electron acceptor in the electron transport chain. Adapted from (Hu et al., 2016) and (Rafalski et al., 2012). OXPHOS, oxidative phosphorylation; TCA, tricarboxylic acid cycle; HRE, hypoxia response element; HIF, hypoxia-inducible factor.
However, hypoxic culture of hESCs enhances the expression of hexokinase and PDK1.

Hexokinase expression is upregulated by HIF-1α and hESCs have, also, demonstrated high levels of hexokinase expression (Semenza, 2000a; Varum et al., 2011). Expression of one pyruvate dehydrogenase kinase isoform, PDK1, is also upregulated by HIF-1α and hESCs have been shown to have inactive PDH complexes (Semenza, 2000a; Varum et al., 2011). Therefore, it has been suggested that high levels of hexokinase and an inactivated PDH complex may be a mechanism through which hESCs maintain a high level of glycolysis (Varum et al., 2011).

OXPHOS is the metabolic pathway where cells use enzymes to oxidise nutrients, and therefore releasing energy in the form of ATP which occurs inside the mitochondria, unlike glycolysis which occurs in the cytoplasm. During OXPHOS, electrons are transferred from electron donors to electron acceptors, where oxygen is the terminal electron acceptor in what is called the electron transport chain (ETC). It is these redox reactions that generate the net gain of 36 ATP molecules (Figure 1.6), which are carried out by a series of protein complexes in the inner mitochondrial membrane (Lehninger et al., 1993). Some key components of the mitochondrial respiratory chain complexes, such as NDUFC1 and UQCRB which are parts of complex I and complex III respectively and cytochrome c oxidase, have been shown to be upregulated upon differentiation. However, the majority of the ETC machinery is expressed in hESCs, and hence emphasises that although OXPHOS cannot occur in hESCs, it is in a poised state (Abu Dawud et al., 2012). This evidence supports the previous mentioned metabolic switch from reliance on glycolysis to OXPHOS upon the initiation of differentiation (Prigione and Adjaye, 2010).

1.4.2 Glycolysis & pluripotency

Safe use of pluripotent stem cell derivatives in regenerative medicine requires an enhanced understanding and control of factors that optimise *in vitro* reprogramming and differentiation protocols, especially as several recent studies have linked changes in energy metabolism with the fate of hESCs (Folmes et al., 2011; Prigione et al., 2011; Zhou et al., 2012; Folmes and Terzic, 2016; Gu et al., 2016; Zhang et al., 2016). Relative shifts in metabolism from naïve to primed pluripotent states and lineage-directed differentiation place variable demands on mitochondrial biogenesis and function for cell types with distinct energetic and biosynthetic requirements. In this context, mitochondrial respiration, hypoxia, TF network dynamics, TCA cycle function, and glycolytic rate all have the potential to influence reprogramming and differentiation outcomes, and therefore the maintenance of the pluripotent state.

While the reliance on glycolysis in tissue-specific stem cells fits with the lower energy demands of their quiescent state and aids the limitation of oxidative metabolism-dependent ROS production to ensure tissue renewal, the importance of utilising glycolysis in highly proliferative cells, such as hESCs, is less obvious, yet still remains a consistent feature. It is well-documented that glycolysis is less efficient in terms of energy production, as it only produces a fraction of the 36 molecules of ATP that can be generated via OXPHOS, but it enables a faster rate of ATP generation compared with oxidative metabolism. Therefore, in the presence of abundant resources, for example in cell culture systems where hESCs are exposed to high levels of glucose, a heavy reliance on glycolytic metabolism may be advantageous as it maintains pools of carbon intermediates required for the biosynthesis of cellular contents that will enable the generation of new daughter cells.

As previously discussed, HIFs regulate approximately 200 genes, where metabolic genes feature extensively including those involved in glucose uptake and glycolytic enzymes, such as LDHA (Hu et al., 2003; Hu et al., 2006). In fact, it was observed that increases in expression of some glycolytic genes, including *GLUT1* and *LDHA*, precede the increases in expression of the pluripotency genes *OCT4*, *SOX2* and *NANOG*, suggesting that metabolism plays an important part in pluripotency and reprogramming (Folmes et al., 2011). GLUTs are a family of structurally related and conserved proteins involved in the passive and facilitative transport of glucose down the concentration gradient. GLUT1 and GLUT4 have been found to be upregulated by HIFs, which allows the cells to meet the increased demand for glucose after the metabolic switch to a more glycolytic-based metabolism (Hu et al., 2006). Additionally, GLUT3 has been documented to play a role in regulating OCT4 expression and therefore, maintenance of the pluripotent state of hESCs. Silencing GLUT3 in hESCs cultured at 5% oxygen displayed a reduction in glucose uptake and a decrease in lactate production, as well as a reduction in OCT4 expression. This correlation between GLUT3 and OCT4 expression suggests that hESC self-renewal is regulated by the rate of glucose uptake (Christensen et al., 2015). Pyruvate kinases are the enzymes that catalyse the final step of glycolysis; the conversion of phosphoenolpyruvate and adenosine diphosphate (ADP) into pyruvate and ATP. There are two different splice variants of pyruvate kinase enzymes, M1 and M2 (PKM1/2), where PKM2 is able to translocate into the nucleus and dimerise. PKM2 dimers are able to bind to promoter regions, such as HRE sites of *OCT4*, and initiate their transcription

(Lee et al., 2008) after the tetramerisation of PKM2 is inhibited by binding to JMJD5 (Wang et al., 2014). The nuclear translocation of PKM2 is also correlated with hydroxylation by PHD3 at Pro-403 and Pro-408, of which PHD3 itself is a HIF-1α transcriptional target (D'Angelo et al., 2003; Luo et al., 2011). HIF-1α activation, also, affects metabolic regulators such as PKM2, which leads to increased glycolysis. An increase in PKM2 coupled with the decreased PDH activity occurs in hESCs, as well as iPSCs (Prigione et al., 2014). OCT4 and PKM2 are known to interact via the POU DNA –binding domain in the pluripotency marker, and the transcriptional activity of OCT4 is positively regulated by PKM2, suggesting that PKM2 has an alternative function as a TF, particularly as silencing PKM2 in hESCs had no effect on the glycolytic flux, whereas PKM1 is likely to be responsible for the enzymatic functions (Lee et al., 2008; Christensen et al., 2015). Silencing PKM2 in hESCs, also, displayed reduced levels of OCT4 expression, re-emphasising the role of PKM2 in transcriptional activation of core pluripotency factors (Christensen et al., 2015). Moreover, a recent study in mESCs have revealed that core pluripotency factors directly regulate glycolysis by controlling the expression of key glycolytic enzymes in a positive feedback loop to maintain high glycolytic levels, and therefore the pluripotent state (Kim et al., 2015). OCT4 was found to occupy the promoter regions of hexokinase 2 (*Hk2*) and *Pkm2*, and aids in their transcriptional activation. Additionally, sustaining high levels of glycolytic flux through overexpression of Hk2 and Pkm2 displayed delayed ESC differentiation upon OCT4 depletion demonstrating the significance of metabolic state in maintaining a pluripotent state (Kim et al., 2015). Similarly, inhibition of the mitochondrial ETC has been shown to support pluripotency and self-renewal in hESCs and prevents differentiation (Chung et al., 2007; Mandal et al., 2011; Varum et al., 2011).

These shifts in cellular metabolism affect enzymes and cofactors that control epigenetic configuration, which impacts chromatin reorganisation and gene expression changes during hESC pluripotency maintenance and reprogramming. hESCs demonstrate unique epigenetic features involved in the regulation of stem cell pluripotency, including a heavily euchromatic state and hyper-dynamic associations of chromatin proteins with DNA which are both mediated by histone acetylation, histone methylation or DNA methylation. There is accumulating evidence demonstrating that intermediate metabolites such as acetyl-coA, S-adenosylmethionine (SAM), ATP and NAD^+, also, function as substrates or cofactors for chromatin modifications to regulate epigenetic changes and

couple cellular metabolic state with gene expression (Etchegaray and Mostoslavsky, 2016).

Histone acetyltransferases (HATs) transfer the acetyl group from the metabolite acetyl-coA to the lysine residues of histones and facilitate histone acetylation, so the availability of acetyl-coA is a major influence in histone acetylation and HAT activity, and therefore gene expression. Changes in glucose metabolism alter the availability of glycolysis-generated acetyl-coA; the essential cofactor for protein acetylation (Wellen et al., 2009). More specifically, reduced acetyl-coA production is linked with hESC differentiation and therefore, the loss of histone H3K9 and H3K27 acetylation, which suggests that acetyl-coA facilitates histone acetylation and an open chromatin state in hESCs, thus supporting the pluripotent state (Moussaieff et al., 2015).

NAD^+ is involved in various oxidative metabolic pathways including glycolysis and OXPHOS, however NAD^+ also functions as a cofactor for class III histone deacetylase (HDAC) enzymes called sirtuins. Studies of NAD^+-dependent sirtuins which target both histone and non-histone proteins have demonstrated that deacetylation is responsive to metabolic cues. Sirtuins are dependent on NAD^+ hydrolysis for their deacetylase activity, which is also sensitive to changes in the intracellular NAD^+/NADH ratio.

Together, this data suggests that modulation of the levels of these metabolites can influence the balance between pluripotency and the initiation of differentiation through epigenetic modifications.

These studies support the idea that the hypoxia-induced response can maintain the pluripotent state through its control and regulation of metabolism, as it will work to prevent the metabolic switch associated with differentiation. If glucose metabolism plays an important role in the maintenance of the pluripotent state, then it may be possible to devise a more appropriate culture medium for long-term culture of hESCs for regenerative medicine purposes. Altogether, this supports the idea that changes in environmental oxygen tensions and, therefore, the HIF-mediated response to hypoxia may support the maintenance of a pluripotent state by significantly impacting hESC metabolism through its support of a glycolytic-based metabolism, either by regulating the rate of glucose uptake or through transcriptional activation of glycolytic or pluripotency-associated genes.

1.5 C-terminal binding proteins

C-terminal binding proteins (CtBPs) are a family of glycolytic sensors that link changes in metabolism to gene expression, and function primarily as transcriptional corepressors in association with sequence-specific DNA-binding transcription factors (TF), however there is increasing evidence that CtBPs, also, act as transcriptional co-activators (Fang et al., 2006; Bajpe et al., 2013; Itoh et al., 2013; Ray et al., 2014). They were initially identified by their ability to interact with the carboxy-terminal domain of the E1A adenovirus (Boyd et al., 1993; Schaeper et al., 1998), as mutating the site of CtBP-binding saw a decrease in its transcriptional repression effects, where cells became immortalised as CtBPs demonstrated a pro-survival role by suppressing the expression of pro-apoptotic genes (Subramanian et al., 1989; Subramanian et al., 1991). Subsequently, CtBPs were first defined as transcriptional corepressors in a normal cellular function in *Drosophila*, by identifying functional CtBP-binding consensus sequences in *Drosophila* transcriptional repressors Hairy, Knirps and Snail (Nibu et al., 1998a; Nibu et al., 1998b; Poortinga et al., 1998).

1.5.1 CtBP isoforms – structure & function

In humans, there are two CtBP gene loci; aptly called *CtBP1* and *CtBP2*, which are widely expressed and essential throughout development. *CtBP1* maps to chromosome 4p16 (Chinnadurai, 2007a), whereas *CtBP2* maps to chromosome 21q21.3 (Katsanis and Fisher, 1998). Transcripts from both *CtBP1* and *CtBP2* are widely expressed throughout embryogenesis, vertebrate development and in adult tissue (Katsanis and Fisher, 1998; Furusawa et al., 1999; Sewalt et al., 1999; Hildebrand and Soriano, 2002), where *CtBP1*-deficient mice are viable but are approximately 30% smaller than their wild-type counterparts and die early and *CtBP2*-deficient mice display an embryonic lethal phenotype (Chinnadurai, 2003). However, *CtBP1* is often expressed at higher levels and in a wider range of tissues compared with *CtBP2* (Furusawa et al., 1999; Sewalt et al., 1999). The CtBP proteins are highly homologous and exhibit functionally redundant and unique roles throughout animal development (Hildebrand and Soriano, 2002).

The proteins encoded by *CtBP1* and *CtBP2* share 78% amino acid identity and 83% similarity (Katsanis and Fisher, 1998) and can function interchangeably. The *CtBP1* locus produces two protein isoforms; CtBP1-S and CtBP1-L, as a result of differential RNA splicing (Figure 1.8), which differ by 13 amino acids at the N-terminus (Bergman et al., 2006; Chinnadurai, 2007b). Whereas the *CtBP2* locus produces three protein variants;

CtBP2-S, CtBP2-L and a retina-specific variant called RIBEYE generated using both alternative splicing and alternative promoter usage (Figure 1.8) (Katsanis and Fisher, 1998; Schmitz et al., 2000; Verger et al., 2006). RIBEYE contains a large N-terminal domain, which is unrelated to CtBPs, linked to a truncated variant of CtBP2, where this form lacks 20 N-terminal amino acids (Schmitz et al., 2000). RIBEYE is expressed using a tissue-specific promoter within an intron of the *CtBP2* locus, while CtBP2 is ubiquitously expressed from a different 5' promoter. CtBP1-L and CtBP2-L are highly similar proteins of 440 and 445 amino acids in length, respectively (Bergman et al., 2009) and widely expressed in normal tissues.

CtBPs have a conserved domain structure, where each monomer includes an NAD(H) binding domain, PXDLS-binding domain and dimerisation domain (Figure 1.8) (Chinnadurai, 2007b). CtBPs are characterised through their conserved central dehydrogenase homology domain, whose primary function is NADH-dependent dimerisation, and shares high amino acid homology with NAD-dependent D2-hydroxy acid dehydrogenases (D2-HDHs) (Schaeper et al., 1995; Chinnadurai, 2002). There is a high degree of homology between D2-HDHs and CtBP NAD(H)-binding domains, specifically a NAD(H)-binding motif GXGXXG, which extends over a Rossman-fold motif; a parallel β-sheet flanked either side by α-helices characteristic of NAD^+ dependent dehydrogenases, required for NAD(H) binding and a catalytic triad of histidine-glutamine-arginine (His/Glu/Arg) at the active site (Schaeper et al., 1995). It is the NAD^+ /NADH binding within the dimerisation domain that mediates most of the dimerisation contacts on the dimer interface (Kumar et al., 2002).

CtBPs are recruited to promoter elements through interactions with TFs that contain a PXDLS motif. Crystallography studies have revealed the PXDLS-binding domain is lined with hydrophobic residues, while the cleft it forms consists of a β-sheet formed by two β strands and a α2 helix (Kumar et al., 2002; Nardini et al., 2003). Additionally to PXDLS-mediated binding, some TFs interact with CtBPs through a redundant binding motif called the RRT motif, which is located within the dinucleotide-binding domain (Quinlan et al., 2006a). Many proteins that contain a RRT motif, also, contain one or two PXDLS-like motifs, therefore it is possible that the RRT motif has a role in stabilising the interactions mediated by the PXDLS motif (Chinnadurai, 2007b). Crystallographic studies have demonstrated that, like D2-HDHs, CtBPs form dimers (Kumar et al., 2002; Nardini et al., 2003). Each dimer, therefore, contains two PXDLS-binding motifs and two RRT-binding

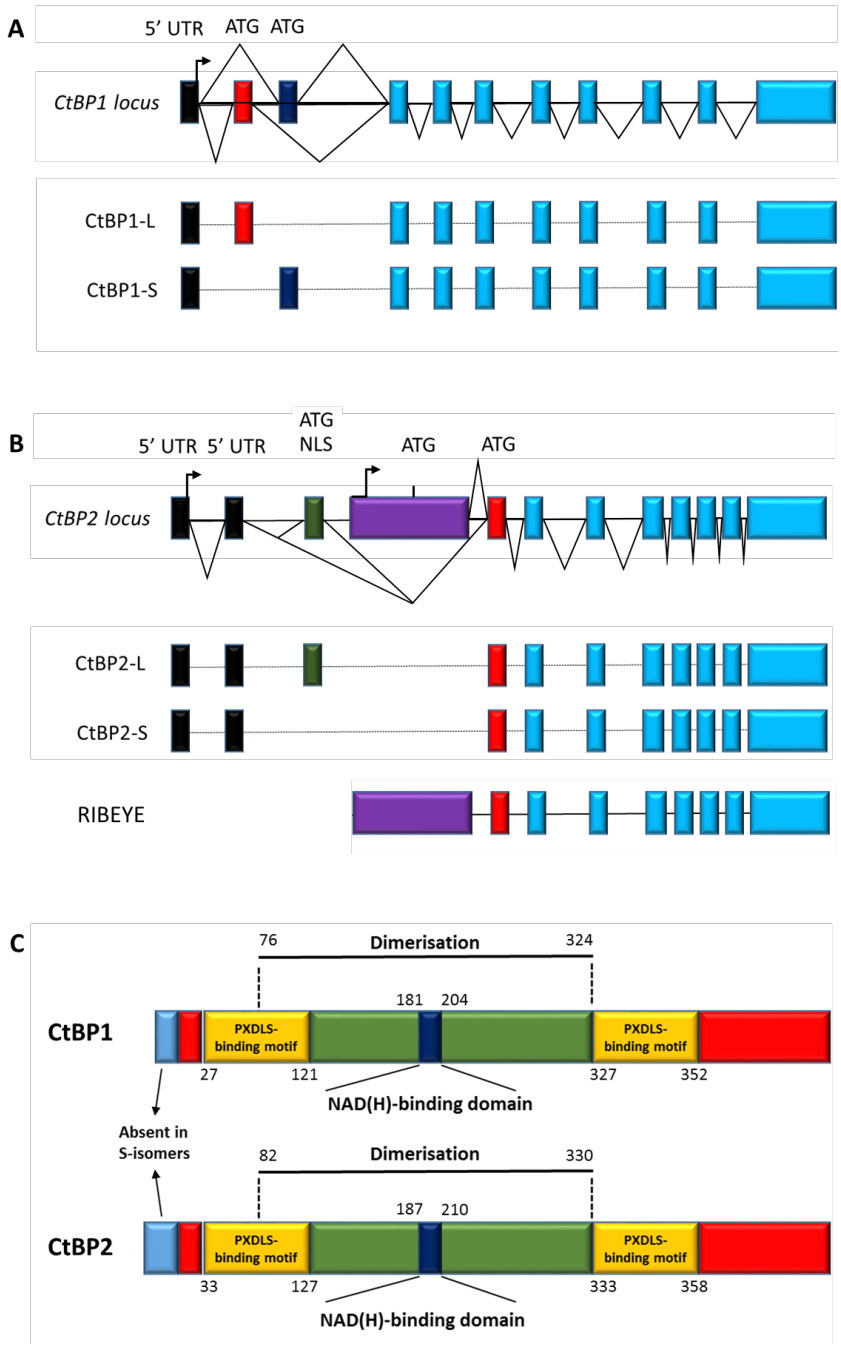

Figure 1.8. Schematic representation of the exon structure of the CtBP genomic loci, splicing patterns and protein domain structure.

(A) Schematic representation of the CtBP1 exon structure and splicing pattern. Each isoform is generated through alternative splicing where there is one exon including an ATG start site for CtBP1-L (red) and one for the CtBP2-S isoform (dark blue). (B) Schematic representation of the CtBP2 exon structure and splicing pattern. CtBP2 splice variants are generated using alternative promoter usage and alternative splicing. The unique N-terminal domain of the RIBEYE variant (purple) is under the influence of a different promoter and contains its own ATG start site. The unique nuclear localisation signal (NLS) of CtBP2 is indicated (green). (C) Simplified model of the protein domain structure of CtBP1 and CtBP2 isoforms. Both CtBP1 splice variants are highly homologous with the corresponding CtBP2 variants. Sequences that make up the PXDLS-binding motifs are shown by the yellow domains. The blue domains show the region which binds NAD^+/NADH, which is surrounded by the dimerisation domains as indicated. The N-terminal domains (blue) are absent from the CtBP1-S and CtBP2-S isoforms and account for the reduction in amino acid length. Adapted from (Chinnadurai, 2007b) and (Verger et al., 2006).

clefts. Furthermore, the PXDLS-binding motif of one CtBP monomer and the RRT-binding motif from the other monomer sit on the same dimer face within close proximity of each other. This suggests that a CtBP-interacting protein with both motifs would bind across the dimer (Quinlan et al., 2006b). The three-dimensional structure of CtBPs consists of a single globular domain and is a bent L-shaped configuration which is characteristic of other NAD^+ dehydrogenases. This is formed by its N-terminal and C-terminal domains, linked to the core dimerisation domain by two flexible hinges (Kumar et al., 2002; Nardini et al., 2003), where the PXDLS-binding motif is contained within the N-terminal region and the C-terminal region plays a regulatory role as it comprises many post-translational modification sites.

CtBPs have been assigned two distinct functions. They are primarily known for their role in the nucleus as short-range transcriptional co-repressors (Turner and Crossley, 2001; Chinnadurai, 2002, 2007a) but both variants have been shown to possess cytosolic functions too, as regulators of Golgi apparatus fission, and additionally, play important roles in visual and auditory Ribbon synapses as well as conventional chemical synapses (Schmitz et al., 2000; Bonazzi et al., 2005; Corda et al., 2006; Chinnadurai, 2007a). CtBPs are functionally interchangeable and can form homo- and heterodimers (Kumar et al., 2002; Nardini et al., 2003), However, there are differences in their regulation through post-translational modifications (Hildebrand and Soriano, 2002; Lin et al., 2003), particularly in the control of their subcellular distribution, with only CtBP2-L containing a nuclear localisation sequence (NLS) located at its unique N-terminus (Bergman et al., 2006; Verger et al., 2006; Zhao et al., 2006), which is key for regulating the nuclear-cytoplasmic distribution of the protein (Bergman et al., 2006). This NLS is evolutionarily conserved and has been shown to function by promoting nuclear accumulation of CtBP2; particularly nuclear retention rather than nuclear import (Verger et al., 2006; Zhao et al., 2006).

Conversely, CtBP1 subcellular distribution has been shown to be regulated with a variety of post-translational modifications. For example, phosphorylation of CtBP1 at Ser158 by p21-activated kinase 1 (PAK1) results in an accumulation of CtBP1 in the cytoplasm, hence inhibiting its transcriptional repression activities (Barnes et al., 2003), whereas certain transcriptional repressors, such as NET, can recruit CtBP1 to the nucleus (Criqui-Filipe et al., 1999). Additionally, an evolutionarily conserved PDZ-binding domain with the conserved motif DXL can be found in the C-terminal region of CtBP1 exclusively. It

is involved in nuclear export when associated with PDZ-containing proteins, such as neuronal nitric oxide synthase, in conjunction with sumoylation at K428 (Riefler and Firestein, 2001; Lin et al., 2003), where both of these sites are absent in CtBP2. SUMOylation is another post-translational modification proposed to be involved in the nuclear retention and therefore the activity of CtBPs. Human Polycomb protein 2 (HPC) was found to interact with CtBPs originally in yeast two-hybrid screens (Sewalt et al., 1999) and is implicated in the assembly of higher-order chromatin structures. HPC2 enhances SUMOylation at K428 of CtBP1 by acting as a SUMO E3 ligase. Yet, there are contrasting reports in the literature of SUMOylation of CtBP2 by HPC (Kagey et al., 2003; Lin et al., 2003). However, the role of CtBP SUMOylation is yet to be fully characterised. It is possible that the translocation of CtBP proteins is a regulatory event to disrupt any CtBP-mediated transcriptional activity, or simply to provide CtBP proteins for the aforementioned cytoplasmic functions.

1.5.2 Regulation of CtBP transcriptional activity by NAD(H) dinucleotides

The transcriptional activity of CtBPs is regulated by the nuclear NAD^+ /NADH ratio, hence appears to be influenced by the metabolic status of the cell, and so may differentially modulate the repressive activities of CtBP-recruited factors. The compelling sequence and structural homology between D2-HDHs and CtBPs predicted the critical role of NAD(H) dinucleotides in CtBP activity, and was supported when mutations in the NAD(H) binding motif of a Gal4-dCtBP chimeric construct abolished its repressive activity (Sutrias-Grau and Arnosti, 2004).

CtBPs bind both NAD^+ and NADH (Balasubramanian et al., 2003) to enhance their oligomerisation. CtBPs have >100 fold higher affinity for binding NADH compared to NAD^+ (Zhang et al., 2002; Fjeld et al., 2003). This postulates CtBPs as a redox sensor linking cellular metabolic status with transcriptional regulation.

As previously mentioned, CtBPs can form and act as heterodimers and homodimers. Critically, this dimerisation is initiated when the ligand, preferably NADH, is occupying the dinucleotide-binding site within the dimerisation domain (Kumar et al., 2002; Balasubramanian et al., 2003; Thio et al., 2004). The NAD(H) binding induces a conformational change promoting its dimerisation, binding to PXDLS-containing proteins and consequently its ability to repress transcription from a set of target promoters (Zhang et al., 2001; Fjeld et al., 2003; Thio et al., 2004). Notably, a CtBP dimer has the

potential to form the core of two complexes containing two PXDLS-containing proteins. Yet, the NADH-unbound form of CtBP binds Hdm2, which represses p53-dependent transcription, and p300/CBP, so may, also, affect p300-dependent gene transcription (Mirnezami et al., 2003; Kim et al., 2005a).

Levels of intracellular NADH dramatically change, for example, in response to ethanol, cellular hypoxia and in metabolic diseases, such as diabetes. Therefore, CtBPs may potentially regulate broad-ranging gene expression changes in response to sensing alterations in cellular metabolism. NADH is produced through glycolysis, and therefore the rate of glycolysis can increase the levels of intracellular NADH. As these levels increase, there is more NADH to bind the dinucleotide-binding site within the dimerisation domain of CtBP monomers and promote their dimerisation. Consequently, there are more functionally active CtBP dimers that can translocate to the nucleus to recruit chromatin modifying complexes to specific gene promoters and change the epigenetic signature of the cell (Figure 1.9). For example, treating cells with chemicals that induce a hypoxic environment and increase glycolysis lead to increased levels of NADH and stimulated CtBP binding to target TFs resulting in enhanced transcriptional repression (Chinnadurai, 2003). However, the role of CtBPs in hESCs and particularly pluripotency maintenance has received little attention.

Additionally, CtBPs are phosphoproteins and have, also, been shown to be phosphorylated in a cell-cycle dependent manner (Boyd et al., 1993). This phosphorylation status plays a key role in induction of apoptosis and therefore the regulation of CtBP activity.

1.5.3 Mechanisms of CtBP-mediated repression

Transcriptional repression is an important mechanism in the regulation of gene expression, where DNA sequence-specific repressors often mediate their effects by recruiting corepressors through various mechanisms, but primarily through targeting components of the basal transcription machinery or altering the chromatin structure.

The most well-documented function of CtBPs is as a transcriptional corepressor. They are thought to be recruited to promoters by sequence-specific TFs through direct physical interactions or indirectly through bridging proteins. Subsequently, CtBPs mainly function as a scaffold to recruit chromatin-modifying enzymes, including histone deacetylases (HDAC), histone methyltransferases (HMT) and Polycomb group (PcG) proteins, to TFs

containing a PXDLS-binding motif to form a CtBP corepressor complex in order to change the local chromatin state (Kuppuswamy et al., 2008; Shi et al., 2003). However, the exact mechanisms involved in CtBP-mediated gene repression remain to be elucidated.

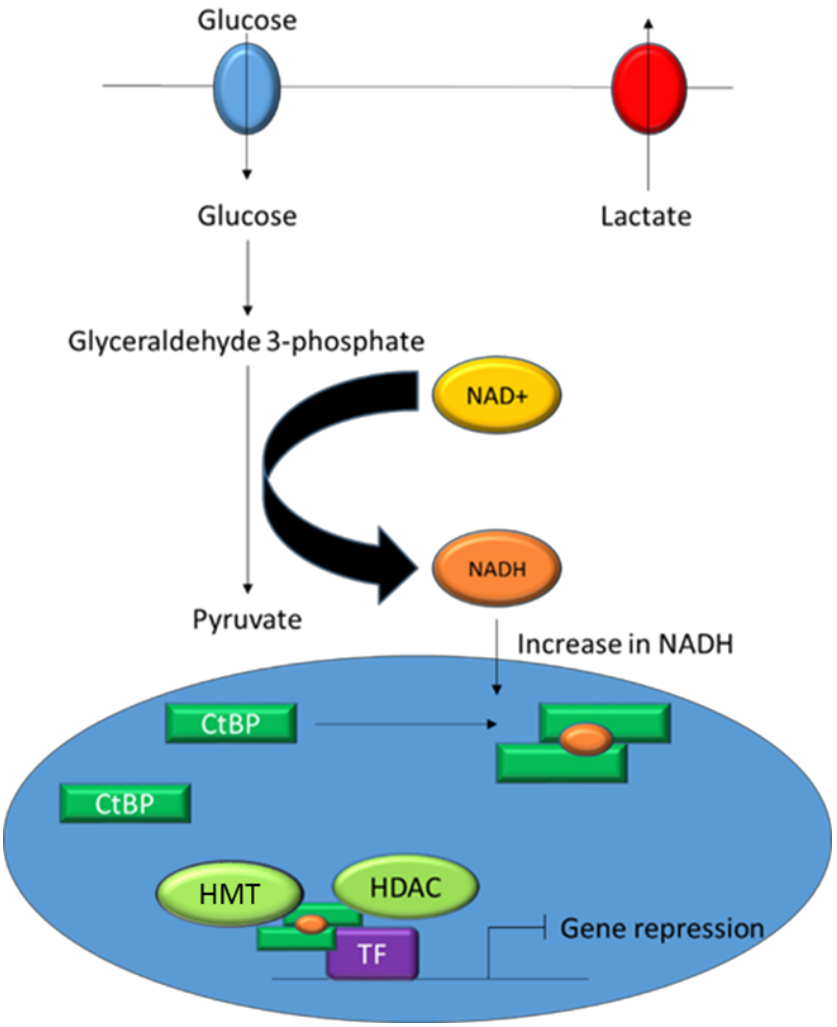

Figure 1.9. Regulation of C-terminal binding protein activity by NAD(H) dinucleotides. Within a cell undergoing glycolysis, NAD^+ is converted into NADH. An increase in the rate of glycolysis will consequently see an increase in the levels of free NADH. NADH binds to CtBPs and promotes dimerisation and activation. Activated CtBP dimers can, then, translocate to the nucleus and bind to DNA-binding transcription factors that are bound to relevant gene promoters. CtBPs, subsequently, act as a scaffold for components of the corepressor complex and recruit chromatin-modifying complexes, such as histone deacetylases (HDACs) and histone methyltransferases (HMTs), to the gene promoter to condense the chromatin and induce gene repression.

CtBP recruitment has been implicated in the modulation of more than 30 different transcriptional regulators, with the best characterised being SLUG and ZEB/δEF1, which repress the expression of epithelium-specific genes (Furusawa et al., 1999; Postigo and Dean, 1999; Grooteclaes et al., 2003; Tripathi et al., 2005). However, the majority of these transcriptional regulators are sequence-specific TFs, which emphasises the role of CtBPs as a transcriptional corepressor (Turner and Crossley, 2001; Chinnadurai, 2002). One important target for gene specific CtBP-mediated repression is the E-cadherin promoter (Grooteclaes and Frisch, 2000; Grooteclaes et al., 2003; Alpatov et al., 2004; Ichikawa et al., 2015). E-cadherin is a transmembrane glycoprotein that mediates calcium-dependent, homophilic cell-cell adhesion in all epithelial tissues, including hESCs (Oda and Takeichi, 2011). Additionally, it is thought of as a marker for undifferentiated hESCs, as the generation of iPSCs displays an increase in E-cadherin expression to form compact colonies (Takahashi and Yamanaka, 2006; Takahashi et al., 2007), but also actively contributes to the self-renewal and pluripotent state of hESCs (Li et al., 2010a; Li et al., 2010b; Xu et al., 2010; Li et al., 2012). E-cadherin expression is repressed at the transcriptional level by repressors such as the ZEB and Snail families of zinc-finger proteins. Of these repressors, ZEB1, ZEB2 and Snail2 have one or more PXDLS-like motif which allows binding of the CtBPs (Chinnadurai, 2009). Therefore, ZEB and Snail repressors are bound directly to the DNA at specific sequences called E-boxes, and the CtBP dimers are bridging them to chromatin-remodelling enzymes, therefore altering the pattern of histone modifications to create a repressive chromatin signature at the E-cadherin promoter (Bergman et al., 2006; Chinnadurai, 2009; Ichikawa et al., 2015). Additionally, the silencing of *CDH1* can be reversed through regulation by ERK signalling, where an ERK signalling substrate called MCRIP1 inhibits CtBP-ZEB binding, and therefore E-cadherin repression (Ichikawa et al., 2015), however phosphorylation of MCRIP1 allows CtBP-mediated repression of E-cadherin to be restored.

Analysis of the CtBP1 corepressor complex revealed the presence of several binding proteins, including ZEB1/2, HPC2 and Znf217 which all bind directly to the DNA sequence of promoter elements (Shi et al., 2003). Furthermore, each of these binding proteins interact directly with CtBPs whether through the PXDLS-binding motif, as with ZEB, or through the RRT motifs, as with Znf217 (Postigo and Dean, 1999; Cowger et al., 2007). Additionally, the CtBP corepressor complex contained enzymatic constituents

which were implicated in catalysing different histone modifications, such as the class I HDACs (HDAC1/2), HMTs and a histone lysine-specific demethylase called LSD1 (Shi et al., 2003). Class I HDACs do not possess any CtBP-binding motifs, but are instead linked to CtBPs, like LSD1, through various other corepressors, such as CoREST (Ballas et al., 2001; Shi et al., 2005), whereas class II HDACs are more likely to bind directly to CtBPs either through PXDLS motifs or the SUMO post-translational modification (Zhang et al., 2001). Together, this evidence suggests that gene-specific CtBP-mediated repression requires a large CtBP complex to facilitate stepwise, coordinated, enzymatic reactions resulting in the conversion of an active chromatin state into a repressed state. However, the precise mechanisms of which remain poorly understood.

As well as gene-specific repression, CtBPs are thought to be involved with global gene repression. CtBPs are postulated to antagonise the function of histone acetyltransferase (HAT) coactivators, such as p300, and therefore any associated HATs, such as p300/CBP-associated factor (P/CAF), thus inhibiting the acetylation of nucleosomal histones. CtBP1 was found to directly interact with p300 through binding to the PXDLS binding domain within a bromodomain of p300 (Kim et al., 2005a). Although, the precise interaction and mechanisms of CtBP-mediated HAT inhibition remains to be elucidated, this data suggests that CtBPs have a role as metabolic-sensing repressor of HATs and thus affects general gene transcription.

In addition to the role that CtBPs play in short range localised repression, CtBPs may, also, influence transcriptional silencing across extended regions of the chromatin through Polycomb group (PcG) proteins, which are known to be implicated in long-term hereditary gene silencing (Lund and van Lohuizen, 2004). This critical role for CtBP repression mediated by PcG proteins was originally identified from studies with transgenic Drosophila embryos, where the repressor YY1, a mammalian PcG protein, repressed PcG-responsive promoters in a CtBP-dependent manner (Atchison et al., 2003; Srinivasan and Atchison, 2004; Basu and Atchison, 2010). As discussed previously, HPC2 is a prominent member of the mammalian CtBP corepressor complex and has been reported to recruit CtBPs to PcG bodies, and therefore play a role in chromatin silencing due to its potential interactions with methylated histones (Kagey et al., 2003).

Together, it has been heavily documented that there are several potential mechanisms by which CtBPs may exert its transcriptional repression effects, where the majority of the underlying mechanisms are still uncharacterised.

1.5.4 CtBP as a transcriptional co-activator

The role of CtBPs as transcriptional co-repressors is well established. However, there is now increasing evidence that CtBPs, also, have a role as transcriptional co-activators, where they function, again, through TFs that contain a conserved PXDLS-binding motif in a gene specific manner (Chinnadurai, 2007b).

The potential role for CtBPs in transcriptional activation was first noticed when E10.5 *CtBP2*$^{-/-}$ mouse embryos displayed lower expression of *Brachyury* compared to E9.5 mouse embryos (Hildebrand and Soriano, 2002). This observation suggested that CtBP2 might function as a transcriptional activator of Brachury expression. More recent studies have demonstrated that CtBPs in *Drosophila* can directly activate transcription of Wnt target genes after stimulation with the Wnt ligand (Fang et al., 2006) and activate the expression of E-box clock genes (Itoh et al., 2013).

Little is known about the possible mechanisms of CtBP-mediated transcriptional activation, however one potential mechanism of activation by CtBPs has recently been characterised. One member of the CtBP1 corepressor complex was identified as LSD1, which has dual functions to either repress or increase transcription depending on the promoter context (Shi et al., 2004; Wang et al., 2007; Ray et al., 2014). A recent study identified CtBPs and its associated proteins, LSD1 and CoREST, co-occupied the promoter regions of with the TF NeuroD1 at actively transcribed genes in human gastrointestinal endocrine cells (Ray et al., 2014). Thus, this re-emphasises that transcriptional activation involving CtBPs requires the presence of an 'activation' complex containing enzymatic constituents and their associated cofactors, much like the analysed CtBP1 corepressor complex (Shi et al., 2003). In addition, if that complex comprises many of the same proteins as the corepressor complex, it suggests that transcriptional activation is highly dependent on promoter context. However, as the mechanism is poorly characterised, it is not clear how the gene is determined to be activated or repressed when a component or components of the CtBP complex are the same. Thus, it might involve the recruitment of different chromatin-modifying complexes, different consensus sequences or binding to different TFs.

1.5.5 CtBPs and pluripotency

The link between CtBPs and pluripotency has received very little attention, although a recent study identified a role for CtBP2 during the exit of pluripotency in mESCs (Tae Wan et al., 2015). CtBP2 was found to regulate nucleosome remodelling and deacetylation of H3K27 by the nucleosome and deacetylation (NuRD) complex, which facilitated the recruitment of polycomb repressive complex 2 (PRC2)-mediated H3K7 trimethylation at active ESC genes to extinguish the core pluripotency network in an orderly manner.

Core pluripotency factors tend to occupy actively transcribed genes in ESCs, which are usually genes associated with a pluripotent state. Yet, this study, also, found that CtBP2 was enriched at actively transcribed genes in undifferentiated mESCs suggesting that CtBPs may have an additional role in the maintenance of pluripotency.

1.6 Epigenetic remodelling and stem cells

While recent studies have reported changes in gene expression and variations in the DNA sequence of hESCs during long term culture, very little is known about the epigenetic regulation in hESCs.

Epigenetics is broadly defined as heritable traits that do not involve changes to the DNA sequence itself, but rather chemical changes within the chromatin. Chromatin is a complex made up of DNA, histones and other proteins (Kornberg, 1974). The fundamental unit of chromatin is the nucleosome, which is comprised of two copies of each of the four core histones (H2A, H2B, H3 and H4) to form a histone octamer with 147bp of genomic DNA wrapped around in 1.7 super-helical turns. The first level of chromatin organisation is described as the 'beads on a string' model; a fibre 11nm in diameter consisting of a series of nucleosomes. Adjacent nucleosomes are connected through the interaction between linker DNA and the linker histone (H1); which organises the chromatin into a more compact fibre 30nm thick. Furthermore, higher order chromatin structures condense the 30nm fibre into metaphase chromosomes up to 100nm in diameter

Chromatin is folded into dynamically regulated structures, and changes to the chromatin state directly influences gene expression programmes. The regulation between an open, transcriptionally permissive and less condensed state and a closed, highly condensed and often repressed chromatin state; termed euchromatin and heterochromatin respectively, involves an array of nucleosome remodelling and post-translational modifications, such as methylation, acetylation, phosphorylation and ubiquitination, of the histone proteins and the DNA. The establishment of such epigenetic signatures is accomplished by specific sets of enzymes that add or remove different types of post-translational modifications such as acetyl or methyl groups and therefore, directly influence gene transcription.

Maintenance of the pluripotent state and self-renewal capacity in hESCs is conferred by a unique transcriptional regulation, and is a consequence of a balance between the dynamic structures of euchromatin and heterochromatin (Meshorer et al., 2006). Regions of chromatin in hESCs is highly euchromatic and transcriptionally active due to the presence of acetylated histones which increase nuclease accessibility (Levings et al., 2006; Meshorer and Misteli, 2006). Furthermore, several of these acetylated histone rich regions in hESCs, also, contain a repressive histone mark; a situation termed bivalency.

While bivalent promoters are not unique to pluripotent stem cells, they are relatively enriched in these cell types and are associated with lineage-specific genes which are silenced but poised for activation upon the initiation of differentiation (Pan et al., 2007; Zhao et al., 2007). As hESCs differentiate, the chromatin begins to condense to a more compact and repressive state due to the dynamic incorporation of specific histone variants and structural proteins (Dai and Rasmussen, 2007). It is this plasticity displayed by hESC chromatin that is crucial for the rapid transcriptional changes which occur upon initiating differentiation. As discussed previously, OCT4, SOX2 and NANOG biochemically interact with each other and co-regulate the expression of themselves and each other, as well as many target genes which include several chromatin-modifying complexes (Boyer et al., 2005; Kuroda et al., 2005; Rodda et al., 2005; Loh et al., 2006). Therefore, it is necessary to investigate the epigenetic changes behind pluripotency maintenance in hESCs to better understand the underlying mechanisms.

1.6.1 Chromatin remodelling complexes & pluripotency

Differentiation of hESCs in vitro or cells of the ICM in vivo into lineage specific derivatives is accompanied by global epigenetic changes of chromatin structure and consequent changes in gene expression. Pluripotency associated genes are gradually silenced throughout differentiation as expression of subsets of lineage-specific genes is activated. This developmental transition occurs, in part, through chromatin regulation which includes covalent histone modifications, DNA methylation and their remodelling complexes.

1.6.1.1 Histone modifications

Post-translational modifications of histone residues are associated with transcriptional activation or repression (Kouzarides, 2007; Vermeulen et al., 2010). There are several modifications that histones may be subjected to including acetylation, methylation, phosphorylation and ubiquitination, however histone acetylation and methylation are the most well characterised. In most cases, acetylation of histones is associated with transcriptional activation, while histone methylation can either promote activation or repression depending on the targeted amino acid residue within a particular histone.

1.6.1.1.1 Histone modifications at active promoters

Histone H3 or H4 acetylation (H3/H4Ac) or histone H3 lysine 4 dimethylation or trimethylation (H3K4me2/H3K4me3) are histone modifications associated with

transcriptional activation and have been observed in the promoter regions of all transcribed genes. Other histone modifications such as H3K36me3 and H3K79me3 were found only in actively transcribed genes, therefore it is essential that a dynamic balance between methylation and demethylation is maintained for the correct gene activation and silencing. Previous studies have discovered that the demethylation of H3K4me2/3, H3K27me2/3 or H3K29me2/3 is important for hESC self-renewal and pluripotency maintenance. Histone methylation is catalysed by histone methyltransferases (HMT), such as the SET domain of the Trithorax group, and reversed through the action of histone demethylases (HDM) such as the Jumonji domain (Jmjd) containing family. Acetylation of H3 and H4 is associated with active gene expression and this modification is catalysed by histone acetyltransferases (HAT) and reversed by histone deacetylases (HDAC). These enzymes interact with chromatin remodelling proteins which allows the chromatin to be in an open conformation and accessible to TFs and these modifying enzymes.

HIF regulation is well established in the literature, but the epigenetic changes that are associated with the hypoxic response are poorly characterised. A previous study demonstrated that HIF-2α directly interacted with the OCT4, SOX2 and NANOG promoters in hESCs, which induced an array of histone modifications associated with a more euchromatic state (Petruzzelli et al., 2014).

1.6.1.1.2 Histone modifications at repressed promoters

Methylation of the specific histone lysine residues H3K9, H3K27 and H4K20 is associated with transcriptional repression. The chromatin modifying enzymes that catalyse these modifications are poorly characterised, compared to those involved at active promoters. However, it is known that H3K9me3 is catalysed by various lysine HMTs, such as Set DB and G9a, which methylate the DNA through interactions with methyl-binding domain (MBD) proteins and HDACs to form a more highly condensed chromatin state that is inaccessible to transcriptional machinery. H3K27 is trimethylated by subunits of the Polycomb group and is a marker for silenced genes, hence is important for lineage commitment in hESCs.

1.6.1.2 DNA methylation and pluripotency

DNA methylation consists of a covalent modification of the DNA involving the addition of a methyl group to the cytosine C5 of CpG island dinucleotides, and is essential for mammalian development (Bird, 2002). This modification is catalysed by DNA

methyltransferases (DNMT) and usually occur on 70-80% of the cytosines preceding guanine in the DNA sequence of the CpG island dinucleotides. DNMT3a and DNMT3b are *de novo* methylases and responsible for adding methyl groups to the unmethylated DNA sequence, whereas DNMT1 is responsible for the maintenance of the methylation mark and favours hemi-methylated DNA, therefore methylates the complementary DNA strand after cell division for example (Jia et al., 2007; Avvakumov et al., 2008). The methylation status of all genes with CpG island rich promoters is inversely correlated with gene expression, so DNA methylation is associated with gene silencing.

Previous studies have suggested the DNA methylation may have a key role in determining cell fate, and thus pluripotency (Reik and Dean, 2001). DNMT1 and DNMT3b KO mice display an embryonic lethal phenotype, whereas DNMT3a deficient mice suffer from severe malformations and usually die within a few weeks (Li et al., 1992; Panning and Jaenisch, 1996). Despite the expression of 5 DNMTs in hESCs and 60-80% of all CpG in a methylated state, hESCs can be established and maintained in the absence of DNMTs and DNA methylation. However, hESCs deficient in DNMTs lack the ability to efficiently differentiate, probably due to their inability to silence genes encoding OCT4 and NANOG during the differentiation process (Jackson et al., 2004; Feldman et al., 2006). In particular, DNMT1 deficient ESCs are viable but undergo apoptosis upon the initiation of differentiation. Previous genome-wide studies showed that DNA methylation at CpG-rich sequences is very low in ESCs where OCT4, SOX2 and NANOG promoters were unmethylated and, interestingly, many of the genes that underwent *de novo* methylation upon differentiation were pluripotency-associated genes, including the core pluripotency factors (Farthing et al., 2008; Meissner et al., 2008; Mohn et al., 2008). Together, this suggests that DNA methylation is involved in the gradual loss of pluripotency upon lineage specification which is supported by the discovery that hESCs display a unique epigenetic signature (Bibikova et al., 2006).

1.6.1.3 Chromatin remodelling complexes

NuRD and PcG complexes are two of the chromatin-remodelling complexes involved in the rapid transitioning between chromatin states.

Mammalian nucleosome remodelling deacetylase (NuRD) complexes contain at least six subunits which possess both ATP-dependent chromatin-remodelling and HDAC activity (Denslow and Wade, 2007). The activity of HDAC1 and HDAC2 within this complex

requires the presence of a SNF2/SW12-related chromatin remodelling ATPase called Mi-2, a member of the MBD family called MBD3, the metastasis-associated protein termed Mta1/2/3, histone binding proteins called RbAP46 and RbAP48 and two zinc finger proteins called p66a and p66b to possess both the transcriptional repressive and activating functions that are important for hESC pluripotency and differentiation (Wade et al., 1999; Yoshida et al., 2008). ESCs lacking Mbd are viable but fail to form a stable NuRD complex. They display a defect in differentiation and hence results in persistent self-renewal (Kaji et al., 2006). Another study demonstrated that Mbd3 was required for the ICM to develop into mature epiblasts after implantation. The expression of the core pluripotency factors was unaffected by the expression of genes typically expressed in the preimplantation stage failed to be effectively repressed (Kaji et al., 2007). Hence, this suggests that Mbd3 is required for the development of pluripotency cells. Furthermore, NuRD complexes physically interact with LSD1 and leads to the silencing of gene enhancers that are essential for the lineage-specific genes in ESCs, suggesting a role for LSD1 in the transition of ESCs into cell of the three germ layers (Whyte et al., 2012).

A subfamily of NuRD complexes called Nanog and OCT4-associated deacetylase (NODE), as the name suggests, interacts with NANOG and OCT4 to maintain the pluripotent state. NODE HDAC activity appears to be comparable to NuRD, where NODE is recruited to NANOG/OCT4 target genes independently of Mbd3 in ESCs. In contrast to Mbd3 loss-of-function, knockdown of NODE subunits in ESCs promoted differentiation (Liang et al., 2008). The mechanisms behind NODE complexes and their interactions with pluripotency markers remain to be fully characterised, so it is unclear whether they are directly involved in hESC self-renewal.

Polycomb group (PcG) genes regulate pluripotency by suppressing developmental and metabolic pathways (Lessard and Crabtree, 2010). They are an evolutionarily conserved family of chromatin regulators. Mammalian PcG proteins assemble into three distinct complexes; PRC1, PRC2 and PhoRC. The fore core subunits of PRC1 are PHC, CBX, Bmil and RING1 and acts as an E3 ubiquitin ligase responsible for chromatin condensation and gene silencing. Mammalian PRC2 complexes contain EED, SUZ12 and either EZH1 or EZH2. The SET-domain-containing EZH1 and EZH2 of PRC2 are crucial for the initiation of gene silencing through the di- or trimethylation of H3K27 (Valk-Lingbeek et al., 2004). This mark recruits the PRC1 complex to initiate the formation of higher order chromatin structures.

Genome wide analyses have demonstrated that a significant subset of PcG target genes were co-occupied by OCT4, SOX2 and NANOG suggesting a functional interaction (Boyer et al., 2006; Lee et al., 2006b). Additionally, previous studies revealed that Jumonji C domain protein family member, JARID2, forms a stable complex with PRC2 in ESCs and promotes its recruitment to target genes while inhibiting its HMT activity (Peng et al., 2009; Pasini et al., 2010). These interactions remain to be fully characterised but appear to be essential in the balance between the expressions of pluripotency associated genes and lineage-specific genes in ESCs.

1.6.2. Jumonji-C domain-containing dioxygenases (JMJDs)

JMJDs are a family of histone demethylases and composed of 30 members in humans based on the presence of the roughly 150 amino acid long Jumonji C (JmjC) domain. They act through a dioxygenase reaction utilising Fe^{2+}, oxygen and 2-oxoglutarate to demethylate histones, and this reaction allows JMJDs to demethylate tri-, di- and mono-methylated lysine residues, particularly H3K4, H3K9, H3K27, H3K36 or H4K20 (Kooistra and Helin, 2012).

1.6.2.1. JMJDs, hypoxia & glycolysis

JMJD expression is well-documented to be enhance by hypoxia in a variety of cell types. In particular, JMJD1a, JMJD2b, JMJD2c, JMJD3 and JMJD5 expression has all been shown to be regulated by HIF-1α (Beyer et al., 2008; Pollard et al., 2008; Lee et al., 2014; Wang et al., 2014). Additionally, JMJD4b has previously been demonstrated to be regulated by HIF-2α (Guo et al., 2015).

Moreover, JMJD5 has been shown to directly interact with the glycolytic enzyme PKM2 to modulate glycolytic flux in cancer cells. This interaction also influences the translocation of PKM2 dimers to the nucleus and promotes HIF-1α-mediated transactivation, particularly of target genes involved in glucose metabolism (Wang et al., 2014). Additionally, JMJD1a contributes to bladder cancer progression by also enhancing glycolysis through the coactivation of HIF-1α target genes such as *GLUT1, HK2* and *LDHA* specifically by removing H3K9me2 histone modifications (Wan et al., 2017).

1.6.2.2. JMJDs and pluripotency

JMJDs have previously been implicated in supporting pluripotency. For example, JMJD5 was shown to regulate the cell cycle and pluripotency in hESCs by maintained a short G1 cell cycle phase (Ishimura et al., 2012; Zhu et al., 2014). Additionally, JMJD1a and

JMJD2c have been shown to be positively regulated by the pluripotency factor OCT4 themselves too (Loh et al., 2007). While other studies have reported that the absence of certain JMJD family members extends self-renewal and accelerates cellular reprogramming by playing a role in differentiation (Kidder et al., 2013).

Together, the previous literature strongly supports that JMJDs support self-renewal by increasing glycolysis, but the exact molecular mechanisms behind this observation remain to be fully characterised.

1.7 Human embryonal carcinoma cells

Teratocarcinomas are a subset of germ cell tumours (GCT) that occur in the testis (Dixon and Moore, 1952). Testicular GCTs account for 1% of all cancers and most commonly affect males between the ages of 15 and 34 (Clark, 2007). They, also, provide a striking model of the stem cell concept of cancer in the form of human embryonal carcinoma cells (hECCs).

The popularity of hECCs as a key model of pluripotency was short-lived and ended with the establishment of mESC lines, and more recently with iPSC advances. However, hECCs are of continued interest to cancer biologists as they provide a glimpse into the interface between stem cell biology and tumourigenesis. In particular, the former is fascinating to stem cell researchers because, unlike hESCs, hECCs are much easier to culture, cheaper and generally do not require feeder layers. As previously mentioned, hESCs have enormous potential for regenerative medicine applications, however there is a risk that they will escape from growth and differentiation control, much like the process that occurs in teratomas, which is a significant concern for clinical translation. Yet, hECCs may hold the key to understanding how pluripotency is secured versus how unrestrained growth and differentiation is initiated in hESCs, and overcome hurdles allowing cells are to be used clinically.

1.7.1 Derivation of hECCs

Although many types of stem cells have been identified, germ cells are grouped into a class of their own as they retain their potential to develop into a complete organism whilst undergoing an elaborate differentiation process. This underlying potential is generally repressed while the germ cells undergo sex-specific differentiation to form male and female gametes. Testicular teratocarcinomas arise from germ cells as a result of a loss of the mechanisms that repress their underlying pluripotency.

Testicular GCTs are typically divided into seminomas and non-seminomas (Damjanov, 1990, 1993). Seminomas are comprised of cells that resemble primordial germ cells, whereas non-seminomas are histologically heterogeneous and often contain somatic tissues such as bone, muscle and nerves, where these cells are often organised to closely resemble that of an early embryo (Andrews, 2002). hECCs are derived from non-seminoma cells of testicular GCTs, as these tumours often contain histologically undifferentiated elements. These tumours are unique in that the normal germ cell from

which it is derived has specific stem cell characteristics. These tumours are highly malignant and comprised of an array of disorganised somatic and extraembryonic cells, nestled amongst embryonal carcinoma cells. Differentiated derivatives of ECCs are usually non-malignant, therefore the ability of the tumour to regenerate itself is a characteristic of the embryonal carcinoma stem cells. This was demonstrated experimentally when a single ECC was transplanted into a new host mouse and was sufficient to generate a new complex teratocarcinoma, that could again be transplanted into another host with the same result (Kleinsmith and Pierce, 1964). This finding was crucial to the derivation and characterisation of mouse and human cell lines that could retain their pluripotent state (Holden et al., 1977; Evans and Kaufman, 1981; Martin, 1981).

Human teratocarcinoma cell lines were first isolated in the 1950s from xenografts in hamster cheek pouches (Pierce et al., 1957), and several cell lines were established subsequently in the 1970s, most notably TERA2 (Fogh and Trempe, 1975).

1.7.2 Characteristics of hECCs

hECCs are the 'pluripotent' stem cells of these tumours and exhibit several characteristics, much like their hESC counterparts, including:

- Derived from germ cell tumours
- Express pluripotency markers
- Capacity to indefinitely self-renew
- Unstable aneuploid karyotype
- High nuclear to cytoplasmic ratio

It is heavily documented that hECCs express OCT4, SOX2 and NANOG (Ezeh et al., 2005), where their downregulation resulted in differentiation of hECCs into any cells of the three developmental germ layers (Matin et al., 2004). These cells, also, express the characteristic surface antigens associated with pluripotency, including alkaline phosphatase, whilst growing in a monolayer of clusters of tightly packed cells with relatively little cytoplasm and prominent nucleoli (Benham et al., 1981; Andrews et al., 1984; Andrews, 2002; Greber et al., 2007b). The expression of these core pluripotency markers in hECCs is essential for their self-renewal capability. This control of self-renewal, again, appears to be very similar between hECCs and hESCs as a previous study demonstrated that silencing of either OCT4, SOX2 or NANOG in hECCs displayed a

consequent decrease in the expression of the other two core pluripotency factors and hence decreased self-renewal, confirming that the reciprocal activation between OCT4, SOX2 and NANOG is maintained in hECCs. Additionally, the observed decreased self-renewal was accompanied by a downregulation of genes involved in the FGF/ERK signalling pathway and so emphasised that the signalling pathways involved in the extended pluripotency network are crucial for maintaining an undifferentiated state of hECCs and hESCs alike (Greber et al., 2007b).

Although hECCs are the stem cells of teratocarcinomas, a striking feature of many hECC lines is their inability to differentiate into recognisable cell types. This may, in part, reflect their tumour origins as the acquisition of this inability to efficiently differentiate may provide a selective advantage. hECCs are highly aneuploid and are susceptible to many chromosomal aberrations (Andrews et al., 2005), hence it is easy to understand how genetic changes could occur to inhibit differentiation. However, there are several hECC lines that can differentiate effectively after their removal from their feeder layers in culture. Additionally, the NTERA-2 (NT2) hECC line does not require feeder layers and can still differentiate extensively in response to retinoic acid where they form a variety of cell types, including neurons, and can also form teratomas when grown as xenografts in mice (Andrews, 1984; Pera et al., 1989).

1.7.3 Hypoxia and metabolism in hECCs

Solid tumours have regions that are subjected to hypoxia; of which cancer stem cells such as hECCs are associated, therefore it is unsurprising that solid tumours often display high levels of HIF-1α (Bertout et al., 2008). The importance of HIFs in various cancer types has been proven through a correlation of elevated HIF-1α levels with a poor clinical prognosis (Birner et al., 2000; Aebersold et al., 2001; Birner et al., 2001a; Birner et al., 2001b; Bos et al., 2001; Schindl et al., 2002). Furthermore, pharmacological HIF inhibition significantly limits tumour growth and progression (Shay et al., 2014). However, to our knowledge, there is no evidence currently describing elevated HIF-1α expression levels in hECCs, but previous data suggests that there may be a correlation with HIF-1α being the predominant regulator of the hypoxic response in hECCs, compared to HIF-2α in hESCs.

Additionally, several studies have demonstrated the similarities between the metabolic status of hESCs and hECCs. Unlike normal differentiated cells that acquire most of their

energy through OXPHOS, most cancer cells rely on a glycolytic metabolism even under normoxic oxygen tensions. This phenomenon is known as the Warburg effect (Warburg, 1956). A recent study demonstrated that the pluripotent state of a hECC line strongly correlated with a glycolytic metabolism and decreased mitochondrial biogenesis and round, low-polarised and inactive mitochondria. Conversely, stimulation of mitochondrial function reduced their glycolytic phenotype and induced a loss of their pluripotent state (Vega-Naredo et al., 2014). Furthermore, it has been previously documented that hECCs express pluripotency markers. However, a recent study has demonstrated that hECCs may use the expression of these TFs, particularly NANOG, to influence hECC metabolism, and therefore maintain their pluripotent state. NANOG was involved in the regulation of expression of genes involved in mitochondrial OXPHOS by repressing their expression and thus supporting the self-renewal of hECCs (Chen et al., 2016). Together, this provides more evidence that the highly glycolytic metabolism of an undifferentiated cell supports the maintenance of its pluripotent state.

1.8 Hypotheses & Aims

Hypothesis: Glycolysis is intrinsic for the epigenetic and metabolic regulation of hESC self-renewal maintenance under hypoxia.

Aims & Objectives:

The objective of this thesis is to enhance understanding of how hESCs maintain self-renewal, and how that compares to their malignant counterparts hECCs

The specific objectives of the chapter within this thesis are:

- To characterise hESCs cultured at either 5% or 20% oxygen
- To investigate the effect of environmental oxygen tension on CtBP expression in hESCs
- To determine the effect of inhibiting glycolysis on CtBP, HIF-2α and pluripotency marker expression in hESCs
- To determine the role of JMJDs and chromatin state in maintaining hESC self-renewal
- To investigate whether the metabolic sensors CtBPs play a role in supporting hESC self-renewal
- To compare the mechanism regulating self-renewal in hESCs with the malignant equivalents hECCs

The specific aims to achieve each of these objectives will be described in each results chapter.

Chapter 2
Materials & Methods

Chapter 2: Materials & Methods

2.1 Cell culture

2.1.1 Derivation of mouse embryonic fibroblasts

12.5 day old (E12.5) mouse embryos were obtained from University of Southampton (derived from a primary source after obtaining approval from the University of Southampton ethical review committee in accordance with UK Home Office regulations using institutional facilities). E12.5 embryos were acquired from wild type mice; either MF-1 or CF-1 strains. Embryos were removed from the embryonic sac, decapitated and eviscerated. Embryos were washed three times in PBS without Ca^{2+} or Mg^{2+} (Invitrogen) before being transferred to a clean petri dish and finely shredded with scalpels. Tissue was collected in 15ml Trypsin/EDTA (Invitrogen) and mixed thoroughly before incubating for 5 minutes at 37˚C, and this was repeated twice more. After a total of 15 minutes incubating, 200µl DNase at 10mg/ml stock in water and 15ml MEF media (high glucose Dulbecco's modified eagle medium (DMEM; Invitrogen) supplemented with 10% fetal bovine serum (FBS; Invitrogen) and 1% penicillin-streptomycin (Invitrogen; Table 2.1) were added to the mixture before incubating at 37˚C until liquid throughout (approximately 10-15 minutes). The total volume was made up to 50ml with MEF medium before centrifuging the mixture for 5 minutes at 1000rpm. The supernatant was discarded and the pellet resuspended in 15 ml MEF medium before adding 5ml of cell suspension per T175 flask. MEFs were incubated at 5% CO_2 at 37˚C overnight or until confluent, where media was change after 25 hours or cells collected. Prior to cell collection, medium samples were taken for mycoplasma testing, otherwise confluent cells were washed in PBS and trypsinised before centrifugation at 1500rpm for 4 minutes. Cell pellets were resuspended in freezing solution (90% FBS and 10% dimethyl sulphoxide (DMSO)) for cryopreservation. Each T175 flask resulted in approximately 6 cryovials. All volumes stated were based on 9 embryos per tube.

Table 2.1. Composition of MEF culture medium.

High glucose DMEM (Invitrogen) supplemented with:	
10% fetal bovine serum (FBS; sterile filtered)	Invitrogen
1% penicillin-streptomycin (sterile filtered)	Invitrogen

2.1.1.1 Mycoplasma testing of MEFs

Cell and medium samples taken from MEFs during derivation were centrifuged at 1500rpm for 5 minutes. The supernatant was discarded and the pellet resuspended in 1ml PBS, transferred into a 1.5ml Eppendorf and centrifuged at 1500rpm for 1 minute before washing twice in PBS. The pellet was resuspended in 100µl PBS and subsequently incubated at 95˚C for 10 minutes, vortexed for 5-10 seconds and centrifuged at 13000rpm for 2 minutes. 10µl of the supernatant was added to each tube of the Mycoplasma PCR Detection Kit (Intronbio) and resuspended in 10µl of sterile water for a total PCR reaction volume of 20µl. PCR was performed using the following programme: initial denaturation at 94˚C for 1 minute, followed by 35 cycles of 30 seconds at 94˚C, 20 seconds at 60˚C and 1 minute at 72˚C with an extension step at 72˚C for 5 minutes and final hold at 10˚C. 7µl of PCR product was loaded on a 1.5% agarose gel (Invitrogen) in 1x TAE buffer (Fisher Bioreagents) containing 0.005% Nancy-520 (Invitrogen) and was run at 90A for approximately 1 hour, alongside a 100bp ladder (New England BioLabs). The agarose gel was imaged with Syngene Bio ImagingINgenuis and compared to the negative and positive controls provided with the Mycoplasma PCR Detection Kit (Figure 2.1).

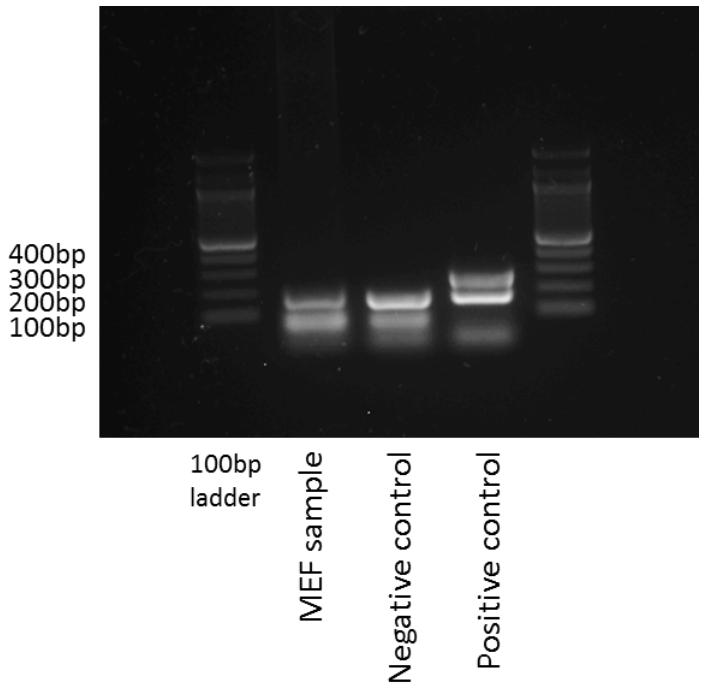

Figure 2.1. Typical PCR products of uncontaminated samples from primary un-irradiated MEF culture using the Mycoplasma PCR Detection Kit (Intronbio).

2.1.2 Culture of MEFs

Mycoplasma-free MEFs were thawed in 1ml pre-warmed MEF culture medium (Table 2.1) and centrifuged at 1500rpm for 4 minutes. The pellet from one vial was resuspended in 2ml of MEF medium and transferred to a T175 tissue culture flask containing 20ml MEF culture medium. MEFs were cultured at 5% CO_2 at 37˚C until 90% confluence was reached. MEF culture medium was removed before cells were passaged using 6ml 1x trypsin-EDTA (Invitrogen) and incubated for approximately 5 minutes until cells had detached from tissue culture plastic. Once cells had detached, 6ml MEF medium was added per flask to inactivate trypsin and subsequently transferred to a 50ml tube before centrifugation at 1500rpm for 4 minutes. Each pellet was resuspended in 4ml MEF medium, and 1ml cell suspension transferred into 4xT175 tissue culture flasks containing 19ml MEF media. MEFs were cultured to 90% confluence before passaging a second time, where each flask generated two new flasks. MEFs were further cultured until 90% confluence, before passaging and collecting MEFs from all eight flasks into 50ml Falcon tubes where the cells were centrifuged for 4 minutes at 1500rpm before each pellet was resuspended in 10ml MEF culture medium. MEFs were pooled and made up to a total volume of 50ml with MEF media. MEFs were γ-irradiated (50Gy) for 23.6 minutes. γ-irradiated cells were centrifuged for 4 minutes at 1500rpm before resuspending in 12ml freezing solution (90% FBS and 10% DMSO) to produce 12x1ml cryovials of γ-irradiated MEFs for cryopreservation.

2.1.3 Preparation of MEFs for hESC culture

One vial of γ-irradiated MEFs was thawed per two 6-well plates. Thawed MEFs were diluted in 15ml MEF culture medium and centrifuged for 4 minutes at 1500rpm before resuspending the pellets in 12ml MEF medium. Each 6-well plate was pre-coated with 0.1% gelatin and incubated at room temperature for 30 minutes. Gelatin was aspirated from 6-well plates and 1ml of MEFs were added to each well of the 6-well plates. After 24 hours, MEF medium was aspirated and 2ml hESC culture medium (Table 2.2) was added to each well of the MEF plates 24 hours prior to use as MEF-conditioned medium (CM) or for use in culturing hESCs.

2.1.4 Preparation of Matrigel-coated plates for hESC culture

Matrigel (BD Biosciences) was thawed and diluted to 6mg/ml concentration using knockout (KO) DMEM (Invitrogen) and stored as 400µl aliquots at -20˚C for a maximum of 3 months. One aliquot per 6-well plate was thawed overnight at 4˚C and each aliquot

added to 5.6ml of cold knockout DMEM. 1ml of Matrigel solution was added to each well and stored at 4˚C overnight prior to use and for up to 7 days.

2.1.5 Culture of hESC lines

Hues-7 (Cowan et al., 2004) or Shef3 hESCs were maintained in feeder-free conditions on Matrigel-coated plates in knockout DMEM (Invitrogen), supplemented with 15% knockout serum replacement (Invitrogen), 1% essential amino acids (Invitrogen), 1% penicillin-streptomycin (Invitrogen), 1% L-glutamax (Invitrogen), 55μM β-mercaptoethanol (Sigma) and 10ng/ml basic fibroblast growth factor (bFGF; Peprotech Ltd.; Table 2.2), that had been conditioned overnight on γ-irradiated MEFs as described in Section 2.1.3, at both 5% and 20% oxygen tensions. The basal medium is high glucose, but exact glucose concentrations are proprietary. Cells were passaged on day 3 post-passage where cells were treated with 160U/ml collagenase (Life Technologies) in KO DMEM (Invitrogen) with no additional supplements and incubated for 4 minutes at either 5% or 20% oxygen. 3ml MEF-conditioned media (CM) was added per well before cells were scraped off of the tissue culture plastic and diluted 1:3 with fresh CM. Cells were maintained for a minimum of 3 passages on Matrigel at both oxygen tensions prior to experimental use and experiments were performed using cells on day 3 post-passage.

Table 2.2. Composition of hESC culture medium.

Reagent (Final concentration)		**Volume**
KO DMEM	Invitrogen	410ml
15% Knockout replacement serum	Invitrogen	75ml
1% non-essential amino acids 100x	Invitrogen	5ml
1% penicillin-streptomycin 100x	Invitrogen	5ml
1% L-glutamax 100x	Invitrogen	5ml
55μM β-mercaptoethanol	Sigma	500μl
10ng/μl bFGF	Peprotech Ltd.	50μl

2.1.6 siRNA transfection of hESC or hECC lines

For siRNA transfections of Hues-7 or Shef3 hESCs, cells were routinely cultured and passaged at 37˚C under 5% oxygen tension until they reached a minimum of 3 passages in feeder-free conditions using Matrigel-coated plates to ensure the absence of MEFs. Hues-7 or Shef3 cells were transfected on day 1 post-passage, using 1 well of a 6-well plate per condition for RNA isolation and 3 wells of a 6-well plate per condition for protein isolation. siRNAs used throughout this thesis can be found in Table 2.3.

For siRNA transfections of NT2 hECCs, cells were again routinely cultured and passaged in KO DMEM supplemented with 10% fetal bovine serum (FBS; Invitrogen) and 1% penicillin-streptomycin (Invitrogen) at 37˚C under 5% oxygen tension until they reached a minimum of 3 passages (approximately 14 days) at 5% oxygen before experimental use. NT2 cells were seeded at a density of $3.3x10^6$ cells per well of a 6-well plate on the day of passage, and transfected on day 1 post-passage, where either 1 well or 3 wells of a 6-well plate per condition were used for RNA and protein isolation, respectively.

On the day of transfection, a transfection mix for each condition was prepared in Eppendorf tubes as following. For each well of a 6-well plate, 3.75µl siRNA was added to 200µl pre-warmed KO DMEM (Invitrogen) for both the Allstars negative control and each test siRNA. Transfection mixes were vortexed briefly, before adding 10µl of the transfection reagent InterferIN (Polyplus), except for HIF-1α and HIF-2α siRNAs which used the transfection reagent HiPerfect (Qiagen), per well of a 6-well plate and incubated at room temperature for 10 minutes. Culture medium was removed from the cells and replaced with 1.3ml of MEF-conditioned medium, and subsequently 200µl of transfection mix added per well in a drop-wise manner for a final concentration of 50nM siRNA. MEF-conditioned medium was replaced 24 hours post-transfection. hESCs or hECCs were collected for either RNA or protein isolation 48 hours post-transfection, unless otherwise stated. All volumes indicated are per well to be transfected, unless otherwise stated.

Transfection mixes containing two individual siRNAs, such as CtBP1+CtBP2, contained a total concentration of 100nM siRNA. Therefore, the Allstars negative control transfection mix was prepared with 7.5µl siRNA for these samples, instead of the 3.75µl siRNA for all other experiments, to have a final concentration of 100nM siRNA per well.

Table 2.3. siRNAs used for transfection experiments.
Table denotes all siRNA products used to transfect Hues-7 hESCs and NT2 hECCs and the relevant transfection reagent required. Allstars negative control siRNA was used as a negative control in all experiments. CtBP1/2 siRNA is a single siRNA that simultaneously targets both CtBP isoforms, whereas CtBP1+2 siRNA transfections describe two siRNAs (Qiagen) that target each CtBP isoform individually combined in one transfection mix to target both isoforms.

siRNA	Transfection reagent	Sense strand	Antisense strand
Allstars negative control (Qiagen)	InterferIN/HiPerfect	Sequence not provided	
CtBP1/2 (Ambion)	InterferIN	GGGAGGACCUG GAGAAGUUtt	AACUUCUCCAGGU CCUCCCtt
CtBP1 (Qiagen)	InterferIN	ACGACUUCACCG UCAAGCAtt	UGCUUGACGGUGA AGUCGUtt
CtBP1 (Ambion)	InterferIN	GUUUGUGACUG UAACCAUUtt	AAUGGUUACAGUC ACAAACtt
CtBP2 (Qiagen)	InterferIN	GCGCCUUGGUCA GUAAUAGtt	CUAUUACUGACCA AGGCGCtt
CtBP2 (Ambion)	InterferIN	GGAAAAUCACA UUACUACtt	UGUAGUAAUGUG AUUUUCCta
HIF-1α (Qiagen)	HiPerfect	Sequence not provided	
HIF2α (Qiagen)	HiPerfect	Sequence not provided	
JMJD2A (Qiagen)	InterferIN	Sequence not provided	
PKM2 (Qiagen)	InterferIN	Sequence not provided	

2.1.7. Pharmacological treatment of hESC and hECC cell lines

hESCs and hECCs maintained on Matrigel coated plates at either 5% or 20% oxygen were passaged and incubated overnight. Cells were treated with MEF-conditioned medium supplemented with either 0mM, 0.2mM, 1mM, 5mM, 10mM or 30mM 2-deoxyglucose (2-DG; Sigma); or 0μM or 25μM 3-brompyruvate (3-BrP; Sigma). 2-DG or 3-BrP-supplemented media was prepared fresh each day. Cells were fed with 2ml of 2-DG or 3-BrP-supplemented conditioned media per well of a 6-well plate on day 1 and day 2 post-passage, before collecting samples for either RNA or protein analysis on day 3 post-passage.

2.2 Gene expression analysis

2.2.1 RNA isolation

RNA was isolated from 1 well of Hues-7 hESCs or NT2 hECCs cultured under feeder-free conditions on Matrigel-coated plates per sample on day 3 post-passage using the TRIzol isolation method adapted from Invitrogen.

Culture medium was removed and 1ml TRIzol (Invitrogen) applied directly on to the cells. Cells were scraped and harvested and either stored at -80˚C or directly used for RNA isolation. 200µl chloroform was added per sample and incubated at room temperature for 15 minutes, before samples were centrifuged at 13000g for 30 minutes at 4˚C to allow phase separation. The upper colourless aqueous phase contained the RNA and was transferred into a fresh tube. Half of the total volume of the aqueous layer (~200µl) of isopropanol and 40µl glycogen (5mg/ml, Ambion) was added to each sample prior to incubation at room temperature for 10 minutes and subsequent incubation at -80˚C for at least 30 minutes. Samples were centrifuged at 13000g for 30 minutes at 4˚C before discarding the supernatant and washing the RNA pellet in 1ml of ice cold 100% ethanol before centrifugation at 7500g for 10 minutes at 4˚C. Pellets were subsequently washed in 70% of ice cold molecular grade ethanol and incubated on ice for 15 minutes before centrifugation as previous. Ethanol was aspirated completely and RNA pellets allowed to semi-dry in the air. The pellet was resuspended in 30µl of DEPC water containing 1µl of RNAsin (Promega). RNA concentrations were determined using the Nanodrop ND-1000 spectrophotometer and ND-1000 software v3.7.1. Samples with a 260/280 ratio of 1.8-2.0 were used in experiments. All volumes are per 1ml of TRIzol, unless otherwise stated. Samples were stored at -80˚C prior to subsequent steps.

2.2.2 DNAse treatment of RNA samples

RNA samples were treated with a DNAse I enzyme to remove any genomic DNA contamination. 1µg RNA was incubated in a 10µl total reaction volume containing 1µl 10x Reaction buffer (Invitrogen), 1µl DNAse I (Invitrogen) and DEPC water for 15 minutes at room temperature. The reaction was stopped with the addition of 1µl of 25mM EDTA (Invitrogen) and incubated for 10 minutes at 65˚C before immediately cooling on ice. Samples were stored at -80˚C or directly reverse transcribed.

2.2.3 cDNA synthesis using random hexamer primers

RNA was reverse transcribed into cDNA using Moloney murine leukaemia virus (MMLV) reverse transcriptase (Promega). 3µl DEPC water and 1µl 10x random hexamer primers (Promega) was added to 11µl DNAse treated RNA and heated at 70˚C for 10 minutes before immediately cooling on ice. 8µl MMLV 5x reaction buffer (Promega), 5µl 10mM pre-mixed dNTPs (Promega), 1µl MMLV reverse transcriptase (RT; Promega) and 11µl DEPC water was added to make a total reaction volume of 40µl and incubated at 42˚C for 60 minutes before immediately cooling on ice. All volumes indicated are per sample. cDNA samples were stored at -20˚C, or directly used in real-time quantitative PCR (qPCR) reaction once confirmed genomic DNA contamination free.

2.2.3.1 Genomic contamination check

cDNA samples were analysed with a PCR reaction to test for genomic DNA (gDNA) contamination using intron spanning primers. The reaction was performed in 25µl reaction volumes consisting of 1µl cDNA, 0.5µl 10mM dNTPs (Promega), 5µl of 1x Go-Taq buffer, 0.5µl of each primer at 5µM (OAZ1, forward primer 5'-GGCGAGGGAATAGTCAGAGG-3', reverse primer 5'-GGACTGGACGTTGAGAATCC-3'), 0.375µl Go-Taq polymerase (Promega) and 17.125µl dH_2O. A negative control reaction was performed simultaneously by substituting cDNA for DEPC water and all volumes indicated are per sample.

The following cycling parameters were used: 95˚C for 5 minutes, followed by 30 cycles of 1 minute at 94˚C, 1 minute at 58˚C and 1 minute at 72˚C and concluding at 72˚C for 10 minutes. 25µl of PCR products and 5µl QuickLoad® 100bp DNA ladder (New England Biolabs) were loaded onto a 2% agarose gel (Invitrogen) in 1x TAE buffer (Fisher Bioreagents) containing 0.005% Nancy-520 (Invitrogen) and was run at 80V for 1 hour. An amplicon of 122bp was expected for cDNA, while any gDNA contamination produced a 373bp product (Figure 2.2).

2.2.4 Reverse transcription quantitative PCR (RT-qPCR)

cDNA samples was used to analyse the relative expression levels of protein coding genes using qPCR with commercially available Taqman Gene expression Assay probes (Applied Biosystems, Table 2.4) or using SYBR Green and primers (Table 2.5). Reactions were performed in a 96-well plate using a 7500 Real-Time PCR system and 7500 software v2.0.6 (Applied Biosystems).

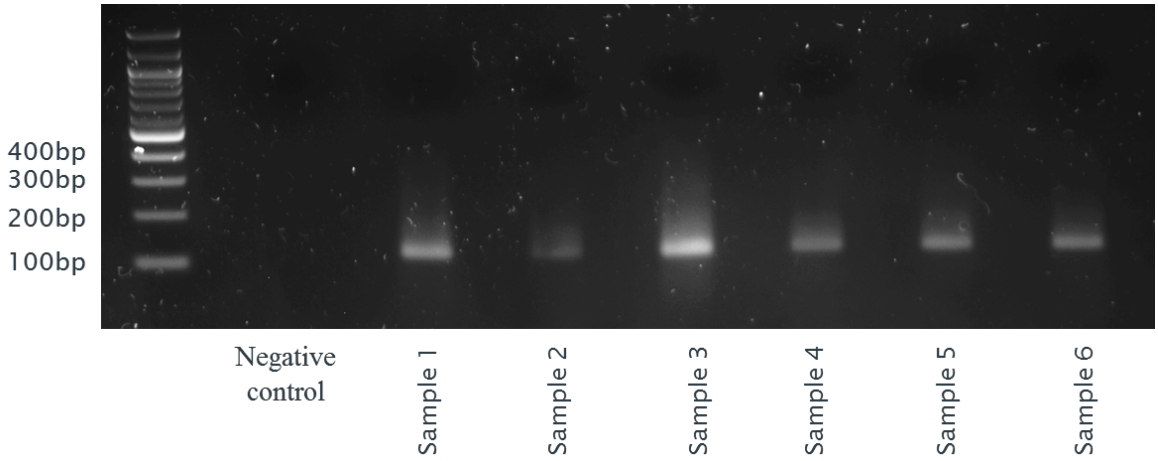

Figure 2.2. Typical PCR products of cDNA samples uncontaminated with genomic DNA.

RT-qPCR was performed in 20µl reactions prepared on ice containing 14µl Taqman Universal PCR Mastermix (Applied Biosystems), 1µl of each 20x probe (Applied Biosystems), 1µg cDNA and DEPC water, or containing 10µl Power Up SYBR Green Mastermix (Thermo Scientific), 2µl of 5µM forward primer, 2µl of 5µM reverse primer, 1µg cDNA and DEPC water. The following cycling parameters were used: 50˚C for 2 minutes, 95˚C for 10 minutes, followed by 45 cycles of 95˚C for 15 seconds and 60˚C for 1 minute. All samples were analysed in duplicate and then normalised to the housekeeping control gene Ubiquitin C (UBC) for Taqman probes or β-actin for SYBR green.

2.2.5 RT-qPCR analysis

Relative gene expression was calculated as previously described using the comparative Ct method ($2^{-\Delta\Delta Ct}$) (Livak and Schmittgen, 2001). This was calculated by subtracting the Ct of the treated group from the Ct value of the control group for each gene of interest and housekeeping gene respectively. Relative expression analysis was performed where gene expression was made relative to the endogenous control gene UBC, depicted as $2^{-\Delta\Delta Ct}$.

Table 2.4. TaqMan gene expression assay probes used for RT-qPCR analysis.

Gene	TaqMan gene expression assay
POU5F1 (Applied Biosystems)	Hs01895061_u1
SOX2 (Applied Biosystems)	Hs00602736_s1
NANOG (Applied Biosystems)	Hs02387400_g1
CtBP1 (Applied Biosystems)	Hs00972288_g1
CtBP2 (Applied Biosystems)	Hs00949547_g1
UBC (Applied Biosystems)	Hs00824723_m1
EPAS1 (Applied Biosystems)	Hs01026142_m1
HIF-1α (Applied Biosystems)	Hs00153153_m1
CXCR4 (Applied Biosystems)	Hs00607978_s1
KDR (Applied Biosystems)	Hs00911700_m1
LIN28B (Applied Biosystems)	Hs01013729_m1
SALL4 (Applied Biosystems)	Hs00360675_m1
LDHA (Applied Biosystems)	Hs01378790_g1
JMJD1A (Applied Biosystems)	Hs00218331_m1
JMJD2A (Applied Biosystems)	Hs00206360_m1
JMJD2B (Applied Biosystems)	Hs00943636_m1
JMJD2C (Applied Biosystems)	Hs00909579_m1
JMJD5 (Applied Biosystems)	Hs00227070_m1
TLN1 (Applied Biosystems)	Hs00196775_m1
CDH1 (Applied Biosystems)	Hs01023894_m1

Table 2.5. Primer sequences used for RT-qPCR analysis.

Gene	Forward primer sequence (5' – 3')	Reverse primer sequence (5' – 3')
SOX17	CTGCCACTTGAACAGTTTGG	GAGGAAGCTGTTTTGGGACA
GATA4	CAGTTCCTCCCACGCATATT	CATGGCCAAGCTCTGATACA
AFP	ACACAAAAAAGGAAGTCCAG	GGTGCATACAGGAAGGGATG
CLD6	TGGGCTTCCCTAGATGTCAC	AGGACGGAGGAAACAGAGGT
SOX1	GGAATGGGAGGACAG	AACAGCCGGAGCAGAAGATA
PAX6	ACTGCACAGCAGCACATTTC	CTGACAGTTCCCTCAGCACA
NODAL	GAGATTTTCCACCAGCCAAA	AGGTGACCTGGGACAAAGTG
BMP4	TCCACAGCACTGGTCTTGAG	GGGATCTGCTGAGGTTAAA
FOXC1	GCGAACAGAATATCCCTCCA	AAAGTCGAGGTGGCTCTGAA
GLUT1	CTCATGGGCTTCTCGAAACT	GAACACCTGGGCGATGAG
GLUT3	TGCCCTGAAAGTCCCAGATTT	ACCGCTGGAGGATCTGGCTTA
β-actin	GGCATCCTCACCCTGAAGTA	AGGTGTGGTGCCAGATTTTC

2.3 Protein expression analysis

2.3.1 Immunocytochemistry

hESCs or hECCs were plated onto MEF-containing chamber slides and cultured for 24 hours. Culture medium was removed from the wells, washed twice in PBS and fixed in 4% paraformaldehyde (PFA) prepared in PBS for 15 minutes at room temperature. Cells were washed in PBS twice and incubated with 100mM glycine in PBS for 10 minutes at room temperature. Cells were permeabilised with 0.2% Triton-X (Fluka Bio Chemika) in PBS for 10 minutes, if necessary, and subsequently washed. OCT4, SOX2, NANOG, CtBP1 and CtBP2 are all intracellular, so cell membranes were permeabilised to analyse their expression. SSEA-1 and TRA-1-60 are surface markers and do not require membrane permeabilisation, so cells were incubated in PBS only for this step. Non-specific antibody binding was blocked with 10% w/v fetal calf serum (FCS) for 30 minutes and then cells were incubated with the appropriate primary antibody in 0.6% w/v bovine serum albumin (BSA) for 90 minutes in a humidified container at room temperature (Table 2.6). Negative controls were secondary antibody only controls.

Cells were washed twice prior to incubation with the secondary antibody prepared in 0.6% w/v BSA in a dark, humid environment for 90 minutes. Cells were washed twice in PBS and once with water before mounting with Vectashield with DAPI (Vector Laboratories) for nuclear staining. Slides were covered with a coverslip and sealed. Slides were stored in the dark at 4˚C until imaging using a Zeiss fluorescence microscope and Axiovision imaging software (Zeiss).

Table 2.6. Primary and secondary antibodies used for immunocytochemistry with relevant dilutions.

Primary antibody	Working dilution	Secondary antibody
Mouse-IgG2b anti-OCT4 (Santa Cruz)	1:100	Anti-mouse IgG FITC (1:100; Sigma)
Rabbit anti-SOX2 (Cell Signalling Technology)	1:200	Alexa Fluor 488 goat anti-rabbit IgG (1:700, Invitrogen)
Rabbit anti-NANOG (AbCam)	1:100	Alexa Fluor 488 goat anti-rabbit IgG (1:700, Invitrogen)
Mouse-IgG anti-CtBP1 (BD Biosciences)	1:200	Anti-mouse IgG FITC (1:100; Sigma)
Mouse-IgG anti-CtBP2 (BD Biosciences)	1:250	Anti-mouse IgG FITC (1:100; Sigma)
Mouse-IgM anti-SSEA-1 (Santa Cruz)	1:100	Anti-mouse IgM FITC (1:200; Molecular Probes)
Mouse-IgM anti-TRA-1-60 (Santa Cruz)	1:100	Anti-mouse IgM FITC (1:200; Molecular Probes)
Rabbit-IgG anti-HIF-1α (GeneTex)	1:100	Alexa Fluor 488 goat anti-rabbit IgG (1:700, Invitrogen)
Rabbit-IgG anti-HIF-2α (Novus Biologicals)	1:100	Alexa Fluor 488 goat anti-rabbit IgG (1:700, Invitrogen)

2.3.2 Western blotting

2.3.2.1 Protein isolation

Protein was isolated from 3 wells of Hues-7 cells from a Matrigel-coated 6-well plate per sample. Cells were washed twice in PBS and isolated in 100µl radio immuno-precipitation assay (RIPA) lysis buffer (Sigma). The samples were collected on ice for 20 minutes before sonicating for 30 seconds and centrifuged at 13,000g for 10 minutes at 4˚C. Supernatants were collected and stored at -80˚C.

Alternatively, protein was isolated from T25 flask of NT2 cells at 90% confluence per sample, or 3 wells of NT2 cells seeded at $3.3x10^5$ cells per well of a 6-well plate per sample. Cells were washed twice as previously described and isolated in either 200µl or 300µl RIPA buffer, respectively, before samples were subsequently processed as described above.

2.3.2.2 Protein quantification

Protein concentration was quantified using the Bradford assay (Bradford, 1976). BSA standards were prepared (0.1-1.4 µg/µl) and 20µl of each standard was added to a well of a 96-well plate in triplicate to form the standard curve (Figure 2.3). Protein samples were diluted 1:20 in water prior to adding 20µl to respective wells in triplicate. 200µl of Bradford reagent (Biorad) was added to each well before absorbance at 595nm was measured using a BMG spectrophotometer and Optima software, and used to calculate the protein concentration using a standard curve.

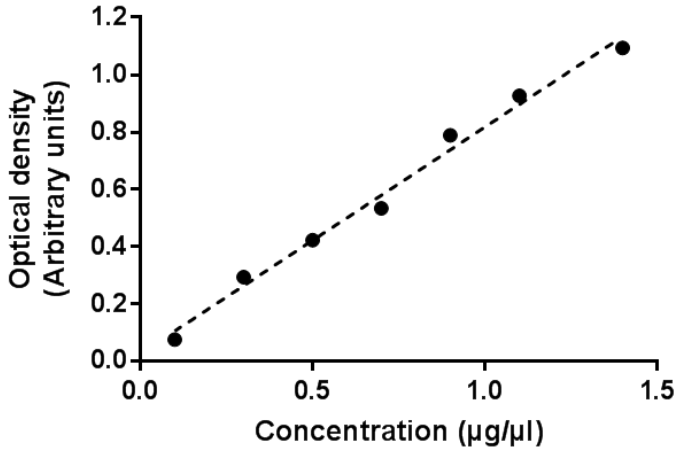

Figure 2.3. Typical BSA standard curve used to estimate protein concentration of samples.

2.3.2.3 SDS polyacrylamide gel electrophoresis (SDS-PAGE)

8%, 12% or 15% resolving gels with a thickness of 0.75mm were prepared, with a 5% stacking gel containing 10 wells unless otherwise stated (Table 2.7). 50µg protein lysate from Section 2.3.2 was resolved on sodium dodecyl sulphate (SDS) acrylamide gels alongside 5µl of EZ-Run Pre-stained Rec Protein Ladder (Fisher Bioreagents) in one well of each electrophoresis gel. These are pre-stained molecular weight markers used to aid visualisation of protein separation through the gel during electrophoresis, evaluate transfer efficiency and allow estimation of molecular weight of protein of interest. 50µg of protein lysate was added to 7.5µl 4X Nu-PAGE LDS-sample buffer (Invitrogen), 7.5µl 1M DL-dithiothreitol (DTT) solution (Sigma) and RIPA buffer (Sigma) to make a total volume of 30µl per sample. Mixed samples were incubated at 95˚C for 5 minutes, and placed back on ice prior to loading 25µl of each sample onto the electrophoresis gel. The electrophoresis tank (BioRad) was filled with 1x running buffer that has been diluted from 5x stock solution (Table 2.8). Electrophoresis was performed at a constant 55mA for between 60-90 minutes, and stopped once the relevant molecular weight markers had travelled a sufficient distance through the gel.

Table 2.7. Preparation of acrylamide gels for Western blotting.
Table denotes the required volumes to make either an 8%, 12% or 15% acrylamide gel with 5% stacking gel. Volumes indicated are for 2x0.75mm gels.

Reagent	**8%**	**12%**	**15%**	**5%**
	Resolving gel			**Stacking gel**
1.5M Tris pH8.8	2.5ml	2.5ml	2.5ml	-
10% SDS	100µl	100µl	100µl	50µl
40% acrylamide-bis (Sigma)	2ml	3ml	4ml	625µl
dH_2O	5.3ml	5ml	4ml	3.63ml
0.5M Tris pH6.8	-	-	-	695µl
10% ammonium persulphate (Sigma)	100µl	100µl	100µl	50µl
TEMED	7.5µl	7.5µl	7.5µl	7.5µl

Table 2.8. Preparation of 5x running buffer and transfer buffer for Western blotting.

Reagent	5x running buffer	Transfer buffer
Tris	15.1g	-
Glycine	94g	2.93g
dH_2O	900ml	-
10% SDS	50ml	-
1.5M Tris pH 8.3	-	32ml
Methanol	-	200ml
	Make up to 1000ml with dH_2O and pH 8.3	Make up to 1000ml with dH_2O

2.3.2.4 Western blotting

Nitrocellulose membranes (Amersham Hybond-ECL) were used for protein transfer from electrophoresis gel. Blotting apparatus was assembled as follows; ice, cathode, sponge, filter paper (Thermo Scientific), electrophoresis gel, membrane, filter paper, sponge, anode; in a BioRad electrophoresis tank. Sponges, filter paper and membrane had been pre-soaked in transfer buffer at 4˚C prior to assembly. Transfer was run at a constant 250mA for two hours with the tank filled with freshly prepared transfer buffer (Table 2.8).

Membranes were subsequently blocked with 5% w/v milk in PBS containing 0.1% Tween-20 (PBS-T, Fisher Bioreagents), except for SOX2 Western blots which were blocked in 5% w/v milk in 1x Tris-buffered saline containing 0.1% Tween-20 (TBS-T) which had been diluted from a 10x stock solution (Table 2.9), for one hour at room temperature prior to incubation with primary antibody diluted in blocking buffer overnight at 4˚C (Table 2.10) with the exception of SOX2 primary antibody which was diluted in 5% w/v BSA in TBS-T. Membranes were washed three times in PBS-T/TBS-T before incubation with relevant horseradish peroxidase (HRP) labelled secondary antibody prepared in blocking buffer (Table 2.10) for one hour at room temperature.

Table 2.9. Preparation of 10x TBS stock.

Reagent	10x TBS stock
200mM Tris	24.2g
1.5M Sodium chloride	87.66g
Make up to 1000ml with dH_2O and pH 7.6	

Membranes were, again, washed three times in PBS-T/TBS-T before being treated with 1ml electrochemiluminescence (ECL) detector solution (GE Healthcare) per blot for 5 minutes in a dark container for visualisation of protein bands using films (Carestream). The ECL treated membranes were placed in light excluding cassettes and exposed to films, where the exposure time varied between different proteins. Films were developed in a 1:5 dilution of GBX developer/replenisher solution (Kodak) in water until bands became visible. Films were subsequently washed in water, fixed in a 1:5 dilution of GBX fixer/replenisher solution (Kodak) in water and washed in water again before being allowed to dry.

After detection of the primary antibody, membranes were washed three times in PBS-T/TBS-T and subsequently incubated with an HRP-tagged antibody against β-actin (Table 2.10) prepared in 5% w/v milk in PBS-T/TBS-T for one hour at room temperature. Membranes were washed three times in PBS-T/TBS-T before treatment with ECL and film development as previously described.

Films were scanned and the integrated density of the bands were measured using ImageJ (National Institutes of Health) as well as the integrated density of the background staining. Background integrated density was subtracted from the integrated density of the band for the protein of interest, and repeated for the β-actin bands. The resulting integrated density for the protein band was divided by the resulting integrated density for the β-actin band for the same sample to give the relative expression of the protein of interest, which was compared between samples run on the same electrophoresis gel.

Table 2.10. Primary and secondary antibodies used for Western blotting.
Table denotes all the primary and secondary antibodies used for Western blotting analysis with the relevant dilutions. Table, also, denotes which percentage gel samples were run on depending on the protein to be probed for and indicates the relevant blocking buffer and primary antibody dilution buffer used for each specific antibody.

Primary antibody	% gel	Working dilution	Blocking buffer	Dilution buffer	Secondary antibody
Mouse-IgG2b anti-OCT4 (Santa Cruz)	12	1:1000	5% milk-PBS/T	5% milk-PBS/T	Anti-mouse IgG HRP (1:100,000; Sigma)
Rabbit-IgG anti-SOX2 (Cell Signalling Technology)	12	1:3000	5% milk-TBS/T	5% BSA-TBS/T	Anti-rabbit IgG HRP (1:50,000; GE Healthcare)
Rabbit-IgG anti-NANOG (AbCam)	12	1:500	5% milk-PBS/T	5% milk-PBS/T	Anti-rabbit IgG HRP (1:50,000; GE Healthcare)
Mouse-IgG anti-CtBP1 (BD Biosciences)	15	1:2000	5% milk-PBS/T	5% milk-PBS/T	Anti-mouse IgG HRP (1:100,000; Sigma)
Mouse-IgG anti-CtBP2 (BD Biosciences)	15	1:2000	5% milk-PBS/T	5% milk-PBS/T	Anti-mouse IgG HRP (1:100,000; Sigma)
Rabbit-IgG anti-HIF-1α (GeneTex)	8	1:250	5% milk-PBS/T	5% milk-PBS/T	Anti-rabbit IgG HRP (1:50,000; GE Healthcare)
Rabbit-IgG anti-HIF-2α (Novus Biologicals)	8	1:250	5% milk-1% BSA-TBS/T	5% milk-1% BSA-TBS/T	Anti-rabbit IgG HRP (1:50,000; GE Healthcare)
Rabbit-IgG anti-E-cadherin (Cell Signalling Technology)	12	1:500	5% milk-PBS/T	5% milk-PBS/T	Anti-rabbit IgG HRP (1:50,000; GE Healthcare)

Rabbit-IgG anti-PHD1 (AbCam)	12	1:5000	5% milk-PBS/T	5% milk-PBS/T	Anti-rabbit IgG HRP (1:50,000; GE Healthcare)
Rabbit-IgG anti-PHD2 (Novus Biologicals)	12	1:2000	5% milk-PBS/T	5% milk-PBS/T	Anti-rabbit IgG HRP (1:50,000; GE Healthcare)
Rabbit-IgG anti-PHD3 (AbCam)	12	1:2000	5% milk-TBS/T	5% milk-TBS/T	Anti-rabbit IgG HRP (1:50,000; GE Healthcare)
Rabbit-IgG anti-PKM2 (Novus Biologicals)	12	1:1000	5% milk-PBS/T	5% milk-PBS/T	Anti-rabbit IgG HRP (1:50,000; GE Healthcare)
Mouse-IgG1 anti-β-actin-HRP (Sigma)	-	1:50,000	-	5% milk-PBS/T	-

2.4 Analysis of hESC metabolism

2.4.1 Preparation of glucose cocktail

Glucose assay cocktail was prepared every 2 months, and stored at -20˚C. The glucose cocktail consisted of 417μM DTT, 3.1mM magnesium sulphate (Sigma), 417μM ATP (Roche), 1.25mM NADP (Roche) and 1ml of a 2:1 mix of hexokinase:glucose-6-phosphate dehydrogenase (G6PDH; Roche) that gave a final concentration of the two enzymes of 14.2 U/ml and 7.1 U/ml respectively, in EPPS buffer (Table 2.11).

Table 2.11. Preparation of EPPS buffer

EPPS buffer consisted of:
2.52g EPPS
10mg penicillin
10mg streptomycin
200ml water to pH8 with NaOH

2.4.2 Measurement of glucose concentrations

Hues-7 hESCs or NT2 hECCs maintained at either 5% or 20% oxygen were seeded into 12 well plates with an approximate density of $3.3x10^4$ cells/ml. hESCs and hECCs were fed with fresh media in the presence or absence of either 10mM 2-DG, 25μM 3-BrP, 10mM oxamate or transfected with 50nM siRNA on day 1 post-passage, and fed again either fresh media supplemented with or without a glycolytic inhibitor on day 2 post-passage. Spent medium samples were collected from either hESCs or hECCs cultured at either 5% or 20% oxygen 48 hours post-transfection or post-addition of inhibitors, before cells were trypsinised to perform a cell count.

Glucose concentration was determined by coupling a hexokinase-catalysed reaction with reduction of $NADP^+$ (Figure 2.4), which was measured spectrophotometrically with fluorescence excitation of NADPH at 340nm and emission at 460nm:

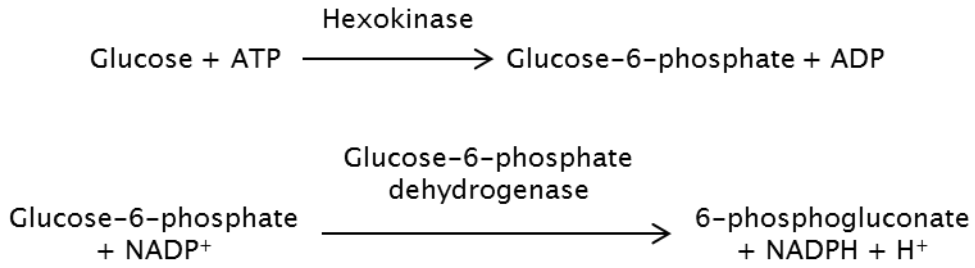

Figure 2.4. Reaction of glucose assay.

A glucose standard curve was prepared using glucose concentrations ranging from 0.1mM to 2mM (Figure 2.5). 5µl of glucose standards and diluted CM samples were mixed with 45µl of glucose cocktail in triplicate in a 96 well plate and left to incubate at room temperature for 10 minutes. All samples were excited at 340nm and the fluorescence measured at 460nm using a Fluostar Optima microplate reader (BMG Labtech) and Optima software.

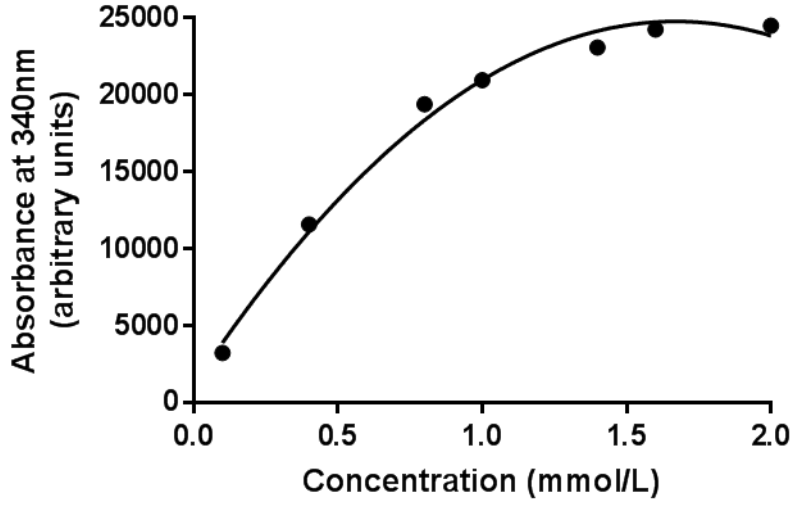

Figure 2.5. Typical standard curve of standards for glucose assay.

2.4.3 Preparation of lactate cocktail

A glycine-hydrazine buffer (Table 2.12) was prepared every 2 months, and stored at 4˚C. The lactate cocktail was prepared in this buffer as follows: 9ml glycine-hydrazine buffer diluted with 8ml water and 0.5ml LDH (final concentration of 72.4U/ml; Roche) and 1.5ml 40mg/ml NAD (final concentration of 4.76U/ml; Roche) was added. Lactate cocktail was stored at -20˚C for up to 2 months.

Table 2.12. Preparation of hydrazine buffer.

Glycine hydrazine buffer consisted of:
1M glycine
400nM hydrazine sulphate
5mM EDTA
Water pH to 9.4 with 2M NaOH

2.4.4 Measurement of lactate concentrations

Hues-7 hESCs or NT2 hECCs maintained at either 5% or 20% oxygen were seeded into 12 well plates with an approximate density of $3.3x10^4$ cells/ml. hESCs and hECCs were fed with fresh media in the presence or absence of either 10mM 2-DG, 25µM 3-BrP, 10mM oxamate or transfected with 50nM siRNA on day 1 post-passage, and fed again either fresh media supplemented with or without a glycolytic inhibitor on day 2 post-passage. Spent medium samples were collected from either hESCs or hECCs cultured at either 5% or 20% oxygen 48 hours post-transfection or post-addition of inhibitors, before cells were trypsinised to perform a cell count.

Lactate concentration was determined using an assay in which the lactate dehydrogenase enzyme catalyses the oxidation of lactate to produce pyruvate, while also reducing NAD^+ to NADH. The concentration of lactate is proportional to the increase in fluorescence at 460 nm as NAD^+ is reduced to NADH (Figure 2.6).

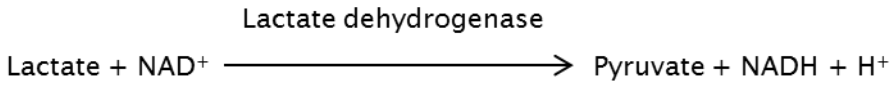

Figure 2.6. Reaction of lactate assay.

Addition of hydrazine to the reaction allows the reaction to run to completion as the pyruvate is removed by reacting with hydrazine sulphate to produce pyruvate hydrazone (Lundholm et al., 1963).

Lactate standards were prepared in the range of 0.1mM to 1mM concentration (Analex; Figure 2.7). 45µl of lactate cocktail was mixed with 5µl of each lactate standard and diluted CM samples in triplicate in a 96 well plate and incubated for 25 minutes at room temperature.

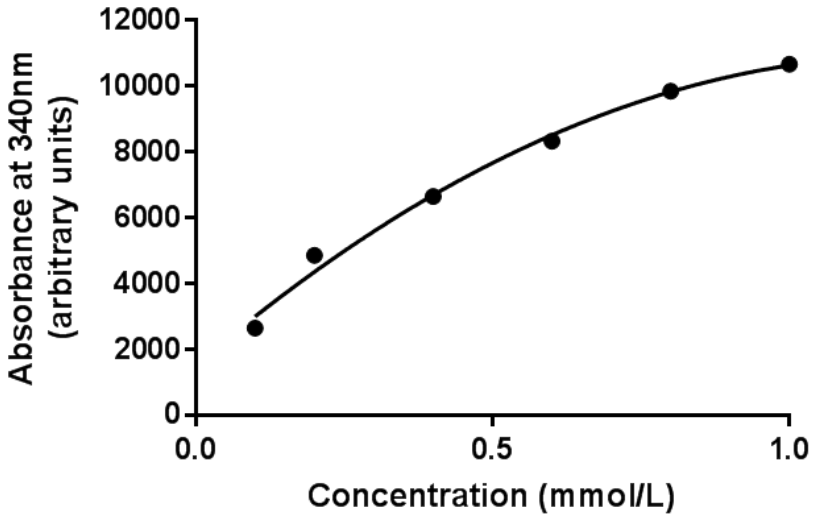

Figure 2.7. Typical standard curve of standards for lactate assay.

2.5 Chromatin Immunoprecipitation (ChIP)

ChIP assays were performed using the Active Motif ChIP-IT Express Enzymatic kit. All volumes indicated are for one sample collected from two 6-well plates.

2.5.1 Cross-linking and nuclei preparation from cell cultures

Chromatin for Hues-7 hESCs was isolated from two 6-well plates on day 3 post-passage. Proteins were crosslinked to DNA by adding 16% methanol-free formaldehyde (Pierce) to cell culture medium for 10 minutes shaking at room temperature. Cells were washed with ice-cold PBS and blocked with 1x glycine buffer for 5 minutes shaking at room temperature. Cells were washed with ice-cold PBS before being scraped into 5ml ice-cold PBS supplemented with 100mM PMSF and collected by centrifugation at 4˚C for 10 minutes at 2500rpm. Nuclei were lysed in ice-cold lysis buffer supplemented with PIC and 100mM PMSF and incubated on ice for 30 minutes.

2.5.2 Enzymatic shearing of chromatin

Hues-7 hESCs were transferred to an ice-cold dounce homogeniser and dounced on ice to aid with nuclei release before centrifugation at 4˚C at 5,000rpm for 10 minutes. The supernatant was discarded, the nuclei pellet resuspended in digestion buffer supplemented with PIC and 100mM PMSF and incubated at 37˚C for 5 minutes. 200U/ml working stock of Enzymatic Shearing Cocktail was added to the pre-warmed nuclei and incubated at 37˚C for 7.5 minutes to allow optimal chromatin shearing while vortexing the tubes every 2 minutes to increase the enzymatic shearing efficiency. 0.5M EDTA was added to stop the reaction before samples were incubated in ice for 10 minutes. Sheared chromatin samples were centrifuged at 13,300 rpm for 12 minutes at 4˚C and supernatant transferred to a fresh tube. Sheared chromatin samples were stored at -80˚C prior to subsequent steps.

2.5.2.1 DNA clean-up for determining shearing efficiency & DNA concentration

50µl aliquots of sheared chromatin samples were diluted in water supplemented with NaCl and incubated at 65˚C overnight to reverse cross-links. 10µg/µl RNase A was added to samples before incubating at 37˚C for 15 minutes. 0.5µg/µl Proteinase K was added to each sample and incubated at 42˚C for 90 minutes. DNA extraction was performed with an equal amount of phenol:chloroform:isoamyl alcohol (25:24:1) (Life Technologies) for each sample, mixed and centrifuged at room temperature at 13,300 rpm for 5 minutes. The aqueous phase was transferred to a fresh tube before adding 3M sodium acetate pH5.5 and 100% ethanol. Samples were incubated at -80˚C for at least 1 hour and subsequently

centrifuged at 13,300 rpm for 10 minutes at 4˚C. The supernatant was discarded and the pellet washed in 75% ice-cold ethanol before spinning at 13,300rpm for 5 minutes at 4˚C. Ethanol was aspirated completely and pellets allowed to air-dry. Pellets were resuspended in 30µl water before determining DNA concentration using the Nanodrop ND-1000 spectrophotometer and ND-1000 software v3.7.1. Shearing efficiency was analysed by loading 10µl sheared chromatin sample diluted in 6x loading buffer and 5µl QuickLoad 100bp DNA ladder (New England Biolabs) and a 1kb DNA ladder (Promega) on a 1% agarose gel (Invitrogen) in 1x TAE buffer (Fisher Bioreagents) containing 0.005% Nancy-520 (Invitrogen) and was run at 100V for approximately 1 hour. Optimal enzymatic shearing resulted in a 200-1500bp banded pattern.

2.5.3 Immunoprecipitation and washing

10µl per sample was collected as 'Input' sample and stored at -20˚C prior to subsequent steps. ChIP assays were performed using 3-15µg sheared chromatin in a reaction including Protein G magnetic beads, ChIP Buffer 1, PIC, water and 3µg of the following antibodies: HIF-2α (Novus Biologicals), H3K9me3 (AbCam), H3K36me3 (AbCam) and normal rabbit IgG (Santa Cruz), as described in Table 2.13. Samples were immuno-precipitated overnight with gentle rotation at 4˚C.

Table 2.13. Preparation of chromatin immunoprecipitation reactions.

Reagent	One reaction (if using less than 60µl chromatin)	One reaction (if using more than 60µl chromatin)
Protein G Magnetic Beads	25µl	25µl
ChIP buffer 1	10µl	20µl
Sheared chromatin	-	-
PIC	1µl	2µl
dH_2O	Make up to 100µl total volume	Make up to 200µl total volume
Antibody	3µg	3µg

Immuno-precipitated samples were placed on a magnetic stand to allow magnetic beads to pellet. Supernatant was discarded before washing the beads twice for 3 minutes in ChIP buffer 1. Supernatant was discarded before washing beads twice in ChIP buffer 2 for 3 minutes per wash.

2.5.4 Elution and Reversal of Formaldehyde crosslinks

After the completion of the wash steps, the supernatant was discarded and washed beads resuspended in Elution buffer to elute the antibody/protein/DNA complexes and incubated at room temperature for 15 minutes with gentle rotation. Reverse cross-linking buffer was added to the eluted chromatin and mixed thoroughly. Samples were placed on a magnetic stand to allow magnetic beads to pellet and the supernatant containing the chromatin was transferred into a fresh tube.

Input DNA was processed by adding 88µl ChIP buffer 2 and 2µl 5M NaCl to the 10µl aliquot set aside in Chapter 2.5.3. Both Input and ChIP samples were incubated at 95˚C for 15 minutes before adding 2µl 0.5µg/µl Proteinase K. Samples were thoroughly mixed and incubated at 37˚C for 1 hour before the addition of Proteinase K Stop Solution. Samples were cleaned up for use in PCR reactions using the QIAquick PCR Purification kit (Appendix 1; Qiagen). DNA samples were stored at -20˚C until required for subsequent analysis steps.

All the steps to the ChIP protocol are illustrated in Figure 2.8.

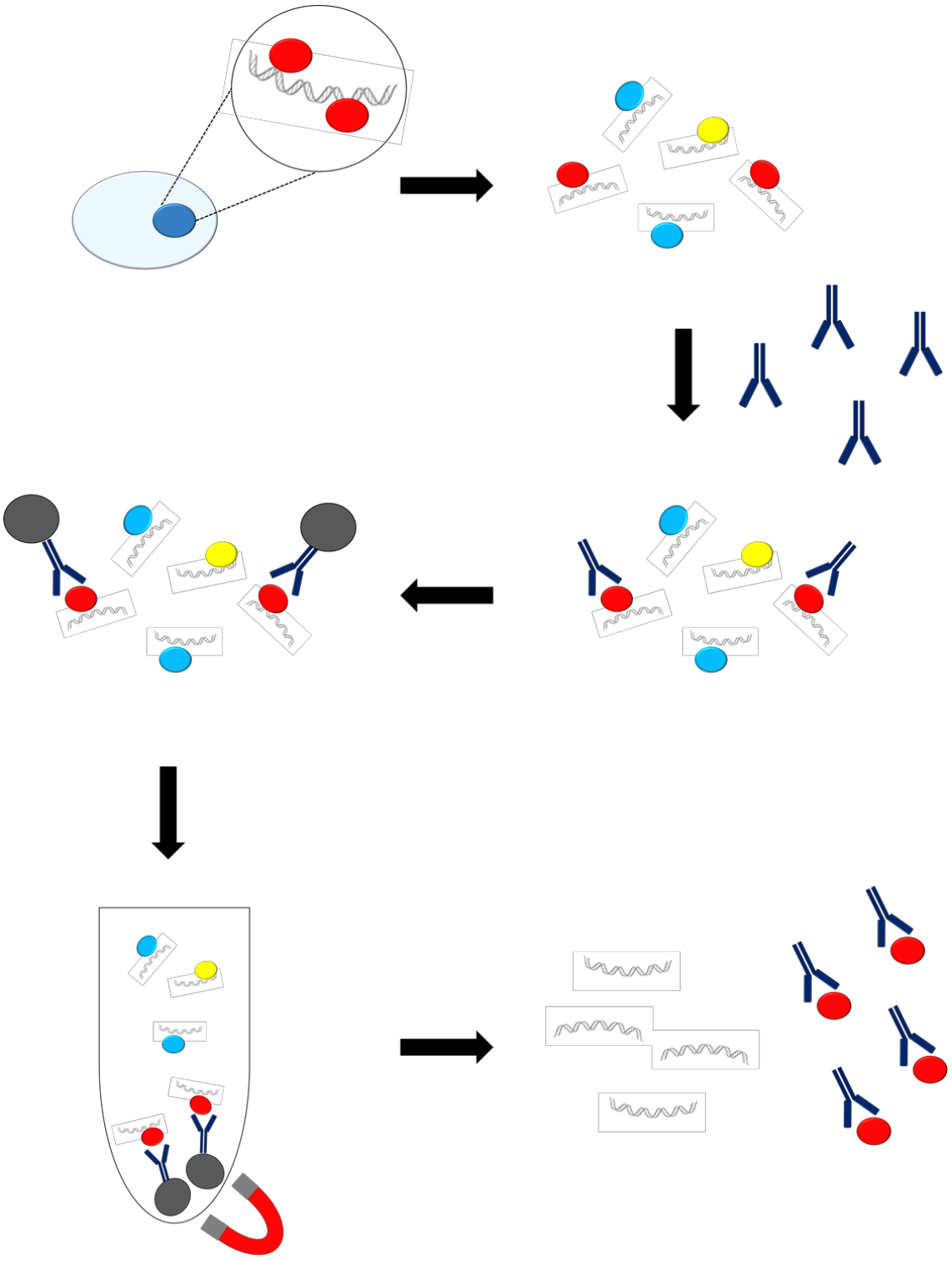

Figure 2.8. Schematic of chromatin immunoprecipitation assay.
Cells were fixed with paraformaldehyde to crosslink DNA with any bound proteins. Chromatin was isolated from cell nuclei and sheared enzymatically. Sheared chromatin was incubated with antibodies against the protein of interest. The protein-DNA complexes are captured by Protein G magnetic beads and immunoprecipitated. Crosslinks were reversed and DNA fragments purified before analysis by qPCR.

2.6 Hypoxia Response Element (HRE) Amplification

2.6.1 Primer and probe design

All primer and probe sequences, that overlap the potential HRE sites in the proximal promoter region of the genes of interest, were designed using the Primer Express 3.0 software and analysed through bioinformatics software such as BLAST to test for their specificity.

2.6.2 HRE Real time PCR Analysis

PCR detection of the CtBP proximal promoter regions or the potential HRE site in the GLUT1 proximal promoter was performed in 20µl reactions containing PowerUp SYBR Green MasterMix (Thermo Scientific), 5µM of each primer (Table 2.14), nuclease-free water and 2µl volume of DNA. PCR amplification of the proximal promoter regions containing a potential HRE in the OCT4, SOX2, NANOG and GLUT1 or a region between two potential HREs in the FOXP3 genes was performed in 20µl reactions containing Taqman Universal Mastermix (Thermo Scientific), 1µl 20x custom Taqman probe (Table 2.15), nuclease-free water and 2µl of DNA. Reactions were performed in a 96-well plate using a 7500 Real-Time PCR system and 7500 software v2.0.6 (Applied Biosystems).

The following cycling parameters were used: 50˚C for 2 minutes, 95˚C for 10 minutes, followed by 45 cycles of 95˚C for 15 seconds and 60˚C for 1 minute. All samples were analysed in duplicate.

Percentage of Input (non-immunoprecipitated chromatin) was calculated as $100x2^{[Ct(Input) - Ct(IP)]}$ for each sample from three independent ChIP assays on chromatin isolated from hESCs cultured at either 5% or 20% oxygen, or hESCs cultured at 5% oxygen in the presence of absence of 10mM 2-DG or JMJD2a siRNA. Relative enrichment of histone modifications was calculated as above, but normalising % enrichment to either the 0mM 2-DG control or the Allstars negative control siRNA. Undetermined values were given an arbitrary Ct value of 40.

Table 2.14. Table of primers used in ChIP assays.

Gene	Forward primer sequence (5' – 3')	Reverse primer sequence (5' – 3')	Amplicon size
CtBP1_HRE	ACACGTGTTCCCTCCTTCATG	CAGGTGTCACCAGAGCTTTGG	80bp
CtBP2_HRE	CCTATGAAGGTCACGCGAAAA	TTGCCCGCTAGTCCACGTA	69bp
GLUT1 _HRE	CCTCCCTTCCAAGGGTAACT	CCAGCATAGGCTAGGACCAC	249bp

Table 2.15. Table of custom designed Taqman probes used in ChIP assays.

Gene	Forward primer sequence (5' – 3')	Reverse primer sequence (5' – 3')	Probe sequence (5' - 3')	Amplicon size
OCT4_CR3	TGAGAAGCCTTACTTAAGTCGACAGA	TTCGAAGCTGTGGGGAGC	TCAGCGTGCCCAGTC	96bp
SOX2_G	CGGCCACCACAATGGAAA	TCCCTCCCACGCAGAGTTC	AGGCTGGTTCTGCT	96bp
SOX2_A	AACGGACGTGCTGCCATT	TGTCCCGACGTAAAGATTTCAA	CCCTCCGCATTGAG	85bp
NANOG	TGGAAACGTGGTGAACCTAGAA	AACCGAGCAACAGAACCTGAA	TATTTGTTGCTGGGTTTGT	83bp
GLUT3_HRE	TCCTGGGCTCAAGTGATCCT	AAATTAGCTGGACGTGGTAATGG	CCACCTCAGCCTCC	87bp
FOXP3	CCCCAGAGACCCTCAAATATCC	CCCGAGGCAGGCAGAGA	CTCACTCACAGAATGGT	56bp

2.7 Statistical analysis

An Anderson-Darling normality test was performed in Minitab 18 and used to confirm that the data was normally distributed. Differences in relative gene and protein expression and relative chromatin enrichment between control and test conditions in either Hues-7, Shef3 and NT2 cells were analysed using a one-sample t-test. A one-way ANOVA was performed to compare the expression of both CtBP isoforms with the expression of either CtBP2-L or CtBP2-S after normalisation to 5% oxygen. Differences in glucose consumption and lactate production along with the percentage of Input DNA and relative chromatin enrichment were analysed by unpaired t-test.

All data represent a minimum of 3 independent experiments and are presented as mean ± SEM, unless otherwise stated. $p<0.05$ was considered statistically significant.

Chapter 3

Characterisation and hypoxic regulation of CtBP expression in hESCs

Chapter 3: Characterisation and hypoxic regulation of CtBP expression in hESCs

3.1 Introduction

3.1.1 Human embryonic stem cells

hESCs are derived from the inner cell mass of the blastocyst and can differentiate into cells of the three developmental germ layers (Evans and Kaufman, 1981; Thomson et al., 1998). Due to this capability, hESCs have the potential to be used in a variety of regenerative medicine applications. However, in standard culture at 20% oxygen, hESCs have a tendency to spontaneously differentiate, making them particularly difficult to maintain in culture. Therefore, it is vital to undertake research to improve the culture conditions for hESCs in order for them to reach their full potential for the benefit of regenerative medicine.

hESCs are characterised by the expression of pluripotency markers; OCT4, SOX2 and NANOG. In addition to the expression of these transcription factors, hESCs can be characterised with the expression of several surface markers, such as TRA-1-60 and SSEA-4. In contrast, SSEA-1 is expressed during early hESC differentiation.

3.1.2 Hypoxia and HIFs

Derivation and culture of hESCs are most commonly performed under atmospheric oxygen tensions. However, preimplantation embryos are exposed to much lower oxygen tensions *in vivo*, and when this is mimicked during *in vitro* culture of hESCs, it is found to be beneficial to hESC maintenance in terms of increased expression of pluripotency markers, such as OCT4, SOX2, NANOG and SSEA-4, and a reduced rate of spontaneous differentiation. Furthermore, hESCs cultured under hypoxic oxygen tensions display a more rounded and defined colony morphology, compared to those cultured at 20% oxygen tensions which were more enlarged and diffuse (Ezashi et al., 2005; Forsyth et al., 2006; Westfall et al., 2008; Chen et al., 2010; Forristal et al., 2010; Forristal et al., 2013).

Hypoxic conditions leads to the stabilisation of the α subunits of the HIF transcription factors, which regulate the expression of more than 200 genes, including many involved in energy metabolism and oxygen homeostasis (Wang and Semenza, 1993b; Wang et al., 1995; Semenza, 2000b). One of the HIF-α subunits (HIF-1α, HIF-2α and HIF-3α)

heterodimerise with the constitutively expressed HIF-1β subunit before translocating to the nucleus, where all three HIF-α subunits can bind a canonical recognition sequence 5'-(A/G)CGTG-3' termed a hypoxic response element (HRE) in the proximal promoter or enhancer of HIF target genes (Semenza and Wang, 1992; Wang and Semenza, 1993a, 1995; Semenza, 1996). Previously identified targets of HIF-1α are the glucose transporters GLUT1 and GLUT3, while targets of HIF-2α include the pluripotency markers OCT4, SOX2 and NANOG (Semenza, 2000b; Chen et al., 2001; Covello et al., 2006; Hu et al., 2006; Forristal et al., 2010; Forristal et al., 2013; Petruzzelli et al., 2014). In hESCs, HIF-1α is only transiently expressed under hypoxic conditions, whereas HIF-2α is thought to be responsible for the long term adaptation to hypoxia (Forristal et al., 2010).

3.1.3 hESC metabolism

Metabolism is fundamental to all cell types for energy but also to fulfil biosynthetic demands. However, the metabolic state of different cells types differs greatly depending on the needs of the cell. Glycolysis involves the enzymatic conversion of glucose into lactate with the production of NADH and 2 molecules of ATP per molecule of glucose, compared to the 36 molecules of ATP generated by OXPHOS. However, hESCs have been documented to rely heavily on glycolysis for their energetic demands and consume little oxygen (Kondoh et al., 2007; Prigione and Adjaye, 2010; Folmes et al., 2011; Varum et al., 2011; Forristal et al., 2013).

hESC metabolism is notably different in cells cultured under hypoxic conditions compared to those maintained under atmospheric oxygen tensions, suggesting a hypoxic environment may support a more glycolytic metabolism and therefore maintain the pluripotent state. As previously mentioned, several genes involved in glycolysis and its regulation are regulated by HIFs, such as GLUTs and PKM2, which provides evidence that hypoxic culture supports the predominantly glycolytic metabolism of hESCs (Forristal et al., 2013; Prigione et al., 2014; Christensen et al., 2015). In addition, previous studies have demonstrated that throughout differentiation, the energetic demands of hESCs change to a reliance on OXPHOS (Cho et al., 2006; Ramalho-Santos et al., 2009; Prigione and Adjaye, 2010). In contrast, the production of iPSCs increases the expression of genes associated with glycolysis. These studies demonstrate that hypoxia is supporting the maintenance of the pluripotent state by enhancing glycolytic metabolism in hESCs

(Prigione and Adjaye, 2010; Folmes et al., 2011; Varum et al., 2011; Kim et al., 2015; Folmes and Terzic, 2016).

3.1.4 C-terminal binding proteins

C-terminal binding proteins (CtBPs) are a family of glycolytic sensors which link cellular metabolism to gene expression. There are two highly homologous proteins in humans called CtBP1 and CtBP2. Each *CtBP* gene locus generates several protein isoforms as a result of alternative splicing and alternative promoter usage to generate the following proteins with evolutionarily conserved functional domains; CtBP1-L, CtBP1-S, CtBP2-L and CtBP2-S (Chinnadurai, 2002).

CtBPs link the metabolic state of the cell to gene transcription through a conserved NAD(H)-binding domain in the CtBP monomers. CtBP activity is predominantly regulated through the binding of NADH, which is produced during glycolysis. The binding of NAD(H) induces a conformational change which allows CtBP monomers to dimerise and therefore become active (Kumar et al., 2002; Balasubramanian et al., 2003). The active dimers can, then, translocate into the nucleus to bind to PXDLS motif-containing TFs, either directly or indirectly through bridging proteins, and recruit chromatin-modifying complexes to specific promoters (Zhang et al., 2001; Fjeld et al., 2003). CtBPs are primarily known for their roles as transcriptional corepressors, but variants of both CtBPs have additional cytosolic functions.

There is increasing evidence that energy metabolism is a key regulator of the pluripotent state, but how the metabolic state of hESCs may impact gene expression is not fully understood, but CtBPs may have a role.

3.1.5 Chapter Aims

The aims of this chapter are:

- To characterise hESC pluripotency at either 5% or 20% oxygen tension using immunocytochemistry, RT-qPCR and Western blotting.
- To quantify the expression and localisation of CtBP1 and CtBP2 in Hues-7 and Shef3 hESCs maintained at either 5% or 20% oxygen using immunocytochemistry, RT-qPCR and Western blotting.
- To determine whether endogenous HIF-2α regulates CtBP expression in Hues-7 hESCs cultured at 5% oxygen, using siRNA
- To determine whether HIF-2α binds directly to potential HRE sites in the proximal promoters of CtBP genes in Hues-7 hESCs cultured at 5% oxygen using ChIP.

3.2 Results

3.2.1 Characterisation of pluripotency marker expression in Hues-7 and Shef3 hESCs cultured at either 5% or 20% oxygen

To characterise pluripotency marker expression in either Hues-7 or Shef3 hESCs cultured at both 5% and 20% oxygen tensions, immunocytochemistry was performed.

Phase contrast images were obtained to demonstrate representative morphologies of Hues-7 hESCs cultured at either 5% or 20% oxygen. Cells at both oxygen tensions formed compact, rounded colonies of a typical cobblestone morphology (Figure 3.1, 3.2, 3.5 and 3.6).

Hues-7 hESCs cultured at either oxygen tension were labelled with antibodies against the pluripotency markers OCT4, SOX2, NANOG and TRA-1-60, and an early differentiation marker SSEA-1 (Figure 3.1 – 3.8). A strong nuclear signal was observed for the transcription factors OCT4, SOX2 and NANOG expression throughout hESC colonies cultured at both 5% and 20% oxygen (Figure 3.1B, J and N; Figure 3.3B, H and K; Figure 3.5 B, J and N; and Figure 3.7B, H and K). Expression of the surface marker TRA-1-60 was observed in most cells of a given colony at either 5% or 20% oxygen tension (Figure 3.2B; Figure 3.4B; Figure 3.6B; and Figure 3.8B). The apparent heterogeneity of TRA-1-60 expression is largely due to the cell surfaces being in different optical planes. Only a few SSEA-1 positive hESCs were observed, primarily around the edges of colonies at both oxygen tensions (Figure 3.2F; Figure 3.4E; Figure 3.6F; and Figure 3.8E), however there appears to be slightly more SSEA-1 positive cells at 20% oxygen (Figure 3.6F and Figure 3.8E) compared to 5% oxygen.

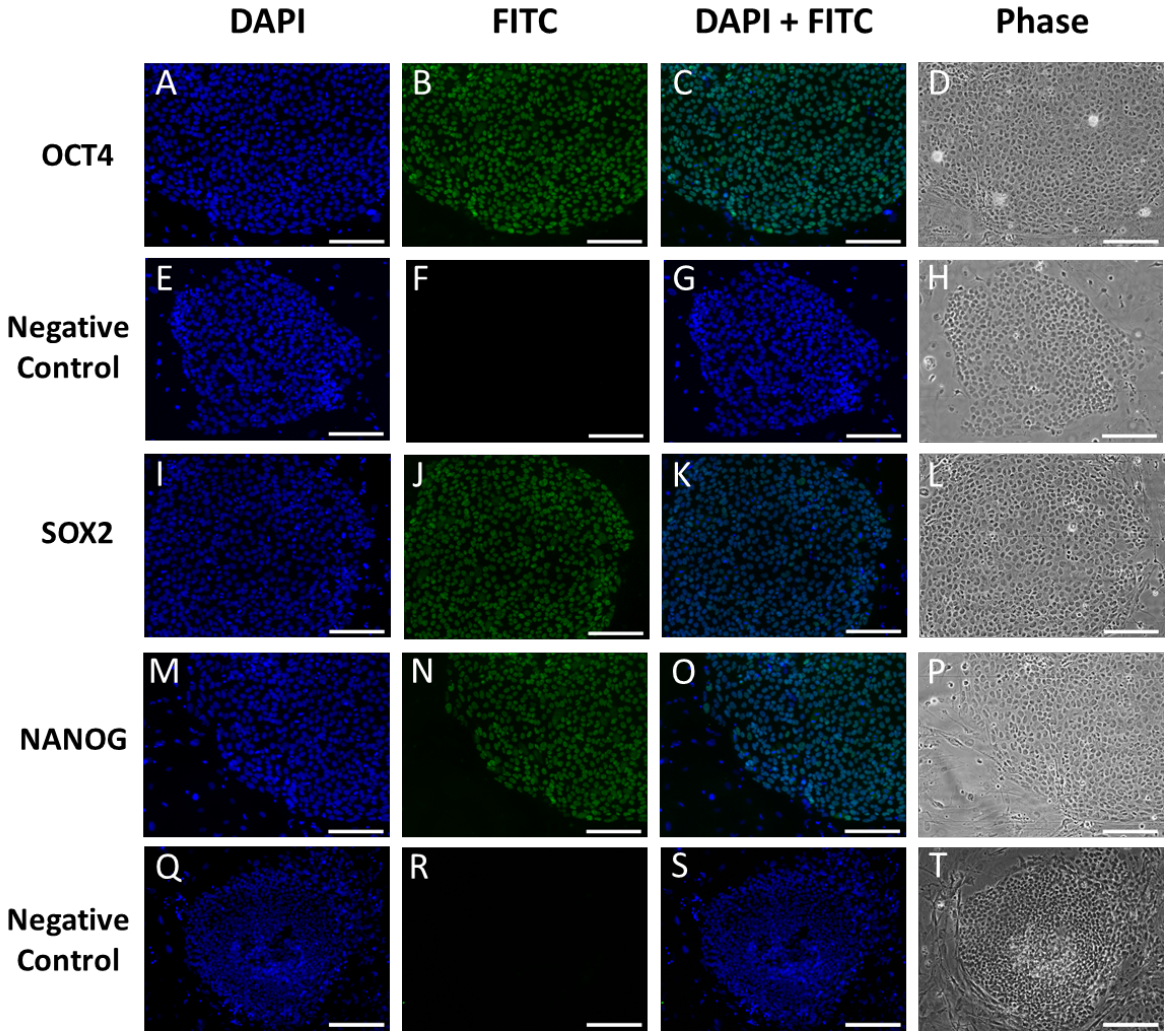

Figure 3.1. Characterisation of Hues-7 hESCs maintained at 5% oxygen.
Representative images of OCT4 (A-D), SOX2 (I-L) and NANOG (M-P) protein expression in Hues-7 hESCs cultured at 5% oxygen on MEF feeder layers. An anti-mouse-IgG FITC-conjugated secondary antibody was used to detect OCT4 expression and its negative control (E-H), whereas an anti-rabbit-IgG FITC-conjugated secondary antibody was used to detect SOX2 and NANOG expression and their negative control (Q-T). DAPI staining was performed to label the nuclei. DAPI (blue; A, E, I, M, Q), FITC (green; B, F, J, N, R) and phase contrast images (D, H, L, P, T) were taken. Scale bar indicates 200µm.

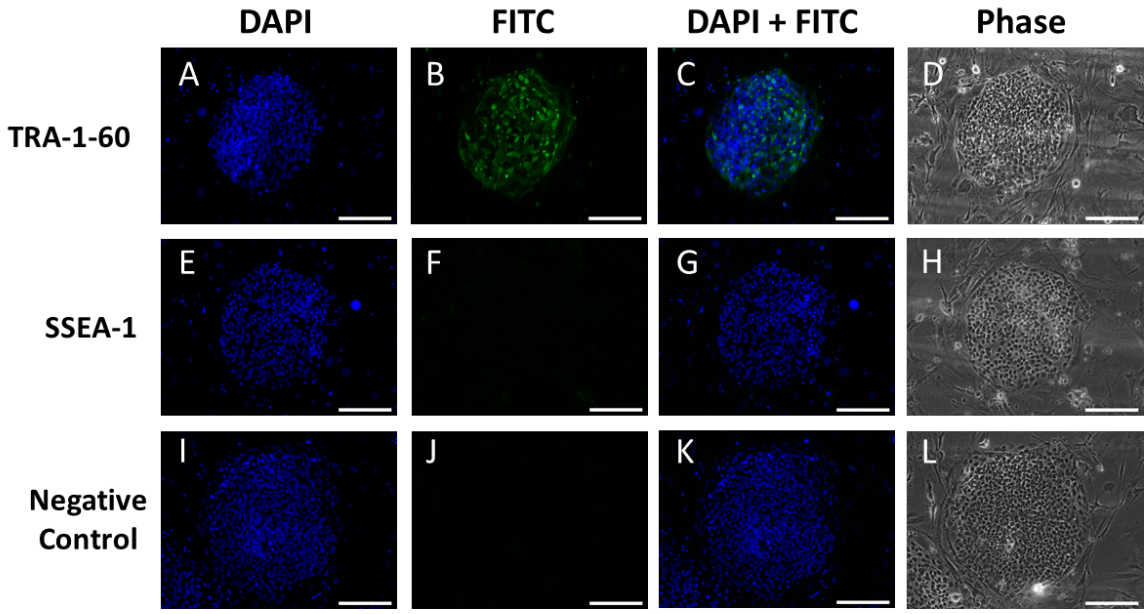

Figure 3.2. Characterisation of surface markers in Hues-7 hESCs cultured at 5% oxygen. Representative images of TRA-1-60 (A-D) and SSEA-1 (E-H) protein expression in Hues-7 hESCs cultured at 5% oxygen on MEF feeder layers. An anti-mouse-IgM FITC-conjugated secondary antibody was used to detect both TRA-1-60 and SSEA-1 expression and the negative control (I-L). DAPI staining was performed to label the nuclei. DAPI (blue; A, E, I), FITC (green; B, F, J) and phase contrast images (D, H, L) were taken. Scale bar indicates 200µm.

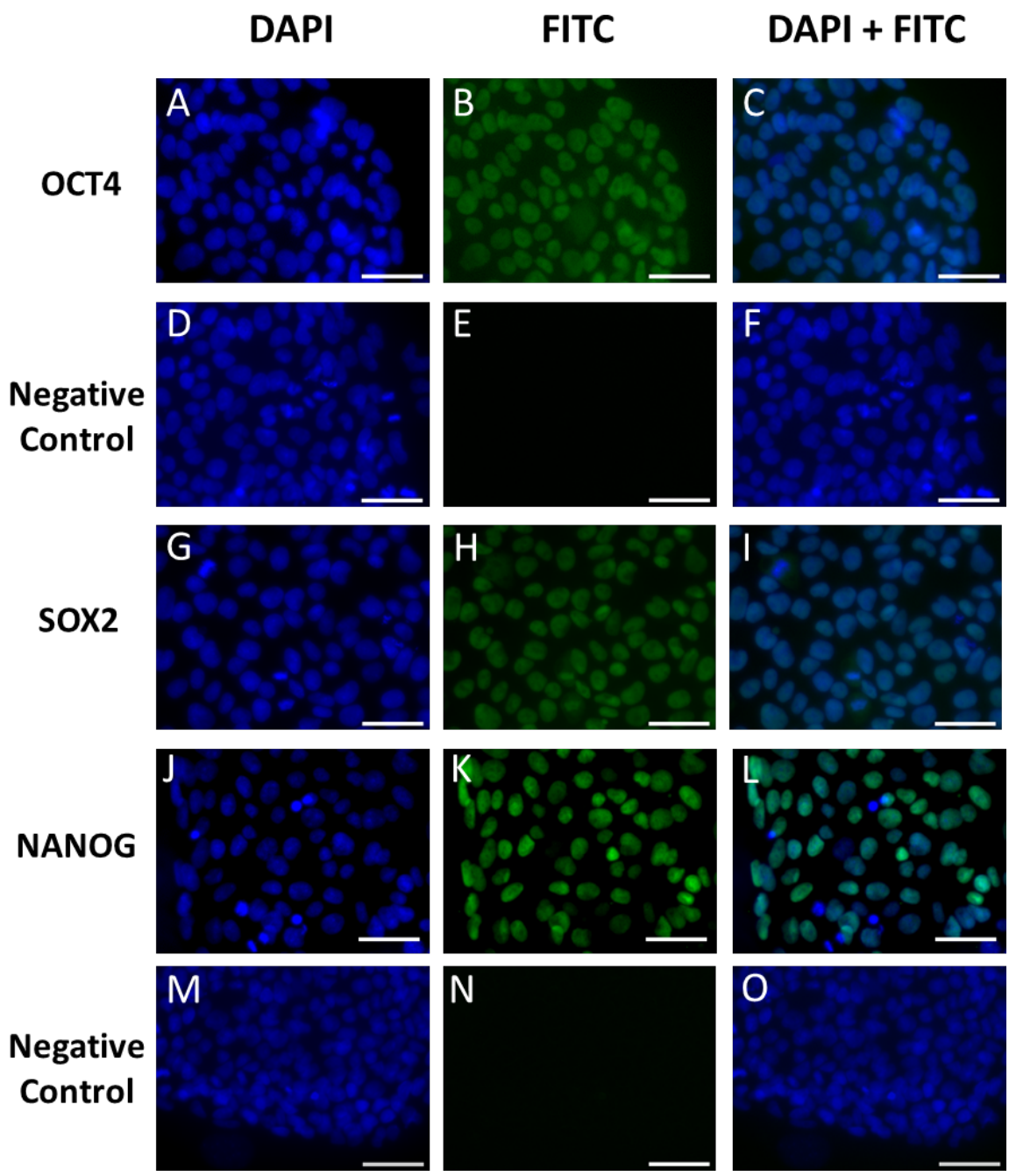

Figure 3.3. Subcellular localisation of pluripotency markers in Hues-7 hESCs cultured at 5% oxygen.

Representative images of OCT4 (A-C), SOX2 (G-1) and NANOG (J-L) protein expression in Hues-7 hESCs cultured at 5% oxygen on MEF feeder layers. An anti-mouse-IgG FITC-conjugated secondary antibody was used to detect OCT4 expression and its negative control (D-F), whereas an anti-rabbit-IgG FITC-conjugated secondary antibody was used to detect SOX2 and NANOG expression and their negative control (M-O). DAPI staining was performed to label the nuclei. DAPI (blue; A, D, G, J, M) and FITC (green; B, E, H, K, N) images were taken. Scale bar indicates 50μm.

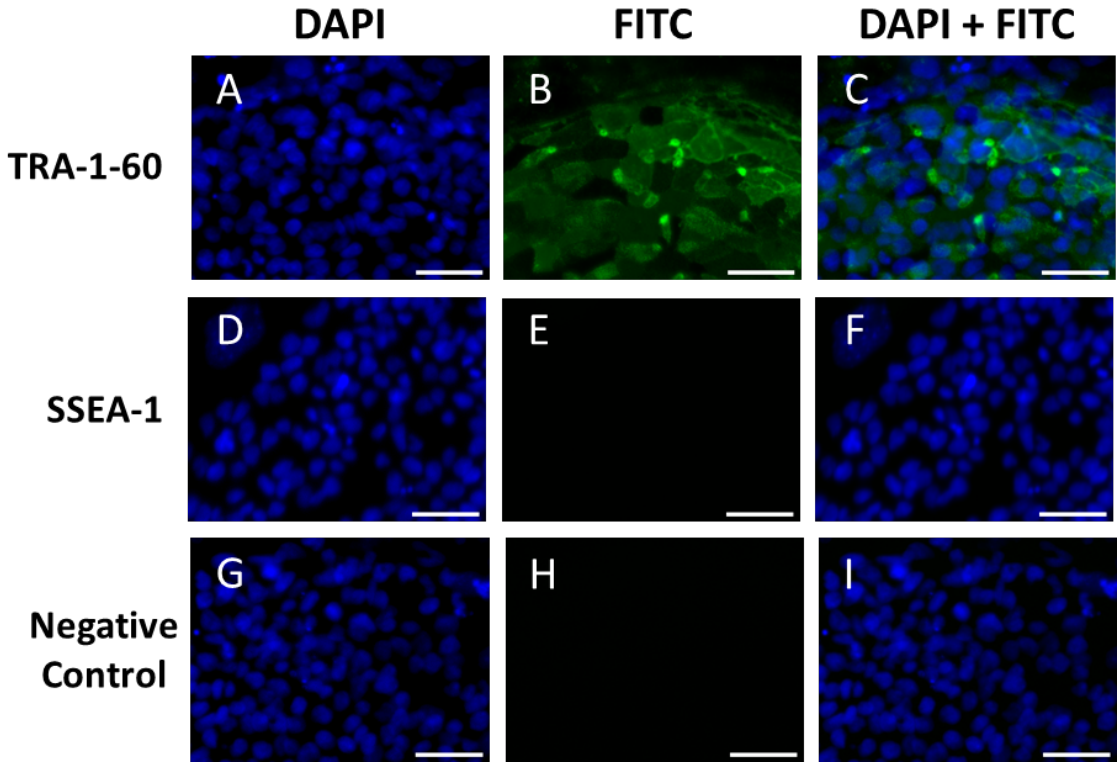

Figure 3.4. Characterisation of surface markers in Hues-7 hESCs cultured at 5% oxygen. Representative images of TRA-1-60 (A-C) and SSEA-1 (D-F) protein expression in Hues-7 hESCs cultured at 5% oxygen on MEF feeder layers. An anti-mouse-IgM FITC-conjugated secondary antibody was used to detect both TRA-1-60 and SSEA-1 expression and the negative control (G-1). DAPI staining was performed to label the nuclei. DAPI (blue; A, D, G) and FITC (green; B, E, H) images were taken. Scale bar indicates 50μm.

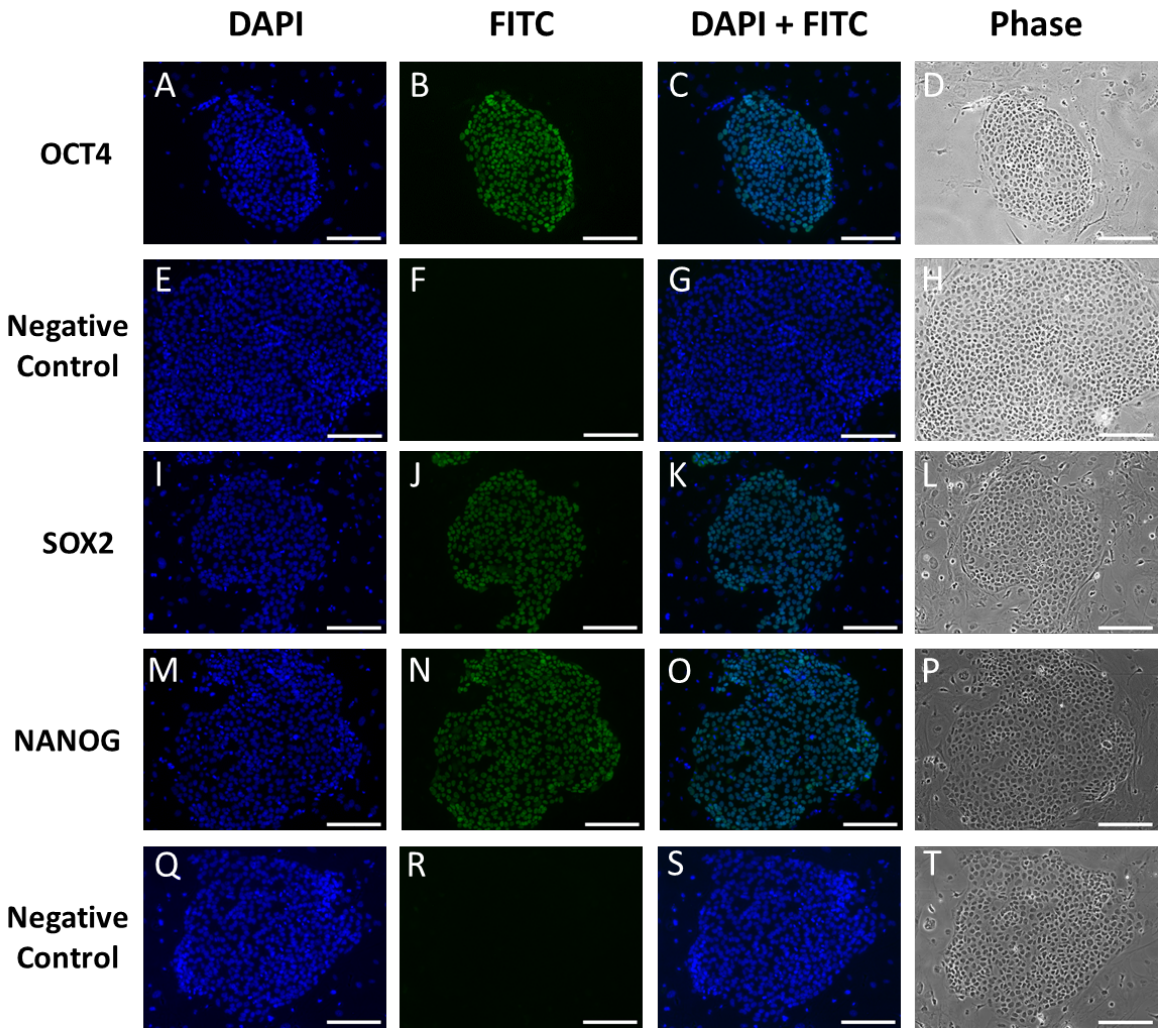

Figure 3.5. Characterisation of Hues-7 hESCs cultured at 20% oxygen.
Representative images of OCT4 (A-D), SOX2 (I-L) and NANOG (M-P) protein expression in Hues-7 hESCs cultured at 20% oxygen on MEF feeder layers. An anti-mouse-IgG FITC-conjugated secondary antibody was used to detect OCT4 expression and its negative control (E-H), whereas an anti-rabbit-IgG FITC-conjugated secondary antibody was used to detect SOX2 and NANOG expression and their negative control (Q-T). DAPI staining was performed to label the nuclei. DAPI (blue; A, E, I, M, Q), FITC (green; B, F, J, N, R) and phase contrast images (D, H, L, P, T) were taken. Scale bar indicates 200µm.

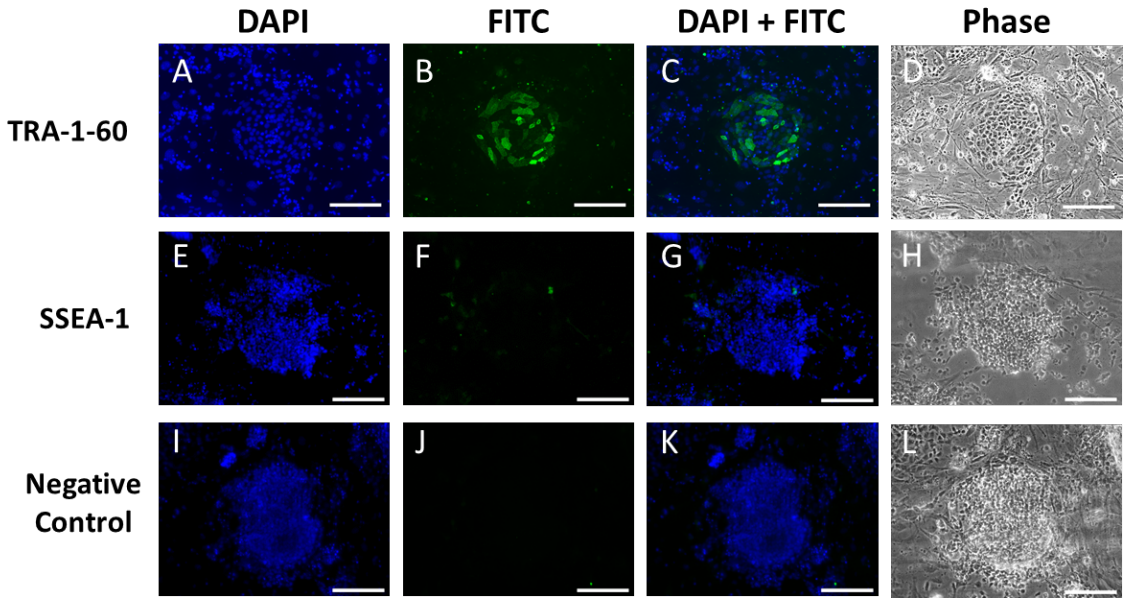

Figure 3.6. Characterisation of surface markers in Hues-7 hESCs cultured at 20% oxygen. Representative images of TRA-1-60 (A-D) and SSEA-1 (E-H) protein expression in Hues-7 hESCs cultured at 20% oxygen on MEF feeder layers. An anti-mouse-IgM FITC-conjugated secondary antibody was used to detect both TRA-1-60 and SSEA-1 expression and the negative control (I-L). DAPI staining was performed to label the nuclei. DAPI (blue; A, E, I), FITC (green; B, F, J) and phase contrast images (D, H, L) were taken. Scale bar indicates 200µm.

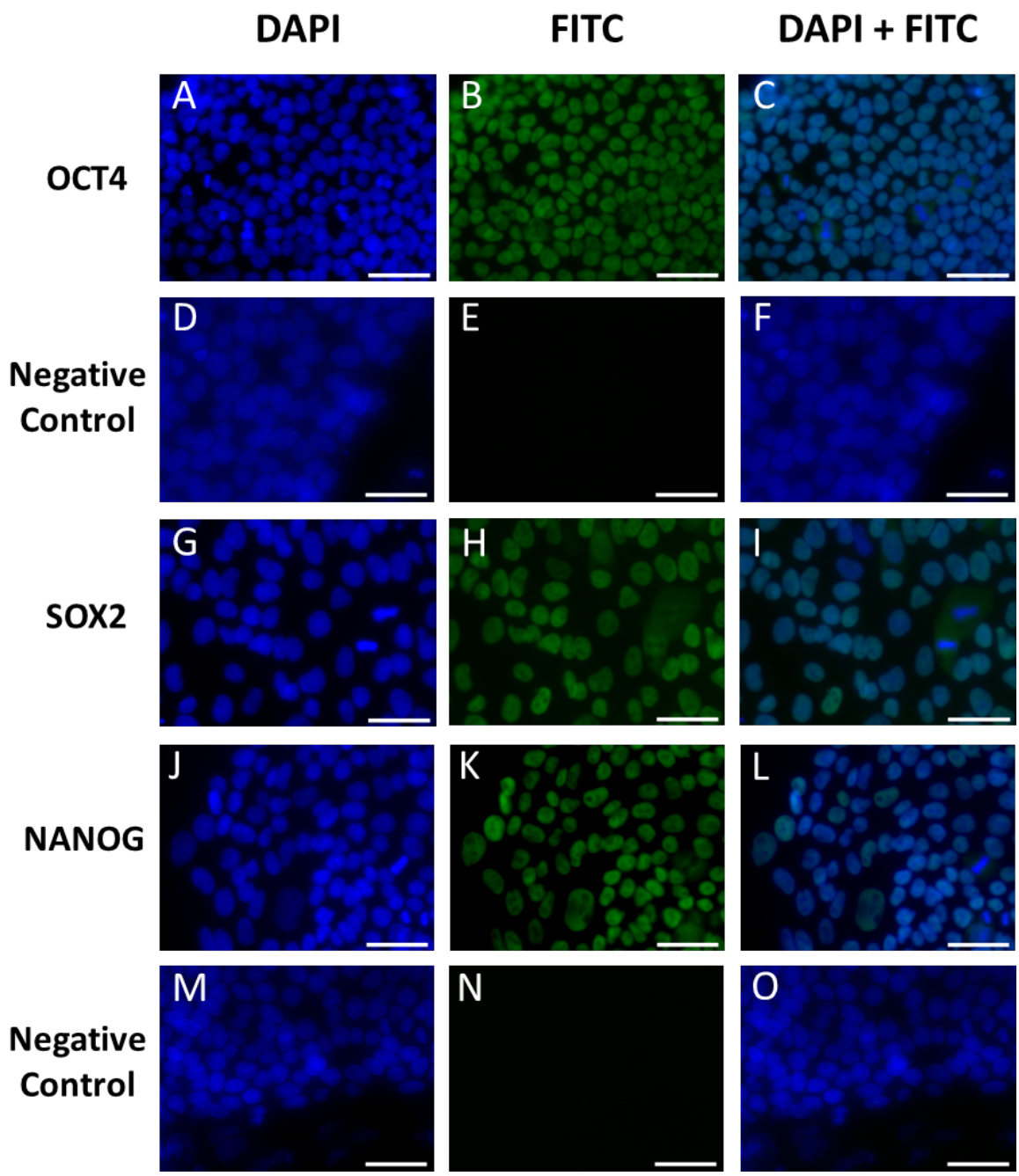

Figure 3.7. Subcellular localisation of pluripotency markers in Hues-7 hESCs cultured at 20% oxygen.

Representative images of OCT4 (A-C), SOX2 (G-1) and NANOG (J-L) protein expression in Hues-7 hESCs cultured at 20% oxygen on MEF feeder layers. An anti-mouse-IgG FITC-conjugated secondary antibody was used to detect OCT4 expression and its negative control (D-F), whereas an anti-rabbit-IgG FITC-conjugated secondary antibody was used to detect SOX2 and NANOG expression and their negative control (M-O). DAPI staining was performed to label the nuclei. DAPI (blue; A, D, G, J, M) and FITC (green; B, E, H, K, N) images were taken. Scale bar indicates 50μm.

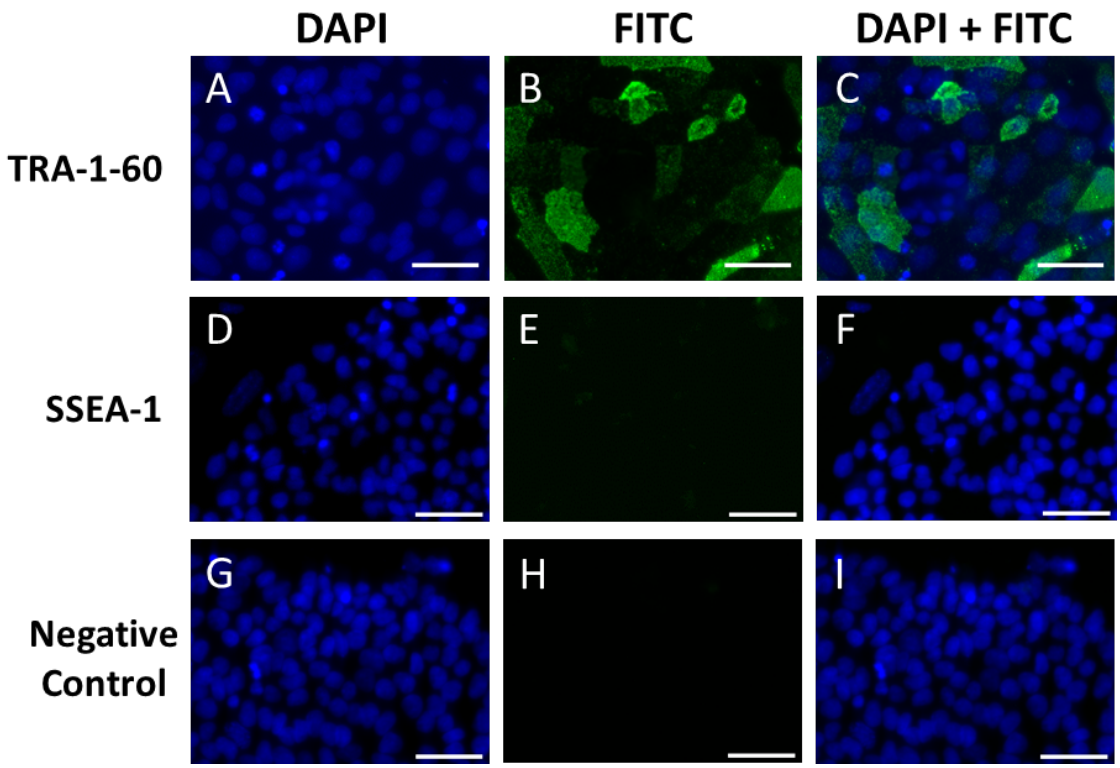

Figure 3.8. Characterisation of surface markers in Hues-7 hESCs cultured at 20% oxygen. Representative images of TRA-1-60 (A-C) and SSEA-1 (D-F) protein expression in Hues-7 hESCs cultured at 5% oxygen on MEF feeder layers. An anti-mouse-IgM FITC-conjugated secondary antibody was used to detect both TRA-1-60 and SSEA-1 expression and the negative control (G-1). DAPI staining was performed to label the nuclei. DAPI (blue; A, D, G) and FITC (green; B, E, H) images were taken. Scale bar indicates 50μm.

Phase contrast images were also obtained to demonstrate representative morphologies of Shef3 hESCs cultured at either 5% or 20% oxygen. Cells at both oxygen tensions formed compact colonies of a typical cobblestone morphology (Figure 3.9 and 3.11).

Shef3 hESCs cultured at either oxygen tension were labelled with antibodies against the pluripotency markers OCT4 and TRA-1-60, and an early differentiation marker SSEA-1 (Figure 3.9 – 3.12). A strong nuclear signal was observed for OCT4 expression throughout hESC colonies cultured at both 5% and 20% oxygen (Figure 3.9B, 3.10B, 3.11B and 3.12B). Expression of the surface marker TRA-1-60 was observed in most cells of a given colony at either 5% or 20% oxygen tension (Figure 3.9J; Figure 3.10H; Figure 3.11J; and Figure 3.12H). Only a few SSEA-1 positive hESCs were observed, primarily around the edges of colonies at both oxygen tensions (Figure 3.9N; Figure 3.10K; Figure 3.11N; and Figure 3.12K), however there were more SSEA-1 positive cells at 20% oxygen (Figure 3.11N and Figure 3.12K) compared to 5% oxygen.

Taken together, these results demonstrate that the majority of hESCs cultured at either 5% or 20% oxygen express markers associated with pluripotency, but some differentiation occurs predominantly around the edges of hESC colonies. However, upon initial comparison between hESCs cultured at either oxygen concentration, there appeared to be no overt difference in the relative expression of pluripotency markers.

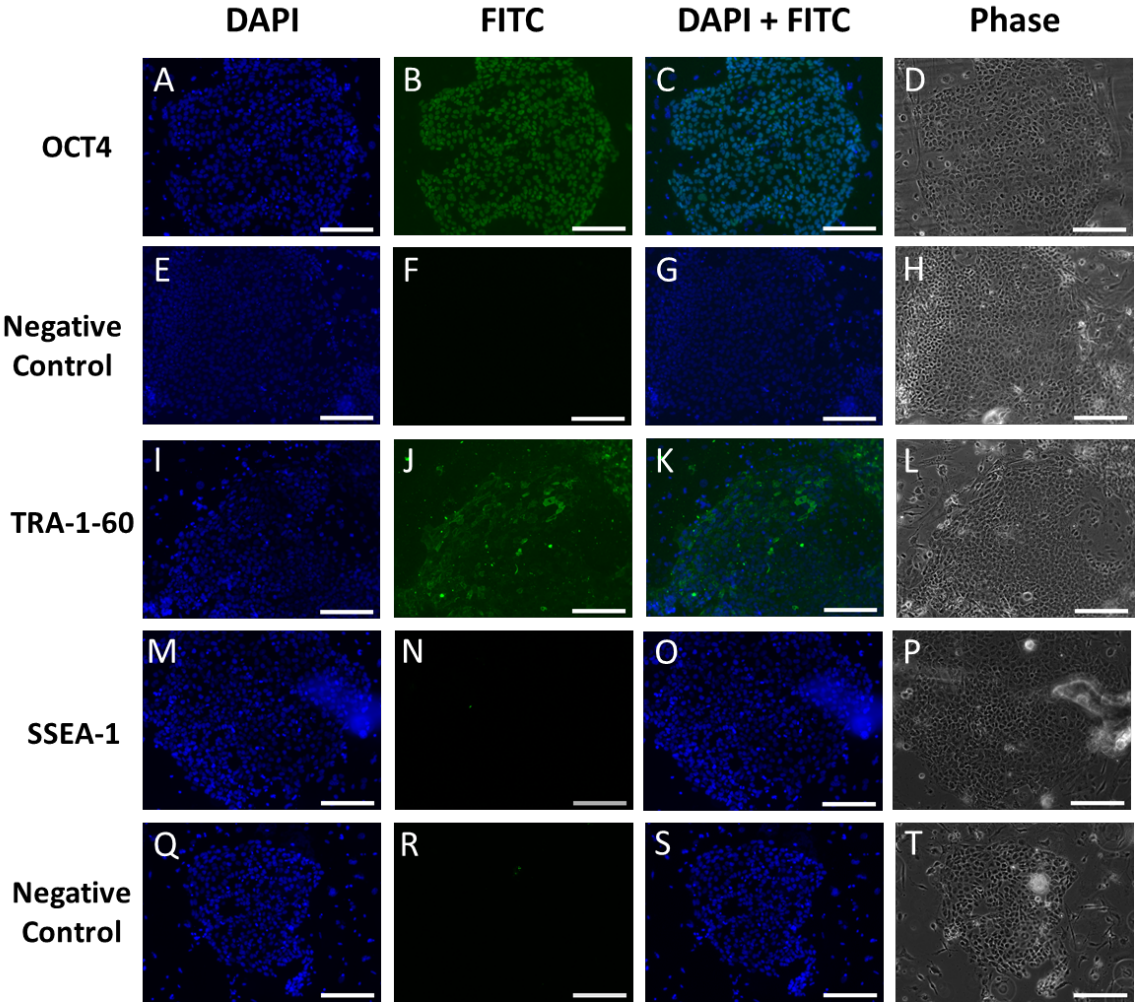

Figure 3.9. Characterisation of Shef3 hESCs maintained at 5% oxygen.
Representative images of OCT4 (A-D), TRA-1-60 (I-L) and SSEA-1 (M-P) protein expression in Shef3 hESCs cultured at 5% oxygen on MEF feeder layers. An anti-mouse-IgG FITC-conjugated secondary antibody was used to detect OCT4 expression and its negative control (E-H), whereas an anti-rabbit-IgM FITC-conjugated secondary antibody was used to detect TRA-1-60 and SSEA-1 expression and their negative control (Q-T). DAPI staining was performed to label the nuclei. DAPI (blue; A, E, I, M, Q), FITC (green; B, F, J, N, R) and phase contrast images (D, H, L, P, T) were taken. Scale bar indicates 200μm.

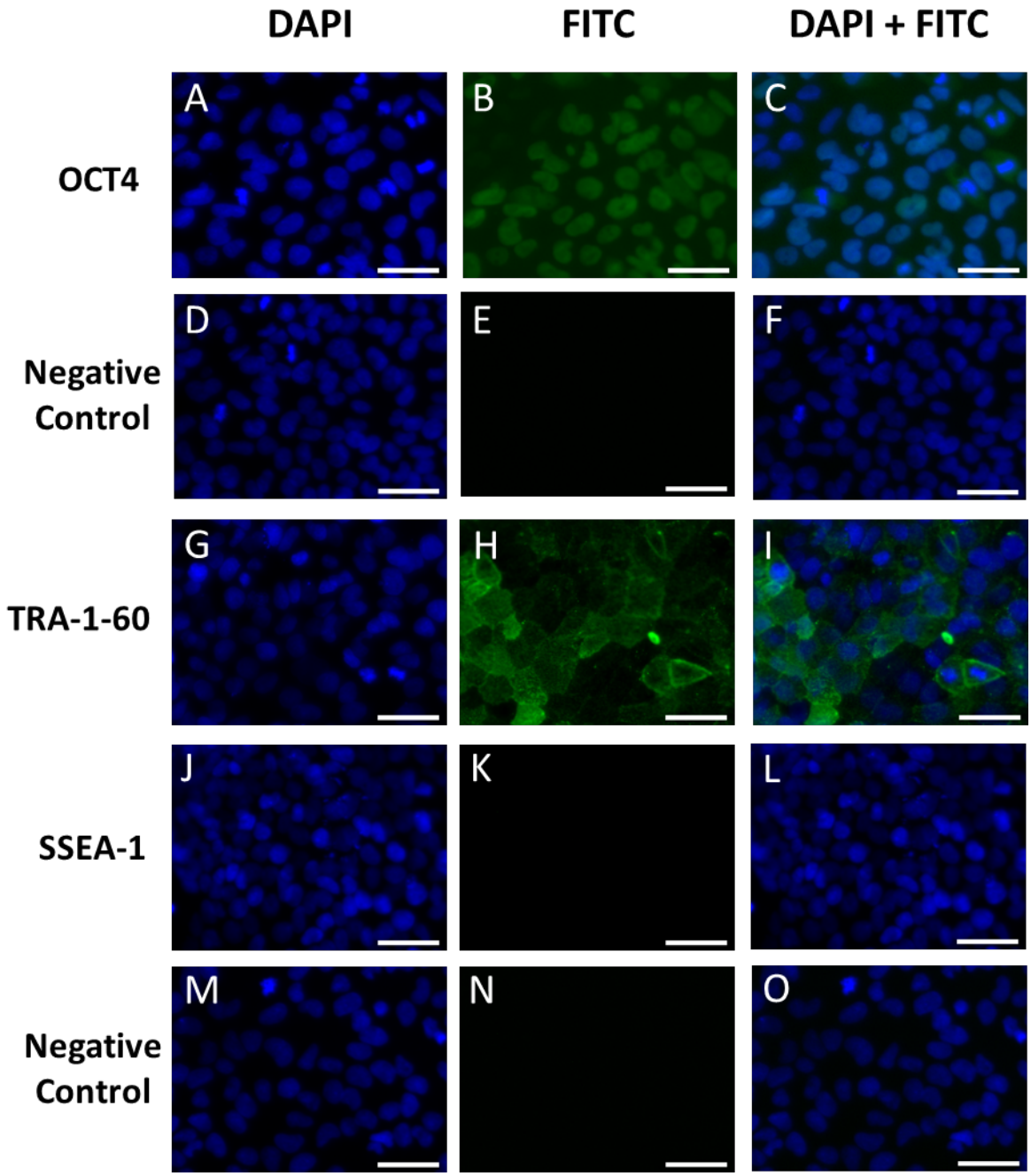

Figure 3.10. Subcellular localisation of pluripotency markers in Shef3 hESCs cultured at 5% oxygen.

Representative images of OCT4 (A-C), TRA-1-60 (G-1) and SSEA-1 (J-L) protein expression in Shef3 hESCs cultured at 5% oxygen on MEF feeder layers. An anti-mouse-IgG FITC-conjugated secondary antibody was used to detect OCT4 expression and its negative control (D-F), whereas an anti-rabbit-IgM FITC-conjugated secondary antibody was used to detect TRA-1-60 and SSEA-1 expression and their negative control (M-O). DAPI staining was performed to label the nuclei. DAPI (blue; A, D, G, J, M) and FITC (green; B, E, H, K, N) images were taken. Scale bar indicates 50μm.

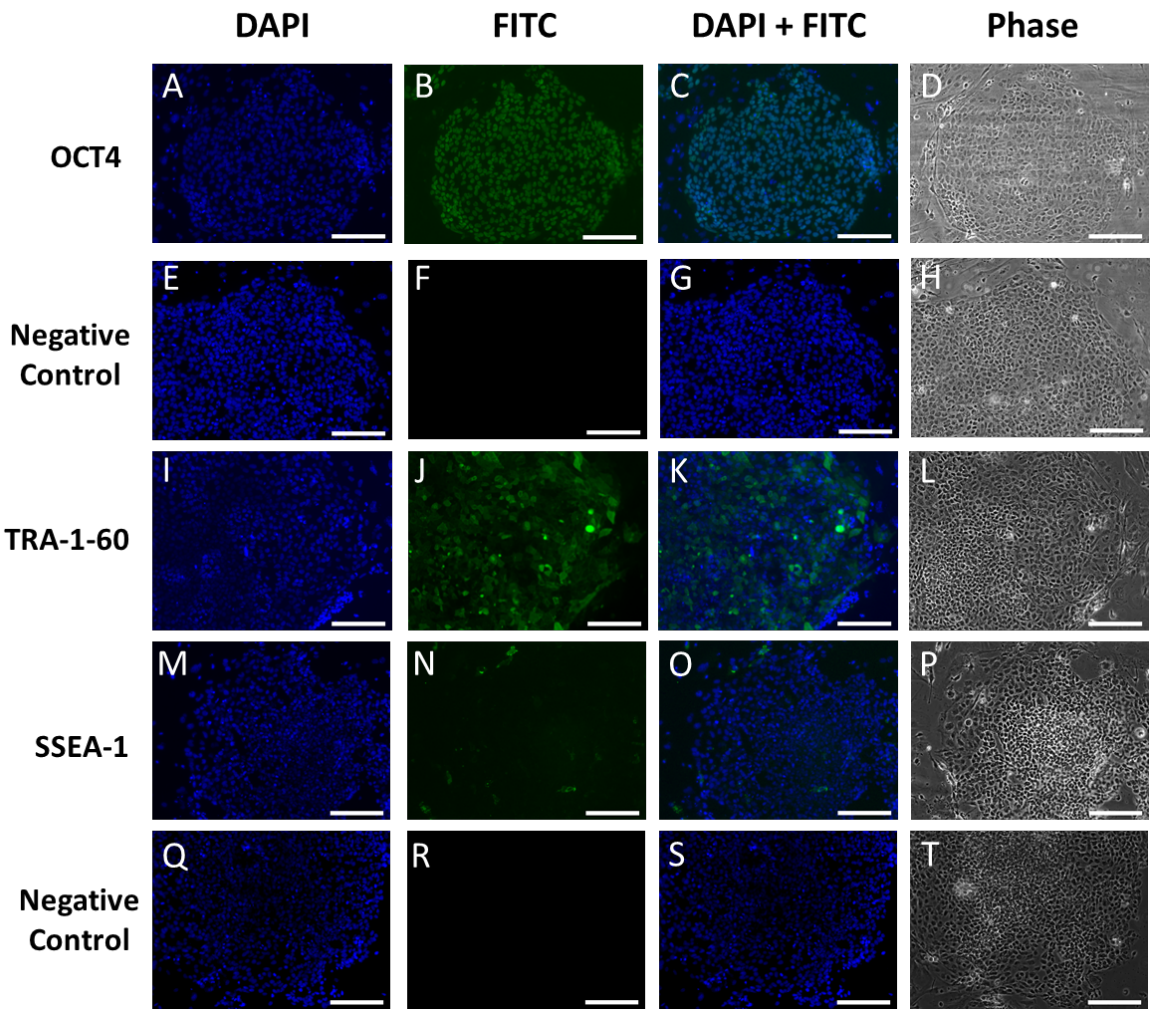

Figure 3.11. Characterisation of Shef3 hESCs maintained at 20% oxygen.
Representative images of OCT4 (A-D), TRA-1-60 (I-L) and SSEA-1 (M-P) protein expression in Shef3 hESCs cultured at 20% oxygen on MEF feeder layers. An anti-mouse-IgG FITC-conjugated secondary antibody was used to detect OCT4 expression and its negative control (E-H), whereas an anti-rabbit-IgM FITC-conjugated secondary antibody was used to detect TRA-1-60 and SSEA-1 expression and their negative control (Q-T). DAPI staining was performed to label the nuclei. DAPI (blue; A, E, I, M, Q), FITC (green; B, F, J, N, R) and phase contrast images (D, H, L, P, T) were taken. Scale bar indicates 200μm.

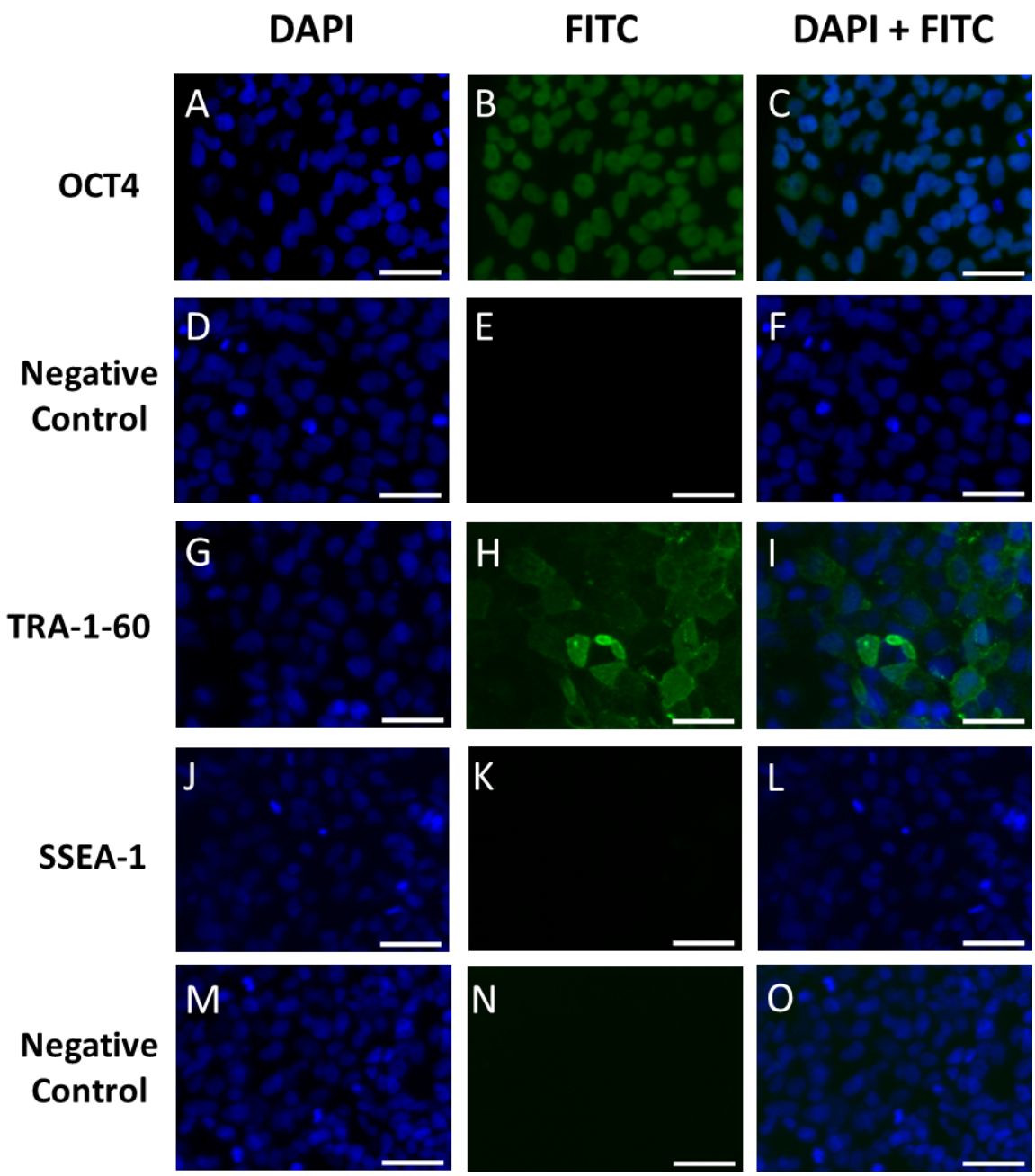

Figure 3.12. Subcellular localisation of pluripotency markers in Shef3 hESCs cultured at 20% oxygen.

Representative images of OCT4 (A-C), TRA-1-60 (G-1) and SSEA-1 (J-L) protein expression in Shef3 hESCs cultured at 20% oxygen on MEF feeder layers. An anti-mouse-IgG FITC-conjugated secondary antibody was used to detect OCT4 expression and its negative control (D-F), whereas an anti-rabbit-IgM FITC-conjugated secondary antibody was used to detect TRA-1-60 and SSEA-1 expression and their negative control (M-O). DAPI staining was performed to label the nuclei. DAPI (blue; A, D, G, J, M) and FITC (green; B, E, H, K, N) images were taken. Scale bar indicates 50μm.

3.2.2 Effect of environmental oxygen tension on pluripotency marker expression in hESCs

Previous studies have demonstrated an increase in the expression of pluripotency markers in Hues-7 hESCs cultured at 5% oxygen compared to cells cultured at 20% oxygen (Forristal et al., 2010). This difference was unclear from the immunocytochemistry results, therefore to quantify any changes in pluripotency marker expression between normoxic and hypoxic culture of hESCs more accurately, RT-qPCR analysis was performed to analyse *OCT4, SOX2, NANOG, LIN28B* and *SALL4* mRNA expression.

Quantification of pluripotency marker mRNA expression levels in Hues-7 hESCs maintained at 5% oxygen revealed a significant increase in *OCT4, SOX2, NANOG, LIN28B* and *SALL4* expression compared to hESCs maintained at 20% oxygen (Figure 3.13). Hues-7 hESCs maintained at 5% oxygen displayed a significant and approximate 130% increase in *OCT4* ($p=0.0174$), a 200% increase in *SOX2* ($p=0.0286$) and a 90% increase in *NANOG* ($p=0.0473$) mRNA expression. Additionally, LIN28B mRNA expression increased by approximately 180% ($p=0.0481$) and SALL4 expression increased by approximately 200% ($p=0.0397$) in hESCs maintained under hypoxia compared to hESCs cultured under a 20% oxygen tension.

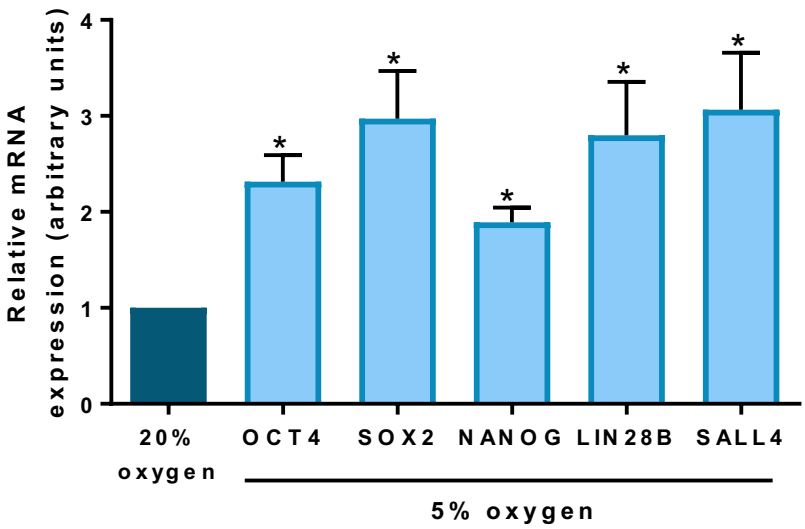

Figure 3.13. Hypoxia increases the mRNA expression of pluripotency markers in Hues-7 hESCs.
Quantification of *OCT4, SOX2, NANOG, LIN28B* and *SALL4* mRNA levels in Hues-7 hESCs maintained at either 5% oxygen or 20% oxygen. Data were normalised to *UBC*, and then to 1 for 20% oxygen. Bars represent mean ± SEM. (n=4).

Western blotting was used to quantify the expression of OCT4, SOX2 and NANOG protein levels in hESCs cultured at either 5% or 20% oxygen. Protein bands of approximately 43kDa, 34kDa and 40kDa were observed for OCT4, SOX2 and NANOG, respectively, in Hues-7 hESCs cultured at both oxygen tensions, but the bands appeared less intense at 20% oxygen (Figure 3.14A).

Quantification of the bands revealed a significant increase in the protein expression of the three core pluripotency markers in Hues-7 hESCs cultured at 5% oxygen compared to those maintained at 20% oxygen. Hues-7 hESCs cultured at 5% oxygen displayed an approximate 130% increase in OCT4 ($p=0.0294$), a 140% increase in SOX2 ($p=0.0277$) and a 90% increase in NANOG ($p=0.0424$) protein expression compared to cells cultured at 20% oxygen (Figure 3.14B).

Quantification of OCT4 protein expression in Shef3 hESCs cultured at either 5% or 20% oxygen revealed the same trend as Hues-7 hESCs. OCT4 expression significantly increased by approximately 64% ($p=0.0423$) in hESCs cultured under 5% oxygen compared to those maintained under normoxic conditions (Figure 3.15).

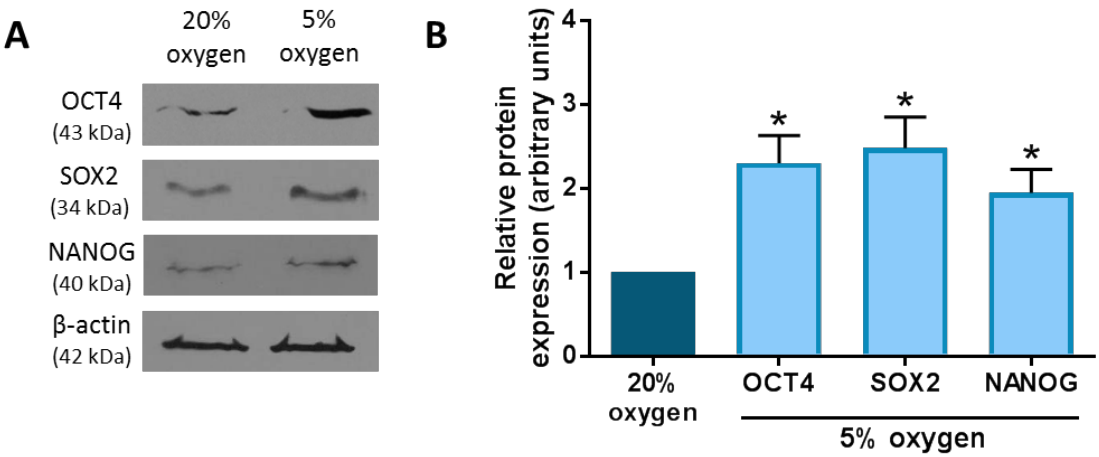

Figure 3.14. Hypoxia increases the protein expression of the three core pluripotency factors in Hues-7 hESCs.
(A) Representative Western blots of OCT4, SOX2 and NANOG expression in Hues-7 hESCs cultured at either 5% or 20% oxygen. (B) Quantification of the protein expression levels of OCT4, SOX2 and NANOG Western blots in Hues-7 hESCs cultured at 5% oxygen compared to 20% oxygen tension. Data were normalised to β-actin, and then to 1 for 20% oxygen tension. Bars represent mean ± SEM (n=4).

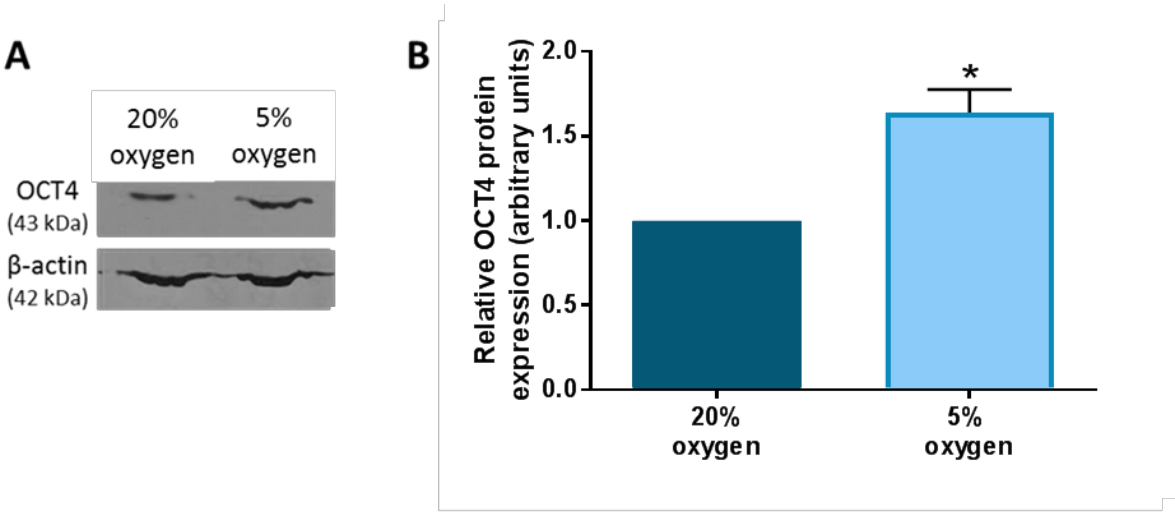

Figure 3.15. Hypoxia increases the protein expression of OCT4 in Shef3 hESCs.
(A) Representative Western blots of OCT4 expression in Shef3 hESCs cultured at either 5% or 20% oxygen. (B) Quantification of OCT4 Western in Shef3 hESCs cultured at 5% oxygen compared to 20% oxygen tension. Data were normalised to β-actin, and then to 1 for 20% oxygen tension. Bars represent mean ± SEM (n=3).

3.2.3 hESCs cultured at 5% and 20% oxygen tensions express both CtBP isoforms

CtBPs are widely expressed throughout development and different tissues and have displayed nuclear and cytoplasmic functions. However, CtBP expression and localisation has not previously been demonstrated in hESCs. Using the characterised Hues-7 and Shef3 hESCs, the expression and subcellular localisation of CtBP1 and CtBP2 was determined in hESCs cultured at either 5% or 20% oxygen using immunocytochemistry.

Hues-7 and Shef3 hESCs clearly expressed both CtBP isoforms at 5% and 20% oxygen tensions throughout colonies (Figure 3.16 – 3.23). However, CtBP1 protein levels appear to be lower at 5% oxygen (Figure 3.16B and Figure 3.17B) compared to 20% oxygen (Figure 3.18B and Figure 3.19B), but no clear difference in CtBP2 expression was observed between hESCs maintained at different oxygen tensions (Figure 3.16F; Figure 3.17E; Figure 3.18F; and Figure 3.19E). Furthermore, no obvious difference in CtBP expression were observed between cells cultured at either 5% or 20% oxygen in Shef3 hESCs (Figure 3.20 – 3.23). Higher magnification of Hues-7 and Shef3 hESCs at both 5% and 20% oxygen revealed that both CtBP1 and CtBP2 expression was largely confined to the nucleus (Figure 3.17B and E; Figure 3.19B and E; Figure 3.21B and E; and Figure 3.23B and E).

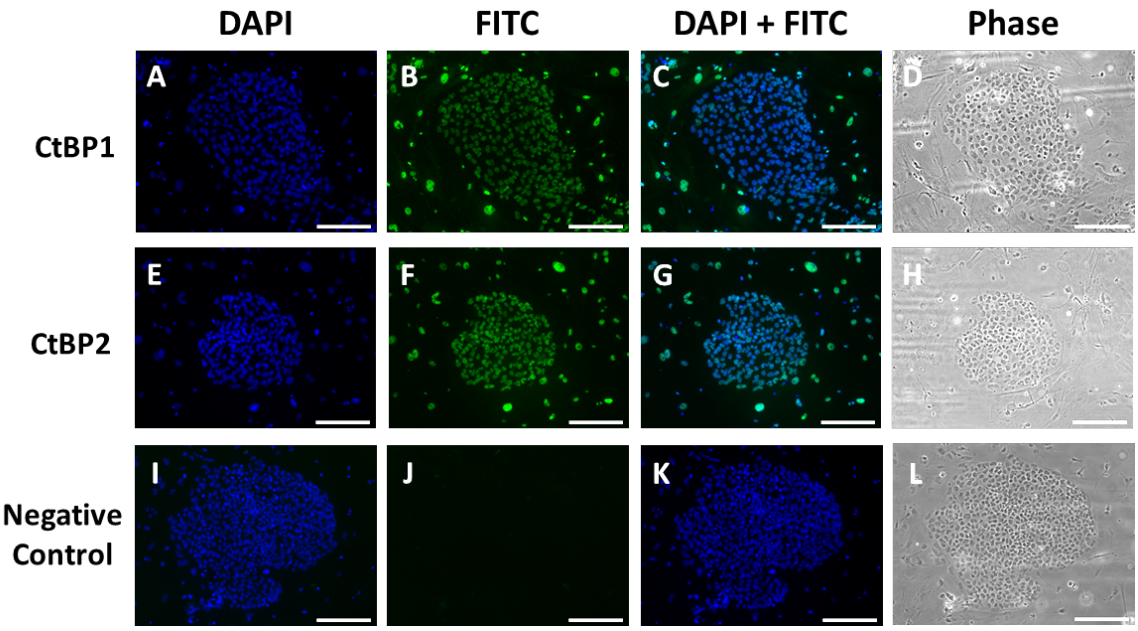

Figure 3.16. Characterisation of CtBP expression in Hues-7 hESCs cultured at 5% oxygen. Representative images of CtBP1 (A-D) and CtBP2 (E-H) protein expression in Hues-7 hESCs cultured at 5% oxygen on MEF feeder layers. An anti-mouse-IgG FITC-conjugated secondary antibody was used to detect both CtBP1 and CtBP2 expression and its negative control (I-L). DAPI staining was performed to label the nuclei. DAPI (blue; A, E, I), FITC (green; B, F, J) and phase contrast images (D, H, L) were taken for both isoforms and the control. Scale bar indicates 200μm.

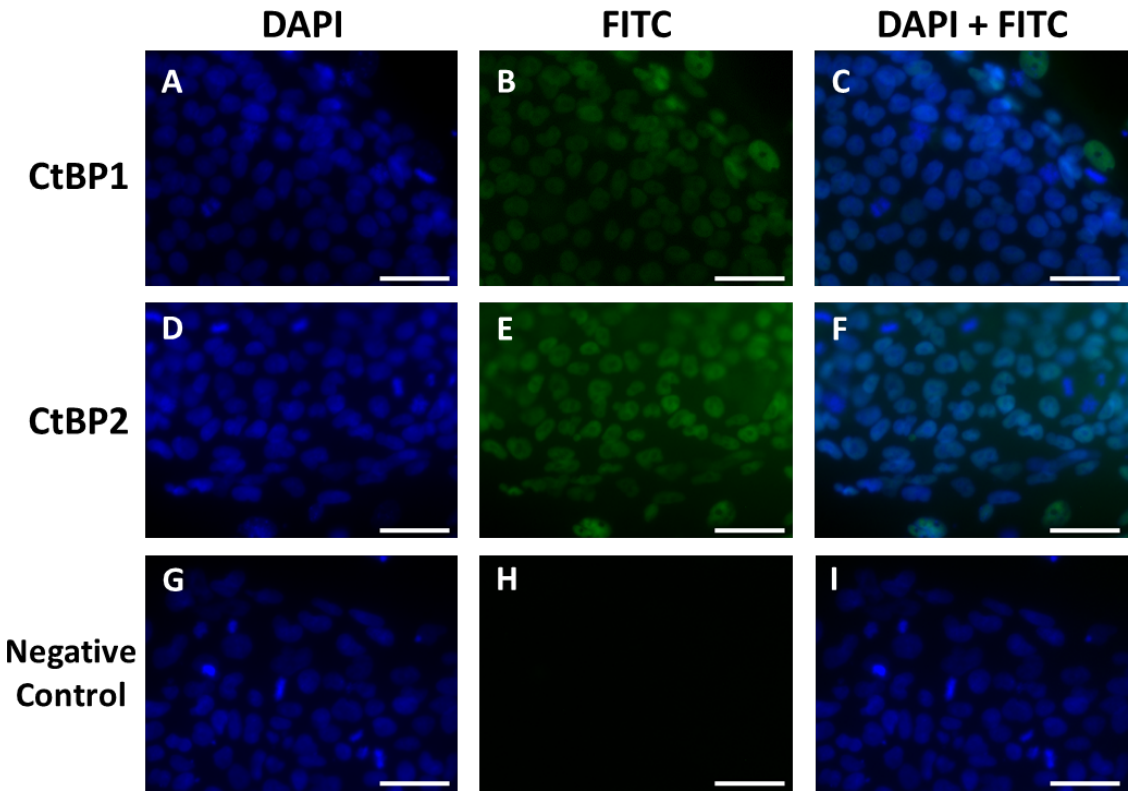

Figure 3.17. Subcellular localisation of CtBP proteins in Hues-7 hESCs maintained at 5% oxygen.
Representative images of CtBP1 (A-C) and CtBP2 (D-F) protein expression in Hues-7 hESCs cultured at 5% oxygen on MEF feeder layers. An anti-mouse-IgM FITC-conjugated secondary antibody was used to detect both CtBP1 and CtBP2 expression and the negative control (G-I). DAPI staining was performed to label the nuclei. DAPI (blue; A, D, G) and FITC (green; B, E, H) images were taken for both proteins and the control. Scale bar indicates 50μm.

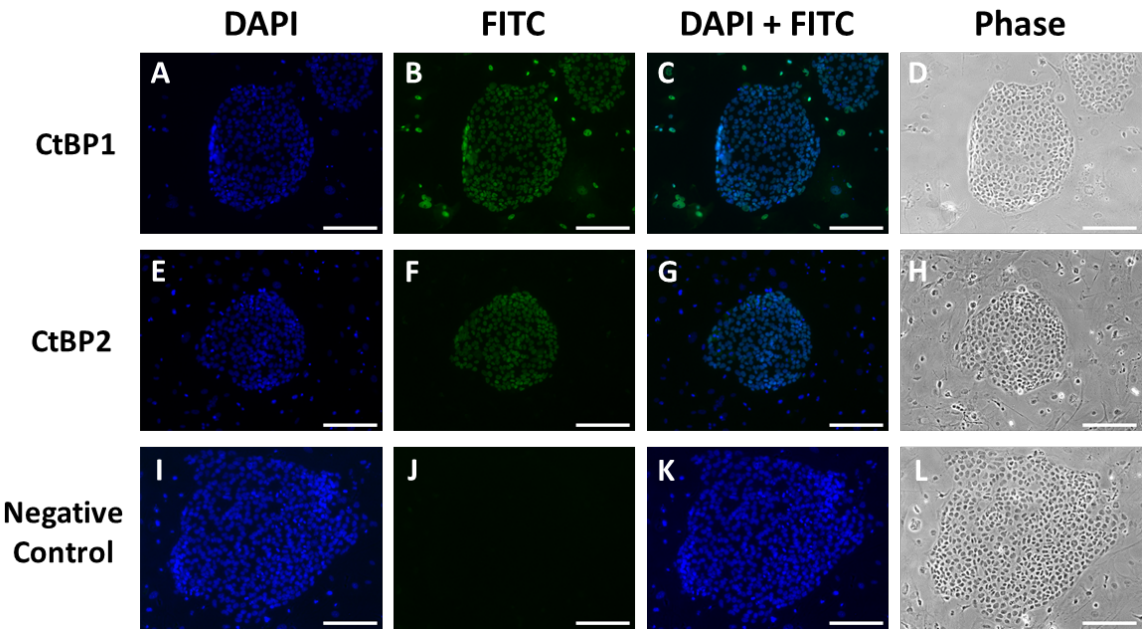

Figure 3.18. Characterisation of CtBP expression in Hues-7 hESCs cultured at 20% oxygen. Representative images of CtBP1 (A-D) and CtBP2 (E-H) protein expression in Hues-7 hESCs cultured at 20% oxygen on MEF feeder layers. An anti-mouse-IgG FITC-conjugated secondary antibody was used to detect both CtBP1 and CtBP2 expression and its negative control (I-L). DAPI staining was performed to label the nuclei. DAPI (blue; A, E, I), FITC (green; B, F, J) and phase contrast images (D, H, L) were taken for both isoforms and the control. Scale bar indicates 200μm.

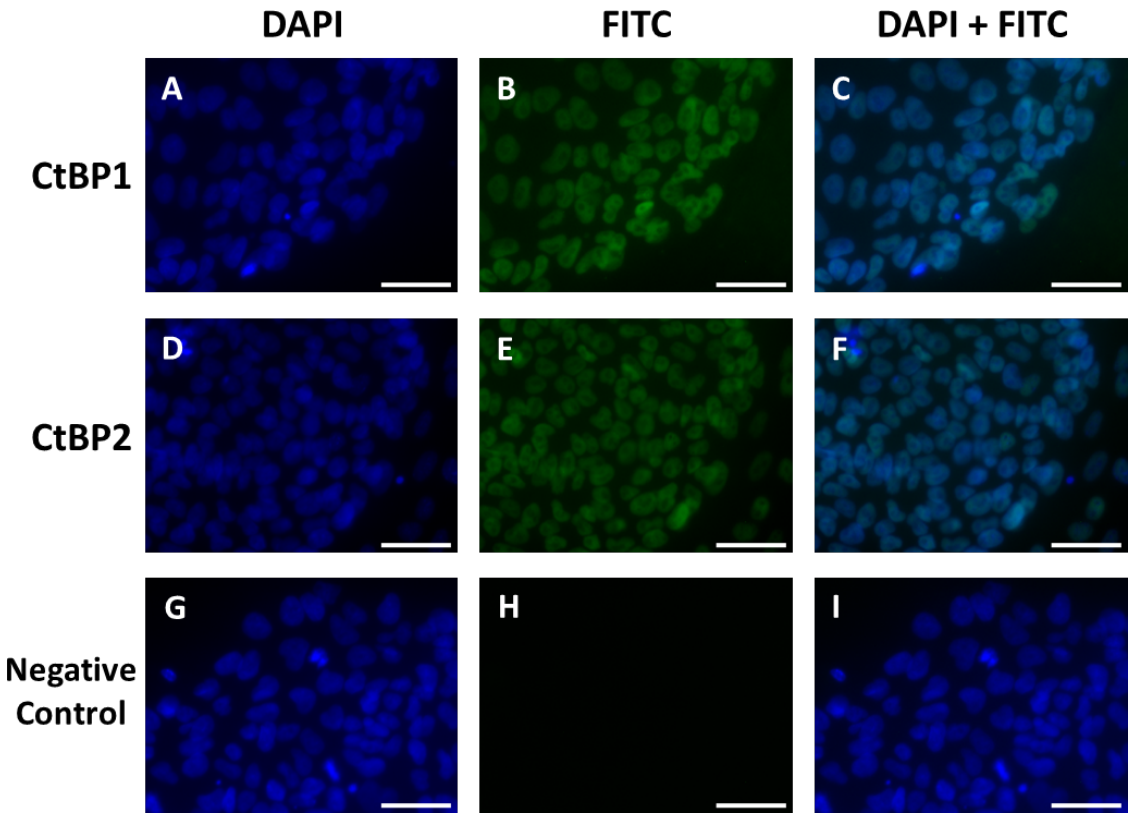

Figure 3.19. Subcellular localisation of CtBP proteins in Hues-7 hESCs maintained at 20% oxygen.

Representative images of CtBP1 (A-C) and CtBP2 (D-F) protein expression in Hues-7 hESCs cultured at 20% oxygen on MEF feeder layers. An anti-mouse-IgM FITC-conjugated secondary antibody was used to detect both CtBP1 and CtBP2 expression and the negative control (G-I). DAPI staining was performed to label the nuclei. DAPI (blue; A, D, G) and FITC (green; B, E, H) images were taken for both proteins and the control. Scale bar indicates 50μm.

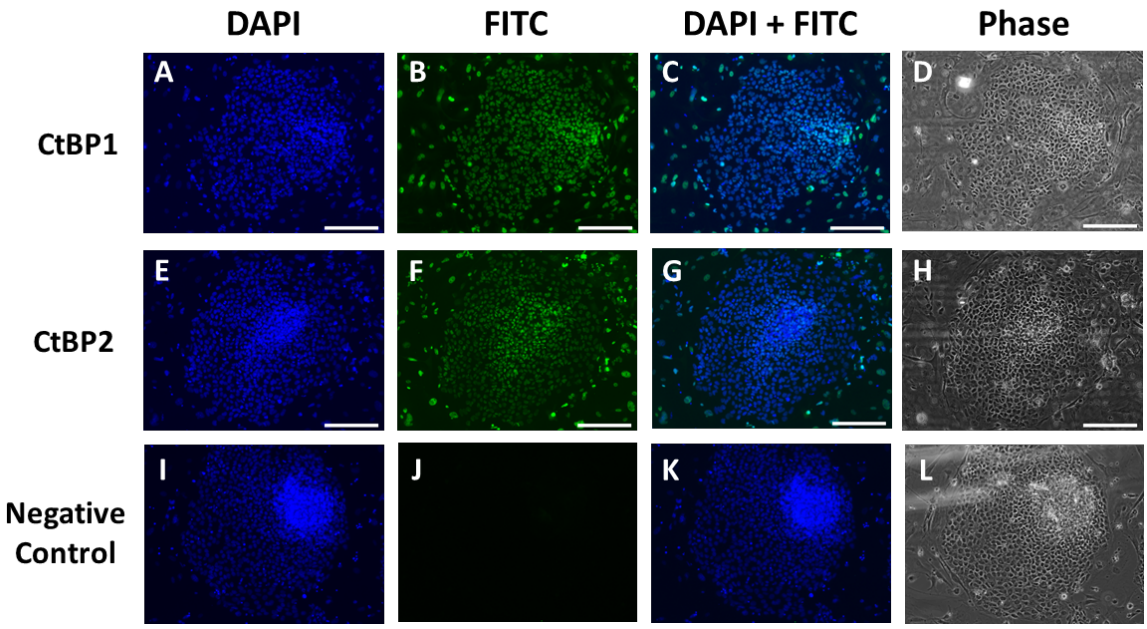

Figure 3.20. Characterisation of CtBP expression in Shef3 hESCs cultured at 5% oxygen. Representative images of CtBP1 (A-D) and CtBP2 (E-H) protein expression in Shef3 hESCs cultured at 5% oxygen on MEF feeder layers. An anti-mouse-IgG FITC-conjugated secondary antibody was used to detect both CtBP1 and CtBP2 expression and its negative control (I-L). DAPI staining was performed to label the nuclei. DAPI (blue; A, E, I), FITC (green; B, F, J) and phase contrast images (D, H, L) were taken for both isoforms and the control. Scale bar indicates 200μm.

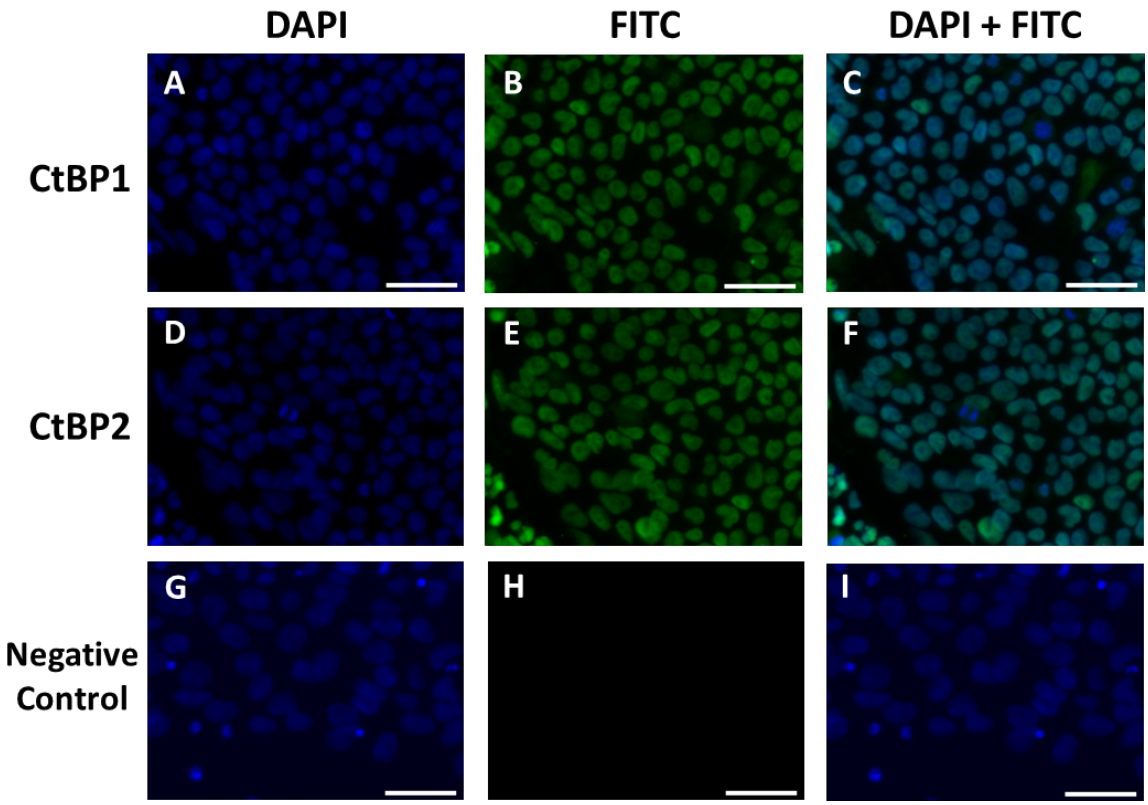

Figure 3.21. Subcellular localisation of CtBP proteins in Shef3 hESCs maintained at 5% oxygen.

Representative images of CtBP1 (A-C) and CtBP2 (D-F) protein expression in Shef3 hESCs cultured at 5% oxygen on MEF feeder layers. An anti-mouse-IgM FITC-conjugated secondary antibody was used to detect both CtBP1 and CtBP2 expression and the negative control (G-I). DAPI staining was performed to label the nuclei. DAPI (blue; A, D, G) and FITC (green; B, E, H) images were taken for both proteins and the control. Scale bar indicates 50μm.

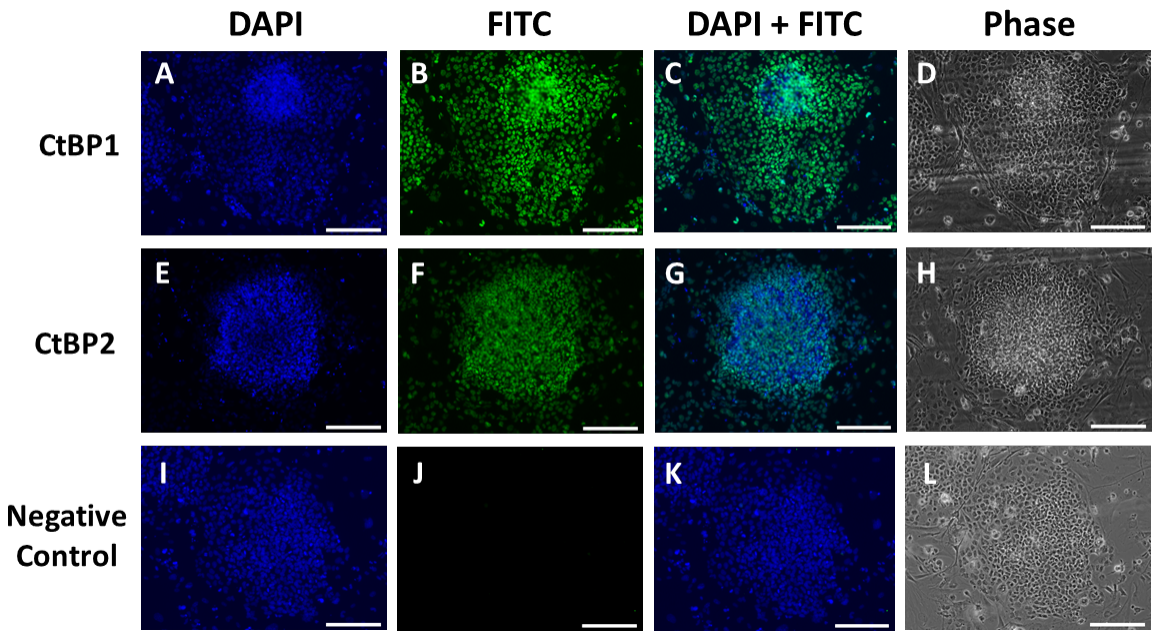

Figure 3.22. Characterisation of CtBP expression in Shef3 hESCs cultured at 20% oxygen. Representative images of CtBP1 (A-D) and CtBP2 (E-H) protein expression in Shef3 hESCs cultured at 20% oxygen on MEF feeder layers. An anti-mouse-IgG FITC-conjugated secondary antibody was used to detect both CtBP1 and CtBP2 expression and its negative control (I-L). DAPI staining was performed to slabel the nuclei. DAPI (blue; A, E, I), FITC (green; B, F, J) and phase contrast images (D, H, L) were taken for both isoforms and the control. Scale bar indicates 200µm.

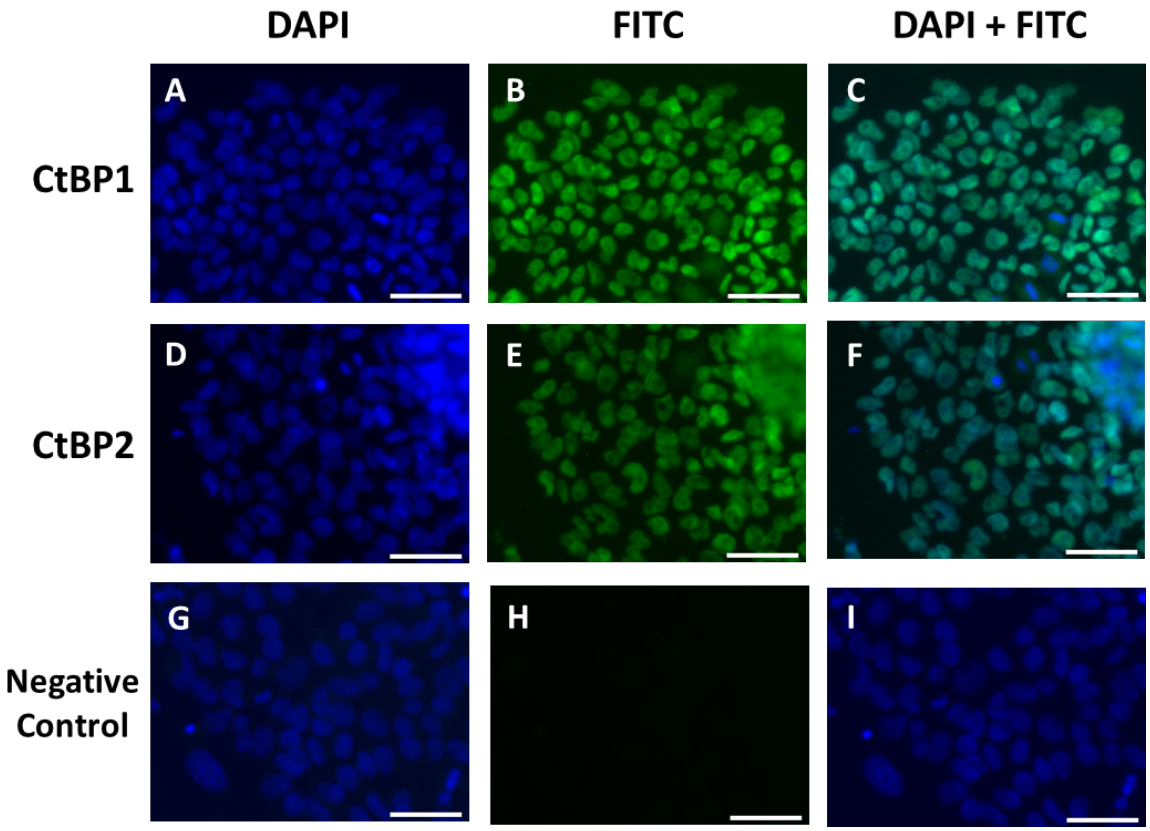

Figure 3.23. Subcellular localisation of CtBP proteins in Shef3 hESCs maintained at 20% oxygen.

Representative images of CtBP1 (A-C) and CtBP2 (D-F) protein expression in Shef3 hESCs cultured at 20% oxygen on MEF feeder layers. An anti-mouse-IgM FITC-conjugated secondary antibody was used to detect both CtBP1 and CtBP2 expression and the negative control (G-I). DAPI staining was performed to label the nuclei. DAPI (blue; A, D, G) and FITC (green; B, E, H) images were taken for both proteins and the control. Scale bar indicates 50μm.

3.2.4 Effects of environmental oxygen tension on CtBP expression in hESCs

To analyse any potential effect of hypoxia on the mRNA and protein expression levels of CtBP1 and CtBP2 in hESCs cultured at either 5% or 20% oxygen, RT-qPCR and Western blotting were performed.

Quantification of mRNA levels in Hues-7 hESCs maintained at either oxygen tension revealed a significant 122% increase in *CtBP1* expression (p=0.0481) and a significant 44% increase in *CtBP2* (p=0.0097) mRNA expression in those cells cultured at 5% compared to those maintained at 20% oxygen (Figure 3.24).

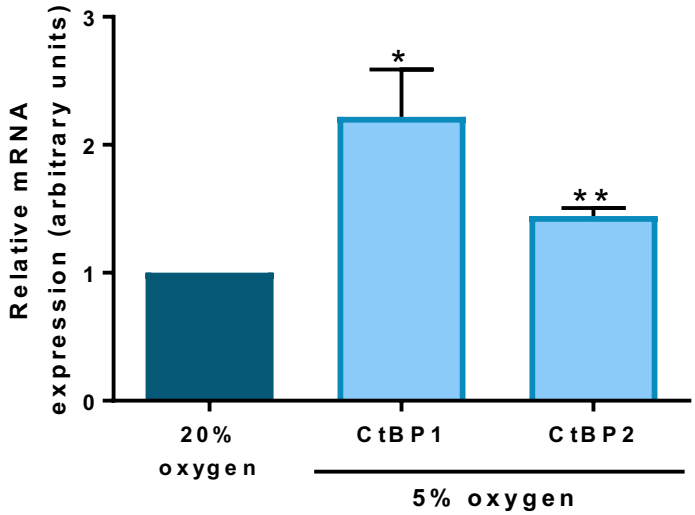

Figure 3.24. CtBP mRNA expression is increased under hypoxia in Hues-7 hESCs.
Quantification of *CtBP1* and *CtBP2* mRNA levels in Hues-7 hESCs maintained at either 5% oxygen or 20% oxygen. Data were normalised to *UBC*, and then to 1 for 20% oxygen. Bars represent mean ± SEM. (n=3 for CtBP1 and n=4 for CtBP2).

3.2.4.1 Validation of the quantification of CtBP2 Western blots

As protein levels are regulated at the transcriptional level, but also post-transcriptionally, it is important to follow up measurements of relative mRNA expression with analysis of protein expression levels. Prior to quantifying CtBP2 protein expression, validation of the quantification method was required as two distinct protein bands were obtained using Western blotting representing CtBP2-S and CtBP2-L. A clear demonstration that there would be no bias between quantifying both CtBP2-L and CtBP2-S bands together (Figure

3.25A, black box) compared to individually (Figure 3.25A, white & red boxes) was required, and so confirming that any effect seen was not affecting one isoform more than the other.

A significant and approximate 50% increase was observed for total CtBP2 expression between hESCs maintained at 5% compared to those at 20% oxygen (p=0.0035). A similar increase in CtBP2-L (p=0.0058) and CtBP2-S protein expression (p=0.004) was also observed between oxygen tensions. Furthermore, no significant difference was found between total CtBP2 expression compared to that of either CtBP2-L or CtBP2-S following normalisation to 5% oxygen (Figure 3.25). Together, quantification of CtBP2 protein expression revealed that both quantification methods resulted in a significant increase in CtBP2 expression and that neither CtBP2 splice variant was influenced more than the other. All subsequent quantification of CtBP2 protein expression shows the expression of both isoforms quantified together.

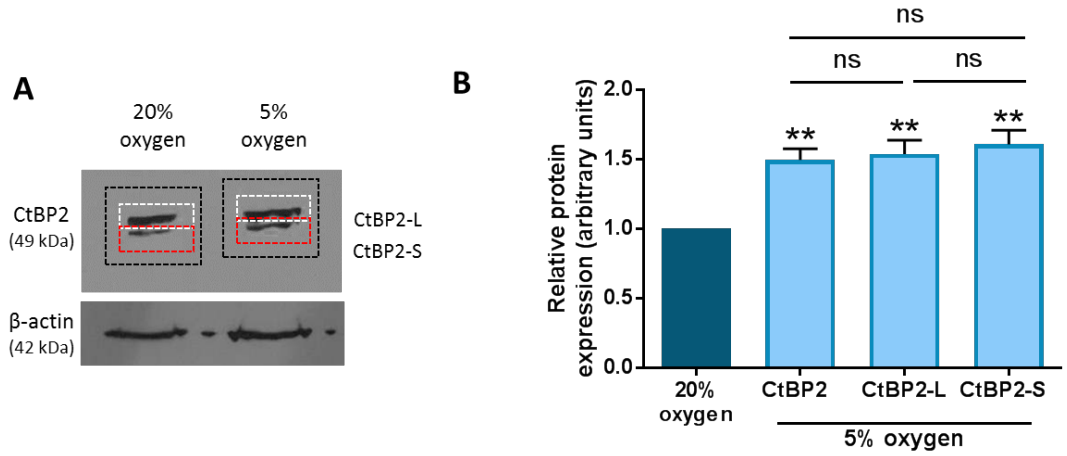

Figure 3.25. Validation of quantification of CtBP2 Western blots.
(A) Representative Western blot of CtBP2-L and CtBP2-S protein expression in Hues-7 hESCs maintained at either 5% or 20% oxygen. Black box indicates a representative area measured for densitometry analysis for total CtBP2 expression, white boxes indicate a representative area measured for densitometry analysis for CtBP2-S expression and red boxes indicate a representative area measured for densitometry analysis for CtBP2-L expression. (B) Quantification of CtBP2, CtBP2-L and CtBP2-S protein in Hues-7 hESCs maintained at 5% oxygen compared to 20% oxygen. Data were normalised to β-actin and then to 1 for 20% oxygen tension. Bars represent mean ± SEM. (n=5)

3.2.4.2 Quantification of CtBP protein expression by Western blotting

CtBP1 and CtBP2 protein expression in Hues-7 and Shef3 hESCs cultured at either 5% or 20% oxygen was quantified using Western blotting.

One protein band of approximately 48kDa and two protein bands of approximately 49kDa were observed for CtBP1 and CtBP2, respectively, at both oxygen tensions where the bands appeared to be less prevalent at 20% oxygen (Figure 3.26A). Interestingly, the protein expression of both CtBP isoforms was significantly increased in Hues-7 hESCs cultured at 5% oxygen compared to those maintained at 20% oxygen (Figure 3.26B). CtBP1 expression had increased by approximately 40% (p=0.005), whereas CtBP2 protein expression appeared to have increased by about 45% (p=0.0061) in Hues-7 hESCs maintained at 5% oxygen compared to those cultured under 20% oxygen tensions.

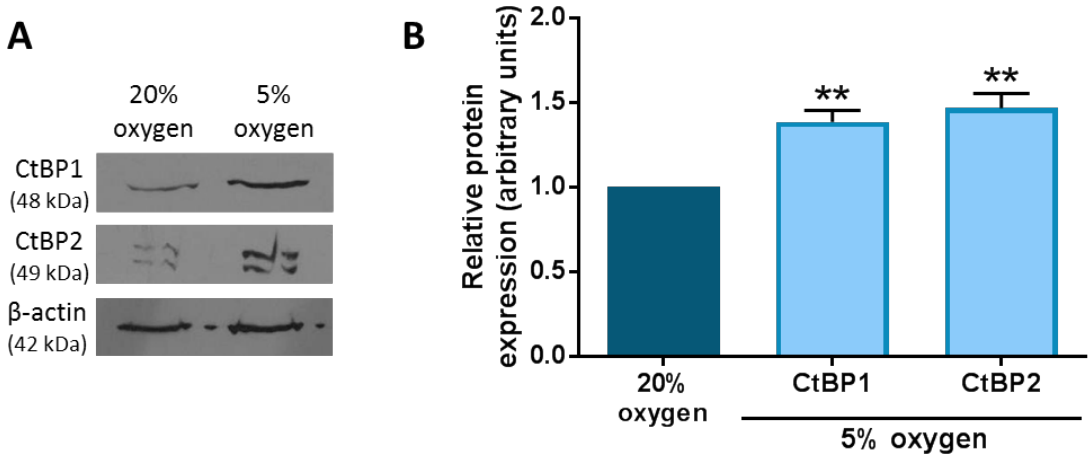

Figure 3.26. CtBP protein expression is increased under hypoxia in Hues-7 hESCs.
(A) Representative Western blots of CtBP1 and CtBP2 expression in Hues-7 hESCs cultured at either 5% or 20% oxygen. (B) Quantification of CtBP1 and CtBP2 Western blots revealed a significant decrease in the protein expression of both CtBP isoforms in Hues-7 hESCs cultured at 20% oxygen compared to those maintained at 5% oxygen. Data were normalised to β-actin, and then to 1 for 20% oxygen tension. Bars represent mean ± SEM (n=5).

Similarly, one band of approximately 48kDa and two bands of approximately 49kDa were observed for CtBP1 and CtBP2 expression in Shef3 hESCs cultured at either 5% or 20% oxygen. Quantification of the CtBP Western blots again revealed a significant increase in both CtBP isoforms in hESCs cultured at 5% oxygen compared to those maintained under normoxic conditions (Figure 3.27). An approximate 30% increase in expression was observed for both CtBP1 ($p=0.0068$) and CtBP2 ($p=0.0059$) in Shef3 hESCs cultured under hypoxic oxygen conditions compared to 20% oxygen.

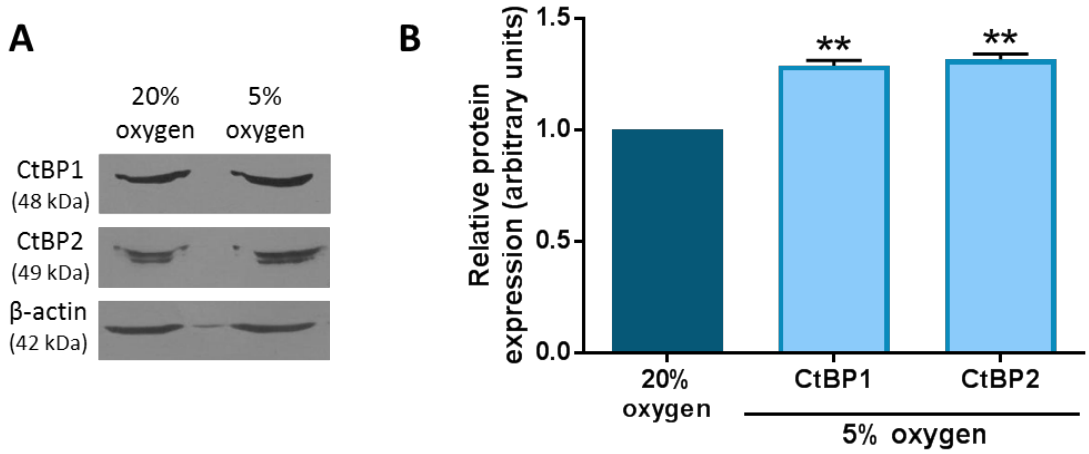

Figure 3.27. CtBP protein expression is increased under hypoxia in Shef3 hESCs.
(A) Representative Western blots of CtBP1 and CtBP2 expression in Shef3 hESCs cultured at either 5% or 20% oxygen. (B) Quantification of CtBP1 and CtBP2 Western blots in Shef3 hESCs cultured at 5% oxygen compared to those maintained at 20% oxygen. Data were normalised to β-actin, and then to 1 for 20% oxygen tension. Bars represent mean ± SEM (n=3)

3.2.5 Effect of silencing HIF-2α in Hues-7 hESCs under hypoxia on pluripotency, CtBP expression and glycolytic flux

To investigate whether HIF-2α might be responsible for the increased expression of CtBPs in hESCs cultured under low oxygen tensions, siRNA transfections were performed. Hues-7 hESCs cultured at 5% oxygen were transfected on day 1 post-passage with 50nM HIF-2α siRNA, and the cells collected on day 3 post-passage for analysis by RT-qPCR or Western blotting.

Phase contrast images demonstrate that there was no morphological difference between cells transfected with either the Allstars negative control siRNA or HIF-2α siRNA as both formed compact colonies of typical cobblestone morphology (Figure 3.28).

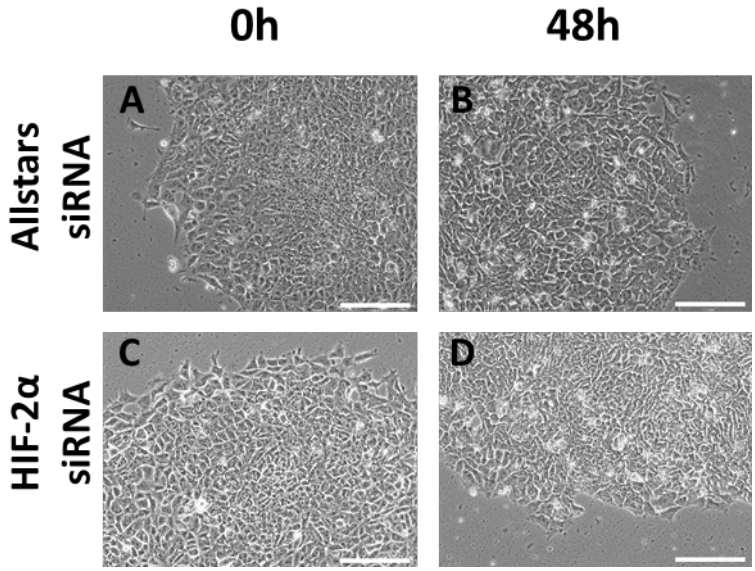

Figure 3.28. Phase contrast images demonstrating colony morphology of Hues-7 hESCs cultured at 5% oxygen transfected with HIF-2α siRNA.
Representative phase contrast images of Hues-7 hESCs cultured at 5% oxygen transfected with either Allstars negative control siRNA (A-B) or HIF-2α siRNA (C-D) after 0 (A, C) and 48 hours (B, D). Scale bar indicates 200μm.

RT-qPCR revealed that *HIF-2α* was successfully silenced in Hues-7 hESCs after transfection with HIF-2α siRNA (Figure 3.29A; p=0.0185) compared to those transfected with the Allstars negative control siRNA. After successfully silencing *HIF-2α* in Hues-7 hESCs maintained under hypoxic conditions, quantification of *OCT4. SOX2, NANOG, LIN28B* and *SALL4* mRNA expression levels significantly decreased by 54% (p=0.0165), 62% (p=0.0111), 49% (p=0.0358), 53% (p=0.001) and 65% (p=0.0107) respectively compared to the control cells (Figure 3.29B). Intriguingly, *CtBP1* and *CtBP2* mRNA expression was significantly decreased in Hues-7 hESCs transfected with HIF-2α siRNA compared to those transfected with Allstars negative control siRNA (Figure 3.29C). An approximate 35% and 40% reduction in *CtBP1* (p=0.0174) and *CtBP2* mRNA (p=0.0297) expression respectively in Hues-7 hESCs transfected with HIF-2α siRNA compared to the control.

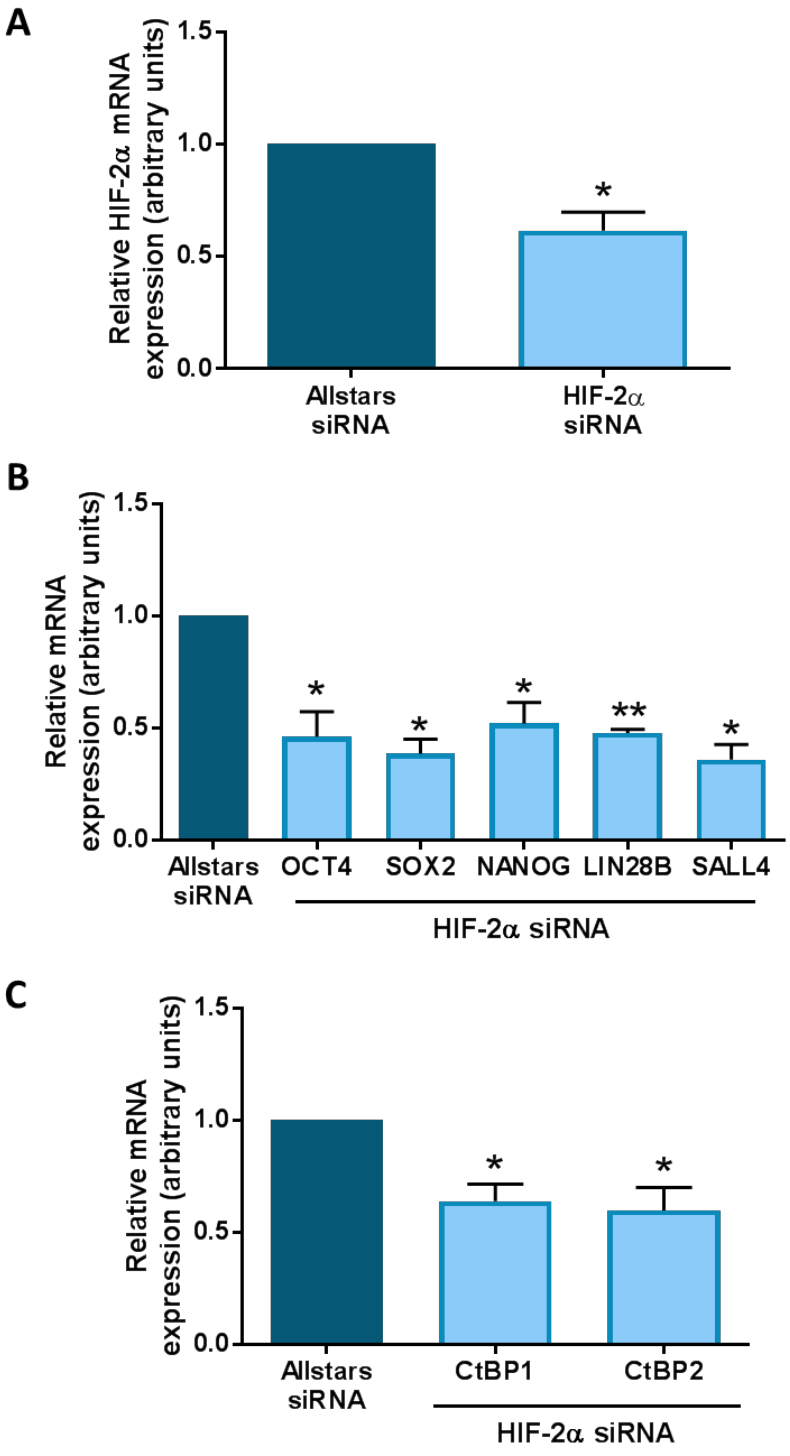

Figure 3.29. HIF-2α regulates pluripotency marker and CtBP expression in hESCs.
(A) Quantification of *HIF-2α* mRNA in Hues-7 hESCs transfected with HIF-2α siRNA revealed a significant decrease in *HIF-2α* expression compared to the control. (B) Quantification of *OCT4, SOX2, NANOG, LIN28B* and *SALL4* mRNA revealed a significant decrease in the mRNA expression of all the pluripotency markers in Hues-7 hESCs transfected with HIF-2α siRNA compared to the Allstars control. (C) Quantification of *CtBP1* and *CtBP2* mRNA expression levels in Hues-7 hESCs transfected with HIF-2α siRNA revealed a significant decrease in the expression of both CtBP isoforms compared to the control. Data were normalised to *UBC*, and then to 1 for Allstars negative control. Bars represent mean ± SEM. (n=4)

To determine whether there was any impact of silencing HIF-2α on the glycolytic phenotype of Hues-7 hESCs cultured under hypoxia, lactate production was measured using the spent conditioned media samples from cells transfected with either Allstars negative control siRNA or HIF-2α siRNA for 48 hours from day 2 to day 3 post-transfection (Figure 3.30).

Transfection with HIF-2α siRNA resulted in a significant and approximate 43% decrease ($p=0.0013$) in the rate of lactate production in Hues-7 hESCs maintained under hypoxic conditions.

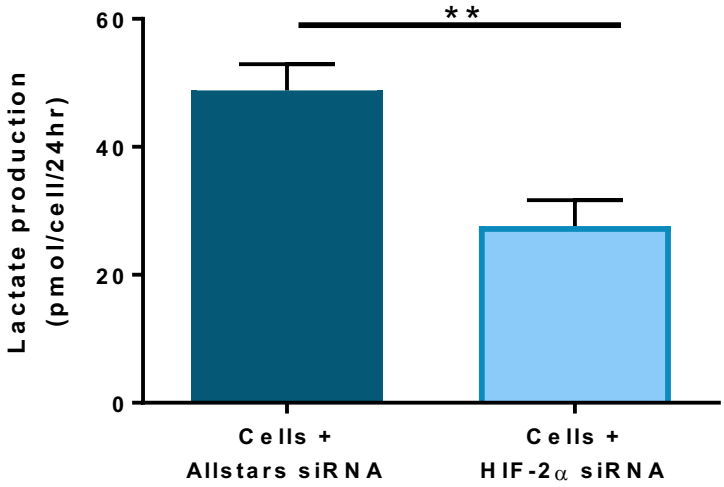

Figure 3.30. Silencing HIF-2α expression reduces the rate of flux through glycolysis in hESCs under hypoxia.
Enzyme-linked assays were performed to measure lactate production in Hues-7 hESCs cultured under 5% oxygen and transfected with either Allstars siRNA or HIF-2α siRNA for 48 hours prior to collecting conditioned media samples. Bars represent mean ± SEM. (n=12)

In an attempt to decipher why the rate in lactate production is significantly decreased in Hues-7 hESCs when HIF-2α is silenced, the expression of a panel of genes associated with glycolysis was investigated in cells transfected with either Allstars negative control or HIF-2α siRNA.

No significant decrease was observed in *LDHA* mRNA expression in Hues-7 hESCs transfected with either Allstars of HIF-2α siRNA. However, the expression of *GLUT1* and *GLUT3* was significantly reduced when HIF-2α was silenced (Figure 3.31). A

decrease of 70% and 69% was observed for *GLUT1* (p=0.0219) and *GLUT3* (p=0.0157) mRNA expression respectively when HIF-2α was silenced compared to the control cells.

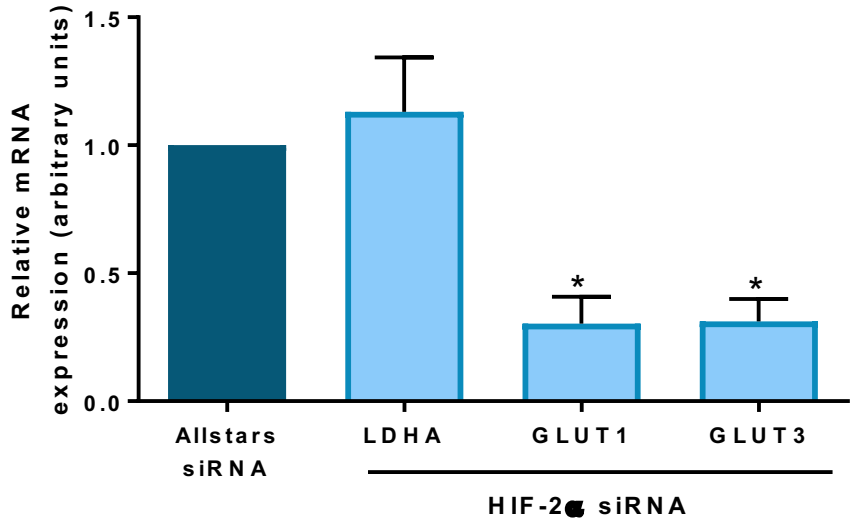

Figure 3.31. HIF-2α regulates expression of glucose transporters, but not glycolytic enzyme LDHA in hESCs under hypoxia.
Quantification of *LDHA, GLUT1* and *GLUT3* mRNA levels in Hues-7 hESCs maintained at 5% oxygen and transfected with either Allstars negative control or HIF-2α siRNA for 48 hours. Data were normalised to *β-actin* for primers and *UBC* for probes, and then to 1 for Allstars siRNA. Bars represent mean ± SEM. (n=3)

Western blotting revealed single protein band of approximately 118kDa was observed for HIF-2α protein expression in hESCs transfected with either the Allstars negative control siRNA or the HIF-2α siRNA, but the bands appeared less strong after transfection with HIF-2α siRNA (Figure 3.32A). Quantification of these bands revealed that HIF-2α protein expression was successfully silenced in Hues-7 hESCs after transfection with HIF-2α siRNA, displaying an approximate 60% decrease in HIF-2α expression (p=0.0381) compared to cells transfected with the Allstars negative control siRNA (Figure 3.32B).

After successfully silencing HIF-2α in Hues-7 hESCs cultured at 5% oxygen, Western blots were performed to evaluate the effect on CtBP protein expression. Quantification of CtBP protein expression revealed a significant and approximate 40% decrease in the expression of both CtBP1 (p=0.0145) and CtBP2 (p=0.0418) isoforms in cells transfected with HIF-2α siRNA (Figure 3.32C).

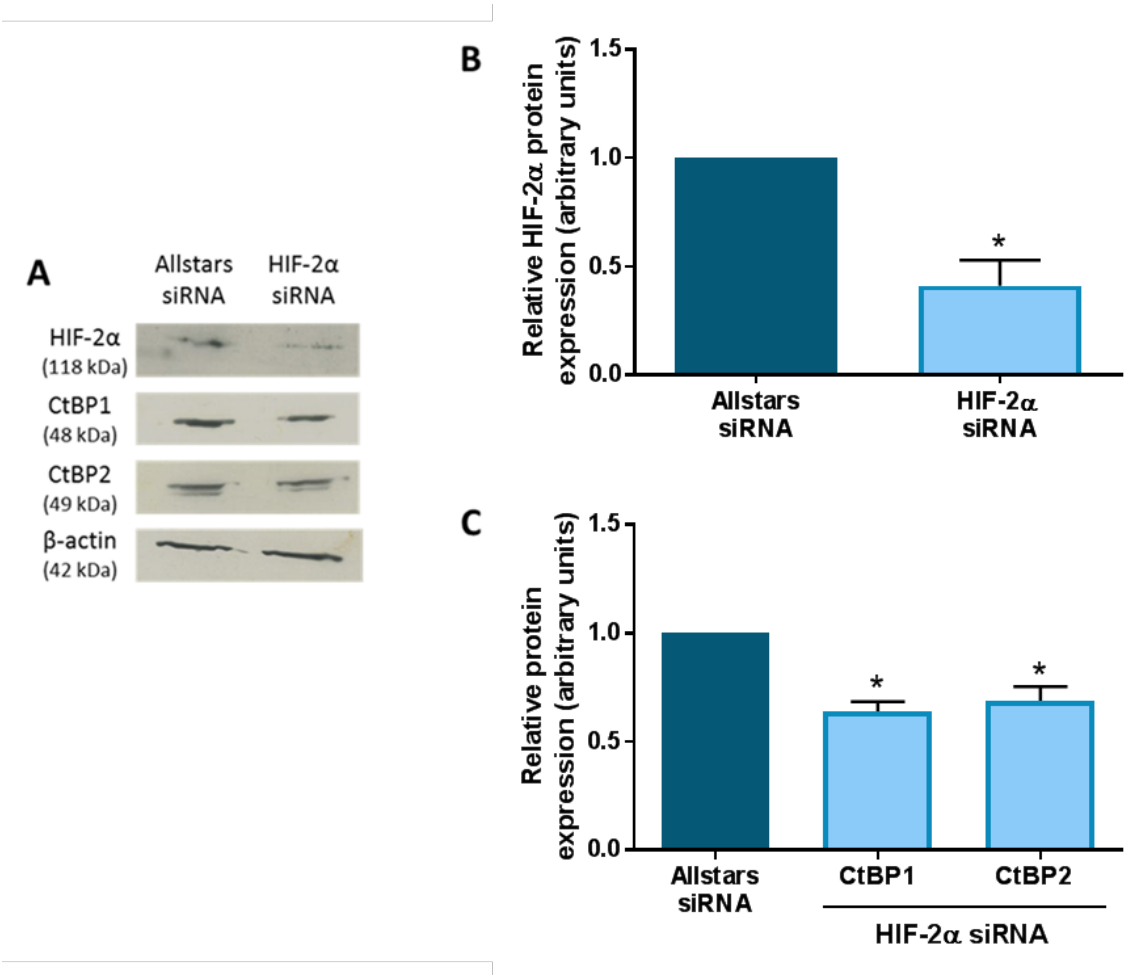

Figure 3.32. CtBP protein expression is regulated by HIF-2α.
(A) Representative Western blots of HIF-2α, CtBP1 and CtBP2 protein expression in Hues-7 hESCs maintained at 5% oxygen and transfected with either Allstars negative control siRNA or HIF-2α siRNA. (B) Quantification of HIF-2α Western blots revealed successful silencing of HIF-2α protein expression after transfection with HIF-2α siRNA. (C) Quantification of CtBP1 and CtBP2 blots revealed a significant decrease in the protein expression of both CtBP isoforms in Hues-7 hESCs maintained at 5% oxygen and transfected with HIF-2α siRNA. Data were normalised to β-actin, and then to 1 for Allstars control. Bars represent mean ± SEM. (n=3)

A BLAST search within the proximal promoters of both the *CtBP1* and *CtBP2* genes reinforced the potential role of HIF-2α in the regulation of CtBP expression by revealing several potential HRE binding sites in the proximal promoter regions of both genes (Figure 3.33-3.34). Primers were designed to specifically cover a potential HRE in the promoters of the genes of interest using the Applied Biosystems Design Software.

GGCTCTGAGTCCTGATTATCAATTGTCATCAAAACTGTTTCTGTCTCACAGAACCACAACAGGCAGGCAAACACAGAACCATCCTGTTG
TCTTCCTGTTCCTGTGGGCACACTCATTCACATCTCTCCTGATGGCGTAGCCCTTTGAGTGCCCTTGTTCCAGTTCCTGATTCACGTGGA
TCCAGGGAGGCCTCGTCTCCTTTCCCATGTGAGTGTGGAGACTTAAACCCCGGGGCTCCAGACGAACACTCTCCTGGGCTGCTGCCCT
TTGGCTCTCACACTTTAAGACCTGGTTTTCAGCCTTCTGTTTGTCTCTGGTTCCTGTCACATCCCTGACCTCCTTGTGAGCTCAGCTCTGC
ATCAAGTTTGTTGTTTCTATCTTGTGCTCACAAGTTCTGTTCTGGGAGGCTTTTGGGGTTAGACCATCACAGGTAAAGACAGAAGGGG
AAATCTACTTTTGCACCATTTCTAAGATCAATTTCTAGGCTTGTTTTCAGAACATTTGCCATCCCCCTCTGTTCTGGTTTGAATAATTGTC
CCCTCCAAAATTCATGAAGTTTGATTGTCATTGTGATGATCTTGAGAGGTGGAACCTTTGAGAGGCGATGCAGCCACGAGGGCTTTGC
CCTCCTGAATGGGCTGGTGCTATTATCATGGGAGTGGGCTTCTTATCAAAGGGTGGGTTCAGCACTCTTTTCTCTCTCTCCTTGCCCT
TCTGCTATTCTGCGATGTGATGATGCAACAAGAAAGCCCTCACCAGATGCAGCCCCTTGAGGTTGGACTTCCCAGCCTCCAGAACCAT
AAGCCAACAAGCTTCTGTAAGCTGTCAGTTACCCAGTGTGCAGGAGTCTGCTATAGCAGCACAGAATGGATGAAGACATCATTTTGCA
ATCCTACAAGAAAGGTGTTCTTTTGTACTCATTTCATCACTGGCTAAACTGGACTCTGGATGGCTAAAGTAACAAGGCAGGTCTGTCTG
CTTCCAGAGGACCTGTCCTGCTGCGGCGGTTCTGGGCTCCCCTGCGCTTTGTGGCATTTTACAGCTTGCAGTCATCCTGCAAGGTAGAT
GTTACTTCTCTTCCCATCTTATGGCTGAAAACCAAGCCTTACAGCAGTTATACAAGTTATGTGGCAGTTTTCAGCGATTGTATTAAAAAA
TATTTTAGGTAAACAATGTGGTGTATATACGCAATGGTATACCAGTCAGCCTTACAAAGGAAGACAATGCTACCATATATGACAATAT
AGATGAACCAGAAGGGCATTATGTGAAAAAACCCAGGCACAGAAAGACAAATGCTGCACAATCTCACTCACAGGTGAAATCTAGAAA
AGCTGAACTCACAGAAGCAGAGGGTAGAATGGTGTTTACCTGGGGCTGGGGCCGGGCAGTGATGTTGGTCAAGGGATACATTTCAG
TTACATTGGAGGAATATGTTCTAGGGATCTATAGTAGGACATGGTGACTGGAAAATTGCTAAGAGAGTAGATGTTAAGTGTCCTCACC
ACACCAAAAAACAAAAAGTATGTGAGTTAATGCATGTTAATTAACTTGATTTAGCCATTCCACAATGTATTCATACTTTAAAACAAGTT
GTAAACAATATATACAAGTATTATTTGCCAATTAAAATACATACATTTAAAAATATTTTAGATATTTGTCCATTTTTGTTTCAAGTTTACT
TGCTGGTCATTTTATTGTTAAAAAATTCTTGGTTGTTTTCGGCTGGGCACAGTGGTTCATGCCTGTAATCTCAGCACTTTGGGAGCCTG
ACGTGGGTGGATCACCTGAGGTCAGGAGTTCAAGACCAGCCTGACCAACATGGTGAAACCCCATCTCTACTAAAAATACATAAAATTA
GCTGGGCGCGTGGTGATGGGTGTCTGCAATTCCAGCTACTCGGGAGGCTGAGACAGGAGAATTGCTTGAATCCGGGTGGCAGAGATTG
CAGTGAGCTGAAATTGCACCATTGCACTCCAGCCTGGGCAACAAGAGCGAAACTCTGTCTCAAAAAATAAAAATAAAAATGACTGGTT
TTTTTTTCTGTGTGTACATGACTGACAAGACCAGTGGTTTCCTTTAATACCTCATCGACGTTCCCAGGCACTTTTTGTATTTGAGGTGTG
TGAAGTAATAGGTTGGCCCTTGTCTTGAGCGTGATACTGAACACACCGACTAATAAAATGGGGGCCTTTGGCTGCACACCAGGCGCTC
TGGGTACTGATGAGCTCGCCCCCAACTCCATGCCAGGAATCAGAACGGTTGCCCGGGAGAGTCGGCAGAAAGAGGAGGAACCGGAT
GCAGTGATCTACCTGGTTTGTCCTGGTGTCCAGTAACTTGGAGTTCTTCTTTCACACGTGGCTGGCACAGAGGAGACACTCATAAATAC
CCGAGTTGAATAAAATAGTCCATTGACATGGAGTCGCATGAAGCAGCATTCGTCCATCCAAAACGCCGATGCTTCTTTAGAGTGGACT
GAGTTTTCCCCCAATACTAGGTTGTCCCACGCGATGGACAAAAATAGCCCATGTGGCAACGGAGGCTGGCCGGGGGGACCTAATGCC
CATGCCTCTGGCATTCCCACCAAGGTGACTGTCCAGTAGCTCCCAGGACAGCCCATCCGTGTAGGGCAAACGCCATGAGCCACTCCTG
TGTGCAGGCACAGGGCAGGCCCAGGCACAGGGAGGCGGGTGGGCAGGCACACAAACAGCCAAACGCTGACCCTGGAGGGCGGTG
GTCATCTGCTCATCACAGGGGAAAGACTGGAGGTGGGAGAGGCAGGTGCCACCCGCAGGAGTTGGGACGAGCTGTGCACACGGCT
GGGCACACGCAAAGCTGAGCCTTCTTCGTGAGCAACACGGTCACATTTGGGTGTAGGAATCTTGGCTGGAGTTGCCCACACGTGGGGA
GCAGACAGCTCTGCAGCCAGGACCCCAGTTGGAGAAGGCAGCGCTTGGAACAAGCCAGGACAGTGGACAGACGGGCCGGTGCCAA
ATAGAAGTCATGATAACGCGCTGACAAGCTGTGCAGACGAACACTGTGTGTAGACGGAGGCCATGGAGAGTGACGATGGGGAAGA
CGCTGGATCCCTGGCTGGCCTGCATCCCTCTCCGTTCTCAGTTGCCTGTGGAATTCCGGGGAGCTCTGCTCCAGCTACACTGCACATAA
AAGTGCGCAGGAAGTGGATCCTGGAGAGGAACTGTTCTTCTGGACTGAGCTTGCTGCTCATGGCAGCCCCACCTGCAGGACCCAAAG
CCTTATGTGATGTTTGCTGGACACTCAGCCACGTGGCTGCCTGTTGAGCTCTGCAAGTCCACGCGGGAGCCAGGAATTCCTCCCCAGA
AGTCTCTCCATTATATTCACCACCCCCTAGTAAATCACAACCTGACTTGCTGCAGAGGATGGAGTGCCTGGGACTCGTCTGACCCCAGC
TCCCCTGGGGAAGTGGGGGTGGTACGTCCCTGCACCCGGCCACGTGCTGCCTTCTCCTGGGCTGCCTGTCCATGCTGAGCAGACAGG
AAAGTCCAGTGAGGTCCCTGCCTGTGCACTCCACCAACCACATCGTCCCTTCCCGGCAGCCTCACCTAGGCCCCTCCAGCTACGACCCC
TTGTCCCCTGCACCGATGCCTGGCCTTGGAGGTTGCTGCTCATTTTTCTGGAATTTTTTCTTAGATCTCTGCAGGGCTGCCCCTCCCCCT
ACAAGGGCTCCACACGTGTTCCCTCCTTCATGACTCCCACTGGGCTTCCCCGACAGGGCCTCACCCTCCCCAAAGCTCTGGTGACACCT
GCCAGGTTTCCTCCAGGCCACAGCTCGGCAGCCCGATCTTAGAACAGAACGTGGCACGCAGGGCAGGTCTGGCTGAGGGCCCAGCAT
TGTCAGCGGGGTTGGAGGTCTTCCCGGGCCTCGAAGGGGAGACGTAGGCTTCTCAGGGCAGCCCAGGACGCGTCCTCACGAACCAC
AGCGAAATTACAGCAGGTATCTCGCGGATAGGAGTCTGCATCATTCCGTCTCCATGCCGTGGTTTCTGAAATTATGCAACTATCTCGGC
ATTCCAGAGGGCTCAGAGTAGCCACGCGCAGAGGCCCTCCCCATGGGGTGGATGGAAGCGTCCACTCGCGGCGCGAGGAATATCCC
TGGGCCCCTCGGGAGAGTCTGCAGGGGCAGCCCCTGGGTGAGCAGGCCCAGTGCGGCCTCTCCCTGAAGGGACTTTCGGGCCCTCCC
GGGTCGGGGCTTCACCGGTAGCAGGCAGGGCTTTGATATTAATGCTTAAAGGGAAAGCAGAGCTGAGCTGTCAGGACGTTGGTTAG
CTACAAACCCTACTCTTGTTAAAAGAGAAATGGGGTCGGGGAAGGGGTTCTCCAGCCCTGAACTTCCCGGGCCGGGCAGGACGCGGT
CCCTCCAGGAGTCGGGGCTCCCCCGCCTGGGGACGCACTGGGGCAGGCGCGCTTCTCCTCTCGGGGTCCCATGTGCCGCCGGCTCTC
GGACGGTAAATCAGGGCTCGGGTGGGGGCGATGGGGGGCCCGCGGCCTCGGTGCCCCTGGCCAGCCTCGGAGGCGCACGGGCCAG
GCCGCGGGGCGAGAAGCGAGCGCGGGAGGGCGGCAGCTGGCGGAGCGGGAAGGGAGCGGGGCGGCTGCGGCTGCGGCGCGGA
GGAGCGCCATTTACGTTCGGGCCCGCGCCAGGCGCTGACGTGGGCGGCCCTGTCTCGGCTTCCGGGCCCGCAGGGTCCTCGGGGCG
GACGGCGCTCCCGCCAGCGGCGCTGAGTCCGGCCCGACCCTGCCCGACTTCCTCGGGGACAGGCGGTTTAGAACGTGCGGAACACCA
GGCCCGGGGCCTCCGCCGGGCTGCAGCCCCGCGAGCTTCCCGCCAGGCTCCCGCCCCGCCCCGCCCCGCAGCCGCGTCCCGGCCGGG
CGGGCCCTGAGCCGCCCGCGTGAGTCCGTGCGCCGCCCGCGCTGGGAACCAGGAGACCAACCGCGAGGCCCCGCCCGCGCGCCCG
CCG

Figure 3.33. Proximal promoter sequence of *CtBP1* gene indicating potential HRE sites. Resulting sequence of BLAST search for proximal promoter of *CtBP1* gene – 5kb upstream of the gene start site. Potential HRE consensus motifs are the ACGTG motif (yellow) and the GCGTG motif (blue).

AGAGTGTGTGTGTGTGTGTGTGTGTGTATTTAATTAAAAAATAAAAGTGATGGGCTTAAACCCAAATGCCAATTCAATCCTGAA
ACTGACAGCTTCAACCACTCCAGTTTTGCACCCCTTACTGCGTATGTCGGGCATGAGCACAGAGTTTTGCTCTGTCACCAGGTTGGAGT
GCAGTGGCGTGATCTTGTCTCACTGCAGCCTCCGCCTCCCTGGTTCAAGCGATTCTGCTGCCTCAGCCTCCCGAGTAGCTGGGATTACA
GGCATGCACCACCATGCCCAGCTAATTTTTGTATTTTTTTAGTAGAGATGGGGTTTCACCATGTTGGCCAGGATGGTCTCAATCTCCTG
ACCTCGTGATCCACCCACCTCTGTCTCCCAAAGTGCTGGGATTACAGGCGTGAGCCACCTTGCCCGGCCGAGCCTAGGATTTTCAATG
CATAGTTGGAAAGGGCCATGGCATCTATAAAAGCAATATGTATTCACTGATTAGAATTAATTATGAATCACATAGTGATTATATTATAG
CCAAAGAGAGCACTGTTATTCTATAAAACATTGCAACAAAATTCCCACATCCACTGAGGACAGCAACTGAGAGCTTCAGATAATTGCG
GTTCTGAAGTGAGCTGAACCCTGAATAACAGAGATAGGTGAGTAACAATACAGTTAAGTCCAACTCCCAGTAACTCTCGCTGCACAGA
CCCTTGAAATACTCAAGTGCACACAACTAGTCCATTTTATTGCACAAAACAGTTCCGATAAAAGGACCCACCATTATCTAGGGCCACTA
TCTTTTTTTTCTACAACCATTGGTTCCTGGAAATGAAATAGGAAAGATAGGAAGCTGAGAAATAAGAACCTCGGTTAGAGGTCTTTGA
TTGTAGCGGGGGAGGCAGGCTGTGATGCAGCCGCAGGCCGGTCCCACGGGCCTTTTTCAGCCCCTGGGTTCCTACAGACATCAGAAG
TGCTCCCGAGGAGGTATAAAGTAGGGAAGGAATTATGCCATCCTGTTTAAAGGCTGCCAGACGGAAGAAAATAAGTGCCTTACAAAC
TCAACGCTCCACACTGGGGCTGTGGATCTCTCTTTTCTTTCACTACTTTTTTTTTTTTTTTTGATGGAGTTTCACTCTTGTTGCCCAGGCT
GGAGTGCAATGGCGCGATCTTGGCTCACTGCAACCTCCGCCTCCCAGGTTCAAGCGATTCTCCTACCTCAGCCTCCCCAGTAGCTGGA
AATACAGGCACGTGCACCACGCCTGGCTAATTTTTAGTATTTTTAGTTTCACCGTGTTGACCAGGCTGGTCTCAAACTCCCGACCTCAG
GTGATCTGCCCACCTTGGCCTCCCAAAGTGTTGGGATTACAGGCATGAGCCACTGTGCCAGTCCAAGGGTTCCCATTTCTCCACATCCT
CCTCAATACACGTTTTTTTCTCTTTTGTTGATAAAAGACATCCCGGTGGACATGAAGTAGTAACTTATCGTGGTTTTGATTTGCATGTCT
CTAATGACCAGTGAGGCCAACCATCTTTTCATGTGCTTACTGGCCGTTGGCCATTTGTCTACCTTCCTTGGAGAAATGCCTATTGAGTCT
TTGGCCATTTTTGAATTGGGTTTTTTGTTTGCAACATCTTAAAAAAAAATAGTATGAAATAATTCACATGTTGGGGGCAAATGAGCTCCA
TATTTTAAAATGCAGGTAAAGTGAAGTGAGAAATACTTTTCAGCTCTCAGGATGCCTTGCTTTTAATGTCTTCAAAACAAATAATATATT
AATAATACTTTCTCGGCCGGGCACAGTGGCTCACGCCGGTAATCCCAGCACTTTGGGAGGCCAAGGCAGGCGGATCACAAGGTCAGG
AGATAGAGACCATCCTGGCTAACACGGTGAAACCCTGTCTGTACTAAAAATACAAAAAAAAAAAATTAGCCGGGCATGGTGGCGGGCG
CCTGTAGTCCCAGCTACTTGGGAGGCCGAGGCAGGAGAATGGCTTGAACCCGGGGGGCGAAGCTTGCAGTGAGCAGAGATCGCGCC
ACTGCACGCCAGCCGGTGACAGACTGAGACTCCGTCTCAATAATAATAATAATAATTATACTTTCTCTTTTTTTTTTCTTGAGACGGAGT
TTCGCTCTGTCGCCCAGGCTGGAATGCAGTGGTGCAATCTTGGCTCACTGCAACCTCCACCTCCCTGGTTCAAGCGATTCTGCTGCCTC
AGCCTCCCGAGTAGCTGGGATTACAGGCATGCGCCACCAGGCCTAGCTAATTTTTGTATTTTTTTTTTTTTAGTAGAGACGGGGTTTCA
CCATGTTGGCCAGGATGGTCTTGATCTCCTGACTTCGTGTTCTGCCCCGCCTTGGCCTCCCAAAGTGCTGGGATAACAGGCGTGAGCC
ACCGTGCCCGGCCAAGAACATGTTAGTAATACTTTCTAAGTCAGAATTCAAATTTATAGAACACGTGAAAGTGAAGGAGTGATATGGA
AAATCAGGCTTTTTGTGGTTTCTTCCTGAGAAAAGAAGACCACTCAGAACCAAAGACTTCTGTGAAATAAGGAAGCAGAAAATCTTTA
TTTGTAGTTCTTATAGTTTATGCCTAAGAAACTCCGAAGAACAGGTACTGGTAACCCGGTAGCCTGGCGGTGGCCGCGGTTTGTTTAC
AGCCAAAAACTAGCTGAGGCGCCATGCCCTTGAGGCAAAACTGCTGAAGAGAGAAGCACCCTGAAGATCAGTTTGTGGAGATCCAG
GGTTGCCAGAAGACGAGACAACCGTGATTGCATGTGCGGAGGTTCCTCGATGGAAGCGCAGCCCGGCGCGCCCCTCAGCTGGCCTG
GCCAGGCCCTATGAAGGTCACGCGAAAACCCTGCTGCGGGCTTCTTAGCGACCGCATTACGTGGACTAGCGGGCAAGAAAAGCCTGG
TCGGCGCTGCCCTCACAGGTAGGCGGTCTTCAATCACGTTTTAAAATCTTGTTGAGTGATTAAGCAATCTTCGATAGTCCCGGCCCCTC
CACTGCAGGCCGCTCAGGCCGCAACGCACCTGGTGCGCTTTGGCAAACAAGCCCCGCGGCGGGCTGGGGCAGGATTTAAGAAATGT
TTAATGAAGACTGGGAGGCCTGGAGCAACGCTCTTTGGGATGCAGAAAAGGGTCGTGCAGCTCGGTGGCCTCTCCTCCGGCCCCCTG
GCCCTGGCTGTAAGTTTCCTCGGCTCTGCAGGGCGCGGGGCACTCAGGGATGGAGGAGACCACACCGCGCGGCTGGGTTCGCGGAA
TGGCGGTCCCTGCGGCCTCCAAAGGCGGGACCTCAGACCCCTCCCACTCCTTTCCTGCTCGACATCTCAATCCAGCTCCTAATATCTCA
ATAGGGTTTTTAAACAAATCGATCCTAAGGGCTCAGTTCAGCCCACCCAGGGATTCTTGGAGGACGCACGCCGAACTCAGGGTAGTG
AGAAGAGTTTGGGGGGCCCTGGGGCGCAGGGAGAAGACCCCACACTCCACGGCCACCAGCTCCCTTCCGGAGACGGCGCTCGGACG
TCGCGGGTCACGGGCGGGGAATTTAGCCCAGGTGCTCGTTGGGCCGCGAGCGGCCGCTGGGCCTGGATTCCCAGGCTCGCTGTGCA
GACTCCAACCTTGAGACGTCAGGACGGCGTGGGCTCCGGGCCGCCGCGCAAGCCCAGGACCCCGAGTCGCGGGCCCCCACGCCGCA
GCGCGCCTCCCTCCTCGAGACCCGGGGCTCCGACCCAACACAGGGCTTCTCAAATGCCCCGGCGAGATCCAGGCAGCAAGAGGGAAC
CTTTTTTTTTTTTTTCAATGTGTAAGAATGTTTTGCTTCTTTTAGGGCACAGCACTGCTGCAACTTGCAGCACAGAGGGCCCTTCCCTGC
GCACCCACAGCGGTCGCCGCCTCTCCGGCACGGTCTCCCGGATCTGGATTTGGGGAGCGCAAGTGCCCCCTGTGGCCGGCCCGCGCC
TGACCCCGCGGGCCTGAGAAGGCAGAAGCGGCCGGTGCGGGGCACCAGGAGGAAGTTGGAGCCCGGGGGCCGGGAAGGGGGCTG
GTTGGCGCCGCTGGCTGGGCGGGGCCCCATGGGACCGGGGCCACCCGGGGCTCGCGTTCCCCCACGTGGCCGGCTGCCCGGTACCC
CACGTGGAAGGGGCGGAGGAGGATGAAGGGCCAGGGGAGCAGCGGACCCCGAGCCACCGCGACAGGACCTCGGCCCCTGCCACC
GAGGCCCCCGCGCCTCCCGAGGGCCTCCCGGGCGGGGCCGGGCTAGGGAGTGCCCGCCGCGCCCGGCCCCTGGCCCTCCCGCCCGC
CGCGCTTGTGTGCACTTTCGCGGAGCCACTAATCCCCCGAGAGAGCCGATTTGTAGTGAGGAGTATCTGAAGGGGGCGAGGCCGGC
CCATGTGGGGTTGTGTCATTGGTTTGCAAAAAGAGACCCCGCCTTTGCCCCCCCCCCCCCAAAAACAGGAGCGAGGAGTGAGCGAGCG
GCGACCCTCACCTCGCCTCCCGCCTAGCTCCTGCGCAGCCAGCGGGTACCGGGAGCTGCGGCCAGCGCCGCTTCTTTCCTTTCCTTTTC
TCTCCGTTTTCCTTCTCCTTCCCCGGAGGAGAAAACAAATAAAGAAGAGCAAATAGCCGGGAGGCGCTCGGCATCCAGGACGTTCCCT
CCCCCGATCCAAGTTGGAATTAGCATCCTCTCGGGGGTGAGCGCGGCGCGGGGCGGGCCCGGGCCGGGGACCCCCAGCGCAGCCCC
CTCTCGGCGGGCGGGAGGGCGCGGGGCCGGGACGCGGGGGGAATTGGGAACCGGGTGGGCGGAGGAAGGGGGTGGGGTGGGT
GGGGAAGTAGGAAGAGGCTCGGCGGCGAGGGGAGGAGGTGGAAGGGAAGGGAGGGGTAGGGTGGGGAGGGGAGGGGAGCGG
AGGGAGGGTGGGGAGGGCGGGAGGGGGAGGGGCGGGGAGCTGGAGAGATTAAGTTTTTGTGTGTGTGTCCCTGTGTGCGTGTGT
CATTTTAAGGTGGCTC

Figure 3.34. Proximal promoter sequence of *CtBP2* gene indicating potential HRE sites. Resulting sequence of BLAST search for proximal promoter of *CtBP2* gene – 5kb upstream of the gene start site. Potential HRE consensus motifs are the ACGTG motif (yellow) and the GCGTG motif (blue).

3.2.6 Optimisation of chromatin immunoprecipitation assay (ChIP) methodology

Prior to using the chromatin immunoprecipitation (ChIP) assay to determine whether HIF-2α directly binds to the proximal promoters of CtBP1 and CtBP2, the enzymatic shearing method was optimised.

Chromatin was isolated from Hues-7 hESCs maintained at either 5% or 20% oxygen and incubated with the enzymatic shearing cocktail (ChIP-IT Express Enzymatic Kit, Active Motif) for either 5, 7.5, 10, 12.5 or 15 minutes at 37˚C before running the sheared chromatin products on a 2% agarose gel (Figure 3.35).

The banding pattern of the sheared chromatin revealed fragments of DNA from approximately 250bp to 1kb with 5 minutes of shearing. As the incubation time with the enzymatic shearing cocktail increased, there was a corresponding increase in the amount of smaller DNA fragments from hESCs cultured at either 5% or 20% oxygen. Chromatin shearing was decided to be optimal with a 7.5 minute incubation time (Figure 3.36).

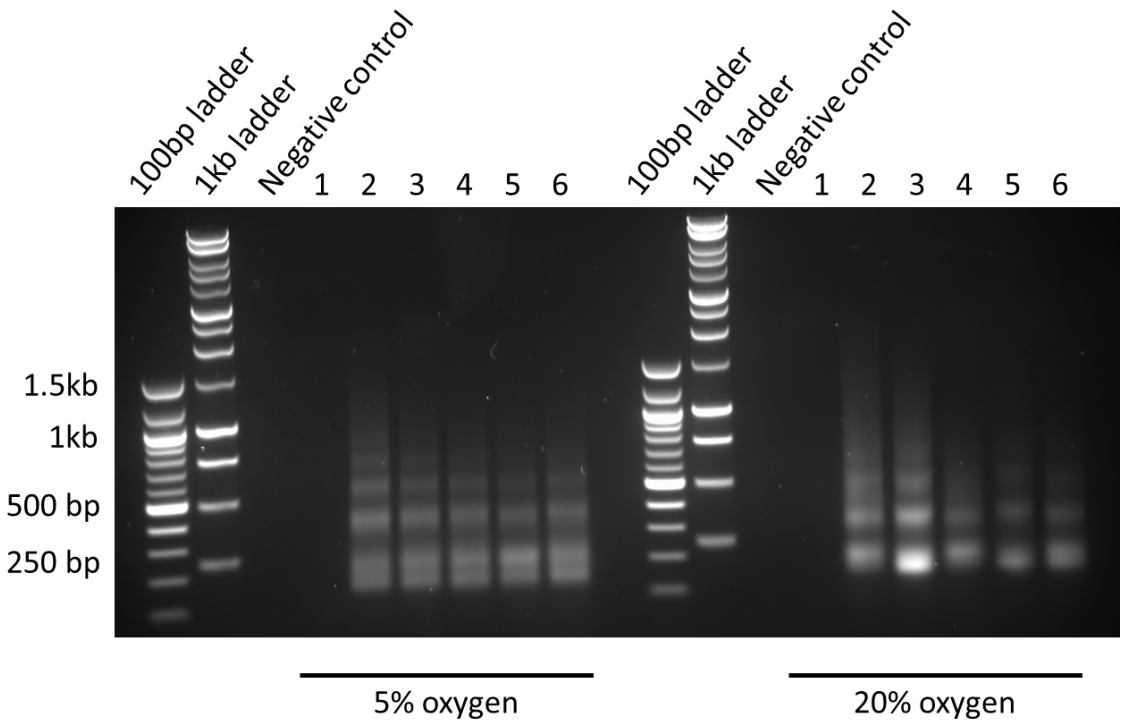

Figure 3.35. Optimisation of chromatin shearing for ChIP assays in Hues7 hESCs.
Representative sheared chromatin isolated from Hues-7 hESCs cultured at either 5% or 20% oxygen. Lane 1: chromatin + water, incubated for 10 minutes; Lane 2: chromatin + enzymatic shearing cocktail, incubated for 5 minutes; Lane 3: chromatin + enzymatic shearing cocktail, incubated for 7.5 minutes; Lane 4: chromatin + enzymatic shearing cocktail, incubated for 10 minutes; Lane 5: chromatin + enzymatic shearing cocktail, incubated for 12.5 minutes; Lane 6: chromatin + enzymatic shearing cocktail, incubated for 15 minutes. Sheared chromatin was run on a 2% agarose gel.

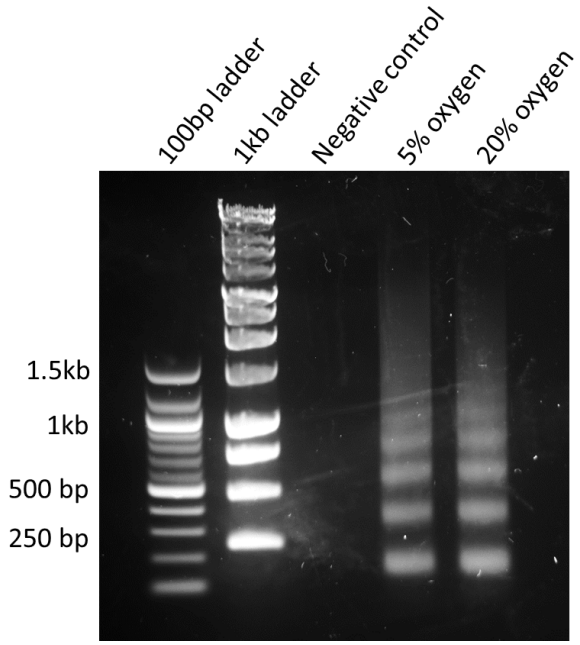

Figure 3.36. Optimised shearing of chromatin isolated from Hues7 hESCs cultured at either 5% or 20% oxygen.
Representative image of sheared chromatin isolated from Hues-7 hESCs cultured at either 5% or 20% oxygen. Chromatin was incubated with enzymatic shearing cocktail for 7.5 minutes and run on a 2% agarose gel.

3.2.7 Chromatin immunoprecipitation assay (ChIP) to examine whether CtBP expression is regulated by HIF-2α

To determine whether HIF-2α directly interacts in vivo with the proximal promoters of *CtBP1* and *CtBP2* genes, ChIP assays were performed on Hues-7 hESCs cultured at either 5% or 20% oxygen tensions.

Chromatin isolated from hESCs was sheared as per the optimised protocol to obtain fragments of approximately 250bp – 1kb in length and immunoprecipitated with an anti-HIF-2α antibody. A rabbit immunoglobin G antibody was used as a negative control. qPCR was performed on immunoprecipitated samples to determine the level of enrichment in HIF-2α immunoprecipitated chromatin from hESCs cultured at either 5% or 20% oxygen for the potential HREs in the *SOX2*, *FOXP3*, *CtBP1* and *CtBP2* proximal promoters, compared to the IgG negative control immunoprecipitated chromatin.

HIF-2α has previously been shown to directly bind to the *SOX2* proximal promoter (Petruzzelli et al., 2014) in hESCs under hypoxia, so was used here as a positive control.

Furthermore, primers designed to amplify a region between two potential HRE sites within the *FOXP3* proximal promoter was used as a negative control.

Specific binding of HIF-2α was observed at the HRE at -1100bp in the proximal promoter of *SOX2*. ChIP analysis revealed a 10-fold increase in enrichment of *SOX2* proximal promoter in hESCs cultured under hypoxic conditions compared to the IgG control ($p=0.0098$). There was no significant difference in the enrichment of *SOX2* between cells maintained at 20% oxygen immunoprecipitated with HIF-2α antibody compared to the IgG negative control. However, HIF-2α was found to significantly bind to the HRE in *SOX2* proximal promoter in hESCs cultured under hypoxia relative to those maintained under normoxic conditions ($p=0.0082$; Figure 3.37). This data agreed with previous literature that HIF-2α directly binds to the *SOX2* proximal promoter and confirms that the ChIP protocol was working correctly.

To further verify the specificity of HIF-2α binding, a negative control probe specific to the *FOXP3* promoter was used. This probe did not amplify a HRE site but instead was designed to amplify a region in the proximal promoter situated between 2 predicted HREs at -670bp and +104bp from the transcription start site. In agreement with Petruzzelli et al. (2014) no significant enrichment by HIF-2α was observed in this *FOXP3* promoter region in hESCs cultured at either 5% or 20% oxygen or with chromatin immunoprecipitated with either a HIF-2α or IgG negative control antibody from cells maintained at either 5% or 20% oxygen. This data, also, confirms that the ChIP protocol is working correctly as no enrichment was seen for this negative control (Figure 3.38).

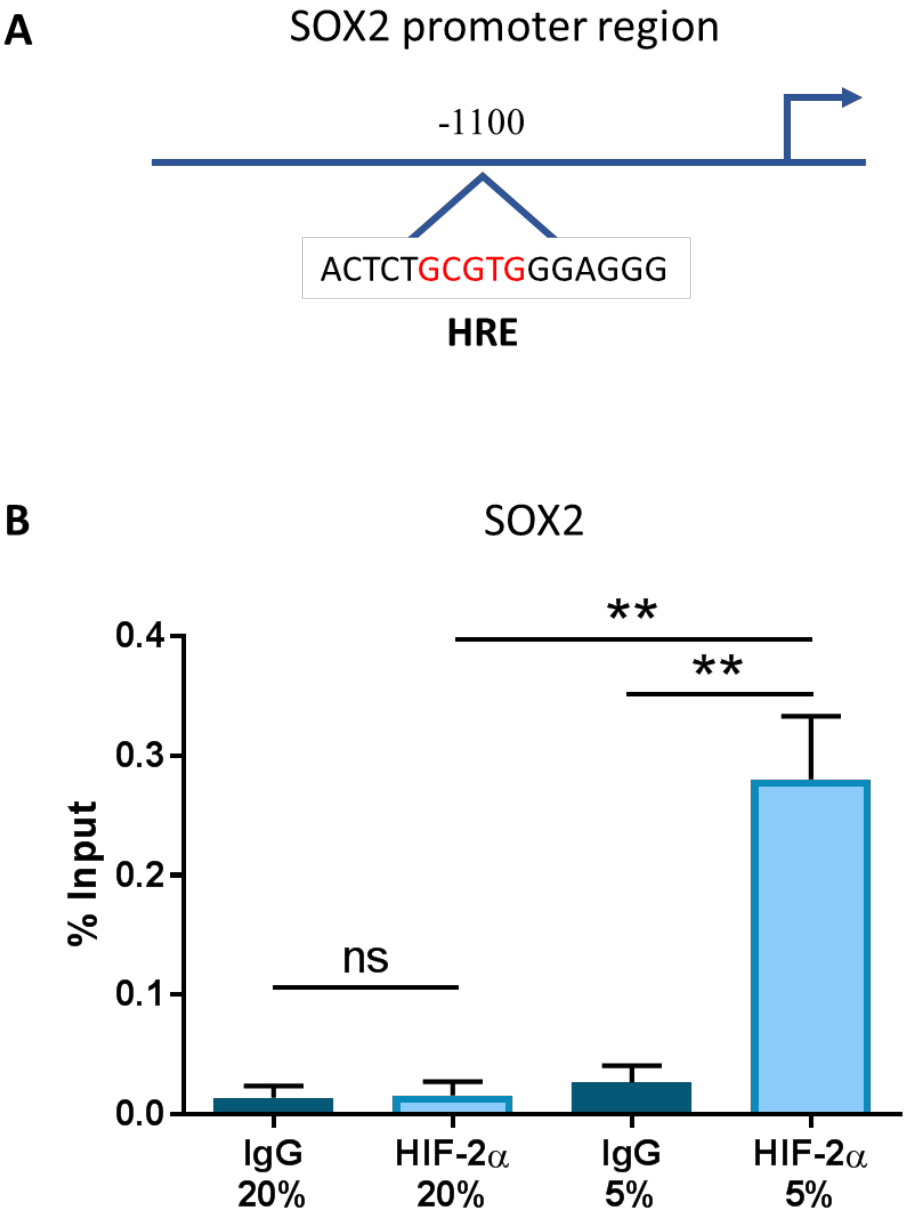

Figure 3.37. HIF2a binds SOX2 promoter in hESCs maintained under hypoxia.
(A) Schematic representation of the SOX2 proximal promoter and the putative HRE located at -1100 from the transcription start site. ChIP assays were performed with either an anti-HIF-2α or IgG control antibodies incubated with chromatin isolated from hESC cultured at either 5% or 20% oxygen. (B) SOX2 proximal promoter DNA enrichment is expressed as a percentage of Input (non-immunoprecipitated chromatin). Bars represent mean ± SEM. (n=3).

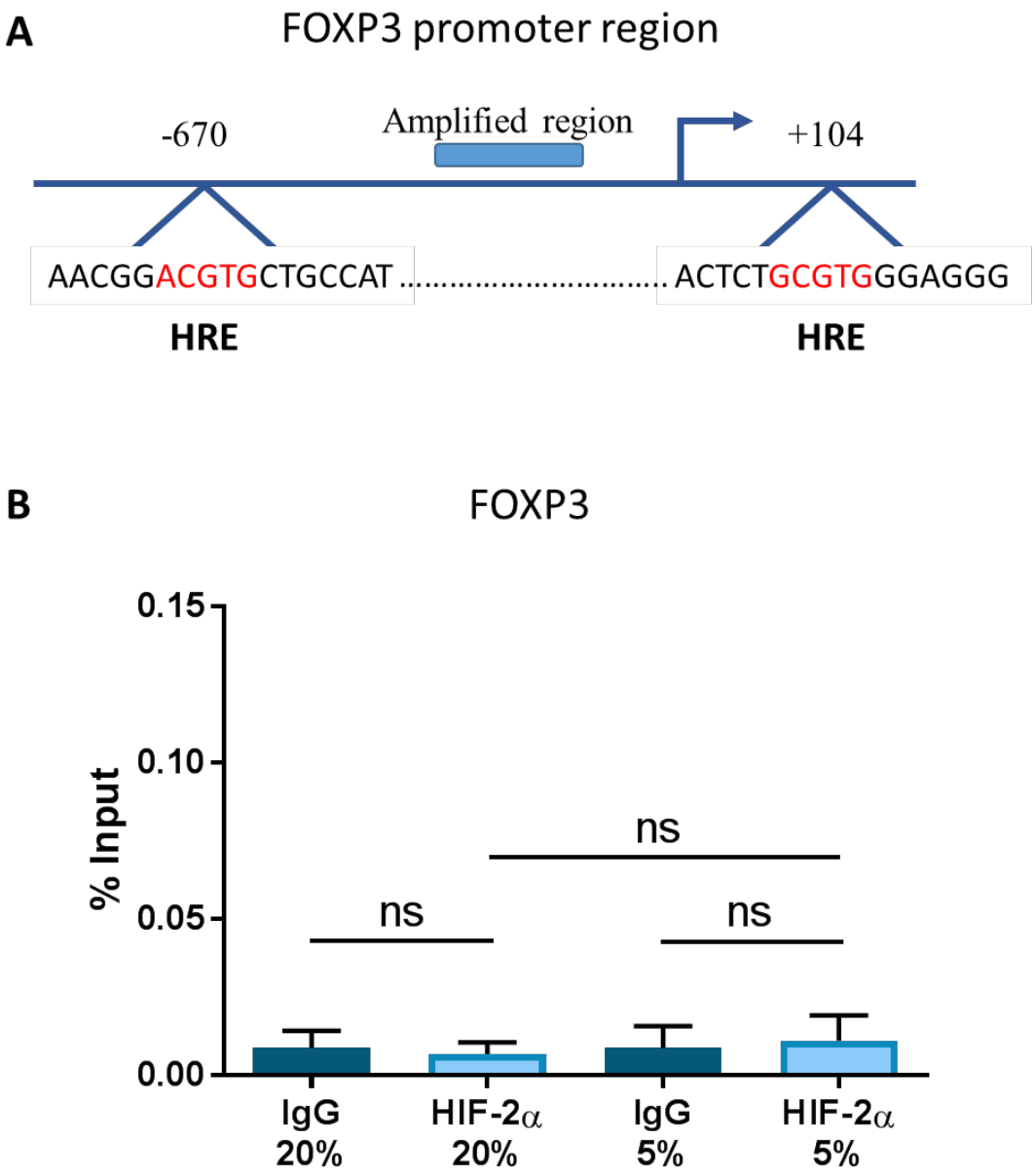

Figure 3.38. HIF-2a does not bind FOXP3 promoter in hESCs maintained under hypoxia. (A) Schematic representation of the FOXP3 proximal promoter and the putative HREs located either at -670 or +104 from the transcription start site. Note that the amplified region is between the two potential HRE sites. ChIP assays were performed with either an anti-HIF-2α or IgG control antibodies incubated with chromatin isolated from hESC cultured at either 5% or 20% oxygen. (B) FOXP3 proximal promoter DNA enrichment is expressed as a percentage of Input (non-immunoprecipitated chromatin). Bars represent mean ± SEM. (n=3).

To determine whether HIF-2α binds directly to potential HRE sites in the proximal promoters of CtBP1 and CtBP2, ChIP assays were performed on chromatin isolated from hESCs cultured at either 5% or 20% oxygen.

Specific binding of HIF-2α was observed at the HRE at -1287bp in the proximal promoter of CtBP1. qPCR revealed a 10-fold increase in enrichment of CtBP1 proximal promoter with HIF-2α antibody in hESCs cultured under hypoxic conditions compared to the IgG control ($p=0.0355$). HIF-2α was found to significantly bind to the HRE in the CtBP1 proximal promoter in hESCs maintained under 5% oxygen compared to those maintained under 20% oxygen ($p=0.0418$) suggesting that HIF-2α is only binding to that HRE in hESCs cultured under hypoxia (Figure 3.39)

Specific binding of HIF-2α was observed at the HRE at -2114bp in the proximal promoter of CtBP2. Amplification of a potential HRE in the CtBP2 proximal promoter sequence revealed a 4-fold increase ($p=0.0389$) in enrichment in chromatin isolated from hESCs maintained under hypoxia with the HIF-2α antibody compared to the IgG control. Comparison between immunoprecipitated sample for HIF-2α in hESCs maintained at 5% oxygen compared to 20% oxygen showed a significant enrichment ($p=0.026$) meaning that HIF-2α is again only binding under hypoxic conditions (Figure 3.40).

In contrast, no significant enrichment of either CtBP1 or CtBP2 proximal promoters was observed in hESCs maintained under 20% oxygen immunoprecipitated with HIF-2α antibody compared to the IgG negative control.

Together, these data reveal a specific interaction between HIF-2α and a HRE in the proximal promoters of CtBP1 and CtBP2 only in hESCs maintained in hypoxic conditions.

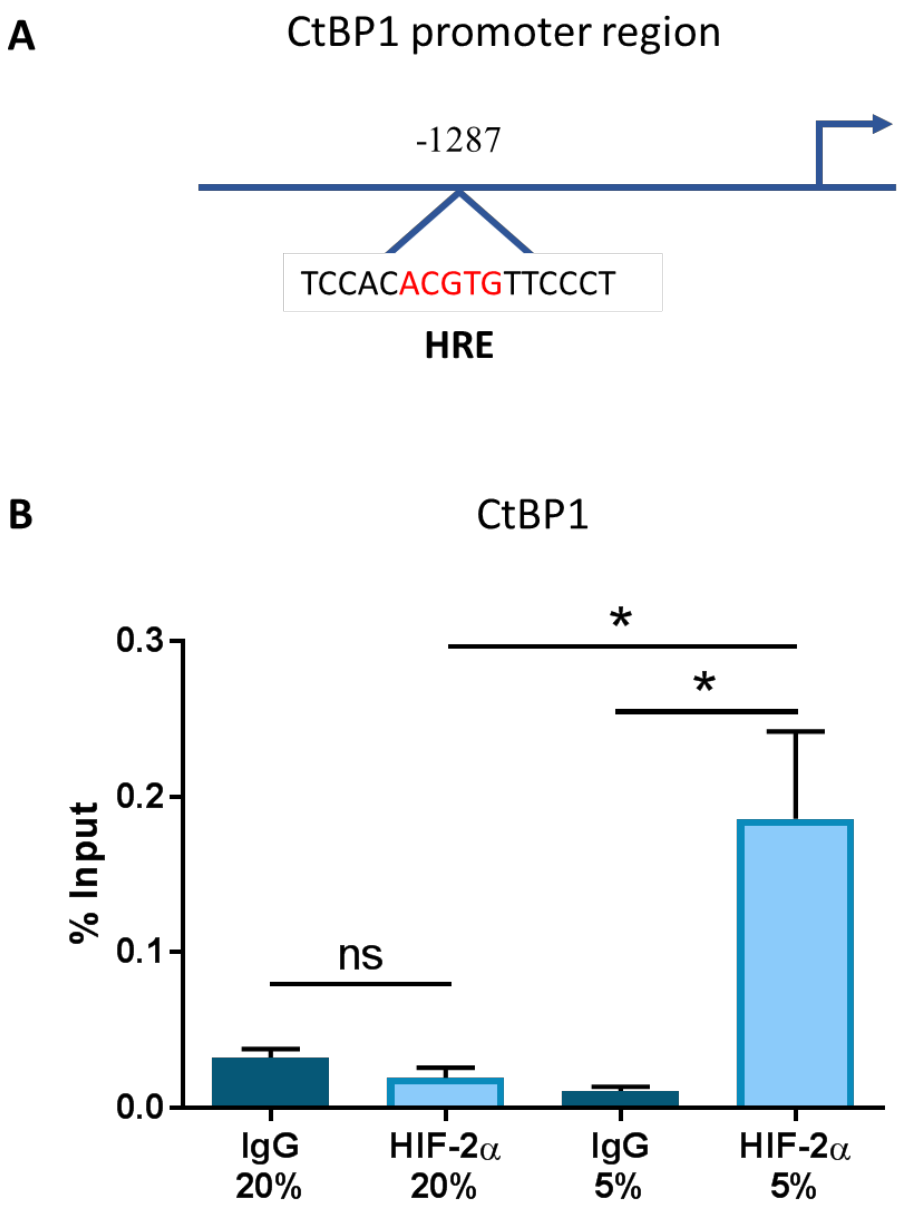

Figure 3.39. HIF-2a binds CtBP1 proximal promoter in hESCs maintained under hypoxia. (A) Schematic representation of the CtBP1 proximal promoter and the putative HRE located at -1287 from the transcription start site. ChIP assays were performed with either an anti-HIF-2α or IgG control antibodies incubated with chromatin isolated from hESC cultured at either 5% or 20% oxygen. (B) CtBP1 proximal promoter DNA enrichment is expressed as a percentage of Input (non-immunoprecipitated chromatin). Bars represent mean ± SEM. (n=3).

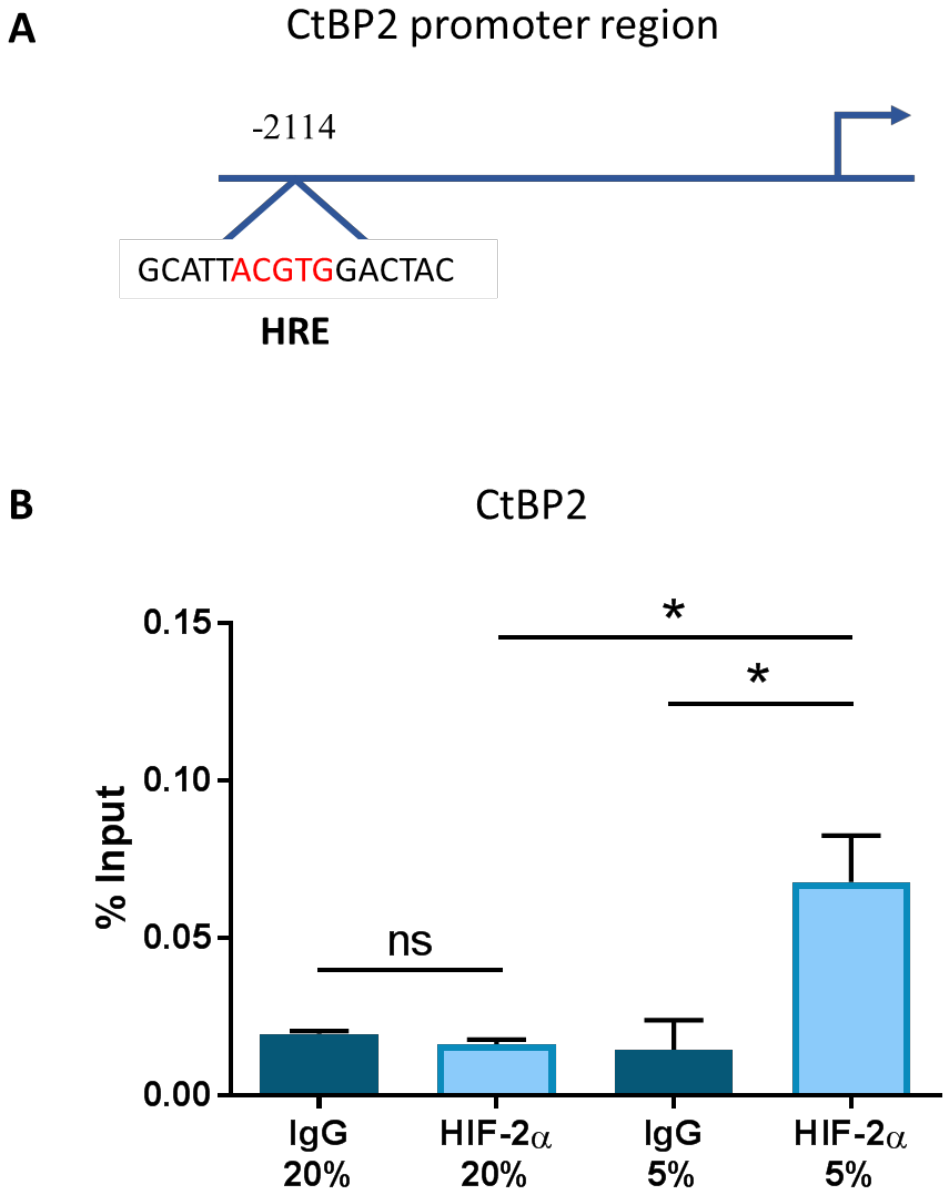

Figure 3.40. HIF-2a binds CtBP2 proximal promoter in hESCs maintained under hypoxia. (A) Schematic representation of the CtBP2 proximal promoter and the putative HRE located at -2114 from the transcription start site. ChIP assays were performed with either an anti-HIF-2α or IgG control antibodies incubated with chromatin isolated from hESC cultured at either 5% or 20% oxygen. (B) CtBP2 proximal promoter DNA enrichment is expressed as a percentage of Input (non-immunoprecipitated chromatin). Bars represent mean ± SEM. (n=3).

3.3 Discussion

Increasing evidence demonstrating that energy metabolism is a key influence on the maintenance of pluripotency is restricted by the lack of knowledge of how the metabolic state affects gene expression. Work in this chapter aimed to investigate whether CtBPs may have a role in connecting metabolic alterations to changes in gene expression in hESCs.

3.3.1 Characterisation of pluripotency marker expression in hESCs

hESCs cultured at either 5% or 20% oxygen expressed the nuclear transcription factors OCT4, SOX2 and NANOG, as well as the surface marker TRA-1-60, as expected, however no clear differences in expression levels between oxygen tensions were observed, probably due to the sensitivity of the technique. The observed expression patterns were indicative of hESC identity and typical cobblestone colony formation was observed (Thomson et al., 1998) confirming the presence of pluripotent hESCs. Additionally, very few hESCs expressed the early differentiation surface marker, SSEA-1. However, it was noted that there appeared to be slightly more SSEA-1 expression in hESCs maintained at 20% oxygen compared to those cultured at 5% oxygen. This supports previous studies where hESCs cultured under hypoxic conditions display reduced spontaneous differentiation, as hESCs cultured under 5% oxygen in this study displayed lower expression levels of the early differentiation marker SSEA-1 (Ezashi et al., 2005).

The significantly increased expression of *OCT4, SOX2, NANOG, LIN28B* and *SALL4* in hESCs cultured at 5% oxygen compared to those cultured at 20% oxygen agrees with previous work that has investigated the effect of hypoxic culture of hESCs on pluripotency (Forristal et al., 2010). Quantification of pluripotency marker protein expression revealed significantly enhanced expression of OCT4, SOX2 and NANOG in hESCs under hypoxic culture. This observation is, again, consistent with previous work investigating the effect of hypoxic culture on pluripotency maintenance (Ezashi et al., 2005; Westfall et al., 2008; Forristal et al., 2013), where hESCs appear to gradually lose their pluripotent state before any clear morphological changes are displayed. Together, this data demonstrated that the hESCs used in this study express markers associated with self-renewal and highlights the importance of hypoxic culture of hESCs for maintaining a pluripotent state, hESC morphology and preventing spontaneous differentiation.

3.3.2 Expression of CtBPs in hESCs

Increasing evidence emphasises the importance of metabolism for maintaining a pluripotent state, but how any changes in metabolism translate into changes in gene expression that supports a pluripotent state are yet to be elucidated. CtBPs may provide an insight into the link between metabolic shifts and changes in gene expression, but as the expression patterns of CtBPs in hESCs were previously uncharacterised, this chapter investigated CtBP expression and localisation in hESCs and how these are affected by changes in oxygen tension.

hESCs cultured at either 5% or 20% oxygen expressed both CtBP1 and CtBP2 in the nucleus. Despite the additional cytoplasmic functions of CtBPs previously noted, this observation suggests that CtBPs are acting as either transcriptional coactivators or corepressors in hESCs due to their nuclear localisation independent of oxygen tension. No clear difference was observed in CtBP2 expression between oxygen tensions, however CtBP1 expression in Hues-7 hESCs cultured under 5% oxygen appeared lower compared to cells maintained under 20% oxygen.

Analysis of CtBP mRNA levels between hESCs maintained at either 5% or 20% oxygen, interestingly, revealed a significant increase in expression in cells cultured under hypoxia compared to those maintained at 20% oxygen. Prior to quantification of CtBP expression, Western blots displayed only one band for CtBP1 expression, whilst clearly showing a doublet for CtBP2 expression in hESCs. Previous results indicate that the doublet band displayed both splice variants; CtBP2-L and CtBP2-S which differ in size by 25 amino acids (Verger et al., 2006). The additional amino acids contained in the CtBP2-L isoform include a basic KVKRQR motif, which could contribute to the altered mobility of the two protein isoforms during SDS-PAGE (Bergman et al., 2006; Verger et al., 2006; Zhao et al., 2006; Birts et al., 2010). However, two distinct bands representing the two CtBP1 isoforms were not observed; a trend which was previously seen in a study using human breast cancer cell lines (Birts et al., 2010). It is assumed that both CtBP1 splice variants are expressed in hESCs, as previous studies have demonstrated that one CtBP1 protein band still represents both CtBP1 variants (Birts et al., 2010). The very small difference in size between CtBP1-S and CtBP1-L may explain why two CtBP1 bands cannot be visualised on an acrylamide gel as the additional amino acids present in the CtBP1-L isoform do not contain a motif that changes the electrophoretic mobility of the isoforms, so both CtBP1 isoforms move together as one band during SDS-PAGE. As a result of

observing two distinct protein bands in CtBP2 Western blots, the method of CtBP2 Western blot quantification was validated to determine that one CtBP2 isoform was not being influenced more than the other. Quantification of both CtBP2 bands together and quantification of the CtBP2-L and CtBP2-S bands individually all displayed a significant increase in their expression in Hues-7 hESCs cultured at 5% oxygen compared to those cultured at 20% oxygen. Furthermore, no difference in expression was seen between total CtBP2, CtBP2-L and CtBP2-S expression that it was assumed that both CtBP2 isoforms are influenced equally and therefore, subsequent results indicate any changes in CtBP2 expression as a result of quantifying both protein bands simultaneously.

In addition to CtBP expression patterns being previously uncharacterised in hESCs, mechanisms that may regulate CtBP expression in hESCs were also previously unknown. *CtBP1* and *CtBP2* mRNA expression levels were significantly increased in Hues-7 hESCs maintained at 5% oxygen compared with those cultured at 20% oxygen. This is a novel observation describing the hypoxic regulation of the expression of CtBPs, which has not previously been demonstrated in any other cell type. Previous studies have documented that the expression of pluripotency factors and glycolytic enzymes is influenced by oxygen tension in hESCs, but this regulatory mechanism has never been documented for a metabolic sensor. Interestingly, quantification of CtBP protein expression revealed a similar significant enhancement in CtBP expression under 5% oxygen compared to 20% oxygen in Hues-7 and Shef3 hESCs. This data suggests that CtBP expression is affected by hypoxic culture at both the mRNA and protein levels. However, this result conflicts the trend observed for CtBP1 immunocytochemistry. An explanation behind these conflicting results is currently unclear. It could be that CtBP1 expression is more dispersed throughout hESCs cultured at 5% oxygen, or additionally, there could be an antibody binding efficiency problem with cells fixed at 5% oxygen, although cells at 20% and 5% oxygen were fixed in exactly the same way so the same trend would be expected in cells fixed at 20% oxygen too. However, the immunocytochemistry was performed to localise protein expression and is not quantitative, in contrast to Western blotting, thus, the result from Western blotting quantification is likely to be more reflective of true results.

This data revealed a novel observation by suggesting that CtBP mRNA and protein expression is, like the pluripotency markers, affected by hypoxia either directly or indirectly. The finding that pluripotency marker and CtBP expression are both higher in

hESCs maintained under hypoxic oxygen tension suggests a correlation between their expression levels in a similar manner to the correlation seen previously between GLUT3 expression and OCT4 expression (Christensen, 2015). This, in turn, suggests there may be parallels between the regulatory mechanisms behind pluripotency factor and CtBP expression, and that metabolism is directly influencing hESC pluripotency.

3.3.3 Hypoxic culture increases hESC pluripotency and CtBP expression through HIF-2α in hESCs

After the finding that hypoxia regulates CtBP expression in hESCs, investigations into whether HIFs were directly influencing this hypoxic regulation of CtBPs were conducted.

HIF-2α is a key regulator of the hypoxic response in hESCs and has been shown to have a role in the maintenance of the pluripotent state. Previous studies revealed that silencing HIF-2α in hESCs significantly decreases the expression of OCT4, SOX2 and NANOG through direct interaction with their proximal promoters (Forristal et al., 2013; Petruzzelli et al., 2014); an observation that was found again in this study. It is well documented in the literature that HIFs, particularly HIF-2α in terms of hESCs, regulate the expression of glycolytic genes. Therefore, lactate assays and qPCR analysis revealed that the significant reduction in HIF-2α at both the mRNA and protein levels resulted in a functional change in hESC metabolism. Specifically, silencing HIF-2α resulted in a significant reduction in the rate of flux through glycolysis under hypoxia by decreasing the expression of GLUT transporters and potentially the expression of other glycolytic enzymes such as hexokinase that were not analysed but are known to be regulated by HIF-2α.

Intriguingly, quantification of CtBP mRNA and protein expression revealed a significant decrease in both isoforms as a result of silencing HIF-2α. This suggests that the increased hypoxic expression of CtBPs is regulated by HIF-2α, but it remained to be determined whether this was a direct or indirect effect of HIF-2α on CtBP expression. However, the presence of several potential HRE sites in the proximal promoter of both CtBP genes offered a possible mechanistic explanation for the hypoxic regulation of CtBPs in hESCs and suggested that CtBP expression may be directly regulated by HIF-2α under hypoxic conditions.

HIF-2α is the predominant regulator of the long term hypoxic response in hESCs. Previous published data has demonstrated that HIF-2α significantly reduces the expression of the core pluripotency markers, which has also been reemphasised in this

study, but the molecular mechanisms that underlie how this might benefit CtBP expression had not previously been characterised. Therefore, ChIP assays were performed to determine whether endogenous HIF-2α interacts *in vivo* with the proximal promoter regions of *CtBP1* and *CtBP2*, but also the proximal promoter regions of the *SOX2* gene which is also upregulated under hypoxia (Petruzzelli et al., 2014).

ChIP results showed that endogenous HIF-2α binds to the predicted HRE in the *SOX2*, *CtBP1* and *CtBP2* proximal promoter regions under hypoxia, but also no significant interaction between HIF-2α and the HREs under atmospheric oxygen conditions was observed. These data suggest that the environmental oxygen tension can influence the chromatin dynamics and accessibility of transcription factors to change gene expression that determine the metabolic phenotype, pluripotent state and ultimately the differentiation of hESCs.

Mechanisms that regulate CtBP expression in hESCs were previously unknown. However, data presented in this study have demonstrated that CtBP1 and CtBP2 expression is hypoxia regulated. This was verified by demonstrating that HIF-2α directly interacts with a putative HRE site in the proximal promoters of both *CtBP1* and *CtBP2* in hESCs maintained under hypoxic conditions only. This is the first report describing the hypoxic regulation of CtBP expression in any cell type. HIF-2α is the key regulator of the hypoxic response in hESCs and has been shown to bind directly to the proximal promoters of *OCT4*, *SOX2* and *NANOG* (Petruzzelli et al., 2014). Although HIFs directly regulate GLUTs and glycolytic enzymes (Wang and Semenza, 1993b; Semenza et al., 1994; Semenza, 2000; Forristal et al., 2013; Christensen et al., 2015), this data represents the first documentation that HIF-2α directly regulates the expression of the glycolytic sensors, CtBPs.

Given that a HRE can be bound by any of the HIF-α subunits and different HIF-α subunits are the predominant regulator of the hypoxic response between cell types, the hypoxic regulation of CtBPs is probably not unique to hESCs. This suggestion is supported by the differential expression of both CtBP expression in the MEF feeder layers observed after immunocytochemistry, where CtBP1 and CtBP2 expression appears to be enhanced in MEFs under 5% oxygen compared to those maintained under 20% oxygen tensions. However, this expression has not been quantified. Therefore, the hypoxic regulation of CtBP expression is likely to extend to other pluripotent and differentiated cell types and

had not been identified previously as research in other cell types has focused on cells cultured under either hypoxic or atmospheric oxygen tensions, and has not involved a direct comparison between oxygen tensions.

Taken all together, the ChIP results are particularly significant as they have revealed a novel and specific interaction between endogenous HIF-2α and the proximal promoter regions of the glycolytic sensors CtBP1 and CtBP2 only in hESCs maintained under hypoxia but also genes involved in hESC self-renewal. This confirms a role for HIF-2α as a direct regulator of the hypoxic response (Figure 3.41). Furthermore, this work suggests a role for HIF-2α in the regulation of glucose uptake in hESCs maintained under hypoxia and offers a potential mechanistic explanation behind the highly glycolytic phenotype associated with a pluripotent state.

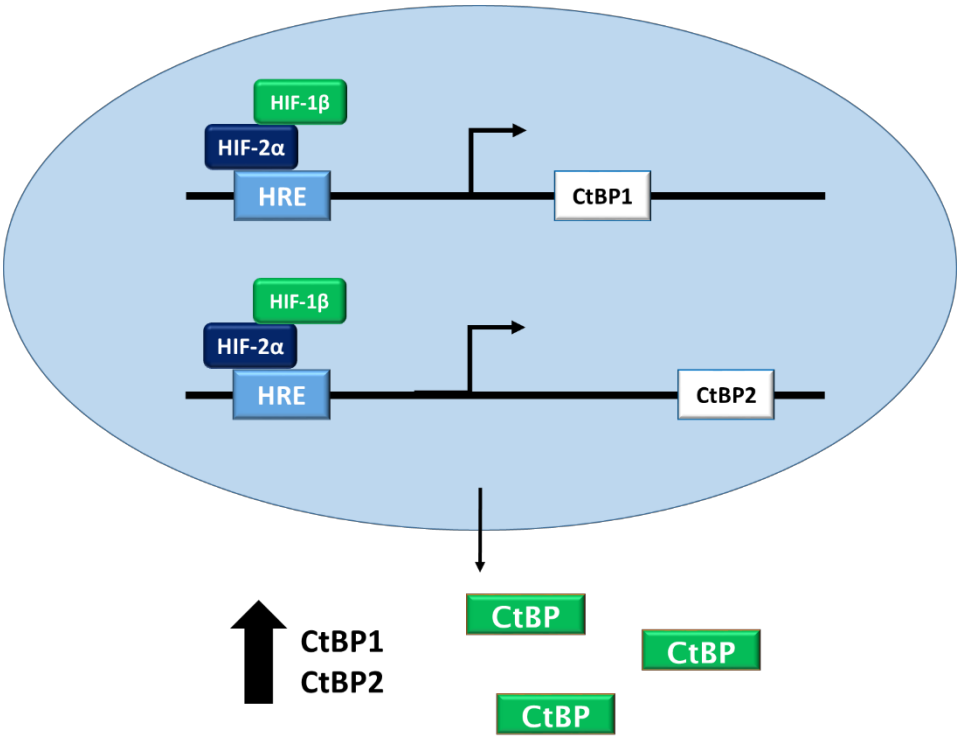

Figure 3.41. Schematic representation of hypoxic regulation of CtBPs in hESCs.
Schematic demonstrating that in hESCs maintained under hypoxia HIF-2α directly binds to the HREs in the proximal promoter region of both the CtBP1 and CtBP2 genes. That direct interaction leads to an increase in the mRNA and protein levels of CtBPs in hESCs under hypoxia.

3.4 Conclusions

In conclusion, data from this chapter has revealed that:

- Hues-7 and Shef3 hESCs express the characteristic markers associated with pluripotency at both 5% and 20% oxygen, but the expression of the core pluripotency markers are regulated by hypoxia.
- Hues-7 and Shef3 hESCs express CtBP1 and CtBP2 at both 5% and 20% oxygen in the nucleus,
- CtBP1 and CtBP2 expression is regulated by hypoxia in Hues-7 and Shef3 hESCs.
- CtBP expression is regulated by HIF-2α in Hues-7 hESCs maintained at 5% oxygen.
- HIF-2α directly binds to the proximal promoters of CtBP1 and CtBP2 to drive their expression in Hues-7 hESCs under hypoxia.

Results in this chapter have looked at how the hypoxic environment enhances influences hESC self-renewal. The next chapter is going to investigate how the metabolism of hESCs influences self-renewal, and how that builds on and links with the hypoxic effects from the results in this chapter.

Chapter 4

Glycolytic regulation of self-renewal in hESCs under hypoxia

Chapter 4: Glycolytic regulation of self-renewal in hESCs under hypoxia

4.1 Introduction

4.1.1. Glycolysis, hypoxia and pluripotency

hESCs have been shown to rely heavily on glycolysis for their energetic and biosynthetic needs. During differentiation, there is a metabolic switch from a predominantly glycolytic based metabolism to a reliance on OXPHOS (Cho et al., 2006; St John et al., 2006; Varum et al., 2011). Interestingly, the opposite switch is observed during cellular programming to produce iPSCs, where there is an increase in the amount of glucose converted into lactate and also an upregulation of genes involved in glycolysis such as GLUT1 and LDHA (Folmes et al., 2011; Panopoulos et al., 2012), followed by the increase in pluripotency marker expression. Together, this demonstrates how the metabolic state of the cell must shift to allow a change in cell identity. However, the exact mechanisms behind how glycolysis supports the acquisition of a pluripotent state in hESCs remains to be elucidated.

Both HIF-1α and HIF-2α have been extensively shown to support a glycolytic metabolism by enhancing the expression of genes involved with glycolysis including various glycolytic enzymes but also glucose transporters such as GLUTs.

4.1.2. PKM2

PKM2 regulates the 'rate-limiting' step of glycolysis at which phosphoenolpyruvate is catalysed into pyruvate. The PKM gene produces two products by alternative splicing; PKM1 and PKM2, where a key difference between the two splice isoforms is that PKM1 is only found in a tetrameric form, whereas PKM2 can be found as either a dimer or a tetramer. Interestingly, the dimeric and tetrameric forms of PKM2 have different enzymatic properties, where the dimeric form is comparatively less enzymatically active due to a much lower affinity for phosphoenolpyruvate. PKM2 is predominantly found in the dimeric form in cancer cells (Luo and Semenza, 2012). This is thought to enhance tumour growth as the lower enzymatic activity of dimeric PKM2 leads to an accumulation of glycolytic intermediates which is needed to meet the biosynthetic demands of the cell. Additionally, PKM2 has also been documented to have other functions, particularly in transcriptional regulation after previous studies found PKM2 localised to the nucleus of

cancer cells (Yang et al., 2011). Interestingly, this appeared to be only the dimeric form of PKM2 also.

Furthermore, PKM2 has previously been demonstrated to enhance the activation of HIF-1α target genes in cancer cells (Kress et al., 1998). HIF-1α has previously been demonstrated to modulate cell fate reprogramming by upregulating PKM2 in iPSCs (Prigione et al., 2014) and PKM2 has been shown to also interact with and regulate the pluripotency marker OCT4 (Lee et al., 2008; Christensen et al., 2015). However, the exact mechanisms of how PKM2 may support hESC self-renewal need to be fully characterised.

4.1.3. Chapter aims

The aims of this chapter are:

- To investigate whether inhibiting the rate of glycolysis in Hues-7 hESCs cultured at 5% oxygen affects hESC pluripotency and CtBP expression using the glycolytic inhibitors 2-deoxyglucose (2-DG), 3-bromopyruvate (3-BrP) and sodium oxamate.
- To determine whether any effects on hESC self-renewal and CtBP expression with the glycolytic inhibitors are via HIF-2α

4.2. Materials and Methods

siRNA transfections were performed as described previously in Section 2.1.6 and pharmacological treatment of hESCs with either 2-DG or 3-BrP was conducted as per Section 2.1.7. Glucose and lactate assays were performed as described in Section 2.4.2 and Section 2.4.4. qPCR and Western blotting analysis were used to identify the effects of glycolytic inhibitor addition (Figure 4.1) and siRNA transfection in Hues-7 hESCs as described in Section 2.2 and Section 2.3 respectively.

4.2.1 Treatment of Hues-7 hESCs with sodium oxamate

Hues-7 hESCs maintained on Matrigel coated plates cultured at 5% oxygen were passaged and incubated overnight in hESC culture medium. Cells were incubated with either 0mM or 10mM oxamate-supplemented CM for 48 hours in 6-well plates. Sodium oxamate stock (Sigma) was prepared fresh each day. Cells were supplied with 2ml of fresh oxamate-supplemented media per well of a 6-well plate on day 1 and day 2 post-passage, before collecting samples for either RNA or protein analysis on day 3 post-passage.

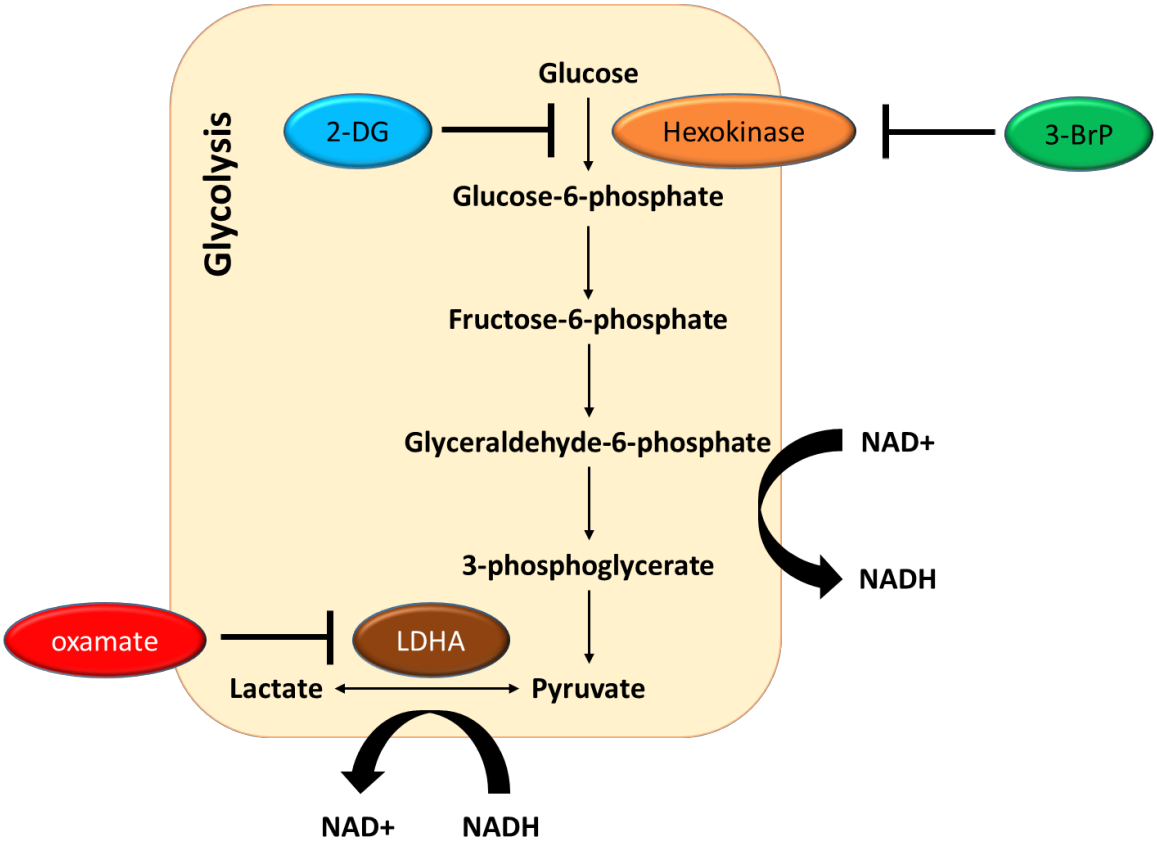

Figure 4.1. Schematic of glycolytic inhibitors used and their targets.
Schematic demonstrating the action of the glycolytic inhibitors. 2-deoxyglucose (2-DG) and 3-bromopyruvate (3-BrP) both target hexokinase. 2-DG reduces the rate of flux through glycolysis by acting as a glucose analogue and a competitive inhibitor of hexokinase, whereas 3-BrP inhibits hexokinase by alkylation. Sodium oxamate functions further downstream in the glycolysis pathway and is a pyruvate analogue to inhibit the action of lactate dehydrogenase A (LDHA).

4.3 Results

4.3.1 Effects of inhibiting glycolytic metabolism in hESCs cultured at 5% oxygen with 2-deoxyglucose

It is well documented that hESCs use glycolysis to maintain pluripotency, and previous studies have demonstrated that hESCs cultured in a less glycolytic environment expressed lower levels of the core pluripotency factors OCT4, SOX2 and NANOG (Ezashi et al., 2005; Westfall et al., 2008; Forristal et al., 2010). To investigate whether altering the rate of glycolysis in Hues-7 hESCs affected the expression of pluripotency markers, Hues-7 hESCs maintained at 5% oxygen were cultured with MEF-conditioned medium (CM) supplemented with increasing concentrations of the glycolytic inhibitor 2-deoxyglucose (2-DG) for 48 hours before collecting cells for RT-qPCR analysis and Western blotting.

4.3.1.1. Morphological characterisation of Hues-7 hESCs incubated with 2-deoxyglucose

Cells treated with either 0.2mM, 1mM or 10mM 2-DG formed compact colonies with typical cobblestone morphology that were comparative to the 0mM 2-DG control after both 24 hours and 48 hours of treatment as demonstrated through representative phase contrast images, where there appeared to be no clear effect on growth rate (Figure 4.2A-H and Figure 4.3A-H). However, cells treated with 30mM 2-DG revealed distinctly smaller colonies compared to the 0mM 2-DG dose. Furthermore, cells treated with 30mM 2-DG formed ‘patchy’ colonies with a distinctly more fibroblastic morphology, indicative of that concentration being toxic to hESCs (Figure 4.2J and Figure 4.3J).

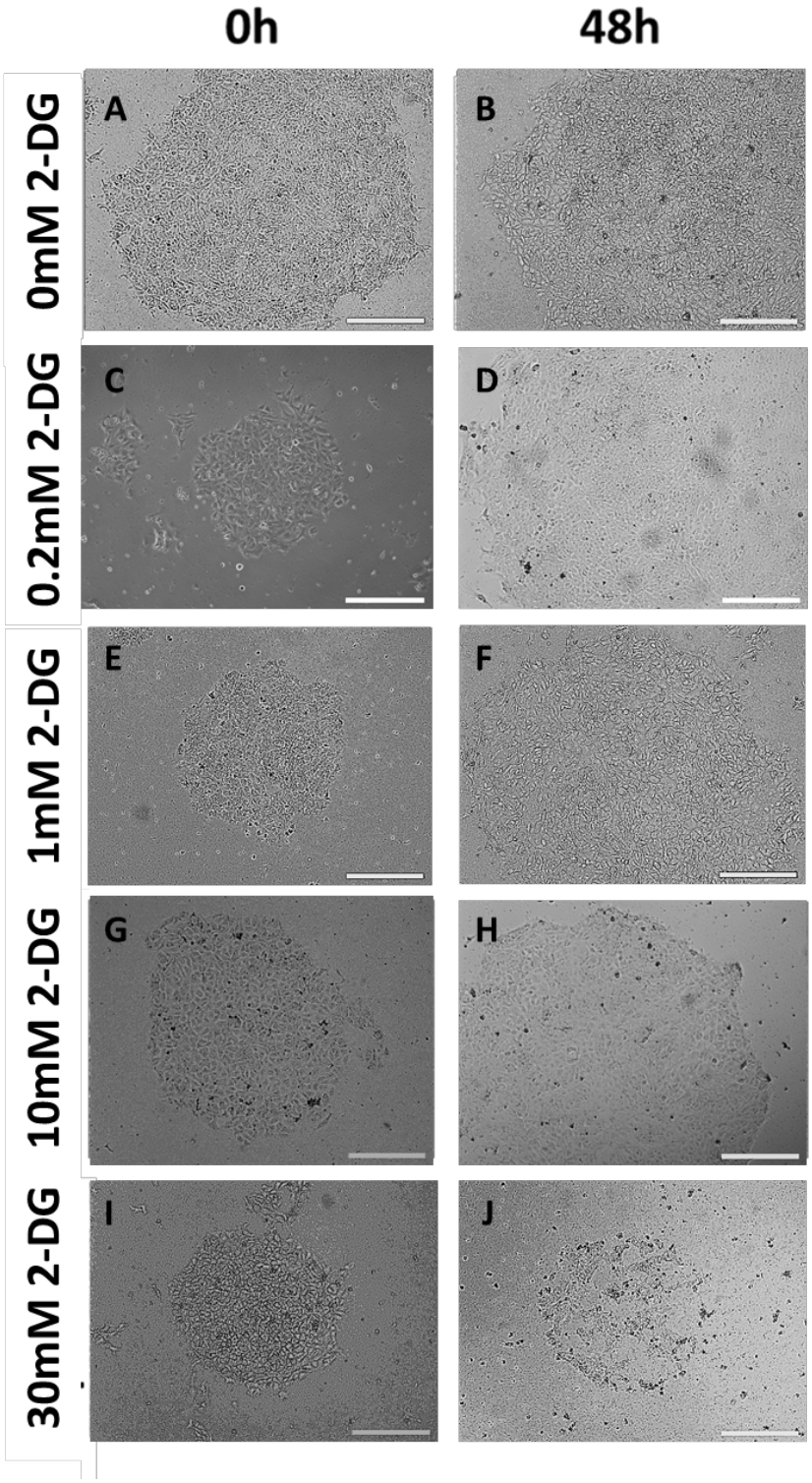

Figure 4.2. Phase contrast images demonstrating colony morphology of Hues-7 hESCs cultured at 5% oxygen in 2-DG supplemented MEF-conditioned medium.
Representative phase contrast images of Hues-7 hESCs cultured at 5% oxygen in MEF-conditioned medium supplemented with either 0mM (A-B) 0.2mM (C-D), 1mM (E-F), 10mM (G-H) or 30mM 2-DG (I-J) after 0 and 48 hours. Scale bar indicates 200μm.

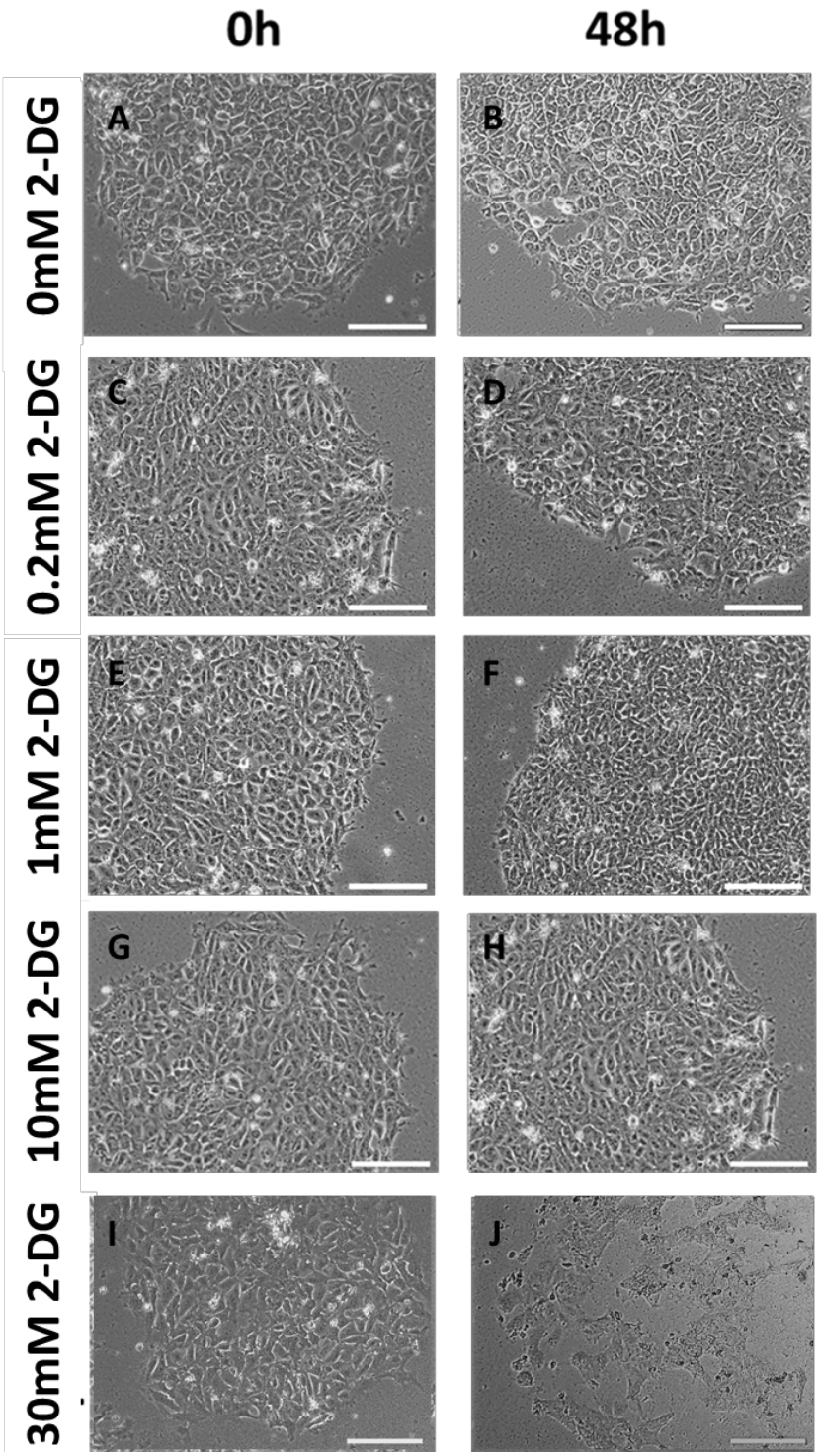

Figure 4.3. Phase contrast images demonstrating the cellular morphology of Hues-7 hESCs cultured at 5% oxygen in 2-DG supplemented MEF-conditioned medium.
Representative phase contrast images of Hues-7 hESCs cultured at 5% oxygen in MEF-conditioned medium supplemented with either 0mM (A-B) 0.2mM (C-D), 1mM (E-F), 10mM (G-H) or 30mM 2-DG (I-J) after 0 and 48 hours. Scale bar indicates 100μm.

4.3.1.2. Measurement of lactate production in Hues-7 hESCs incubated with 2-deoxyglucose

To determine whether there was any impact of increasing 2-DG concentrations on the rate of lactate production in Hues-7 hESCs maintained at 5% oxygen, a dose response curve of lactate production was produced using the optimised lactate assay.

A significant reduction in lactate production in Hues-7 hESCs maintained at 5% oxygen was only observed at the highest, 10mM, concentration of 2-DG, and this conclusion was used for further investigation.

No significant difference in lactate production was measured with the addition of 0.2mM (p=0.8189) or 1mM 2-DG (p=0.5864) compared to cells cultured in the absence of 2-DG. However, the rate of lactate production did appear to be starting to decrease with an approximate 11% decrease in lactate production in Hues-7 hESCs incubated with 1mM 2-DG compared to the control cells. A significant and approximate 67% reduction (p=0.0046) in the rate of lactate production was observed in Hues-7 hESCs incubated with 10mM 2-DG compared to hESCs cultured in the absence of 2-DG (Figure 4.4).

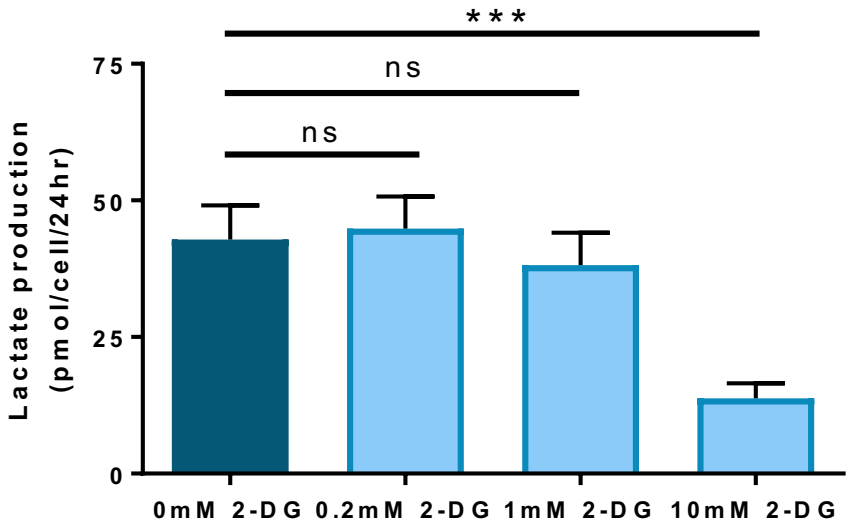

Figure 4.4. Lactate production is significantly reduced in Hues-7 hESCs cultured at 5% oxygen treated with 2-DG.
Quantification of the rate of lactate production in Hues-7 hESCs maintained with either 0mM, 0.2mM, 1mM or 10mM 2-DG for 48 hours prior to collecting media samples for use in the enzyme-linked assays. Bars represent mean ± SEM. (n=15)

4.3.1.3. Characterisation of pluripotency and differentiation marker expression in Hues-7 hESCs incubated with 2-deoxyglucose

To investigate the effects of glycolytic rate on the mRNA expression levels of pluripotency markers, RT-qPCR was performed using Hues-7 cells maintained at 5% oxygen treated with either 0mM, 0.2mM, 1mM or 10mM 2-DG for 48 hours. *OCT4*, *SOX2*, *NANOG, LIN28B* and *SALL4* were expressed in Hues-7 hESCs treated with all 2-DG concentrations. However, quantification of the relative mRNA expression levels revealed a significant decrease in the mRNA expression of all pluripotency markers only in 10mM 2-DG treated cells compared to those treated with 0mM 2-DG (Figure 4.5).

There was no significant difference in the expression of any of the pluripotency markers in Hues-7 hESCs incubated with either 0.2mM or 1mM 2-DG. However, it was observed that in hESCs treated with 1mM 2-DG the expression of *OCT4*, *SOX2*, *NANOG* and *SALL4* was beginning to decrease similarly to the rate of lactate production. hESCs treated with 10mM 2-DG displayed a 58% decrease in *OCT4* expression ($p=0.0009$), a 51% decrease in *SOX2* expression ($p=0.0121$), a 45% reduction in *NANOG* mRNA levels ($p=0.0197$), a 52% decrease in *LIN28B* expression ($p=0.0441$) and a 57% reduction in *SALL4* mRNA expression ($p=0.0426$) compared to hESCs incubated in the absence of 2-DG under hypoxia.

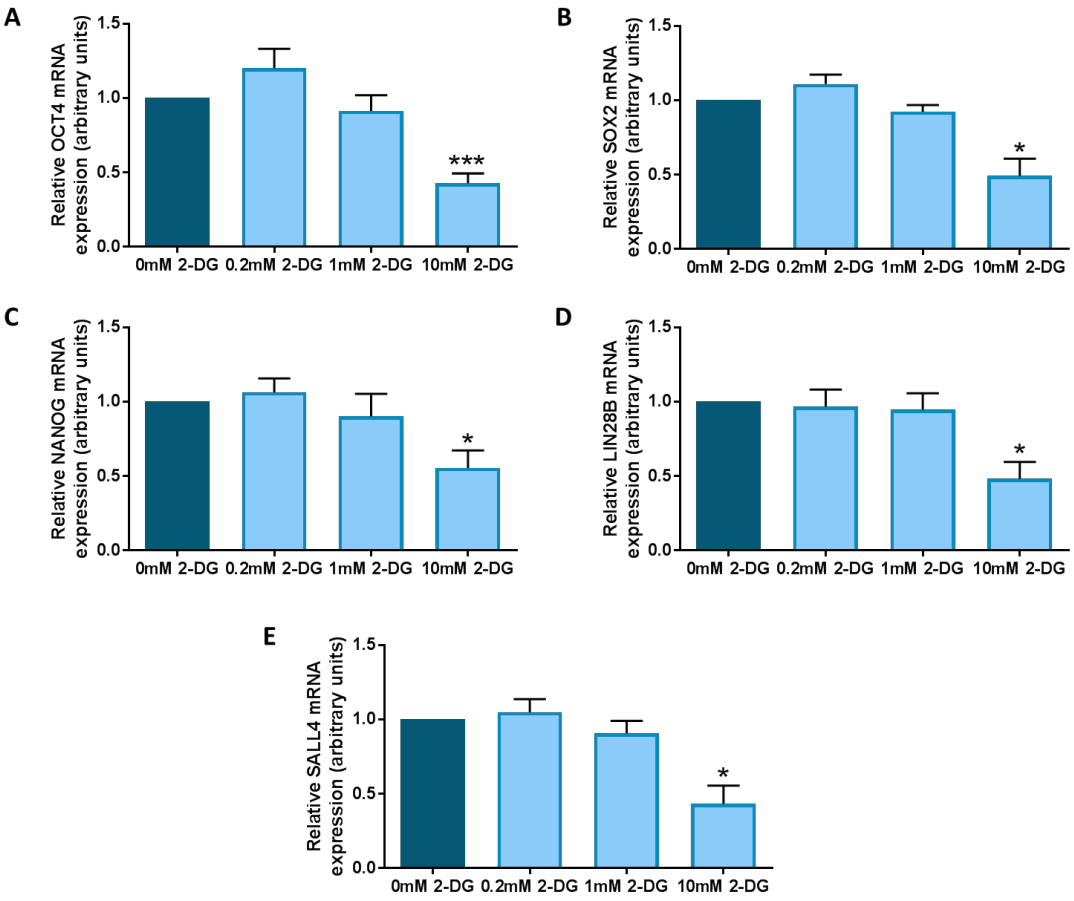

Figure 4.5. Decreasing the rate of glycolysis in Hues-7 hESCs cultured at 5% oxygen using the glycolytic inhibitor 2-DG reduces the mRNA expression levels of pluripotency markers. Hues-7 hESCs cultured at 5% oxygen in MEF-conditioned media supplemented with 10mM 2-DG only displayed a significant decrease in *OCT4* (A), *SOX2* (B), *NANOG* (C), *LIN28B* (D) and *SALL4* (E) mRNA expression levels compared to the 0mM 2-DG control. Data were normalised to *UBC*, and then to 1 for 0mM 2-DG control. Bars represent mean ± SEM. (n=3-5)

Quantification of the OCT4, SOX2 and NANOG protein expression revealed a significant dose-dependent decrease in the protein expression of the three core pluripotency markers in Hues-7 hESCs maintained at 5% oxygen cultured with increasing 2-DG concentration (Figure 4.6B). Hues-7 hESCs cultured with 10mM 2-DG for 48 hours displayed an approximate 60% reduction in OCT4 (p=0.0318), SOX2 (p=0.0479) and an approximate 80% decrease in NANOG (p=0.0041) protein expression compared to cells treated with 0mM 2-DG. Furthermore, Hues-7 hESCs treated with 30mM 2-DG for 48 hours displayed an approximate 80% decrease in OCT4 (p=0.0011), 70% decrease in SOX2 (p=0.0386) and 90% reduction in NANOG (p=0.0015) protein expression compared to the 0mM 2-DG control.

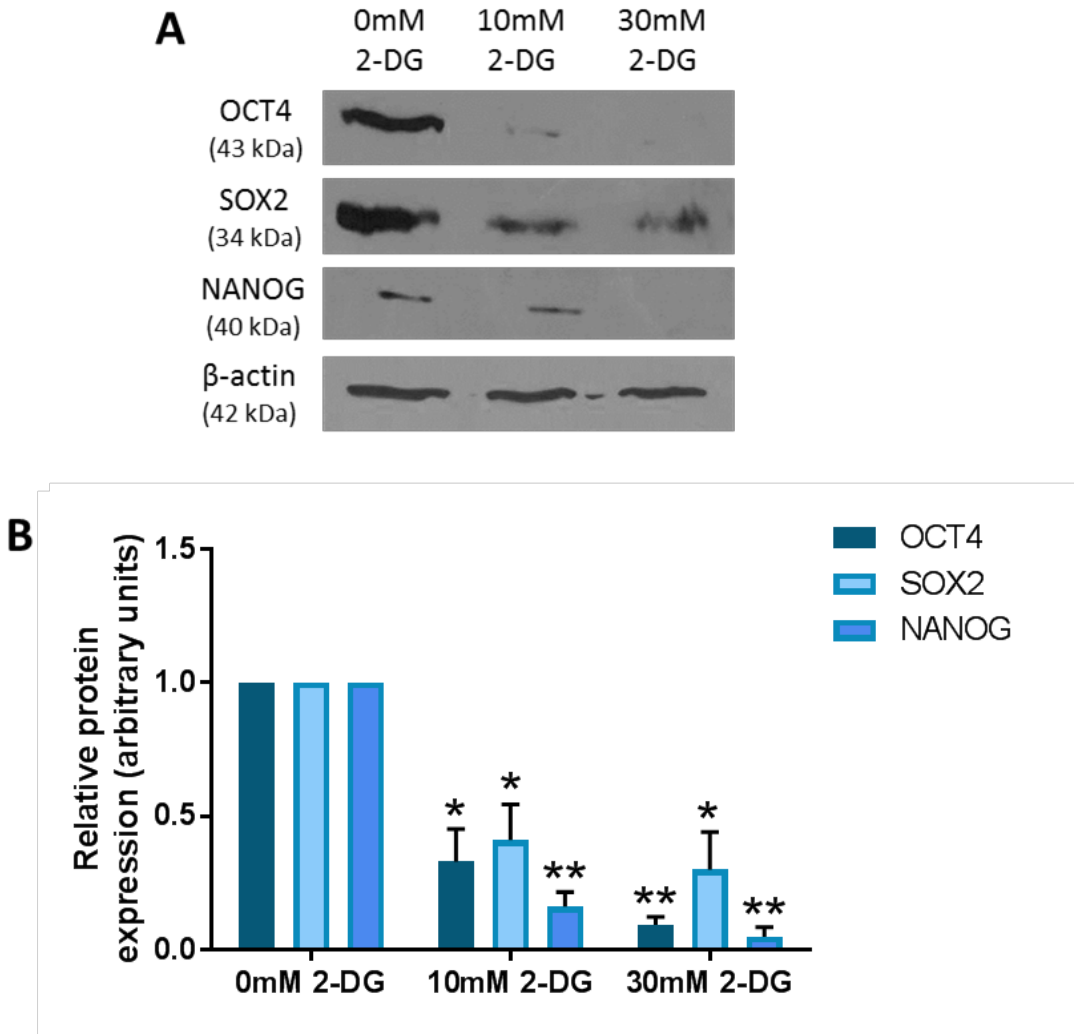

Figure 4.6. Pluripotency marker protein expression is affected by changes in glycolytic rate using the glycolytic inhibitor 2-DG in Hues-7 hESCs cultured at 5% oxygen in a dose-dependent manner.

(A) Representative Western blots of OCT4, SOX2 and NANOG expression in Hues-7 hESCs cultured at 5% oxygen in MEF-conditioned media supplemented with either 0mM, 10mM or 30mM 2-DG. (B) Quantification of OCT4, SOX2 and NANOG Western blots revealed a dose-dependent significant decrease in the protein expression of the three pluripotency factors with increasing 2-DG concentration. Data were normalised to β-actin, and then to 1 for 0mM 2-DG control. Bars represent mean ± SEM. (n=3)

To further support the observed loss of pluripotency in Hues-7 hESCs maintained under hypoxia and incubated with 10mM 2-DG, RT-qPCR was performed to analysis the expression of a panel of early differentiation markers representing all three developmental germ layers.

In concordance with the pluripotency gene expression, the expression of *SOX17* (Figure 4.7A), *GATA4* (Figure 4.7B), *SOX1* (Figure 4.7C), *PAX6* (Figure 4.7D), *BMP4* (Figure 4.7E), *CXCR4* (Figure 4.7F) and *KDR* (Figure 4.7G) significantly increased in Hues-7 hESCs incubated only with 10mM 2-DG compared to those cultured without 2-DG.

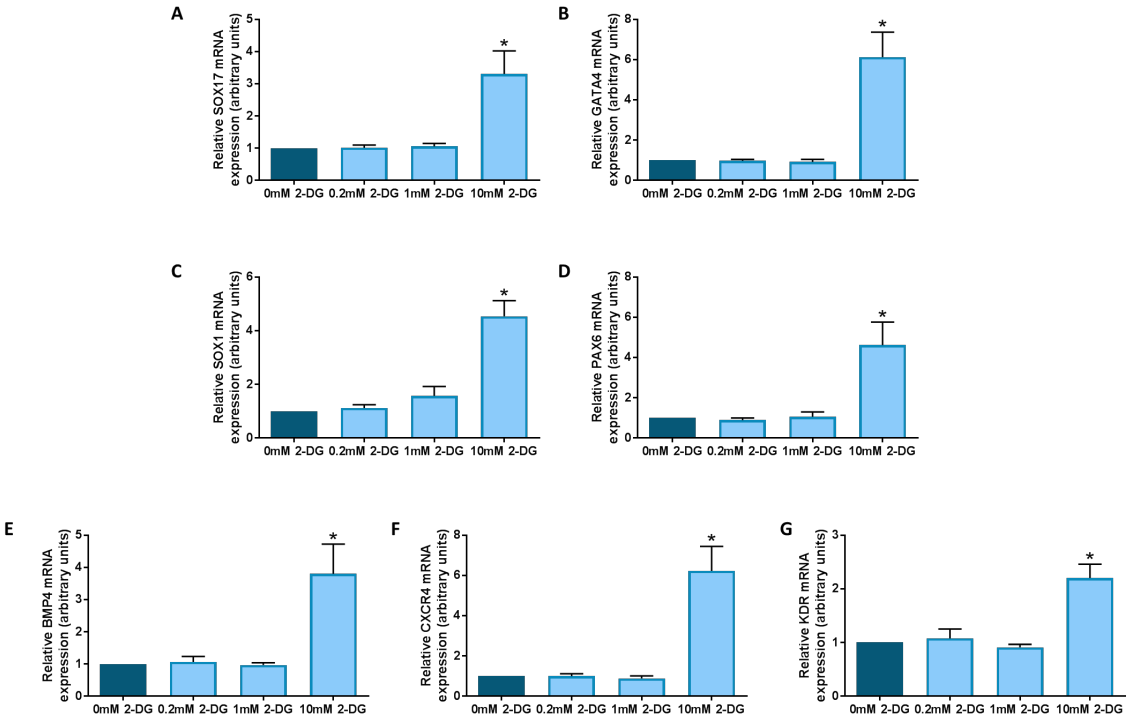

Figure 4.7. Expression of a panel of early differentiation markers increases in Hues-7 hESCs treated with 2-DG at 5% oxygen.
Hues-7 hESCs cultured at 5% oxygen in MEF-conditioned media supplemented with 10mM 2-DG only displayed a significant increase in *SOX17* (A), *GATA4* (B), *SOX1* (C), *PAX6* (D), *BMP4* (E), *CXCR4* (F) and *KDR* (G) mRNA expression levels compared to the 0mM 2-DG control. Data were normalised to *β-actin* for primers and *UBC* for probes, and then to 1 for 0mM 2-DG control. Bars represent mean ± SEM. (n=3-5)

4.3.1.4. Characterisation of gene expression associated with glycolysis in Hues-7 hESCs incubated with 2-deoxyglucose

To evaluate whether reducing the rate of flux through glycolysis affected the expression of glycolytic enzymes, glucose transporters or the metabolic sensors CtBPs, RT-qPCR and Western blotting were performed in Hues-7 hESCs incubated for 48 hours with increasing concentrations of 2-DG under hypoxic conditions.

RT-qPCR analysis revealed that the mRNA expression of the glycolytic enzyme *LDHA*, and the glucose transporters *GLUT1* and *GLUT3* significantly decreased in Hues-7 hESCs treated with only 10mM 2-DG compared to those incubated with 0mM 2-DG (Figure 4.8).

No significant difference in the mRNA expression of any of the genes of interest was, again, observed between hESCs incubated with either 0mM, 0.2mM or 1mM 2-DG. However, *LDHA, GLUT1* and *GLUT3* mRNA expression levels was significantly decreased by approximately 65% ($p=0.0027$), 39% ($p=0.029$) and 33% ($p=0.0106$) respectively in hESCs incubated with 10mM 2-DG compared to those in the absence of 2-DG.

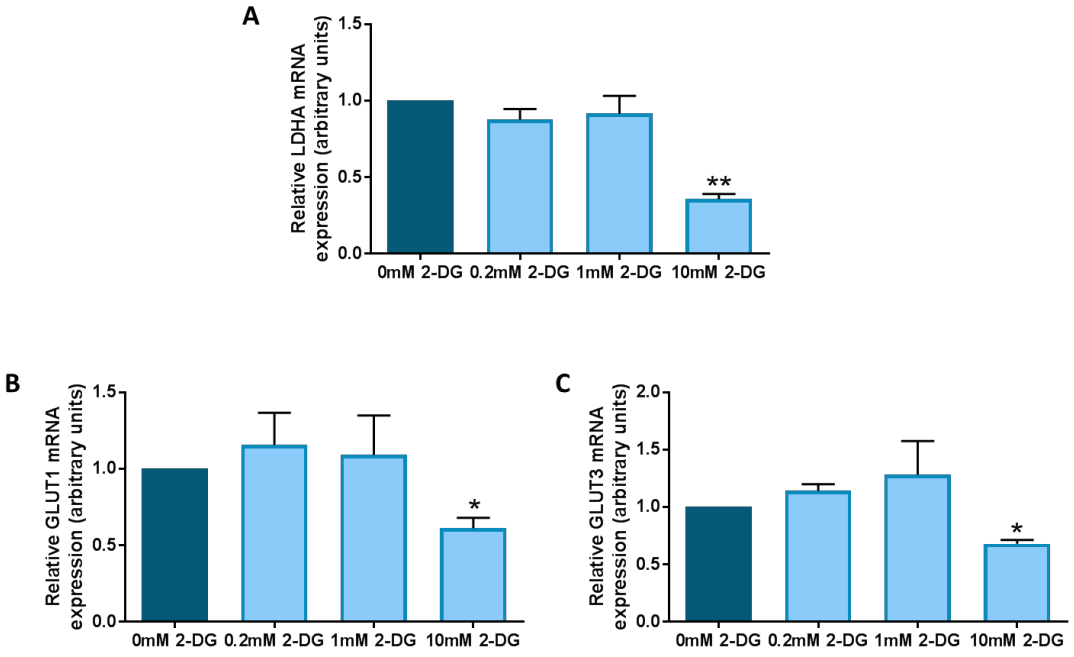

Figure 4.8. Decreasing the rate of glycolysis using the glycolytic inhibitor 2-DG reduces the expression of glycolytic enzymes and glucose transporters in hESCs maintained under hypoxia.
Hues-7 hESCs cultured at 5% oxygen in MEF-conditioned media supplemented with 10mM 2-DG only displayed a significant decrease in *LDHA* (A), *GLUT1* (B) and *GLUT3* (C) mRNA expression levels compared to the 0mM 2-DG control. Data were normalised to *β-actin* for primers and *UBC* for probes, and then to 1 for 0mM 2-DG control. Bars represent mean ± SEM. (n=3-4)

To investigate whether changing the rate of glycolysis in Hues-7 hESCs affected the expression of CtBPs, as well as pluripotency gene expression, CtBP mRNA and protein expression levels were quantified in Hues-7 hESCs cultured at 5% oxygen with CM supplemented with either 0mM, 0.2mM, 1mM, 10mM or 30mM 2-DG concentrations for 48 hours.

Interestingly, quantification of relative *CtBP* mRNA expression revealed the mRNA expression of both *CtBP1* ($p=0.0247$) and *CtBP2* ($p=0.0325$) isoforms was significantly reduced by approximately 50% in 10mM 2-DG treated cells compared to those treated with 0mM 2-DG (Figure 4.9).

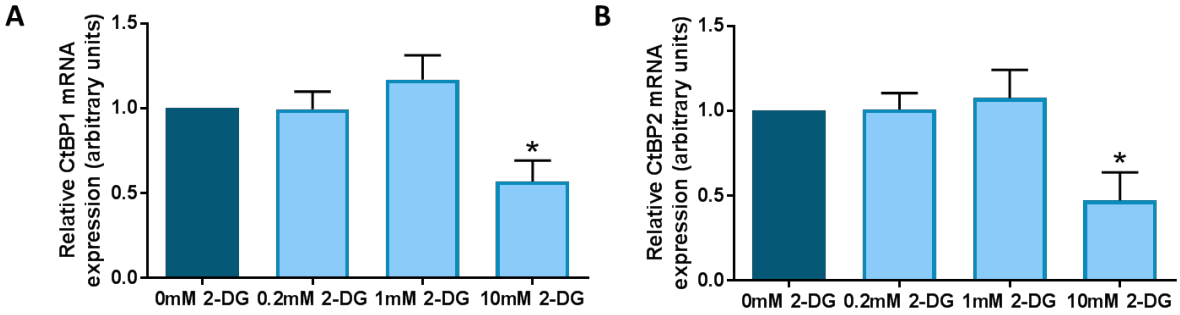

Figure 4.9. Decreasing the rate of glycolysis using the glycolytic inhibitor 2-DG reduces CtBP mRNA expression in Hues-7 hESCs maintained at 5% oxygen.
Hues-7 hESCs cultured at 5% oxygen tension in MEF-conditioned media supplemented with 10mM 2-DG only displayed a significant decrease in both *CtBP1* (A) and *CtBP2* (B) mRNA expression levels compared to the 0mM 2-DG control. Data were normalised to *UBC*, and then to 1 for 0mM 2-DG control. Bars represent mean ± SEM. (n=4-5)

Quantification revealed that CtBP1 and CtBP2 protein levels significantly decreased in a dose-dependent manner in Hues-7 hESCs maintained at 5% oxygen treated with increasing 2-DG concentrations (Figure 4.10B). Hues-7 hESCs treated with 10mM 2-DG for 48 hours displayed an approximate 60% reduction in CtBP1 ($p=0.0410$) and an approximate 80% decrease in CtBP2 ($p=0.0384$) protein expression compared to cells treated with 0mM 2-DG. Moreover, Hues-7 hESCs treated with 30mM 2-DG for 48 hours displayed an approximate 90% and 95% decrease in CtBP1 ($p=0.0043$) and CtBP2 ($p=0.0004$) protein expression respectively compared to the 0mM 2-DG control.

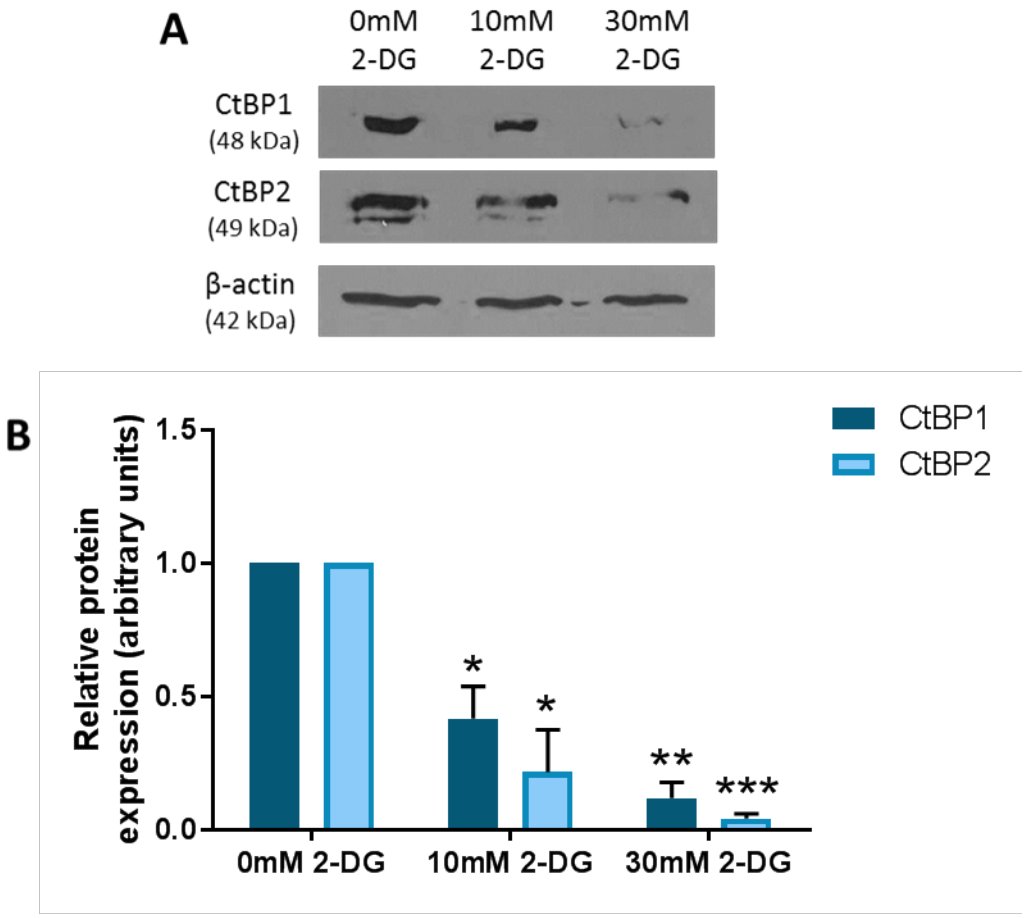

Figure 4.10. CtBP protein expression is affected by changes in glycolytic rate using the glycolytic inhibitor 2-DG in Hues-7 hESCs cultured at 5% oxygen in a dose-dependent manner.

(A) Representative Western blots of CtBP1 and CtBP2 expression in Hues-7 hESCs cultured at 5% oxygen in MEF-conditioned media supplemented with either 0mM, 10mM or 30mM 2-DG. (B) Quantification of CtBP1 and CtBP2 Western blots revealed a dose-dependent significant decrease in the protein expression of both CtBP isoforms with increasing 2-DG concentration. Data were normalised to β-actin, and then to 1 for 0mM 2-DG control. Bars represent mean ± SEM. (n=3)

4.3.1.5. Characterisation of HIF-2α expression in Hues-7 hESCs incubated with 2-deoxyglucose

Previous published studies and data in this thesis have demonstrated that pluripotency marker and glycolysis associated gene expression is directly regulated by HIF-2α. Additionally, data presented in this study has revealed that reducing the rate of glycolytic flux, also regulates the expression of pluripotency and glycolytic gene expression. Therefore, to determine whether these changes in pluripotency marker, glycolytic enzyme, glucose transporter and CtBP expression as a result of reducing the rate of glycolysis was through HIF-2α regulation, the mRNA and protein expression of HIF-2α in Hues-7 hESCs incubated with increasing 2-DG concentrations was analysed.

Interestingly, qPCR analysis of *HIF-2α* expression revealed a significant reduction in *HIF-2α* mRNA expression only with the highest 10mM 2-DG concentration (Figure 4.11). No significant difference was, again, observed in *HIF-2α* expression between hESCs incubated with 0mM, 0.2mM and 1mM 2-DG. However, *HIF-2α* expression significantly reduced by 74% in Hues-7 hESCs maintained under hypoxia and incubated with 10mM 2-DG compared to the control cells.

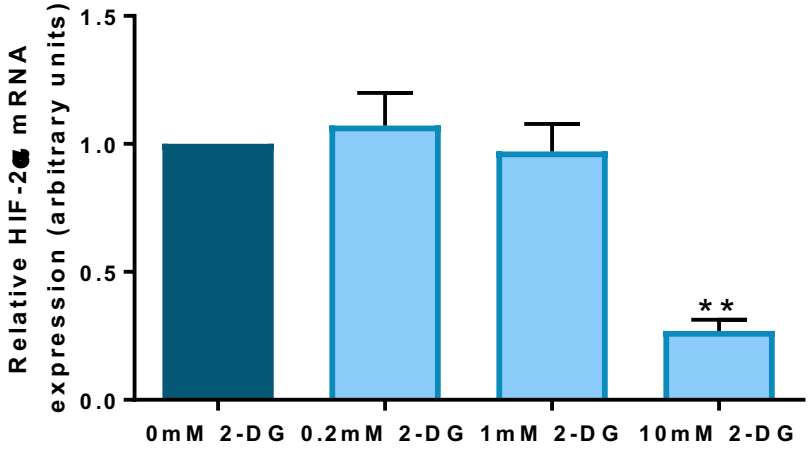

Figure 4.11. Decreasing the rate of glycolysis using 2-DG reduces HIF-2α expression in Hues-7 hESCs maintained at 5% oxygen.
Hues-7 hESCs cultured at 5% oxygen tension in MEF-conditioned media supplemented with 10mM 2-DG only displayed a significant decrease in *HIF-2α* mRNA expression levels compared to the 0mM 2-DG control. Data were normalised to *UBC*, and then to 1 for 0mM 2-DG control. Bars represent mean ± SEM. (n=4-5)

Quantification of HIF-2α protein expression revealed the same trend. HIF-2α protein expression significantly decreased by 85% when Hues-7 hESCs were incubated with 10mM 2-DG compared to when they were incubated without 2-DG (Figure 4.12B).

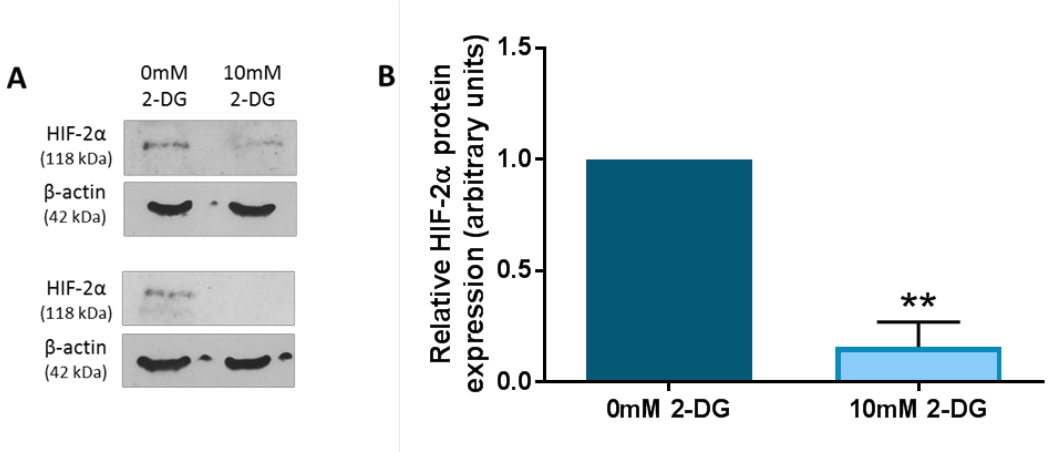

Figure 4.12. HIF-2α protein expression is affected by changes in glycolytic rate using 2-DG in Hues-7 hESCs cultured at 5% oxygen.
(A) Representative Western blots of HIF-2α expression in Hues-7 hESCs cultured at 5% oxygen in MEF-conditioned media supplemented with either 0mM or 10mM 2-DG. (B) Quantification of HIF-2α Western blots revealed a significant decrease in the protein expression of HIF-2α in the presence of 2-DG compared to the control cells. Data were normalised to β-actin, and then to 1 for 0mM 2-DG control. Bars represent mean ± SEM. (n=3)

4.3.1.6. Effects of inhibiting glycolysis with 2-deoxyglucose in Shef3 hESCs

To determine whether the observed effects of inhibiting glycolysis on hESC pluripotency, glycolytic gene and HIF-2α expression were not cell line specific, cells of the Shef3 hESC line were maintained under hypoxia and incubated with either 0mM or 10mM 2-DG before collecting samples for Western blotting analysis.

Shef3 hESCs treated with 10mM 2-DG formed compact colonies with typical cobblestone morphology that were comparative to the control cells incubated in the absence of 2-DG after 48 hours (Figure 4.13).

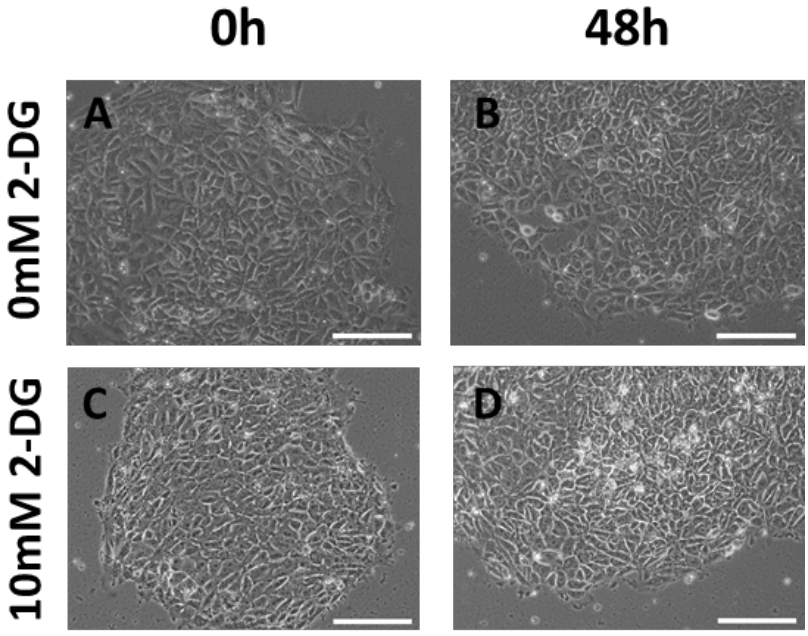

Figure 4.13. Phase contrast images demonstrating colony morphology of Shef3 hESCs cultured at 5% oxygen in 2-DG supplemented MEF-conditioned medium.
Representative phase contrast images of Shef3 hESCs cultured at 5% oxygen in MEF-conditioned medium supplemented with either 0mM (A-B) or 10mM 2-DG (C-D) after 48 hours. Scale bar indicates 200μm.

Quantification of the OCT4, SOX2 and NANOG protein expression revealed a significant decrease in the protein expression of the three core pluripotency markers in Shef3 hESCs maintained at 5% oxygen cultured in the presence of the glycolytic inhibitor 2-DG (Figure 4.14B). Shef3 hESCs cultured with 10mM 2-DG for 48 hours displayed an approximate 55% reduction in OCT4 ($p=0.0155$), an 82% reduction in SOX2 ($p=0.0025$) and an approximate 80% decrease in NANOG ($p=0.0152$) protein expression compared to cells treated with 0mM 2-DG.

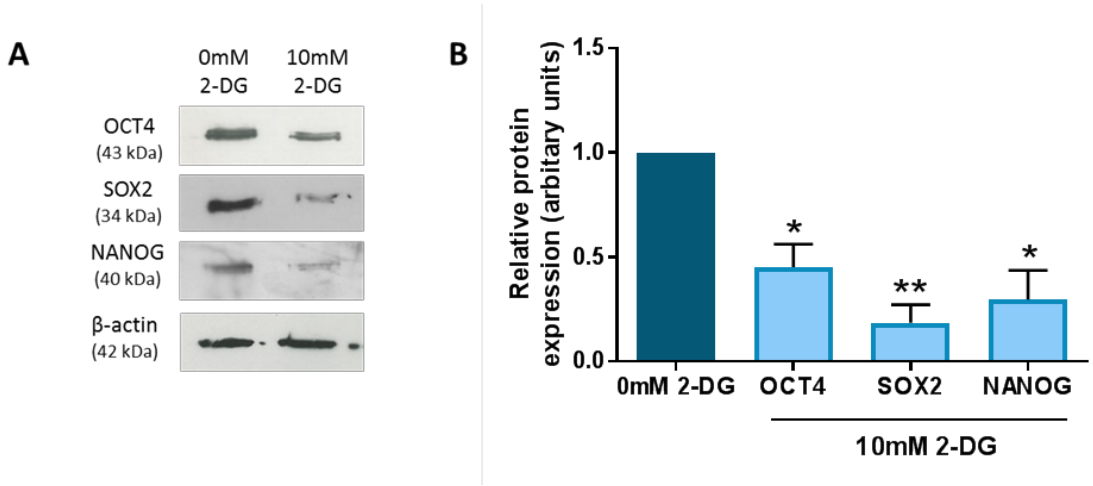

Figure 4.14. Pluripotency marker protein expression is affected by changes in glycolytic rate using the glycolytic inhibitor 2-DG in Shef3 hESCs cultured at 5% oxygen.
(A) Representative Western blots of OCT4, SOX2 and NANOG expression in Shef3 hESCs cultured at 5% oxygen in MEF-conditioned media supplemented with either 0mM or 10mM 2-DG. (B) Quantification of OCT4, SOX2 and NANOG Western blots revealed a significant decrease in the protein expression of the three pluripotency factors in the presence of 2-DG compared to the control cells. Data were normalised to β-actin, and then to 1 for 0mM 2-DG control. Bars represent mean ± SEM. (n=4)

Quantification revealed that CtBP1 and CtBP2 protein levels significantly decreased in Shef3 hESCs maintained at 5% oxygen incubated with 10mM 2-DG compared to the control cells (Figure 4.15B). Shef3 hESCs treated with 10mM 2-DG for 48 hours displayed a 41% reduction in CtBP1 ($p=0.0339$) and a 74% decrease in CtBP2 ($p=0.0197$) protein expression compared to cells treated with 0mM 2-DG.

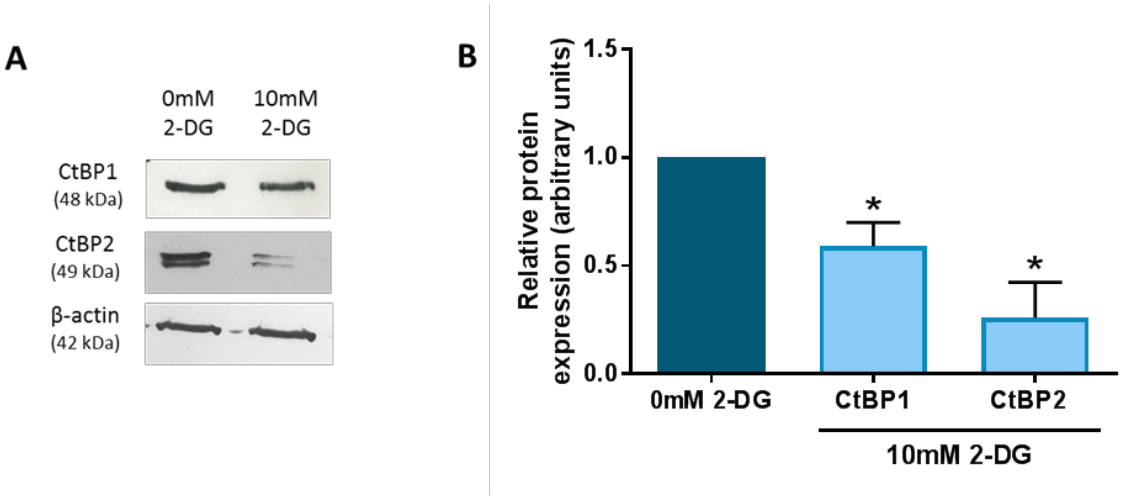

Figure 4.15. CtBP protein expression is affected by changes in glycolytic rate using the glycolytic inhibitor 2-DG in Shef3 hESCs cultured at 5% oxygen in a dose-dependent manner.

(A) Representative Western blots of CtBP1 and CtBP2 expression in Shef3 hESCs cultured at 5% oxygen in MEF-conditioned media supplemented with either 0mM or 10mM 2-DG. (B) Quantification of CtBP Western blots revealed a significant decrease in the protein expression of both CtBP1 and CtBP2 in the presence of 2-DG compared to the control cells. Data were normalised to β-actin, and then to 1 for 0mM 2-DG control. Bars represent mean ± SEM. (n=4)

HIF-2α protein expression was, also, found to be significantly less in Shef3 hESCs incubated with 10mM 2-DG compared to Shef3 hESCs incubated with 0mM 2-DG (Figure 4.16). Quantification of HIF-2α protein expression revealed a significant decreased by 81% ($p=0.0207$) when Shef3 hESCs were incubated with 10mM 2-DG compared to when they were incubated without 2-DG (Figure 4.16B).

Taken together, this data demonstrates that the effects of inhibiting glycolysis under hypoxia are not cell line specific, but common across hESC lines.

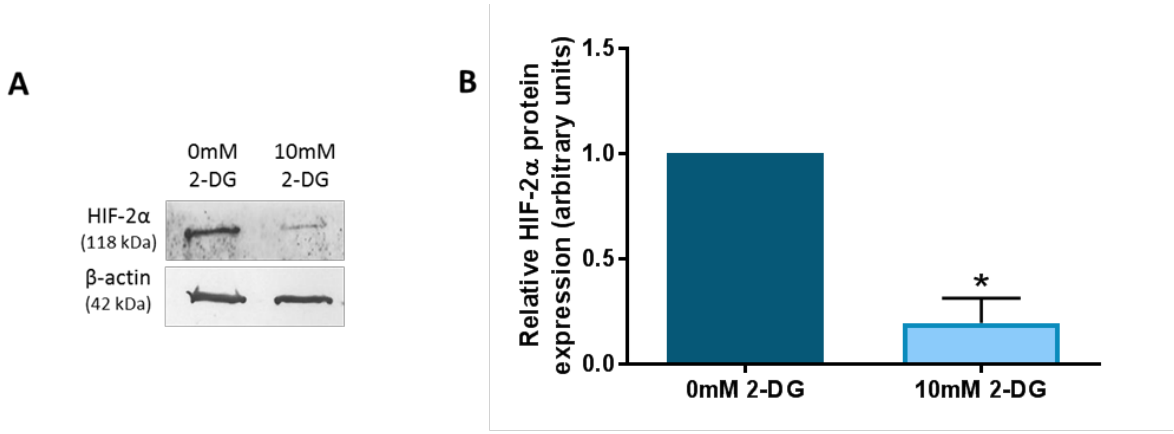

Figure 4.16. HIF-2α protein expression is affected by changes in glycolytic rate using 2-DG in Shef3 hESCs cultured at 5% oxygen.
(A) Representative Western blots of HIF-2α expression in Shef3 hESCs cultured at 5% oxygen in MEF-conditioned media supplemented with either 0mM or 10mM 2-DG. (B) Quantification of HIF-2α Western blots revealed a significant decrease in the protein expression of HIF-2α in the presence of 2-DG compared to the control cells. Data were normalised to β-actin, and then to 1 for 0mM 2-DG control. Bars represent mean ± SEM. (n=3)

4.3.2. Effects of inhibiting glycolytic metabolism in Hues-7 hESCs cultured at 20% oxygen with 2-deoxyglucose

Regardless of environmental oxygen tension, hESCs display a highly glycolytic phenotype. Therefore, experiments were conducted to determine whether the effects of inhibiting glycolysis on pluripotency marker and CtBP expression observed under hypoxia also occurred under normoxic oxygen tensions. To investigate the effects altering the rate of glycolysis in Hues-7 hESCs maintained under 20% oxygen, cells were incubated with the glycolytic inhibitor 2-deoxyglucose (2-DG) for 48 hours before collecting cells for RT-qPCR analysis and Western blotting.

Cells were treated with either 0mM, 5mM or 10mM 2-DG. hESCs incubated with 5mM 2-DG formed compact colonies with clearly defined edges (Figure 4.17C-D) similar to colonies maintained in the absence of 2-DG (Figure 4.17A-B). Furthermore, Hues-7 hESCs maintained under 20% oxygen and incubated with 10mM 2-DG displayed a distinctly smaller colony size compared to the control cells after 48 hours. Additionally, cells cultured with 10mM 2-DG for 48 hours displayed a 'patchy' colony morphology, indicative of that concentration being toxic to cells (Figure 4.17E-F).

It was noted that the 10mM 2-DG concentration used to inhibit glycolysis in Hues-7 hESCs under hypoxia was toxic for Hues-7 hESCs maintained under normoxic oxygen concentrations. This is probably reflected by the fact that although cells maintained under 20% oxygen are still highly reliant on glycolysis, the rate of flux through glycolysis in those cells is significantly less than hESCs maintained under hypoxia. Therefore, the 5mM 2-DG concentration was used for further investigation in hESCs maintained under 20% oxygen.

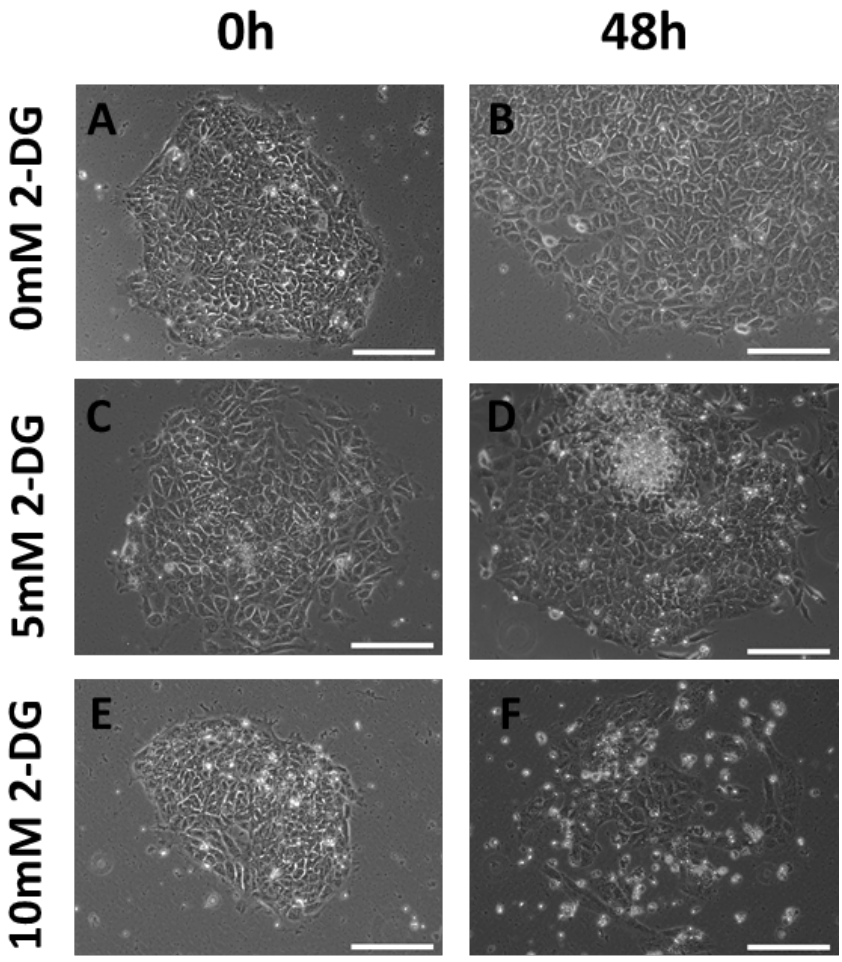

Figure 4.17. Phase contrast images demonstrating colony morphology of Hues-7 hESCs cultured at 20% oxygen in 2-DG supplemented MEF-conditioned medium.
Representative phase contrast images of Hues-7 hESCs cultured at 20% oxygen in MEF-conditioned medium supplemented with either 0mM (A-B), 5mM (C-D) or 10mM 2-DG (E-F) after 48 hours. Scale bar indicates 200μm.

Western blots were performed to analysis the effect of adding 5mM 2-DG on pluripotency marker expression in hESCs at 20% oxygen. Representative Western blots revealed protein bands of approximately 43kDa, 34kDa and 40kDa for OCT4, SOX2 and NANOG respectively in hESCs incubated with either 0mM or 5mM 2-DG. However, those protein bands were much less prevalent in hESCs incubated with 5mM 2-DG compared to the control (Figure 4.18A). Quantification of those bands revealed a significant reduction in the expression of OCT4, SOX2 and NANOG by 72% (p=0.0165), 90% (p=0.0011) and 67% (p=0.0061) respectively in Hues-7 hESCs treated with 5mM 2-DG compared to those cultured in the absence of 2-DG (Figure 4.18B).

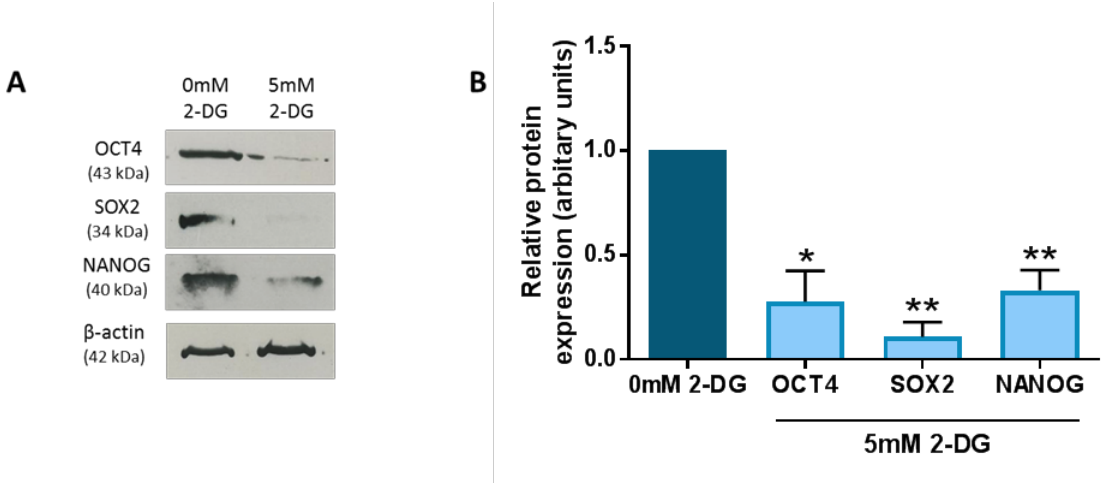

Figure 4.18. Pluripotency marker expression is affected by changes in glycolytic rate using 2-DG in Hues-7 hESCs cultured at 20% oxygen.
(A) Representative Western blots of OCT4, SOX2 and NANOG expression in Hues-7 hESCs cultured at 20% oxygen in MEF-conditioned media supplemented with either 0mM or 5mM 2-DG. (B) Quantification of OCT4, SOX2 and NANOG Western blots revealed a significant decrease in the protein expression of the three pluripotency factors in the presence of 2-DG compared to the control cells under normoxic conditions. Data were normalised to β-actin, and then to 1 for 0mM 2-DG control. Bars represent mean ± SEM. (n=4)

Western blots were performed to analysis the effect of adding 5mM 2-DG on the expression of the metabolic sensors CtBPs in hESCs at 20% oxygen. Representative Western blots revealed one protein band of approximately 48kDa for CtBP1 expression and two protein bands of approximately 49kDa for CtBP2 expression in hESCs incubated with either 0mM or 5mM 2-DG. However, the CtBP protein bands were much less prevalent in hESCs incubated with 5mM 2-DG compared to the control (Figure 4.19A). Quantification of those bands revealed a significant 75% reduction in CtBP1 expression ($p=0.0031$) and a significant 86% decrease in CtBP2 expression ($p=0.0014$) in Hues-7 hESCs treated with 5mM 2-DG compared to those cultured in the absence of 2-DG (Figure 4.19B).

Taken together, these data suggest that the glycolytic regulation of pluripotency marker and CtBP expression remains in Hues-7 hESCs maintained under 20% oxygen, as well as previously shown in hESCs under hypoxia.

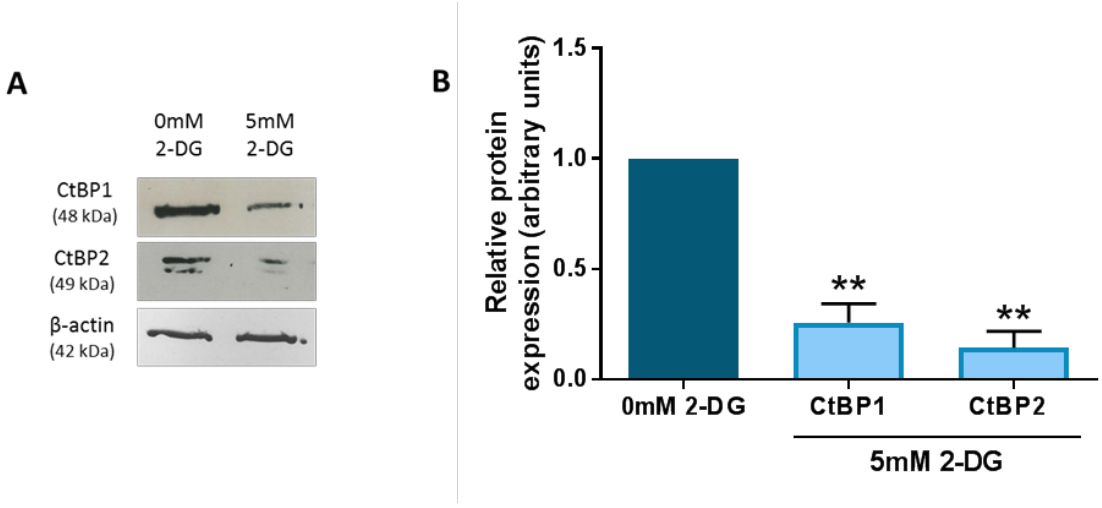

Figure 4.19. CtBP expression is affected by changes in glycolytic rate using 2-DG in Hues-7 hESCs cultured at 20% oxygen.
(A) Representative Western blots of CtBP1 and CtBP2 expression in Hues-7 hESCs cultured at 20% oxygen in MEF-conditioned media supplemented with either 0mM or 5mM 2-DG. (B) Quantification of CtBP Western blots revealed a significant decrease in the protein expression of both CtBP1 and CtBP2 in the presence of 2-DG compared to the control cells under normoxic conditions. Data were normalised to β-actin, and then to 1 for 0mM 2-DG control. Bars represent mean ± SEM. (n=4)

4.3.3. Effects of inhibiting glycolytic metabolism in Hues-7 hESCs cultured at 5% oxygen with 3-bromopyruvate

To confirm that the observed effects on hESC pluripotency, LDHA, GLUT transporter, CtBP and HIF-2α expression when the rate of flux through glycolysis was decreased using the inhibitor 2-DG was not specific to the inhibitor, the experiments were repeated using an alternative glycolytic inhibitor; 3-bromopyruvate (3-BrP). To investigate the effects of inhibiting glycolysis using 3-BrP, Hues-7 hESCs maintained under hypoxic oxygen tensions were incubated with either 0μM or 25μM 3-BrP for 48 hours before collecting samples for analysis of glycolytic rate and use in RT-qPCR and Western blotting.

4.3.3.1. Morphological characterisation of Hues-7 hESCs incubated with 3-bromopyruvate

Hues-7 hESCs treated with 25μM 3-BrP formed compact colonies with typical cobblestone morphology that were comparative to the control cells incubated in the absence of 3-BrP after 48 hours (Figure 4.20).

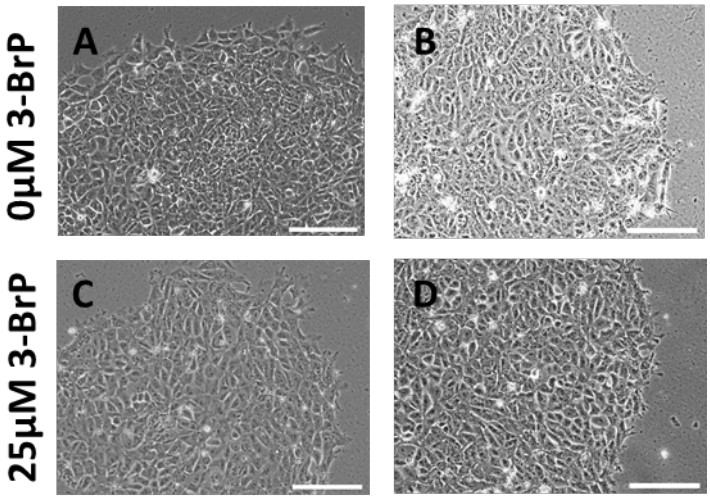

Figure 4.20. Phase contrast images demonstrating colony morphology of Hues-7 hESCs cultured at 5% oxygen in 3-BrP supplemented MEF-conditioned medium.
Representative phase contrast images of Hues-7 hESCs cultured at 5% oxygen in MEF-conditioned medium supplemented with either 0μM (A-B) or 25μM 3-BrP (C-D) after 48 hours. Scale bar indicates 200μm.

4.3.3.2. Measurement of lactate production in Hues-7 hESCs incubated with 3-bromopyruvate

Prior to analysing whether the addition of the glycolytic inhibitor 3-BrP affected the expression of the genes of interest, metabolism assays were performed to confirm whether the rate of glycolysis was reduced by 3-BrP.

Enzyme-linked assays were performed to investigate any effects of lactate production in hESCs incubated with either 0µM or 25µM 3-BrP under hypoxia. A significant reduction in lactate production was also observed in Hues-7 hESCs maintained at 5% oxygen and treated with 25µM 3-BrP. A significant and approximate 55% reduction (p=0.0009) in the rate of lactate production was observed in Hues-7 hESCs incubated with 25µM 3-BrP compared to hESCs cultured in the absence of 3-BrP (Figure 4.21).

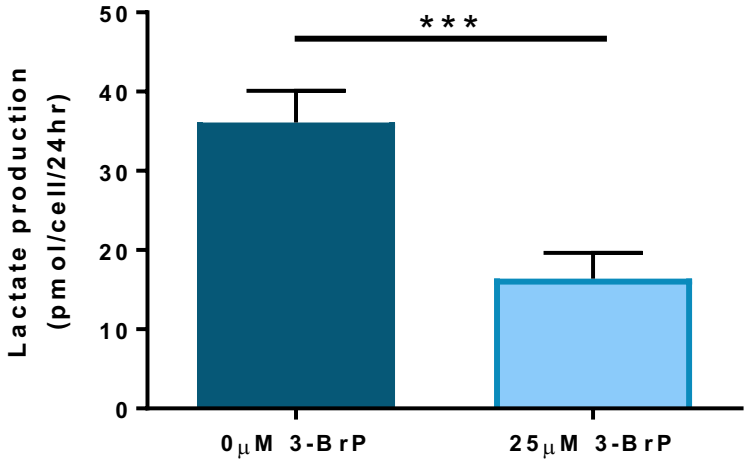

Figure 4.21. Lactate production is significantly reduced in Hues-7 hESCs cultured at 5% oxygen treated with 3-BrP.
Quantification of the rate of lactate production in Hues-7 hESCs maintained either in the presence of absence of 25µM 3-BrP for 48 hours prior to collecting media samples for use in the enzyme-linked assays. Bars represent mean ± SEM. (n=12)

4.3.3.3. Characterisation of pluripotency and differentiation marker expression in Hues-7 hESCs incubated with 3-bromopyruvate

To investigate the effects of glycolytic rate on the mRNA expression levels of pluripotency markers, RT-qPCR was performed using Hues-7 cells maintained at 5% oxygen treated with either 0µM or 25µM 3-BrP for 48 hours. Quantification of the relative mRNA expression levels of *OCT4*, *SOX2*, *NANOG, LIN28B* and *SALL4* revealed a significant decrease in the mRNA expression of all pluripotency markers in 25µM 3-BrP treated cells compared to those treated with 0µM 3-BrP (Figure 4.22).

Hues-7 hESCs treated with 25µM 3-BrP displayed a 60% decrease in *OCT4* expression (p=0.0275), a 38% decrease in *SOX2* expression (p=0.0408), a 57% reduction in *NANOG* mRNA levels (p=0.0331), a 44% decrease in *LIN28B* expression (p=0.0315) and a 23% reduction in *SALL4* mRNA expression (p=0.0486) compared to hESCs incubated in the absence of 3-BrP under hypoxia.

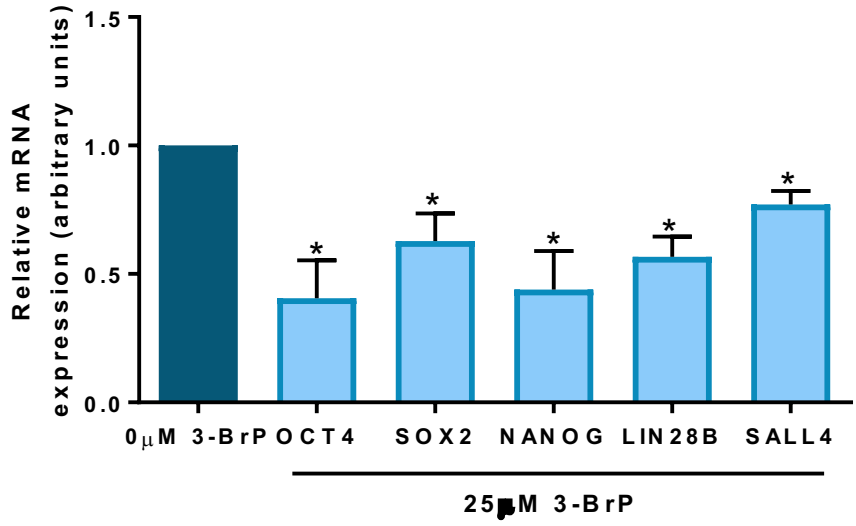

Figure 4.22. Decreasing the rate of glycolysis in Hues-7 hESCs cultured at 5% oxygen using the glycolytic inhibitor 3-BrP reduces the mRNA expression levels of pluripotency markers. Hues-7 hESCs cultured at 5% oxygen in MEF-conditioned media supplemented with 25µM 3-BrP displayed a significant decrease in *OCT4*, *SOX2*, *NANOG*, *LIN28B* and *SALL4* mRNA expression levels compared to the 0µM 3-BrP control. Data were normalised to *UBC*, and then to 1 for 0µM 3-BrP control. Bars represent mean ± SEM. (n=3-4)

Quantification of the OCT4, SOX2 and NANOG protein expression revealed a significant decrease in the protein expression of the three core pluripotency markers also in Hues-7 hESCs maintained at 5% oxygen cultured in the presence of the glycolytic inhibitor 3-BrP (Figure 4.23B). Hues-7 hESCs cultured with 25μM 3-BrP for 48 hours displayed an approximate 50% reduction in OCT4 (p=0.0291), a 55% reduction in SOX2 (p=0.0202) and an approximate 59% decrease in NANOG (p=0.043) protein expression compared to cells treated with 0μM 3-BrP.

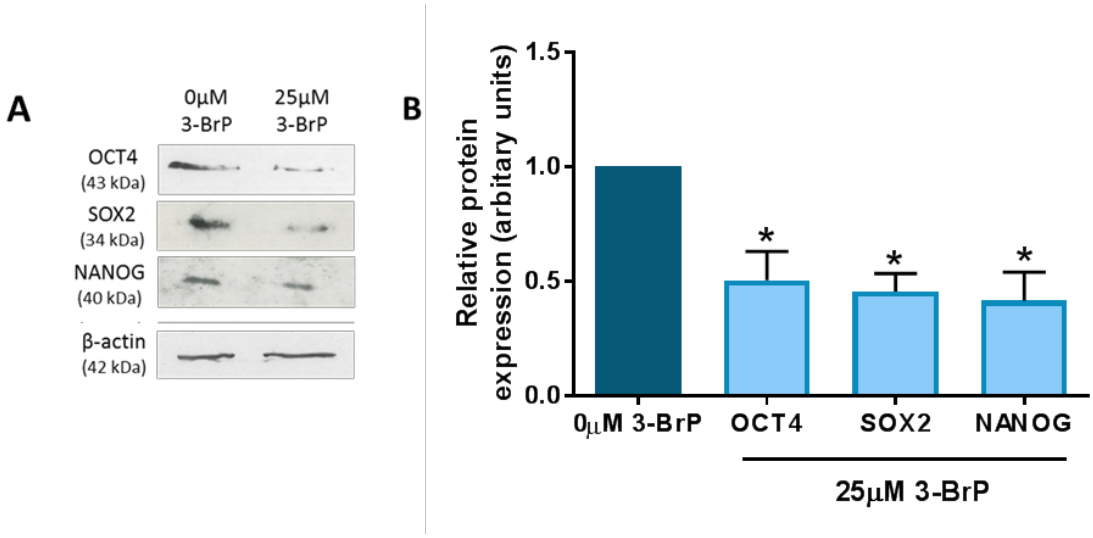

Figure 4.23. Pluripotency marker expression is affected by changes in glycolytic rate using 3-BrP in Hues-7 hESCs cultured at 5% oxygen.
(A) Representative Western blots of OCT4, SOX2 and NANOG expression in Hues-7 hESCs cultured at 5% oxygen in MEF-conditioned media supplemented with either 0μM or 25μM 3-BrP. (B) Quantification of OCT4, SOX2 and NANOG Western blots revealed a significant decrease in the protein expression of the three pluripotency factors in the presence of 3-BrP compared to the control cells. Data were normalised to β-actin, and then to 1 for 0μM 3-BrP control. Bars represent mean ± SEM. (n=3-4)

To further support the observed loss of pluripotency in Hues-7 hESCs maintained under hypoxia and incubated with 25µM 3-BrP, RT-qPCR was performed to analysis the expression of a panel of early differentiation markers representing all three developmental germ layers.

The mRNA expression levels of *GATA4* (p=0.0344), *SOX1* (p=0.0349), *PAX6* (p=0.0338), *BMP4* (p=0.007), *CXCR4* (p=0.0421) and *KDR* (p=0.0498) significantly increased in Hues-7 hESCs incubated with 25µM 3-BrP compared to those cultured without 3-BrP (Figure 4.24).

Together, these data suggest that the addition of the glycolytic inhibitor 3-BrP leads to a loss in hESC pluripotency and the initiation of early differentiation.

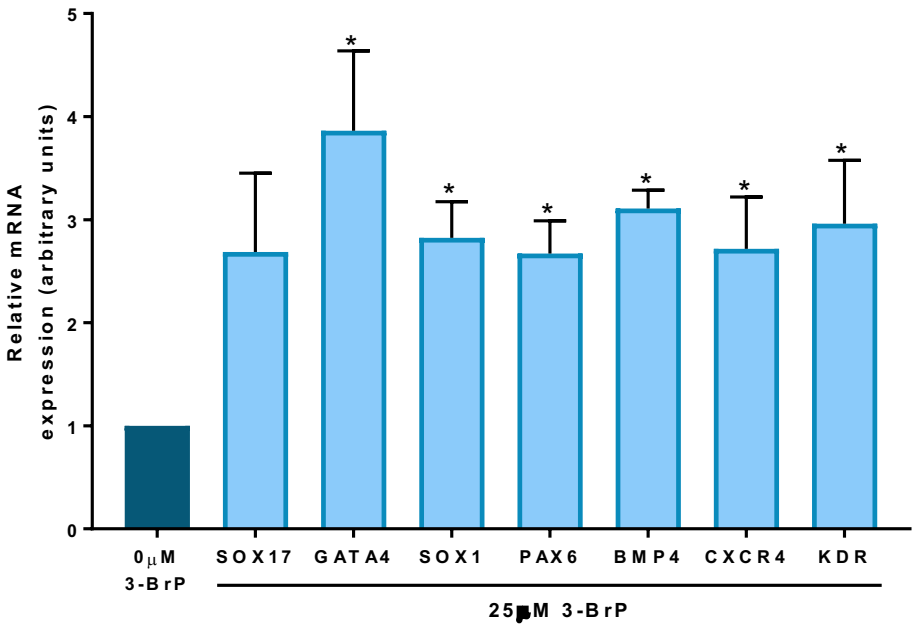

Figure 4.24. Expression of a panel of differentiation markers increases in Hues-7 hESCs treated with 3-BrP at 5% oxygen.
Hues-7 hESCs cultured at 5% oxygen in MEF-conditioned media supplemented with 25µM 3-BrP displayed a significant increase in *SOX17*, *GATA4*, *SOX1*, *PAX6*, *BMP4*, *CXCR4* and *KDR* mRNA expression levels compared to the 0µM 3-BrP control. Data were normalised to β-actin for primers and *UBC* for probes, and then to 1 for 0µM 3-BrP control. Bars represent mean ± SEM. (n=3-4)

4.3.3.4. Characterisation of gene expression associated with glycolysis in Hues-7 hESCs incubated with 3-bromopyruvate

To evaluate whether reducing the rate of flux through glycolysis affected the expression of glycolytic enzymes, glucose transporters or the metabolic sensors CtBPs, RT-qPCR and Western blotting was performed in Hues-7 hESCs incubated for 48 hours with the glycolytic inhibitor 3-BrP under hypoxic conditions.

RT-qPCR analysis revealed that the mRNA expression of the glycolytic enzyme *LDHA*, and the glucose transporters *GLUT1* and *GLUT3* significantly decreased in Hues-7 hESCs treated with 25µM 3-BrP compared to those incubated with 0µM 3-BrP (Figure 4.25).

LDHA mRNA expression was reduced by 44% (p=0.0471) in hESCs incubated in the presence of 3-BrP compared to the control cells. Furthermore, the mRNA expression levels of the glucose transporters *GLUT1* (p=0.0101) and *GLUT3* (p=0.0308) significantly decreased by approximately 60% and 50% respectively when the rate of flux through glycolysis was decreased with 3-BrP compared to hESCs incubated without 3-BrP.

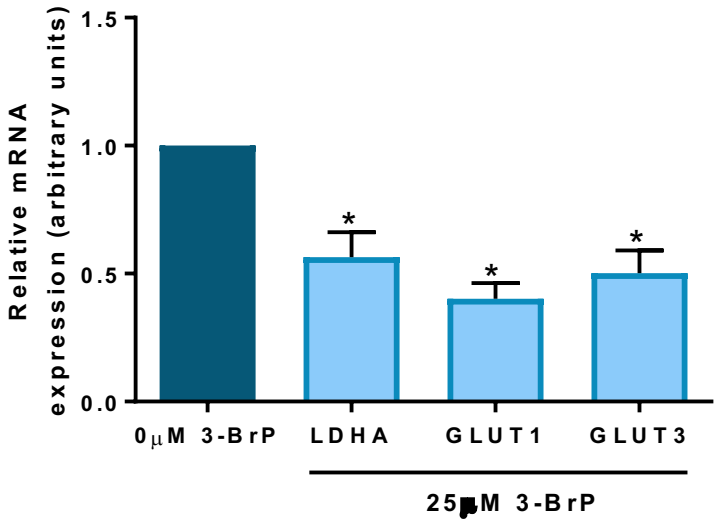

Figure 4.25. Decreasing the rate of glycolysis using the glycolytic inhibitor 3-BrP reduces mRNA expression of glycolytic associated genes in Hues-7 hESCs maintained at 5% oxygen. Hues-7 hESCs cultured at 5% oxygen tension in MEF-conditioned media supplemented with 25µM 3-BrP displayed a significant decrease in *LDHA*, *GLUT1* and *GLUT3* mRNA expression levels compared to the 0µM 3-BrP control. Data were normalised to β-actin for primers and *UBC* for probes, and then to 1 for 0µM 3-BrP control. Bars represent mean ± SEM. (n=3)

To investigate whether changing the rate of glycolysis in Hues-7 hESCs affected the expression of CtBPs, as well as pluripotency gene expression, CtBP mRNA and protein expression levels were quantified in Hues-7 hESCs cultured at 5% oxygen with CM supplemented with either 0µM or 25µM 3-BrP concentrations for 48 hours.

Interestingly, quantification of relative *CtBP* mRNA expression revealed the mRNA expression of both *CtBP1* and *CtBP2* isoforms have been significantly reduced by approximately 52% (p=0.0255) and 65% (p=0.0171) respectively in 25µM 3-BrP treated cells compared to those treated with 0µM 3-BrP (Figure 4.26).

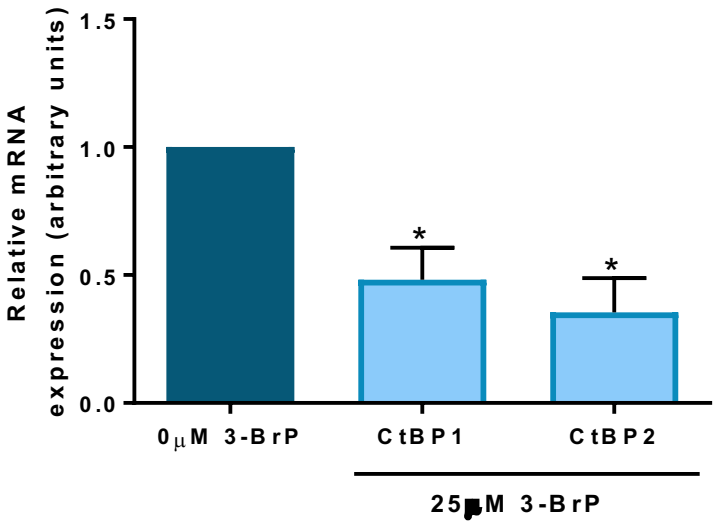

Figure 4.26. Decreasing the rate of glycolysis using the glycolytic inhibitor 3-BrP reduces CtBP mRNA expression in Hues-7 hESCs maintained at 5% oxygen.
Hues-7 hESCs cultured at 5% oxygen tension in MEF-conditioned media supplemented with 25µM 3-BrP displayed a significant decrease in both *CtBP1* and *CtBP2* mRNA expression levels compared to the 0µM 3-BrP control. Data were normalised to *UBC*, and then to 1 for 0µM 3-BrP control. Bars represent mean ± SEM. (n=4)

Quantification revealed that CtBP1 and CtBP2 protein levels, also, significantly decreased in Hues-7 hESCs maintained at 5% oxygen treated with 3-BrP (Figure 4.27B). Hues-7 hESCs treated with 25µM 3-BrP for 48 hours displayed an approximate 39% reduction in CtBP1 (p=0.0491) and an approximate 48% decrease in CtBP2 (p=0.0304) protein expression compared to cells treated with 0µM 3-BrP.

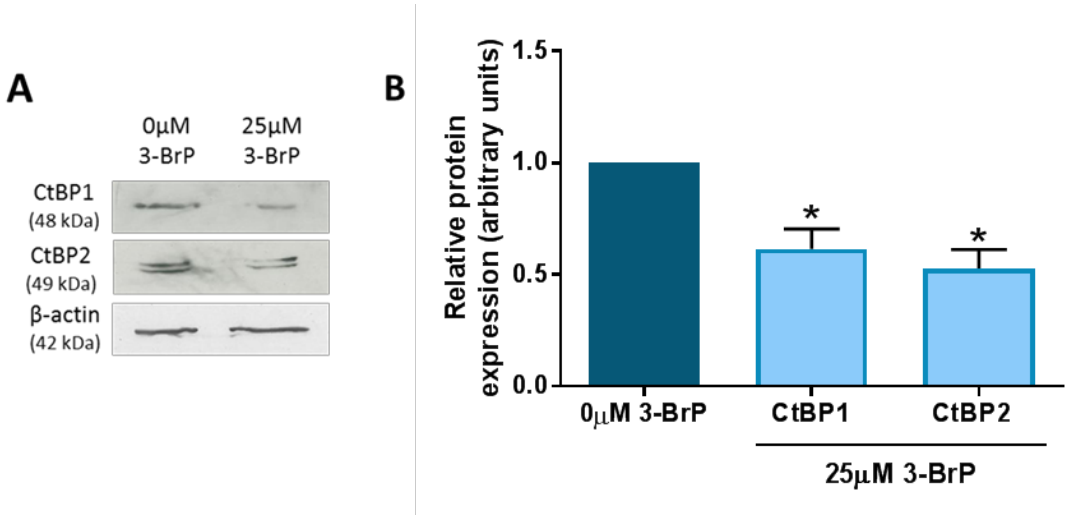

Figure 4.27. CtBP expression is affected by changes in glycolytic rate using 3-BrP in Hues-7 hESCs cultured at 5% oxygen.
(A) Representative Western blots of CtBP1 and CtBP2 expression in Hues-7 hESCs cultured at 5% oxygen in MEF-conditioned media supplemented with either 0µM or 25µM 3-BrP. (B) Quantification of CtBP Western blots revealed a significant decrease in the protein expression of both CtBP1 and CtBP2 in the presence of 3-BrP compared to the control cells. Data were normalised to β-actin, and then to 1 for 0µM 3-BrP control. Bars represent mean ± SEM. (n=3)

4.3.3.5. Characterisation of HIF-2α expression in Hues-7 hESCs incubated with 3-bromopyruvate

To determine whether the addition of another glycolytic inhibitor to reduce the glycolytic rate in Hues-7 hESCs maintained under hypoxia affected HIF-2α expression again, the mRNA and protein expression of HIF-2α in Hues-7 hESCs incubated in the presence of 3-BrP was analysed.

Interestingly, qPCR analysis of *HIF-2α* expression revealed a significant reduction in *HIF-2α* mRNA expression when the rate of flux through glycolysis had been reduced with 3-BrP (Figure 4.28). *HIF-2α* expression significantly reduced by 48% (p=0.0249) in Hues-7 hESCs maintained under hypoxia and incubated with 25μM 3-BrP compared to the control cells.

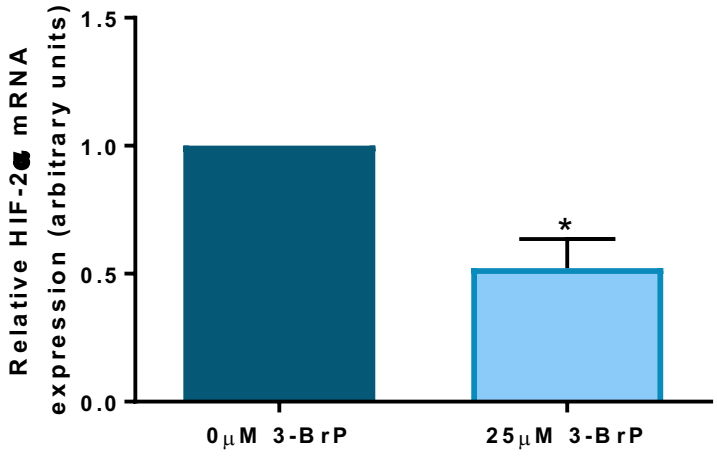

Figure 4.28. Decreasing the rate of glycolysis using 3-BrP reduces HIF-2α expression in Hues-7 hESCs maintained at 5% oxygen.
Hues-7 hESCs cultured at 5% oxygen in MEF-conditioned media supplemented with 25μM 3-BrP displayed a significant decrease in *HIF-2α* mRNA expression levels compared to the 0μM 3-BrP control. Data were normalised to *UBC*, and then to 1 for 0μM 3-BrP control. Bars represent mean ± SEM. (n=4)

Quantification of HIF-2α protein expression revealed the same trend. HIF-2α protein expression significantly decreased by approximately 40% (p=0.0404) when Hues-7 hESCs were incubated with 3-BrP compared to when they were incubated without (Figure 4.29B).

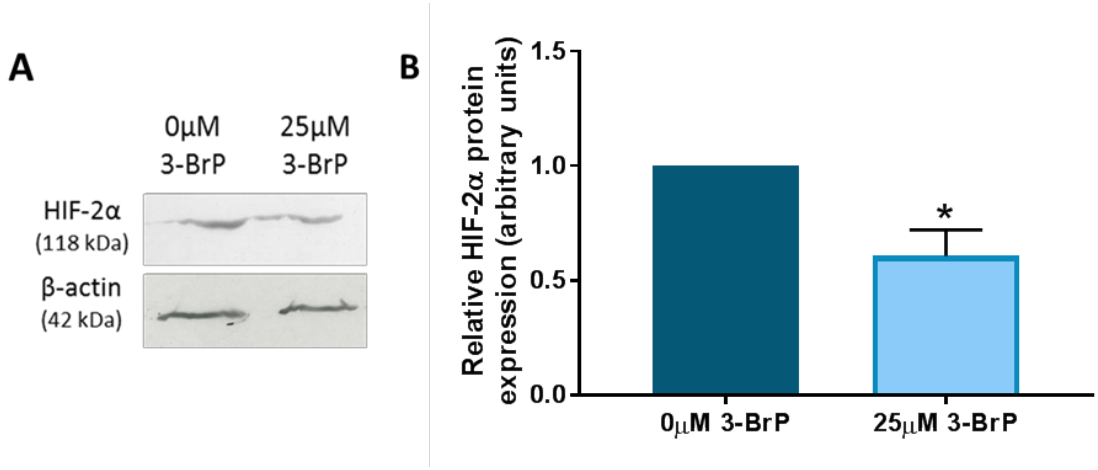

Figure 4.29. HIF-2α expression is affected by a reduction in glycolytic rate using 3-BrP in Hues-7 hESCs cultured under 5% oxygen.
(A) Representative Western blots of HIF-2α expression in Hues-7 hESCs cultured at 5% oxygen in MEF-conditioned media supplemented with either 0μM or 25μM 3-BrP. (B) Quantification of HIF-2α Western blots revealed a significant decrease in the protein expression of HIF-2α in the presence of 3-BrP compared to the control cells. Data were normalised to β-actin, and then to 1 for 0μM 3-BrP control. Bars represent mean ± SEM. (n=4)

4.3.4. Effects of inhibiting glycolytic metabolism in Hues-7 hESCs cultured at 5% oxygen with sodium oxamate

Data presented in this chapter so far has demonstrated that inhibiting the rate of flux through glycolysis using the inhibitors 2-DG and 3-BrP affects the expression of pluripotency markers, glycolysis associated proteins and also HIF-2α. The next aim was no confirm whether these effects were still observed when a glycolytic inhibitor was added that targets further downstream in glycolysis. To investigate this aim, Hues-7 hESCs maintained at 5% oxygen were incubated with either 0mM or 10mM sodium oxamate for 48 hours before analysis of hESC metabolism and collecting samples for analysis by RT-qPCR and Western blotting.

4.3.4.1. Morphological characterisation of Hues-7 hESCs incubated with sodium oxamate

Hues-7 hESCs treated with 10mM sodium oxamate formed compact colonies with typical cobblestone morphology and defined colony edges that were comparative to the control cells incubated in the absence of oxamate after 48 hours (Figure 4.30).

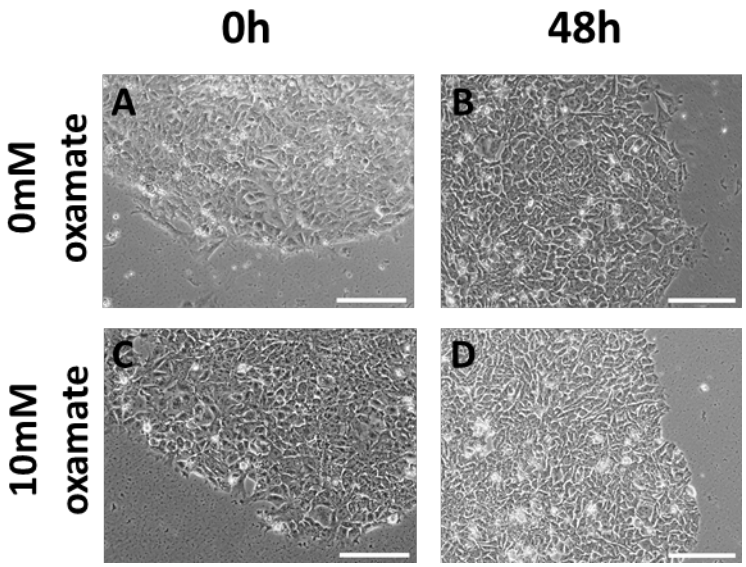

Figure 4.30. Phase contrast images demonstrating colony morphology of Hues-7 hESCs cultured at 5% oxygen in oxamate supplemented MEF-conditioned medium.
Representative phase contrast images of Hues-7 hESCs cultured at 5% oxygen in MEF-conditioned medium supplemented with either 0mM (A-B) or 10mM oxamate (C-D) after 48 hours. Scale bar indicates 200μm.

4.3.4.2. Measurement of lactate production in Hues-7 hESCs incubated with sodium oxamate

To assess whether the addition of 10mM sodium oxamate sufficiently reduced the rate of glycolysis, the rates of glucose consumption and lactate production in Hues-7 hESCs incubated with either 0mM or 10mM oxamate were measured using enzyme linked assays.

Enzyme-linked assays were performed to investigate any effects of lactate production in hESCs incubated with either 0mM or 10mM oxamate under hypoxia. A significant reduction in lactate production was also observed in Hues-7 hESCs maintained at 5% oxygen and treated with the inhibitor. A significant and approximate 46% reduction ($p=0.0006$) in the rate of lactate production was observed in Hues-7 hESCs incubated with 10mM oxamate compared to hESCs cultured in the absence of oxamate (Figure 4.31).

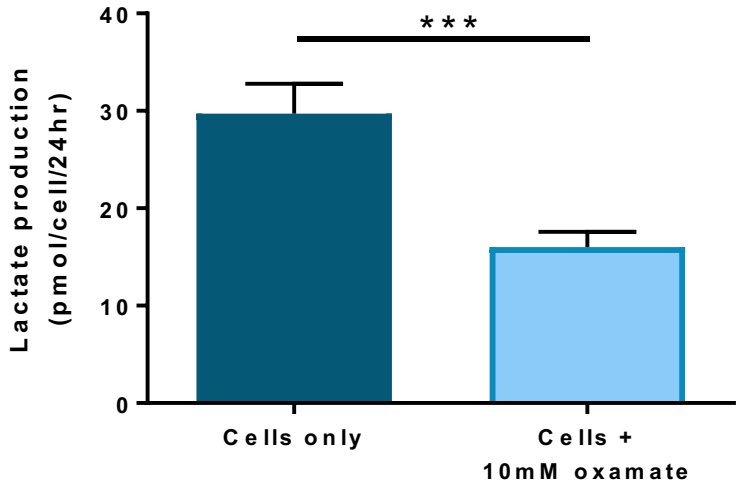

Figure 4.31. Lactate production is significantly reduced in Hues-7 hESCs cultured at 5% oxygen treated with oxamate.
Quantification of the rate of lactate production in Hues-7 hESCs maintained either in the presence of absence of 10mM oxamate for 48 hours prior to collecting media samples for use in the enzyme-linked assays. Bars represent mean ± SEM. (n=12)

4.3.4.3. Characterisation of pluripotency and differentiation marker expression in Hues-7 hESCs incubated with sodium oxamate

To investigate the effects of adding sodium oxamate on the mRNA expression levels of pluripotency markers, RT-qPCR was performed using Hues-7 cells maintained at 5% oxygen treated with either 0mM or 10mM oxamate for 48 hours.

Analysis of *OCT4*, *SOX2*, *NANOG, LIN28B* and *SALL4* mRNA expression levels revealed a significant decrease in 10mM oxamate treated cells compared to those treated with 0mM oxamate (Figure 4.32).

Hues-7 hESCs treated with 10mM oxamate displayed an approximate 20% decrease in *OCT4* expression (p=0.0131), a 31% decrease in *SOX2* expression (p=0.0458), a 42% reduction in *NANOG* mRNA levels (p=0.0469), a 75% decrease in *LIN28B* expression (p=0.0168) and a 63% reduction in *SALL4* mRNA expression (p=0.0346) compared to hESCs incubated in the absence of oxamate under hypoxia.

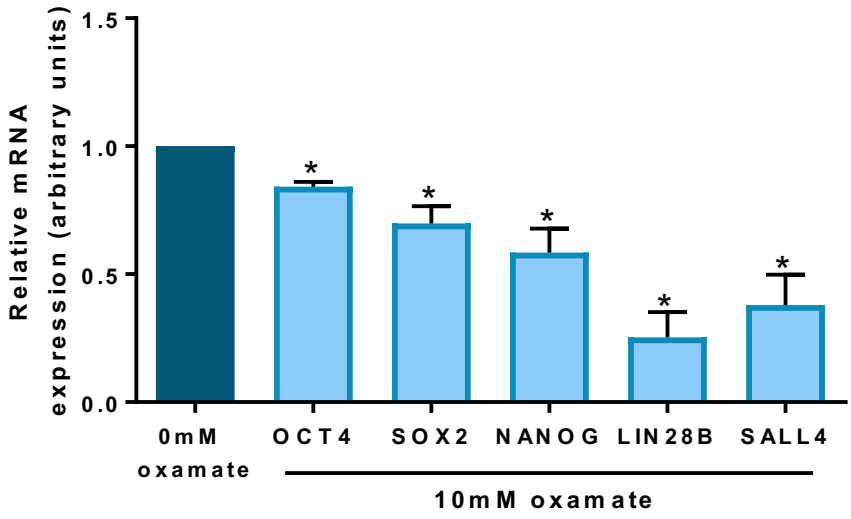

Figure 4.32. Decreasing the rate of glycolysis in Hues-7 hESCs cultured at 5% oxygen using the glycolytic inhibitor oxamate reduces the mRNA expression levels of pluripotency markers.
Hues-7 hESCs cultured at 5% oxygen in MEF-conditioned media supplemented with 10mM oxamate displayed a significant decrease in *OCT4*, *SOX2* and *NANOG* mRNA expression levels compared to the 0mM oxamate control. Data were normalised to *UBC*, and then to 1 for 0mM oxamate control. Bars represent mean ± SEM. (n=3)

One protein band of approximately 43kDa, 34kDa and 40kDa representing OCT4, SOX2 and NANOG expression respectively was observed in hESCs cultured with either 0mM or 10mM oxamate, where the protein bands appeared to be less prevalent in hESCs treated with the glycolytic inhibitor sodium oxamate (Figure 4.33A).

Quantification of the OCT4, SOX2 and NANOG protein expression revealed a significant decrease in the protein expression of the three core pluripotency markers in Hues-7 hESCs maintained at 5% oxygen cultured in the presence of the glycolytic inhibitor oxamate (Figure 4.33B). Hues-7 hESCs cultured with 10mM oxamate for 48 hours displayed an approximate 39% reduction in OCT4 ($p=0.0209$), a 33% reduction in SOX2 ($p=0.0422$) and an approximate 43% decrease in NANOG ($p=0.0375$) protein expression compared to cells incubated in the absence of sodium oxamate.

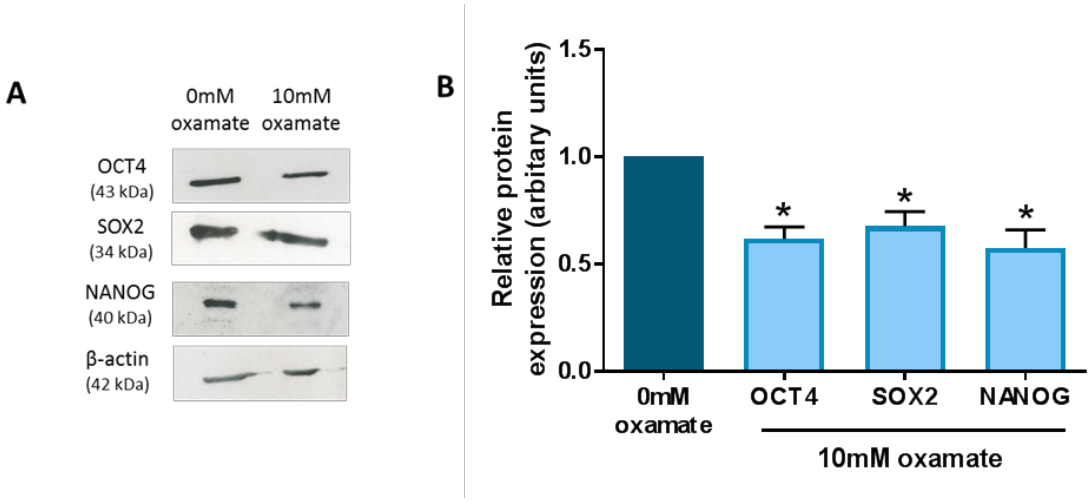

Figure 4.33. Pluripotency marker expression is affected by changes in glycolytic rate using oxamate in Hues-7 hESCs cultured at 5% oxygen.
(A) Representative Western blots of OCT4, SOX2 and NANOG expression in Hues-7 hESCs cultured at 5% oxygen in MEF-conditioned media supplemented with either 0mM or 10mM oxamate. (B) Quantification of OCT4, SOX2 and NANOG Western blots revealed a significant decrease in the protein expression of the three pluripotency factors in the presence of oxamate compared to the control cells. Data were normalised to β-actin, and then to 1 for 0mM oxamate control. Bars represent mean ± SEM. (n=3)

The mRNA expression levels of a panel of early differentiation markers were, also, analysed in Hues-7 hESCs maintained under hypoxia and treated with either 0mM or 10mM sodium oxamate. RT-qPCR analysis revealed a significant increase in the endodermal marker *GATA4* (p=0.0279) by approximately 1.7-fold (Figure 4.34). There was also a significant increase in the ectodermal markers *SOX1* (p=0.0291) and *PAX6* (p=0.0496) by 1-fold and 1.6-fold respectively (Figure 4.34), and also the mesodermal markers *BMP4* (p=0.0345), *CXCR4* (p=0.0129) and *KDR* (p=0.0229) significantly increased by 1.3-fold, 0.7-fold and 0.5-fold respectively in Hues-7 hESCs incubated with 10mM oxamate compared to the control cells (Figure 4.34). No significant difference was observed in the mRNA expression levels of *SOX17* in hESCs incubated with either 0mM or 10mM oxamate.

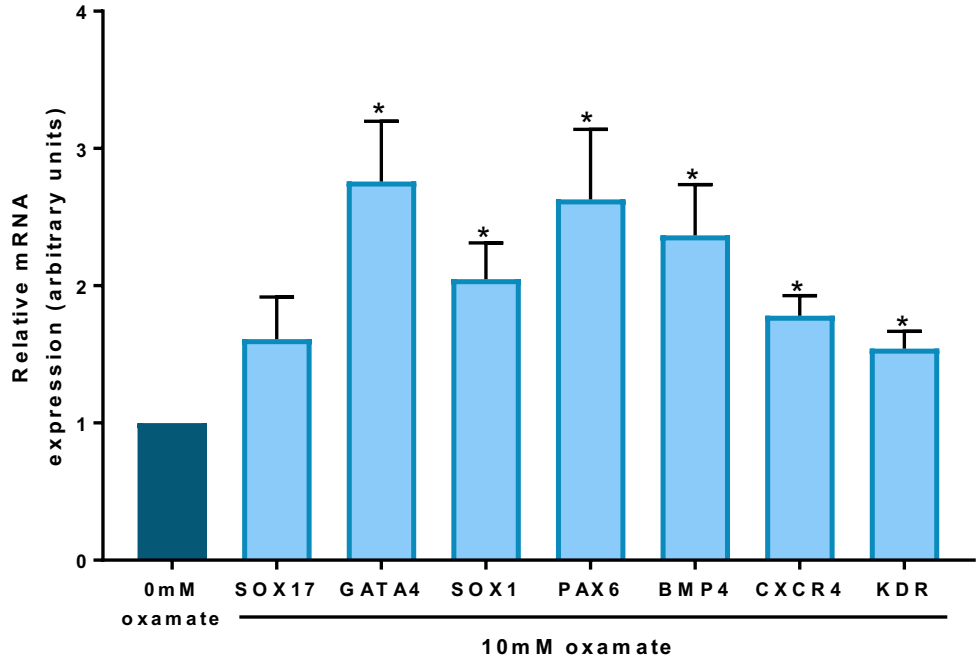

Figure 4.34. Expression of a panel of differentiation markers increases in Hues-7 hESCs treated with oxamate at 5% oxygen.
Hues-7 hESCs cultured at 5% oxygen in MEF-conditioned media supplemented with 10mM oxamate displayed a significant increase in *SOX17*, *GATA4*, *SOX1*, *PAX6*, *BMP4*, *CXCR4* and *KDR* mRNA expression levels compared to the 0mM oxamate control. Data were normalised to *β-actin* for primers and *UBC* for probes, and then to 1 for 0mM oxamate control. Bars represent mean ± SEM. (n=4)

4.3.4.4. Characterisation of gene expression associated with glycolysis in Hues-7 hESCs incubated with sodium oxamate

To investigate the effects of adding sodium oxamate on the mRNA expression levels of *LDHA*, and the glucose transporters *GLUT1* and *GLUT3*, RT-qPCR was performed using Hues-7 cells maintained at 5% oxygen treated with either 0mM or 10mM oxamate for 48 hours.

RT-qPCR analysis revealed that the mRNA expression of the glycolysis associated genes significantly decreased in Hues-7 hESCs treated with 10mM oxamate compared to those incubated with 0mM oxamate (Figure 4.35).

A significant reduction by approximately 77% was observed for *LDHA* expression ($p=0.0093$) in Hues-7 hESCs treated in the presence of the inhibitor oxamate compared to the control cells. Furthermore, the mRNA expression levels of the glucose transporters *GLUT1* ($p=0.0289$) and *GLUT3* ($p=0.0331$) significantly decreased by approximately 76% and 64% respectively when the rate of flux through glycolysis was decreased with oxamate compared to hESCs incubated without oxamate.

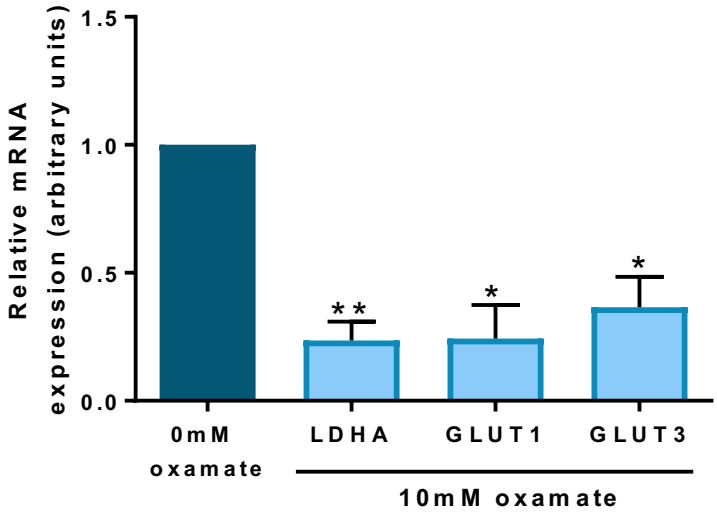

Figure 4.35. Decreasing the rate of glycolysis using the glycolytic inhibitor oxamate reduces mRNA expression of glycolytic associated genes in Hues-7 hESCs maintained at 5% oxygen. Hues-7 hESCs cultured at 5% oxygen tension in MEF-conditioned media supplemented with 10mM oxamate displayed a significant decrease in *LDHA*, *GLUT1* and *GLUT3* mRNA expression levels compared to the 0mM oxamate control. Data were normalised to *β-actin* for primers and *UBC* for probes, and then to 1 for 0mM oxamate control. Bars represent mean ± SEM. (n=3)

To investigate whether changing the rate of glycolysis with the inhibitor sodium oxamate in Hues-7 hESCs affected the expression of CtBPs, mRNA and protein expression levels were quantified in Hues-7 hESCs cultured at 5% oxygen with CM supplemented with either 0mM or 10mM oxamate concentrations for 48 hours.

Quantification of relative *CtBP* mRNA expression revealed the mRNA expression of both *CtBP1* and *CtBP2* isoforms have been significantly reduced by approximately 34% (p=0.0204) and 20% (p=0.0265) respectively in 10mM oxamate treated cells compared to those treated with 0mM oxamate (Figure 4.36).

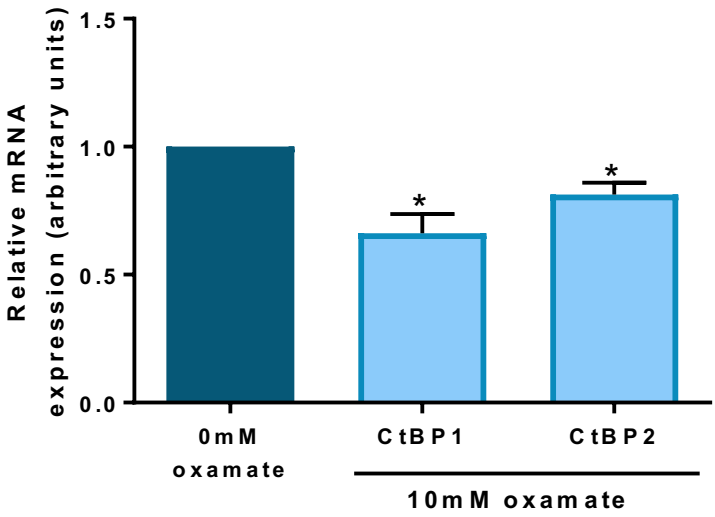

Figure 4.36. Decreasing the rate of glycolysis using the glycolytic inhibitor oxamate reduces CtBP mRNA expression in Hues-7 hESCs maintained at 5% oxygen.
Hues-7 hESCs cultured at 5% oxygen tension in MEF-conditioned media supplemented with 10mM oxamate displayed a significant decrease in both *CtBP1* and *CtBP2* mRNA expression levels compared to the 0mM oxamate control. Data were normalised to *UBC*, and then to 1 for 0mM oxamate control. Bars represent mean ± SEM. (n=4)

Quantification revealed that CtBP1 and CtBP2 protein levels, also, significantly decreased in Hues-7 hESCs maintained at 5% oxygen treated with oxamate (Figure 4.37B). Hues-7 hESCs treated with 10mM oxamate for 48 hours displayed an approximate 61% reduction in CtBP1 ($p=0.0095$) and an approximate 54% decrease in CtBP2 ($p=0.0463$) protein expression compared to cells treated with 0mM sodium oxamate.

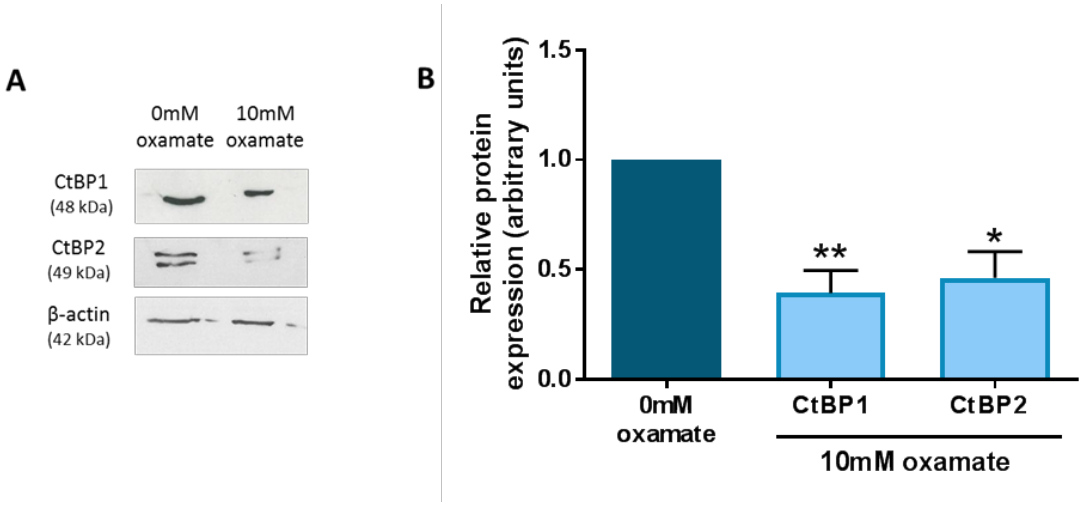

Figure 4.37. CtBP expression is affected by changes in glycolytic rate using oxamate in Hues-7 hESCs cultured at 5% oxygen.
(A) Representative Western blots of CtBP protein expression in Hues-7 hESCs cultured at 5% oxygen in MEF-conditioned media supplemented with either 0mM or 10mM oxamate. (B) Quantification of CtBP Western blots revealed a significant decrease in the protein expression of both CtBP isoforms in the presence of oxamate compared to the control cells. Data were normalised to β-actin, and then to 1 for 0mM oxamate control. Bars represent mean ± SEM. (n=3-4)

4.3.4.5. Characterisation of HIF-2α expression in Hues-7 hESCs incubated with sodium oxamate

To determine whether the addition of another glycolytic inhibitor to reduce the glycolytic rate in Hues-7 hESCs maintained under hypoxia affected HIF-2α expression, HIF-2α mRNA and protein expression levels were analysed between in Hues-7 hESCs incubated in the presence and absence of oxamate.

qPCR analysis of *HIF-2α* expression revealed a significant reduction in *HIF-2α* mRNA expression when the rate of flux through glycolysis had been reduced with the glycolytic inhibitor sodium oxamate (Figure 4.38). *HIF-2α* expression significantly reduced by 34% (p=0.017) in Hues-7 hESCs maintained under hypoxia and incubated with 10mM oxamate compared to the control cells.

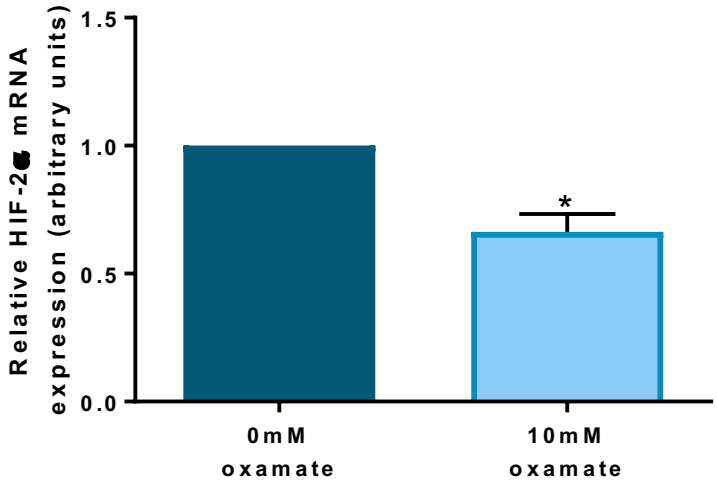

Figure 4.38. Decreasing the rate of glycolysis using oxamate reduces HIF-2α expression in Hues-7 hESCs maintained at 5% oxygen.
Hues-7 hESCs cultured at 5% oxygen in MEF-conditioned media supplemented with 10mM oxamate displayed a significant decrease in *HIF-2α* mRNA expression levels compared to the 0mM oxamate control. Data were normalised to *UBC*, and then to 1 for 0mM oxamate control. Bars represent mean ± SEM. (n=4)

HIF-2α protein expression also significantly decreased by approximately 51% (p=0.0444) when Hues-7 hESCs were incubated with oxamate compared to when they were incubated without (Figure 4.39B).

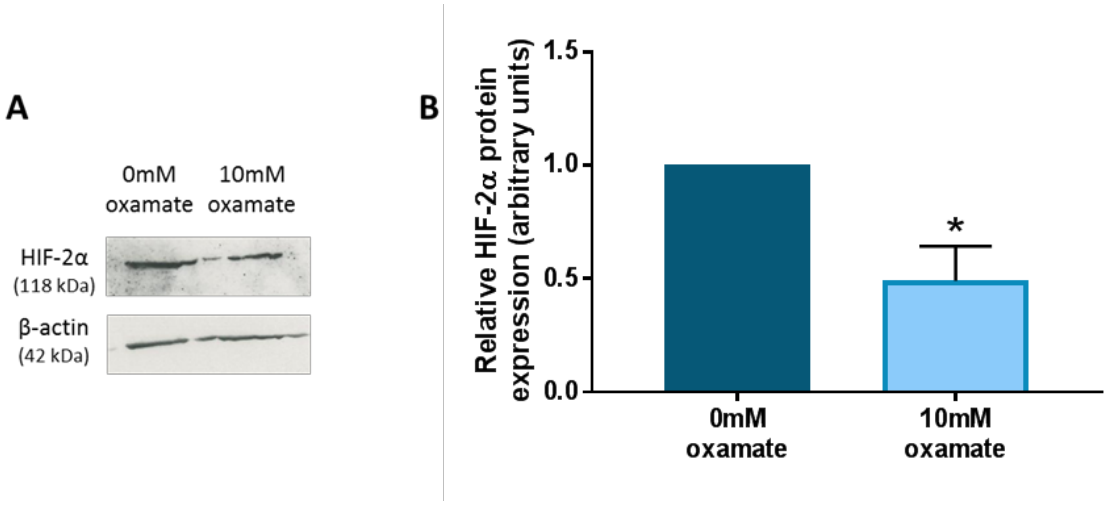

Figure 4.39. HIF-2α expression is affected by a reduction in glycolytic rate using oxamate in Hues-7 hESCs cultured under 5% oxygen.
(A) Representative Western blots of HIF-2α protein expression in Hues-7 hESCs cultured at 5% oxygen in MEF-conditioned media supplemented with either 0mM or 10mM oxamate. (B) Quantification of Western blots revealed a significant decrease in HIF-2α protein expression in the presence of oxamate compared to the control cells. Data were normalised to β-actin, and then to 1 for 0mM oxamate control. Bars represent mean ± SEM. (n=4)

4.3.5. Investigating the glycolytic regulation of HIF-2α in hESCs maintained at 5% oxygen

Previously published studies have demonstrated that HIF-2α regulates the expression of an array of genes associated with glycolysis and results in an increase in the rate of glycolysis. However, data presented in this chapter has interestingly revealed that inhibiting the rate of flux through glycolysis using three independent glycolytic inhibitors is affecting HIF-2α expression in hESCs maintained under hypoxia. The next step was to attempt to decipher the molecular mechanisms behind this observation. The first investigations were aimed to determine whether the reduction in HIF-2α expression as a result of decreasing the rate of flux through glycolysis was due to HIF-2α stability. Prolyl hydroxylases (PHDs) target HIF-2α for degradation under normoxia, so the expression of PHD1, PHD2 and PHD3 in Hues-7 hESCs maintained at 5% oxygen and incubated with either 0mM or 10mM 2-DG was investigated by Western blotting.

No significant difference was found in the protein expression levels of PHD1, PHD2 or PHD3 in hESCs treated either in the presence or absence of the glycolytic inhibitor 2-DG (Figure 4.40). However, there appears to be a trend towards an increase in PHD expression in Hues-7 hESCs incubated with 10mM 2-DG compared to the control cells.

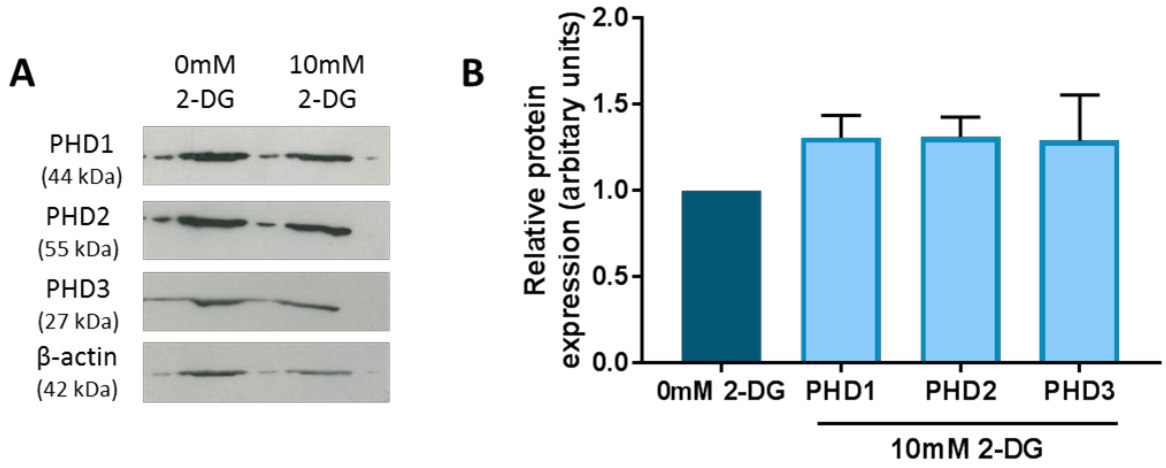

Figure 4.40. PHD expression is not affected by a reduction in glycolytic rate using 2-deoxyglucose in Hues-7 hESCs cultured under 5% oxygen.
(A) Representative Western blots of PHD protein expression in Hues-7 hESCs maintained at 5% oxygen in MEF-conditioned media supplemented with either 0mM or 10mM 2-DG. (B) Quantification of Western blots revealed no difference in the protein expression levels of PHD1, PHD2 or PHD3 in Hues-7 hESCs incubated with 10mM 2-DG compared to control cells. Data were normalised to β-actin, and then to 1 for 0mM 2-DG control. Bars represent mean ± SEM, (n=3-4)

As no significant effect on PHD expression, and therefore HIF-2α protein stability, was observed in hESCs where the rate of flux through glycolysis had been reduced, therefore further investigations in the molecular mechanisms behind the glycolytic regulation of HIF-2α was conducted.

Pyruvate kinase M2 (PKM2) is a glycolytic enzyme involved in the generation of ATP but also the production of pyruvate through the conversion of phosphoenolpyruvate, which also has a key role in tumour metabolism and growth. However, PKM2 has also been shown to localise to the nucleus of cancer cells to play a role in transcriptional regulation functioning as a protein kinase that phosphorylates histones during gene transcription and chromatin remodelling (Chen et al., 2014). Correlations between PKM2 and pluripotency marker expression had also previously been observed highlighting a transcriptional role for PKM2 in OCT4 expression in hESCs (Christensen et al., 2015). Therefore, PKM2 expression in hESCs was investigated to assess whether it may have a role in the glycolytic regulation of HIF-2α expression.

Firstly, PKM2 expression in Hues-7 hESCs maintained at either 5% or 20% oxygen was quantified using Western blotting. Representative Western blots showed that PKM2 was expressed in hESCs maintained under both oxygen tensions, although protein bands were less strong from hESCs maintained under 20% oxygen (Figure 4.41A). Quantification of the PKM2 protein bands revealed a significant 46% increase in expression (p=0.0092) in hESCs cultured under 5% oxygen compared to those maintained under normoxic oxygen tensions (Figure 4.41B). These results agreed with previous published data (Christensen et al., 2015).

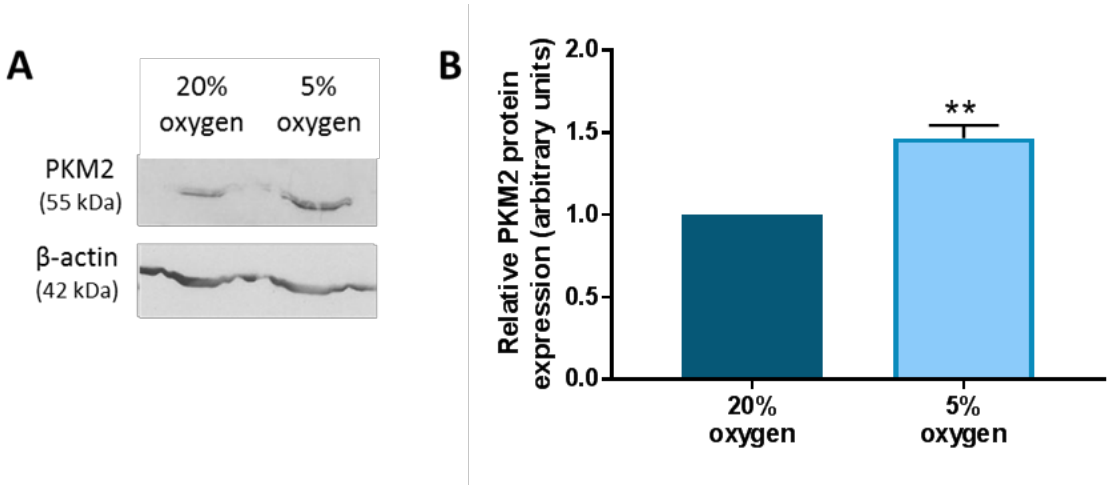

Figure 4.41. Hypoxic culture increase PKM2 protein expression in Hues-7 hESCs.
(A) Representative Western blots of PKM2 protein expression in Hues-7 hESCs maintained at either 5% oxygen or 20% oxygen. (B) Quantification of Western blots of PKM2 protein expression in Hues-7 hESCs maintained at 5% oxygen compared to those maintained at 20% oxygen. Data were normalised to β-actin, and then to 1 for 20% oxygen. Bars represent mean ± SEM, (n=4)

To investigate whether PKM2 may have a role in the transcriptional regulation of HIF-2α, Hues-7 hESCs maintained under hypoxic conditions were transfected with either Allstars negative control of PKM2 siRNA for 48 hours before samples were collected for analysis by Western blotting.

Phase contrast images clearly demonstrate that cells transfected with either the Allstars negative control (Figure 4.42A-B) or PKM2 siRNA (Figure 4.42C-D) display no clear morphological differences 48 hours post-transfection.

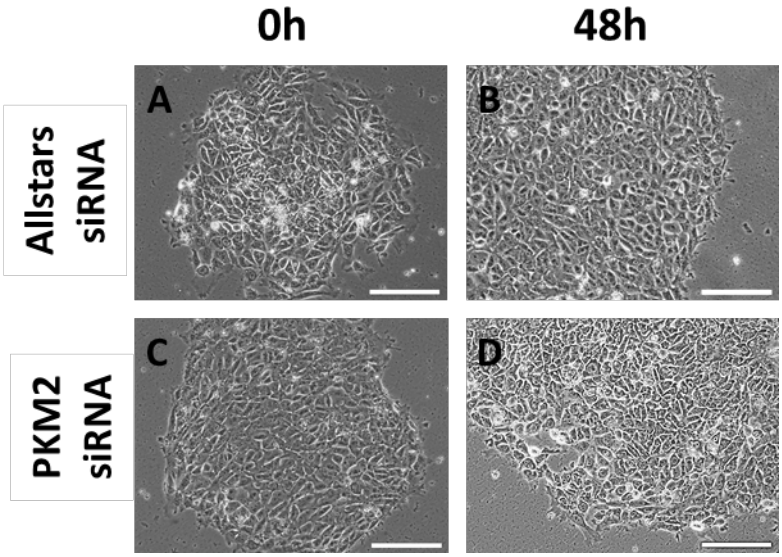

Figure 4.42. Phase contrast images demonstrating colony morphology of Hues-7 hESCs cultured at 5% oxygen transfected with PKM2 siRNA.
Representative phase contrast images of Hues-7 hESCs cultured at 5% oxygen transfected with either Allstars negative control siRNA (A-B) or PKM2 siRNA (C-D) after 0 (A, C) and 48 hours (B, D). Scale bar indicates 200μm.

Analysis of protein expression levels revealed that PKM2 expression was successfully silenced in Hues-7 hESCs after transfection with PKM2 siRNA (Figure 4.43B) compared to those transfected with the Allstars negative control siRNA. PKM2 expression decreased by approximately 43% in Hues-7 hESCs transfected with PKM2 siRNA ($p=0.0352$). After successfully silencing PKM2 expression in Hues-7 hESCs maintained under hypoxic conditions, OCT4 protein expression was quantified to determine whether the approximate 43% decrease in PKM2 expression was enough to elicit a functional response. Western blotting analysis revealed that OCT4 expression was significantly reduced by approximately 31% ($p=0.0138$) in hESCs where PKM2 expression had been silenced compared to the control cells (Figure 4.43C).

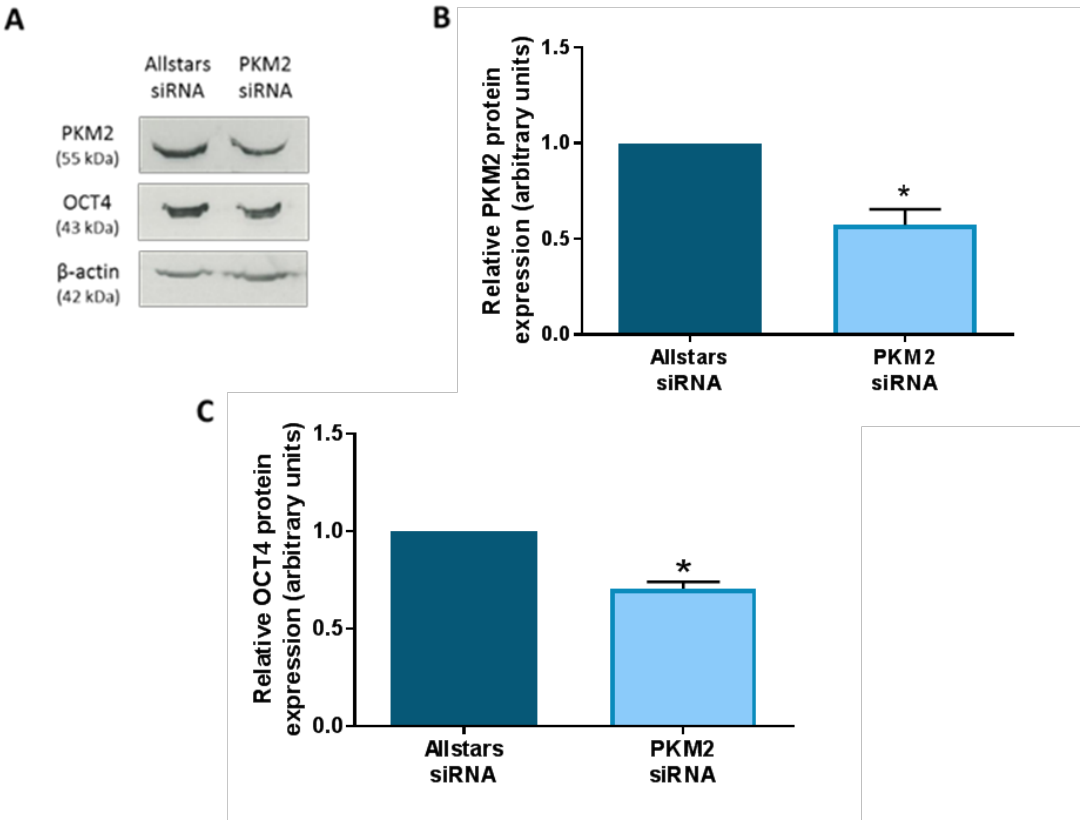

Figure 4.43. PKM2 regulates OCT4 expression in Hues-7 hESCs under 5% oxygen.
(A) Representative Western blots of PKM2 and OCT4 protein expression in Hues-7 hESCs maintained at 5% oxygen and transfected with either Allstars negative control siRNA or PKM2 siRNA. (B) Quantification of PKM2 Western blots revealed successful silencing of PKM2 protein expression after transfection with PKM2 siRNA. (C) Quantification of OCT4 blots revealed a significant decrease in the protein expression of OCT4 in Hues-7 hESCs maintained at 5% oxygen and transfected with PKM2 siRNA. Data were normalised to β-actin, and then to 1 for Allstars control. Bars represent mean ± SEM. (n=3)

To determine whether silencing PKM2 had any effect on the expression of HIF-2α in hESCs maintained under hypoxia, HIF-2α Western blots were performed. Excitingly, transfection with PKM2 siRNA resulted in a significant and approximate 36% decrease in HIF-2α protein expression levels (p=0.0351) in hESCs maintained under hypoxia compared to those cells transfected with the Allstars negative control siRNA (Figure 4.44).

Together, this data suggests that PKM2 may play a role in regulating HIF-2α expression, and therefore the downstream effects on pluripotency marker expression and other HIF-2α target genes in hESCs under hypoxia.

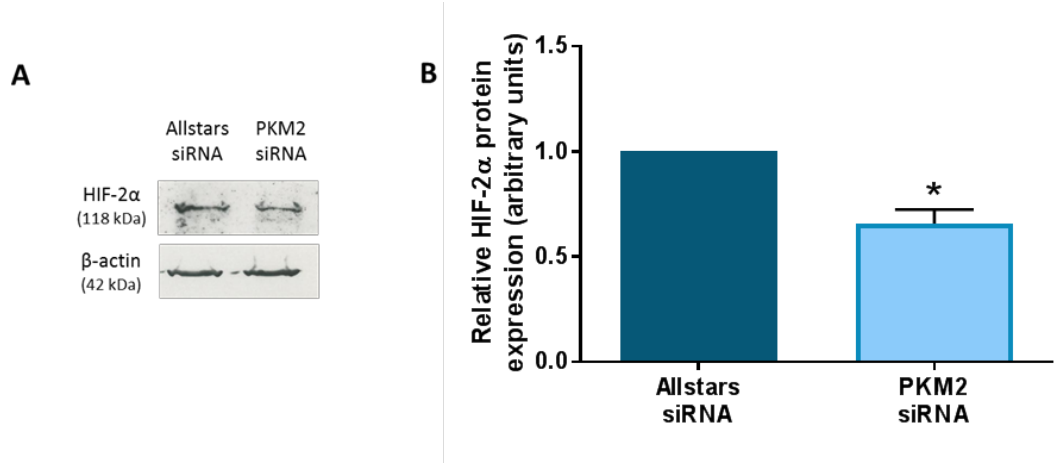

Figure 4.44. PKM2 regulates HIF-2α expression in Hues-7 hESCs under 5% oxygen.
(A) Representative Western blots of HIF-2α protein expression in Hues-7 hESCs maintained at 5% oxygen and transfected with either Allstars negative control siRNA or PKM2 siRNA. (B) Quantification of HIF-2α blots revealed a significant decrease in the protein expression of HIF-2α in Hues-7 hESCs maintained at 5% oxygen and transfected with PKM2 siRNA. Data were normalised to β-actin, and then to 1 for Allstars control. Bars represent mean ± SEM. (n=3)

4.4 Discussion

hESCs rely heavily on glycolytic metabolism for their energetic demands, in part due to their immature mitochondrial phenotype (Sathananthan et al., 2002). In addition, previous studies have demonstrated that a hypoxic environment supports a more glycolytic metabolism as the expression of glycolytic enzymes, such as hexokinase and lactate dehydrogenase, is increased under hypoxic conditions. Moreover, HIF-1α and HIF-2α subunits directly regulate the expression of GLUTs and other glycolytic enzymes (Chen et al., 2001; Forristal et al., 2013; Cui et al., 2017), which together results in an increased rate of flux through glycolysis in hESCs under hypoxia. However, whether this increased flux through glycolysis directly affected hESC pluripotency and CtBP expression was investigated in this study.

Three different glycolytic inhibitors were used and incubated with hESCs maintained at either 5% or 20% oxygen. Inhibiting glycolysis using either 2-DG, 3-BrP or sodium oxamate resulted in the same effects on hESC self-renewal, CtBP and HIF-2α expression highlighting and re-emphasising the importance of metabolism in the maintenance of hESC pluripotency.

A dose-response curve was performed for hESCs incubated with increasing 2-DG concentrations. Phase contrast images clearly demonstrate a toxic effect and any observed consequent decreases in pluripotency marker expression may not have been a reflection of the reduced rate of glycolysis alone, but also influenced by increased cell death and the initiation of early differentiation. Lactate production was only significantly decreased in hESCs treated with 10mM 2-DG compared to the control cells and not in cells incubated with either 0.2mM or 1mM 2-DG. Previous studies have used a wide range of concentrations in different cell types (Zhong et al., 2008; Zhou et al., 2012; Candelario et al., 2013; Vega-Naredo et al., 2014; Moussaieff et al., 2015). Although potential off target effects may be obtained using an inhibitor concentration that is too high, the use of 10mM 2-DG utilised in this thesis was required in order to significantly reduce lactate production. This reflects the high concentration of glucose found in the hESC culture medium and also the increased rate of flux through glycolysis observed in hESCs cultured under hypoxic conditions. This is supported by the fact that hESCs maintained at atmospheric oxygen concentrations only required 5mM 2-DG in order to inhibit lactate production. Furthermore, the observed decreases in pluripotency marker and CtBP expression in hESCs incubated with 2-DG were backed up by the results in hESCs treated

with 3-BrP. Further analysis of the dose response curve showed that there was a significant decrease in pluripotency marker and CtBP expression between either 0.2mM or 1mM and 10mM 2-DG reemphasising that the 10mM 2-DG concentration was the right one to use to effectively inhibit glycolysis.

4.4.1. Glycolytic regulation of hESC self-renewal under hypoxia

Pluripotent hESCs have immature mitochondria (Sathananthan et al., 2002) and hence rely on glycolysis for their energy requirements. A hypoxic environment supports a higher rate of flux through glycolysis by enhancing the expression of PKM2 and the glucose transporter GLUT3 (Christensen et al., 2015) and is associated with an increased expression of pluripotency markers compared to culture at atmospheric oxygen tensions (Forristal et al., 2013). Our data support this observation as inhibiting glycolysis in hESCs maintained at 5% oxygen using any of the glycolytic inhibitors used resulted in a significant decrease in OCT4, SOX2, NANOG, LIN28B and SALL4 and a concomitant increase in the expression of a range of early differentiation markers representing all three germ lineages. This suggests that inhibition of glycolysis results in the loss of self-renewal and onset of early differentiation of hESCs agreeing with a previously published report (Gu et al., 2016). The analysis of differentiation marker expression reemphasised that a loss of glycolytic based metabolism in hESCs results in differentiation rather than apoptosis and thus that the metabolic state of the cell is intrinsic to pluripotency maintenance.

4.4.2. Glycolytic regulation of CtBP and glycolytic associated gene expression in hESCs maintained under hypoxia

As this study has shown that pluripotency marker expression is affected by glycolytic rate in agreement with previous studies, and due to the emerging evidence that CtBP expression may be regulated in similar ways to pluripotency gene expression, CtBP expression in response to changes in glycolytic rate were investigated. Excitingly, data in this study demonstrated that inhibiting glycolysis using either 2-DG, 3-BrP or sodium oxamate significantly decreased the mRNA and protein expression of both CtBP1 and CtBP2 and the glycolytic enzyme *LDHA*.

Glycolysis is known to influence CtBP activity through its production of NADH combined with the consequent activation of CtBP dimers (Zhang et al., 2002; Fjeld et al., 2003). However, this data suggests that CtBP expression is, also, influenced by the

metabolic state of the cell, and not just CtBP activity. This data predicts another novel mechanism of the regulation of CtBP expression in hESCs, but specifically a role for glycolytic metabolism in upregulating the expression of CtBPs, in order to utilise the increased levels of free NADH produced through the higher glycolytic flux displayed by hESCs cultured under hypoxic conditions, and therefore allows CtBP dimers to function and influence changes in target gene expression.

4.4.3 Glycolytic regulation of HIF-2α expression in hESCs maintained under hypoxia

It is well documented from previously published studies and data from this study that HIF-2α is the predominant regulator of the long term hypoxic response in hESCs, and that HIF-2α directly binds to the proximal promoter sequences of pluripotency markers, glycolytic enzymes and metabolic sensors CtBPs. Therefore, it was investigated whether the observed reduction in the mRNA and protein expression of pluripotency marker and glycolysis associated genes was through HIF-2α. Interestingly, HIF-2α expression was found to be regulated by inhibiting glycolysis in hESCs maintained under hypoxia.

This result indicated that the expression of OCT4, SOX2 and NANOG may be regulated directly by glycolysis, but also indirectly through HIF-2α. A previous study in macrophages revealed that PKM2 regulates HIF-1α activity (Palsson-McDermott et al., 2015), and while there are no accounts of how a glycolytic metabolite or glycolytic enzyme may be influencing HIF-α expression, it cannot be ruled out that PKM2 may be a viable option as it shares a correlation with HIF-α activity. Crucially though, this observation reveals a feed forward loop between glycolytic rate and HIF-α expression in hESCs which would be utilised to maintain the highly glycolytic phenotype and as such hESC self-renewal. Furthermore, PKM2 has been shown to bind to different signalling molecules such as β-catenin or STAT3 to increase the activity of target genes (Luo et al., 2011; Yang et al., 2011; Gao et al., 2012; Yang et al., 2012b; Li et al., 2018). Further work would be required to see if any of these signalling pathways may regulate HIF-2α expression.

4.4.4 Glycolytic regulation of hESC self-renewal under 20% oxygen

hESCs display a highly glycolytic phenotype regardless of whether they are cultured under hypoxic or atmospheric oxygen tensions. Therefore, hESCs maintained at 20%

oxygen were treated with the glycolytic inhibitor 2-DG to examine whether the glycolytic regulation of pluripotency marker and CtBP expression was maintained.

Data in this chapter revealed that the expression of OCT4, SOX2, NANOG and CtBPs significantly decreased in hESCs incubated with 5mM 2-DG compared to the control. Phase contrast images revealed that a 2-DG concentration of 10mM was toxic to hESCs maintained at 20% oxygen. This highlights that hESCs maintained at 20% oxygen have a lower rate of flux through glycolysis compared to hESCs maintained under hypoxia and so lower concentrations of glycolytic inhibitors are necessary to significantly inhibit metabolism.

Furthermore, as HIF-2α is not expressed in hESCs maintained at 20% oxygen and yet the glycolytic regulation of pluripotency marker and CtBP expression is maintained in hESCs cultured at 20% oxygen, this confirms that there is a HIF-2α independent metabolic regulation of OCT4, SOX2, NANOG and CtBPs.

4.4.5. Mechanisms behind the glycolytic regulation of HIF-2α in hESCs cultured under hypoxia

Much evidence suggests that HIFs support the glycolytic metabolism of hESCs, by enhancing the expression of glucose transporters and glycolytic enzymes (Semenza, 2000b; Varum et al., 2011; Forristal et al., 2013; Christensen et al., 2015), but data from this study suggests that glycolysis itself promotes HIF-2α protein expression at least in hESCs cultured under hypoxia. Previous studies have reported a similar mechanism by which aerobic glycolysis supports HIF-1α protein stability to activate HIF-1α inducible gene expression in glioma cells (Lu et al., 2002; Lu et al., 2005). However, our data represents a novel observation for the regulation of HIF-2α in any cell type cultured under hypoxic conditions. Lu *et al.* (2005) demonstrated that glycolytic metabolites, such as pyruvate and oxaloacetate, control HIF-1α stability by regulating the activity of HIF prolyl hydroxylases. To establish whether glycolysis supports HIF-2α expression using comparable mechanisms to that of HIF-1α, PHD expression was examined. However, no significant difference was found in the expression of PHD1, PHD2 or PHD3 expression between hESCs maintained at either 5% or 20% oxygen although there appears to be a trend towards an increase in hESCs at 20% oxygen. This suggests that PHD expression in hESCs does not affected HIF-2α protein stability, however it cannot be ruled out that

the activity of PHDs does not differ between hESCs maintained at either 5% or 20% oxygen and would require further investigation.

Furthermore, in attempts to decipher any potential mechanism behind the metabolic regulation of HIF-2α expression, a potential role for PKM2 was examined. PKM2 is a glycolytic enzyme involved in the production of pyruvate and has been shown to have a role in transcriptional regulation as it can phosphorylate histones during gene transcription and chromatin remodelling (Chen et al., 2014). Correlations between PKM2 and pluripotency marker expression had also previously been observed highlighting a transcriptional role for PKM2 in OCT4 expression in hESCs (Christensen et al., 2015).

However, the mechanism of how an increased rate of flux through glycolysis enhances HIF-2α expression in hESCs is currently unclear and further work is required to establish whether this involves comparable mechanisms to those shown for HIF-1α, particularly as HIF-1α is not expressed in hESCs cultured under long term hypoxia (Forristal et al., 2010). Additionally, since HIF-2α itself promotes glycolytic metabolism (Forristal et al., 2013), enhancement of HIF-2α by glycolysis constitutes a potential novel feed forward mechanism that is critical for the acquisition and maintenance of hESC self-renewal.

Together, these data suggest the rate of flux through glycolysis regulates not only CtBP1 and CtBP2 but also OCT4, SOX2 and NANOG expression in hESCs via HIF-2α, since HIF-2α is known to directly bind to the proximal promoters of these genes (Figure 4.45) (Petruzzelli et al., 2014). Much evidence suggests that HIFs support the glycolytic metabolism of hESCs, by enhancing the expression of glucose transporters and glycolytic enzymes (Semenza, 2000b; Varum et al., 2011; Forristal et al., 2013; Christensen et al., 2015). Our data represents the first report of glycolysis promoting HIF-2α protein expression in any cell type cultured under hypoxia. Although the mechanisms which regulate this effect are unclear, it is tempting to speculate that glycolytic metabolites may control HIF-2α stability by regulating the activity of HIF prolyl hydroxylases in a similar way to that observed for HIF-1α (Lu et al., 2002; Lu et al., 2005). Moreover, since HIF-2α itself promotes glycolytic metabolism (Forristal et al., 2013), enhancement of HIF-2α by glycolysis constitutes a potential novel feed forward mechanism that is critical for the acquisition and maintenance of hESC self-renewal. Furthermore, it is worth noting that these data provide evidence that CtBP expression, and not just their activity, is influenced

by the metabolic state of the cell. It is hypothesised that the reduction in CtBP expression in the presence of 2-DG, 3-BrP or sodium oxamate is due to the observed decrease in HIF-2α expression. However, it cannot be ruled out that there could be an unknown direct mechanism where glycolysis is influencing CtBP expression in order to utilise the increased levels of NADH produced in hESCs cultured under hypoxic conditions (Zhang et al., 2002; Fjeld et al., 2003).

4.5 Conclusions

The conclusions from the data presented in this chapter are:

- Hues-7 hESCs have a reduced rate of flux through glycolysis when maintained with either 2-DG, 3-BrP or oxamate under hypoxia.
- Decreasing the rate of flux through glycolysis in hESCs under hypoxia results in the loss of pluripotency and the onset of early differentiation.
- Reducing the rate of flux through glycolysis affects CtBP expression in hESCs cultured at 5% oxygen.
- Interestingly, changes in glycolytic rate, also, affected the expression of HIF-2α in hESCs maintained under hypoxia.
- Reducing the rate of flux through glycolysis also affects pluripotency marker and CtBP protein expression in hESCs maintained under atmospheric oxygen conditions.
- The effects of inhibiting the rate of flux through glycolysis in not cell line specific

Results from this chapter have highlighted the interplay between glycolysis and hypoxia and how they maintain hESC pluripotency, but also how they regulate the metabolic sensors CtBPs. The next chapter in this thesis will investigate how epigenetic changes under hypoxia influence glycolysis and hESC self-renewal.

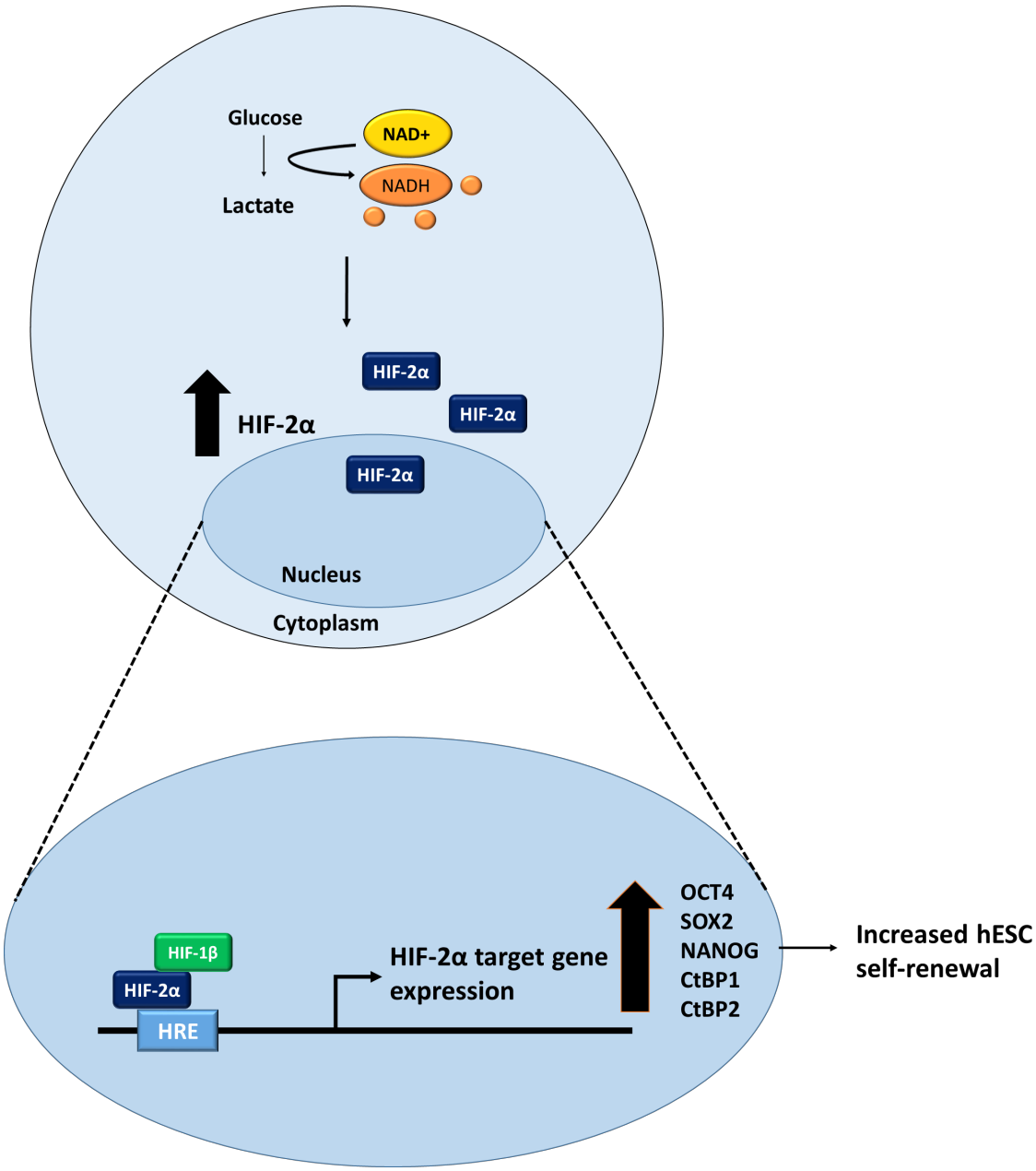

Figure 4.45. Schematic representation of glycolytic regulation of HIF-2α, pluripotency markers and CtBPs in hESCs under hypoxia.
Schematic diagram demonstrating the potential mechanism behind how a glycolytic phenotype is essential for maintained hESC pluripotency. hESCs maintained under hypoxia display a higher rate of flux through glycolysis which leads to an increase in HIF-2α protein expression. The molecular mechanisms behind this regulation of HIF-2α remain to be fully characterised. The increased HIF-2α expression forms a feed forward loop to increase the expression of glycolytic enzymes and glucose transporters to maintain the rate of flux through glycolysis. Moreover, the increased HIF-2α expression enhances hESC self-renewal and CtBP expression by directly regulating their expression.

Chapter 5

Epigenetic regulation of hESC self-renewal under hypoxia

Chapter 5: Epigenetic regulation of hESC self-renewal under hypoxia

5.1. Introduction

5.1.1. Chromatin & histone modifications

Epigenetic regulation including DNA methylation and histone modifications are being studied intensively in hESCs in order to understand the mechanisms of regulation that maintain genes in a poised position for transcription in undifferentiated cells (Meshorer et al., 2006). Furthermore, hESCs are characterised to possess a unique epigenetic signature compared to other cell types that contributes to their pluripotent state and self-renewal (Bibikova et al., 2006).

The epigenetic regulation of hESCs has an essential role in regulating the balance between pluripotency and early differentiation, and thus the role of chromatin modifications to control gene expression has been previously studied (Bernstein et al., 2006; Meshorer and Misteli, 2006). Mapping of histone modification in hESCs revealed that the genome exists in a bivalent state characterised by the presence of both histone modification associated with gene activation (H3K36me3) and silencing (H3K9me3), but leaves genes that are normally repressed in hESCs poised to be expressed upon differentiation (Bernstein et al., 2006; Mikkelsen et al., 2007; Zhao et al., 2007; Gifford et al., 2013).

5.1.2. JMJDs

Histone methylation at lysine (K) or arginine residues is an important modification that regulates gene expression and leads to either an enhancement or repression of gene transcription. Histone H3 methylated at K4, K36 and K79 is associated with active gene transcription, whereas histone H3 methylated at K9 and K27 is an indicator of gene repression. Adding and removing these modifications to regulate gene expression is a process that involves histone methyltransferases (HMTs) or histone demethylases (HDMs) respectively. Among the HDMs is the Jumonji-C (JmjC)-domain containing histone demethylase (JMJD) family.

JMJDs are a family of histone demethylases and composed of 30 members in humans based on the presence of the roughly 150 amino acid long Jumonji C (JmjC) domain. They act through a dioxygenase reaction utilising Fe^{2+}, oxygen and 2-oxoglutarate to demethylate histones, and this reaction allows JMJDs to demethylate tri-, di- and mono-

methylated lysine residues, particularly H3K4, H3K9, H3K27, H3K36 or H4K20 (Kooistra and Helin, 2012).

The expression of several JMJD family members has previously been shown to be enhanced by either HIF-1α or HIF-2α (Beyer et al., 2008; Pollard et al., 2008; Lee et al., 2014; Wang et al., 2014; Guo et al., 2015). This is reported to result in enhanced glycolysis after the increase in the expression of key genes such as *GLUT1, HK2* and *LDHA* (Wang et al., 2014; Wan et al., 2017). Moreover, JMJDs have previously been documented to play a role in either self-renewal, or even differentiation, by removing the active or repressive histone methylation modifications respectively at different lysine residues in the promoter regions (Loh et al., 2007; Kidder et al., 2014; Zhu et al., 2014). However, the exact mechanisms of how certain JMJDs may help maintain hESC self-renewal under hypoxia is not fully characterised.

5.1.3. Metabolepigenetics

The pluripotent epigenome is required to maintain the expression of pluripotency-related genes, but also remain poised for rapid and lineage-specific gene activation upon the initiation of differentiation. Concomitantly, cells constantly modulate their metabolic state in response to extracellular signals to maintain their identity. The availability and activity of various metabolites and cofactors can affect the regulation of transcription by modulating the epigenetic processes such as histone methylation and acetylation.

5.1.4. Chapter Aims

The aims of this chapter were:

- To characterise JMJD expression in hESCs maintained at either 5% or 20% oxygen
- To analyse the hypoxic regulation of JMJD expression in hESCs
- To determine whether glycolysis regulates JMJD expression in hESCs maintained under hypoxia
- To analyse histone modifications around the HRE sites in the proximal promoter regions of OCT4, SOX2, NANOG and GLUTs in response to 2-DG addition
- To investigate whether JMJD expression regulates hESC self-renewal
- To analyse histone modifications around the HRE sites in the proximal promoter regions of OCT4, SOX2, NANOG and GLUTs when JMJDs were silenced

5.2. Materials and Methods

See Section 2.1.6 and 2.2 for JMJD probes and siRNA specific information.

5.2.1. Analysis of gene expression in early hypoxia

To analyse the effects of the first 48 hours of exposure to hypoxia on the expression of genes of interest, Hues-7 hESCs maintained at 20% oxygen were passaged into three single wells of a 6-well plate. One well was maintained at 20% oxygen, whereas the other two wells were moved to 5% oxygen and incubated overnight. MEF-conditioned media was changed daily. RNA samples were collected from cells maintained at 20% oxygen 48 hours post-passage, and from cells maintained at 5% oxygen at both 24 and 48 hours post-passage for analysis by RT-qPCR.

For siRNA transfections, hESCs were passaged and incubated overnight at 20% oxygen. Cells were transfected with siRNA as previously described (Section 2.1.6) before being incubated at 5% oxygen for 48 hours before hESCs were collected and the RNA isolated.

5.3 Results

5.3.1. Hypoxic regulation of JMJDs in Hues-7 hESCs

In attempt to evaluate whether any JMJDs were involved in the hypoxic and glycolytic regulation of hESC pluripotency, JMJD mRNA expression levels in Hues-7 hESCs maintained at either 5% or 20% oxygen were investigated.

RT-qPCR analysis revealed that the expression of *JMJD1a*, *JMJD2a*, *JMJD2b* and *JMJD5* was significantly increased in hESCs cultured under 5% oxygen compared to those maintained under normoxic oxygen tensions (Figure 5.1). A significant and approximate 110%, 70%, 55% and 85% increase in *JMJD1a* (p=0.0441), *JMJD2a* (p=0.0252), *JMJD2b* (p=0.0265) and *JMJD5* (p=0.0454) mRNA expression respectively was observed in hESCs maintained at 5% oxygen compared to those cultured at 20% oxygen. No significant difference was observed in the mRNA expression of *JMJD2c* in hESCs maintained at either 5% or 20% oxygen (Figure 5.1). It is worth noting that the relative abundance of each *JMJD* within each sample was similar, except for *JMJD2b* where Ct values reflected that this was at slightly lower abundance compared to the others.

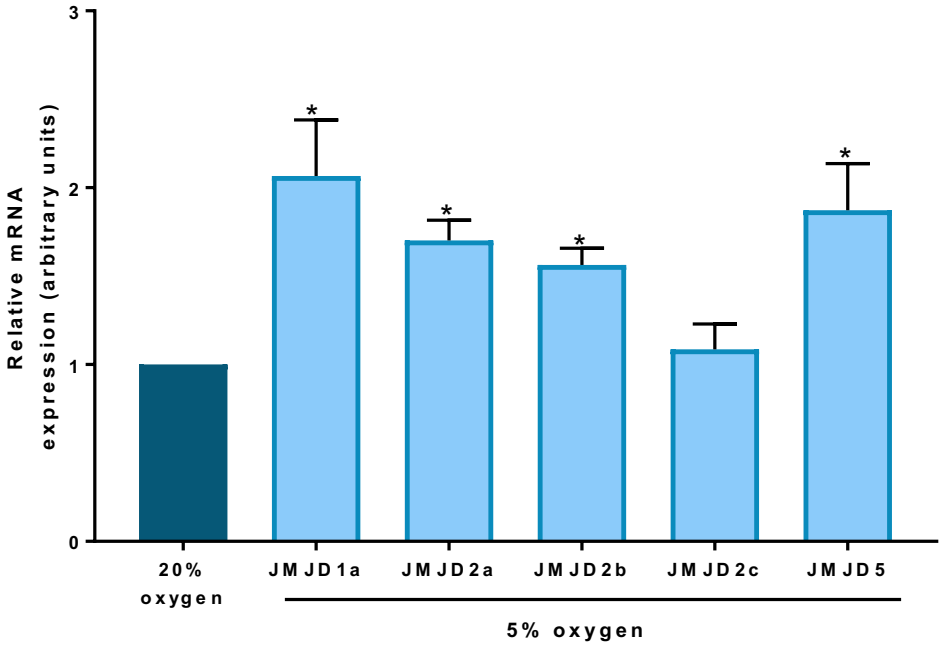

Figure 5.1. Hypoxia increases JMJD protein expression in Hues-7 hESCs.
Quantification of *JMJD1a, JMJD2a, JMJD2b, JMJD2c* and *JMJD5* mRNA levels in Hues-7 hESCs maintained at either 5% oxygen or 20% oxygen. Data were normalised to *UBC*, and then to 1 for 20% oxygen. Bars represent mean ± SEM. (n=3-4).

To determine if the hypoxic regulation of JMJDs was dependent on HIF-2α, hESCs maintained under hypoxic conditions were transfected with either Allstars negative control or HIF-2α siRNA for 48 hours before collecting samples for analysis by RT-qPCR.

RT-qPCR revealed a significant and approximate 65% reduction in *HIF-2α* expression in hESCs transfected with HIF-2α siRNA compared to the control (p=0.0481; Figure 5.2A).

As a consequence of silencing HIF-2α, there was a resulting decrease in *JMJD1a*, *JMJD2a*, *JMJD2b* and *JMJD5* expression (Figure 5.2B). *JMJD1a* (p=0.0105), *JMJD2a* (p=0.0364) and *JMJD2b* (p=0.0477) were all significantly reduced by approximately 60%, whereas *JMJD5* expression was reduced by approximately 39% (p=0.0084) in hESCs transfected with HIF-2α siRNA compared to those transfected with the Allstars negative control siRNA. No significant difference was observed in *JMJD2c* mRNA expression levels in hESCs transfected with either Allstars or HIF-2α siRNA (Figure 5.2B). This was similar to the trend observed when comparing JMJD mRNA expression in hESCs cultured at either 5% or 20% oxygen.

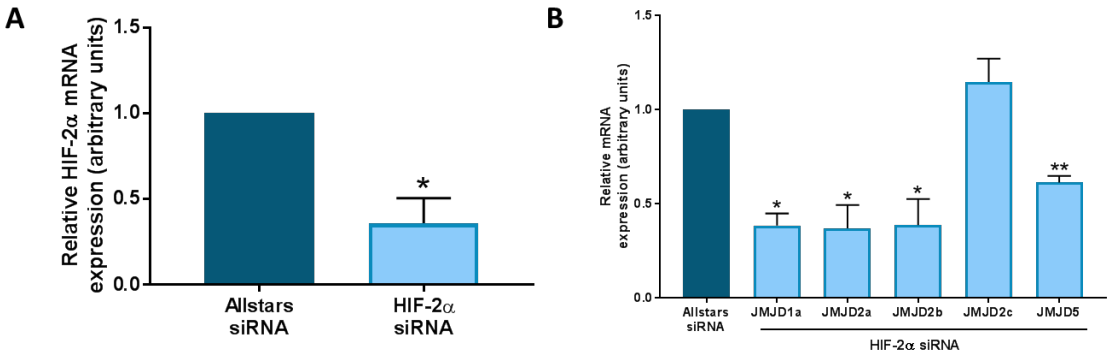

Figure 5.2. JMJD expression is regulated by HIF-2α, except for *JMJD2C*, in Hues-7 hESCs maintained under hypoxia.
(A) Quantification of *HIF-2α* mRNA in Hues-7 hESCs transfected with HIF-2α siRNA revealed a significant decrease in *HIF-2α* expression compared to the control. (B) Quantification of *JMJD* mRNA expression in Hues-7 hESCs transfected with HIF-2α siRNA compared to the Allstars control for 48 hours under hypoxia. Data were normalised to *UBC*, and then to 1 for Allstars negative control. Bars represent mean ± SEM. (n=3)

HIF-2α is responsible for the long term hypoxic response in hESCs, whereas HIF-1α regulates the first 48 hours of exposure to hypoxia (Forristal et al., 2010). Therefore, the next aim was to investigate whether there was any change in *JMJD2c* mRNA expression during the first 48 hours of hypoxia. RNA samples were collected from Hues-7 hESCs maintained at either 20% oxygen or 5% oxygen long-term for more than 3 passages, or from hESCs incubated under hypoxia for 24 and 48 hours before analysing by RT-qPCR.

JMJD2c mRNA expression was found to be significantly increased in a time-dependent manner in hESCs exposed to short term hypoxia compared to cells maintained at 20% oxygen. *JMJD2c* expression was found to increase by approximately 50% after 24 hours of exposure to hypoxia ($p=0.0041$), whereas a significant and approximate 90% increase in *JMJD2c* expression was recorded after 48 hours of exposure to hypoxia ($p=0.0403$) compared to hESCs maintained under 20% oxygen (Figure 5.3A). No difference was observed in *JMJD2c* expression between hESCs maintained at either 5% or 20% oxygen long term for more than 3 passages in agreement with Figure 5.1.

HIF-1α mRNA expression was found to significantly increase within the first 48 hours of hypoxia compared to those cells maintained at 20% oxygen, but no difference was observed between hESCs cultured long term at 5% oxygen compared to those maintained at 20% oxygen. *HIF-1α* mRNA expression increased by approximately 70% ($p=0.0305$) and 35% ($p=0.0495$) after 24 and 48 hours of exposure to hypoxia respectively compared to hESCs maintained at 20% oxygen.

These data reveal that both *JMJD2c* and *HIF-1α* increase upon initial exposure to hypoxia.

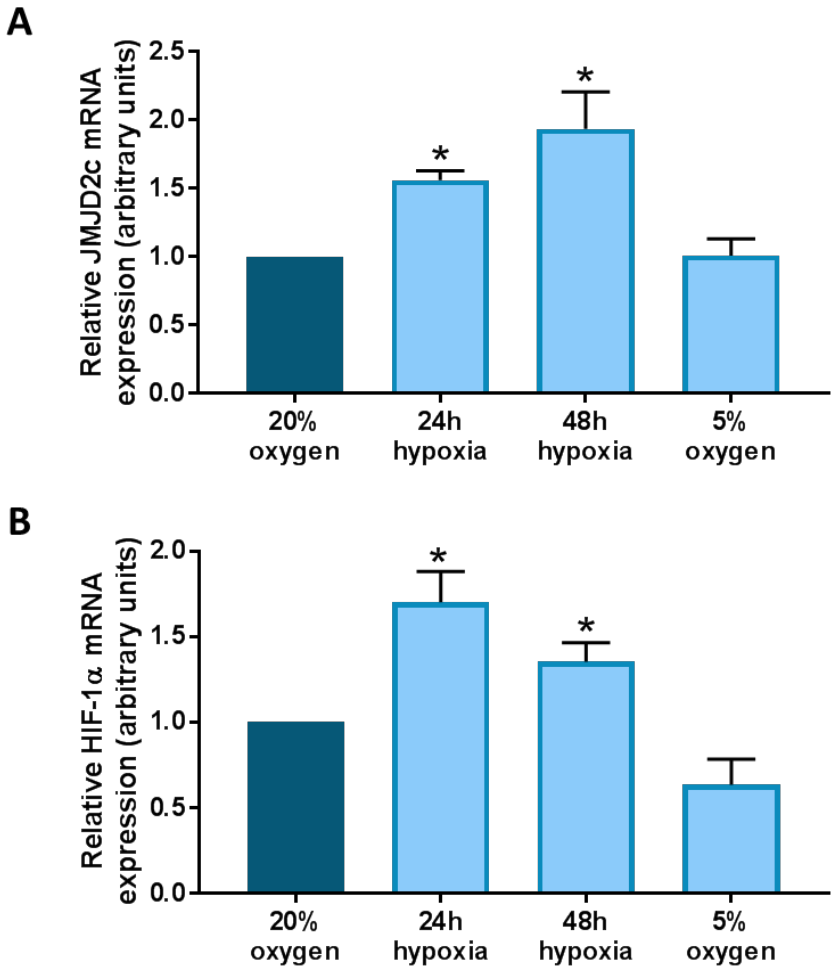

Figure 5.3. *JMJD2c* & *HIF-1α* expression increases within the first 48 hours of exposure to hypoxia.

(A) Quantification of *JMJD2c* expression levels in Hues-7 hESCs maintained either at 20%, or at 5% oxygen for 24 hours, 48 hours or long-term hypoxic culture. (B) Quantification of *HIF-2α* expression levels in Hues-7 hESCs maintained either at 20%, or at 5% oxygen for 24 hours, 48 hours or long-term for more than 3 passages under hypoxic conditions. Data were normalised to *UBC*, and then to 1 for Allstars negative control. Bars represent mean ± SEM. (n=4)

Due to the observed correlating trend between *JMJD2c* and *HIF-1α* expression in hESCs within the first 48 hours of hypoxic culture, the next aim was to examine whether HIF-1α regulates the expression of *JMJD2c* in hESCs maintained at 5% oxygen for only 48 hours by transfecting hESCs with HIF-1α siRNA.

To determine that *HIF-1α* expression was silenced, RT-qPCR analysis was performed on hESCs samples transfected with either Allstars control or HIF-1α siRNA. *HIF-1α* mRNA expression significantly reduced by approximately 45% (p=0.0473) in hESCs transfected with HIF-1α siRNA compared to control cells (Figure 5.4A). After successfully silencing *HIF-1α*, any consequent effects on *JMJD2c* expression was investigated. A significant 47% decrease in *JMJD2c* mRNA (p=0.0455) was revealed in hESCs where *HIF-1α* had been silenced compared to hESCs transfected with the Allstars negative control (Figure 5.4B).

Together, this data suggests that *HIF-1α* regulates *JMJD2c* expression in hESCs.

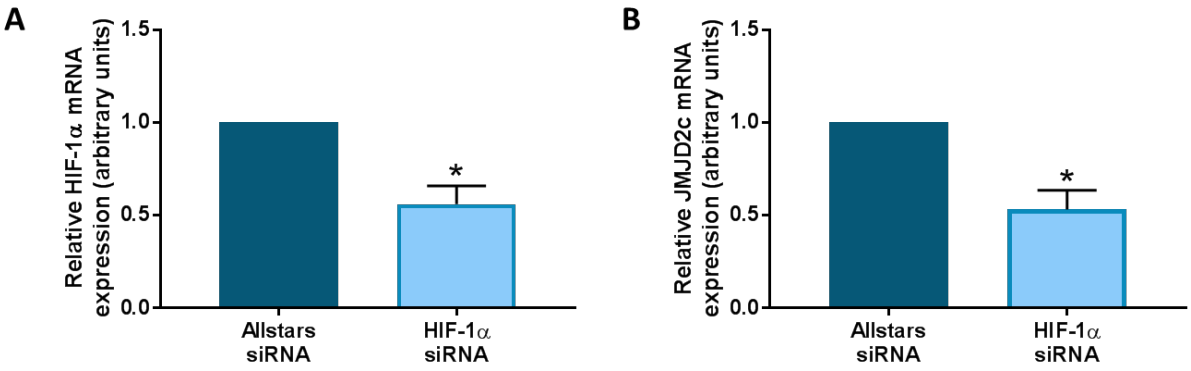

Figure 5.4. HIF-1α regulates JMJD2c mRNA expression within the first 48 hours of exposure to hypoxia in hESCs.
(A) Quantification of *HIF-1α* expression in hESCs transfected with either Allstars negative control or HIF-1α siRNA. (B) Quantification of *JMJD2c* expression in hESCs transfected with either Allstars negative control or HIF-1α siRNA for 48 hours at 5% oxygen. Data were normalised to *UBC*, and then to 1 for Allstars negative control. Bars represent mean ± SEM. (n=3)

5.3.2. Glycolytic regulation of JMJD expression and chromatin state in Hues-7 hESCs under hypoxia.

To determine whether JMJD expression was regulated by the rate of flux through glycolysis, hESCs were incubated with the glycolytic inhibitor 2-DG for 48 hours before collecting samples for RT-qPCR analysis.

The mRNA expression of *JMJD1a, JMJD2a, JMJD2b, JMJD2c* and *JMJD5* all significantly decreased in hESCs incubated with 10mM 2-DG compared to those cultured in the absence of the inhibitor. There was a significant and approximate 35% reduction in *JMJD1a* (p=0.0061), *JMJD2a* (p=0.0024), *JMJD2b* (p=0.0047) and *JMJD2c* (p=0.0214) expression, whereas *JMJD5* expression significantly decreased by 54% (p=0.0286) in cells cultured in the presence of 2-DG (Figure 5.5).

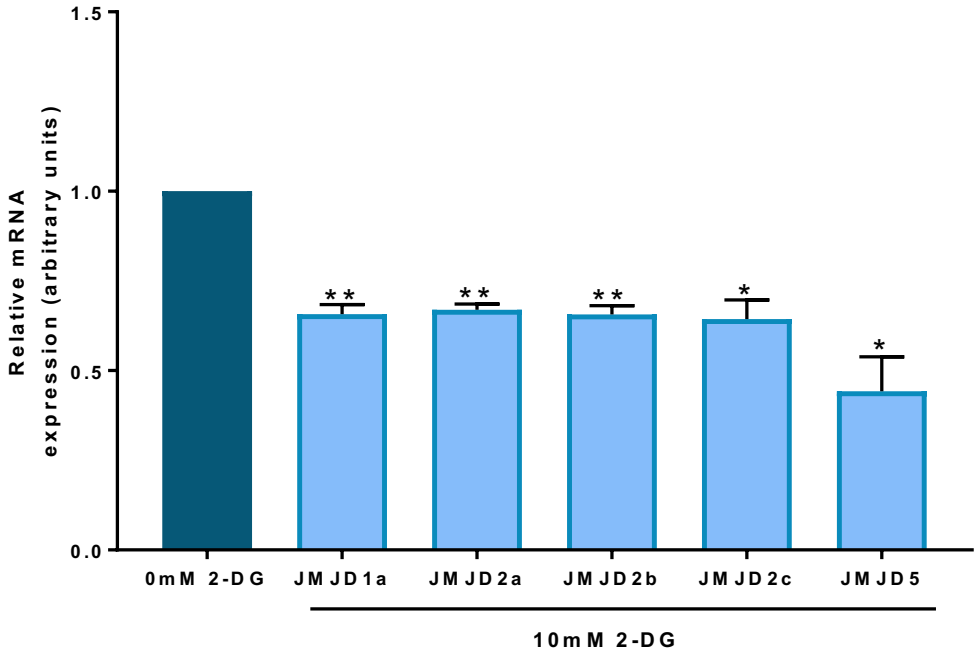

Figure 5.5. JMJD expression decreases after inhibiting glycolysis using the inhibitor 2-DG. Quantification of *JMJD1a*, *JMJD2a*, *JMJD2b*, *JMJD2c* and *JMJD5* expression in Hues-7 hESCs maintained at 5% oxygen and incubated in MEF-conditioned medium supplemented with 10mM 2-DG compared to the 0mM 2-DG control after 48 hours. Data were normalised to *UBC*, and then to 1 for 0mM 2-DG control. Bars represent mean ± SEM. (n=3)

To verify the results obtained for JMJD expression in the presence of 2-DG, the experiment was repeated using a second glycolytic inhibitor; 3-BrP. Hues-7 hESCs maintained under hypoxic oxygen tensions were incubated with either 0µM or 25µM 3-BrP for 48 hours before collecting samples for use in RT-qPCR.

Inhibiting glycolysis with 3-BrP resulted in a significant reduction in JMJD mRNA expression in hESCs (Figure 5.6). *JMJD1a* (p=0.0135) and *JMJD2a* (p=0.0097) mRNA expression decreased by approximately 60% *JMJD2a* expression reduced by approximately 61%. *JMJD2b* (p=0.0029) and *JMJD2c* (p=0.0013) mRNA expression significantly reduced by approximately 65%, whereas *JMJD5* (p=0.0274) mRNA expression decreased by approximately 52% in hESCs treated with 25µM 3-BrP compared to hESCs incubated with 0µM 3-BrP.

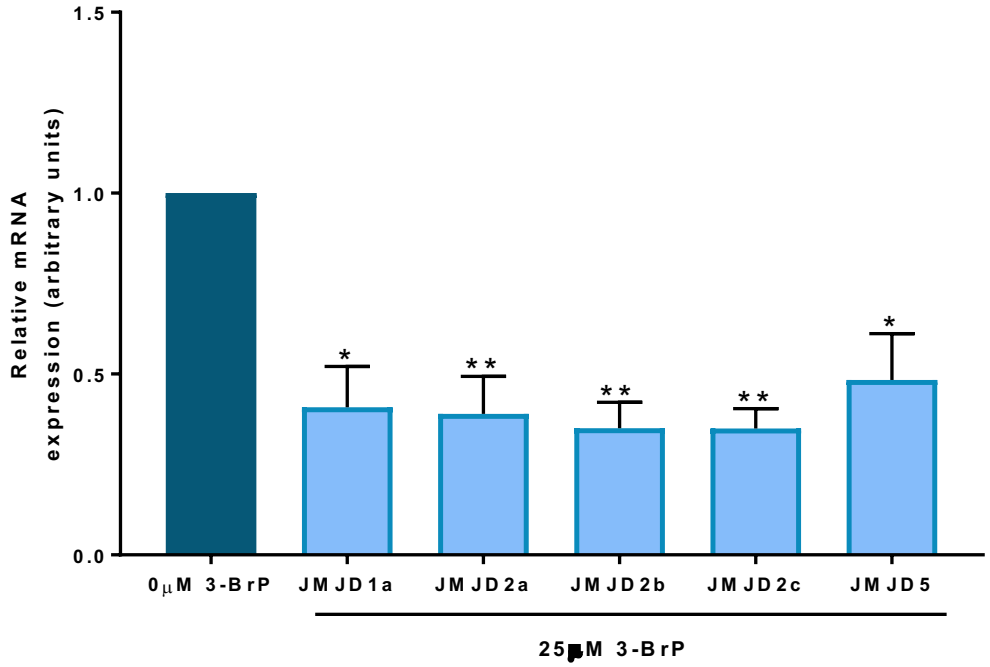

Figure 5.6. JMJD expression decreases after inhibiting glycolysis using the inhibitor 3-BrP. Quantification *JMJD1a*, *JMJD2a*, *JMJD2b*, *JMJD2c* and *JMJD5* mRNA expression in Hues-7 hESCs maintained at 5% oxygen and incubated in MEF-conditioned medium supplemented with 25µM 3-BrP compared to the 0µM 3-BrP control after 48 hours. Data were normalised to *UBC*, and then to 1 for 0µM 3-BrP control. Bars represent mean ± SEM. (n=4)

To investigate whether inhibiting glycolysis affects chromatin state, ChIP analysis was performed to analyse any changes in histone modifications within predicted HRE sites of the hypoxia inducible genes; OCT4, SOX2, NANOG, GLUT1 and GLUT3. Chromatin isolated from hESCs maintained at 5% oxygen and incubated with either 0mM or 10mM 2-DG was sheared and immunoprecipitated with specific antibodies against the histone modifications H3K9me3 and H3K36me3, while immunoprecipitation with a non-specific IgG antibody was used as a negative control.

Using probes designed to cover the HRE site at -1956bp in the OCT4 proximal promoter, percentage enrichment of OCT4 proximal promoter DNA revealed a significant increase in H3K9me3 expression compared to the IgG only control ($p=0.0182$) in hESCs incubated with 10mM 2-DG. H3K9me3 levels in hESCs incubated in the absence of 2-DG were not significantly different to the IgG control. Likewise, no significant difference was observed in H3K36me3 levels compared to the IgG control in hESCs treated in the presence or absence of 2-DG (Figure 5.7A). However, when the relative enrichment of H3K9me3 and H3K36me3 histone modifications around the OCT4 HRE were analysed between hESCs incubated either in the presence or absence of 10mM 2-DG, there was a significant increase in the H3K9me3 repressive histone mark by approximately 1.5-fold ($p=0.0393$) in hESCs incubated with 10mM 2-DG compared to hESCs incubated in the absence of 2-DG. In contrast, relative enrichment of the active H3K36me3 histone marker significantly decreased by 75% ($p=0.0246$) in hESCs cultured in the presence of 2-DG compared to control cells (Figure 5.8A).

Using a probe designed to cover the HRE at -1100bp in the SOX2 proximal promoter (SOX2_G), H3K36me3 histone modification levels were significantly increased compared to the IgG control ($p=0.0267$) in hESCs treated with 10mM 2-DG, whereas no other significant differences in H3K9me3 and H3K36me3 histone modifications were observed in hESCs incubated either in the presence or absence of 2-DG (Figure 5.7B). Additionally, H3K9me3 levels were significantly increased compared to the IgG control ($p=0.0322$) around the HRE at -1450bp in the SOX2 proximal promoter (SOX2_A) in hESCs incubated with 10mM 2-DG. Additionally, H3K36me3 levels at this particular HRE were significantly increased compared to the IgG control in hESCs incubated in the absence of 2-DG ($p=0.0472$) and in the presence of the inhibitor ($p=0.0077$; Figure 5.7C). When the relative enrichment of both H3K9me3 and H3K36me3 modifications at both HREs in the SOX2 proximal promoter in hESCs incubated with 10mM 2-DG compared

to those incubated in the absence of the inhibitor, there was an approximate 4-fold ($p=0.0115$) and 4.5-fold increase ($p=0.0218$) in the relative enrichment of H3K9me3 at SOX_G and SOX2_A respectively in the presence of 2-DG compared to the control cells. Furthermore, the relative enrichment of the histone marker H3K36me3 significantly decreased by 67% ($p=0.0288$) and 72% ($p=0.0037$) at the SOX2_G and SOX2_A HREs respectively in hESCs cultured with 2-DG compared to hESCs maintained without the inhibitor (Figure 5.8B-C).

Finally, using a probe designed to amplify the HRE at -301bp in the NANOG proximal promoter, the percentage enrichment of NANOG proximal promoter DNA revealed a significant increase in H3K9me3 histone modifications compared to the IgG control ($p=0.0041$) in hESC treated with 10mM 2-DG and also a significant increase in H3K36me3 histone modifications compared to the IgG control ($p=0.004$) in hESCs incubated in the absence of the inhibitor. Interestingly, H3K9me3 levels significantly increased when hESCs were treated with 10mM 2-DG compared to cells incubated in the absence of 2-DG ($p=0.0118$), whereas conversely H3K36me3 levels significantly decreased ($p=0.0344$) after the addition of 2-DG (Figure 5.7D). The relative enrichment of H3K9me3 and H3K36me3 levels in hESCs incubated in the presence of 2-DG compared to the absence of the inhibitor reemphasised this observation, where H3K9me3 enrichment increased by 6-fold ($p=0.0219$) and H3K36me3 enrichment decreased significantly by approximately 65% ($p=0.0322$) at the HRE at -301bp in the NANOG proximal promoter in hESCs cultured with 2-DG compared to hESCs maintained without 2-DG (Figure 5.8D).

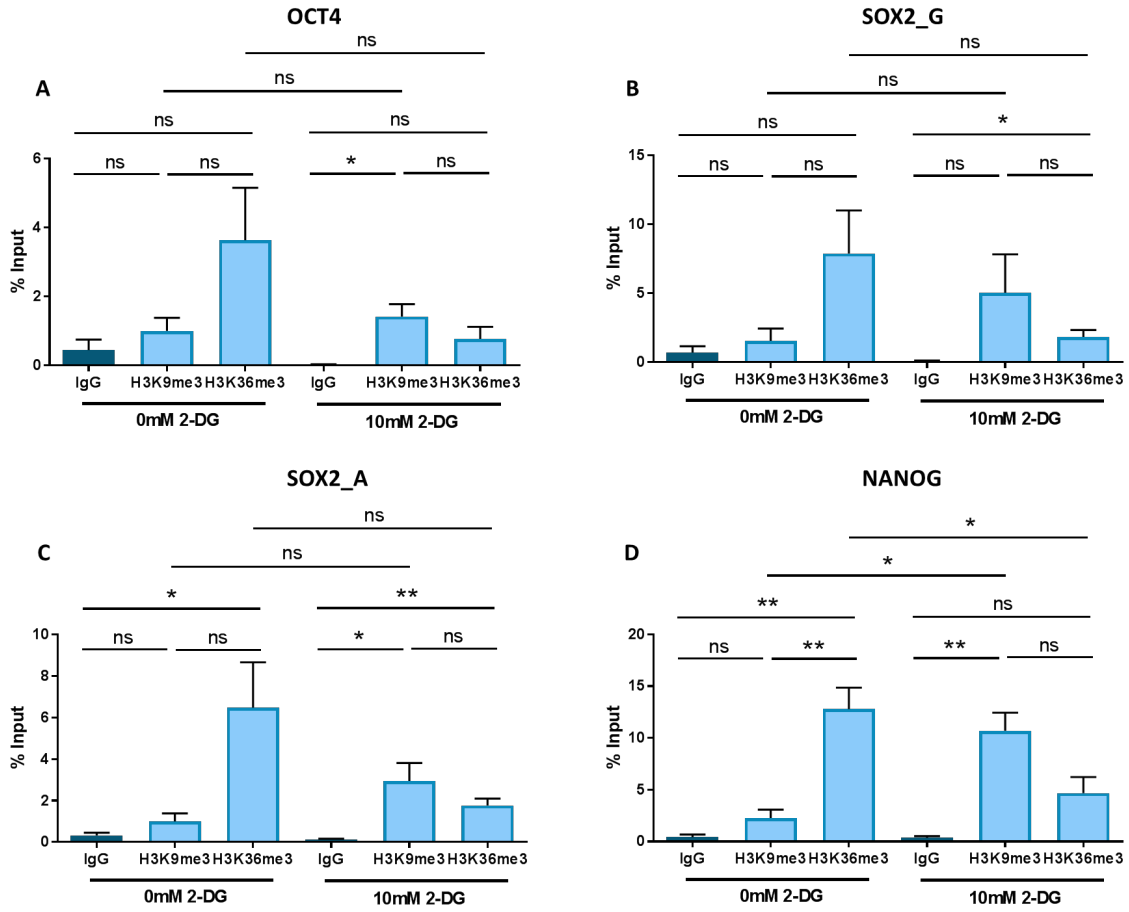

Figure 5.7. Histone modifications within the HREs of OCT4, SOX2 and NANOG proximal promoters in hESCs maintained at 5% oxygen and treated with 2-DG.
ChIP analysis was performed on chromatin isolated from hESCs maintained at 5% oxygen and incubated either in the presence or absence of 10mM 2-DG to reveal the levels of H3K9me3 and H3K36me3 histone marks around the HREs in the OCT4 (A), SOX2_G (B), SOX2_A (C) and NANOG (D) proximal promoters. OCT4, SOX2 and NANOG proximal promoter DNA enrichment is expressed as a percentage of Input (non-immunoprecipitated chromatin). Bars represent mean ± SEM. (n=3).

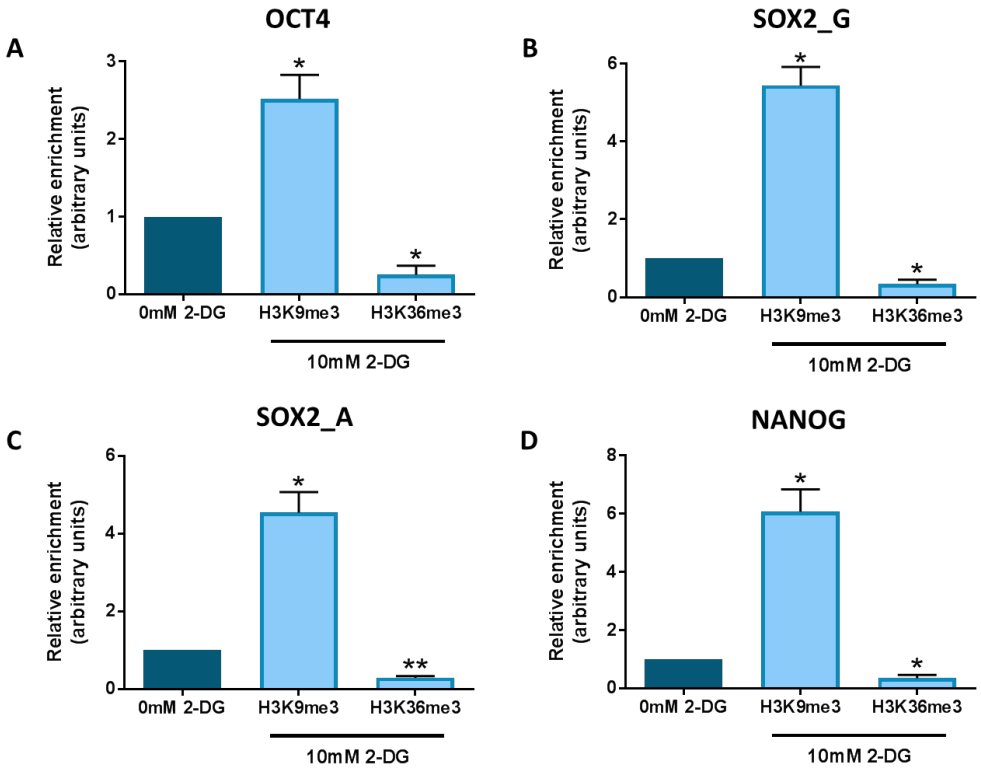

Figure 5.8. Relative enrichment of histone modification markers within the HREs of *OCT4*, *SOX2* and *NANOG* genes in hESCs maintained under hypoxia and treated with 2-DG.
ChIP assays were performed with 3µg of anti-H3K9me3, anti-H3K36me3 or IgG control antibodies immunoprecipitated with chromatin isolated from hESCs cultured at 5% oxygen and incubated with either 0mM or 10mM 2-DG before analysing the relative enrichment at predicted HREs in OCT4 (A), SOX2 (B-C) and NANOG (D) proximal promoters. DNA enrichment is expressed as a percentage of Input (non-immunoprecipitated chromatin) minus the background IgG. All data have been normalised to 1 for 0mM 2-DG control. Bars represent mean ± SEM. (n=3)

Pie charts were used to represent the relative enrichment of each histone marker as a proportion of the total for each predicted HRE of interest. While the bar charts represent a comparison of individual epigenetic marks, the pie charts demonstrate a more global indication of the chromatin state in response to the glycolytic inhibitor 2-DG. Pie charts revealed an increase in the proportion of H3K9me3 bound in hESCs cultured in the presence of 2-DG compared to the 0mM control for OCT4 (Figure 5.9A), SOX2_G (Figure 5.9B), SOX2_A (Figure 5.9C) and NANOG (Figure 5.9D).

This data suggests that inhibiting glycolysis in hESCs maintained under hypoxia leads to a more heterochromatic state around the predicted HRE sites in the OCT4, SOX2 and NANOG proximal promoters.

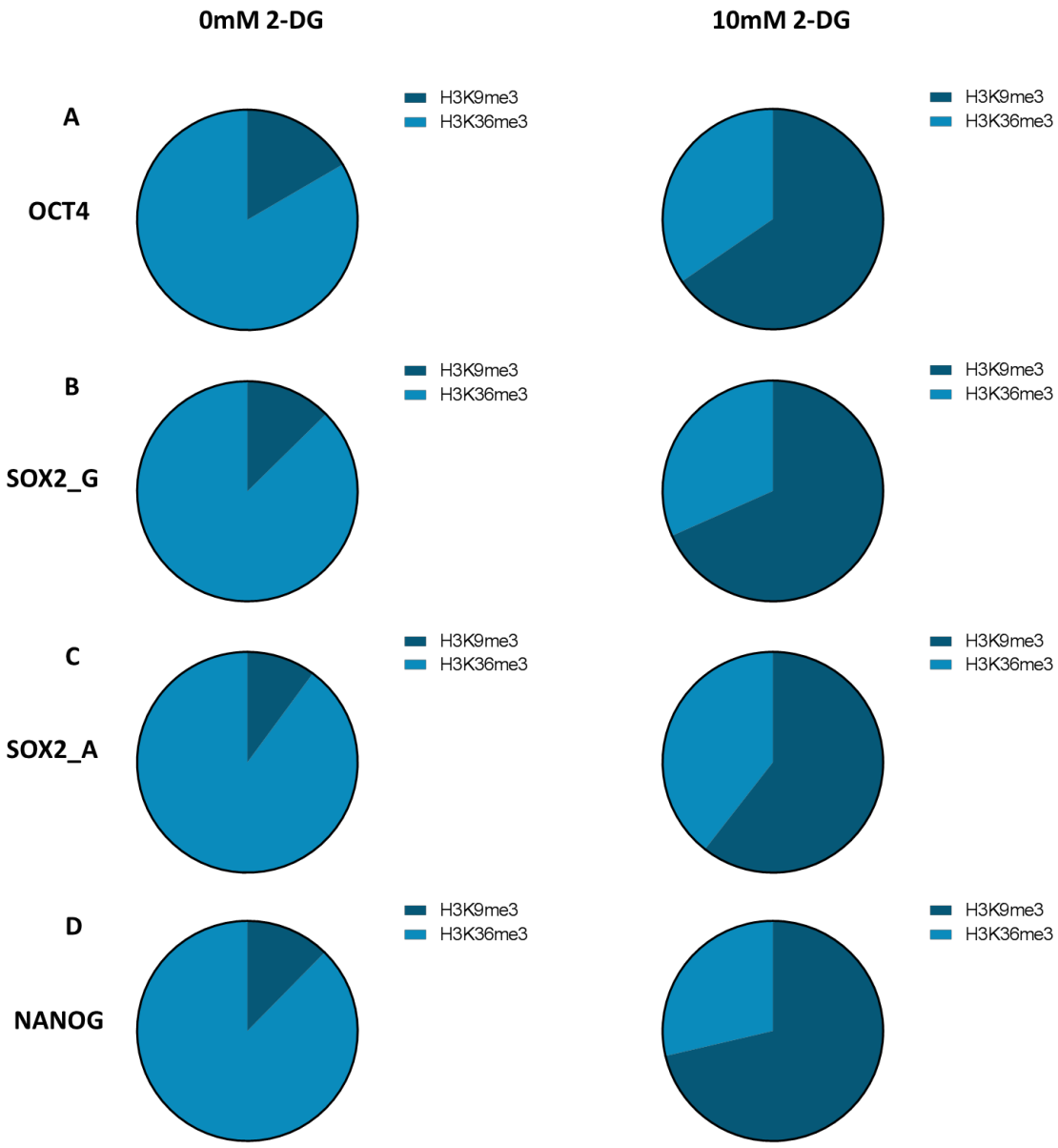

Figure 5.9. Inhibiting glycolysis under hypoxia in hESCs using 2-DG results in a more heterochromatic conformation within the HREs of *OCT4*, *SOX2* and *NANOG*.
Active H3K36me3 and repressive H3K9me3 histone modifications in the predicted HRE sites of the OCT4 (-1956bp; A), SOX2 (-1100bp, B; -1450bp, C) and NANOG (-301bp; D) proximal promoters of chromatin isolated from hESCs maintained at 5% oxygen and incubated with either 0mM or 10mM 2-DG. Pie charts demonstrate a comparison of enrichment in hESCs treated with 10mM 2-DG compared to the 0mM 2-DG control for each HRE site analysed. DNA enrichment is expressed as a percentage of Input (non-immunoprecipitated chromatin) minus the background IgG. All data have been normalised to 1 for 0mM 2-DG control. Bars represent mean ± SEM. (n=3)

ChIP analysis was performed to analyse any changes in histone modifications within HRE sites of GLUT1 and GLUT3 proximal promoters to evaluate whether reducing the rate of glycolysis affected the gene expression of GLUTs by changing the chromatin state.

H3K36me3 histone modification levels were significantly increased at the HRE in the GLUT1 proximal promoter compared to the IgG control in hESCs incubated in both the absence ($p=0.001$) and the presence of 2-DG ($p=0.022$). Interestingly, a significant decrease in H3K36me3 expression was observed around the HRE in the GLUT1 proximal promoter between hESCs incubated in the presence of 10mM 2-DG compared to the absence of 2-DG ($p=0.0049$; Figure 5.10A). Relative enrichment levels of H3K36me3 between hESCs reinforced that trend, but also revealed a significant and approximate 4.2-fold increase ($p=0.0338$) in H3K9me3 in the same DNA region between hESCs incubated with 10mM 2-DG compared to the control cells (Figure 5.11A).

H3K9me3 histone modification levels were significantly increased compared to the IgG control in hESCs incubated either in the absence of 2-DG ($p=0.0356$) or the presence of 10mM 2-DG ($p=0.0009$) at the HRE in the GLUT3 proximal promoter (Figure 5.10B). Relative enrichment of H3K9me3 significantly increased by approximately 5-fold ($p=0.039$) and H3K36me3 significantly reduced by 70% ($p=0.0036$) in chromatin isolated from hESCs incubated with 10mM 2-DG compared to those maintained in the absence of the inhibitor at the HRE in the GLUT3 proximal promoter (Figure 5.11B).

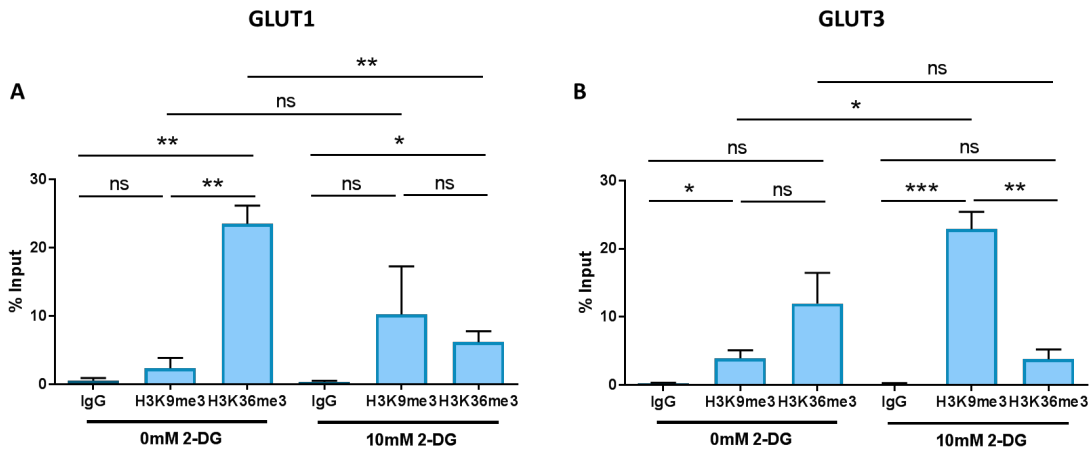

Figure 5.10. Histone modifications within the HREs of GLUT1 and GLUT3 proximal promoters in hESCs maintained at 5% oxygen and treated with 2-DG.
ChIP analysis was performed on chromatin isolated from hESCs maintained at 5% oxygen and incubated either in the presence or absence of 10mM 2-DG to reveal the levels of H3K9me3 and H3K36me3 histone marks around the HREs in the GLUT1 (A) and GLUT3 (B) proximal promoters. GLUT1 and GLUT3 proximal promoter DNA enrichment is expressed as a percentage of Input (non-immunoprecipitated chromatin). Bars represent mean ± SEM. (n=3).

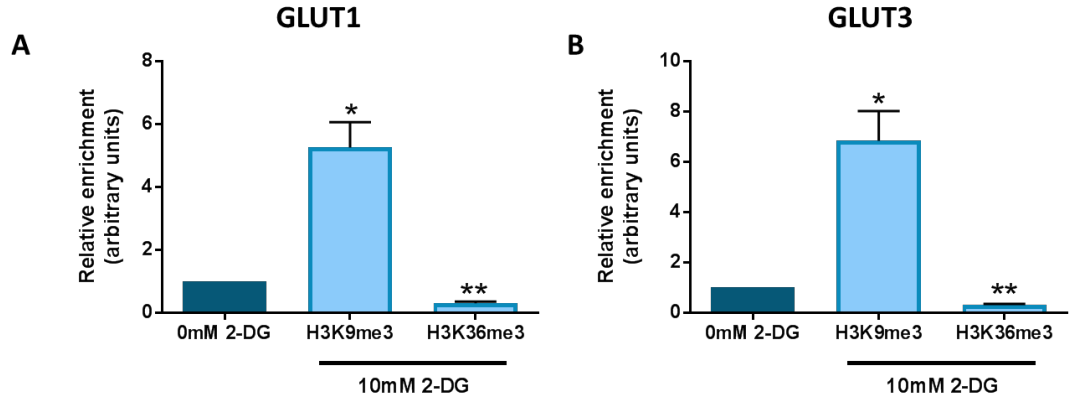

Figure 5.11. Relative enrichment of histone modification markers within the HRE sites of *GLUT1* and *GLUT3* genes in hESCs maintained under hypoxia and treated with 2-DG.
ChIP assays were performed with 3µg of anti-H3K9me3, anti-H3K36me3 or IgG control antibodies immunoprecipitated with chromatin isolated from hESCs cultured at 5% oxygen and incubated with either 0mM or 10mM 2-DG before analysing the relative enrichment at predicted HREs in the GLUT1 (A) and GLUT3 (B) proximal promoters. DNA enrichment is expressed as a percentage of Input (non-immunoprecipitated chromatin) minus the background IgG. All data have been normalised to 1 for 0mM 2-DG control. Bars represent mean ± SEM. (n=3)

Pie charts revealed an increase in the proportion of H3K9me3 bound to the GLUT1 and GLUT3 HRE sites in hESCs cultured in the presence of 2-DG compared to the 0mM control for GLUT1 (Figure 5.12A) and GLUT3 (Figure 5.12B) proximal promoters.

This data suggests that decreasing the rate of flux through glycolysis in hESCs maintained under hypoxia leads to a more heterochromatic state around a HRE site in the GLUT1 and GLUT3 proximal promoters.

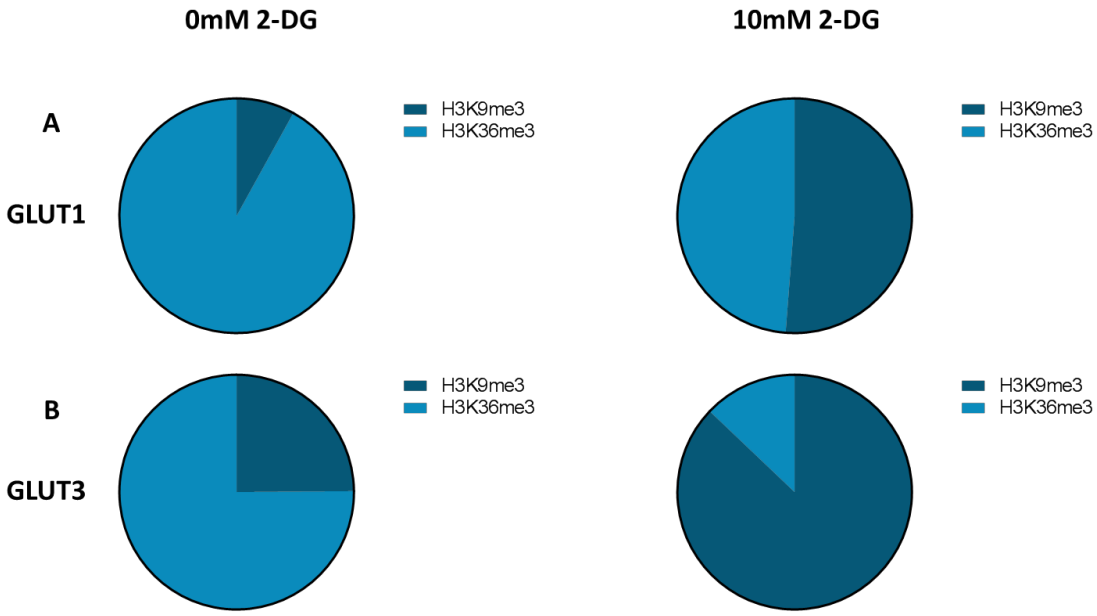

Figure 5.12. Inhibiting glycolysis under hypoxia in hESCs induces a more heterochromatic conformation within the HREs of *GLUT1* and *GLUT3*.
Active H3K36me3 and repressive H3K9me3 histone modifications in the predicted HRE sites of the GLUT1 (A) and GLUT3 (B) proximal promoters of chromatin isolated from hESCs maintained at 5% oxygen and incubated with either 0mM or 10mM 2-DG. Pie charts demonstrate a comparison of enrichment in hESCs treated with 10mM 2-DG compared to the 0mM 2-DG control for each HRE site analysed. DNA enrichment is expressed as a percentage of Input (non-immunoprecipitated chromatin) minus the background IgG. All data have been normalised to 1 for 0mM 2-DG control. Bars represent mean ± SEM. (n=3)

5.3.3. Role of JMJD2a in the maintenance of hESC pluripotency under hypoxia

To investigate whether the histone demethylases JMJDs play a role in pluripotency maintenance, Hues-7 hESCs maintained under 5% oxygen were transfected with either Allstars control or JMJD2a siRNA before collecting samples for use in RT-qPCR 48 hours post-transfection.

RT-qPCR revealed that *JMJD2a* was successfully silenced in Hues-7 hESCs after transfection with JMJD2a siRNA (Figure 5.13A; p=0.0063) compared to those transfected with the Allstars negative control siRNA. Silencing JMJD2a caused a significant reduction in *OCT4* (p=0.0026), *SOX2* (p=0.0066), *NANOG* (p=0.0024), *LIN28B* (p=0.0345) and *SALL4* (p=0.0431) mRNA expression compared to the Allstars negative control siRNA transfected cells (Figure 5.13B).

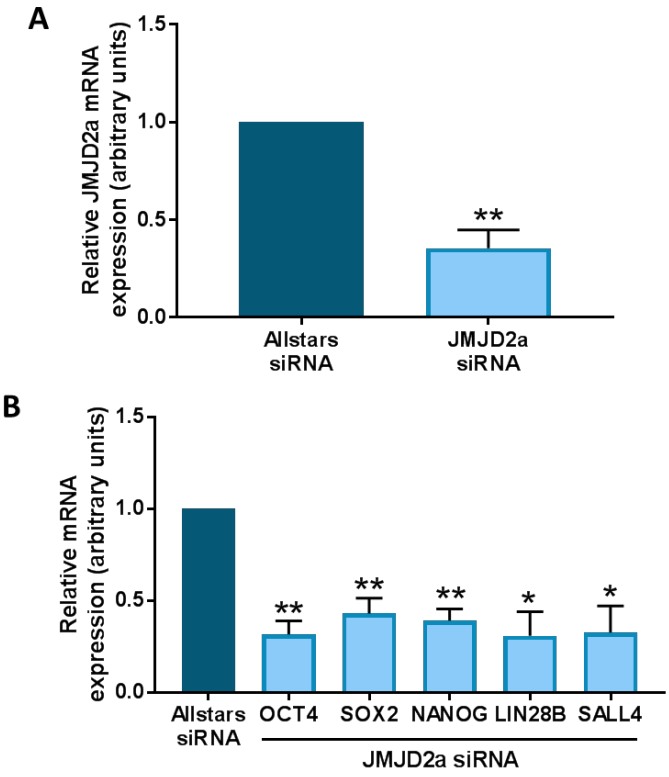

Figure 5.13. Silencing JMJD2a expression decreases pluripotency marker expression. Hues-7 hESCs maintained at 5% oxygen were transfected with either Allstars negative control or JMJD2a siRNA before collecting samples for RNA isolation 48 hours post-transfection. (A) Quantification of *JMJD2a* mRNA in Hues-7 hESCs transfected with either Allstars or JMJD2a siRNA. (B) Quantification of *OCT4, SOX2, NANOG, LIN28B* and *SALL4* mRNA expression in Hues-7 hESCs transfected with JMJD2a siRNA compared to the Allstars control. Data were normalised to *UBC*, and then to 1 for Allstars negative control. Bars represent mean ± SEM. (n=3-4)

To determine whether there was any impact of silencing JMJD2a on the glycolytic phenotype of Hues-7 hESCs cultured under hypoxia, lactate production was measured in the spent conditioned media samples. Cells were transfected with either Allstars negative control or HIF-2α siRNA for 48 hours with the spent medium collected from day 2 to day 3 post-transfection for analysis of glycolytic phenotype.

hESCs transfected with Allstars siRNA produced 38.7 ± 4.6 pmol/cell/24hr of lactate, whereas hESCs transfected with JMJD2a siRNA produced 28.7 ± 3.9 pmol/cell/24hr of lactate. Statistical analysis revealed that silencing JMJD2a did not affect lactate production in Hues-7 hESCs maintained under hypoxic conditions compared to hESCs transfected with Allstars negative control siRNA (p=0.1149; Figure 5.14).

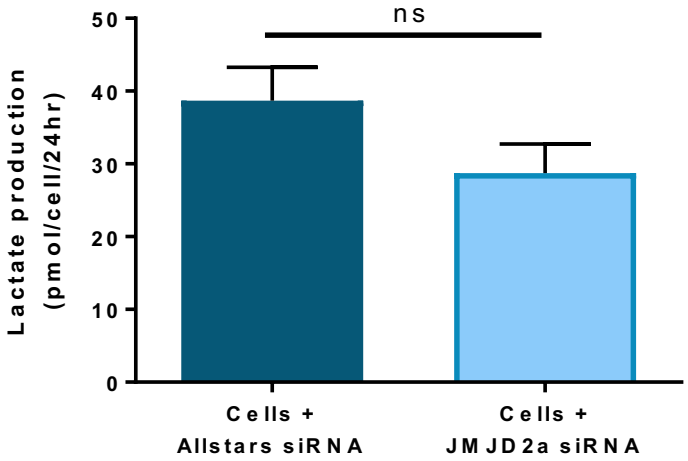

Figure 5.14. Silencing JMJD2a had no effect on lactate production in hESCs under hypoxia. Enzyme-linked assays were performed to measure lactate production in Hues-7 hESCs cultured under 5% oxygen and transfected with either Allstars siRNA or HIF-2α siRNA for 48 hours prior to collecting conditioned media samples. Bars represent mean ± SEM. (n=12)

To investigate whether silencing JMJD2a had any consequent effects on the expression of *LDHA* or the glucose transporters *GLUT1* and *GLUT3*, RT-qPCR analysis was performed.

There was no significant difference in *GLUT1* or *GLUT3* mRNA expression between hESCs transfected with either Allstars control or JMJD2a siRNA. However, silencing JMJD2a resulted in a significant and approximate 65% decrease (p=0.0299) in *LDHA* expression compared to the control cells (Figure 5.15).

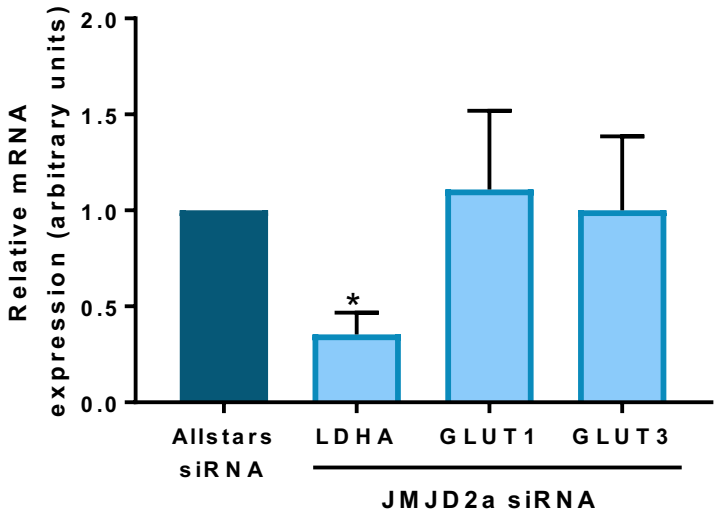

Figure 5.15. Silencing JMJD2a expression decreases expression of the glycolytic enzyme *LDHA*, but not glucose transporters in hESCs under hypoxia.
Quantification of *LDHA, GLUT1* and *GLUT3* mRNA levels in Hues-7 hESCs maintained at 5% oxygen and transfected with either Allstars negative control or JMJD2a siRNA for 48 hours. Data were normalised to *β-actin* for primers and *UBC* for probes, and then to 1 for Allstars siRNA. Bars represent mean ± SEM. (n=3)

To determine whether silencing *JMJD2a* expression in Hues-7 hESCs maintained under hypoxia affected *HIF-2α* expression, RT-qPCR was performed on hESCs transfected with either Allstars negative or JMJD2a siRNA.

HIF-2α expression significantly decreased by approximately 77% (p=0.0032) in Hues-7 hESCs maintained under hypoxia and transfected with JMJD2a siRNA compared to hESCs transfected with Allstars control siRNA (Figure 5.16).

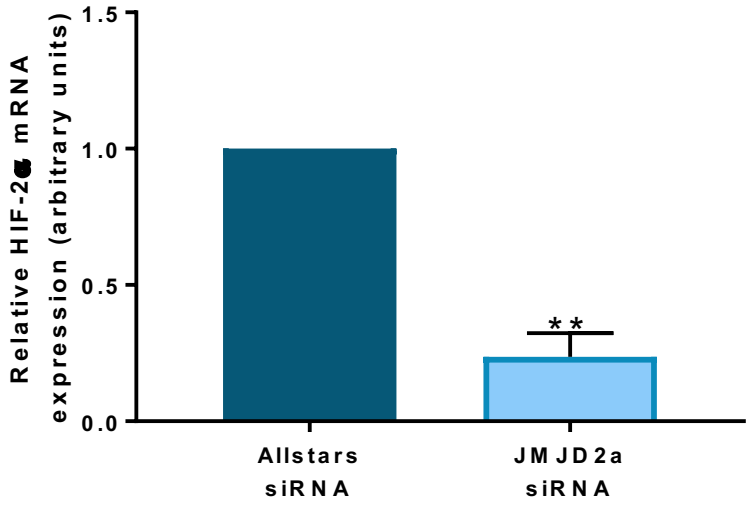

Figure 5.16. Silencing JMJD2a reduces *HIF-2α* expression in hESCs maintained at 5% oxygen.
Quantification of HIF-2α mRNA expression in Hues-7 hESCs maintained at 5% oxygen and transfected with either Allstars negative control siRNA or JMJD2a siRNA for 48 hours. Data were normalised to *UBC*, and then to 1 for Allstars siRNA. Bars represent mean ± SEM. (n=4)

To investigate whether silencing JMJD2a affects chromatin state, ChIP analysis was performed to analyse any changes in histone modifications within predicted HRE sites of the hypoxia inducible genes; OCT4, SOX2, NANOG, GLUT1 and GLUT3. Chromatin isolated from hESCs maintained at 5% oxygen and transfected with either Allstars negative control or JMJD2a siRNA was immunoprecipitated with H3K9me3 and H3K36me3 or a non-specific IgG antibody.

No significant differences were observed in H3K9me3 or H3K36me3 histone modification levels compared to the IgG in either hESCs transfected with Allstars siRNA or JMJD2a siRNA at the HRE in the OCT4 proximal promoter (Figure 5.17A) or the HRE at -1100bp in the SOX2 proximal promoter (SOX2_G; Figure 5.17B). H3K9me3 enrichment was increased compared to the IgG control at the SOX2_A HRE in hESCs incubated with JMJD2a siRNA ($p=0.004$), and was revealed to be significantly higher than H3K36me3 levels ($p=0.0433$) under the same conditions (Figure 5.17C). Finally, only H3K9me3 enrichment levels were found to be significantly increased compared to the IgG control in hESCs transfected with JMJD2a siRNA ($p=0.0266$) in the HRE in the NANOG proximal promoter (Figure 5.17D).

Relative enrichment of histone modification at the HRE in the OCT4 proximal promoter revealed a significant 1.1-fold (p-0.0391) increase in H3K9me3 and an approximate 45% decrease in H3K36me3 ($p=0.0435$) histone modifications in hESCs transfected with JMJD2a siRNA compared to the control cells (Figure 5.18A).

A substantial increase in the relative enrichment of the repressive H3K9me3 mark was also revealed at both the HRE sites at -1100bp (Figure 5.18B) and -1450bp (Figure 5.18C) in the SOX2 proximal promoter in hESCs transfected with JMJD2a siRNA compared to the control. No significant difference was again observed in the relative enrichment of the H3K36me3 histone modification within both the HRE sites in the SOX2 proximal promoter sequence analysed between hESCs transfected with either Allstars control or JMJD2a siRNA.

Finally, relative enrichment of the histone modifications at the HRE in the NANOG proximal promoter revealed a significant 2.6-fold increase ($p=0.0185$) in H3K9me3 modifications in hESCs transfected with JMJD2a siRNA compared to those transfected with the Allstars negative control siRNA, whereas no significant difference in the relative enrichment of H3K36me3 was observed (Figure 5.18D).

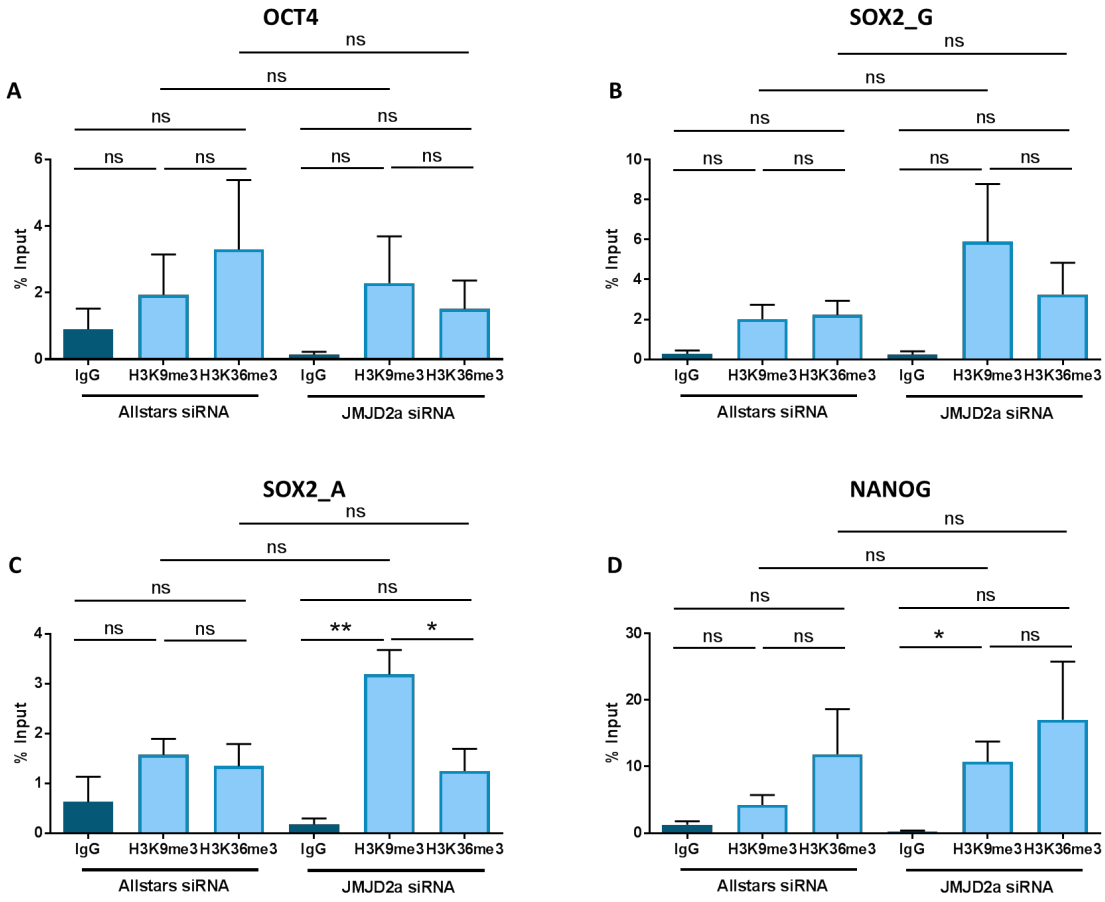

Figure 5.17. Histone modifications within the HREs of OCT4, SOX2 and NANOG proximal promoters in hESCs maintained at 5% oxygen and transfected with JMJD2a siRNA.
ChIP analysis was performed on chromatin isolated from hESCs maintained at 5% oxygen and transfected with either Allstars control or JMJD2a siRNA for 48 hours to reveal the levels of H3K9me3 and H3K36me3 histone marks around the HREs in the OCT4 (A), SOX2_G (B), SOX2_A (C) and NANOG (D) proximal promoters. OCT4, SOX2 and NANOG proximal promoter DNA enrichment is expressed as a percentage of Input (non-immunoprecipitated chromatin). Bars represent mean ± SEM. (n=3).

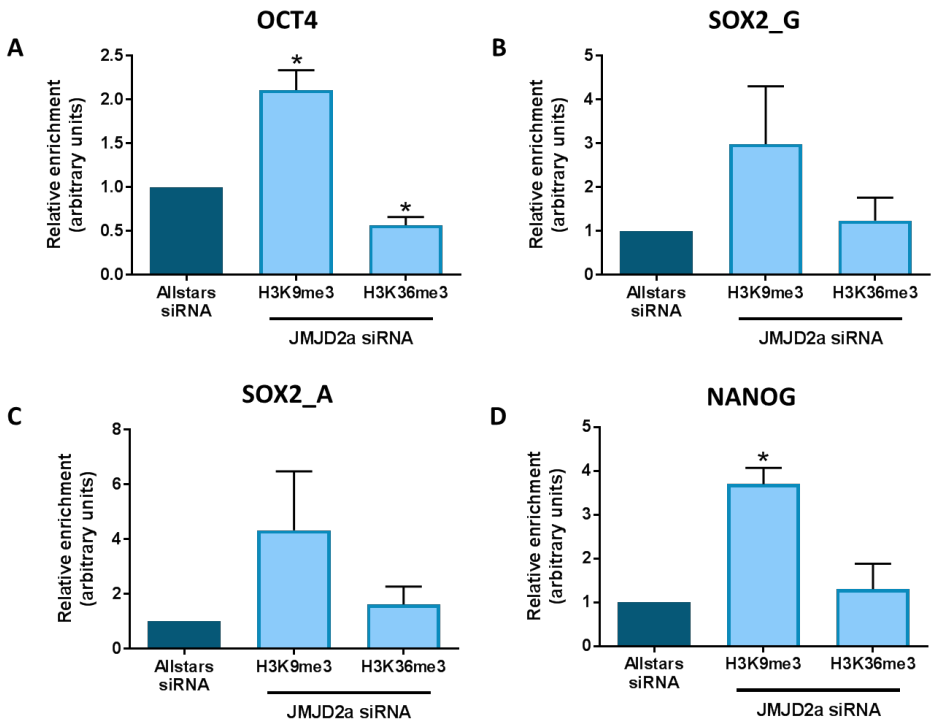

Figure 5.18. Relative enrichment of histone modification markers within the HRE of *OCT4*, *SOX2* and *NANOG* genes in hESCs maintained under hypoxia and transfected with JMJD2a siRNA.
ChIP assays were performed with 3µg of anti-H3K9me3, anti-H3K36me3 or IgG control antibodies immunoprecipitated with chromatin isolated from hESCs cultured at 5% oxygen and transfected with either Allstars control or JMJD2a siRNA before analysing the relative enrichment at predicted HREs in OCT4 (A), SOX2 (B-C) and NANOG (D) proximal promoters. DNA enrichment is expressed as a percentage of Input (non-immunoprecipitated chromatin) minus the background IgG. All data have been normalised to 1 for Allstars negative control. Bars represent mean ± SEM. (n=3)

Pie charts were used to represent the relative enrichment of each histone marker as a proportion of the total for each predicted HRE of interest to demonstrate a more global indication of the chromatin state of the proximal promoters of pluripotency markers in hESCs transfected with JMJD2a siRNA. Pie charts revealed an increase in the proportion of H3K9me3 bound in hESCs transfected with JMJD2a siRNA compared hESCs transfected with Allstars negative control siRNA for OCT4 (Figure 5.19A), SOX2_G (Figure 5.19B), SOX2_A (Figure 5.19C) and NANOG (Figure 5.19D).

This data suggests that although there was no change in the amount of active H3K36me3 histone mark, silencing JMJD2a in hESCs under hypoxia leads to a more heterochromatic state around the predicted HRE sites in the OCT4, SOX2 and NANOG proximal promoters.

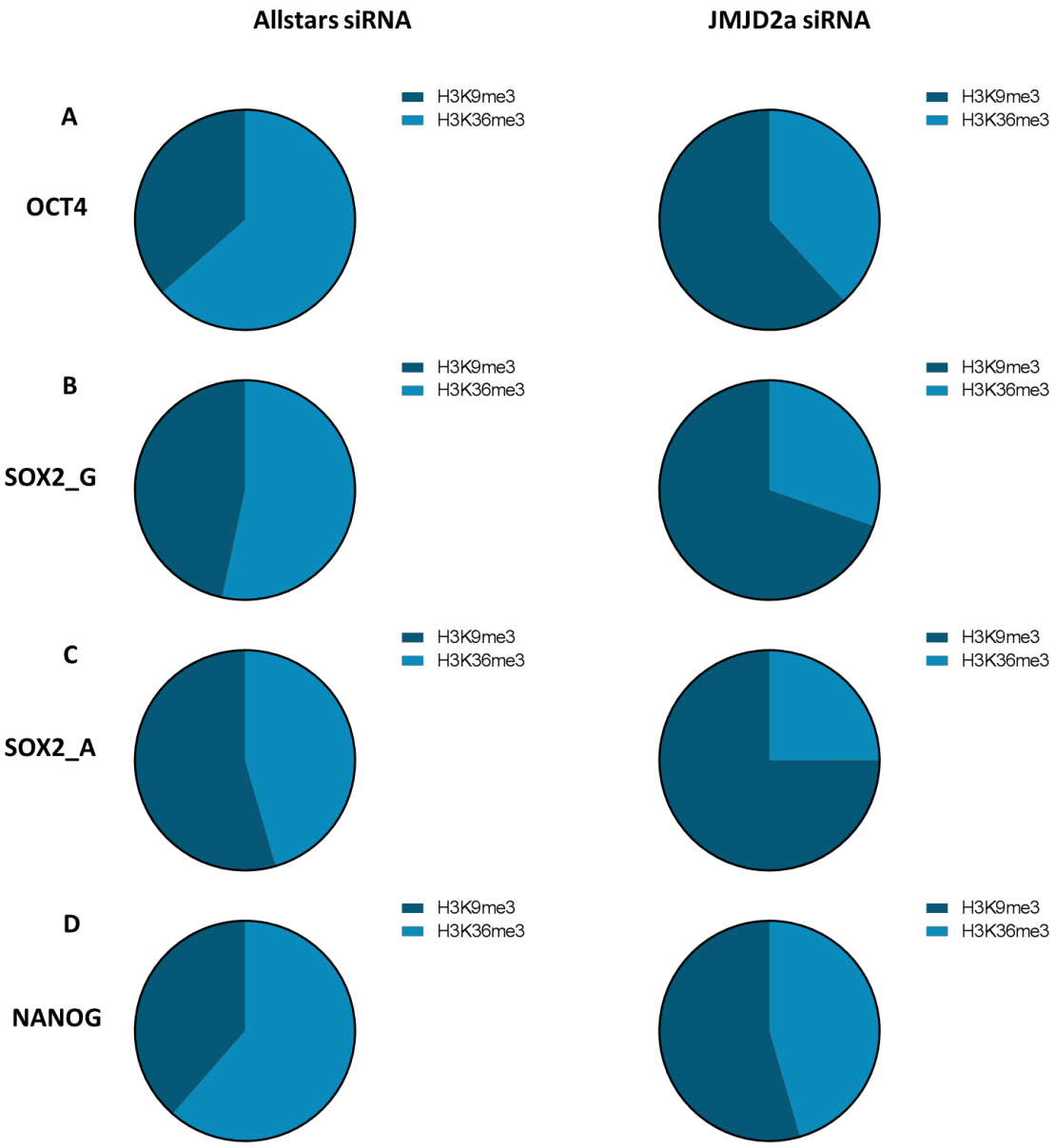

Figure 5.19. Silencing JMJD2a expression in hESCs under hypoxia induces a more heterochromatic conformation within the HREs of *OCT4*, *SOX2* and *NANOG*.
Active H3K36me3 and repressive H3K9me3 histone modifications in the predicted HRE sites of the OCT4 (-1956bp; A), SOX2 (-1100bp, B; -1450bp, C) and NANOG (-301bp; D) proximal promoters of chromatin isolated from hESCs maintained at 5% oxygen and transfected with either Allstars control or JMJD2a siRNA. Pie charts demonstrate a comparison of enrichment in hESCs transfected with JMJD2a siRNA compared to the Allstars control for each HRE site analysed. DNA enrichment is expressed as a percentage of Input (non-immunoprecipitated chromatin) minus the background IgG. All data have been normalised to 1 for Allstars negative control. Bars represent mean ± SEM. (n=3)

ChIP analysis was performed to analyse any changes in histone modifications within predicted HRE sites of GLUT1 and GLUT3 proximal promoters in response to silencing JMJD2a expression in hESCs maintained under hypoxia.

H3K9me3 histone modification levels were significantly increased compared to the IgG control in both hESCs transfected with Allstars siRNA ($p=0.0497$) and JMJD2a siRNA ($p=0.0203$) around the HRE in the GLUT1 proximal promoter. No difference was observed between H3K36me3 levels and the IgG control (Figure 5.20A). Similarly, only H3K9me3 levels were significantly increased compared to the IgG control ($p=0.0384$) within the HRE in the GLUT3 proximal promoter in hESCs transfected with JMJD2a siRNA (Figure 5.20B).

There was a significant increase in the H3K9me3 repressive histone mark by approximately 1.1-fold ($p=0.014$) at the HRE in the GLUT1 proximal promoter in hESCs transfected with JMJD2a siRNA compared to hESCs transfected with Allstars siRNA. However, no significant difference of the active histone marker, H3K36me3, was observed at the potential HRE in the GLUT1 proximal promoter region in hESCs transfected with either Allstars of JMJD2a siRNA (Figure 5.21A).

Additionally, a similar trend in the histone modification was observed at the HRE site in the GLUT3 proximal promoter. Relative enrichment of H3K9me3 significantly increased by approximately 1.4-fold ($p=0.033$)) in chromatin isolated from hESCs where JMJD2a had been silenced compared to the control cells, whereas no significant difference in H3K36me3 was observed between conditions (Figure 5.21B).

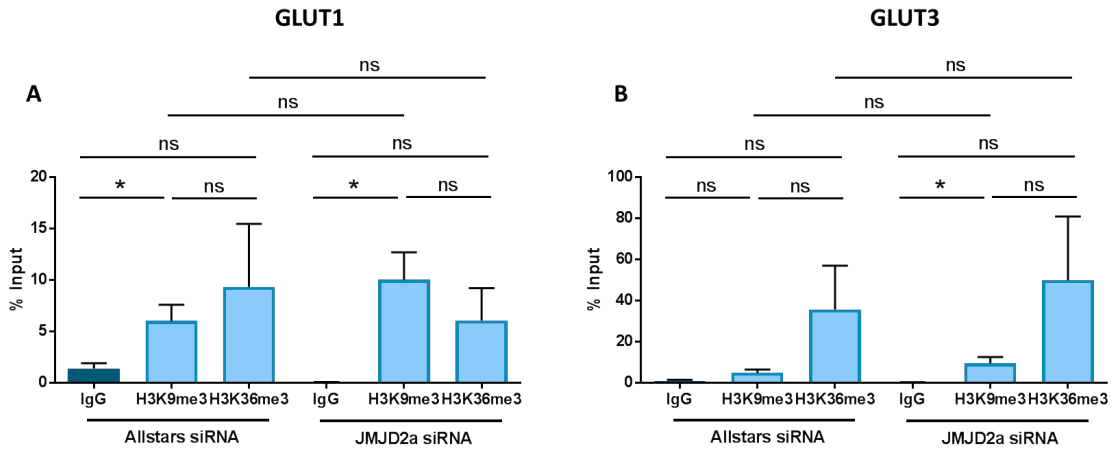

Figure 5.20. Histone modifications within the HREs of GLUT1 and GLUT3 proximal promoters in hESCs maintained at 5% oxygen and transfected with JMJD2a siRNA.
ChIP analysis was performed on chromatin isolated from hESCs maintained at 5% oxygen and transfected with either Allstars control or JMJD2a siRNA for 48 hours to reveal the levels of H3K9me3 and H3K36me3 histone marks around the HREs in the GLUT1 (A) and GLUT3 (B) proximal promoters. GLUT1 and GLUT3 proximal promoter DNA enrichment is expressed as a percentage of Input (non-immunoprecipitated chromatin). Bars represent mean ± SEM. (n=3).

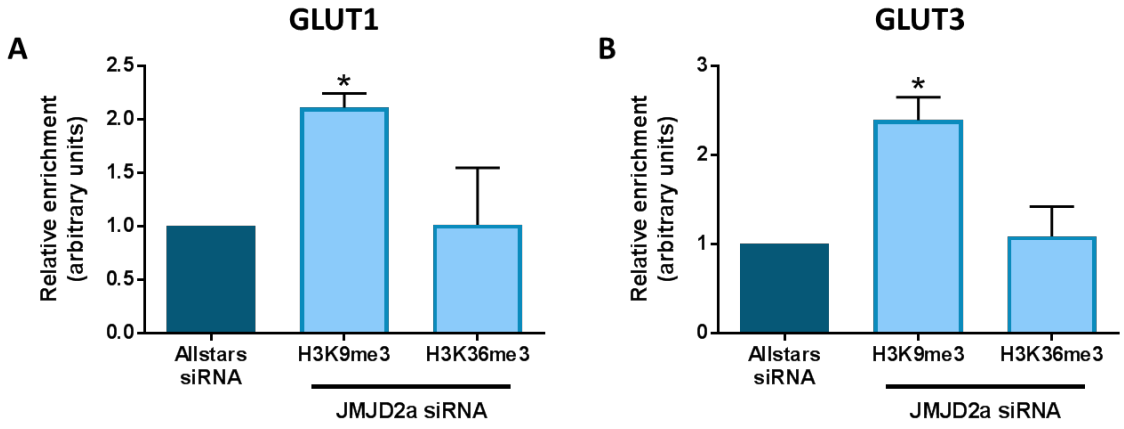

Figure 5.21. Relative enrichment of histone modification markers within the HRE sites of *GLUT1* and *GLUT3* genes in hESCs maintained under hypoxia and transfected with JMJD2a siRNA.
ChIP assays were performed with 3µg of anti-H3K9me3, anti-H3K36me3 or IgG control antibodies immunoprecipitated with chromatin isolated from hESCs cultured at 5% oxygen and transfected with either Allstars control or JMJD2a siRNA before analysing the relative enrichment at predicted HREs in the GLUT1 (A) and GLUT3 (B) proximal promoters. DNA enrichment is expressed as a percentage of Input (non-immunoprecipitated chromatin) minus the background IgG. All data have been normalised to 1 for the Allstars negative control. Bars represent mean ± SEM. (n=3)

Pie charts revealed an increase in the proportion of H3K9me3 bound in hESCs cultured at 5% oxygen and transfected with JMJD2a siRNA compared to the Allstars negative control siRNA for GLUT1 (Figure 5.22A) and GLUT3 (Figure 5.22B) proximal promoters.

This data suggests that silencing JMJD2a expression in hESCs maintained under hypoxia leads to a more heterochromatic state around the predicted HRE sites in the GLUT1 and GLUT3 proximal promoters.

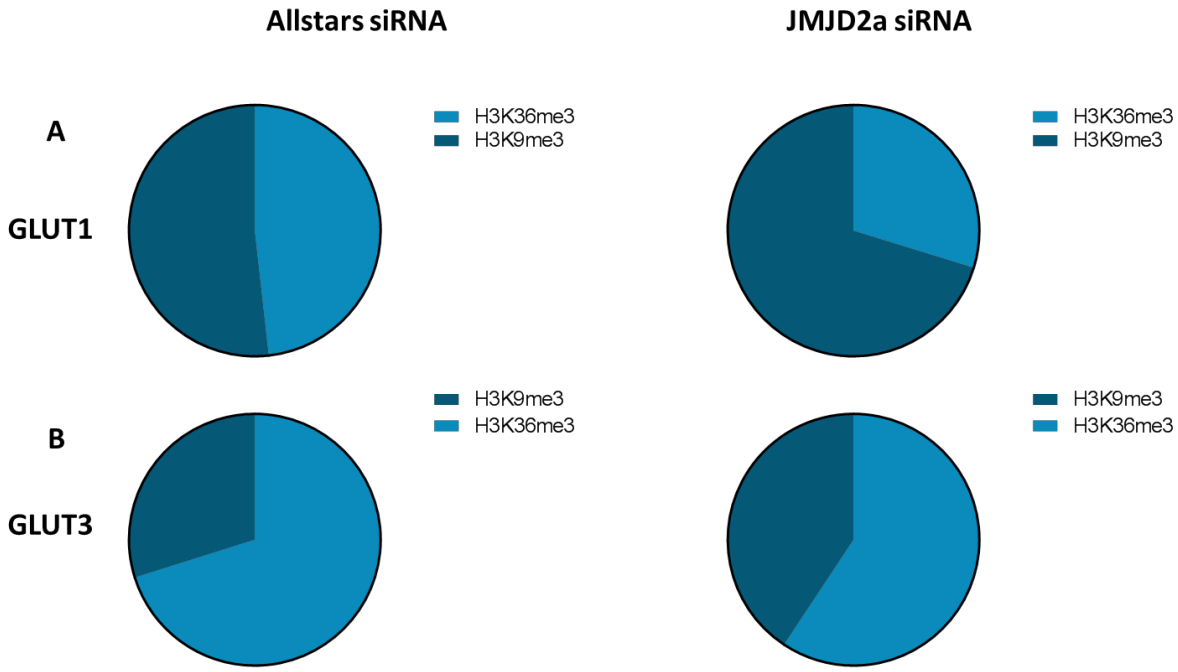

Figure 5.22. Silencing JMJD2a expression in hESCs under hypoxia induces a more heterochromatic conformation within the HREs of *GLUT1* and *GLUT3*.
Active H3K36me3 and repressive H3K9me3 histone modifications in the predicted HRE sites of the GLUT1 (A) and GLUT3 (B) proximal promoters of chromatin isolated from hESCs maintained at 5% oxygen and transfected with either Allstars or JMJD2a siRNA. Pie charts demonstrate a comparison of enrichment in hESCs transfected with JMJD2a siRNA compared to control cells for each HRE site analysed. DNA enrichment is expressed as a percentage of Input (non-immunoprecipitated chromatin) minus the background IgG. All data have been normalised to 1 for the Allstars negative control. Bars represent mean ± SEM. (n=3)

5.4 Discussion

5.4.1. Hypoxic regulation of JMJD expression in hESCs

Hypoxic culture of hESCs is well-documented to increase pluripotency marker expression and thus hESC self-renewal. However, to fully understand any potential role that JMJDs may have in supporting self-renewal, it is critical to understand whether JMJD expression is regulated by hypoxia.

Results from this chapter revealed that the expression of JMJD1a, JMJD2a, JMJD2b and JMJD5 is regulated by hypoxia in hESCs. As HIF-2α is the predominant regulator of the hypoxic response in hESCs, whether that hypoxic regulation of JMJD expression was HIF-2α dependent was investigated and confirmed from the data presented in this chapter. Therefore, this suggests that the adaptation to a hypoxic environment also includes JMJDs in hESCs in addition to the expression of an array of other genes from the literature such as the glucose transporters GLUTs and glycolytic enzymes for example. Previous studies have highlighted that JMJD expression, particularly JMJD1a, was regulated by HIF-1α to enhance a subset of hypoxia-inducible genes that are dependent on JMJD1a in renal cell and colon carcinoma cells (Beyer et al., 2008; Pollard et al., 2008; Krieg et al., 2010). This mechanism present in other cells supports the hypothesis that hypoxic regulation of JMJD expression acts to facilitate hypoxic gene expression in hESCs, particularly as HIF-2α has also been demonstrated to regulate the expression of other members of the JMJD family also (Guo et al., 2015).

However, the expression of JMJD2c was no different in hESCs maintained at either 5% or 20% oxygen. In comparison to the other JMJDs analysed in this chapter, this suggests that JMJD2c expression is not regulated by HIF-2α. Interestingly though, when the expression levels of JMJD2c were examined in hESCs maintained at either 20% oxygen, under short term hypoxia or long term hypoxia, JMJD2c expression peaked and subsequently decreased in a similar manner to HIF-1α expression which is documented in the literature to be responsible for adapting to the hypoxic response for the first 48 hours of exposure in hESCs, but is subsequently lost in hESCs maintained under long-term hypoxia. This correlation between HIF-1α and JMJD2c expression within the first 48 hours of exposure to hypoxia suggested, instead, that JMJD2c expression was regulated by HIF-1α, and not HIF-2α, which was again confirmed from the experiments performed in this chapter. Therefore, this suggests that the increase in HIF-1α upon exposure to hypoxia in hESCs induces JMJD2c expression to allow a more euchromatic

state around JMJD2c-target genes to initiate the long-term hypoxia response. For example, JMJD2c may open up the chromatin and allow the increase in HIF-2α expression and also potentially HIF-3α which is responsible for inhibiting HIF-1α expression acting as a feedback loop (Forristal et al., 2010). Additionally, this would explain the decrease in the expression of both HIF-1α and JMJD2c from hESCs exposed to short term hypoxia to those cells exposed to long term hypoxia. This theory is supported by a previous study conducted in breast cancer cells. That particular study revealed JMJD2c acts as a coactivator for HIF-1α exclusively, and not HIF-2α, by decreasing H3K9 trimethylation to enhance HIF-1α binding to the HREs present in target genes required for the metabolic reprogramming and progression in breast cancer (Luo et al., 2012).

Together, data from this chapter supports previous literature demonstrating that JMJDs are hypoxia regulated whilst also revealing a potential molecular mechanism behind the metabolic switch between hESCs maintained at 20% oxygen before exposure to hypoxia, and molecular insights into how hESCs may potentially alter gene expression programs to adapt to hypoxia.

5.4.2. Glycolytic regulation of JMJD expression in hESCs

The importance of metabolic state in the maintenance of pluripotency marker expression and hESC self-renewal is well-documented in the literature and throughout this thesis. However, as results from this chapter have revealed the potential role of JMJDs in hESC self-renewal, it was critical to investigate whether JMJD expression was regulated by glycolysis in hESCs maintained under hypoxia, and to give further insights into whether metabolism or hypoxia is the predominant regulator of pluripotency maintenance.

Glycolysis was inhibited using the glycolytic inhibitors 2-DG and 3-BrP in hESCs and revealed a significant decrease in the expression of all JMJDs analysed in this chapter. To our knowledge, this is the first report of glycolytic rate regulating JMJD expression in any cell type, particularly hESCs. However, previous studies have highlighted that JMJDs increase the expression of genes associated with glycolysis such as *GLUT1, HK2* and *LDHA* (Wang et al., 2014; Wan et al., 2017), which suggests that there is a feedback loop between JMJD expression and glycolysis.

Notably, these results demonstrated a decrease in all JMJDs analysed, including JMJD2c which was found not to be regulated by hypoxia in this chapter. Results demonstrated in

Chapter 4 revealed that the rate of glycolysis regulated HIF-2α expression in hESCs maintained under hypoxia. As JMJD2c expression revealed to be regulated by HIF-1α, which would not be present in hESCs maintained under long-term hypoxia, the observed decrease in JMJD mRNA expression as a result of inhibiting glycolysis reemphasises that JMJD expression is regulated by metabolism potentially in a HIF independent manner, as well as through a HIF-dependent mechanism.

It is well-documented that metabolites such as S-adenosylmethionine, NAD+ and α-ketoglutarate can inhibit the activity of chromatin modifiers like DNMTs, Sirtuins and JMJDs for example (Etchegaray and Mostoslavsky, 2016), but if and how these metabolites, or even glycolytic enzymes, act to regulate the expression of chromatin modifiers is not well known. However, the glycolytic enzyme PKM2 has also been shown to have nuclear functions involved in gene expression. PKM2 has been demonstrated to interact with β-catenin to bind β-catenin-regulated promoters, bind to HIF-1α to promote the recruitment of HIF-1α and p300 to HIF-1α target genes, but also directly increases the transcriptional activity of signal transducer and activator of transcription 3 (STAT3) (Luo et al., 2011; Yang et al., 2011; Gao et al., 2012; Yang et al., 2012b; Li et al., 2018). Previous studies in microglia and vascular endothelial cells have demonstrated the activation of the NF-κB and STAT3 signalling increased the expression of JMJD3 (Przanowski et al., 2014; Yu et al., 2017). Therefore, it could be that glycolysis is regulating JMJD expression in hESCs indirectly, potentially through PKM2 and then activating the NF-κB or STAT3 signalling pathways.

5.4.3. Maintenance of hESC self-renewal by JMJD2a

Several studies in both mESCs and hESCs have highlighted a role for JMJDs in maintaining pluripotency and self-renewal. However, whether JMJD2a in particular had any role in maintaining hESC self-renewal had not previously been evaluated.

Silencing JMJD2a in hESCs maintained at 5% oxygen decreased the expression of OCT4, SOX2 and NANOG. Although this is the first report of the role JMJD2a plays in hESC self-renewal, this observation agrees with previous literature where various JMJDs regulate pluripotency (Loh et al., 2007; Zhu et al., 2014).

Excitingly, JMJD expression was found to also regulate HIF-2α expression in hESCs maintained under hypoxia, and regulate LDHA expression, but not the expression of the glucose transporters GLUT1 and GLUT3. Data from this chapter has revealed that JMJD

expression is regulated by HIFs in hESCs. Therefore, further data indicating that silencing JMJD2a expression decreased HIF-2α expression suggests that there is a feedback loop between JMJDs and HIFs also. Both HIFs and JMJD expression has also previously been demonstrated to be regulated by and themselves regulate glycolysis too and thus revealing an increasingly complex regulatory loop that helps to maintain hESC self-renewal.

Data in this chapter showed that silencing JMJD2a had no effect on the expression of either GLUT1 or GLUT3 in hESCs maintained under hypoxia. But as previous results have indicated that JMJD2a expression regulates HIF-2α and these GLUTs are known to be HIF target genes, it may be misleading to conclude that GLUT1 and GLUT3 expression is not affected after transfecting hESCs with JMJD2a siRNA. Further experiments would be required to characterise this observation further, particularly as only JMJD2a has been silenced and there may be some compensatory effects occurring between other JMJD family members.

But overall, the results presented in this chapter support previous literature indicating that JMJD2a helps to maintain hESC self-renewal under hypoxia.

5.4.4. Regulation of chromatin state in the maintenance of hESC self-renewal

Previous studies and data presented in this thesis have shown that an increased rate of glycolysis, HIF-2α and JMJD2a expression increase hESC self-renewal. However, how they affected the chromatin state to enhance the expression of OCT4, SOX2 and NANOG was not fully characterised, and so the histone modifications within the HREs in the proximal promoters of the three core pluripotency markers in response to 2-DG and JMJD2a siRNA were analysed.

ChIP analyses revealed that the chromatin around the HREs in the OCT4, SOX2 and NANOG proximal promoters became much more heterochromatic after glycolysis was inhibited and JMJD2a was silenced. This suggests that glycolysis supports hESC self-renewal by opening the chromatin around the HREs in the proximal promoters of OCT4, SOX2 and NANOG to allow the binding of HIF-2α and the activation of pluripotency marker expression. Furthermore, the ChIP analysis suggests that JMJD2a, in particular, is required to open up the chromatin at those regions of DNA to allow HIF-2α binding to the HREs, particularly by removing the H3K9 trimethylation to active gene expression in agreement with a previous report in cancer cells (Berry and Janknecht, 2013). It is worth noting that it is likely that this is not exclusive to JMJD2a, but other JMJD family

members too. Also, JMJDs are probably working in partnership with other chromatin modifiers that are responsible for adding active histone modifications. A previous study in mESCs revealed that JMJD2 demethylases are critical for the continual removal of H3K9 promoter methylation to support self-renewal (Pedersen et al., 2016). Increased H3K9me3 levels were found to compromise the expression of several JMJD2a or JMJD2c target genes which including genes important for self-renewal. This mechanism of continued removal of H3K9 promoter methylation in mESCs is likely to be similar to the underlying mechanism in hESCs to ensure the stability of the pluripotent cell identity and ability to self-renew.

The levels of H3K9me3 and H3K36me3 histone modifications were also evaluated around the HREs in the GLUT1 and GLUT3 proximal promoters in response to 2-DG addition and transfection with JMJD2a siRNA. Results indicated that inhibiting glycolysis and silencing JMJD2a, again resulted in the condensation of the DNA region around the HREs in the GLUT proximal promoters and thus preventing the binding of HIF-2α to enhance GLUT expression. This suggests that glycolysis is increasing JMJD2a expression in order to maintain a highly euchromatic state within the HRE of the GLUT1 and GLUT3 proximal promoters. An open chromatin state would allow an increase in GLUT expression as a result of HIF-2α binding to the HRE and forming a feed forward loop to increase the rate of flux through glycolysis which is known to support hESC self-renewal.

Together, data presented in this chapter suggests that JMJDs and chromatin state are vital for the maintenance of hESC self-renewal by maintaining a euchromatic state to allow the enhanced expression of pluripotency markers, but also increased expression of genes to support a high glycolytic rate (Figure 5.23).

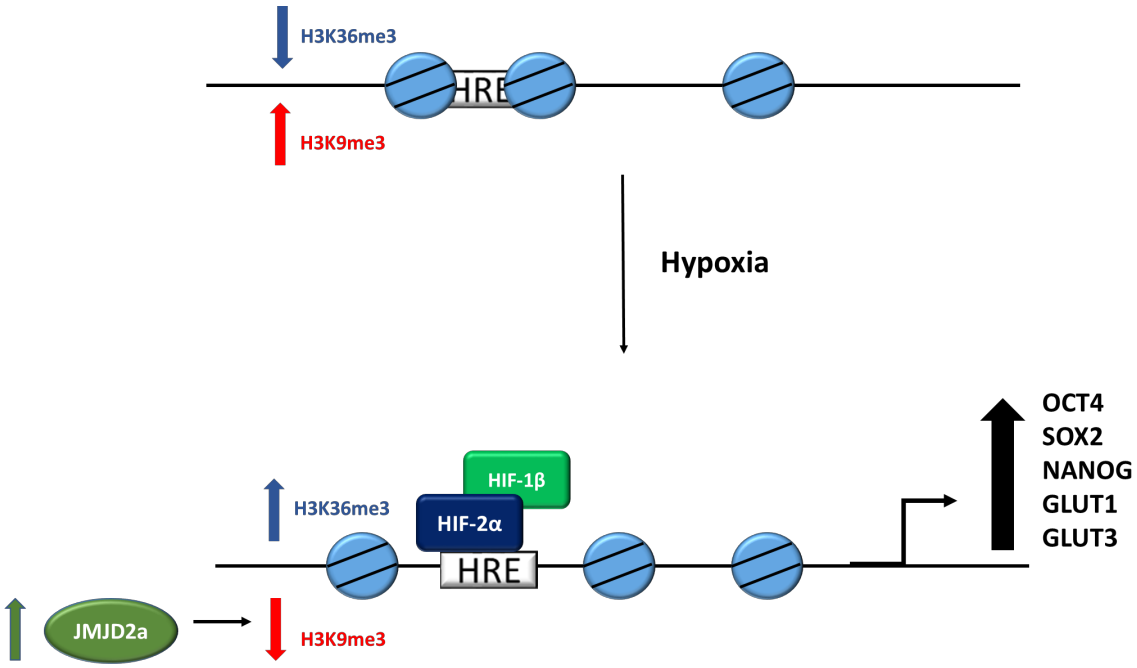

Figure 5.23. Schematic of proposed mechanism of how JMJDs and chromatin state help to maintain hESC self-renewal.
Under normoxia, the chromatin around the HREs in the proximal promoters of OCT4, SOX2, NANOG, GLUT1 and GLUT3 is more heterochromatic preventing the binding of HIF-2α binding. Upon exposure to hypoxia, the expression of JMJDs is increased, notably JMJD2a. JMJD2a is able to reduce the H3K9me3 modifications around the HREs and open the chromatin. This allows HIF-2α access to the HRE binding site to drive the expression of OCT4, SOX2 and NANOG to enhance hESC self-renewal, but also GLUT1 and GLUT3 to maintain a high rate of flux of glycolysis and delay differentiation.

5.5 Conclusions

In conclusion, data from this chapter has revealed that:

- *JMJD1a, JMJD2a, JMJD2b* and *JMJD5* expression is regulated by HIF-2α in hESCs maintained under long term hypoxic culture.
- *JMJD2C* expression is regulated by HIF-1α and is increased in hESCs exposed to hypoxia for up to 48 hours.
- JMJD expression is decreased when the rate of flux through glycolysis is reduced.
- Decreasing the rate of flux through glycolysis leads to a significantly more heterochromatic state around the HREs of pluripotency markers and glucose transporters.
- Silencing *JMJD2a* results in a decrease in pluripotency marker expression, a reduction in lactate production, and interestingly, a decrease in *HIF-2α* expression.
- Silencing *JMJD2a* expression leads to a more 'heterochromatic' state around the HREs of *OCT4, SOX2, NANOG* and *GLUT*s.

Results from this chapter have highlighted how epigenetic changes through JMJDs may affect how glycolysis influences the maintenance of hESC self-renewal; building on Chapters 3 and 4. The next chapter is going to investigate how the metabolism of hESCs influences self-renewal and whether CtBPs play a role, and how that builds on and links with the hypoxic effects from the results demonstrated in previous chapters.

Chapter 6

Role of CtBPs in the regulation of hESC self-renewal

Chapter 6: Role of CtBPs in the regulation of hESC self-renewal

6.1 Introduction

6.1.1 CtBPs as transcriptional corepressors and coactivators

CtBPs are primarily known for their role as transcriptional corepressors. However, there is increasing evidence suggesting a role as transcriptional coactivators. In order for CtBPs to exert their function, they need to dimerise. This is regulated by binding of either NAD^+ or, preferentially, NADH to the dinucleotide-binding site of the CtBP protein (Balasubramanian et al., 2003). CtBPs have >100 fold higher affinity for binding NADH compared to NAD^+ (Zhang et al., 2002; Fjeld et al., 2003). This binding induces a conformational change in the CtBP protein monomers and facilitates the formation of either homo- or heterodimers (Kumar et al., 2002; Balasubramanian et al., 2003). Activated CtBP dimers can, subsequently, translocate to the nucleus and function as either a transcriptional corepressor or coactivator (Zhang et al., 2001; Fjeld et al., 2003; Ray et al., 2014).

The mechanisms involved in CtBP-mediated repression are poorly understood, but can be broadly summarised into gene-specific repression and global repression (Chinnadurai, 2007b). Gene-specific repression is the most well-characterised mechanism. CtBP dimers translocate to the nucleus and bind to TFs containing the consensus motif PXDLS bound to specific promoter regions of a given gene, for example the *CDH1* gene (Grooteclaes et al., 2003; Ichikawa et al., 2015). CtBP dimers act to recruit chromatin-modifying complexes to the specific gene promoter in order to change the chromatin state and induce gene repression (Shi et al., 2003; Kuppuswamy et al., 2008). The mechanism of CtBP-mediated global repression is postulated to antagonise the transactivation function of p300 and associated HATs such as P/CAF (Kim et al., 2005a; Senyuk et al., 2005).

The underlying mechanisms involved in CtBP-mediated transcriptional activation are even less well understood than the repressive mechanisms. Current knowledge suggests that the same basic mechanism involved in gene-specific repression is, also, implicated in CtBP-mediated activation (Ray et al., 2014). However, how CtBPs discriminate between acting as a corepressor or a coactivator has not been fully characterised, but may be context dependent and influenced by different TFs, different components of the CtBP complex and the recruitment of different chromatin modifiers, for example.

Knowledge of the role of CtBPs acting as corepressors in cancer cells and coactivators in other model systems, such as *Drosophila*, is increasing (Fang et al., 2006; Itoh et al., 2013; Ray et al., 2014). However, the role that CtBPs have in hESCs and more specifically in the maintenance of pluripotency, has been largely overlooked.

6.1.2 Chapter Aims

The aim of this chapter was to investigate the role of CtBP1 and CtBP2 expression on hESC self-renewal. The specific chapter aims were:

- To investigate the effect of silencing CtBP1 and CtBP2 simultaneously and individually on pluripotency marker expression in hESCs cultured at 5% oxygen.
- To evaluate the effects of silencing CtBPs on glycolysis in Hues-7 hESCs maintained under 5% oxygen.
- To determine the effect of silencing CtBPs on pluripotency marker expression in Hues-7 maintained at 20% oxygen.
- To investigate the effects of inhibiting CtBP function using the inhibitor MTOB on pluripotency marker expression in Hues-7 hESCs maintained at 5% oxygen.

6.2 Materials and Methods

CtBP siRNA transfections were performed as described previously in Section 2.1.6. RT-qPCR and Western blotting analysis was used to analyse the effects of siRNA transfection and inhibiting CtBP dimerisation on pluripotency marker expression and CtBP expression levels in hESCs as described in Section 2.2 and 2.3 respectively.

6.2.1 Treatment of hESCs with 4-Methylthio 2-oxobutyric acid (MTOB)

MTOB is an inhibitor of CtBP dimerisation. hESCs cultured at 5% oxygen were maintained in either 0mM or 1mM MTOB-supplemented CM for 48 hours in 6-well plates. MTOB stock (Sigma) was prepared as 6mM aliquots in dH_2O and stored at -20˚C until required, when 1ml MTOB stock was diluted 1:6 with sterile filtered CM to create a final concentration of 1mM MTOB. Cells were incubated with 2ml CM containing 1mM MTOB on day 1 post-passage. Medium was replaced with fresh CM containing 1mM MTOB on day 2 post-passage before collecting samples for protein analysis 48 hours after the initial addition of MTOB.

6.3 Results

6.3.1 Effect of silencing CtBPs on pluripotency marker expression in hESCs maintained under hypoxia

Data already presented in this thesis has demonstrated that CtBP expression is significantly higher in hESCs maintained under hypoxia compared to 20% oxygen (Chapter 3.2.4). Therefore, hESC maintained under 5% oxygen were used to investigate whether CtBPs have a role in regulating the pluripotency of hESCs. Hues-7 hESCs maintained under hypoxia were transfected on day 1 post-passage with 50nM of a siRNA that targets both CtBP1 and CtBP2 (CtBP1/2; Qiagen) simultaneously. Cells were collected on day 3 post-passage for analysis using Western blotting.

Cells transfected with CtBP1/2 formed rounded, compact colonies and displayed typical cobblestone morphology. There were no obvious differences in the morphology of cells transfected with either the Allstars control or CtBP1/2 siRNA (Figure 6.1).

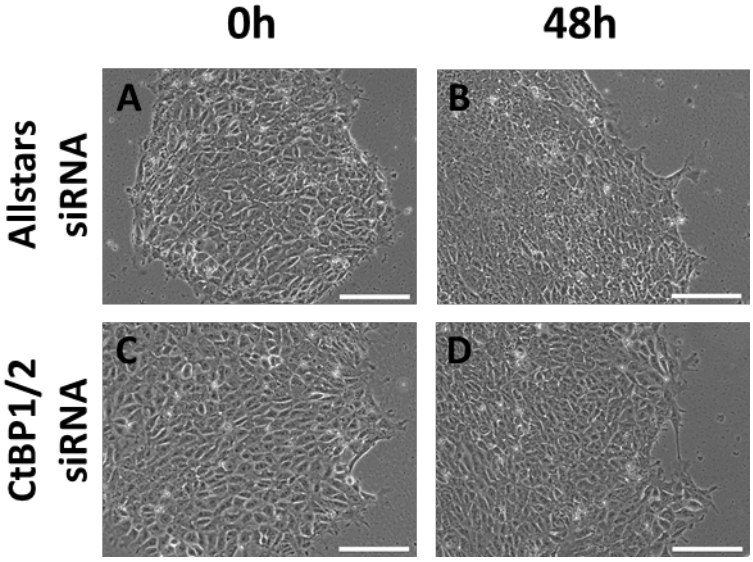

Figure 6.1. Phase contrast images demonstrating colony morphology of Hues-7 hESCs cultured at 5% oxygen transfected with CtBP1/2 siRNA.
Representative phase contrast images of Hues-7 hESCs cultured at 5% oxygen transfected with either Allstars negative control siRNA (A-B) or CtBP1/2 siRNA (C-D) after 0 (A, C) and 48 hours (B, D). Scale bar indicates 200μm.

RT-qPCR analysis revealed that the expression of both CtBP isoforms was significantly reduced in Hues-7 hESCs transfected with CtBP1/2 siRNA (Figure 6.2). Quantification of relative mRNA expression levels revealed a significant 85% and 87% reduction in *CtBP1* (p=0.0195) and *CtBP2* (p=0.015) respectively.

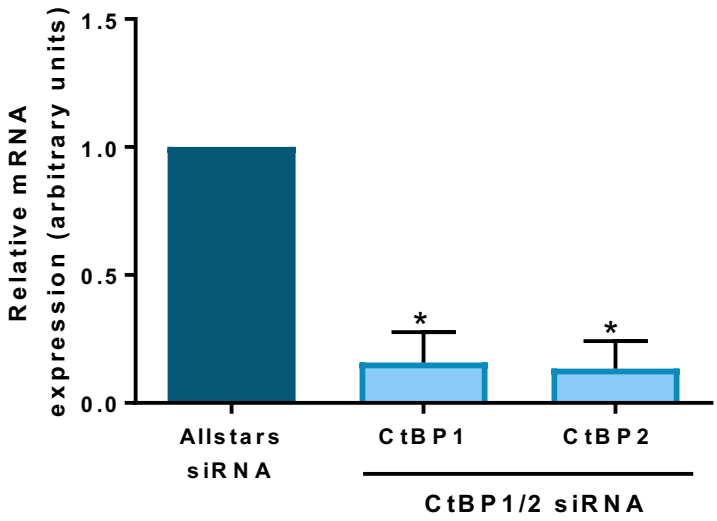

Figure 6.2. CtBP mRNA expression is significantly decreased after transfection with CtBP1/2 siRNA.
Quantification of *CtBP1* and *CtBP2* mRNA levels in Hues-7 hESCs maintained at 5% oxygen and transfected with either Allstars control or CtBP1/2 siRNA. Data were normalised to *UBC*, and then to 1 for Allstars siRNA. Bars represent mean ± SEM. (n=3)

To investigate whether silencing CtBP expression had any effect on the self-renewal of hESCs, the mRNA expression of *OCT4*, *SOX2*, *NANOG*, *LIN28B* and *SALL4* was investigated in hESCs where CtBP expression was silenced. Cells that had been transfected with CtBP1/2 siRNA for 48 hours displayed a significant decrease in pluripotency markers compared to hESCs transfected with the Allstars control siRNA (Figure 6.3). mRNA expression was reduced by 78% (p=0.0166), 74% (p=0.0248), 84% (p=0.0079), 66% (p=0.0447) and 72% (p=0.0284) for *OCT4*, *SOX2*, *NANOG*, *LIN28B* and *SALL4* respectively in hESCs where CtBPs had been silenced compared to the control cells.

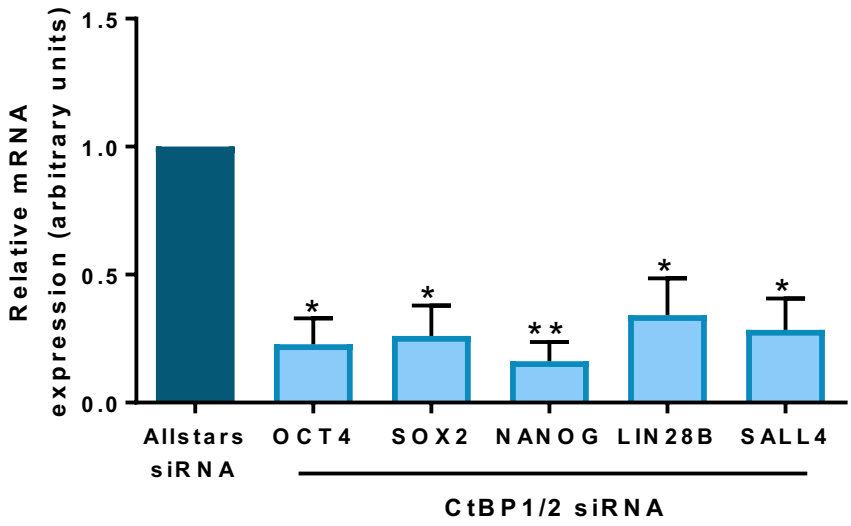

Figure 6.3. The expression of transcription factors regulating self-renewal are significantly decreased in Hues-7 hESCs transfected with CtBP1/2 siRNA.
Quantification of *OCT4, SOX2, NANOG, LIN28B* and *SALL4* mRNA levels in Hues-7 hESCs maintained at 5% oxygen and transfected with either Allstars control or CtBP1/2 siRNA. Data were normalised to *UBC*, and then to 1 for Allstars siRNA. Bars represent mean ± SEM. (n=3)

To further support the observed loss of pluripotency in Hues-7 hESCs maintained under hypoxia and transfected with CtBP1/2 siRNA, RT-qPCR was performed to analysis the expression of a panel of early differentiation markers representing all three developmental germ layers.

In concordance with the pluripotency gene expression, the expression of *SOX17*, *GATA4*, *AFP*, *CLD6* (Figure 6.4A), *SOX1*, *PAX6* (Figure 6.4B), *BMP4*, *FOXC1*, *CXCR4* and *KDR* (Figure 6.4C) were all significantly increased in Hues-7 hESCs transfected with CtBP1/2 siRNA compared to those transfected with Allstars siRNA. No significant difference in the expression of *NODAL* was observed between hESCs transfected with either Allstars negative control or CtBP1/2 siRNA under hypoxia (Figure 6.4C).

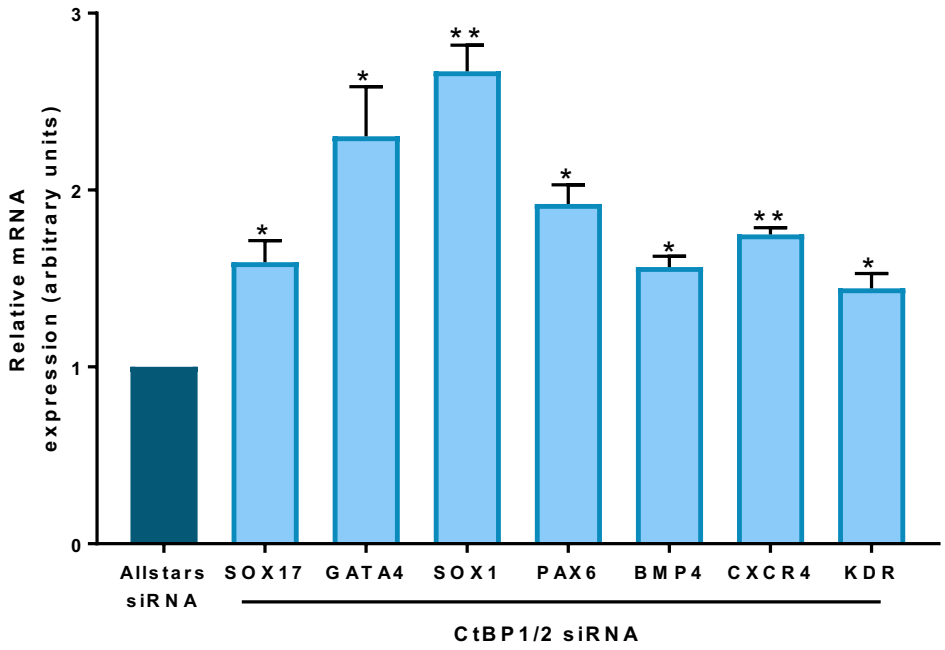

Figure 6.4. Expression of a panel of differentiation markers increases in Hues-7 hESCs transfected with CtBP1/2 siRNA.
Hues-7 hESCs cultured at 5% oxygen in MEF-conditioned media supplemented and transfected with CtBP1/2 siRNA displayed a significant increase in *SOX17*, *GATA4*, *SOX1*, *PAX6*, *BMP4*, *CXCR4* and *KDR* mRNA expression levels compared to the Allstars control siRNA. Data were normalised to *β-actin* for primers and *UBC* for probes, and then to 1 for Allstars negative control siRNA. Bars represent mean ± SEM. (n=3)

Western blotting was performed to analyse any changes in pluripotency marker expression after transfection with CtBP1/2 siRNA. Quantification of the bands revealed that the protein expression of both CtBP1 and CtBP2 was successfully silenced after transfection with CtBP1/2 siRNA. An approximate 50% decrease in CtBP1 (p=0.0468) and CtBP2 (p=0.0360) expression was observed compared to Hues-7 hESCs transfected with the Allstars negative control siRNA (Figure 6.5B).

After successfully silencing both CtBP isoforms, Western blots were performed to evaluate any effects on hESC pluripotency. Quantification of OCT4, SOX2 and NANOG protein bands revealed a significant decrease in expression compared to cells transfected with CtBP1/2 siRNA. OCT4 (p=0.0492) and SOX2 (p=0.0372) expression was decreased by approximately 60%, whereas NANOG (p=0.0006) protein expression was reduced by

approximately 80% when both CtBP1 and CtBP2 were silenced compared to the control siRNA (Figure 6.5C).

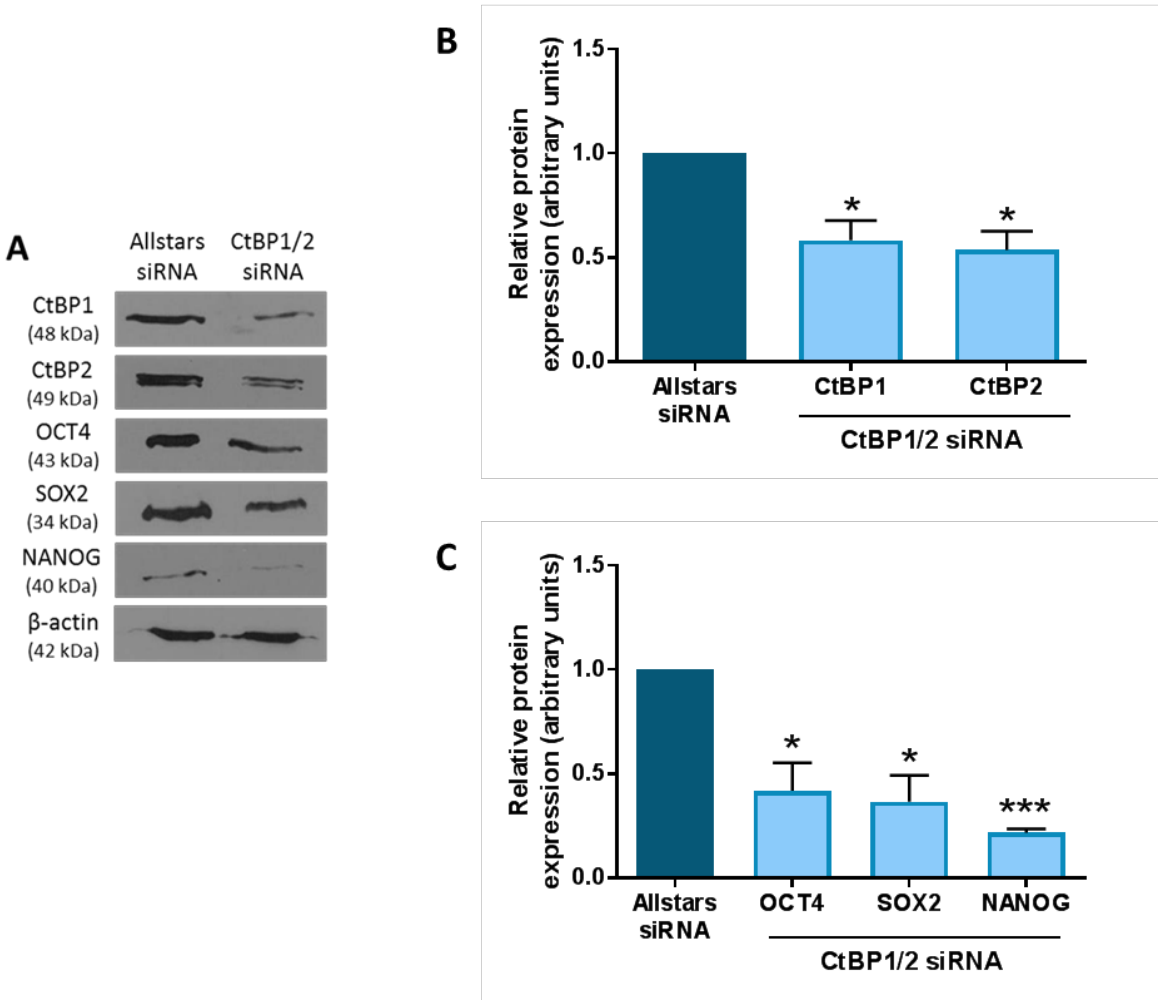

Figure 6.5. Silencing both CtBP isoforms reduces the expression of pluripotency markers in Hues-7 hESCs maintained at 5% oxygen using CtBP1/2 siRNA.
(A) Representative Western blots of CtBP1, CtBP2, OCT4, SOX2 and NANOG expression in Hues-7 hESCs cultured at 5% oxygen and transfected with either Allstars negative control siRNA or CtBP1/2 siRNA. (B) Quantification of CtBP1 and CtBP2 Western blots revealed the successful silencing of both CtBP isoforms in Hues-7 hESCs transfected with CtBP1/2 siRNA compared to the Allstars negative control. (C) Quantification of OCT4, SOX2 and NANOG Western blots revealed a significant decrease in the expression of all three pluripotency markers in Hues-7 hESCs transfected with CtBP1/2 siRNA compared to the control. Data were normalised to β-actin, and then to 1 for Allstars control. Bars represent mean ± SEM. (n=3)

To confirm that these effects were not cell line specific, Shef3 hESCs maintained under hypoxia were transfected with either the Allstars negative control or CtBP1/2 siRNA for 48 hours before collecting samples for protein isolation.

Phase contrast images revealed that there were no clear morphological differences between Shef3 hESCs transfected with either Allstars or CtBP1/2 siRNA after 48 hours. hESC colonies were of typical cobblestone morphology with clearly defined edges (Figure 6.6).

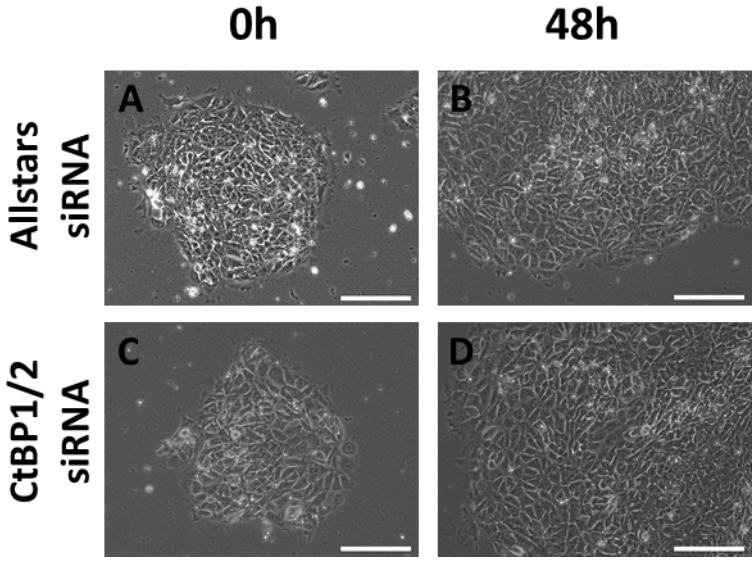

Figure 6.6. Phase contrast images demonstrating colony morphology of Shef3 hESCs cultured at 5% oxygen transfected with CtBP1/2 siRNA.
Representative phase contrast images of Shef3 hESCs cultured at 5% oxygen transfected with either Allstars negative control siRNA (A-B) or CtBP1/2 siRNA (C-D) after 0 (A, C) and 48 hours (B, D). Scale bar indicates 200μm.

CtBP protein expression was quantified using Western blotting. CtBP1 and CtBP2 expression was significantly decreased by approximately 60% ($p=0.0193$) and 70% ($p=0.0034$) respectively in hESCs transfected with CtBP1/2 siRNA compared to those transfected with the Allstars negative control siRNA (Figure 6.7B).

After silencing CtBP expression, Western blotting revealed a significant reduction in the expression of all three core pluripotency markers (Figure 6.7C). OCT4 expression

decreased by 36% (p=0.0489), SOX2 expression reduced by approximately 22% (p-0.0273) and NANOG expression decreased by approximately 25% (p=0.0348) in Shef3 hESCs transfected with CtBP1/2 siRNA compared to the control cells.

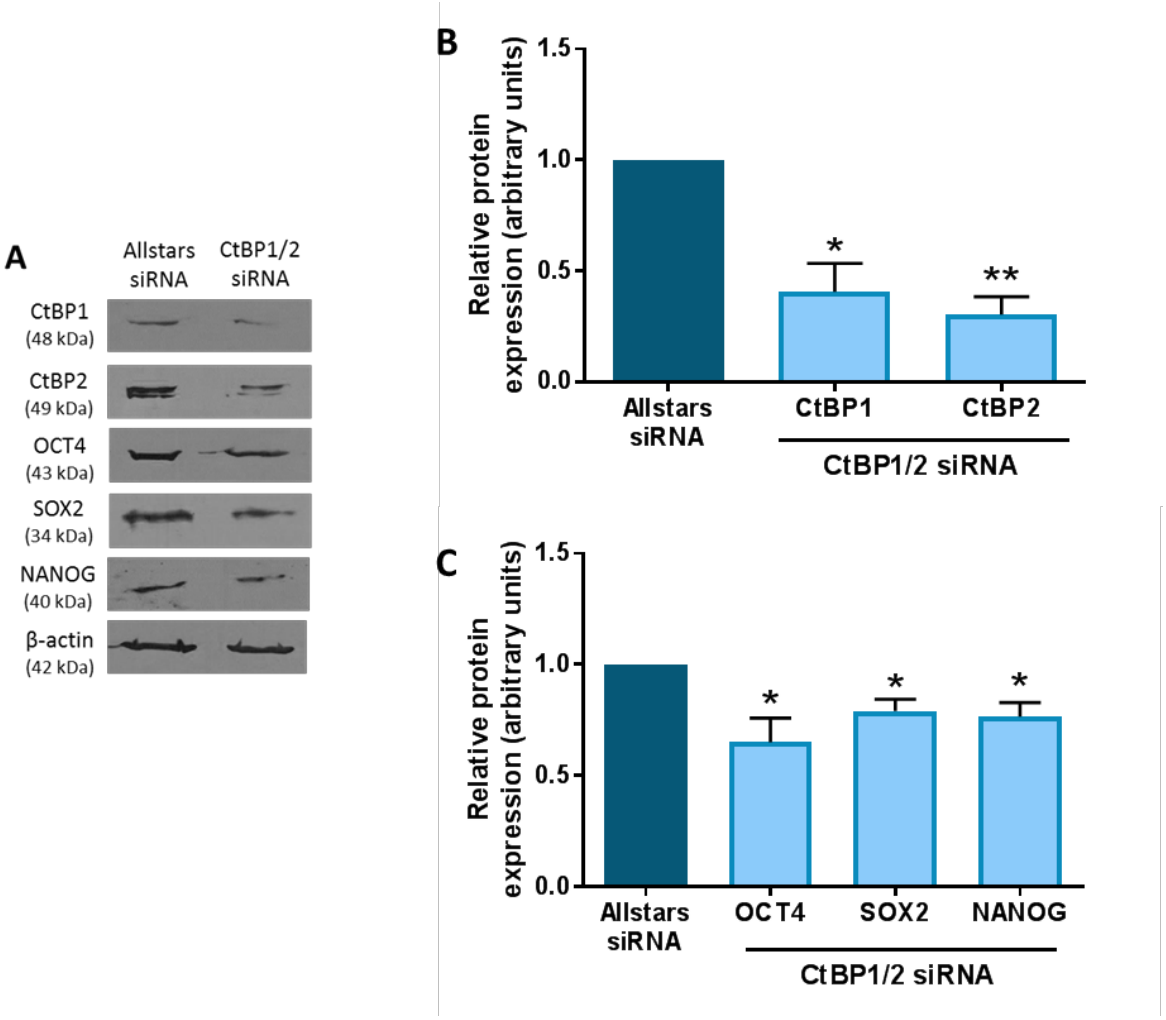

Figure 6.7. Silencing both CtBP isoforms reduces the expression of pluripotency markers in Shef3 hESCs maintained at 5% oxygen using CtBP1/2 siRNA.
(A) Representative Western blots of CtBP1, CtBP2, OCT4, SOX2 and NANOG expression in Shef3 hESCs cultured at 5% oxygen and transfected with either Allstars negative control siRNA or CtBP1/2 siRNA. (B) Quantification of CtBP1 and CtBP2 Western blots revealed the successful silencing of both CtBP isoforms in Shef3 hESCs transfected with CtBP1/2 siRNA compared to the Allstars negative control. (C) Quantification of OCT4, SOX2 and NANOG Western blots revealed a significant decrease in the expression of all three pluripotency markers in Shef3 hESCs transfected with CtBP1/2 siRNA compared to the control. Data were normalised to β-actin, and then to 1 for Allstars control. Bars represent mean ± SEM. (n=4)

6.3.2. Effect of silencing CtBPs on the rate of flux through glycolysis in Hues-7 hESCs maintained under hypoxia

Data in this thesis has already demonstrated that reducing the rate of glycolysis decreases pluripotency marker expression potentially directly and indirectly via HIF-2α (Chapter 4.3). Therefore, to investigate whether the loss of hESC pluripotency and the consequent increase of differentiation marker expression was directly due to the silencing of CtBPs and not due to a reduction in the rate of glycolysis, the mRNA expression of key glycolytic genes was analysed.

RT-qPCR analysis revealed no significant difference in the expression of the glycolytic enzyme *LDHA*, and the glucose transporters *GLUT1* and *GLUT3* was observed between hESCs transfected with either Allstars control or CtBP1/2 siRNA under hypoxia (Figure 6.8). It is worth noting that the large error bars for *LDHA* expression were due to three conflicting experimental replicates, and thus may not be a true reflection of actual results.

However, this data suggests that CtBP expression has no effect on the expression of key glycolytic genes.

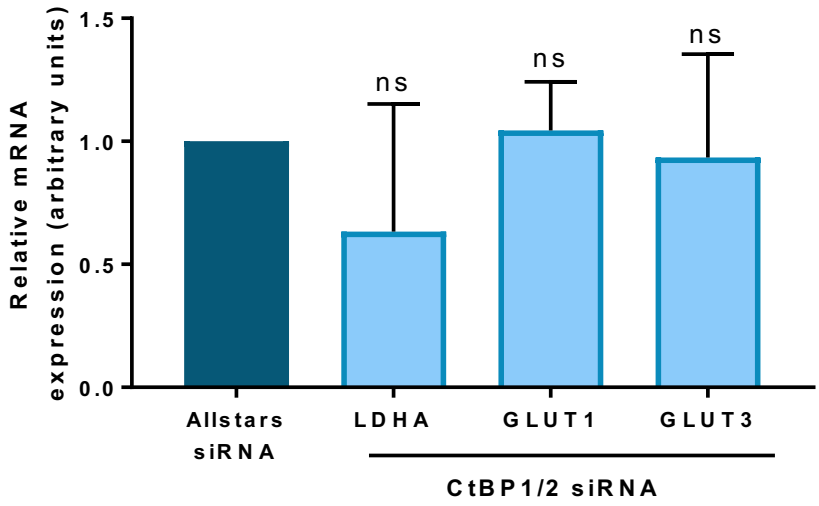

Figure 6.8. Expression of glycolysis associated genes is not affected by silencing CtBPs in hESCs under hypoxia.
Quantification of *LDHA, GLUT1* and *GLUT3* mRNA levels in Hues-7 hESCs maintained at 5% oxygen and transfected with either Allstars control or CtBP1/2 siRNA. Data were normalised to

β-actin for primers and *UBC* for probes, and then to 1 for Allstars negative control siRNA. Bars represent mean ± SEM. (n=3)

To further evaluate whether silencing CtBPs had any effects on the rate of flux through glycolysis, enzyme linked assays were performed to measure the concentration of lactate in the spent MEF-conditioned medium samples from cells transfected with either Allstars negative control or CtBP1/2 siRNA.

Silencing both CtBP isoforms resulted in no significant difference in lactate production (p=0.864) between hESCs transfected with either Allstars control or CtBP1/2 siRNA (Figure 6.9).

Together, this data confirms that silencing the metabolic sensors CtBPs in hESCs maintained under hypoxic conditions does not affect the rate of flux through glycolysis.

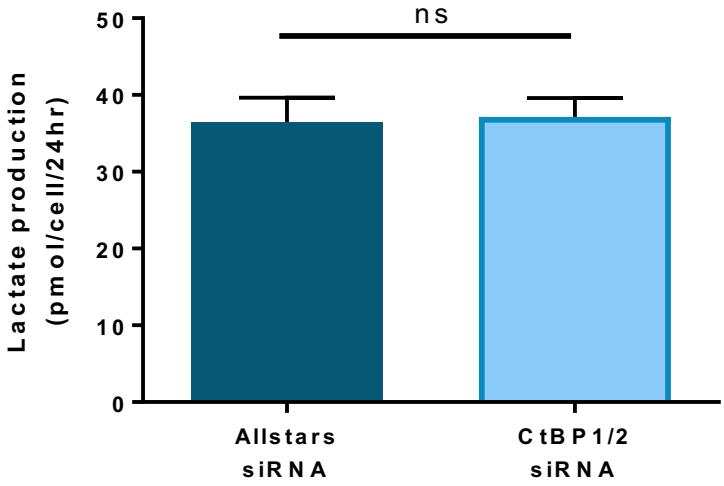

Figure 6.9. Lactate production is not affected by the silencing of CtBP1 and CtBP2 in Hues-7 hESCs at 5% oxygen.
Quantification of the rate of lactate production of Hues-7 hESCs maintained under hypoxic conditions and transfected with CtBP1/2 siRNA for 48 hours compared to the control cells. Bars represent mean ± SEM. (n=12)

6.3.3. Effect of silencing CtBPs on hESC self-renewal under 20% oxygen

The next aim was to investigate whether silencing CtBPs in hESCs also had the same effect on OCT4, SOX2 and NANOG expression in hESCs maintained under 20% oxygen. Therefore, Hues-7 hESCs maintained under 20% oxygen were transfected with either Allstars or CtBP1/2 siRNA for 48 hours before collecting samples for analysis by RT-qPCR and Western blotting.

hESCs displayed typical cobblestone morphology with defined edges regardless of whether they were transfected with Allstars negative control or CtBP1/2 siRNA for 48 hours (Figure 6.10).

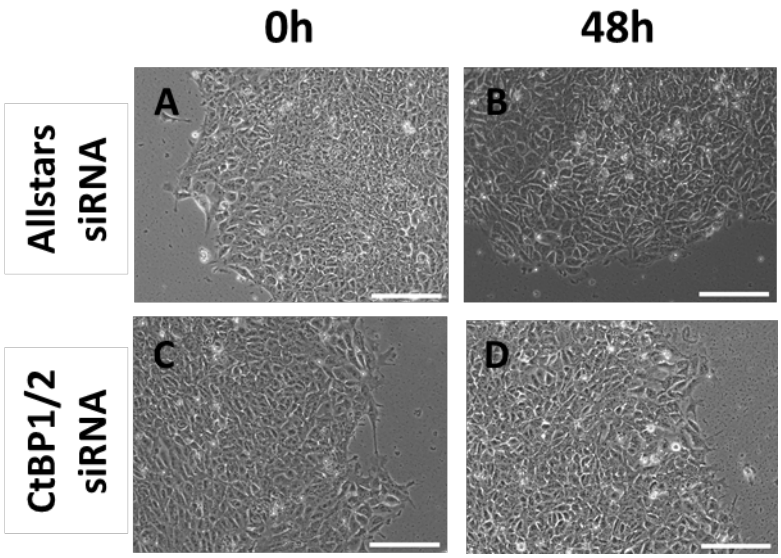

Figure 6.10. Phase contrast images demonstrating colony morphology of Hues-7 hESCs cultured at 20% oxygen transfected with CtBP1/2 siRNA.
Representative phase contrast images of Hues-7 hESCs cultured at 20% oxygen transfected with either Allstars negative control siRNA (A-B) or CtBP1/2 siRNA (C-D) after 0 (A, C) and 48 hours (B, D). Scale bar indicates 200μm.

RT-qPCR analysis revealed that the expression of both *CtBP1* and *CtBP2* was significantly silenced by 75% (p=0.0035) and 69% (p=0.0203) respectively in Hues-7 hESCs maintained at 20% oxygen and transfected with CtBP1/2 siRNA compared to the control (Figure 6.11).

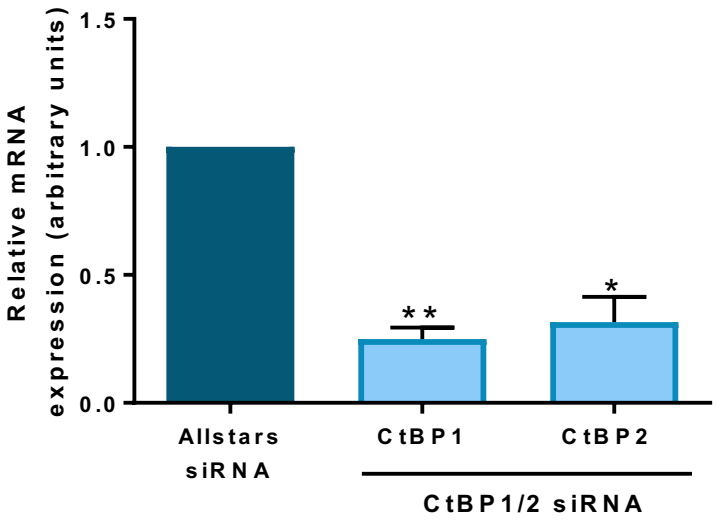

Figure 6.11. CtBP mRNA expression is significantly decreased after transfection with CtBP1/2 siRNA in Hues-7 hESCs maintained under 20% oxygen.
Quantification of *CtBP1* and *CtBP2* mRNA levels in Hues-7 hESCs maintained at 20% oxygen and transfected with either Allstars control or CtBP1/2 siRNA. Data were normalised to *UBC*, and then to 1 for Allstars siRNA. Bars represent mean ± SEM. (n=3)

After silencing the expression of CtBPs in hESCs maintained at 20% oxygen, the effects on the expression of *OCT4*, *SOX2* and *NANOG* was investigated. There was a significant 33% decrease in *OCT4* expression (p=0.0424) and a 39% reduction in both *SOX2* (p=0.0456) and *NANOG* (p=0.0428) expression in hESCs transfected with CtBP1/2 siRNA compared to those transfected with the Allstars negative control siRNA (Figure 6.12).

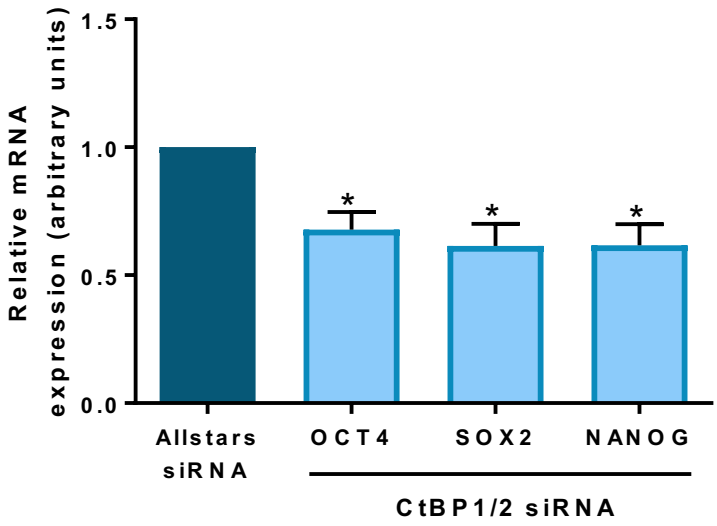

Figure 6.12. Pluripotency marker mRNA expression is significantly decreased in Hues-7 hESCs transfected with CtBP1/2 siRNA under 20% oxygen.
Quantification of *OCT4, SOX2* and *NANOG* mRNA levels in Hues-7 hESCs maintained at 20% oxygen and transfected with either Allstars control or CtBP1/2 siRNA. Data were normalised to *UBC*, and then to 1 for Allstars siRNA. Bars represent mean ± SEM. (n=3)

The expression of a panel of differentiation markers representing all three developmental lineages was analysed by RT-qPCR. A significant increase in the expression of *SOX17* (p=0.0236), GATA4 (p=0.0437), *SOX1* (p=0.0041), *PAX6* (p=0.0182), *BMP4* (p=0.0117), *CXCR4* (p=0.01) and *KDR* (p=0.0054; Figure 6.13) was observed in Hues-7 hESCs maintained at 20% oxygen and transfected with CtBP1/2 siRNA compared to cells transfected with Allstars siRNA. No significant difference was observed in the expression of *CLD6* and *NODAL* in hESCs transfected with either Allstars or CtBP1/2 siRNA.

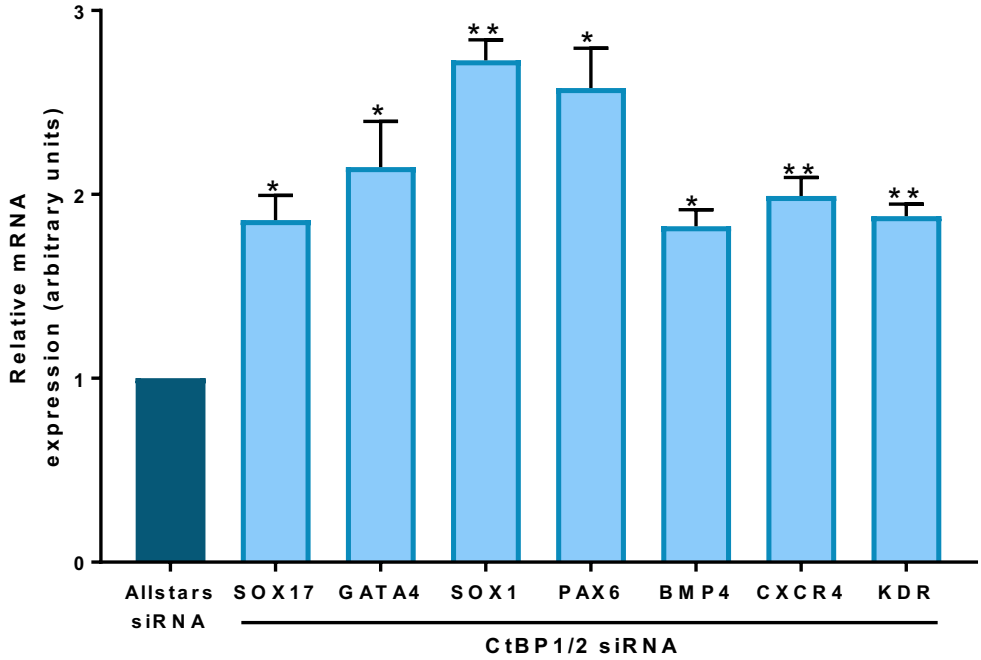

Figure 6.13. Expression of a panel of differentiation markers increases in Hues-7 hESCs transfected with CtBP1/2 siRNA under 20% oxygen.
Hues-7 hESCs cultured at 20% oxygen in MEF-conditioned media supplemented and transfected with CtBP1/2 siRNA displayed a significant increase in *SOX17*, *GATA4*, *SOX1*, *PAX6*, *BMP4*, *CXCR4* and *KDR* mRNA expression levels compared to the Allstars control siRNA. Data were normalised to *β-actin* for primers and *UBC* for probes, and then to 1 for Allstars negative control siRNA. Bars represent mean ± SEM. (n=3)

Western blotting was performed to analyse any changes in pluripotency marker expression in Hues-7 hESCs maintained at 20% oxygen after silencing both CtBP1 and CtBP2. Quantification of the bands revealed that the protein expression of both CtBP1 and CtBP2 was successfully silenced after transfection with CtBP1/2 siRNA. An approximate 48% and 51% decrease in CtBP1 ($p=0.0087$) and CtBP2 ($p=0.0261$) expression respectively was observed compared to Hues-7 hESCs transfected with the Allstars negative control siRNA under 20% oxygen (Figure 6.14B).

After successfully silencing both CtBP isoforms, Western blots were performed to evaluate any effects on hESC self-renewal. Quantification of OCT4, SOX2 and NANOG protein bands revealed a significant decrease in the protein expression of the three pluripotency factors in cells transfected with CtBP1/2 siRNA. Hues-7 hESCs where both CtBP isoforms had been silenced, OCT4 ($p=0.0384$) expression was reduced by approximately 53%, SOX2 ($p=0.0115$) expression was decreased by approximately 45%, whereas NANOG ($p=0.006$) protein expression was reduced by approximately 64% compared to the control (Figure 6.14C).

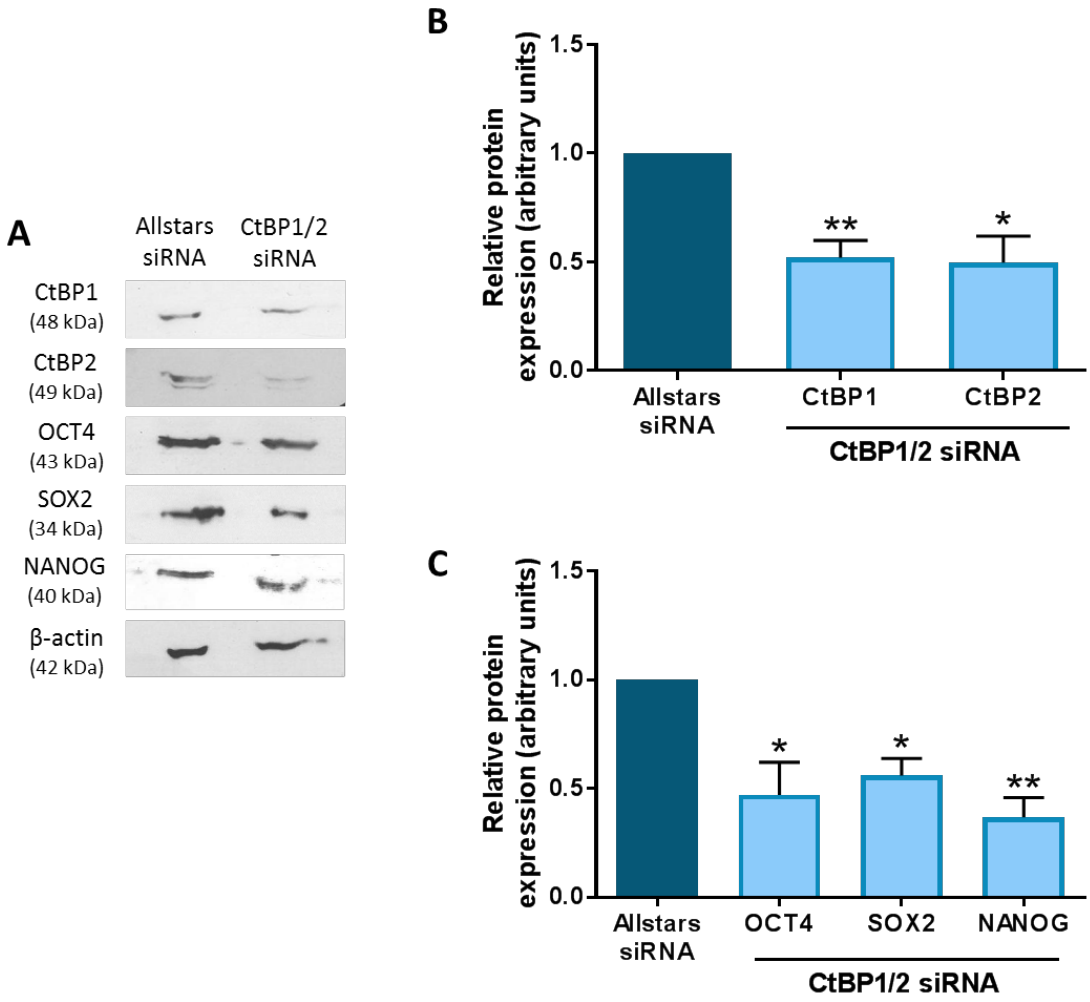

Figure 6.14. Silencing both CtBP isoforms reduces the expression of pluripotency markers in Hues-7 hESCs maintained at 20% oxygen using CtBP1/2 siRNA.
(A) Representative Western blots of CtBP1, CtBP2, OCT4, SOX2 and NANOG expression in Hues-7 hESCs cultured at 5% oxygen and transfected with either Allstars negative control siRNA or CtBP1/2 siRNA. (B) Quantification of CtBP1 and CtBP2 Western blots revealed the successful silencing of both CtBP isoforms in Hues-7 hESCs transfected with CtBP1/2 siRNA compared to the Allstars negative control. (C) Quantification of OCT4, SOX2 and NANOG Western blots revealed a significant decrease in the expression of all three pluripotency markers in Hues-7 hESCs transfected with CtBP1/2 siRNA compared to the control. Data were normalised to β-actin, and then to 1 for Allstars control. Bars represent mean ± SEM. (n=3)

6.3.4. Effect of silencing CtBPs on pluripotency marker expression using CtBP1+2 siRNA under hypoxia

To further verify the results, a different siRNA strategy was used where instead of using a single siRNA that targets both CtBP isoforms, two siRNAs were transfected simultaneously where each siRNA targeted just one CtBP isoform. Therefore, Hues-7 hESCs maintained at 5% oxygen were transfected with 50nM CtBP1 and 50nM CtBP2 (CtBP1+2; Qiagen) siRNA on day 1 post-passage simultaneously. Cells were collected on day 3 post-passage and the protein isolated for analysis using Western blotting.

No morphological differences were observed between cells transfected with either the Allstars negative control siRNA or CtBP1+2 siRNA after 48 hours (Figure 6.15).

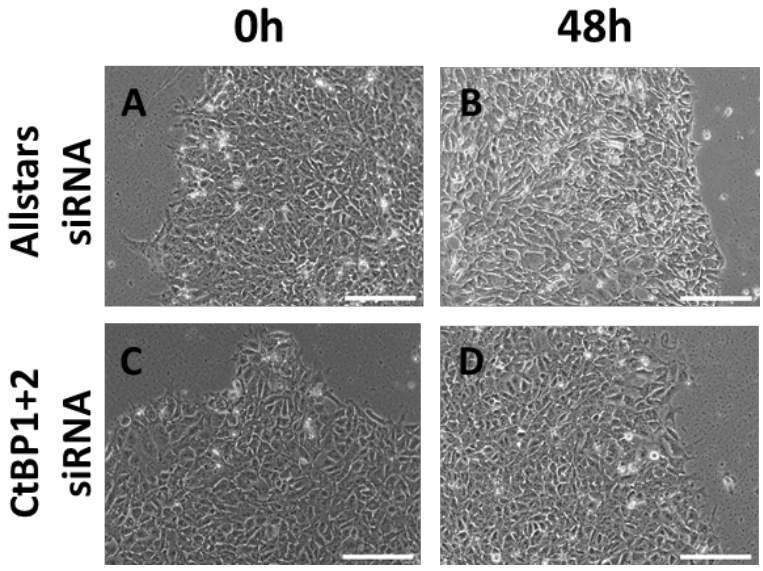

Figure 6.15. Phase contrast images demonstrating colony morphology of Hues-7 hESCs cultured at 5% oxygen transfected with CtBP1+2 siRNA.
Representative phase contrast images of Hues-7 hESCs cultured at 5% oxygen transfected with either Allstars negative control siRNA (A-B) or both CtBP1 and CtBP2 siRNAs (CtBP1+2; C-D) after 0 (A, C) and 48 hours (B, D). Scale bar indicates 200μm.

Quantification of the CtBP protein bands revealed a significant 50% decrease in the protein expression of both CtBP1 ($p=0.0022$) and CtBP2 ($p=0.0019$) compared to the transfection control (Figure 6.16B). Thus, both CtBP isoforms were successfully silenced using two single-targeting siRNAs.

Western blots were performed to evaluate the effect of silencing both CtBP isoforms on the expression of key transcription factors regulating hESC self-renewal. Quantification

of the protein expression revealed a significant decrease in the expression of OCT4, SOX2 and NANOG in cells transfected with CtBP1+2 siRNA. Hues-7 hESCs where both CtBP isoforms had been silenced displayed an approximate 30% decrease in OCT4 (p=0.0371) and an approximate 50% reduction in SOX2 (p=0.0120) and NANOG (p=0.0294) protein expression compared to the Allstars control (Figure 6.16C).

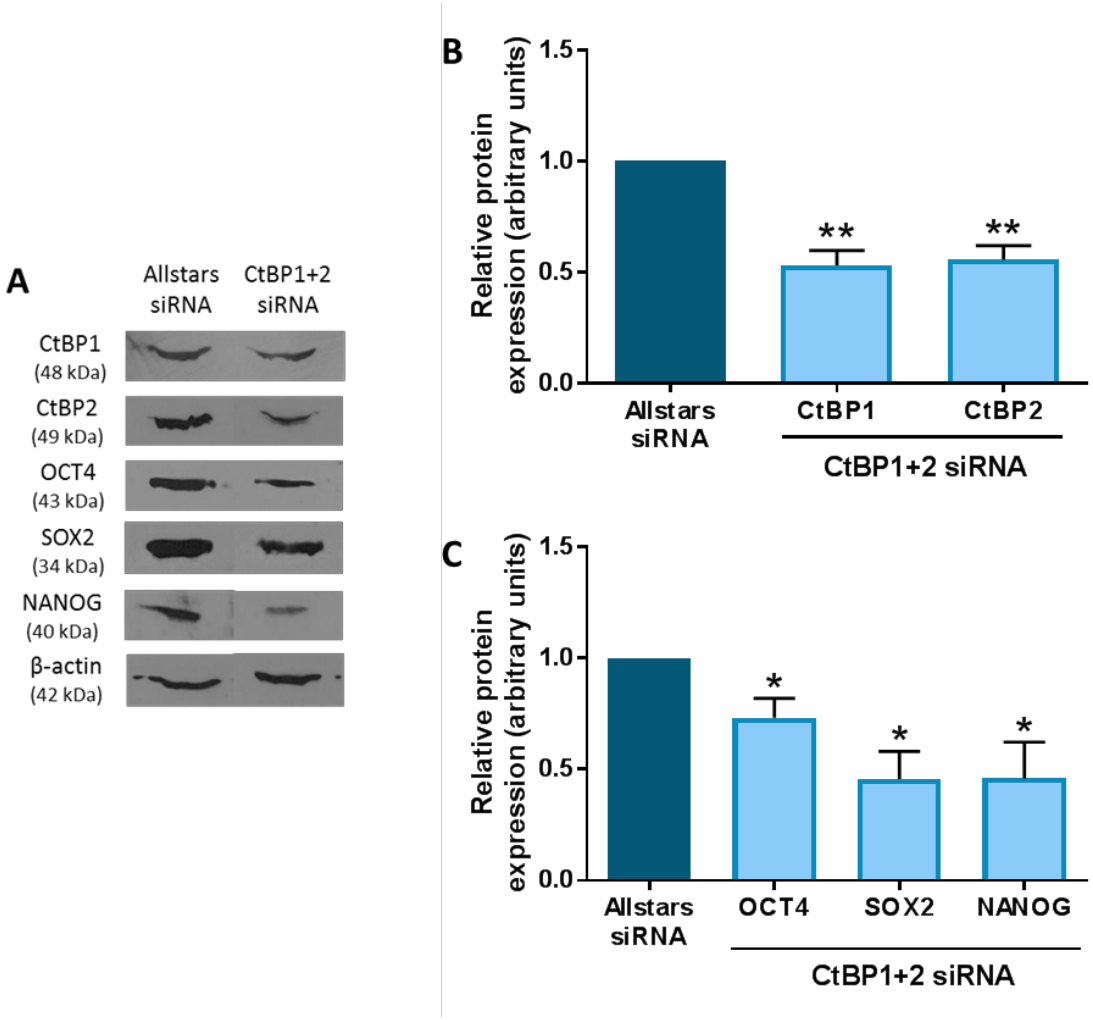

Figure 6.16. Silencing both CtBP isoforms reduces the expression of pluripotency markers in Hues-7 hESCs maintained at 5% oxygen using CtBP1+2 siRNA.
(A) Representative Western blots of CtBP1, CtBP2, OCT4, SOX2 and NANOG expression in Hues-7 hESCs cultured at 5% oxygen and transfected with either Allstars negative control siRNA or CtBP1+2 siRNA. (B) Quantification of CtBP1 and CtBP2 Western blots revealed the successful silencing of both CtBP isoforms in Hues-7 hESCs transfected with CtBP1+2 siRNA compared to the Allstars negative control. (C) Quantification of OCT4, SOX2 and NANOG Western blots revealed a significant decrease in the expression of all three pluripotency markers in Hues-7 hESCs transfected with CtBP1+2 siRNA compared to the control. Data were normalised to β-actin, and then to 1 for Allstars control. Bars represent mean ± SEM. (n=5)

6.3.5. Effect of silencing CtBP isoforms individually on hESC self-renewal under hypoxia

After demonstrating that silencing both CtBP isoforms together significantly reduces the protein expression of all three core pluripotency factors, the next aim was to analyse whether one isoform affects pluripotency marker protein expression more than another. Therefore, Hues-7 hESCs maintained at 5% oxygen were transfected on day 1 post-passage with either 50nM CtBP1 siRNA (Ambion) or 50nM CtBP2 siRNA (Ambion) to silence the CtBP isoforms individually, and cells were collected on day 3 post-passage for protein isolation.

Phase contrast images demonstrated that transfection with either the CtBP1 or CtBP2 siRNA had no adverse effects on the cell or colony morphology of Hues-7 hESCs after 48 hours, but displayed typical morphology comparative to the control (Figure 6.17).

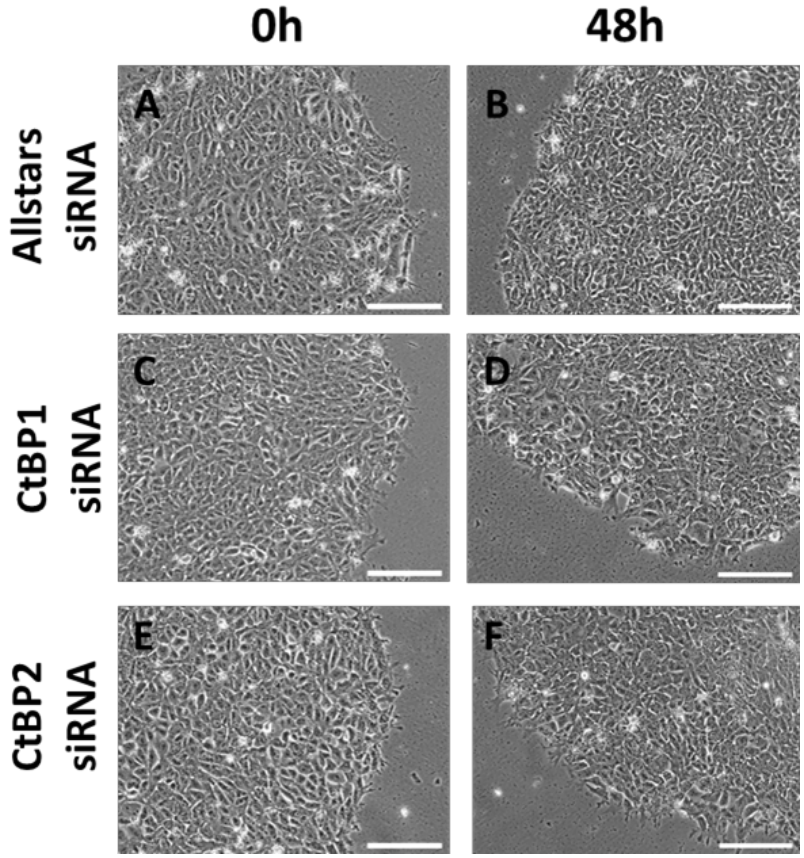

Figure 6.17. Phase contrast images demonstrating colony morphology of Hues-7 hESCs cultured at 5% oxygen transfected with either CtBP1 siRNA or CtBP2 siRNA.
Representative phase contrast images of Hues-7 hESCs cultured at 5% oxygen transfected with either Allstars negative control siRNA (A-B), CtBP1 siRNA (C-D) or CtBP2 siRNA (E-F) after 0 (A, C, E) and 48 hours (B, D, F). Scale bar indicates 200μm.

Silencing CtBP1 significantly decreased CtBP1 protein expression (p=0.0028) compared to the Allstars control siRNA without affecting CtBP2 protein expression. Similarly, silencing CtBP2 decreased CtBP2 protein expression by approximately 70% (p=0.0004) but had no effect on CtBP1 expression (Figure 6.18B). This data suggests that there was no compensatory increase in the expression of either CtBP isoform.

After successfully silencing both CtBP isoforms individually, further Western blots were performed to evaluate the effects of silencing only one isoform on hESC self-renewal under hypoxia. Quantification of the protein bands revealed a significant decrease in the expression of OCT4, SOX2 and NANOG in cells transfected with CtBP1 siRNA compared to the control siRNA. Hues-7 hESCs transfected with CtBP1 siRNA displayed an approximate 50% decrease in OCT4 (p=0.0292), an approximate 40% reduction in SOX2 (p=0.0495) and an approximate 60% decrease in NANOG (p=0.0156) protein expression compared to the Allstars control. Furthermore, quantification of the Western blots revealed a significant 50% and 60% decrease in the protein expression of OCT4 (p=0.0482) and NANOG (p=0.0475) respectively in cells transfected with CtBP2 siRNA, but there was no significant difference in SOX2 protein expression (p=0.6363) compared to the control treated cells (Figure 6.18C).

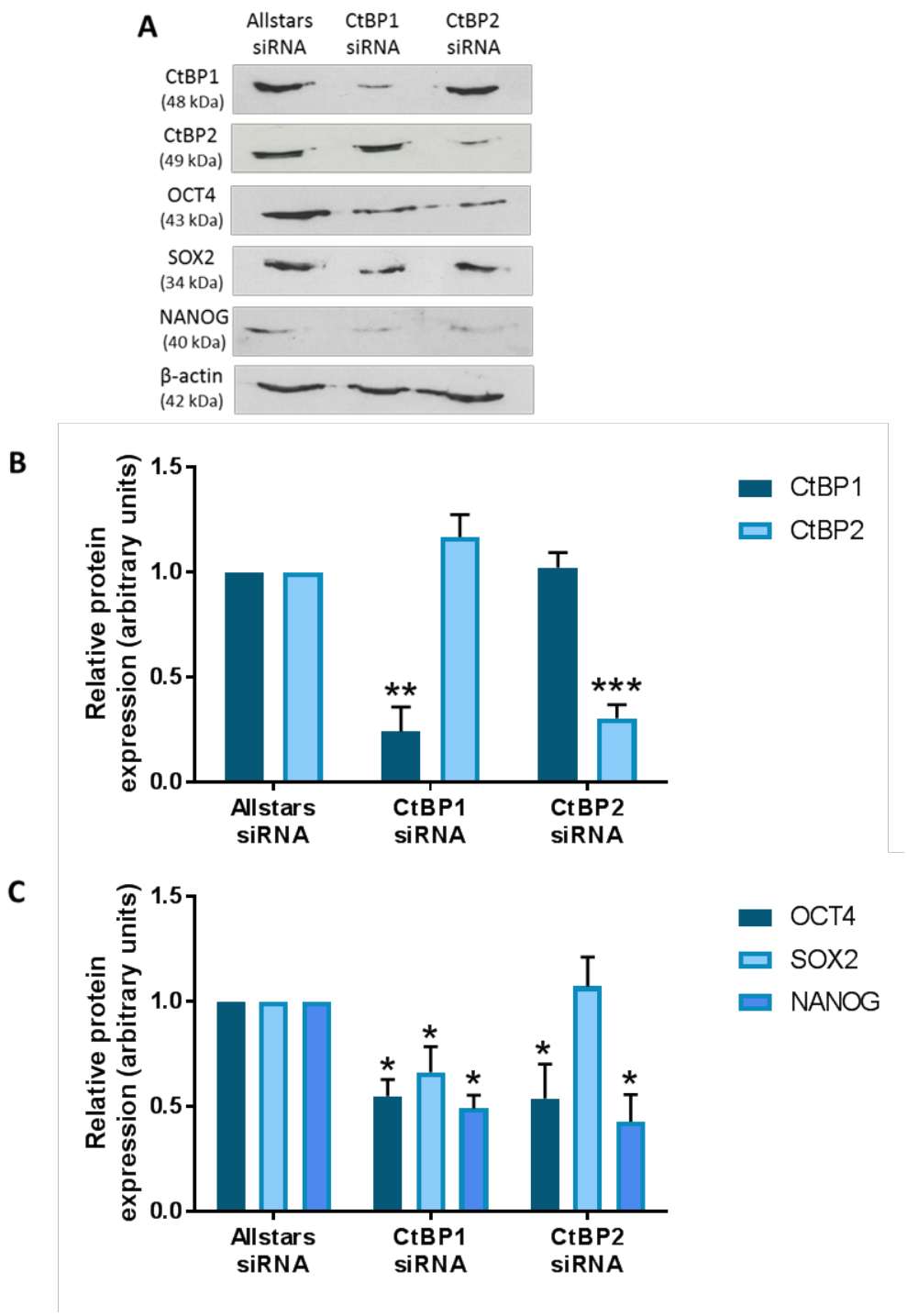

Figure 6.18. Silencing of CtBP isoforms individually in Hues-7 hESCs cultured at 5% oxygen and transfected with either CtBP1 siRNA or CtBP2 siRNA.
(A) Representative Western blots of CtBP1, CtBP2, OCT4, SOX2 and NANOG expression in Hues-7 hESCs cultured at 5% oxygen and transfected with either Allstars negative control siRNA, CtBP1 siRNA or CtBP2 siRNA. (B) Quantification of CtBP1 and CtBP2 Western blots revealed the successful silencing of an individual CtBP isoform in Hues-7 hESCs transfected with either CtBP1 or CtBP2 siRNA compared to the Allstars negative control. (C) Quantification of OCT4 and NANOG Western blots revealed a significant decrease in their expression in Hues-7 hESCs transfected with either CtBP1 or CtBP2 siRNA compared to the control, whereas quantification of SOX2 blots revealed a significant decrease only when CtBP1 was silenced. Data were normalised to β-actin, and then to 1 for Allstars control. Bars represent mean ± SEM. (n=3-5)

6.3.6. Effect of inhibiting CtBP function on the self-renewal of hESCs under hypoxic conditions

To investigate the effects of inhibiting CtBP function on pluripotency marker expression, Hues-7 hESCs maintained at 5% oxygen were treated with CM supplemented with either 0mM or 1mM of the CtBP inhibitor, MTOB, for 48 hours before collecting samples for protein isolation. Previous work within the lab incubated Hues-7 hESCs with MTOB concentrations of greater than 1mM. Analysis of hESC colony morphology revealed that these concentrations of MTOB were toxic to the cells (unpublished data).

Cells treated with 1mM MTOB formed compact, rounded colonies of typical cobblestone morphology comparative to cells cultured in the absence of MTOB after both 24 hours and 48 hours (Figure 6.19).

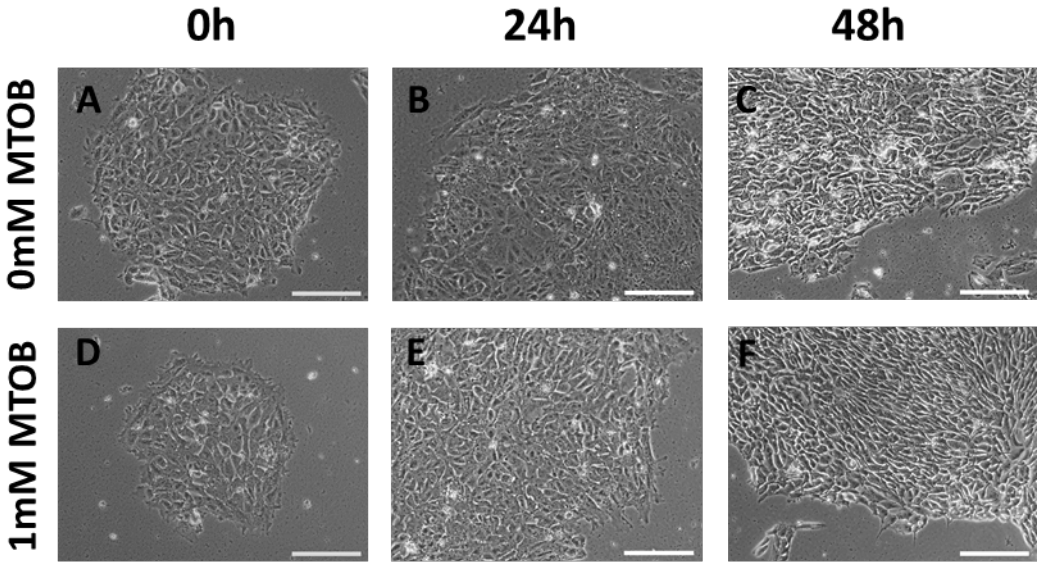

Figure 6.19. Phase contrast images demonstrating colony morphology of Hues-7 hESCs cultured at 5% oxygen in the presence of absence of MTOB supplemented MEF-conditioned medium.

Representative phase contrast images of Hues-7 hESCs cultured at 5% oxygen in MEF-conditioned medium supplemented with either 0mM (A-C) or 1mM MTOB (D-F) after 0 (A, D), 24 (B, E) and 48 hours (C, F). Scale bar indicates 200μm.

MTOB is an inhibitor of CtBP dimerisation and therefore is not expected to affect CtBP protein expression. However, it was not known whether CtBP dimerisation affected the self-renewal of hESCs.

No significant difference was observed in either CtBP1 ($p=0.3888$) or CtBP2 ($p=0.9447$) protein expression between cells treated with 0mM or 1mM MTOB (Figure 6.20B).

To determine whether the addition of the inhibitor MTOB successfully inhibited CtBP function, the expression of the known CtBP-repressed gene E-cadherin was quantified. Western blotting revealed a significant and approximate 50% increase in E-cadherin protein expression ($p=0.039$) in Hues-7 hESCs treated with MTOB under hypoxia compared to the control cells (Figure 6.20C). Together, these data demonstrate that CtBP function, and not expression, was affected by the addition of the inhibitor MTOB.

Subsequently, Western blots were performed to assess any changes in pluripotency marker expression as a result of inhibiting CtBP activity. Inhibiting CtBP function with the addition of MTOB in Hues-7 hESCs resulted in an approximate 30% decrease in OCT4 ($p=0.0241$), a 15% reduction in SOX2 ($p=0.0074$) and an approximate 40% reduction in NANOG ($p=0.0462$) protein expression compared to the control (Figure 6.20D).

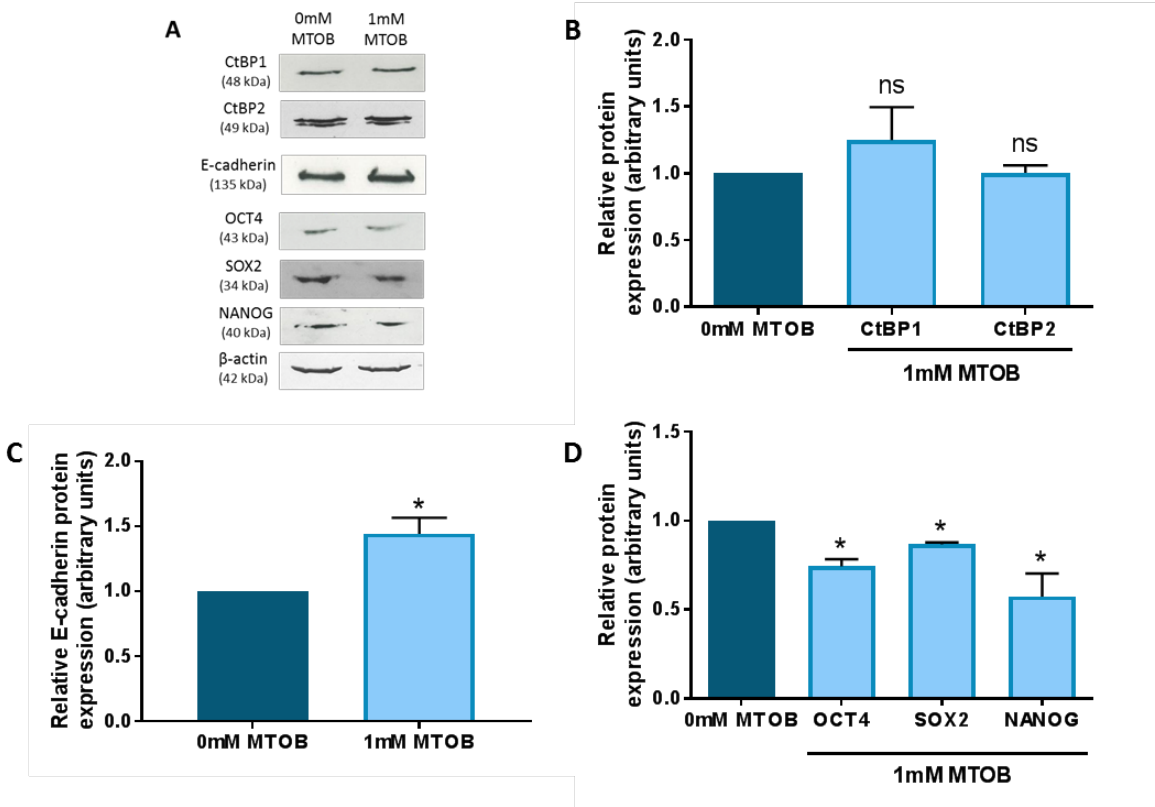

Figure 6.20. Inhibiting CtBP dimerisation using MTOB reduces the expression of pluripotency markers in Hues-7 hESCs maintained at 5% oxygen.
(A) Representative Western blots of CtBP1, CtBP2, OCT4, SOX2 and NANOG protein expression in Hues-7 hESCs cultured at 5% oxygen and treated with either 0mM or 1mM MTOB. (B) Quantification of CtBP1 and CtBP2 Western blots revealed no significant difference in Hues-7 hESCs treated with 1mM MTOB compared to the untreated control. (C) Quantification of E-cadherin Western blots revealed a significant increase in protein expression in Hues-7 hESCs treated with MTOB compared to the control cells. (D) Quantification of OCT4, SOX2 and NANOG Western blots revealed a significant decrease in their expression in Hues-7 hESCs treated with 1mM MTOB compared to the 0mM MTOB control. Data were normalised to β-actin, and then to 1 for Allstars control. Bars represent mean ± SEM. ns; not significant. (n=3-4)

To ensure that these effects were not cell line specific, Shef3 hESCs maintained under 5% oxygen were also incubated with either 0mM or 1mM MTOB for 48 hours before collecting cells for protein isolation.

Shef3 hESCs incubated with either 0mM or 1mM MTOB displayed typical cobblestone morphology and no clear morphological differences were observed between cells incubated in the presence or absence of MTOB (Figure 6.21).

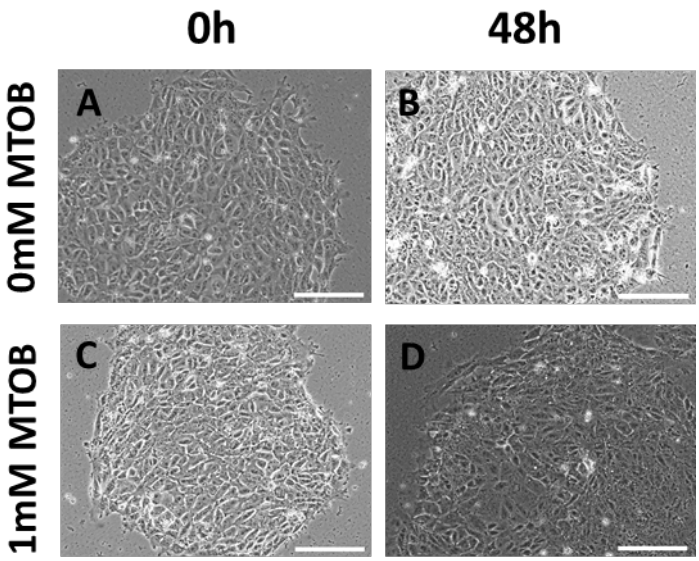

Figure 6.21. Phase contrast images demonstrating colony morphology of Shef3 hESCs cultured at 5% oxygen in the presence of absence of MTOB- supplemented MEF-conditioned medium.
Representative phase contrast images of Shef3 hESCs cultured at 5% oxygen in MEF-conditioned medium supplemented with either 0mM (A-C) or 1mM MTOB (D-F) after 0 (A, D), 24 (B, E) and 48 hours (C, F). Scale bar indicates 200μm.

Western blot analysis revealed no significant difference in CtBP1 and CtBP2 protein expression in Shef3 hESCs incubated with either 0mM or 1mM MTOB (Figure 6.22B). However, a significant and approximate 30% increase in E-cadherin expression ($p=0.016$) was observed in hESCs treated with MTOB compared to those cultured in the absence of the inhibitor (Figure 6.22C).

Furthermore, a significant decrease was observed in the protein expression of the three core pluripotency markers in Shef3 hESCs incubated with 1mM MTOB compared to the 0mM control (Figure 6.22D). A significant 32% decrease in OCT4 (p=0.0488), a 43% reduction in SOX2 (p=0.0448) and a 38% decrease in NANOG (p=0.0432) expression was observed when CtBP function was inhibited with the addition of MTOB compared to the control.

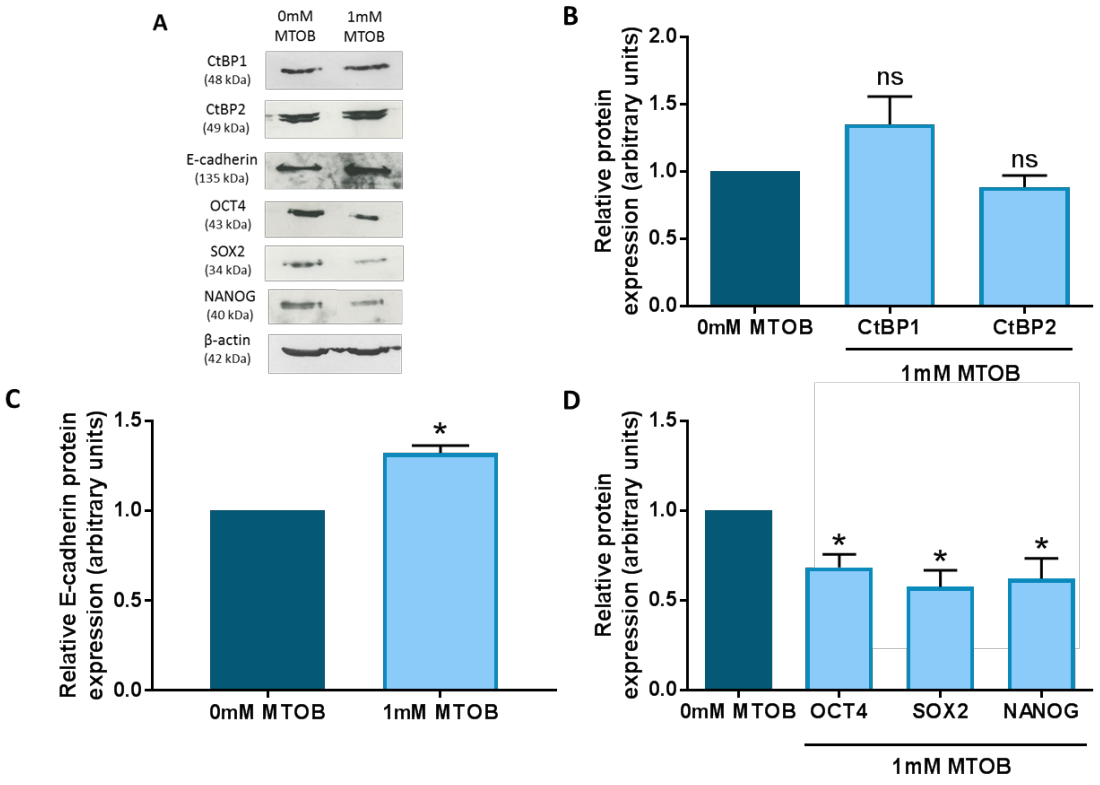

Figure 6.22. Inhibiting CtBP dimerisation using MTOB reduces the expression of pluripotency markers in Shef3 hESCs maintained at 5% oxygen.
(A) Representative Western blots of CtBP1, CtBP2, OCT4, SOX2 and NANOG protein expression in Shef3 hESCs cultured at 5% oxygen and treated with either 0mM or 1mM MTOB. (B) Quantification of CtBP1 and CtBP2 Western blots revealed no significant difference in Shef3 hESCs treated with 1mM MTOB compared to the untreated control. (C) Quantification of E-cadherin protein expression in Shef3 hESCs treated with MTOB compared to the control cells. (D) Quantification of OCT4, SOX2 and NANOG Western blots in Shef3 hESCs treated with 1mM MTOB compared to the 0mM MTOB control. Data were normalised to β-actin, and then to 1 for Allstars control. Bars represent mean ± SEM. ns; not significant. (n=3-4)

6.4 Discussion

Hypoxic culture of hESCs leads to an increase in the rate of flux through glycolysis and an increase in pluripotency marker expression (Ezashi et al., 2005; Westfall et al., 2008; Forristal et al., 2010; Forristal et al., 2013). However, it was unclear whether the metabolic state of the cell was influencing the self-renewal of hESCs, or vice versa, although more recent studies suggests it could be the former (Christensen et al., 2015). Data from Chapter 3.2.7 and Chapter 4.3.1.6 revealed that CtBPs, which link cellular metabolism to gene transcription, are expressed in hESCs and CtBP expression is regulated under hypoxia by HIF-2α as well as by glycolysis. Therefore, this chapter aimed to investigate whether CtBP expression and function regulate the self-renewal of hESCs under hypoxic conditions.

6.4.1 CtBPs in the transcriptional activation of pluripotency marker expression in Hues-7 hESCs

hESCs maintained at 5% oxygen were transfected with a double-targeting siRNA to silence both CtBP isoforms simultaneously to investigate whether CtBPs, and therefore metabolism, were involved in regulating the expression of pluripotency markers. A significant decrease in the mRNA and protein expression of both CtBP1 and CtBP2 was observed in hESCs transfected with CtBP1/2 siRNA. This was repeated using an alternative siRNA strategy where two single-targeting siRNAs were transfected simultaneously to, again, silence the expression of both CtBPs in order to repeat and reinforce the effects on OCT4, SOX2 and NANOG expression. hESCs transfected with CtBP1+2 siRNA presented a significant reduction in both CtBP isoforms, mimicking that of the double-targeting siRNA. Consequently, the silencing of both CtBPs, either with CtBP1/2 or CtBP1+2 siRNAs, led to a significant decrease in the mRNA and protein expression of an array of pluripotency markers. Furthermore, the loss of pluripotency when CtBP expression was silenced resulted in the initiation of early hESC differentiation the expression of a panel of differentiation markers significantly increased. The observed reduction in pluripotency marker protein expression and observed increase in differentiation marker expression may be a direct result of the lack of CtBP activity caused by silencing CtBP expression. Therefore, the data suggests that CtBPs play a role in the self-renewal of hESCs, specifically through the transcriptional activation of OCT4, SOX2 and NANOG, or alternatively via the repression of genes associated with early differentiation.

Data previously presented in Chapter 3 and Chapter 4 demonstrated that self-renewal and CtBP expression is also regulated by metabolism and hypoxia. Therefore, experiments were performed to further characterise whether this CtBP regulation of pluripotency was direct. The expression of *LDHA* and GLUT transporters was not affected by silencing CtBP expression and silencing CtBPs did not affect glycolysis. Therefore, CtBP expression has no effect on the rate of flux through glycolysis, and thus the effects of silencing CtBPs on hESC pluripotency are independent of metabolic and hypoxic regulation of CtBPs and pluripotency marker expression.

Although the exact mechanism(s) of regulation remain to be elucidated, it is possible that CtBPs may be activating pluripotency marker expression directly by acting as a coactivator at the promoter regions of all three pluripotency factors. This theory is supported by a previous study which identified both CtBP1 and CtBP2 as OCT4-associated proteins and CtBP2 was identified as a target of NANOG in mESCs (Pardo et al., 2010). Alternatively, CtBPs may still be functioning in a gene-specific manner, but indirectly affecting hESC self-renewal. CtBPs could act as a corepressor by inhibiting the expression of a lineage-specific gene, which results in the observed increase in OCT4, SOX2 and NANOG expression when CtBPs are expressed in hESCs. A recent study described CtBPs interacting with a known component of the CtBP corepressor complex, LSD1, in human gastrointestinal endocrine cells to activate the expression of the protein NeuroD1 (Ray et al., 2014). Although the mechanism behind CtBP-mediated transcriptional activation is not fully characterised, this study demonstrated that a PXDLS motif-containing TF recruited CtBPs to the NeuroD1 promoter region and the associated chromatin—modifying complexes and cofactors including LSD1. LSD1 catalysed the demethylation of H3K9 residues and P/CAF catalysed the subsequent acetylation of these residues to drive gene expression. This is one of the few examples describing CtBPs as transcriptional coactivators in human cell types, but may provide a basis for the mechanism behind CtBPs directly driving pluripotency marker expression in hESCs cultured under hypoxic conditions. Alternatively, CtBPs may be indirectly activating pluripotency marker expression through a different mechanism – potentially through a signalling pathway or by aiding chromatin-modifying enzymes to function and maintain a more euchromatic state.

Furthermore, data presented in this chapter has demonstrated that the regulation of pluripotency marker expression by CtBPs is not cell line specific and is also maintained

in hESCs cultured under 20% oxygen. This suggests that the glycolytic phenotype that is characteristic of the pluripotency state might consequently influence the expression of pluripotency markers in hESCs via CtBPs to promote self-renewal.

When CtBP1 and CtBP2 were silenced individually in hESCs cultured under hypoxia, no compensatory increase in the expression of the other CtBP isoform was observed. Although this demonstrated that the siRNAs were specific to either CtBP1 or CtBP2, this was somewhat unexpected as previous studies have revealed that CtBP2 was found to compensate for CtBP1 expression in human breast cancer cell lines (Birts et al., 2010).

As a result of silencing CtBP1 protein expression alone, the protein expression levels of OCT4, SOX2 and NANOG were significantly decreased. Additionally, silencing CtBP2 protein expression alone in hESCs maintained under hypoxic conditions revealed a significant decrease in OCT4 and NANOG protein expression, but no clear effect on SOX2 expression. This data suggests that only CtBP1 expression is required for the transcriptional activation of SOX2, but whether CtBP1 is acting as a homodimer or a heterodimer of both isoforms is not known. To our knowledge, there is no evidence of either a CtBP1 or CtBP2 homodimer regulating the expression of a target gene alone, however previous studies have indicated CtBP1 functioning as a monomer and interacting with a bromodomain. (Kim et al., 2005a). Although this example describes CtBP1 acting as a monomer to repress p300-mediated transcriptional activation, it is possible that the transcriptional activation of SOX2 may utilise a mechanism where CtBP1 functions as a monomer and blocks the activity of HMTs and HDACs in order to maintain the expression of the pluripotency marker. Conversely, this data suggests that both CtBP isoforms are required for the transcriptional activation of OCT4 and NANOG in hESCs as silencing either CtBP isoform results in a significant decrease in their protein expression levels. Therefore, a CtBP heterodimer must be involved if CtBPs are directly regulating pluripotency marker expression. This suggests that CtBPs are potentially driving OCT4 and NANOG expression in a gene-specific manner using a CtBP complex. However, it would probably require different chromatin-modifying complexes compared to those identified in the CtBP1 corepressor complex as they want to perform the opposite function, so could include HATs, for example, rather than HDACs (Shi et al., 2003). Alternatively, as the hESC epigenome is highly euchromatic (Meshorer and Misteli, 2006), the transcriptional activation of pluripotency markers in hESCs may require a completely novel mechanism involving the maintenance of histone marks at active

promoters rather than the removal of repressive marks in order to enhance their expression.

However, there may be alternative mechanisms through which CtBPs activate the expression of pluripotency markers. CtBPs may still be acting as transcriptional corepressors and exerting their effects on genes associated with differentiation and, as a result, hESCs can maintain their pluripotent state, in either a gene-specific manner or using a global repression mechanism, or additionally through the derepression of corepressors (Grooteclaes and Frisch, 2000). A recent study demonstrated CtBP2 had a role in the exit of pluripotency in mESCs (Tae Wan et al., 2015), which evidently describes conflicting results to those shown in this study. However, this study focused on the role of CtBPs in mESCs that are undergoing differentiation, and so may indicate that CtBPs have different roles. How CtBPs would discriminated between functioning to maintain hESC pluripotency and regulating the differentiation of ESCs is currently unknown, but is likely to be associated with a change in promoter context where different TFs, chromatin modifiers and associated cofactors are recruited to different promoter sequences, or perhaps in response to different environmental cues. Alternatively, it may support the theory that CtBPs are repressing lineage-specific genes, which results in increased pluripotency marker expression.

6.4.2 CtBP function is important for the transcriptional activation of pluripotency markers

To re-emphasise the role of CtBPs in the transcriptional activation of pluripotency marker expression, hESCs were treated with the CtBP inhibitor MTOB. The increase in E-cadherin; a known CtBP repressed gene, confirmed that CtBP function had been inhibited (Furusawa et al., 1999; Chinnadurai, 2009; Ichikawa et al., 2015). Hence, the significant decrease in OCT4, SOX2 and NANOG expression in the presence of MTOB highlights the requirement of CtBP dimerisation to activate the expression of these genes. This data highlights the need for active CtBP dimers in the transcriptional activation of OCT4, SOX2 and NANOG.

Furthermore, this data negates the hypothesis that CtBP1 acts as a monomer to enhance SOX2 expression in hESCs, as treatment with MTOB caused a significant decrease in SOX2 expression. If CtBP1 was acting as a monomer to drive SOX2 expression, no difference on SOX2 expression would have been observed in the presence of MTOB.

Despite the significant decrease in SOX2 expression as a result of MTOB treatment, and it should not be ignored that MTOB would bind to the CtBP monomer (Hilbert et al., 2014) and may block any potential CtBP1 activity as a monomer.

Together, these data demonstrate the first report of CtBPs regulating the expression of OCT4, SOX2 and NANOG in hESCs. CtBPs could be acting either directly by binding to TFs containing a PXDLS consensus motif at the promoters of these genes, or through a novel coactivating mechanism, or indirectly by potentially repressing the expression of other genes resulting in the increase of pluripotency marker expression (Figure 6.23). More specifically, CtBPs need to be in their active dimeric form to exert their effects; either as heterodimers or potentially as a CtBP1 homodimer for the activation of SOX2 expression. As previously mentioned, CtBP activity is regulated primarily through the binding of dinucleotides, such as NADH, to induce a conformational change and promote CtBP dimerisation. hESCs rely on glycolysis to meet their energetic and biosynthetic demands. Under hypoxic conditions, the rate of flux through glycolysis increases and thus the production of NADH. Thus, these data emphasise that CtBPs, and metabolism, regulate the pluripotency of hESCs cultured under hypoxic conditions.

6.5 Conclusions

Data presented in this chapter revealed that:

- Silencing both CtBP isoforms simultaneously and individually significantly decreases OCT4 and NANOG expression in hESCs maintained at 5% oxygen.
- Silencing both CtBP isoforms simultaneously and silencing CtBP1 individually significantly reduces SOX2 expression. However, silencing CtBP2 only had no clear effect on SOX2 expression in hESCs maintained at 5% oxygen.
- Silencing CtBPs in hESCs maintained at 20% oxygen, also, decreased pluripotency marker expression.
- Silencing both CtBP isoforms had no effect on glycolysis in hESCs maintained under hypoxia.
- Inhibiting CtBP dimerisation using MTOB significantly decreases the expression of the three core pluripotency factors in hESCs cultured at 5% oxygen.

Results from this chapter reveal that while hypoxia and metabolism maintain hESC self-renewal, the glycolytic sensors CtBPs play a role in that maintenance. From Chapters 3 to 6, this thesis has built up a better understanding of the roles that hypoxia, glycolysis and CtBPs play in hESC maintenance. However, the next chapter will look to see how similar those mechanisms are in the malignant counterparts of hESCs; hECCs.

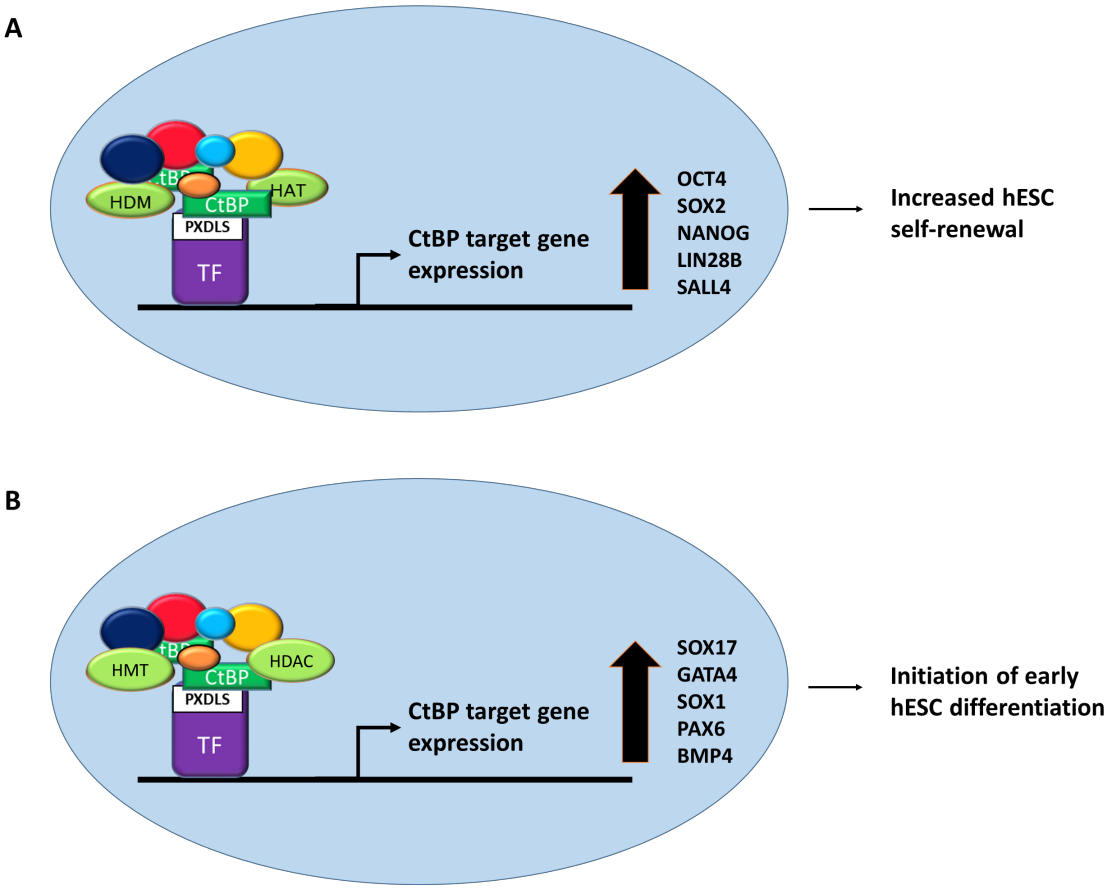

Figure 6.23. Schematic of proposed alternative mechanisms of how CtBPs may increase hESC pluripotency.
Schematic demonstrating the potential mechanisms behind how the glycolytic sensors CtBPs may increase hESC pluripotency. Functional CtBP dimers bind to DNA-binding transcription factors that contain the consensus motif PXDLS. (A) CtBPs could recruit chromatin modifying proteins such as HDMs and HATs to form a coactivator complex that results in a more 'open' chromatin state in the proximal promoter regions of pluripotency genes and leads to an increase in the expression of OCT4, SOX2, NANOG, LIN28B and SALL4. (B) Alternatively, CtBPs could recruit HDACs or HMTs to the proximal promoter regions of differentiation genes and lead to a more repressed chromatin conformation. This could prevent the early initiation of differentiation, hence supporting a pluripotent state. However, the exact molecular mechanisms are yet to be fully characterised.

Chapter 7

Characterisation of hypoxic regulation in human embryonal carcinoma cells

Chapter 7: Characterisation of hypoxic regulation in human embryonal carcinoma cells

7.1 Introduction

7.1.1. Human embryonal carcinoma cells

Human embryonal carcinoma cells (hECCs) are derived from non-seminoma cells of a testicular germ cell tumour. These tumours are unique in that the 'normal' germ cells from which they are derived have specific stem cell characteristics, which they share with pluripotent stem cells such as hESCs. hECCs are the cancer stem cells of teratocarcinomas and are the malignant equivalent of hESCs, so are considered as a potential suitable model for hESC research at the embryonic stage for comparison with tumourigenesis, due to their capability to self-renew and differentiate into a variety of different cell types, much like their 'normal' pluripotent equivalents in hESCs. hECCs express pluripotency markers (Ezeh et al., 2005), and when these cells lose the expression of such pluripotency markers, differentiation is induced (Matin et al., 2004).

hECCs are associated with the hypoxic regions of solid tumours which display high HIF-1α expression levels (Bertout et al., 2008). This correlates with a poor clinical prognosis, and although there is no evidence specifically describing these elevated HIF-1α expression levels in hECCs, it could provide evidence that HIF-1α acts as the predominant regulator of the hypoxic response in hECCs.

Several studies have, also, documented the similarities between the metabolic state of hESCs and hECCs (De Miguel et al., 2015). Many cancer cell types generate most of their energy through glycolysis even under atmospheric oxygen tensions in a phenomenon known as the Warburg effect. The pluripotent state of hECCs correlates with an increased glycolytic metabolism, where upon differentiation, this reliance on a glycolytic metabolism is lost (Vega-Naredo et al., 2014). hECCs, also, utilise the expression of pluripotency markers to maintain that highly glycolytic metabolism and thus support pluripotency maintenance (Chen et al., 2016).

7.1.2. Nitric oxide

Nitric oxide (NO) is a free radical synthesised from L-arginine by the NO synthases (NOS); neuronal NOS (nNOS), inducible NOS (iNOS) and endothelial NOS (eNOS) (Moncada et al., 1991; Alderton et al., 2001), and an essential signalling molecule. NO

and the reactive nitrogen species that are derived from it are important signalling molecules that function in several different biological pathways including the regulation of stress pathways, the upregulation of hypoxic genes, cancer and normal cell proliferation, stem cell differentiation and apoptosis (Benhar and Stamler, 2005; Castello et al., 2006; Poyton et al., 2009; Mora-Castilla et al., 2010; Tejedo et al., 2010; Ball et al., 2012).

NO is well documented to affect HIF-α activation via several concentration-dependent mechanisms, including NO metabolites and oxygen availability. Particularly, low NO concentrations have been shown to induce HIF-1α in human embryonic kidney (HEK-293) cells. Yet, high levels of NO have been shown to stabilise HIF-1α in cells under normoxia mimicking the hypoxic response (Mateo et al., 2003). NO is capable of modifying many proteins within the cell that regulate HIF-1α expression including PHDs, VHL and signalling molecules in the phosphatidylinositide 3-kinase (PI3K) signalling pathway. The inhibition of PHDs or VHL by nitrosylation of cysteine residues or by binding the catalytic ion prevents the ubiquitination and therefore degradation of HIF-1α (Park et al., 2008; Chowdhury et al., 2011). NO can also stabilise HIF-1α via the PI3-K/Akt signalling pathway where S-nitrosylation of Ras-Cys119 increases its activity and thus enhances HIF-1α expression (Zhou et al., 2004).

7.1.3. Chapter Aims

hECCs are often regarded as a model system for hESC research since they express pluripotency markers and are easier to maintain in culture. The beneficial role of low oxygen tension for the maintenance of hESCs is well-documented, however the role of hypoxia in the maintenance of tumour stem cell characteristics is not as well known.

This chapter aims to investigate the hypoxic regulation of self-renewal in hECCs to determine whether the mechanism was similar to hESCs.

The specific aims of this chapter are:

- To characterise the expression of pluripotency markers and CtBPs in N-TERA-2 (NT2) hECCs cultured at either 5% or 20% oxygen tensions.
- To characterise the expression and localisation of HIF-1α and HIF-2α in NT2 cells maintained at either 5% or 20% oxygen.

- To investigate the mechanisms regulating HIF expression in NT2 hECCs maintained at either 5% or 20% oxygen.

7.2 Materials & Methods

siRNA transfections were performed as described previously (Section 2.1.6). Pharmacological treatment, RT-qPCR and Western blotting analysis were used as described in Section 2.1.7, Section 2.2 and Section 2.3.2 respectively.

7.2.1. Culture of N-TERA-2 (NT2) hECC cell line

NTERA-2 (NT2) human testicular embryonal carcinoma cells were maintained in high glucose DMEM (Invitrogen) supplemented with 10% fetal bovine serum (FBS; Invitrogen) and 1% penicillin-streptomycin (Invitrogen) in T75 tissue culture flasks (Greiner Bio One, Glos, UK). Cells were cultured at 37˚C at both 20% and 5% oxygen tensions and passaged every 3-4 days once 80-90% confluent. Cells were washed in PBS and trypsinised with 2ml 0.05% trypsin-EDTA (Invitrogen) and incubated for approximately 5 minutes at either 5% or 20% oxygen tension to allow cells to detach for passaging. Cells were resuspended in 6ml supplemented DMEM and diluted 1:3 with fresh culture medium (Table 7.1). Cells were maintained for a minimum of 3 passages at both oxygen tensions before experimental use.

Table 7.1. Composition of NT2 culture medium.

High glucose DMEM (Invitrogen) supplemented with:	
10% fetal bovine serum (FBS)	Invitrogen
1% penicillin-streptomycin	Invitrogen

7.2.2. Treatment of NT2 hECCs with L-NAME

NT2 hECCs cultured at either 5% or 20% oxygen seeded at $3.3x10^5$ cells per well of a 6-well plate were maintained in either 0mM, 1mM or 10mM N(G)-Nitro-L-arginine methyl ester (L-NAME; Sigma)-supplemented media for 48 hours in 6-well plates. Cells were incubated with 2ml of fresh L-NAME-supplemented media per well of a 6-well plate on day 1 and day 2 post-passage, before collecting samples for protein analysis 48 hours after the initial addition of L-NAME.

7.2.3. Labelling of NO with DAF-FM DA

A 1mM stock solution of 4-amino-5-methylamino-2',7'-difluorofluorescein diacetate (DAF-FM DA; Thermo Scientific) was diluted to 1mM stock using anhydrous DMSO and stored in 1µl aliquots at -80˚C until required. NT2 hECCs were passaged and seeded at $3.3x10^4$ cells per well of a 12-well plate and maintained at either 5% or 20% oxygen until ~50% confluent after 48 hours before DAF-FM DA labelling. Alternatively, NT2 hECCs maintained at either 5% or 20% were seeded at $3.3x10^5$ cells per well of a 6-well plate and 10mM L-NAME was added on day 1 post-passage. hECCs were incubated either in the presence or absence of L-NAME for 48 hours before DAF-FM DA labelling.

DAF-FM DA aliquots were diluted to a final concentration of either 5µM or 10µM in culture medium before adding to NT2 hECCs and incubated at either 5% or 20% oxygen for 1 hour in a dark environment at 37˚C. Medium containing DAF-FM DA was removed and fresh culture medium was added to each well before incubation for 30 minutes at 37˚C at either 5% or 20% oxygen and protected from light. Cells were washed with PBS for 5 minutes before fixing with 4% paraformaldehyde for 15 minutes in a dark environment at room temperature. Normal NT2 culture medium was used as a negative control. Cells were imaged using a Zeiss fluorescence microscope and Axiovision imaging software (Zeiss) at an excitation/emission maxima of 495/515nm. The mechanism of DAF-DM DA labelling is shown in Figure 7.1.

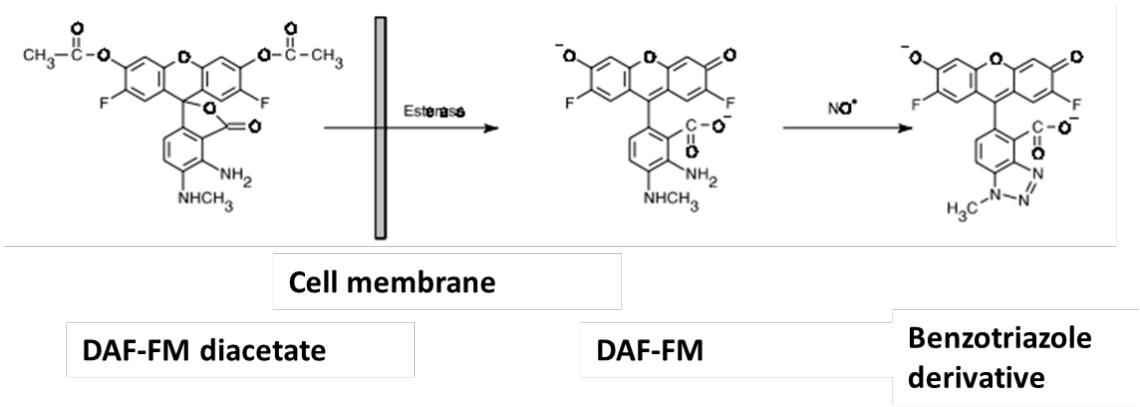

Figure 7.1. Schematic of the DAF-FM DA mechanism of action.
DAF-FM DA is cell-permeant and passively diffuses across cellular membranes. Once inside cells, it is deacetylated by intracellular esterases to become DAF-FM and begins to emit very low levels of fluorescence. After reacting with NO the levels of fluorescence increase significantly with excitation/emission maxima of 495/515nm.

7.2.4. NOS RT-qPCR

RNA was isolated from hECCs samples as previously described in Chapter 2.2 Relative NOS gene expression was analysed as previously described (Section 2.2.5) using Taqman probes (Table 7.2).

Table 7.2. TaqMan gene expression assay probes used for RT-qPCR analysis of NOS expression.

Gene	TaqMan gene expression assay
nNOS (Applied Biosystems)	Hs00167223_m1
iNOS (Applied Biosystems)	Hs01075527_m1
eNOS (Applied Biosystems)	Hs00167166_m1

7.3 Results

7.3.1. Characterisation of pluripotency marker expression in NT2 cells cultured at either 5% or 20% oxygen tensions

Human embryonal carcinoma cells are well-known to express pluripotency markers and are considered to be the malignant counterparts of hESCs. To investigate whether environmental oxygen regulates the expression of OCT4, SOX2 and NANOG in hECCs maintained at either 5% or 20% oxygen, immunocytochemistry was performed.

OCT4, SOX2 and NANOG were expressed in the nucleus of NT2 cells cultured at both 5% (Figure 7.2 – 7.3) and 20% oxygen (Figure 7.4 – 7.5).

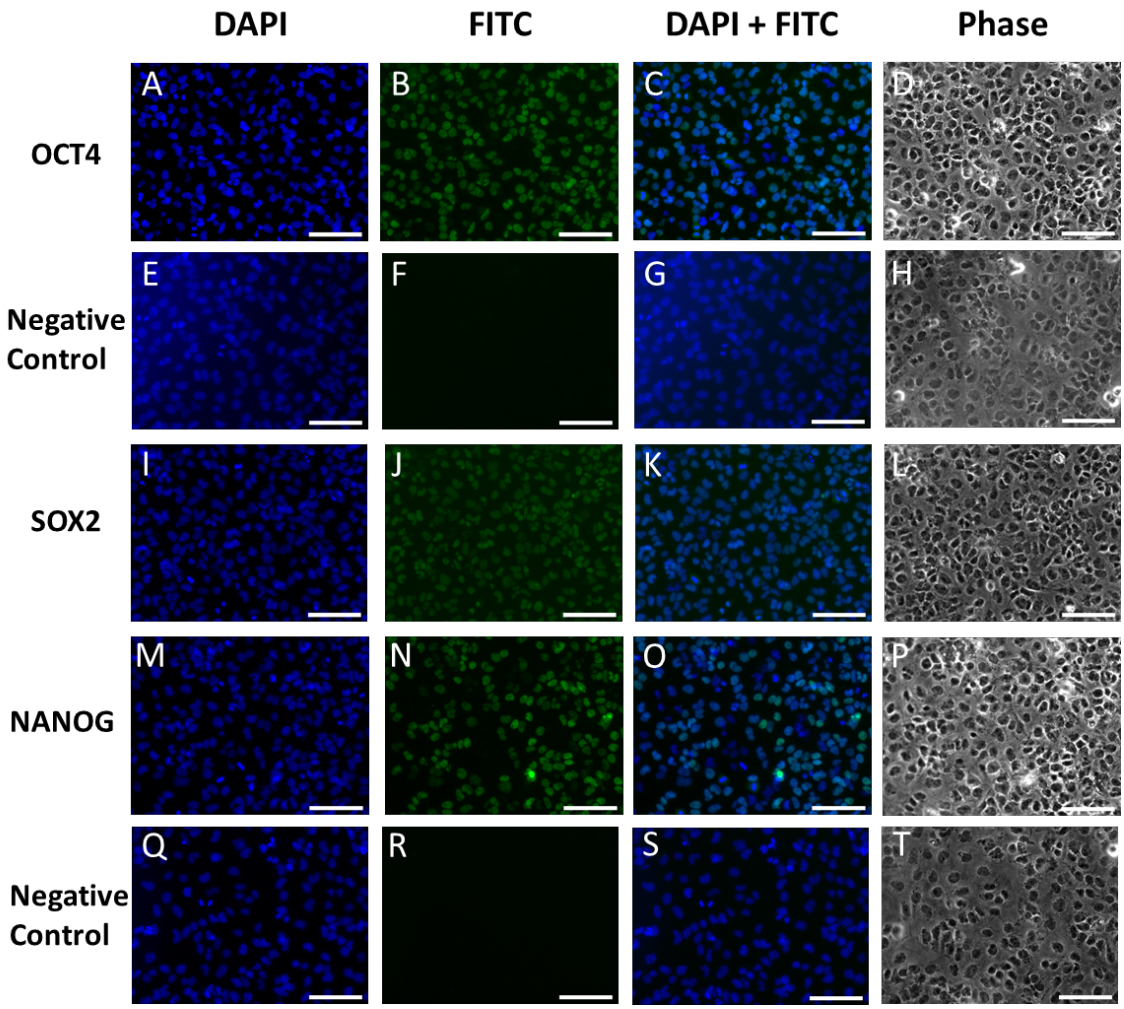

Figure 7.2. Characterisation of pluripotency marker expression in NT2 hECCs maintained at 5% oxygen.

Representative images of OCT4 (A-C), SOX2 (I-K) and NANOG (M-O) protein expression in NT2 hECCs cultured at 5% oxygen. An anti-mouse-IgG FITC-conjugated secondary antibody was used to detect OCT4 expression and its negative control (E-G), whereas an anti-rabbit-IgG FITC-conjugated secondary antibody was used to detect SOX2 and NANOG expression and their negative control (Q-S). DAPI staining was performed to label the nuclei. DAPI (blue; A, E, I, M, Q), FITC (green; B, F, J, N, R) and phase contrast images (D, H, L, P, T) were taken. Scale bar indicates 200μm.

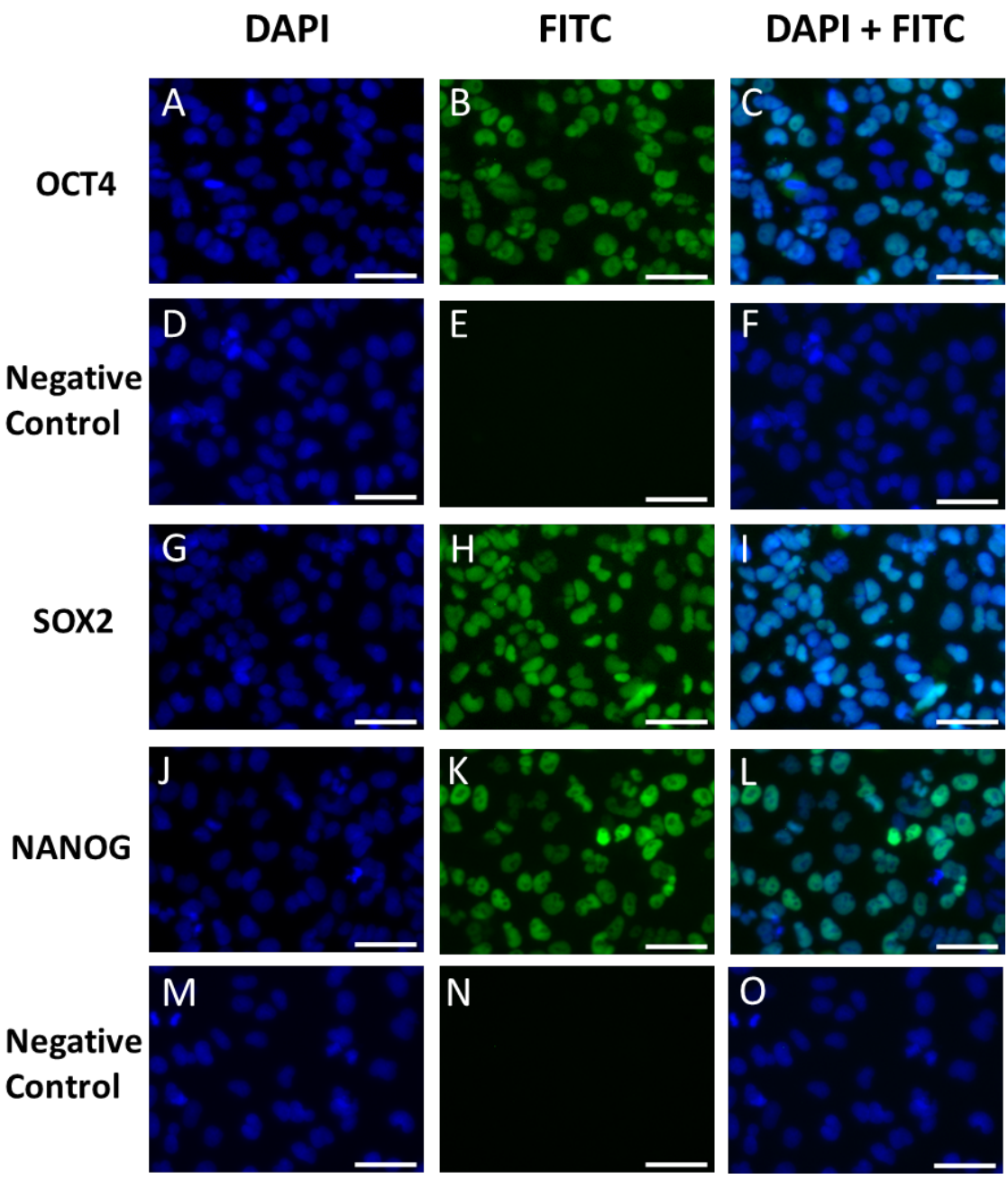

Figure 7.3. Subcellular localisation of pluripotency markers in NT2 hECCs cultured at 5% oxygen.

Representative images of OCT4 (A-C), SOX2 (G-I) and NANOG (J-L) protein expression in NT2 hECCs cultured at 5% oxygen. An anti-mouse-IgG FITC-conjugated secondary antibody was used to detect OCT4 expression and its negative control (D-F), whereas an anti-rabbit-IgG FITC-conjugated secondary antibody was used to detect SOX2 and NANOG expression and their negative control (M-O). DAPI staining was performed to label the nuclei. DAPI (blue; A, D, G, J, M) and FITC (green; B, E, H, K, N) images were taken. Scale bar indicates 50μm.

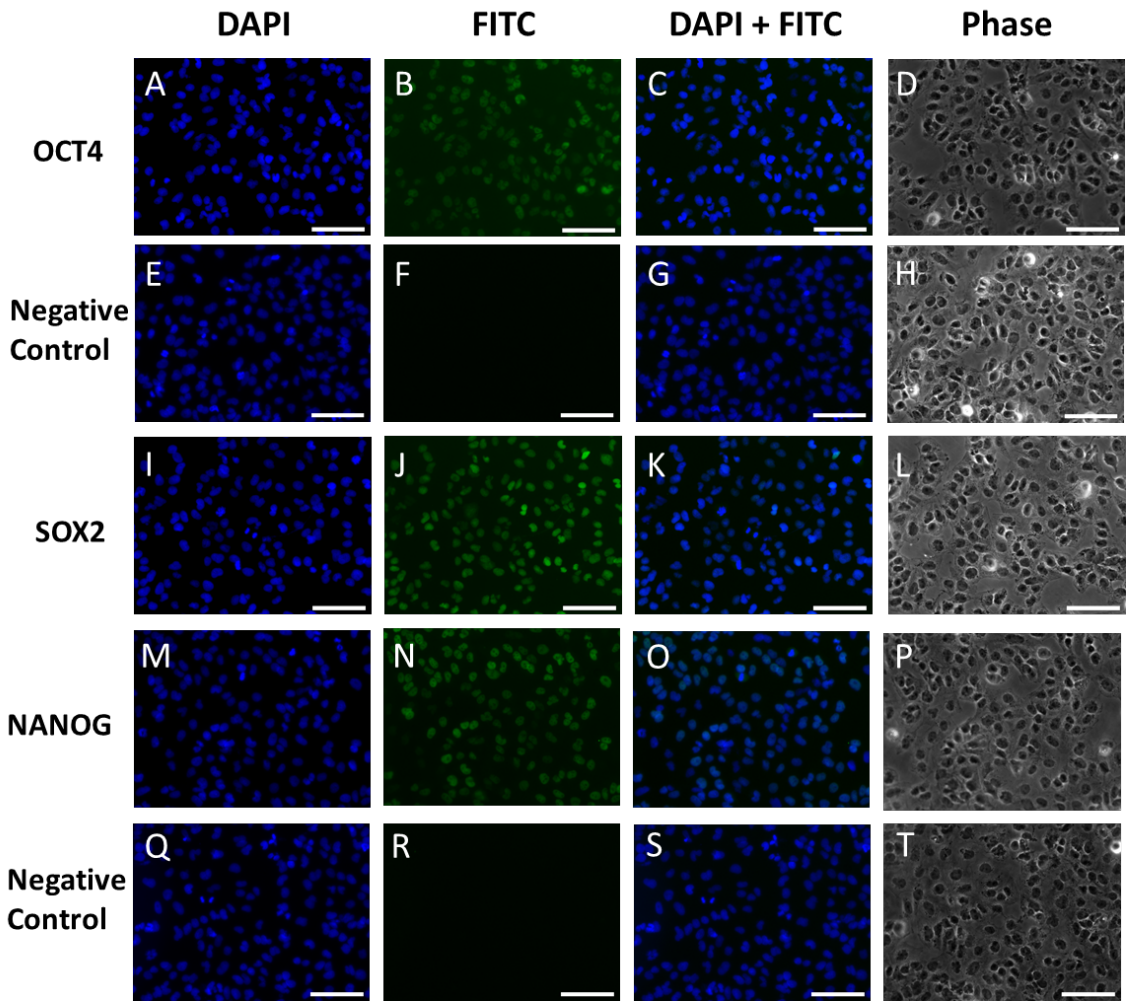

Figure 7.4. Characterisation of pluripotency marker expression in NT2 hECCs maintained at 20% oxygen.
Representative images of OCT4 (A-C), SOX2 (I-K) and NANOG (M-O) protein expression in NT2 hECCs cultured at 20% oxygen. An anti-mouse-IgG FITC-conjugated secondary antibody was used to detect OCT4 expression and its negative control (E-G), whereas an anti-rabbit-IgG FITC-conjugated secondary antibody was used to detect SOX2 and NANOG expression and their negative control (Q-S). DAPI staining was performed to label the nuclei. DAPI (blue; A, E, I, M, Q), FITC (green; B, F, J, N, R) and phase contrast images (D, H, L, P, T) were taken. Scale bar indicates 200μm.

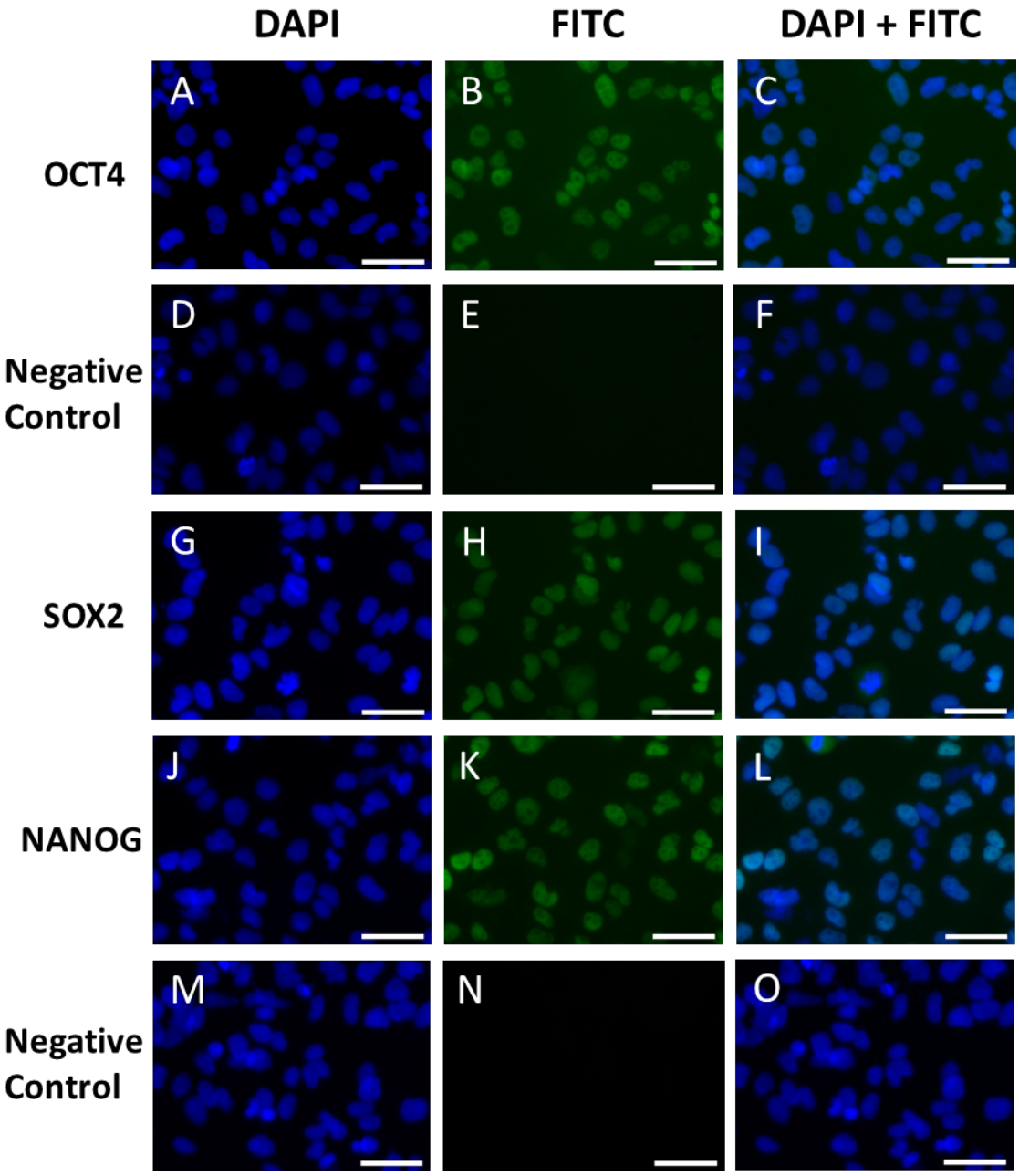

Figure 7.5. Subcellular localisation of pluripotency markers in NT2 hECCs cultured at 20% oxygen.

Representative images of OCT4 (A-C), SOX2 (G-I) and NANOG (J-L) protein expression in NT2 hECCs cultured at 20% oxygen. An anti-mouse-IgG FITC-conjugated secondary antibody was used to detect OCT4 expression and its negative control (D-F), whereas an anti-rabbit-IgG FITC-conjugated secondary antibody was used to detect SOX2 and NANOG expression and their negative control (M-O). DAPI staining was performed to label the nuclei. DAPI (blue; A, D, G, J, M) and FITC (green; B, E, H, K, N) images were taken. Scale bar indicates 50μm.

Previous studies have demonstrated an increase in the expression of pluripotency markers in Hues-7 hESCs cultured at 5% oxygen compared to cells cultured at 20% oxygen (Forristal et al., 2010; Forristal et al., 2013). Therefore, the expression of OCT4, SOX2 and NANOG was determined in NT2 hECCs cultured at both 5% and 20% oxygen tensions using RT-qPCR and Western blotting.

Quantification of OCT4, SOX2 and NANOG mRNA expression revealed no significant difference between NT2 hECCs maintained at 5% oxygen compared to hECCs maintained under normoxic oxygen tensions (Figure 7.6).

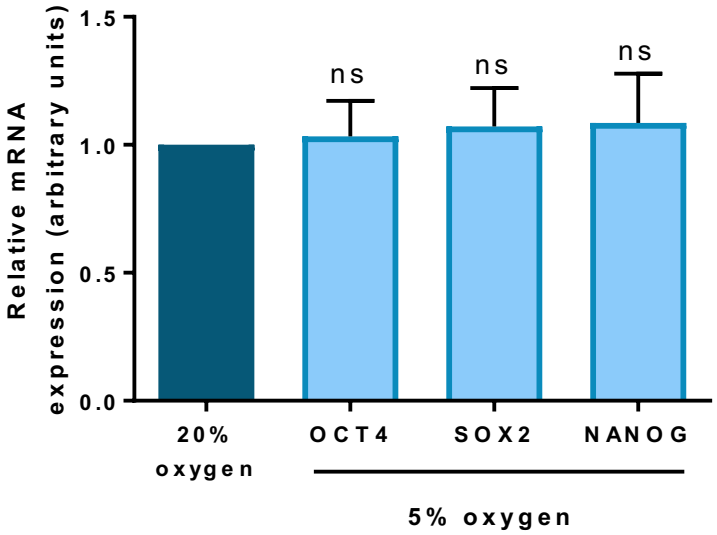

Figure 7.6. Pluripotency marker mRNA expression is not affected by oxygen tension in NT2 hECCs.
Quantification of *OCT4, SOX2* and *NANOG* mRNA expression in NT2 hECCs maintained at either 5% oxygen or 20% oxygen. Data were normalised to *UBC*, and then to 1 for 20% oxygen. Bars represent mean ± SEM. (n=4).

Similarly, at the protein level, there was no significant difference in the expression of OCT4 (p=0.9041), SOX2 (p=0.1353) and NANOG (p=0.7665) in NT2 cells maintained at 5% oxygen compared to those cultured at 20% oxygen (Figure 7.7). It was noted that there was great variation in the protein expression of all three core pluripotency markers from an approximate 90% decrease to a 210% increase in expression in NT2 cells maintained at 20% oxygen compared to those maintained under hypoxia. Together, this

data suggests that, unlike hESCs, pluripotency marker expression is no longer regulated by hypoxia in NT2 hECCs.

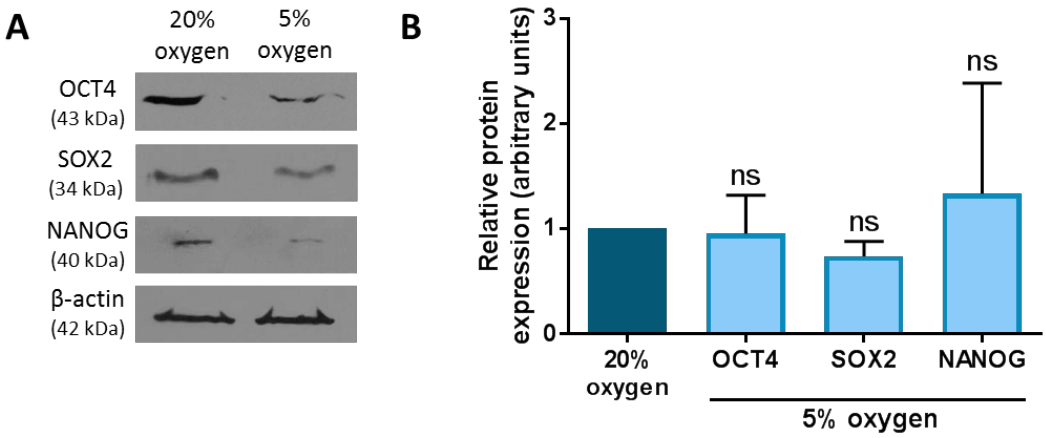

Figure 7.7. Pluripotency marker protein expression is not affected by oxygen tension in NT2 hECCs.
(A) Representative Western blots of OCT4, SOX2 and NANOG expression in NT2 hECCs cultured at either 5% or 20% oxygen. (B) Quantification of OCT4, SOX2 and NANOG expression in NT2 hECCs cultured at 5% oxygen compared to 20% oxygen tension. Data were normalised to β-actin, and then to 1 for 20% oxygen tension. Bars represent mean ± SEM (n=5)

7.3.2. Characterisation of CtBP expression in NT2 cells cultured at 5% and 20% oxygen

To investigate the expression and subcellular localisation of CtBP1 and CtBP2 in NT2 hECCs cultured at either 5% or 20% oxygen immunocytochemistry was performed.

NT2 cells clearly expressed both CtBP isoforms at 5% and 20% oxygen tensions (Figure 7.8 – 7.11). No obvious difference in CtBP1 and CtBP2 expression were observed between NT2 cells cultured at either 5% (Figure 7.8) or 20% oxygen (Figure 7.10). Higher magnification of NT2 hECCs at both 5% (Figure 7.9) and 20% oxygen (Figure 7.11) revealed that both CtBP1 and CtBP2 expression was contained in the nucleus.

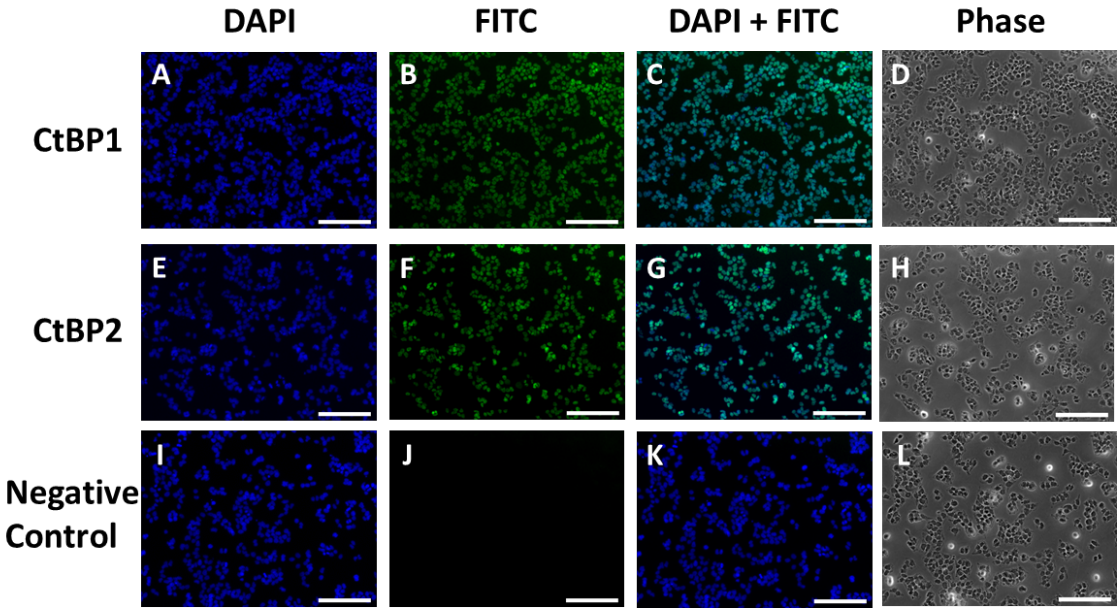

Figure 7.8. Characterisation of CtBP expression in NT2 hECCs cultured at 5% oxygen. Representative images of CtBP1 (A-C) and CtBP2 (E-G) protein expression in NT2 hECCs cultured at 5% oxygen. An anti-mouse-IgG FITC-conjugated secondary antibody was used to detect CtBP expression and the negative control (I-K). DAPI staining was performed to label the nuclei. DAPI (blue; A, E, I), FITC (green; B, F, J) and phase contrast images (D, H, L) were taken. Scale bar indicates 200μm.

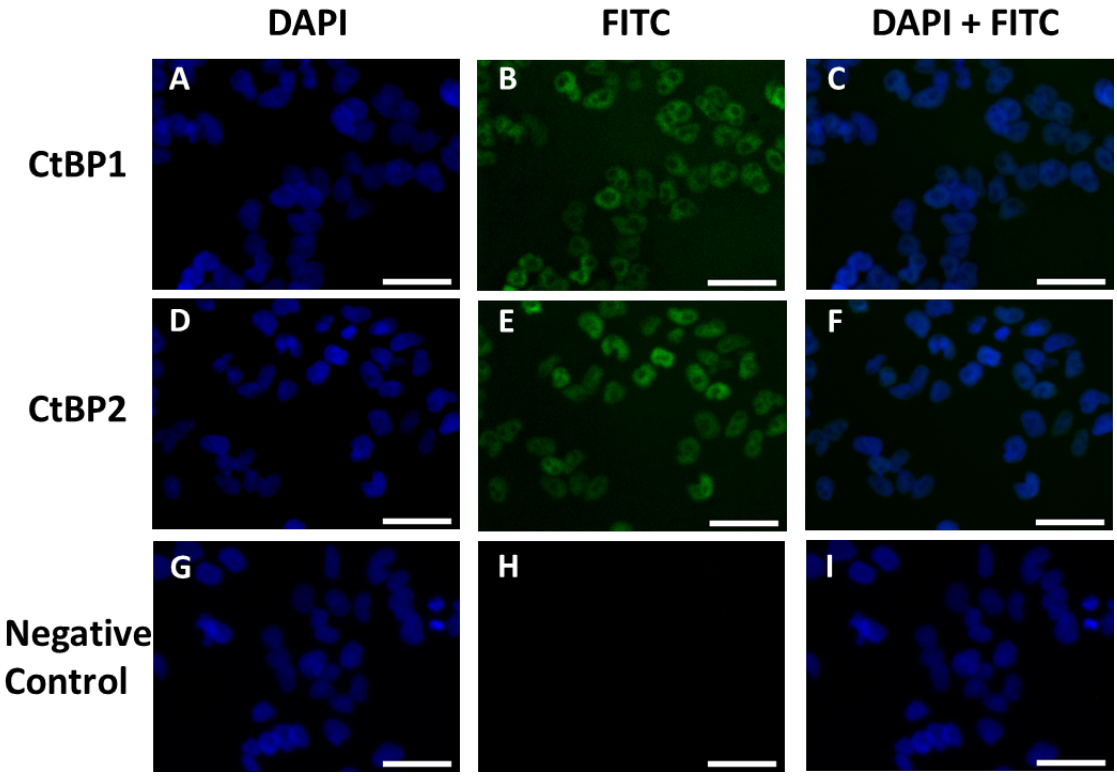

Figure 7.9. Subcellular localisation of CtBP expression in NT2 hECCs cultured at 5% oxygen.

Representative images of CtBP1 (A-C) and CtBP2 (D-F) protein expression in NT2 hECCs cultured at 5% oxygen. An anti-mouse-IgG FITC-conjugated secondary antibody was used to detect CtBP expression and the negative control (G-I). DAPI staining was performed to label the nuclei. DAPI (blue; A, D, G) and FITC (green; B, E, H) images were taken. Scale bar indicates 50μm.

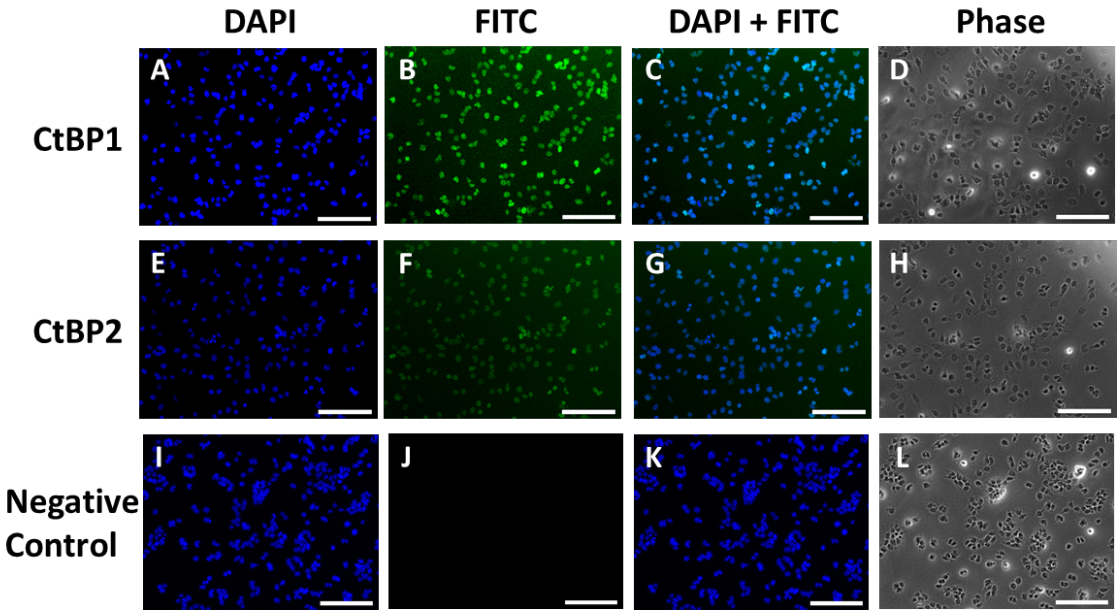

Figure 7.10. Characterisation of CtBP expression in NT2 hECCs cultured at 20% oxygen. Representative images of CtBP1 (A-C) and CtBP2 (E-G) protein expression in NT2 hECCs cultured at 20% oxygen. An anti-mouse-IgG FITC-conjugated secondary antibody was used to detect CtBP expression and the negative control (I-K). DAPI staining was performed to label the nuclei. DAPI (blue; A, E, I), FITC (green; B, F, J) and phase contrast images (D, H, L) were taken. Scale bar indicates 200μm.

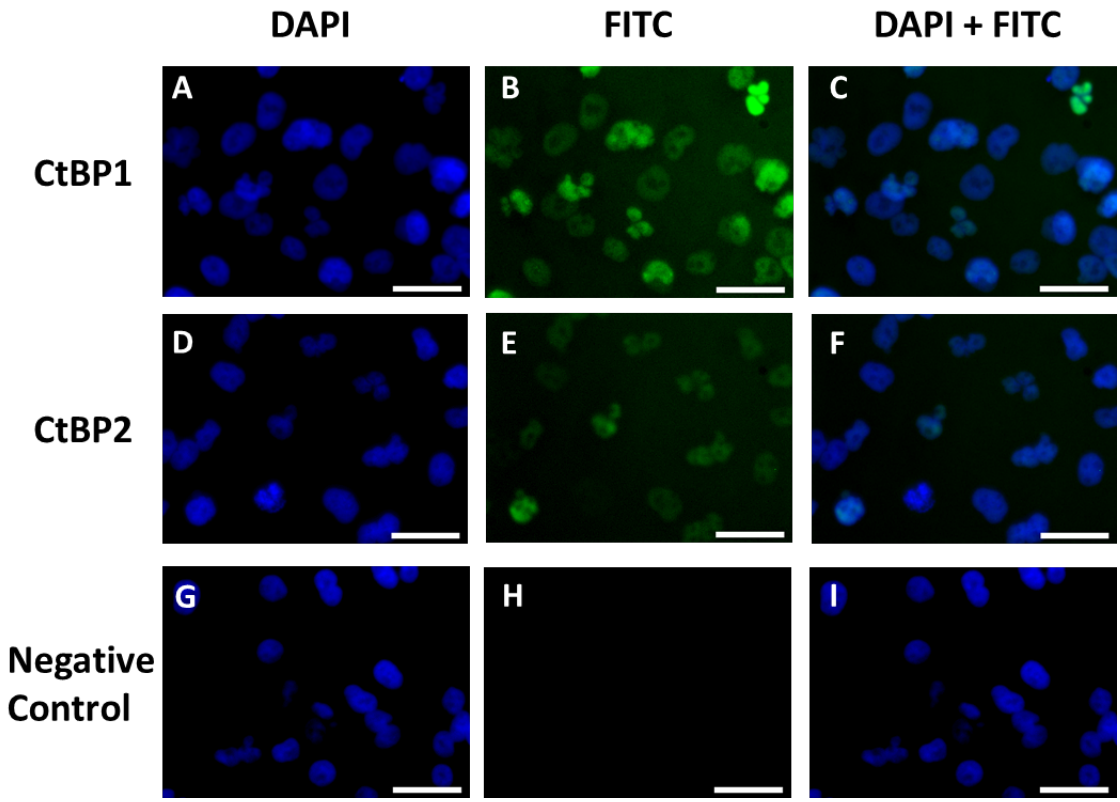

Figure 7.11. Subcellular localisation of CtBP expression in NT2 hECCs cultured at 20% oxygen.

Representative images of CtBP1 (A-C) and CtBP2 (D-F) protein expression in NT2 hECCs cultured at 20% oxygen. An anti-mouse-IgG FITC-conjugated secondary antibody was used to detect CtBP expression and the negative control (G-I). DAPI staining was performed to label the nuclei. DAPI (blue; A, D, G) and FITC (green; B, E, H) images were taken. Scale bar indicates 50μm.

To analyse any potential effect of hypoxia on the mRNA and protein expression levels of CtBP1 and CtBP2 in hECCs cultured at either 5% or 20% oxygen, RT-qPCR and Western blotting were performed.

Quantification of mRNA levels in NT2 cells maintained at either oxygen tensions revealed a significant 87% increase in *CtBP1* (p=0.0179) and a significant 66% increase in *CtBP2* (p=0.0168) mRNA expression in those cells cultured at 5% compared to those maintained at 20% oxygen (Figure 7.12).

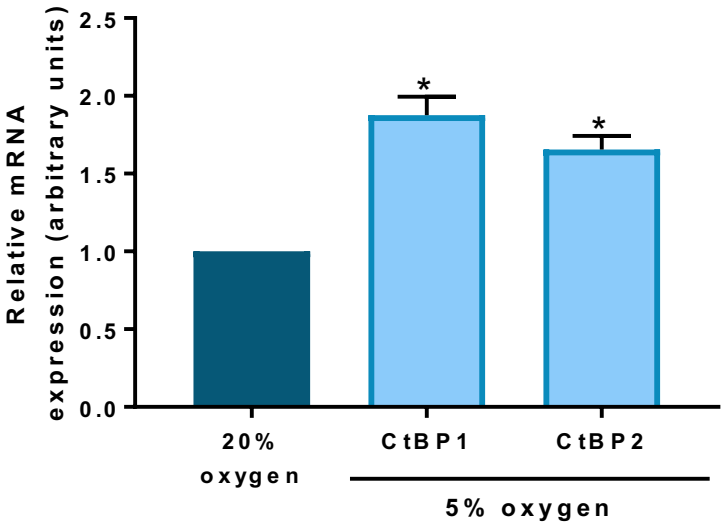

Figure 7.12. CtBP mRNA expression is enhanced by hypoxia in NT2 hECCs.
Quantification of *CtBP1* and *CtBP2* mRNA levels in NT2 hESCs maintained at either 5% oxygen or 20% oxygen. Data were normalised to *UBC*, and then to 1 for 20% oxygen. Bars represent mean ± SEM. (n=3)

Quantification of Western blots revealed a significant increase in the protein expression of both CtBP isoforms in NT2 hECCs cultured at 5% oxygen compared to those maintained under normoxic oxygen tensions. NT2 hECCs cultured at 5% oxygen displayed an approximate 41% increase in CtBP1 (p=0.0073) and an approximate 50% increase in CtBP2 (p=0.0261) protein expression compared to cells cultured at 20% oxygen (Figure 7.13).

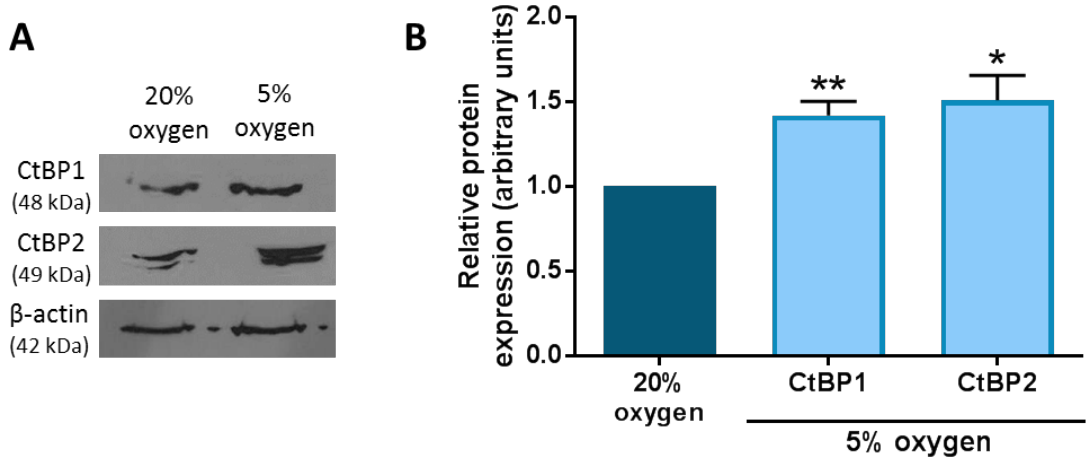

Figure 7.13. CtBP protein expression is increased under hypoxia in NT2 hECCs.
(A) Representative Western blots of CtBP1 and CtBP2 expression in NT2 hECCs cultured at either 5% or 20% oxygen. (B) Quantification of CtBP1 and CtBP2 Western from NT2 hECCs cultured at 5% oxygen compared to 20% oxygen tension. Data were normalised to β-actin, and then to 1 for 20% oxygen tension. Bars represent mean ± SEM. (n=5)

7.3.3. Characterisation and regulation of HIFs in NT2 cells

Data presented in this chapter has revealed that, in contrast to hESCs, the expression of pluripotency markers OCT4, SOX2 and NANOG is no longer regulated by environmental oxygen tension in NT2 hECCs. However, the CtBP family of glycolytic sensors still remain hypoxia regulated. To investigate a potential mechanism which may regulate this effect, the expression of HIF-1α and HIF-2α in NT2s maintained at either 5% or 20% oxygen was characterised using immunocytochemistry.

Using immunocytochemistry, NT2 cells clearly expressed both HIF-1α and HIF-2α at 5% oxygen as expected (Figure 7.14), but also both HIF-α subunits were expressed at 20% oxygen also (Figure 7.16). Higher magnification of NT2 hECCs cultured at either 5% (Figure 7.15) or 20% oxygen (Figure 7.17) revealed that HIF-1α expression was cytoplasmic. In contrast, HIF-2α expression was solely nuclear in NT2 cells cultured at both 5% (Figure 7.15) and 20% oxygen (Figure 7.17).

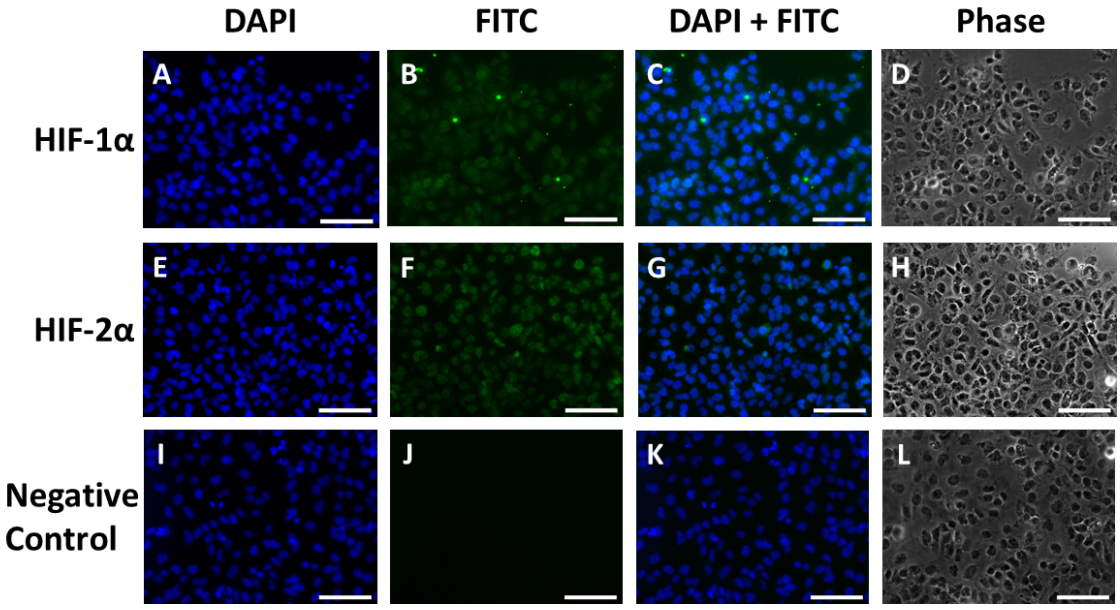

Figure 7.14. Characterisation of HIF-α subunit expression in NT2 hECCs cultured at 5% oxygen.

Representative images of HIF-1α (A-C) and HIF-2α (E-G) protein expression in NT2 hECCs cultured at 5% oxygen. An anti-rabbit-IgG FITC-conjugated secondary antibody was used to detect both HIF-1α and HIF-2α expression and its negative control (I-K). DAPI staining was performed to label the nuclei. DAPI (blue; A, E, I), FITC (green; B, F, J) and phase contrast images (D, H, L) were taken for both subunits and the control. Scale bar indicates 200μm.

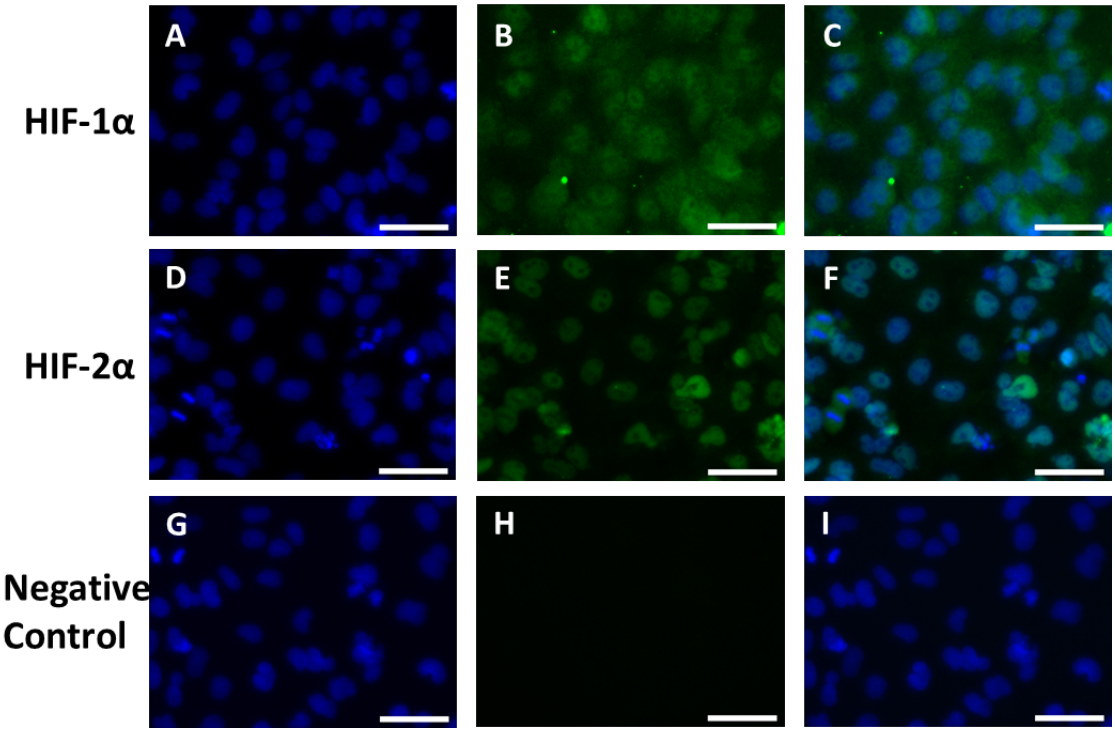

Figure 7.15. Subcellular localisation of HIF-α subunits in NT2 hECCs maintained at 5% oxygen.
Representative images of HIF-1α (A-C) and HIF-2α (D-F) protein expression in NT2 hECCs cultured at 5% oxygen. An anti-rabbit-IgG FITC-conjugated secondary antibody was used to detect both HIF-1α and HIF-2α expression and the negative control (G-I). DAPI staining was performed to label the nuclei. DAPI (blue; A, D, G) and FITC (green; B, E, H) images were taken for both proteins and the control. Scale bar indicates 50μm.

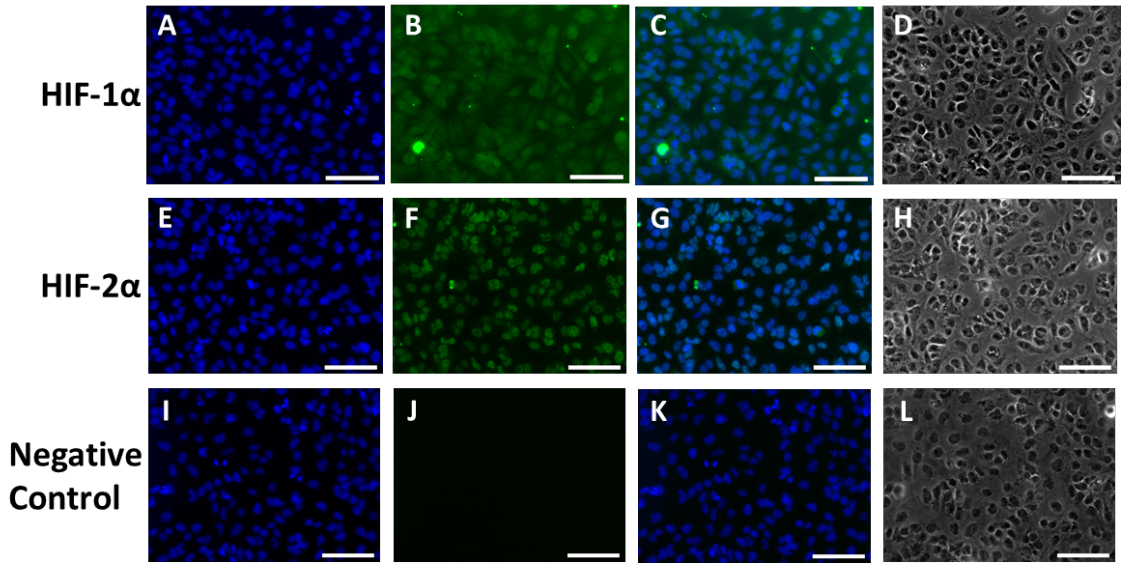

Figure 7.16. Characterisation of HIF-α subunit expression in NT2 hECCs cultured at 20% oxygen.

Representative images of HIF-1α (A-C) and HIF-2α (E-G) protein expression in NT2 hECCs cultured at 20% oxygen. An anti-rabbit-IgG FITC-conjugated secondary antibody was used to detect both HIF-1α and HIF-2α expression and its negative control (I-K). DAPI staining was performed to label the nuclei. DAPI (blue; A, E, I), FITC (green; B, F, J) and phase contrast images (D, H, L) were taken for both subunits and the control. Scale bar indicates 200μm.

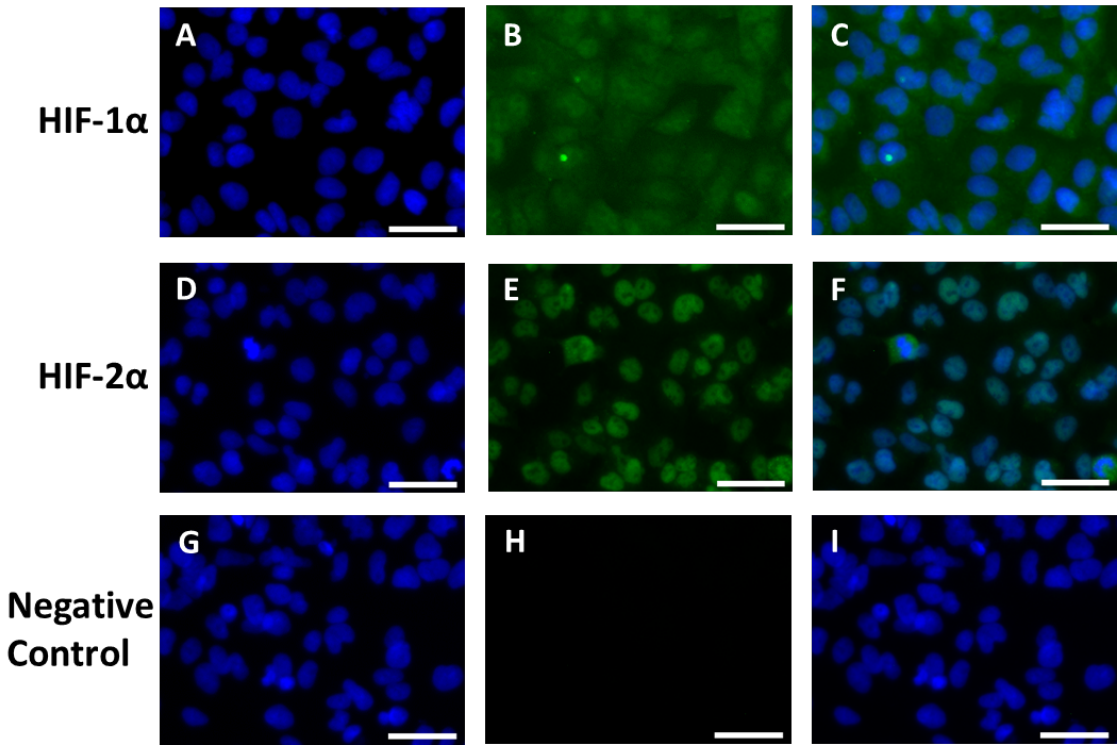

Figure 7.17. Subcellular localisation of HIF-α subunits in NT2 hECCs maintained at 20% oxygen.

Representative images of HIF-1α (A-C) and HIF-2α (D-F) protein expression in NT2 hECCs cultured at 20% oxygen. An anti-rabbit-IgG FITC-conjugated secondary antibody was used to detect both HIF-1α and HIF-2α expression and the negative control (G-I). DAPI staining was performed to label the nuclei. DAPI (blue; A, D, G) and FITC (green; B, E, H) images were taken for both proteins and the control. Scale bar indicates 50μm.

Although there were no obvious differences in the expression levels of HIF-1α and HIF-2α from the immunocytochemistry, Western blotting was performed to quantify HIF expression.

A single protein band of about 120kDa was observed for HIF-1α expression and another single band was observed at around 118kDa for HIF-2α expression in samples isolated from NT2 hECCs cultured at either 5% or 20% oxygen with no obvious difference in band density (Figure 7.18). Quantification of protein bands revealed no significant difference in the expression of either HIF-1α (p=0.7174) and HIF-2α (p=0.8507) between NT2 hECCs cultured at either 5% or 20% oxygen (Figure 7.18).

This suggests that HIF-α subunits are expressed equally in NT2 cells cultured under 5% and 20% oxygen.

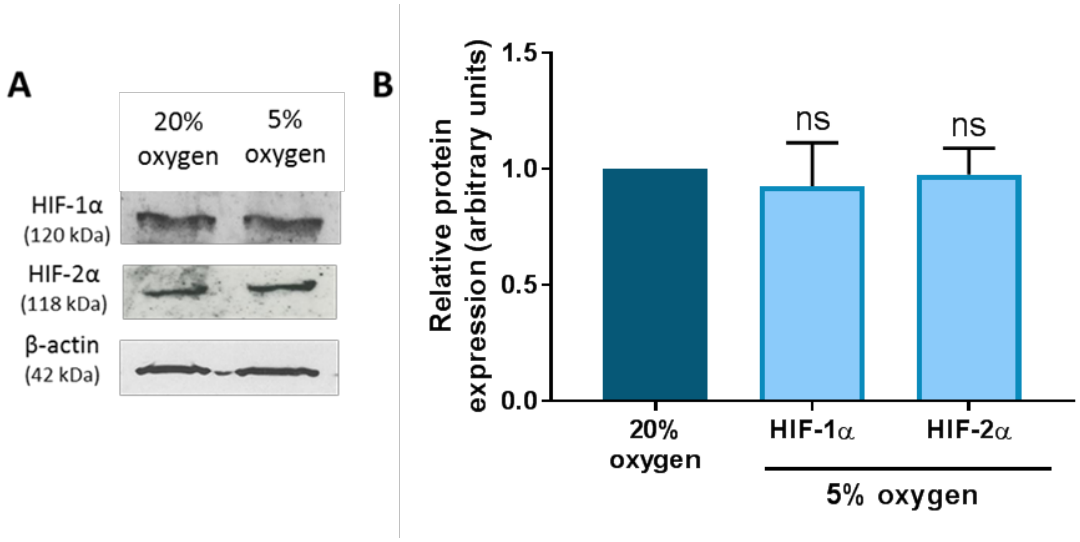

Figure 7.18. HIF-1α and HIF-2α expression is not different in NT2 hECCs cultured at either 5% or 20% oxygen.
(A) Representative Western blots of HIF-1α and HIF-2α expression in NT2 hECCs cultured at either 5% or 20% oxygen. (B) Quantification of HIF-1α and HIF-2α protein expression in NT2 hECCs cultured at 5% oxygen compared to 20% oxygen tension. Data were normalised to β-actin, and then to 1 for 20% oxygen tension. Bars represent mean ± SEM (n=3-4); ns; not significant.

7.3.3.1. Effect of silencing HIF-1α and HIF-2α in NT2 hECCs maintained under 5% oxygen

To investigate whether HIF-1α and HIF-2α were still functional in NT2 cells cultured at either 5% or 20% oxygen, NT2s were transfected with either HIF-1α siRNA or HIF-2α siRNA before analysing the effects of silencing HIF-α subunits on pluripotency marker and CtBP expression.

Phase contrast images demonstrate that there are no obvious morphological changes or effects on cell number in NT2 cells transfected with either Allstars negative control siRNA or HIF-1α siRNA at 5% oxygen (Figure 7.19).

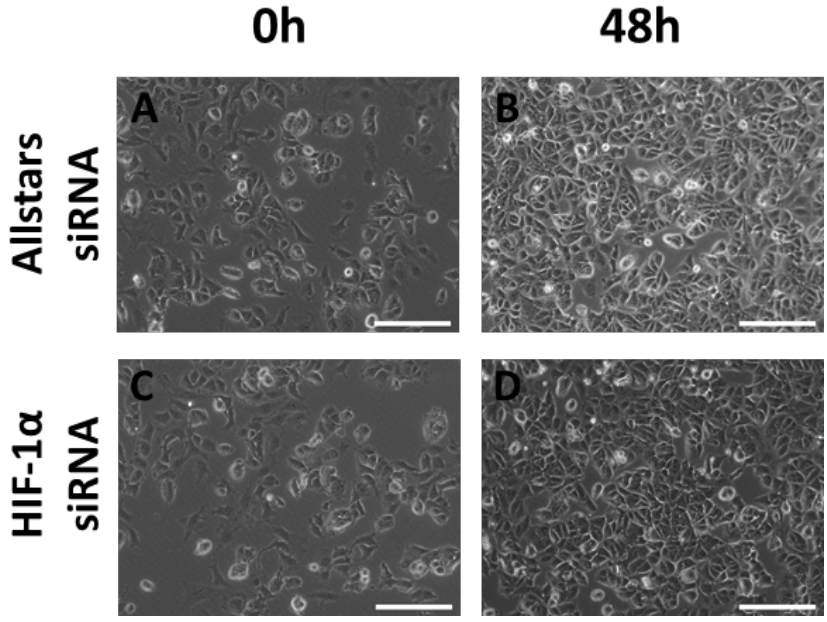

Figure 7.19. Phase contrast images demonstrating colony morphology of NT2 hECCs cultured at 5% oxygen transfected with HIF-1α siRNA.
Representative phase contrast images of NT2 hECCs cultured at 5% oxygen transfected with either Allstars negative control siRNA (A-B) or HIF-1α siRNA (C-D) after 0 (A, C) and 48 hours (B, D). Scale bar indicates 200μm.

HIF-1α protein expression was successfully silenced in NT2 hECCs after transfection with HIF-1α siRNA, displaying an approximate 87% decrease in HIF-1α expression ($p=0.0005$) compared to cells transfected with the Allstars negative control siRNA (Figure 7.20B).

After successfully silencing HIF-1α in NT2 cells cultured at 5% oxygen, quantification of OCT4, SOX2 and NANOG expression revealed a significant reduction in the expression of all three core pluripotency markers in cells transfected with HIF-1α siRNA (Figure 7.20C). OCT4 expression was reduced by approximately 32% ($p=0.029$), SOX2 expression decreased by approximately 58% ($p=0.0218$) and NANOG expression reduced by 42% ($p=0.0306$).

Furthermore, quantification of CtBP protein expression revealed a significant and approximate 67% and 50% decrease in the expression of both CtBP1 ($p=0.0441$) and CtBP2 ($p=0.029$) isoforms respectively in cells transfected with HIF-1α siRNA compared to those transfected with Allstars negative control siRNA (Figure 7.20D).

To determine whether HIF-2α was still functional in NT2 cells maintained under hypoxia, NT2 cells were transfected with HIF-2α siRNA.

Phase contrast images demonstrate that there are no obvious morphological changes or effects on growth rate in NT2 cells transfected with either Allstars negative control siRNA or HIF-2α siRNA at 5% oxygen (Figure 7.21).

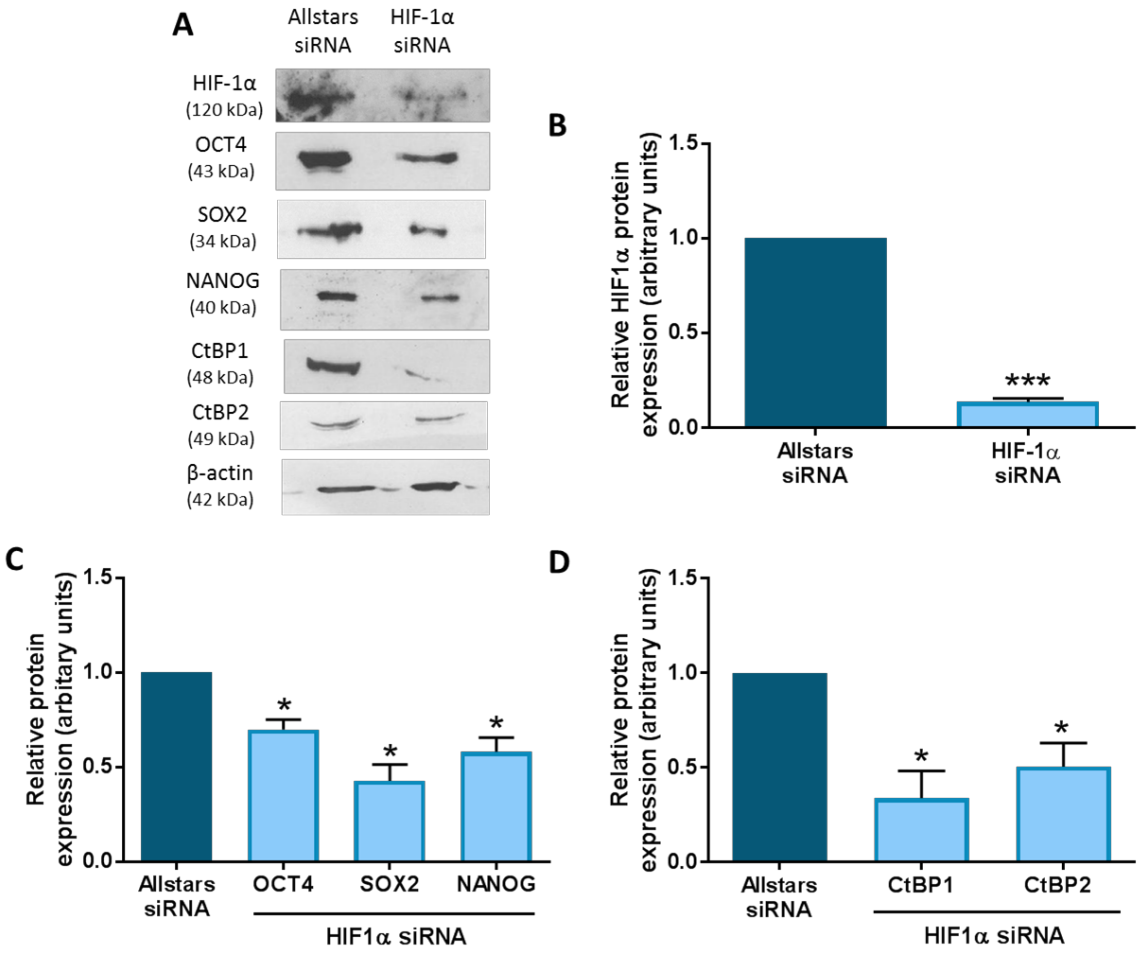

Figure 7.20. HIF-1α regulates pluripotency marker and CtBP expression in NT2 hECCs under 5% oxygen.

(A) Representative Western blots of HIF-1α, OCT4, SOX2, NANOG, CtBP1 and CtBP2 protein expression in NT2 hECCs maintained at 5% oxygen and transfected with either Allstars negative control siRNA or HIF-1α siRNA. (B) Quantification of HIF-1α Western blots revealed the successful silencing of HIF-1α protein expression after transfection with HIF-1α siRNA. (C) Quantification of OCT4, SOX2 and expression in NT2 hECCs maintained at 5% oxygen and transfected with HIF-1α siRNA. (D) Quantification of CtBP1 and CtBP2 expression in NT2 hECCs maintained at 5% oxygen and transfected with HIF-1α siRNA. Data were normalised to β-actin, and then to 1 for Allstars control. Bars represent mean ± SEM. (n=3-4)

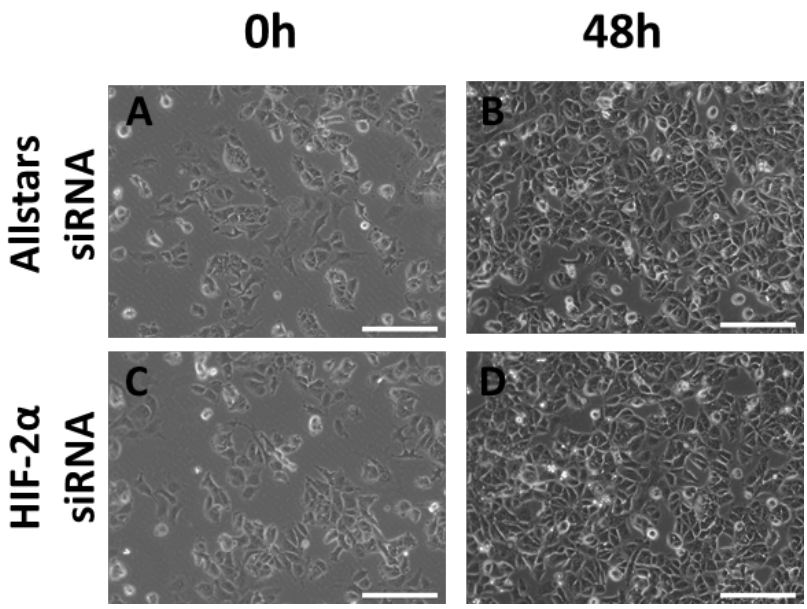

Figure 7.21. Phase contrast images demonstrating colony morphology of NT2 hECCs cultured at 5% oxygen transfected with HIF-2α siRNA.
Representative phase contrast images of NT2 hECCs cultured at 5% oxygen transfected with either Allstars negative control siRNA (A-B) or HIF-2α siRNA (C-D) after 0 (A, C) and 48 hours (B, D). Scale bar indicates 200μm.

HIF-2α protein expression was successfully silenced in NT2 hECCs after transfection with HIF-2α siRNA, displaying an approximate 57% decrease in HIF-2α expression ($p=0.0004$) compared to cells transfected with the Allstars negative control siRNA (Figure 7.22).

After successfully silencing HIF-2α in NT2 cells cultured at 5% oxygen, Western blots were performed to evaluate the effect on pluripotency marker and CtBP protein expression. Quantification of OCT4, SOX2 and NANOG expression revealed a significant reduction in the expression of all three core pluripotency markers in cells transfected with HIF-2α siRNA (Figure 7.22C). OCT4 expression was reduced by approximately 30% ($p<0.0001$), SOX2 expression decreased by approximately 50% ($p=0.0281$) and NANOG expression reduced by approximately 40% ($p=0.0168$).

Furthermore, quantification of CtBP protein expression revealed a significant 27% and 33% decrease in the expression of both CtBP1 ($p=0.0105$) and CtBP2 ($p=0.0068$) isoforms respectively in cells transfected with HIF-2α siRNA compared to those transfected with Allstars negative control siRNA (Figure 7.22).

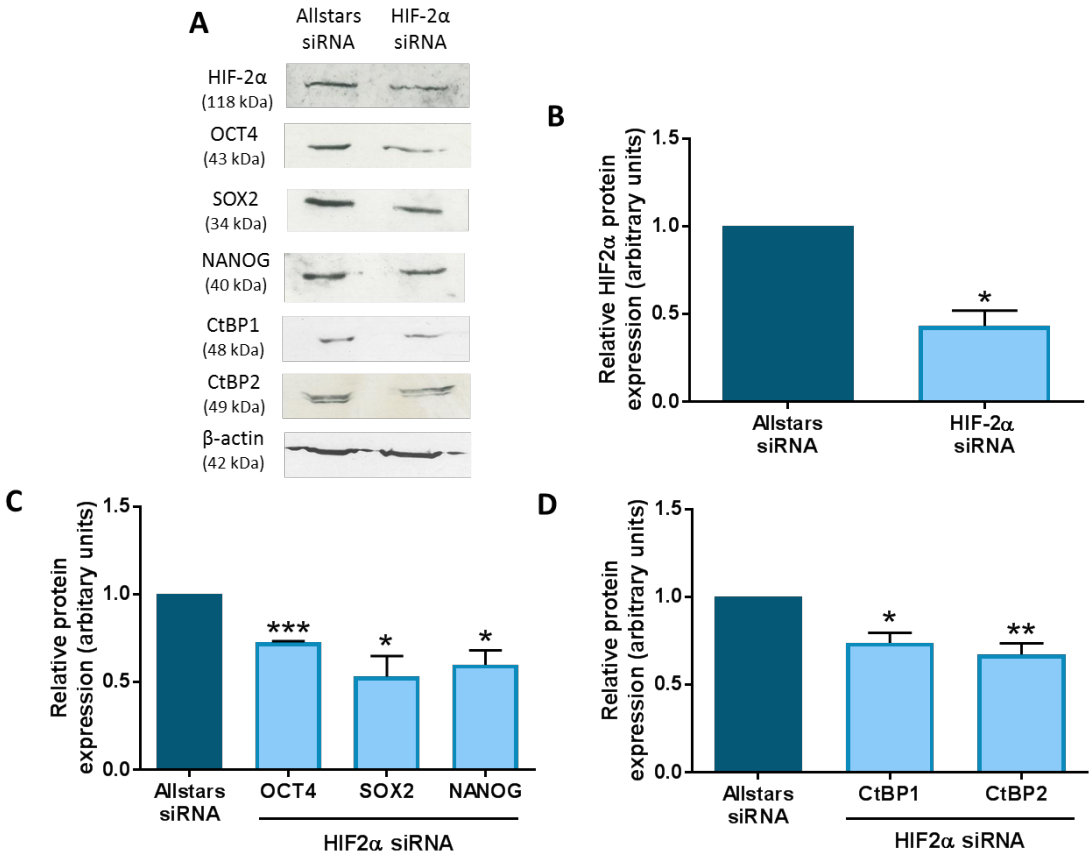

Figure 7.22. HIF-2α regulates pluripotency marker and CtBP expression in NT2 hECCs under 5% oxygen.

(A) Representative Western blots of HIF-2α, OCT4, SOX2, NANOG, CtBP1 and CtBP2 protein expression in NT2 hECCs maintained at 5% oxygen and transfected with either Allstars negative control siRNA or HIF-2α siRNA. (B) Quantification of HIF-2α Western blots revealed successful silencing of HIF-2α protein expression after transfection with HIF-2α siRNA. (C) Quantification of OCT4, SOX2 and NANOG expression in NT2 hECCs maintained at 5% oxygen and transfected with HIF-2α siRNA. (D) Quantification of CtBP1 and CtBP2 Western blots in NT2 hECCs maintained at 5% oxygen and transfected with HIF-2α siRNA. Data were normalised to β-actin, and then to 1 for Allstars control. Bars represent mean ± SEM. (n=4-5)

7.3.3.2. Effect of silencing HIF-1α and HIF-2α in NT2 hECCs maintained under 20% oxygen

To investigate whether HIF-1α and HIF-2α were still functional in NT2 cells cultured at 20% oxygen, cells were transfected with either HIF-1α siRNA or HIF-2α siRNA before analysing the effects of silencing HIF-α subunits on pluripotency marker and CtBP expression.

Phase contrast images demonstrate that there are no obvious morphological changes or effects on growth rate in NT2 cells transfected with either Allstars negative control siRNA or HIF-1α siRNA at 20% oxygen (Figure 7.23).

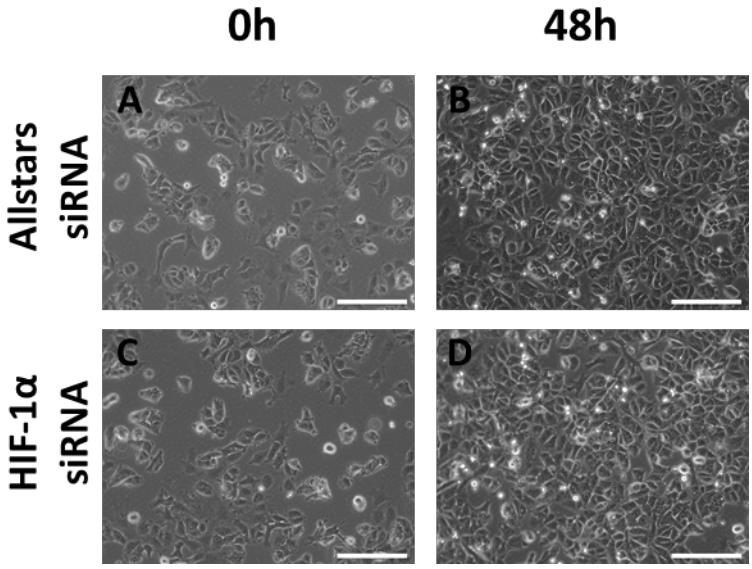

Figure 7.23. Phase contrast images demonstrating colony morphology of NT2 hECCs cultured at 20% oxygen transfected with HIF-1α siRNA.
Representative phase contrast images of NT2 hECCs cultured at 20% oxygen transfected with either Allstars negative control siRNA (A-B) or HIF-1α siRNA (C-D) after 0 (A, C) and 48 hours (B, D). Scale bar indicates 200μm.

HIF-1α protein expression was successfully silenced in NT2 hECCs maintained at 20% oxygen after transfection with HIF-1α siRNA, displaying an approximate 40% decrease in HIF-1α expression (p=0.0201) compared to cells transfected with the Allstars negative control siRNA (Figure 7.24B).

Quantification of OCT4, SOX2 and NANOG expression revealed a significant reduction in the expression of all three core pluripotency markers in cells transfected with HIF-1α siRNA (Figure 7.24C). OCT4 expression was reduced by approximately 30% (p=0.0015), SOX2 expression decreased by approximately 58% (p=0.0375) and NANOG expression reduced by 27% (p=0.0362).

Furthermore, quantification of CtBP protein expression revealed a significant and approximate 54% and 63% decrease in the expression of both CtBP1 (p=0.0368) and CtBP2 (p=0.0322) isoforms respectively in cells transfected with HIF-1α siRNA compared to those transfected with Allstars negative control siRNA (Figure 7.24D).

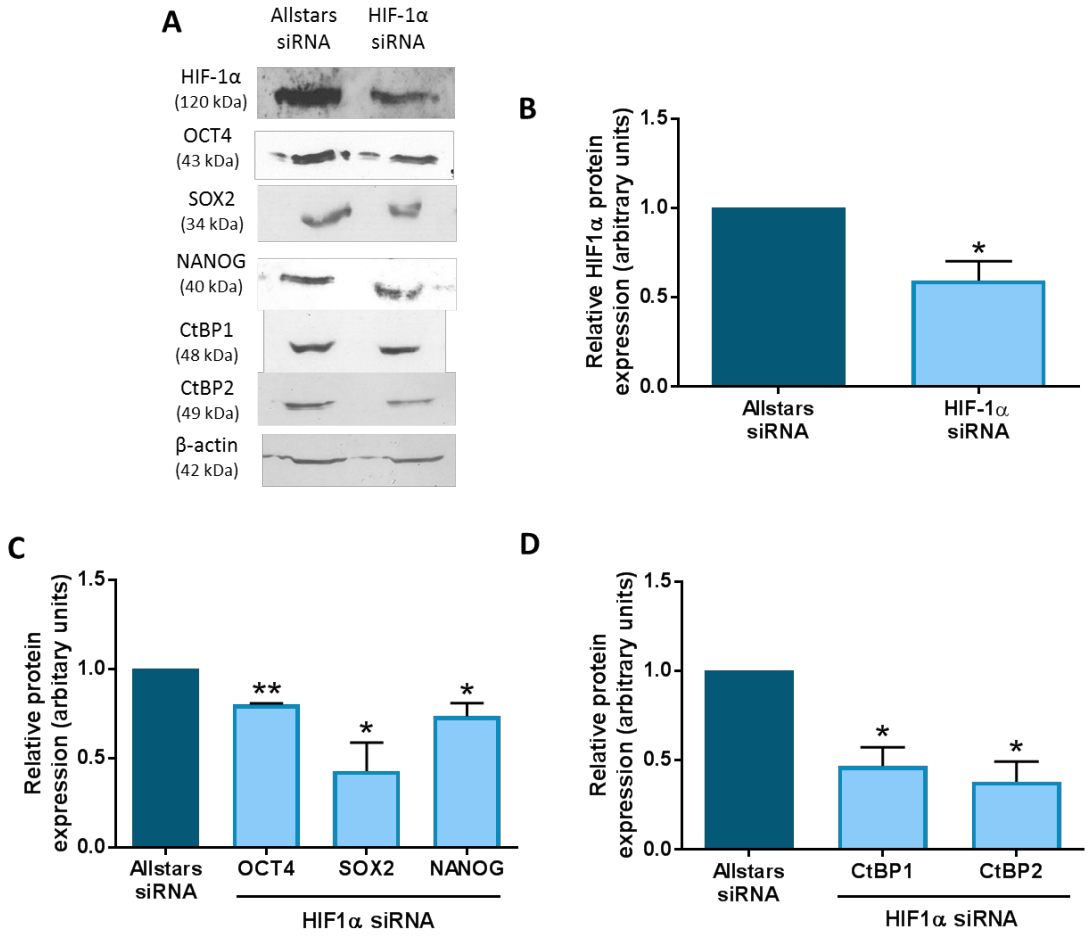

Figure 7.24. HIF-1α regulates pluripotency marker and CtBP expression in NT2 hECCs under 20% oxygen.

(A) Representative Western blots of HIF-1α, OCT4, SOX2, NANOG, CtBP1 and CtBP2 protein expression in NT2 hECCs maintained at 20% oxygen and transfected with either Allstars negative control siRNA or HIF-1α siRNA. (B) Quantification of HIF-1α Western blots revealed the successful silencing of HIF-1α protein expression after transfection with HIF-1α siRNA. (C) Quantification of OCT4, SOX2 and NANOG in NT2 hECCs maintained at 20% oxygen and transfected with HIF-1α siRNA. (D) Quantification of CtBP1 and CtBP2 expression in NT2 hECCs maintained at 20% oxygen and transfected with HIF-1α siRNA. Data were normalised to β-actin, and then to 1 for Allstars control. Bars represent mean ± SEM. (n=4-5)

To determine whether HIF-2α was still functional in NT2 cells maintained at 20% oxygen, NT2 cells were transfected with HIF-2α siRNA.

Phase contrast images demonstrate that there are no obvious morphological changes or effects on growth rate in NT2 cells transfected with either Allstars negative control siRNA or HIF-2α siRNA at 2% oxygen (Figure 7.25).

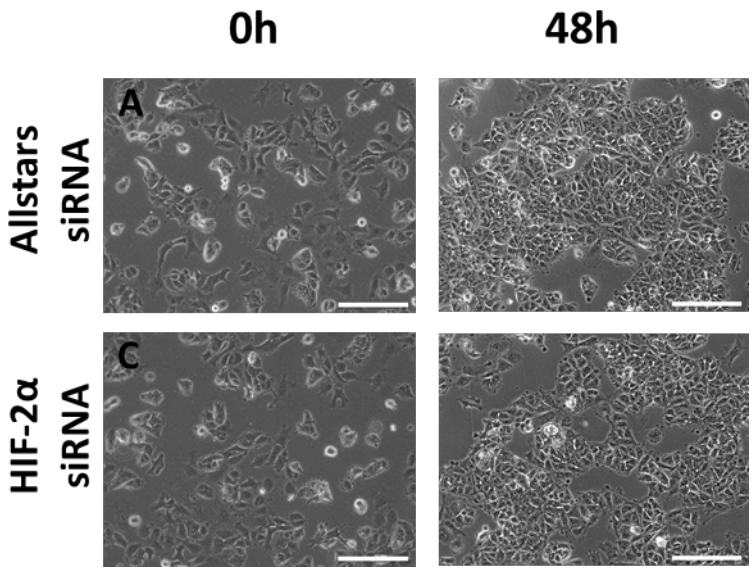

Figure 7.25. Phase contrast images demonstrating colony morphology of NT2 hECCs cultured at 20% oxygen transfected with HIF-2α siRNA.
Representative phase contrast images of NT2 hECCs cultured at 20% oxygen transfected with either Allstars negative control siRNA (A-B) or HIF-2α siRNA (C-D) after 0 (A, C) and 48 hours (B, D). Scale bar indicates 200μm.

Quantification of protein bands revealed that HIF-2α protein expression was successfully silenced in NT2 hECCs at 20% oxygen after transfection with HIF-2α siRNA, displaying an approximate 35% decrease in HIF-2α expression ($p=0.015$) compared to cells transfected with the Allstars negative control siRNA (Figure 7.26B).

Quantification of OCT4, SOX2 and NANOG expression revealed a significant reduction in the expression of all three core pluripotency markers in cells transfected with HIF-2α siRNA (Figure 7.26C). OCT4 expression was reduced by 26% ($p=0.0295$), SOX2 expression decreased by approximately 43% ($p=0.0201$) and NANOG expression reduced by approximately 52% ($p=0.0273$).

Furthermore, quantification of CtBP protein expression revealed a significant and approximate 40% decrease in the expression of both CtBP1 (p=0.0453) and CtBP2 (p=0.0472) isoforms in cells transfected with HIF-2α siRNA compared to those transfected with Allstars negative control siRNA (Figure 7.26D).

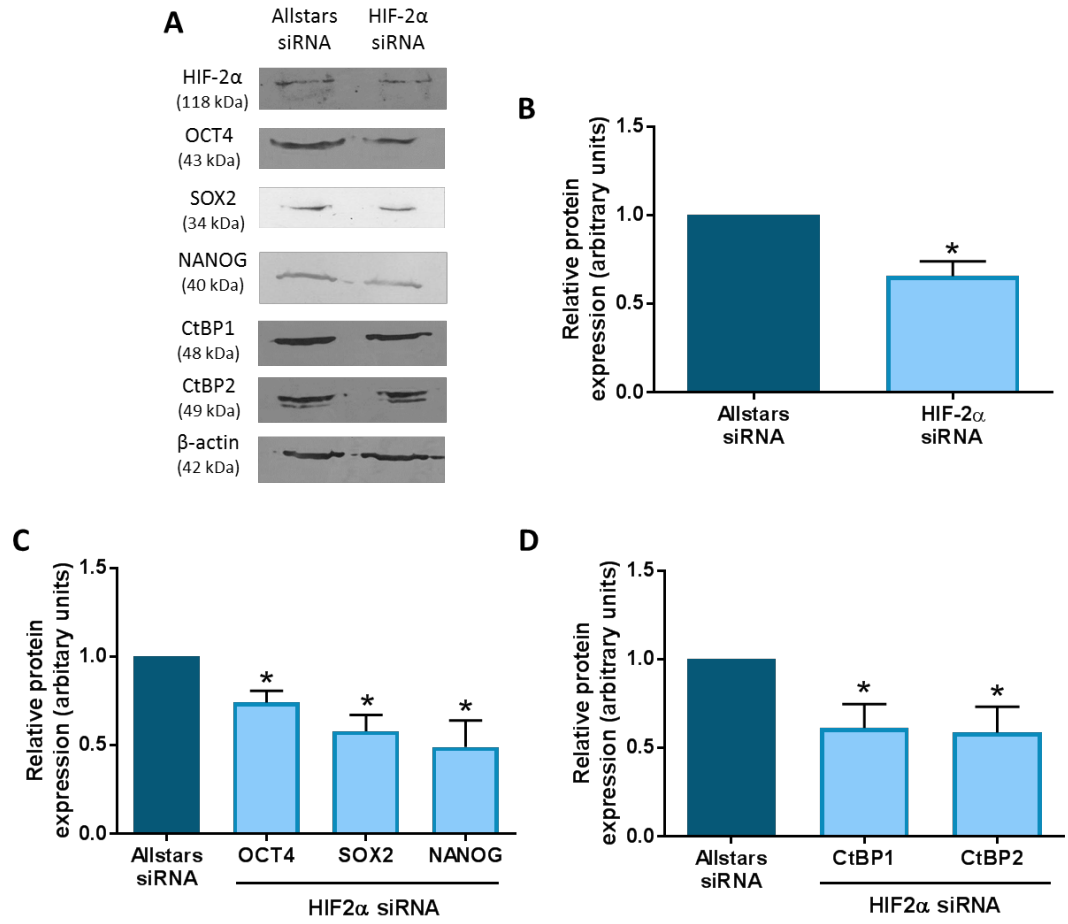

Figure 7.26. HIF-2α regulates pluripotency marker and CtBP expression in NT2 hECCs under 20% oxygen.

(A) Representative Western blots of HIF-2α, OCT4, SOX2, NANOG, CtBP1 and CtBP2 protein expression in NT2 hECCs maintained at 20% oxygen and transfected with either Allstars negative control siRNA or HIF-2α siRNA. (B) Quantification of HIF-2α Western blots revealed successful silencing of HIF-2α protein expression after transfection with HIF-2α siRNA. (C) Quantification of OCT4, SOX2 and NANOG blots in NT2 hECCs maintained at 20% oxygen and transfected with HIF-2α siRNA. (D) Quantification of CtBP1 and CtBP2 blots in NT2 hECCs maintained at 20% oxygen and transfected with HIF-2α siRNA. Data were normalised to β-actin, and then to 1 for Allstars control. Bars represent mean ± SEM. (n=4-5)

7.3.3.3. Characterisation of PHD expression in NT2s in response to environmental oxygen tension

As both HIF-1α and HIF-2α are expressed in NT2 cells maintained at either 5% or 20% oxygen and that both HIF-α subunits are functional independent of oxygen tension, the next aim was to investigate why the HIF-α subunits were still expressed in NT2 cells cultured at 20% oxygen. HIF-α expression is usually regulated under normoxic conditions via PHDs and VHL, therefore PHD expression in NT2 hECCs maintained at either 5% or 20% oxygen was characterised by Western blotting.

Quantification of Western blots revealed no significant difference in the expression of PHD1 (p=0.4582), PHD2 (p=0.9772) and PHD3 (p=0.2892) in NT2 hECCs cultured at either 5% or 20% oxygen (Figure 7.27).

This data suggests that PHD expression plays no role in the observed HIF expression in NT2 cells at 20% oxygen.

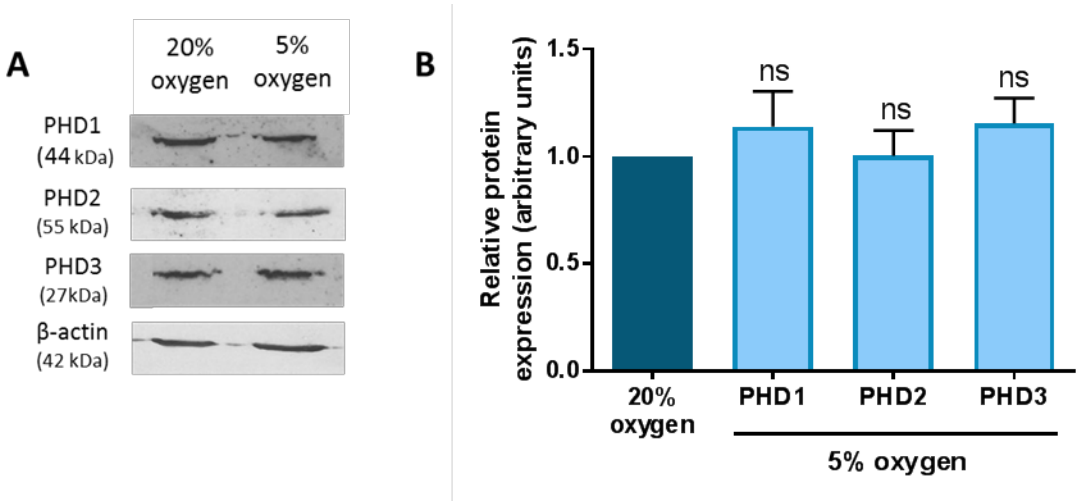

Figure 7.27. PHD expression is not regulated by oxygen tension in NT2 hECCs.
(A) Representative Western blots of PHD1, PHD2 and PHD3 expression in NT2 hECCs cultured at either 5% or 20% oxygen. (B) Quantification of PHD1, PHD2 and PHD3 Western blots in NT2 hECCs cultured at 5% oxygen compared to 20% oxygen tension. Data were normalised to β-actin, and then to 1 for 20% oxygen tension. Bars represent mean ± SEM (n=4); ns; not significant.

7.3.3.4. Characterisation of NO levels in NT2s in response to environmental oxygen tension

Previously in the literature, studies have demonstrated that nitric oxide (NO) can regulate PHD expression, despite that effect not being observed in this study. Therefore, to further investigate the potential mechanism behind the observed expression of functional HIF-α in NT2 cells maintained at 20% oxygen, NO levels were investigated in hECCs maintained at either 5% or 20% oxygen using DAF-FM DA labelling.

NT2 hECCs were incubated with either 0μM, 5μM or 10μM DAF-FM DA for 1 hour before imaging. Images revealed that NO is expressed in hECCs at both 5% and 20% oxygen (Figure 7.28). NO expression appears to be located throughout the entire cell and also NO levels appear to be higher in NT2 cells maintained at 5% oxygen compared to those maintained at 20% oxygen (Figure 7.29).

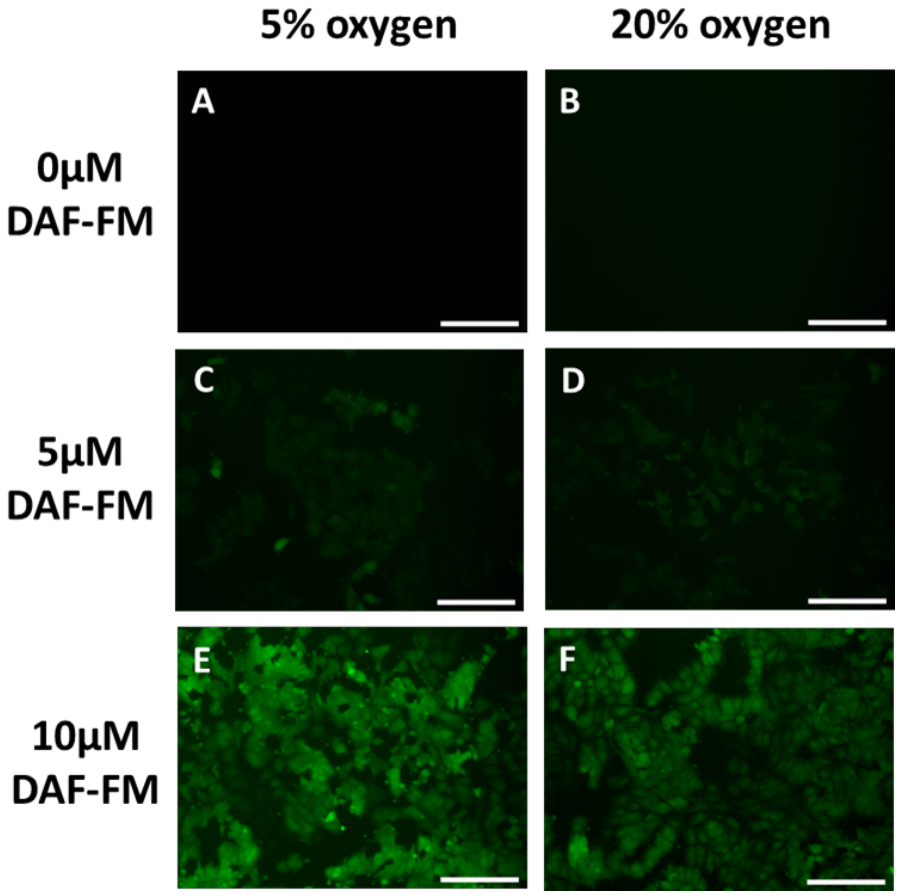

Figure 7.28. NO levels in NT2 hECCs cultured at either 5% or 20% oxygen.
Representative images of DAF-FM DA labelling of NO expression in NT2 cells maintained at either 5% or 20% oxygen and incubated with either 0μM (A-B), 5μM (C-D) and 10μM DAF-FM DA (E-F). Scale bar indicates 200μm.

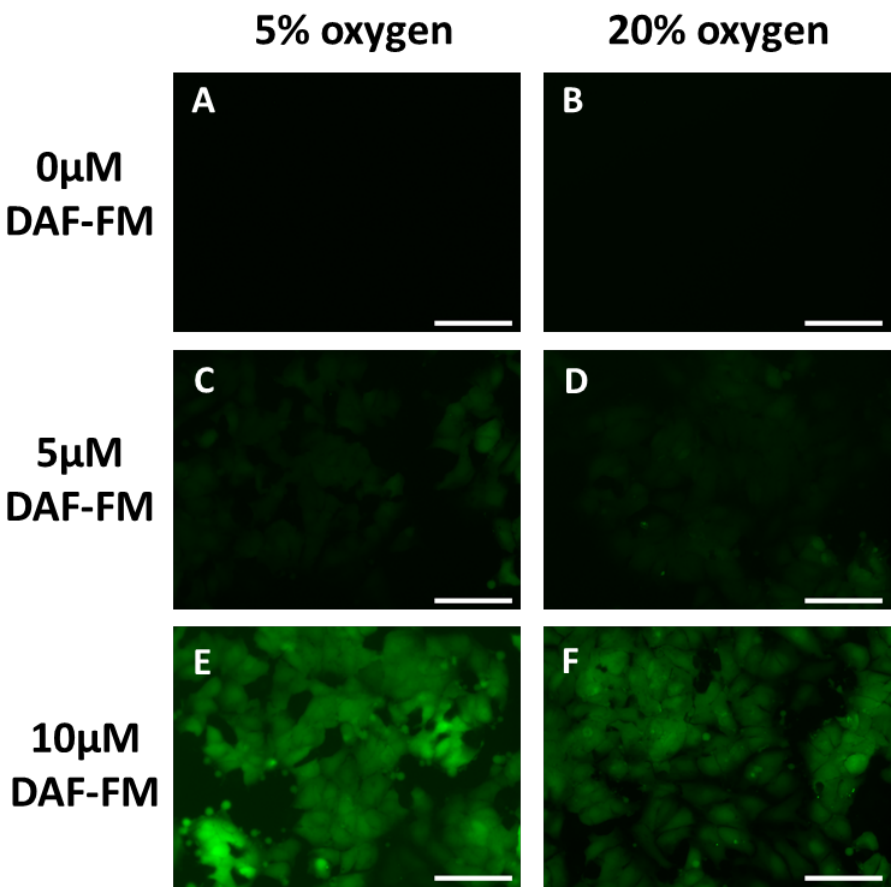

Figure 7.29. Subcellular localisation of NO expression in NT2 hECCs cultured at either 5% or 20% oxygen.
Representative images of DAF-FM DA labelling of NO expression in NT2 cells maintained at either 5% or 20% oxygen and incubated with either 0µM (A-B), 5µM (C-D) and 10µM DAF-FM DA (E-F). Scale bar indicates 50µm.

The expression levels of nitric oxide synthases (NOS) *nNOS, iNOS* and *eNOS* in NT2 hECCs cultured at either 5% or 20% oxygen were also investigated by RT-qPCR.

Quantification of NOS mRNA expression revealed a significant decrease in *nNOS, iNOS* and *eNOS* expression in NT2 cells maintained at 20% oxygen compared to those maintained at 5% oxygen tension (Figure 7.30). *nNOS* expression decreased by 56% ($p=0.0324$), whereas *iNOS* ($p=0.0216$) and *eNOS* ($p=0.0108$) expression reduced by approximately 42% in NT2 cells maintained at 20% oxygen compared to those cultured under hypoxia.

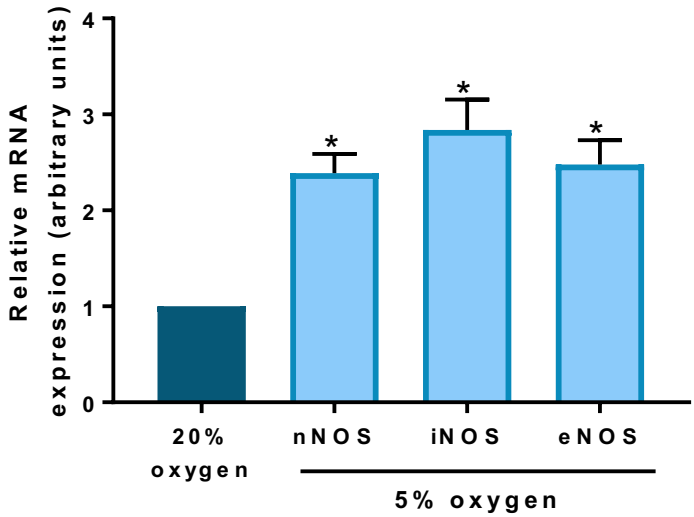

Figure 7.30. NOS expression is increased under hypoxia in NT2 hECCs.
Quantification of *nNOS, iNOS* and *eNOS* mRNA expression levels in NT2 hECCs maintained at either 5% or 20% oxygen. Data were normalised to *UBC*, and then to 1 for 20% oxygen. Bars represent mean ± SEM. (n=3)

7.3.3.5. Characterisation of HIF expression in NT2s in response to decreasing NO levels

To investigate whether decreasing the NO levels in NT2s resulted in any changes to HIF-2α expression, NT2 cells maintained at either 5% or 20% oxygen were incubated with either 0mM, 1mM, 10mM or 30mM L-NAME; an inhibitor of nitric oxide synthesis, for 48 hours before collecting cells for protein isolation.

Phase contrast images reveal that NT2 cells incubated with either 1mM or 10mM L-NAME display no clear morphological differences compared to cells incubated in the absence of the inhibitor independent of oxygen tension. However, incubating NT2 cells with 30mM L-NAME was toxic to cells cultured at both oxygen tensions as cell numbers were noticeably lower compared to cells treated with either 0mM, 1mM or 10mM L-NAME after 48 hours (Figure 7.31). Therefore, further experiments were performed using the 1mM and 10mM L-NAME.

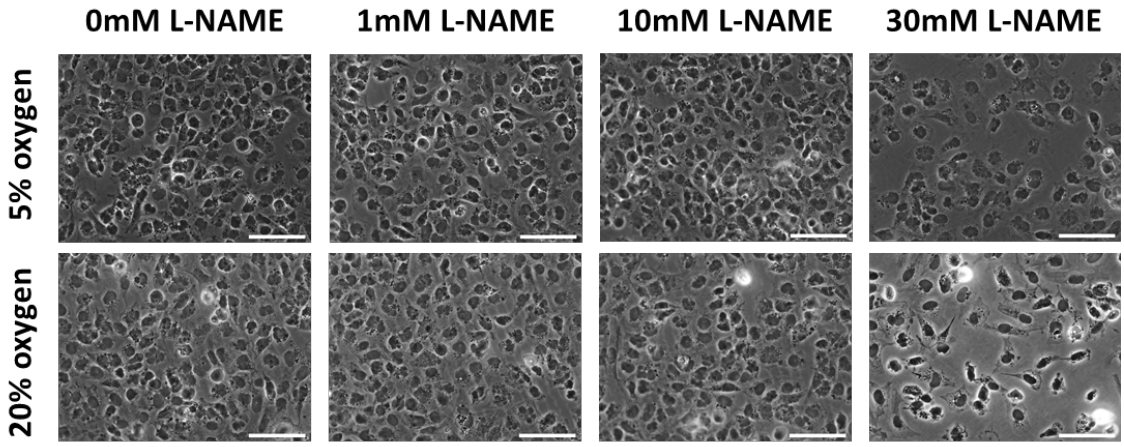

Figure 7.31. Phase contrast images demonstrating cellular morphology of NT2 hECCs cultured in L-NAME supplemented media.
Representative phase contrast images of NT2 hECCs cultured at either 5% or 20% oxygen and incubated with medium supplemented with either 0mM (A-B), 1mM (C-D), 10mM (E-F) or 30mM L-NAME after 48 hours. Scale bar indicates 100μm.

To investigate whether reducing NO levels affected HIF-2α expression in NT2 hECCs at both 5% and 20% oxygen, cells were incubated with L-NAME for 48 hours before performing immunocytochemistry.

NT2 hECCs expressed HIF-2α expression under hypoxic (Figure 7.32) and normoxic oxygen tensions (Figure 7.33). There was no obvious difference in HIF-2α expression between NT2 cells treated with 0mM and 1mM L-NAME at both 5% (Figure 7.32) and 20% oxygen (Figure 7.33). However, HIF-2α expression appeared reduced in NT2 cells incubated with 10mM L-NAME compared to the control cells incubated in the absence of the inhibitor at 5% oxygen. This reduction in HIF-2α was even greater in NT2 cells maintained at 20% oxygen (Figure 7.33).

As there was no overt difference in HIF-2α expression between NT2 cells incubated with either 0mM or 1mM L-NAME, all subsequent experiments were performed with 10mM L-NAME.

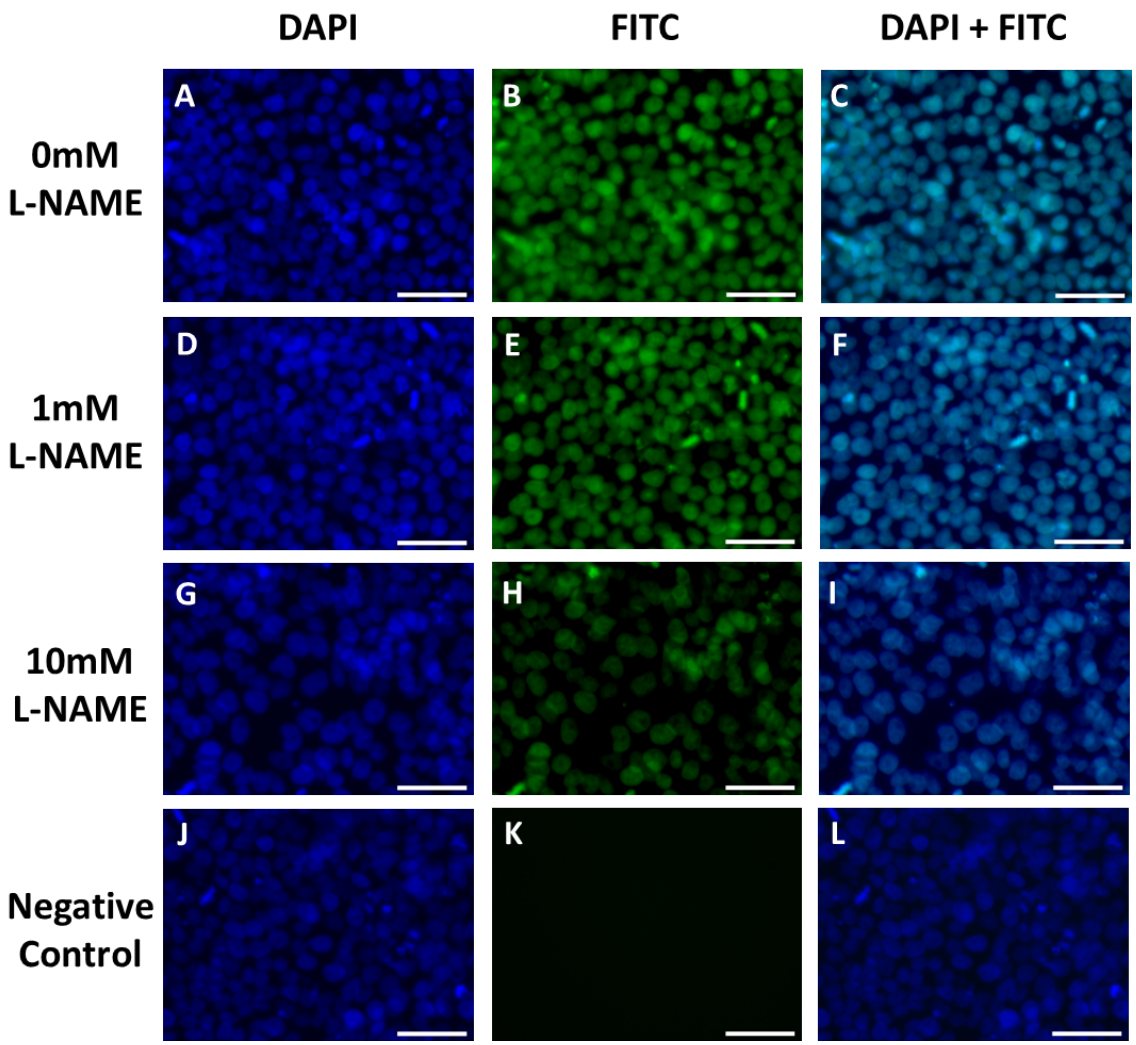

Figure 7.32. HIF-2α expression in NT2 hECCs cultured in L-NAME supplemented medium at 5% oxygen.

Representative images of HIF-2α protein expression in NT2 hECCs cultured at 5% oxygen and treated with either 0mM (A-C), 1mM (D-F) or 10mM L-NAME (G-I). An anti-rabbit-IgG FITC-conjugated secondary antibody was used to detect HIF-2α expression and the negative control (J-L). DAPI staining was performed to label the nuclei. DAPI (blue; A, D, G, J) and FITC (green; B, E, H, K) images were taken. Scale bar indicates 100μm.

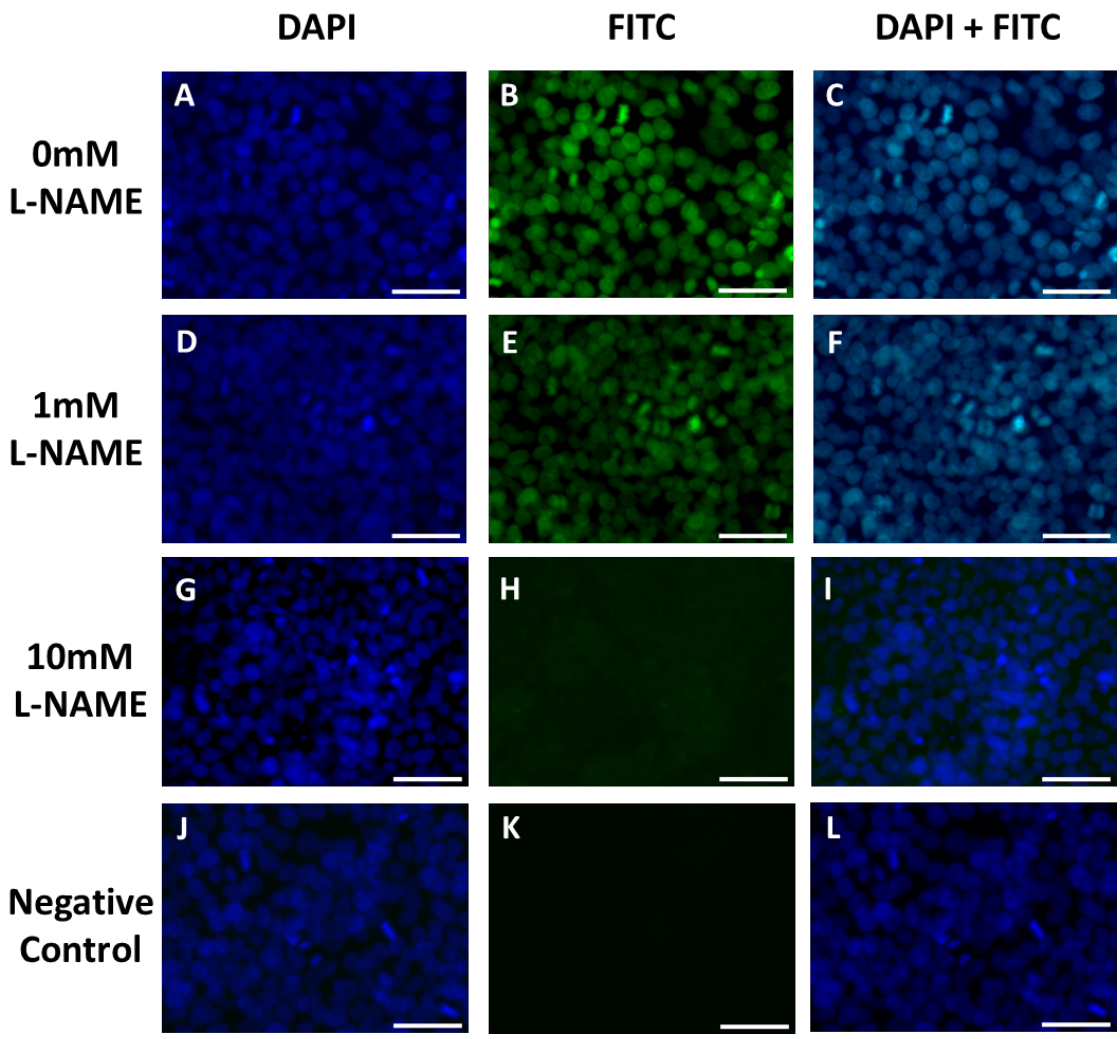

Figure 7.33. HIF-2α expression in NT2 hECCs cultured in L-NAME supplemented medium at 20% oxygen.

Representative images of HIF-2α protein expression in NT2 hECCs cultured at 20% oxygen and treated with either 0mM (A-C), 1mM (D-F) or 10mM L-NAME (G-I). An anti-rabbit-IgG FITC-conjugated secondary antibody was used to detect HIF-2α expression and the negative control (J-L). DAPI staining was performed to label the nuclei. DAPI (blue; A, D, G, J) and FITC (green; B, E, H, K) images were taken. Scale bar indicates 100μm.

To confirm whether decreasing NO levels using the inhibitor L-NAME in NT2 cells maintained under 5% oxygen affected HIF-2α expression, Western blotting was performed.

Quantification revealed a non-significant trend towards reduced HIF-2α expression in cells treated with 10mM L-NAME compared to cells maintained in the absence of L-NAME (p=0.1576; Figure 7.34).

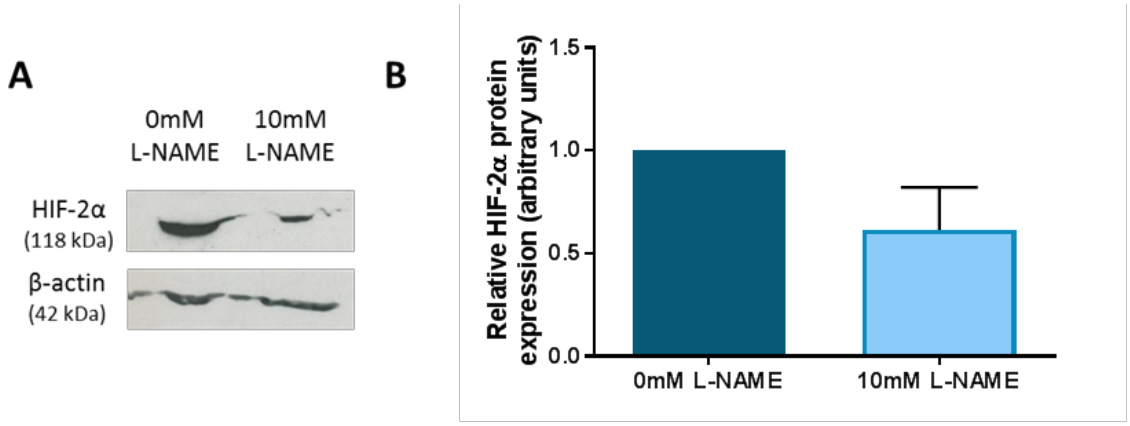

Figure 7.34. HIF-2α protein expression in NT2 hECCs maintained at 5% oxygen after treatment with L-NAME.
(A) Representative Western blots of HIF-2α protein expression in NT2 hECCs maintained at 5% oxygen and treated with either 0mM or 10mM L-NAME for 48 hours. (B) Quantification of HIF-2α protein expression in NT2 hECCs cultured under hypoxic conditions and treated with either 0mM or 10mM L-NAME. Data were normalised to β-actin, and then to 1 for 0mM L-NAME. Bars represent mean ± SEM (n=4)

To investigate a potential mechanistic reason and consequence to support the observed non-significant effect on HIF-2α expression, the effects of incubating NT2 hECCs maintained under 5% oxygen with 10mM L-NAME and decreasing NO levels on PHD and pluripotency marker expression were also analysed.

Quantification of Western blots revealed no significant difference in the protein expression of PHD1 (p=0.1162), PHD2 (p=0.9433) or PHD3 (p=0.9238) in NT2 hECCs incubated with either 0mM or 10mM L-NAME (Figure 7.35).

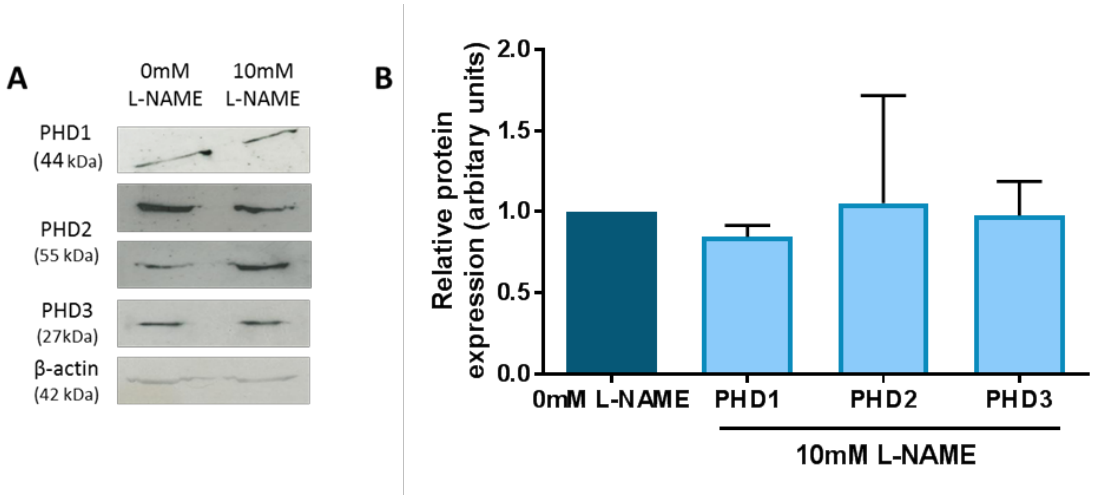

Figure 7.35. PHD protein expression in NT2 hECCs maintained at 5% oxygen after treatment with L-NAME.
(A) Representative Western blots of PHD1, PHD2 and PHD3 protein expression in NT2 hECCs maintained at 5% oxygen and treated with either 0mM or 10mM L-NAME for 48 hours. (B) Quantification of PHD protein expression in NT2 hECCs cultured under hypoxic conditions and treated with either 0mM or 10mM L-NAME. Data were normalised to β-actin, and then to 1 for 0mM L-NAME. Bars represent mean ± SEM (n=3-4)

Furthermore, quantification of pluripotency marker expression revealed that the protein expression of either OCT4 (p=0.7983), SOX2 (p=0.1915) and NANOG (p=0.1137) was not significantly different between hECCs incubated with either 0mM or 10mM L-NAME (Figure 7.36).

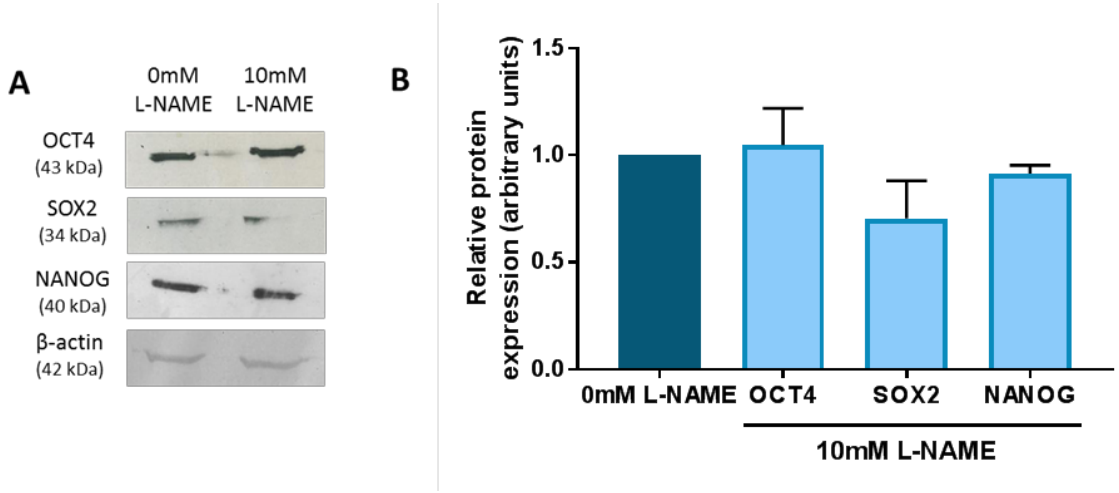

Figure 7.36. Pluripotency protein expression in NT2 hECCs maintained at 5% oxygen after treatment with L-NAME.
(A) Representative Western blots of OCT4, SOX2 and NANOG protein expression in NT2 hECCs maintained at 5% oxygen and treated with either 0mM or 10mM L-NAME. (B) Quantification of pluripotency marker expression in NT2 hECCs cultured under hypoxic conditions and treated with either 0mM or 10mM L-NAME for 48 hours. Data were normalised to β-actin, and then to 1 for 0mM L-NAME. Bars represent mean ± SEM (n=4)

As no significant effect was observed in cells treated with L-NAME, the next aim was to confirm that adding L-NAME to hECCs maintained at 5% oxygen decreased NO levels. Therefore, NT2 cells were incubated with either 0mM or 10mM L-NAME for 48 hours before labelling with DAF-FM DA.

Representative images of NT2 hECCs revealed that NO was expressed in cells incubated with both 0mM and 10mM L-NAME, however NO levels in NT2 hECCs treated with 10mM L-NAME appeared lower than cells incubated in the absence of the inhibitor suggesting that NO levels were reduced (Figure 7.37).

Together, this data suggests that reducing NO levels in NT2 cells maintained at 5% oxygen has no effect on HIF-2α expression and also pluripotency marker expression.

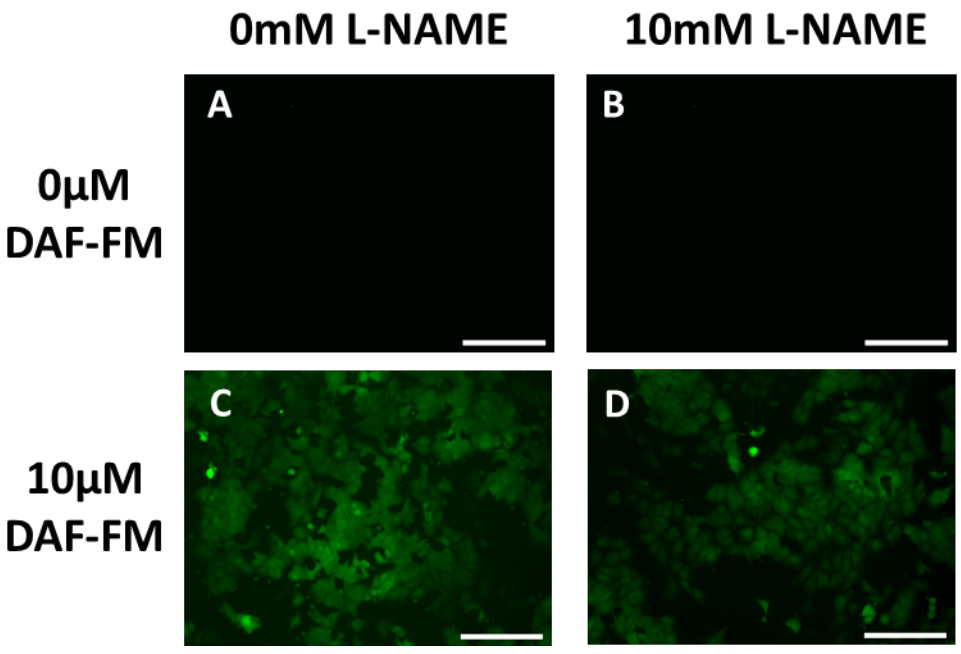

Figure 7.37. NO levels in NT2 hECCs maintained at 5% oxygen and incubated with L-NAME.
Representative images of DAF-FM DA labelling of NO expression in NT2 cells maintained at 5% oxygen and incubated with either 0μM (A-B) or 10μM DAF-FM DA (C-D) after treatment with either 0mM (A, C) or 10mM L-NAME (B, D) for 48 hours. Scale bar indicates 100μM.

As NO levels appeared lower in NT2 cells maintained at 20% oxygen and was inhibited by 10mM L-NAME, the effect on HIF-2α expression was investigated.

HIF-2α expression decreased by approximately 60% (p=0.474) in NT2 cells treated with 10mM L-NAME compared to cells cultured in the absence of L-NAME (Figure 7.38).

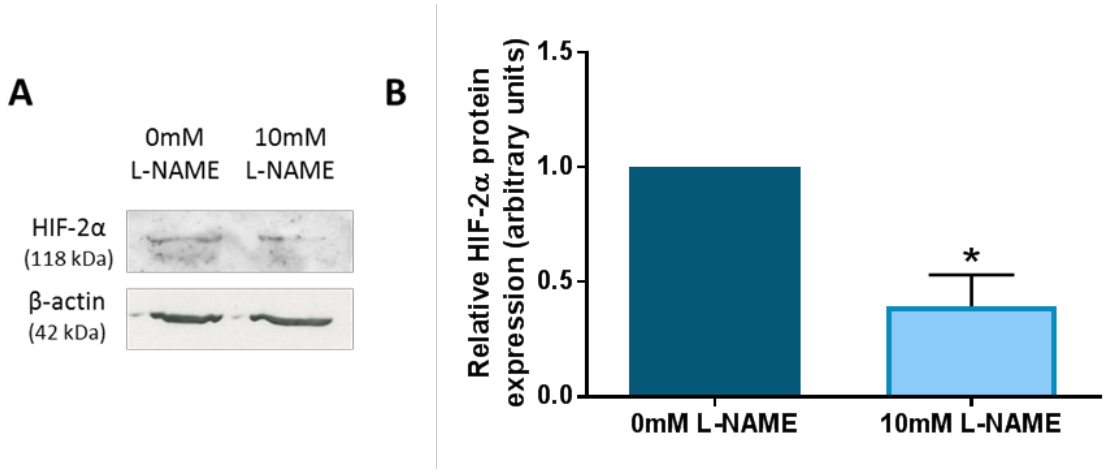

Figure 7.38. HIF-2α protein expression is regulated by NO in NT2 hECCs maintained at 20% oxygen.
(A) Representative Western blots of HIF-2α protein expression in NT2 hECCs maintained at 20% oxygen and treated with either 0mM or 10mM L-NAME. (B) Quantification of HIF-2α protein expression in NT2 hECCs cultured under normoxic conditions and treated with either 0mM or 10mM L-NAME for 48 hours. Data were normalised to β-actin, and then to 1 for 0mM L-NAME. Bars represent mean ± SEM (n=3)

To investigate whether inhibiting NO production in NT2 cells maintained at 20% oxygen altered PHD expression or pluripotency marker expression, Western blotting was performed.

PHD1 expression decreased by approximately 40% (p=0.0068), PHD2 expression significantly reduced by 55% (p=0.0399) and PHD3 expression reduced by approximately 60% (p=0.0247) in hECCs treated with 10mM L-NAME compared to cells incubated in the absence of the inhibitor (Figure 7.39).

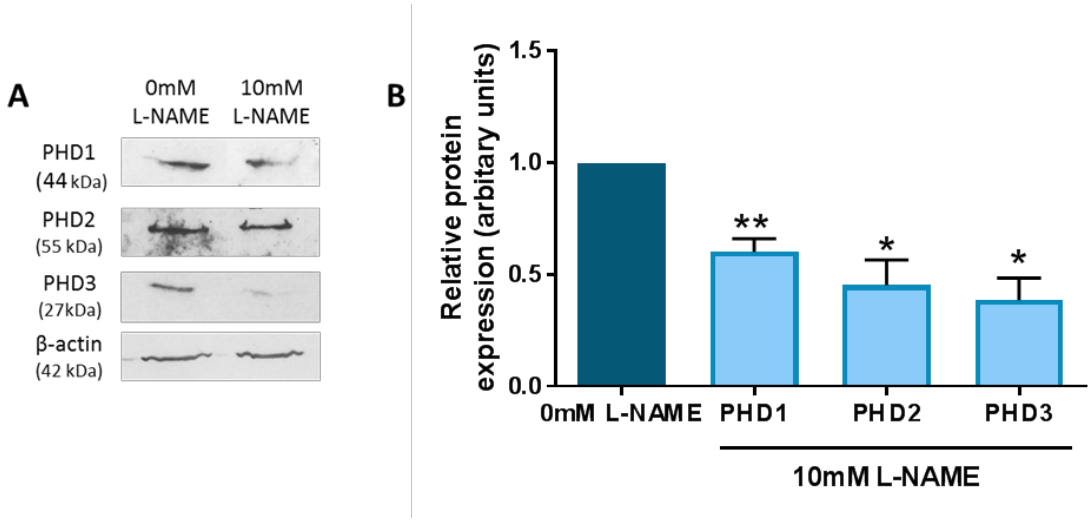

Figure 7.39. PHD protein expression in NT2 hECCs maintained at 20% oxygen after treatment with L-NAME.
(A) Representative Western blots of PHD1, PHD2 and PHD3 protein expression in NT2 hECCs maintained at 20% oxygen and treated with either 0mM or 10mM L-NAME for 48 hours. (B) Quantification of PHD protein expression in NT2 hECCs cultured under normoxic conditions and treated with either 0mM or 10mM L-NAME. Data were normalised to β-actin, and then to 1 for 0mM L-NAME. Bars represent mean ± SEM (n=3-4)

Furthermore, OCT4, SOX2 and NANOG protein expression was significantly decreased by approximately 45% (p=0.0155), 95% (p=0.0016) and 69% (p=0.0326) respectively in NT2 hECCs incubated in the presence of 10mM L-NAME compared to cells incubated in the absence of the inhibitor (Figure 7.40).

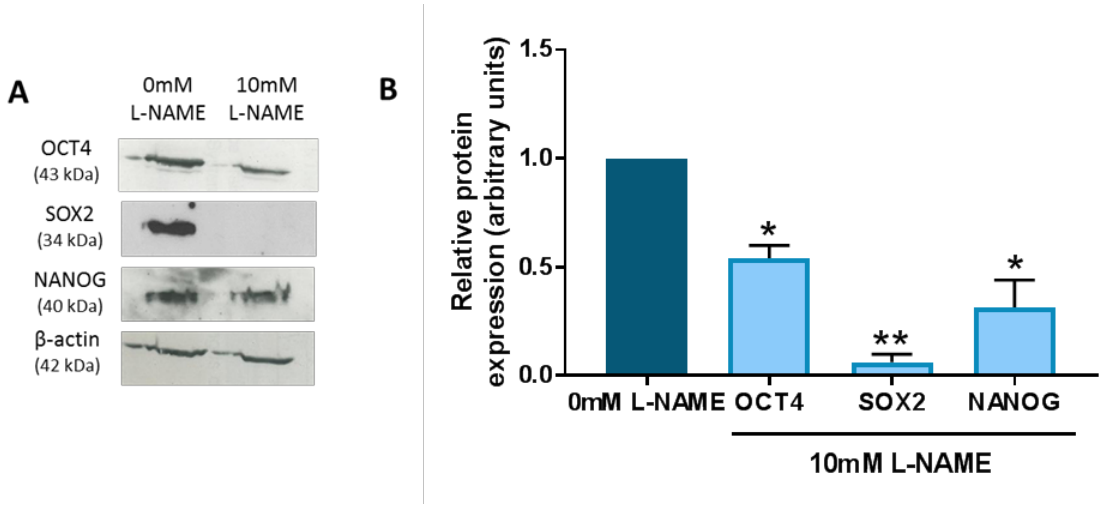

Figure 7.40. Pluripotency protein expression in NT2 hECCs maintained at 20% oxygen after treatment with L-NAME.
(A) Representative Western blots of OCT4, SOX2 and NANOG protein expression in NT2 hECCs maintained at 5% oxygen and treated with either 0mM or 10mM L-NAME for 48 hours. (B) Quantification of pluripotency marker expression in NT2 hECCs cultured under normoxic conditions and treated with either 0mM or 10mM L-NAME. Data were normalised to β-actin, and then to 1 for 0mM L-NAME. Bars represent mean ± SEM (n=3)

To confirm that NO levels were decreased in NT2 cells maintained at 20% oxygen, cells were treated with 10mM L-NAME for 48 hours before labelling with DAF-FM DA.

Representative images reveal that after 48 hours of L-NAME treatment, NO levels were substantially reduced in NT2 cells treated with 10mM L-NAME compared to those incubated with 0mM L-NAME (Figure 7.41).

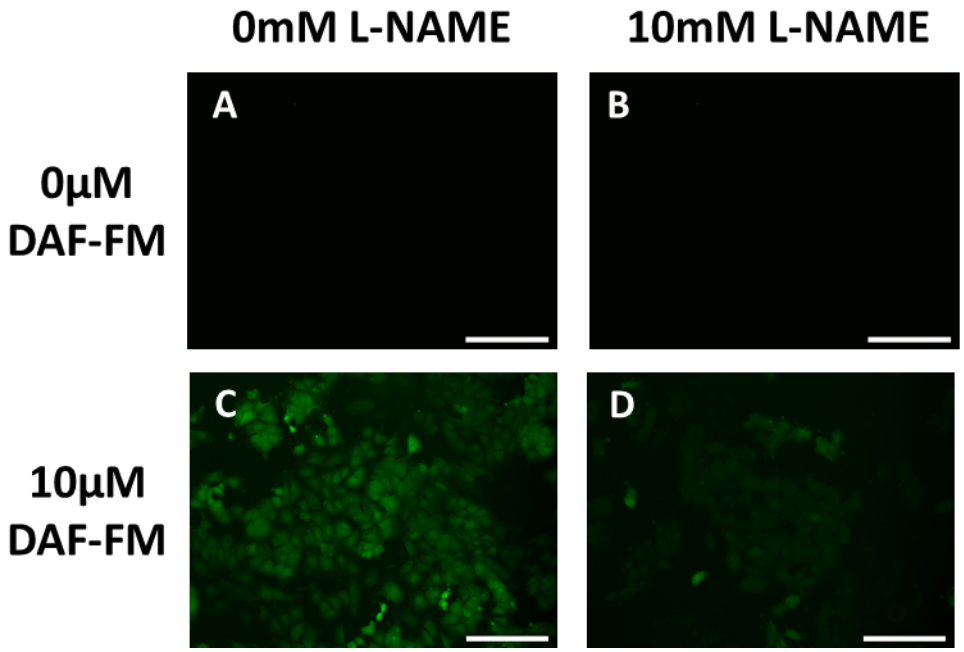

Figure 7.41. NO levels in NT2 hECCs maintained at 20% oxygen and incubated with L-NAME.
Representative images of DAF-FM DA labelling of NO expression in NT2 cells maintained at 20% oxygen and incubated with either 0µM (A-B) or 10µM DAF-FM DA (C-D) after treatment with either 0mM (A, C) or 10mM L-NAME (B, D) for 48 hours. Scale bar indicates 100µM.

7.4 Discussion

Culture under hypoxia is known to be beneficial for a highly proliferative population of hESCs (Ezashi et al., 2005; Forristal et al., 2010; Varum et al., 2011; Forristal et al., 2013; Petruzzelli et al., 2014; Christensen et al., 2015). It is well documented that hECCs express pluripotency markers, particularly OCT4, SOX2 and NANOG (Andrews, 2002; Matin et al., 2004; Andrews et al., 2005; Ezeh et al., 2005; Greber et al., 2007b). However, how their expression is regulated in NT2 hECCs is poorly understood, yet appears to be affected by hypoxia in other pluripotent stem cell types.

7.4.1. Characterisation of pluripotency marker expression in NT2 hECCs between oxygen tensions

The expression of the core pluripotency markers is significantly increased in hESCs cultured under hypoxia compared to hESCs maintained at 20% oxygen. But surprisingly, no significant difference was observed in either the mRNA or protein expression of OCT4, SOX2 and NANOG in NT2 hECCs cultured at either 5% or 20% oxygen. This may be explained by a different HIF-α subunit acting as the predominant regulator of the hypoxic response in hECCs. A recent study demonstrated that HIF-2α directly binds to the promoter regions of OCT4, SOX2 and NANOG in hESCs (Petruzzelli et al., 2014) and previous studies have indicated that there is a correlation between elevated HIF-1α expression levels and cancer cells under hypoxia (Birner et al., 2000; Aebersold et al., 2001; Birner et al., 2001a; Birner et al., 2001b; Bos et al., 2001; Schindl et al., 2002; Bertout et al., 2008; Shay et al., 2014). This suggests that HIF-1α may be the predominant regulator of the long term hypoxic response in hECCs, and that HIF-1α cannot bind to a HRE binding site in the proximal promoters of OCT4, SOX2 and NANOG most likely due to chromatin state and the heterochromatic nature of that region of DNA being inaccessible to the transcription factor. However, due to the homology between HIF-1α and HIF-2α, it is highly likely that both HIF-α subunits are capable of binding to the same HRE site. This is supported by data presented in this chapter when silencing either HIF-1α or HIF-2α regardless of oxygen tension resulted in a significant decrease in pluripotency marker expression. Therefore, it is hypothesised that both HIF-α subunits can bind a given HRE to drive the expression of OCT4, SOX2 and NANOG, although further experiments are currently required to determine if HIF-1α directly binds to the HRE in the proximal promoter regions of the core pluripotency factors. It is also evident from the literature that there is a correlation between HIF-2α and aggressive tumours.

Assuming that germ cell tumours, from which hECCs are derived, are regarded as highly aggressive tumours and therefore HIF-2α is still the predominant regulator of the hypoxic response, this data suggests that there may be an uncoupling of the mechanism where hypoxia influences pluripotency marker expression via HIFs in hECCs. Alternatively, there may be an alternative mechanism by which the ability to self-renew is enhanced in hECCs as an increased expression of OCT4, SOX2 and NANOG would allow these malignant cancer stem cells to exploit the pluripotent state to maintain the rapid growth and proliferation rates characteristic of cancer cells in order to enhance invasive potential and tumourigenic capacity (Mathieu et al., 2011).

This data suggests that hECCs possess molecular mechanisms to gain a pluripotent state and the ability to self-renew regardless of the oxygen levels they are exposed to in the tumour microenvironment.

7.4.2. Characterisation of CtBP expression in NT2 hECCs between oxygen tensions

CtBP expression is widely documented throughout different cancer types. However, this study represents the first report of CtBP expression in NT2 cells.

CtBPs were expressed in the nucleus of NT2 hECCs cultured at either 5% or 20% oxygen tensions, where both CtBP mRNA and protein expression was significantly decreased in cells cultured under 20% oxygen compared to 5% oxygen. Although OCT4, SOX2 and NANOG expression was not affected by oxygen tension in hECCs, CtBPs appeared to be regulated by hypoxia in both hESCs and hECCs. CtBP expression was also found to be significantly decreased after silencing either HIF-1α or HIF-2α regardless of oxygen tension. Even though whether HIF-1α directly binds to the same HREs in the CtBP proximal promoters as HIF-2α (Chapter 3) is not fully characterised, this data further supports that both HIF-α subunits can bind to a given HRE. However, it does raise the question as to why CtBP expression is regulated by hypoxia in hECCs and pluripotency marker expression is not given that both HIF-1α and HIF-2α regulate the expression of CtBPs, OCT4, SOX2 and NANOG. It is possible that it might be an epigenetic effect, where the DNA region around the HRE in the CtBP proximal promoters condensed and becomes more heterochromatic under 20% oxygen, whereas that condensation within the proximal promoters of OCT4, SOX and NANOG is absent and maintains access to the HRE for HIF-α subunits to increase the expression of pluripotency markers in hECCs at

20% oxygen. Alternatively, this may be a metabolic phenotype rather than a HIF-dependent mechanism.

This data re-emphasises the hypothesis previously drawn in Chapter 3.3.2 that CtBP expression is regulated by hypoxia and that hypoxic regulation is not unique to hESCs. However, any potential role for CtBPs in the regulation of hECC self-renewal remains to be elucidated.

7.4.3. Regulation of HIF-α expression in NT2 hECCs between oxygen tensions

The expression of HIFs is usually decreased in cells maintained under normoxic conditions due to degradation by PHDs and VHL. However, results in this study indicate that both HIF-1α and HIF-2α are expressed in NT2 cells maintained at either 5% or 20% and both isoforms are functional as silencing HIF expression resulted in the loss of pluripotency marker expression at both oxygen tensions. These results clearly suggested that there is a different mechanism of HIF regulation in hECCs, compared to hESCs, leading to the accumulation of HIFs in NT2 hECCs maintained under normoxic conditions and similar levels of pluripotency marker expression observed in NT2 hECCs maintained at either 5% or 20% oxygen.

It is worth noting that HIF-1α expression was more cytoplasmic in hECCs maintained at either 5% or 20% oxygen and HIF-2α expression was localised to the nucleus in hECCs regardless of oxygen tension. Given that the localisation of either HIF-α isoform was maintained between oxygen concentrations, it would suggest that the regulation of HIF-1α and HIF-2α was maintained between oxygen tensions. Additionally, the fact that HIF-1α was observed to be localised in the cytoplasm of NT2 hECCs suggests that this HIF-α subunit may not be acting as a transcription factor. However, HIF-1α expression was not found exclusively in the cytoplasm of hECCs but was much more dispersed throughout hECCs compared to HIF-2α expression, which was found exclusively in the nucleus as expected.

Previous studies have indicated that HIF-α subunits require a bipartite nuclear localisation signal and the binding of the nuclear transport receptors, importins, in order to regulate the nucleocytoplasmic shuttling and therefore transcriptional activity of HIF-1α, HIF-2α and even HIF-3α (Luo and Shibuya, 2001; Depping et al., 2008; Chachami et al., 2009). Therefore, there could be an issue with the shuttling of HIF-1α into the nucleus either via a mutated nuclear localisation signal, or the absence of a particular importin to leave HIF-

1α expression in the cytoplasm. Alternatively, there may be a role for HIF-3α in the regulation of HIF-1α and HIF-2α localisation in NT2 hECCs as HIF-3α has been previously reported to regulate the expression of both other HIF-α isoforms (Forristal et al., 2010).

To analyse why HIF-1α and HIF-2α were expressed in hECCs maintained at either 5% or 20% oxygen and with no significant difference in HIF-α expression between oxygen tensions, experiments were conducted to investigate whether this was due to impaired HIF regulation via PHDs. PHD expression was observed to be no different between NT2 cells maintained at either 5% or 20% oxygen suggesting that PHD expression had no role in the accumulation of HIF-α subunits in cells cultured under normoxia.

Previous studies have demonstrated that PHD3 mRNA and protein expression increased in a time-dependent manner in human cardiovascular cells when exposed to hypoxia or a hypoxia mimic; cobalt chloride. This increase in PHD expression also correlated with an increase in HIF-1α expression. Furthermore, overexpression of PHD3 in cells maintained in both normoxic and hypoxic conditions influenced HIF-1α stability implicating PHD3 in a potential feedback loop controlling HIF activity (Cioffi et al., 2003). As no increase in PHD3 was observed in this study, it suggests that HIF-1α, and likely HIF-2α, stability is regulated in a PHD-independent manner in hECCs cultured under long-term hypoxia.

However, although differential PHD expression was not the reason for HIF accumulation in hECCs maintained under normoxia, the activity of PHDs was still a possibility. It is well-documented that NO targets PHDs and suggests that attenuation of prolyl hydroxylation is the underlying mechanism of NO-induced HIF-1α accumulation in cells under normoxia (Metzen et al., 2003). Results in this chapter revealed that decreasing NO levels in hECCs maintained at 20% oxygen resulted in a decrease in HIF-2α expression and a subsequent decrease in the expression of the pluripotency markers OCT4, SOX2 and NANOG. This suggests that HIF-2α accumulation in cells maintained under normoxia is NO concentration dependent. This is in agreement with the previously reported mechanism of HIF-1α accumulation under normoxia. However, results in this study also revealed that PHD expression decreased in NT2 cells maintained under 20% oxygen and incubated with the NO inhibitor L-NAME. This would theoretically result in the opposite consequent effect to the observed effect; an increase or accumulation in HIF-

2α in cells with decreased NO levels. However, this may suggest that NO levels regulate HIF accumulation in a PHD-independent manner in NT2 hECCs.

Table 7.3. Summary of hypoxic regulation in hECCs.

	5% oxygen	20% oxygen
Pluripotency marker expression	+	+
CtBP expression	+ +	+
HIF-1α expression	+	+
HIF-2α expression	+	+
PHD expression	+	+
Relative NO expression	+ + +	+
Effect of L-NAME addition	No inhibition of NO No effect on the expression of PHDs, OCT4, SOX2, NANOG or HIF-2α	Inhibition of NO Decrease in the expression of PHDs, OCT4, SOX2, NANOG and HIF-2α

Furthermore, decreasing NO levels in NT2 hECCs cultured at 5% oxygen using the same concentration of L-NAME resulted in no significant difference in HIF-2α, OCT4, SOX2 and NANOG expression in NT2 cells incubated with either 0mM or 10mM L-NAME. The absence of any effect on HIF-2α expression and consequently pluripotency marker

expression in NT2 cells maintained at 5% oxygen compared to cells cultured under normoxia is possibly due to NO levels being higher in NT2 cells cultured at 5% oxygen and backed up by the observed increased expression of NOS in NT2s cultured under hypoxia compared to normoxia.

Therefore, it is likely that the significant decrease in HIF-2α expression observed in NT2 cells incubated with L-NAME at 20% oxygen, and not in cells cultured under hypoxia, was due to the fact that NO levels in cells cultured at 5% oxygen with L-NAME were still high enough to stabilise HIF-2α. It is hypothesised that reducing the NO levels in NT2 hECCs further would result in a significant decrease in HIF-2α expression and consequently reduce the expression of the three core pluripotency markers. Therefore, it appears that the mechanism of regulation of hECC self-renewal by NO is the same between cells maintained at either 5% or 20% oxygen but NO levels are higher in cells cultured under hypoxia.

It is hypothesised that endogenously generated NO in hECCs inhibits the activity of PHDs, as previously shown in colon carcinoma cells (Chowdhury et al., 2012), leading to the stabilisation of HIF-2α, and most likely HIF-1α also, which leads to increased hECC self-renewal. Due to the well-documented metabolic plasticity in hECCs, there could also be a metabolic effect occurring too.

It is well documented throughout the literature that NO has dual functions depending on whether it is present in high or low doses. Furthermore, previous studies have demonstrated that lowering NO levels delays differentiation in mESCs (Tejedo et al., 2010) particularly by increasing the number of H3K4me3 histone marks associated with euchromatin (Tapia-Limonchi et al., 2016). Furthermore, data from a recent study reemphasises this observation where low NO levels on ovary cancer cells increase glycolysis, which in turn supports pluripotency maintenance (Folmes and Terzic, 2016; Li et al., 2017). However, the data presented in this chapter is contradictory to that in the literature as when NO were decreased with L-NAME, pluripotency marker expression decreased and therefore suggests the onset of early differentiation.

However, NO has been shown to induce changes in cancer stem cells by increasing associated markers. Therefore, it could be that NO-induced changes in hECCs include increasing OCT4, SOX2 and NANOG expression in order to become malignant, and as

such there is no dual role for NO in cancer stem cells, but just one function that helps with malignant progression.

7.5 Conclusions

In conclusion, data from this chapter has revealed that:

- Pluripotency marker expression is not affected by hypoxia in NT2 hECCs.
- CtBP expression is affected by hypoxia in NT2 hECCs.
- Both HIF-1α and HIF-2α are expressed and functional in NT2 hECCs maintained at both 5% and 20% oxygen.
- HIF-α expression is stabilised under normoxic conditions due to high basal levels of NO leading to the inactivity of PHDs.

Results from this chapter have revealed that the hypoxic regulation of pluripotency markers is not maintained between hESCs and hECCs. The next chapter will further explore the similarities and differences between the cell types and investigate whether the glycolytic regulation of self-renewal and role of CtBPs is maintained in hECCs as well as hESCs,

Chapter 8

Metabolic regulation of self-renewal in human embryonal carcinoma cells

Chapter 8: Metabolic regulation of self-renewal in human embryonal carcinoma cells

8.1 Introduction

8.1.1. hECC metabolism

Cells constantly adjust their metabolic state to extracellular signals and nutrient availability to meet their bioenergetic demands including providing substrates for post-translational modifications that influence cell signalling, gene expression and epigenetic modifications of histones and DNA.

Unlike normal differentiated cells, which obtain most of their energy they need for cellular processes through OXPHOS in mitochondria, previous studies have observed that most cancer cells rely instead predominantly on glycolysis even under normoxic conditions. This phenomenon is known as the Warburg effect (Warburg, 1956). Thus, knowledge on how metabolism is rewired in cancer stem cells may provide significant insights not only for cancer progression but also the maintenance of self-renewal in hESCs.

While hESCs and hECCs were largely thought to harbour similar metabolic states, recent evidence demonstrates that the metabolic dependency in each cell type is distinctly different. While hECCs share the glycolytic phenotype of hESCs, hECCs may display more metabolic plasticity. Previous studies have revealed that hECCs may use the expression of pluripotency marker, particularly NANOG, to regulate the genes involved with OXPHOS and hence supporting hECC self-renewal (Chen et al., 2016).

8.1.2. CtBPs

CtBPs are a family of glycolytic sensors that link the metabolic state of the cell to gene expression. NADH binding induces a conformational change in the CtBP monomers which promotes dimerisation. CtBP dimers are active to function as either transcriptional coactivators or corepressors after the formation of a protein complex containing cofactors and chromatin modifying enzymes that can open or condense chromatin in a gene specific manner.

8.1.3. Chapter Aims

The specific aims of this chapter are:

- To compare the effects of inhibiting glycolysis on pluripotency marker and CtBP expression in NT2 hECCs with 2-DG.
- To investigate whether CtBPs regulate OCT4, SOX2 and NANOG expression in NT2 cells using siRNA.

8.2. Results

8.2.1. Effect of glycolytic rate on pluripotency marker expression in NT2 cells cultured at 5% oxygen

Results from Chapter 4 indicated that glycolysis maintains hESC pluripotency. However, whether that metabolic regulation of OCT4, SOX2 and NANOG expression is also present in hECCs is unknown. NT2 hECCs were cultured at 5% oxygen in the presence or absence of 10mM, 30mM or 100mM of the glycolytic inhibitor 2-DG for 48 hours before collecting cells for either RNA or protein isolation.

Phase contrast images found that up to 100mM 2-DG had no clear effect on NT2 cell number (Figure 8.1) or cell morphology (Figure 8.2) after 24 hours or 48 hours of exposure.

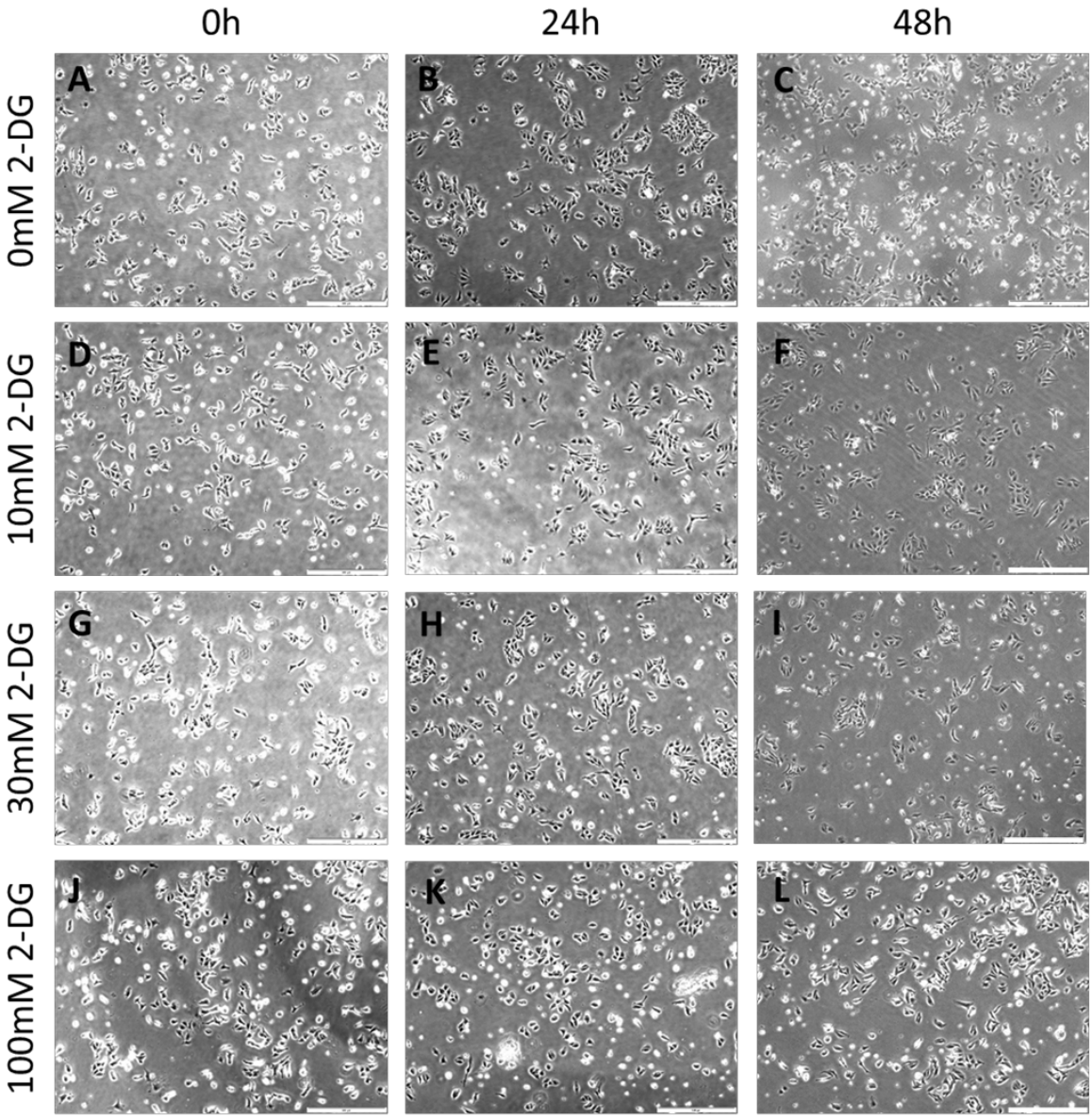

Figure 8.1. Phase contrast images demonstrating effects of 2-DG exposure on NT2 hECC number at 5% oxygen.

Representative phase contrast images of NT2 hECCs cultured at 5% oxygen in 60ml dishes in NT2 culture medium supplemented with either 0mM (A-C), 10mM (D-F) or 30mM (G-I) or 100mM 2-DG (J-L) after 0 (A, D, G, J), 24 (B, E, H, K) and 48 hours (C, F, I, L). Scale bar indicates 500μm.

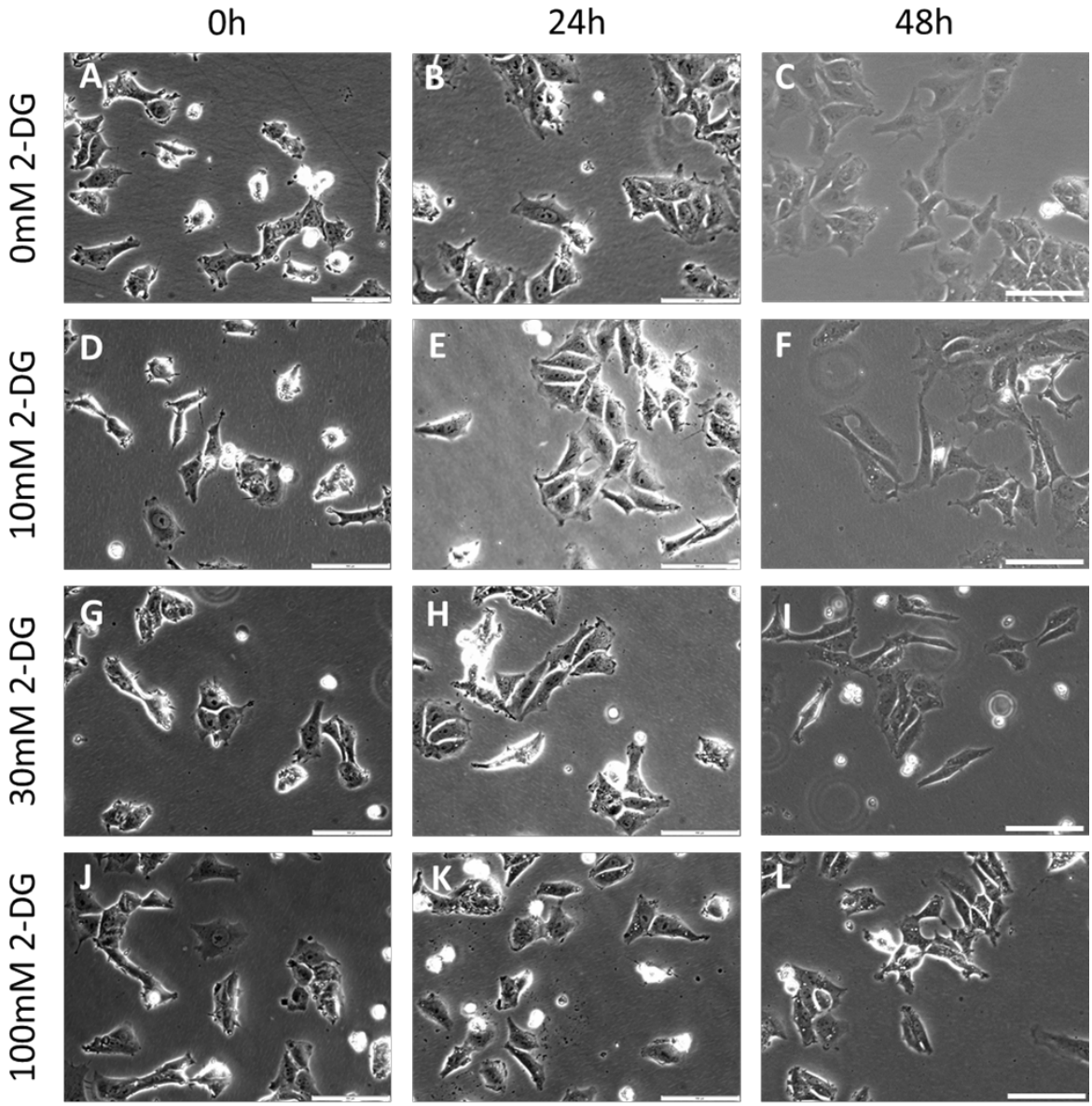

Figure 8.2. Phase contrast images of NT2 hECCs cultured in 2-DG supplemented media display no clear morphological changes.

Representative phase contrast images of NT2 hECCs cultured at 5% oxygen in 60ml dishes in NT2 culture medium supplemented with either 0mM (A-C), 10mM (D-F) or 30mM (G-I) or 100mM 2-DG (J-L) after 0 (A, D, G, J), 24 (B, E, H, K) and 48 hours (C, F, I, L). Scale bar indicates 100μm.

Prior to analysing whether the addition of the glycolytic inhibitor 2-DG affected the expression of the genes of interest, metabolism assays were performed to confirm whether the rate of glycolysis was reduced by 2-DG.

NT2 cells maintained at 5% oxygen and incubated in the absence of 2-DG consumed 31.07 ± 3.09 pmol/cell/24 hours of glucose. In comparison, NT2 cells incubated with 10mM 2-DG consumed 28.77 ± 3.22 pmol/cell/24 hours of glucose, whereas the addition of 30mM 2-DG to NT2 cells resulted in a glucose consumption rate of 26.94 ± 2.28 pmol/cell/24 hours. The addition of either 10mM (p=0.6117) or 30mM 2-DG (p=0.2929) to NT2 hECCs maintained under hypoxia resulted in no significant difference in the rate of glucose consumption compared to NT2 cells maintained in the absence of 2-DG (Figure 8.3).

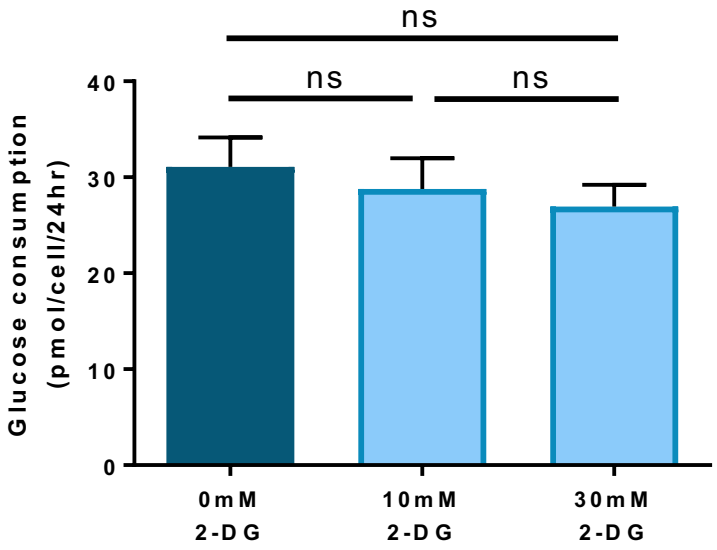

Figure 8.3. Glucose consumption is not affected by the addition of 2-DG in NT2 hECCs at 5% oxygen.
Quantification of the rate of glucose consumption of NT2 hECCs maintained under hypoxic conditions and incubated with either 10mM or 30mM 2-DG for 48 hours compared to the control cells. Bars represent mean ± SEM. (n=12)

Furthermore, NT2 cells maintained at 5% oxygen and in the absence of 2-DG produced 74.95 ± 5.95 pmol/cell/24 hours of lactate. The addition of 10mM 2-DG to NT2 cells resulted in a lactate production rate of 62.75 ± 7.44 pmol/cell/24 hours and thus no significant difference was observed in lactate production between NT2 cells incubated with 10mM 2-DG compared to those maintained in the absence of 2-DG (p=0.2137).

In contrast, a significant reduction in lactate production was observed in NT2 hECCs maintained at 5% oxygen and treated with 30mM 2-DG. A significant and approximate 83% reduction (p<0.0001) in the rate of lactate production to 12.67 ± 2.28 pmol/cell/24 hours was observed in NT2 cells incubated with 30mM 2-DG compared to hECCs cultured in the absence of 2-DG (Figure 8.4).

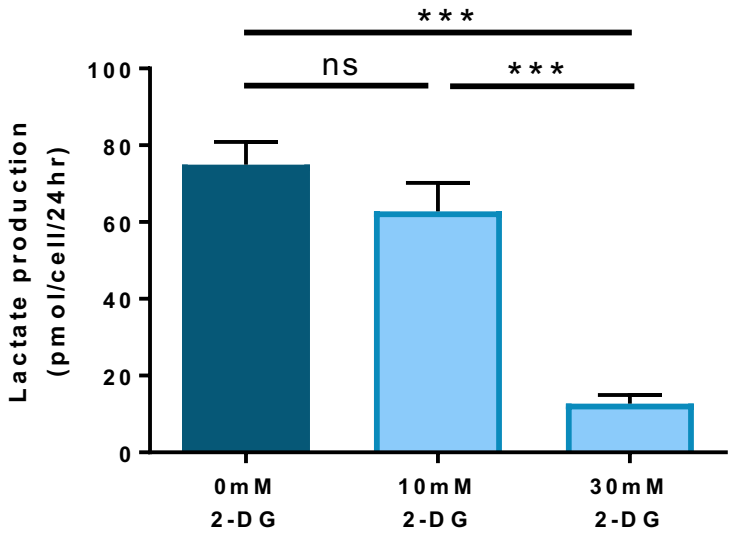

Figure 8.4. Lactate production is significantly reduced in NT2 hECCs cultured at 5% oxygen treated with 2-DG.
Quantification of the rate of lactate production in NT2 hECCs maintained under hypoxia and incubated with either 10mM or 30mM 2-DG for 48 hours compared to the control cells. Bars represent mean ± SEM. (n=12)

The percentage glycolysis was determined from glucose uptake and lactate production according to the following equation:

$$Glycolysis = \frac{\left(\frac{Lactate\ production}{2}\right)}{Glucose\ uptake} \times 100$$

Together, the addition of 30mM 2-DG alone to NT2 hECCs maintained at 5% oxygen resulted in a significant decrease in the rate of glycolysis (p=0.0001) compared to NT2 hECCs maintained in the absence of 2-DG (Figure 8.5). Therefore, future experiments in NT2 hECCs maintained under hypoxia were performed using 30mM 2-DG.

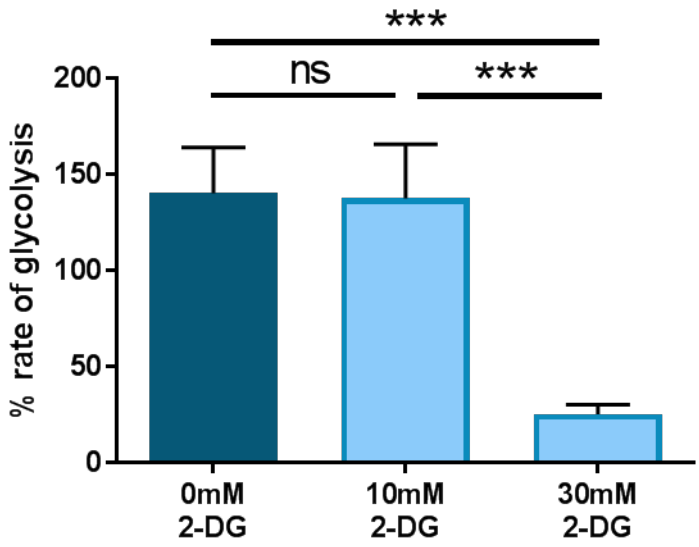

Figure 8.5. Rate of glycolysis decreases in NT2 hECCs incubated with 2-DG under hypoxia. Quantification of the percentage of glycolysis in NT2 hECCs maintained at 5% oxygen and incubated with either 0mM, 10mM or 30mM 2-DG. Bars represent mean ± SEM. (n=12)

To investigate the effects of inhibiting the glycolytic rate on the mRNA expression levels of pluripotency markers, RT-qPCR was performed on NT2 cells maintained at 5% oxygen treated with either 0mM or 30mM 2-DG for 48 hours.

NT2 hECCs treated with 30mM 2-DG displayed an approximate 40% decrease in *OCT4* expression (p=0.0057), a 57% decrease in *SOX2* expression (p=0.0149) and an approximate 50% reduction in *NANOG* mRNA levels (p=0.0044) compared to hECCs incubated in the absence of 2-DG under hypoxia (Figure 8.6).

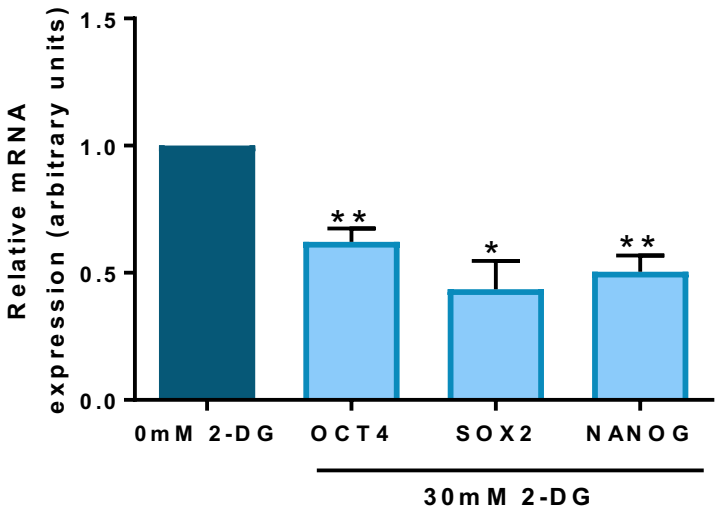

Figure 8.6. Pluripotency marker mRNA expression levels are significantly decreased in NT2 hECCs cultured at 5% oxygen and in the presence of the inhibitor 2-DG.
Quantification of *OCT4, SOX2* and *NANOG* mRNA expression in NT2 hECCs maintained at 5% and cultured either in the presence of 30mM 2-DG after 48 hours compared to the 0mM 2-DG control. Data were normalised to *UBC*, and then to 1 for 0mM 2-DG control. Bars represent mean ± SEM. (n=4)

Quantification of the OCT4, SOX2 and NANOG protein expression revealed a significant decrease in the protein expression of the three core pluripotency markers also in NT2 hECCs maintained at 5% oxygen cultured in the presence of the glycolytic inhibitor 2-DG (Figure 8.7). NT2 cells cultured with 30mM 2-DG for 48 hours displayed an approximate 66% reduction in OCT4 ($p=0.0259$), a 74% reduction in SOX2 ($p=0.0404$) and an approximate 75% decrease in NANOG ($p=0.0074$) protein expression compared to cells treated with 0mM 2-DG.

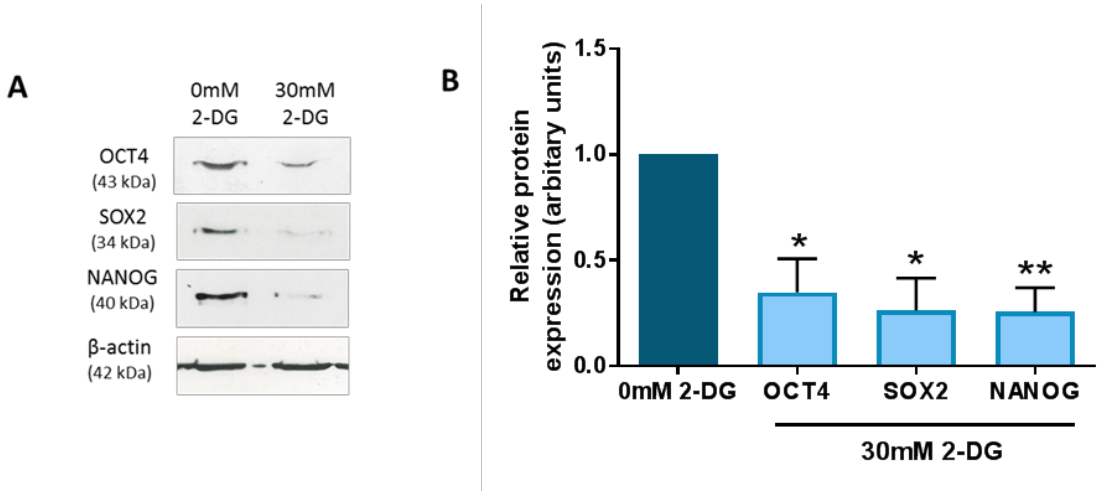

Figure 8.7. Inhibition of glycolysis using 2-DG decreases the protein expression of pluripotency markers in NT2 hECCs maintained at 5% oxygen.
(A) Representative Western blots of OCT4, SOX2 and NANOG expression in NT2 hECCs cultured at 5% oxygen in fresh media supplemented with either 0mM or 30mM 2-DG for 48 hours. (B) Quantification of OCT4, SOX2 and NANOG protein in the presence of 2-DG compared to its absence. Data were normalised to β-actin, and then to 1 for 0mM 2-DG control. Bars represent mean ± SEM. (n=3-4)

8.2.2. Effect of glycolysis on CtBP expression in NT2 cells cultured at 5% oxygen

To investigate whether inhibiting glycolysis in NT2 hECCs affected the expression of CtBPs mimicking previous results observed in hESCs, NT2 hECCs were cultured at 5% oxygen in the presence or absence of either 0mM or 30mM 2-DG for 48 hours before collecting cells for RT-qPCR or Western blotting.

A significant and approximate 33% and 36% reduction in CtBP1 (p=0.0184) and CtBP2 (p=0.0087) mRNA expression respectively in hECCs treated with 30mM 2-DG compared to those treated with 0mM 2-DG (Figure 8.8).

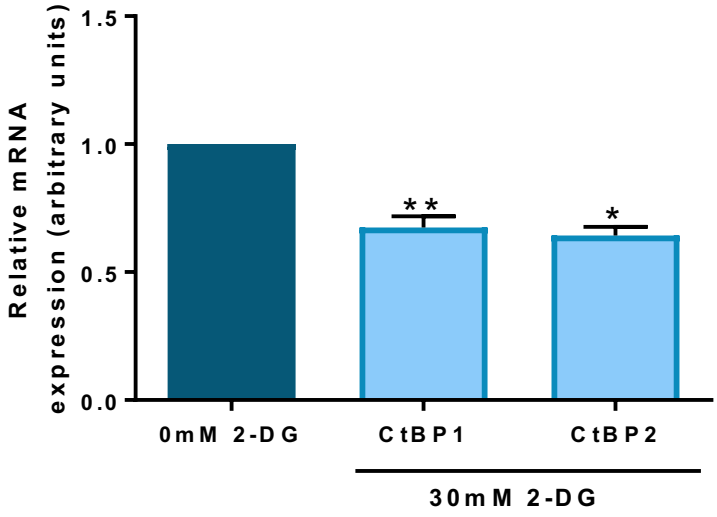

Figure 8.8. CtBP mRNA expression levels are significantly decreased after the inhibition of glycolysis using 2-DG in NT2 hECCs.
Quantification of *CtBP1* and *CtBP2* mRNA expression in NT2 hECCs cultured with 30mM 2-DG compared to the 0mM 2-DG control after 48 hours. Data were normalised to *UBC*, and then to 1 for 0mM 2-DG control. Bars represent mean ± SEM. (n=3)

Quantification of CtBP1 and CtBP2 Western blots revealed a significant reduction in the expression of both CtBP isoforms in NT2 cells incubated with 2-DG (Figure 8.9). CtBP1 expression decreased by 63% (p=0.0332) and CtBP2 expression reduced by approximately 55% (p=0.0047) in NT2 hECCs maintained at 5% oxygen and incubated with 30mM 2-DG compared to cells incubated in the absence of 2-DG.

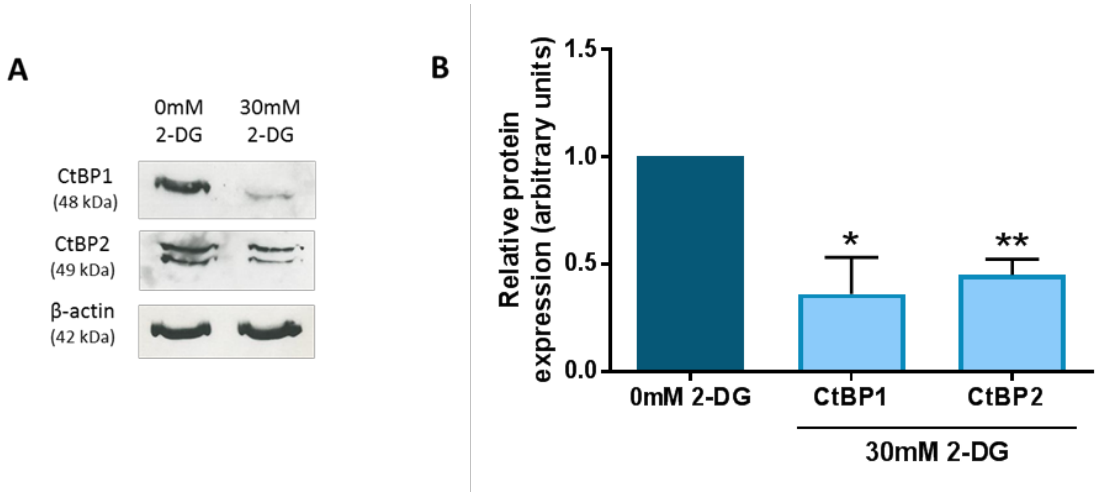

Figure 8.9. CtBP protein expression decreases after inhibiting glycolysis using 2-DG in NT2 hECCs cultured at 5% oxygen.
(A) Representative Western blots of CtBP1 and CtBP2 expression in NT2 hECCs cultured at 5% oxygen in media supplemented with either 0mM or 30mM 2-DG after 48 hours. (B) Quantification of CtBP1 and CtBP2 protein expression in NT2 hECCs incubated with either 0mM or 30mM 2-DG. Data were normalised to β-actin, and then to 1 for 0mM 2-DG control. Bars represent mean ± SEM. (n=4)

8.2.3. Effect of glycolysis on HIF-2α expression in NT2 cells cultured at 5% oxygen

To determine whether inhibiting glycolysis in NT2 hECCs maintained under hypoxia affected HIF-2α expression, Western blotting was performed on NT2 hECCs incubated in the presence or absence of 2-DG.

HIF-2α protein expression decreased by approximately 64% (p=0.0291) when NT2 cells were incubated with 30mM 2-DG compared to when they were incubated without (Figure 8.10).

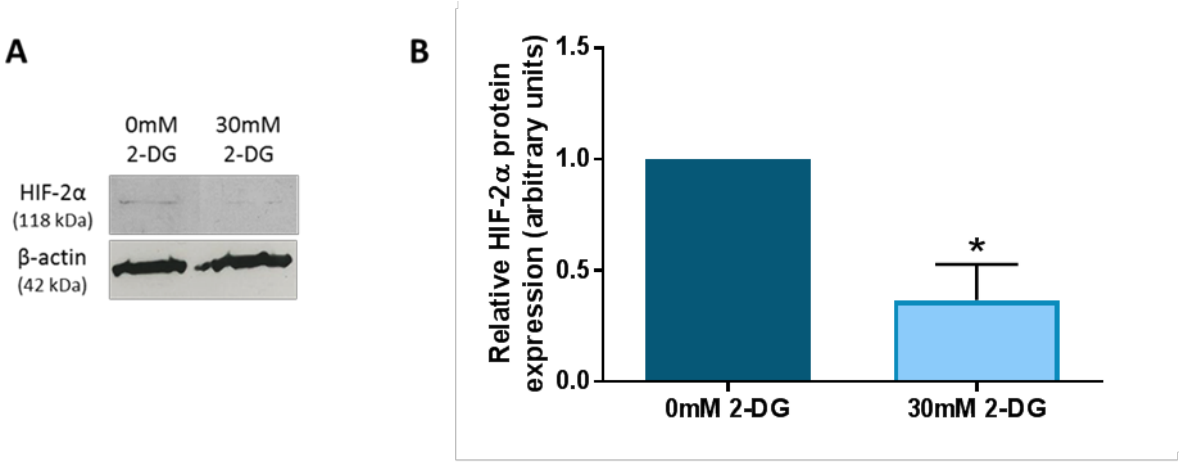

Figure 8.10. HIF-2α protein expression decreases after inhibiting glycolysis using 2-DG in NT2 hECCs cultured at 5% oxygen.
(A) Representative Western blots of HIF-2α expression in NT2 hECCs cultured at 5% oxygen in medium supplemented with either 0mM or 30mM 2-DG after 48 hours. (B) Quantification of HIF-2α protein expression in NT2 hECCs incubated in the presence of 2-DG compared to its absence. Data were normalised to β-actin, and then to 1 for 0mM 2-DG control. Bars represent mean ± SEM. (n=4)

8.2.4. Effect of inhibiting glycolysis in NT2 cells cultured at 20% oxygen

Experiments were conducted to determine whether the effects of inhibiting glycolysis on pluripotency marker, CtBP and HIF-2α expression observed under hypoxia also occurred under normoxic oxygen tensions in NT2 hECCs, like their non-malignant counterparts hESCs (Chapter 4.3.2). To investigate the effects of altering the rate of glycolysis in NT2 hECCs maintained under 20% oxygen, cells were incubated with the glycolytic inhibitor 2-DG for 48 hours before collecting cells for RT-qPCR and Western blotting analysis.

Cells were treated with either 0mM, 10mM or 30mM 2-DG. 30mM 2-DG concentrations were toxic to NT2 cells maintained at 20% oxygen as cells had lifted off tissue culture plastic and were floating in the medium resulting in a clear decrease in cell number after 48 hours of exposure to the inhibitor. However, NT2 cells incubated with 10mM 2-DG displayed no overt differences in cell morphology or cell number after 48 hours compared to cells incubated in the absence of 2-DG (Figure 8.11). Therefore, further experiments were carried out using a 2-DG concentration of 10mM for NT2 cells maintained at 20% oxygen.

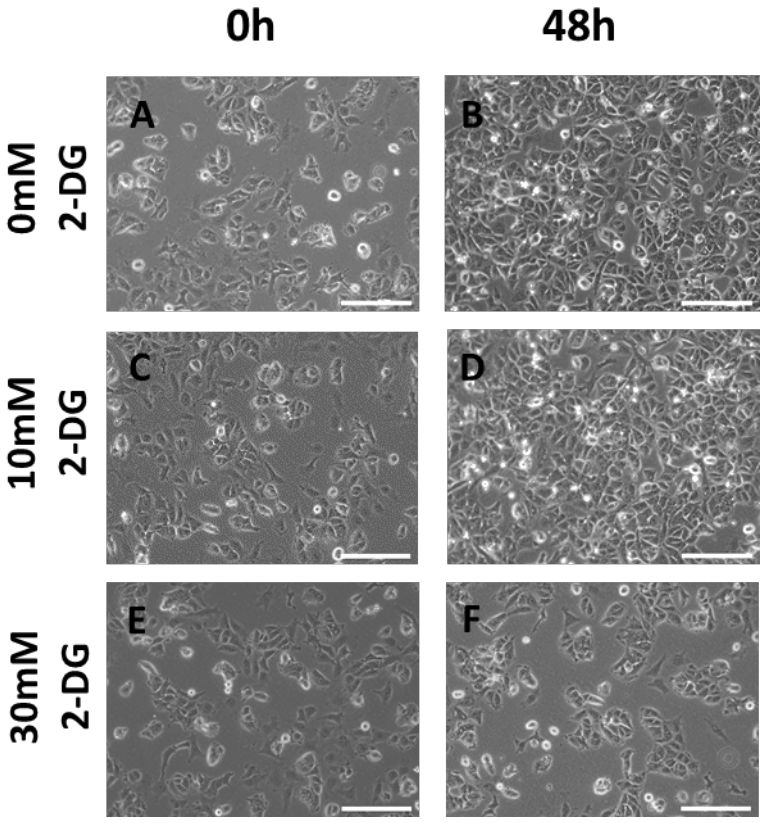

Figure 8.11. Phase contrast images demonstrating cellular morphology of NT2 hECCs cultured in 2-DG supplemented media at 20% oxygen.
Representative phase contrast images of NT2 hECCs cultured at 20% oxygen in fresh medium supplemented with either 0mM (A-B), 10mM (C-D) or 30mM 2-DG (E-F) after 48 hours. Scale bar indicates 200μm.

To determine that a concentration of 10mM 2-DG was enough to reduce the rate of flux through glycolysis in NT2 hECCs maintained at 20% oxygen, enzyme-linked assays assessing metabolism were performed.

Addition of 10mM 2-DG resulted in no significant difference in the rate of glucose consumption ($p=0.7632$) in NT2 cells from 25.27 ± 1.79 pmol/cell/24 hours compared to the control cells at 23.89 ±1.97 pmol/cell/24 hours (Figure 8.12).

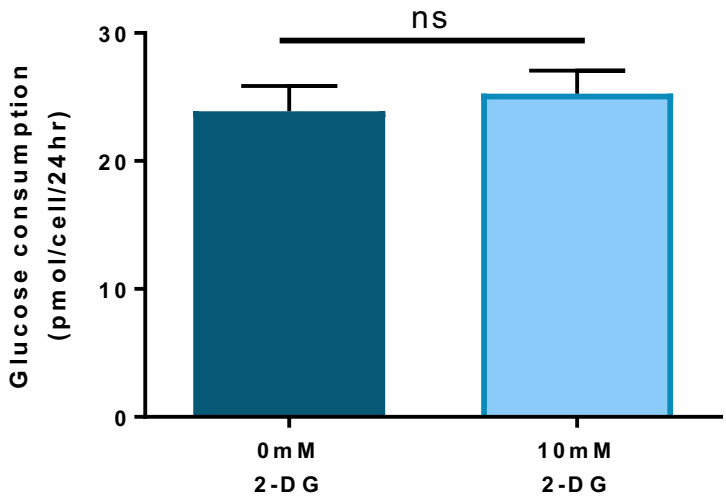

Figure 8.12. Glucose consumption is not affected by the addition of 2-DG in NT2 hECCs at 20% oxygen.
Quantification of the rate of glucose consumption of NT2 hECCs maintained at 20% oxygen and incubated with 10mM 2-DG for 48 hours compared to the control cells. Bars represent mean ± SEM. (n=12)

Moreover, lactate production was significantly reduced from 73.19 ± 2.4 pmol/cell/24 hours in NT2 hECCs incubated in the absence of 2-DG to 24.44 ± 4.6 pmol/cell/24 hours in NT2 hECCs incubated in the presence of 10mM 2-DG; an approximate 66% reduction ($p<0.0001$; Figure 8.13).

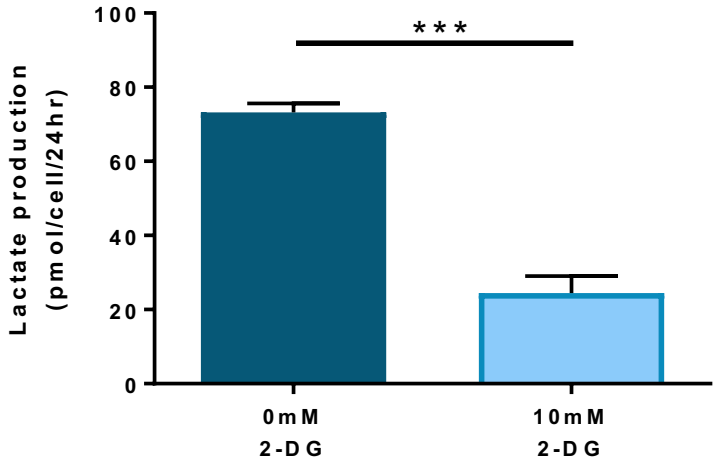

Figure 8.13. Lactate production is significantly reduced in NT2 hECCs cultured at 20% oxygen treated with 2-DG.
Quantification of the rate of lactate production in NT2 hECCs maintained at 20% oxygen and incubated either in the presence of absence of 10mM 2-DG for 48 hours. Bars represent mean ± SEM. (n=12)

Together, the addition of 10mM 2-DG to NT2 cells maintained at 20% oxygen resulted in a significant decrease in the rate of glycolysis compared to NT2 hECCs cultured in the absence of 2-DG ($p<0.0001$; Figure 8.14).

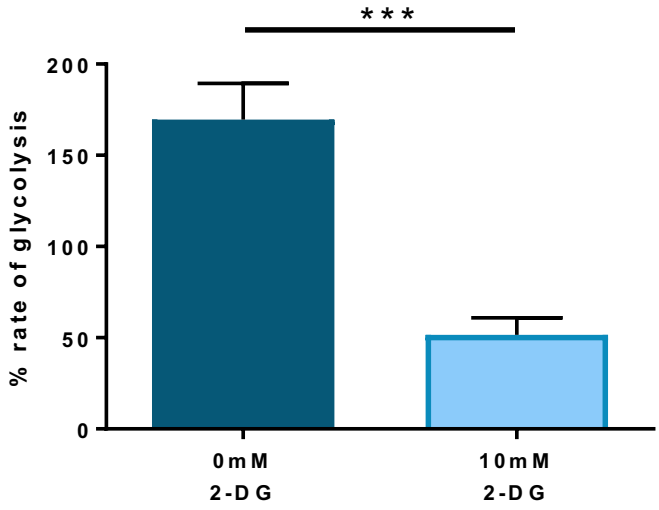

Figure 8.14. Rate of glycolysis significantly decreases in NT2 hECCs incubated with 2-DG under 20% oxygen.
Quantification of the percentage rate of glycolysis in NT2 hECCs maintained at 20% oxygen and incubated with either 0mM, 10mM or 30mM 2-DG. Bars represent mean ± SEM. (n=12)

To evaluate the effect of inhibiting glycolysis using 2-DG in NT2 cells maintained at 20% oxygen on pluripotency marker expression, OCT4, SOX2 and NANOG mRNA and protein levels were analysed by RT-qPCR and Western blotting.

OCT4, SOX2 and NANOG mRNA expression decreased by approximately 55% (p=0.0102), 40% (p=0.001) and 50% (p=0.0019) respectively in NT2 hECCs incubated with 10mM 2-DG compared to the 0mM control cells (Figure 8.15).

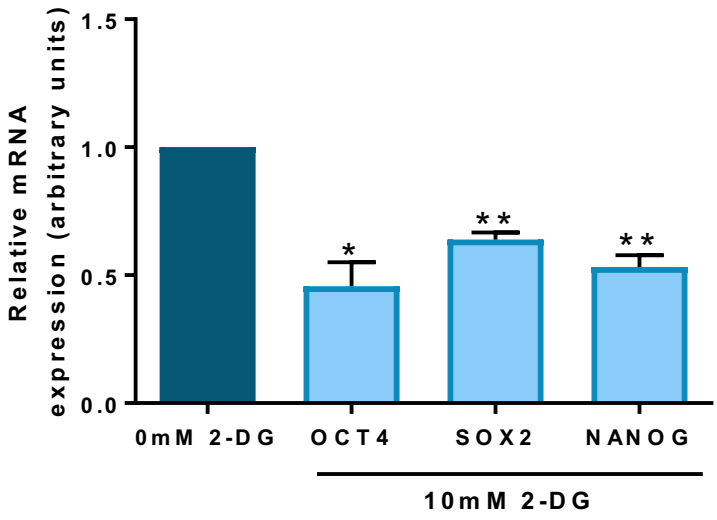

Figure 8.15. Pluripotency marker expression decreases when glycolysis is inhibited with 2-DG in NT2 hECCs at 20% oxygen.
Quantification of *OCT4, SOX2* and *NANOG* expression in NT2 hECCs maintained at 20% oxygen and incubated with either 0mM or 10mM 2-DG. Data were normalised to *UBC*, and then to 1 for 0mM 2-DG control. Bars represent mean ± SEM. (n=4)

Quantification of protein expression revealed a significant decrease in OCT4 expression by approximately 27% (p=0.011), a significant reduction in SOX2 expression by 57% (p=0.0441) and a significant decrease in NANOG expression by approximately 25% (p=0.0229) in NT2 cells incubated with 10mM 2-DG compared to the 0mM control cells (Figure 8.16).

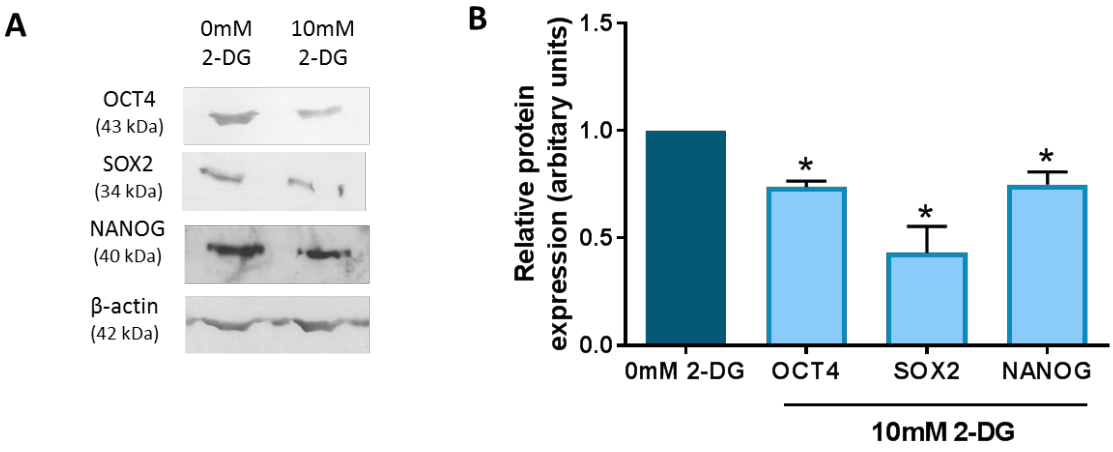

Figure 8.16. Pluripotency marker protein expression decreases after inhibiting glycolysis with 2-DG in NT2 hECCs cultured at 20% oxygen.
(A) Representative Western blots of OCT4, SOX2 and NANOG expression in NT2 hECCs cultured at 20% oxygen in medium supplemented with either 0mM or 10mM 2-DG after 48 hours. (B) Quantification of OCT4, SOX2 and NANOG protein expression in NT2 hECCs maintained at 20% oxygen and incubated in the presence of 2-DG compared to its absence. Data were normalised to β-actin, and then to 1 for 0mM 2-DG control. Bars represent mean ± SEM. (n=3-4)

To evaluate whether glycolysis regulates CtBP expression in NT2 hECCs maintained at 20% oxygen were incubated in the presence or absence of 10mM 2-DG.

RT-qPCR analysis revealed a significant and approximate 54% and 46% reduction in CtBP1 (p=0.0065) and CtBP2 (p=0.0212) mRNA expression respectively in hECCs treated with 10mM 2-DG compared to those treated with 0mM 2-DG (Figure 8.17).

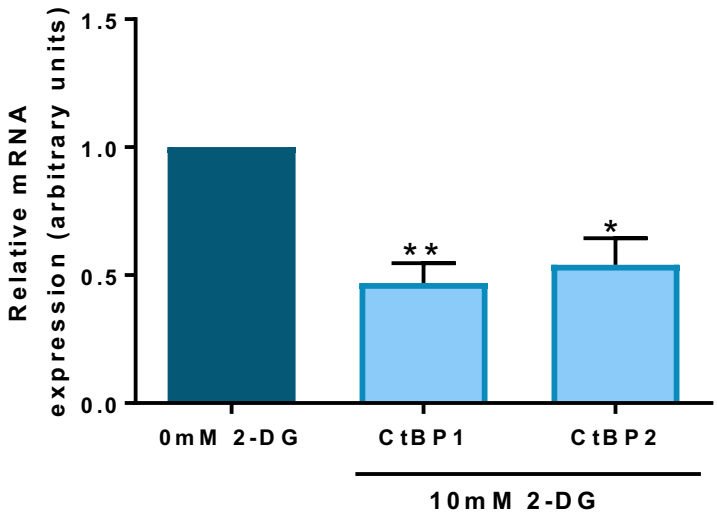

Figure 8.17. CtBP expression decreases when the rate of glycolysis is reduced using 2-DG in NT2 hECCs at 20% oxygen.
Quantification of *CtBP1* and *CtBP2* expression in NT2 hECCs maintained at 20% oxygen and incubated with either 0mM or 10mM 2-DG. Data were normalised to *UBC*, and then to 1 for 0mM 2-DG control. Bars represent mean ± SEM. (n=4)

Quantification of CtBP protein expression revealed a significant 63% and 58% decrease in CtBP1 (p=0.0308) and CtBP2 (p=0.042) expression respectively in NT2 cells maintained at 20% oxygen and treated with 10mM 2-DG compared to cells incubated in the absence of the inhibitor (Figure 8.18).

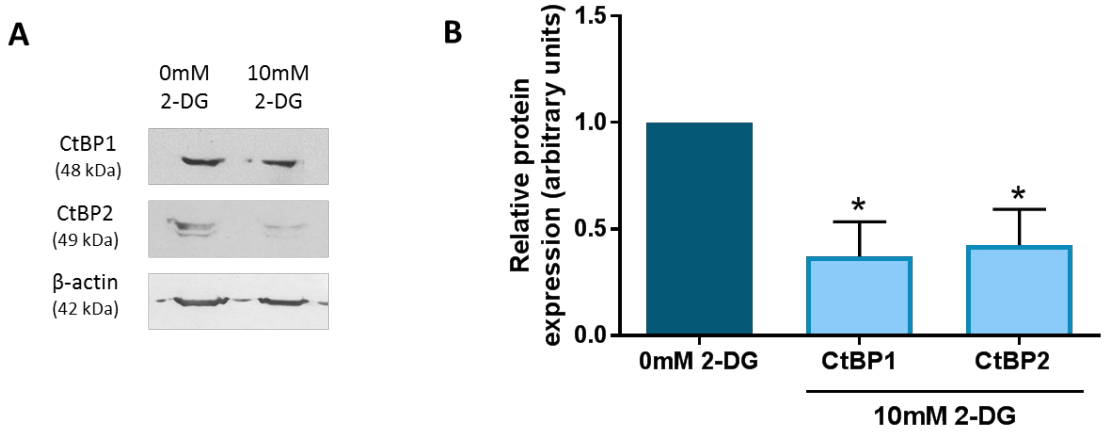

Figure 8.18. CtBP protein expression is reduced when glycolysis is inhibited using the glycolytic inhibitor 2-DG in NT2 hECCs cultured at 20% oxygen.
(A) Representative Western blots of CtBP1 and CtBP2 expression in NT2 hECCs cultured at 20% oxygen in medium supplemented with either 0mM or 10mM 2-DG. (B) Quantification of CtBP1 and CtBP2 protein expression in NT2 hECCs cultured at 20% oxygen and incubated in the presence or absence of 10mM 2-DG. Data were normalised to β-actin, and then to 1 for 0mM 2-DG control. Bars represent mean ± SEM. (n=4)

To determine whether inhibiting the rate of flux through glycolysis using 2-DG in NT2 hECCs maintained at 20% oxygen affected HIF-2α expression, protein expression in NT2 hECCs incubated in the presence of 2-DG was analysed by Western blotting.

HIF-2α protein expression decreased by approximately 40% (p=0.0003) when NT2 cells were incubated with 30mM 2-DG compared to when they were incubated without (Figure 8.19).

Together, these data suggest that inhibiting the rate of flux through glycolysis decreases pluripotency marker, CtBP and HIF-2α expression in NT2 hECCs independent of oxygen tension.

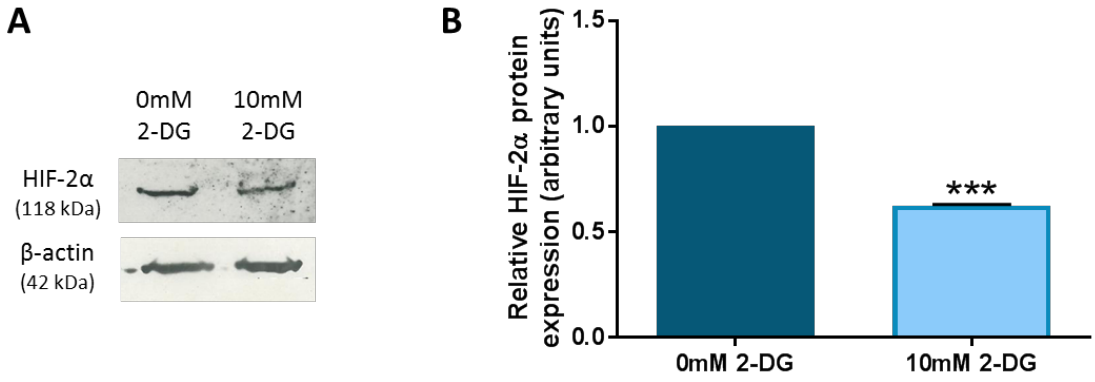

Figure 8.19. HIF-2α protein expression is decreased when glycolysis is inhibited using 2-DG in NT2 hECCs cultured at 20% oxygen.
(A) Representative Western blots of HIF-2α expression in NT2 hECCs cultured at 20% oxygen in fresh media supplemented with either 0mM or 10mM 2-DG. (B) Quantification of HIF-2α protein expression in NT2 hECCs maintained at 20% oxygen and cultured in the presence of 2-DG compared to its absence. Data were normalised to β-actin, and then to 1 for 0mM 2-DG control. Bars represent mean ± SEM. (n=4)

8.2.5. Effect of silencing CtBP expression in NT2 cells at 5% oxygen on pluripotency marker expression

To investigate whether CtBPs had a role in regulating pluripotency marker expression in hECCs, NT2 hECCs maintained at 5% oxygen were transfected on day 1 post-passage with 50nM CtBP1/2 siRNA to silence the expression of both CtBP isoforms. Cells were collected on day 3 post-passage for analysis by RT-qPCR and Western blotting.

Cells transfected with CtBP1/2 siRNA displayed no overt difference in cell number (Figure 8.20) or morphology (Figure 8.21) compared to control cells.

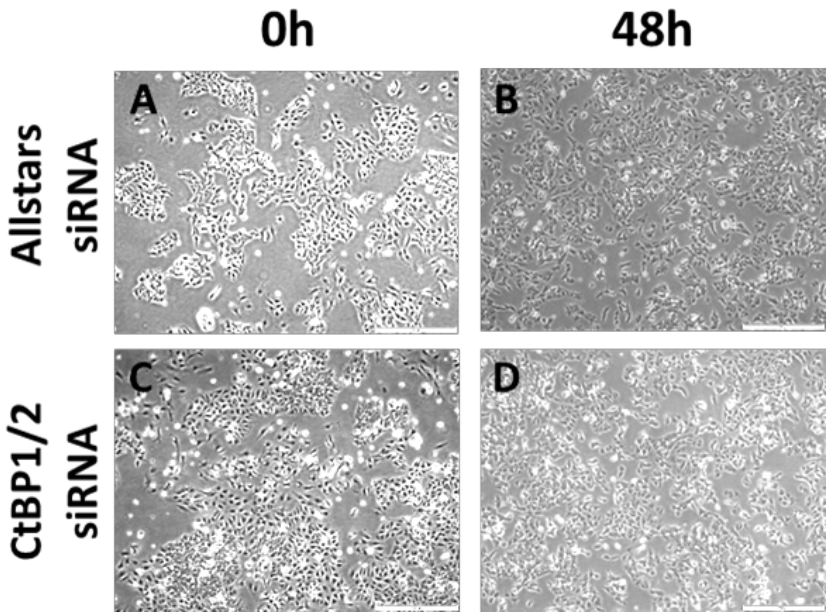

Figure 8.20. Phase contrast images demonstrating morphology of NT2 hECCs cultured at 5% oxygen transfected with CtBP1/2 siRNA.
Representative phase contrast images of NT2 hECCs cultured at 5% oxygen transfected with either Allstars negative control siRNA (A-B) or CtBP1/2 siRNA (C-D) after 0 (A, C) and 48 hours (B, D). Scale bar indicates 500μm.

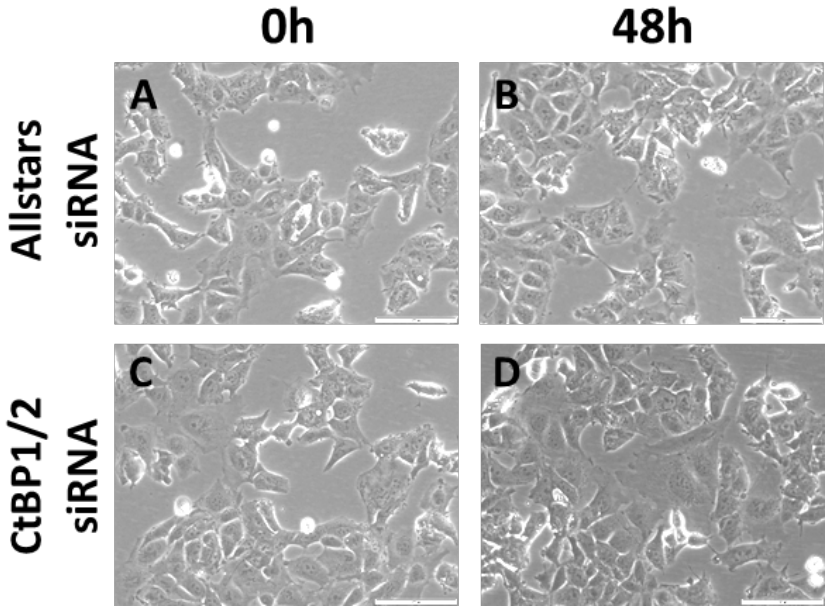

Figure 8.21. Phase contrast images of NT2 hECCs cultured at 5% oxygen transfected with CtBP1/2 siRNA display no clear morphological differences.
Representative phase contrast images of NT2 hECCs cultured at 5% oxygen transfected with either Allstars negative control siRNA (A-B) or CtBP1/2 siRNA (C-D) after 0 (A, C) and 48 hours (B, D). Scale bar indicates 100μm.

Silencing with CtBP1/2 siRNA resulted in a significant, approximate 50% decrease in the mRNA expression of both *CtBP1* ($p<0.0001$) and *CtBP2* ($p=0.0087$) compared to cells transfected with the Allstars negative control siRNA (Figure 8.22). Prior to evaluating any consequent changes in pluripotency marker expression, the expression of two known CtBP-repressed genes; *Talin-1* (*TLN1*) and *E-cadherin* (*CDH1*), were evaluated in response to silencing the expression of both CtBP isoforms. Quantification of *TLN1* and *CDH1* mRNA expression levels in NT2 hECCs transfected with CtBP1/2 siRNA revealed a significant increase in their expression compared with the control (Figure 8.22). NT2 hECCs transfected with CtBP1/2 siRNA displayed an approximate 2.4-fold increase in *TLN1* expression ($p=0.0009$) and an approximate doubling of *CDH1* expression ($p=0.0075$) compared to the transfection control. Subsequently, quantification of pluripotency marker mRNA expression levels in NT2 hECCs transfected with CtBP1/2 siRNA revealed a significant decrease in *OCT4, SOX2* and *NANOG* expression by approximately 60% ($p=0.0099$), 48% ($p=0.017$) and 52% ($p=0.0267$) respectively compared to those transfected with Allstars negative control siRNA (Figure 8.22).

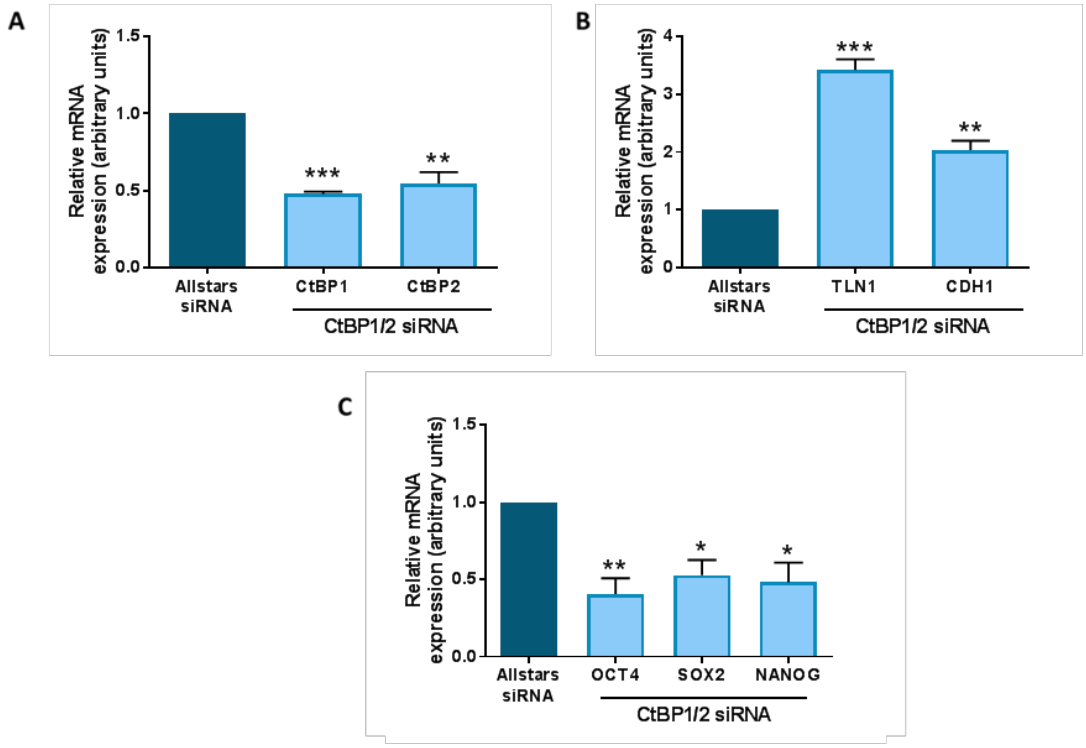

Figure 8.22. Silencing both CtBP isoforms decreases pluripotency marker expression in NT2 hECCs maintained at 5% oxygen using CtBP1/2 siRNA.
Quantification of relative *CtBP1, CtBP2* (A), *TLN1, CDH1* (B), *OCT4, SOX2* and *NANOG* (C) mRNA expression levels in NT2 hECCs transfected with either the Allstars negative control siRNA or CtBP1/2 siRNA where cells were collected 48 hours post-transfection. Data were normalised to *UBC*, and then to 1 for Allstars control. Bars represent mean ± SEM. (n=4)

When expression was investigated at the protein level, both CtBP1 (p=0.0017) and CtBP2 (p=0.0006) protein expression significantly decreased by approximately 60% and 40% respectively after transfection with CtBP1/2 siRNA compared to NT2 cells transfected with Allstars negative control siRNA (Figure 8.23).

Having successfully silenced both CtBP isoforms, the effect on OCT4, SOX2 and NANOG protein expression was investigated. Silencing both CtBP1 and CtBP2 displayed a significant decrease in OCT4, SOX2 and NANOG expression (Figure 8.23). NT2 hECCs transfected with CtBP1/2 siRNA displayed an approximate 15% decrease in OCT4 (p=0.0341), an approximate 50% decrease in SOX2 (p=0.0203), and an approximate 45% reduction in NANOG (p=0.0147) protein expression compared to the control.

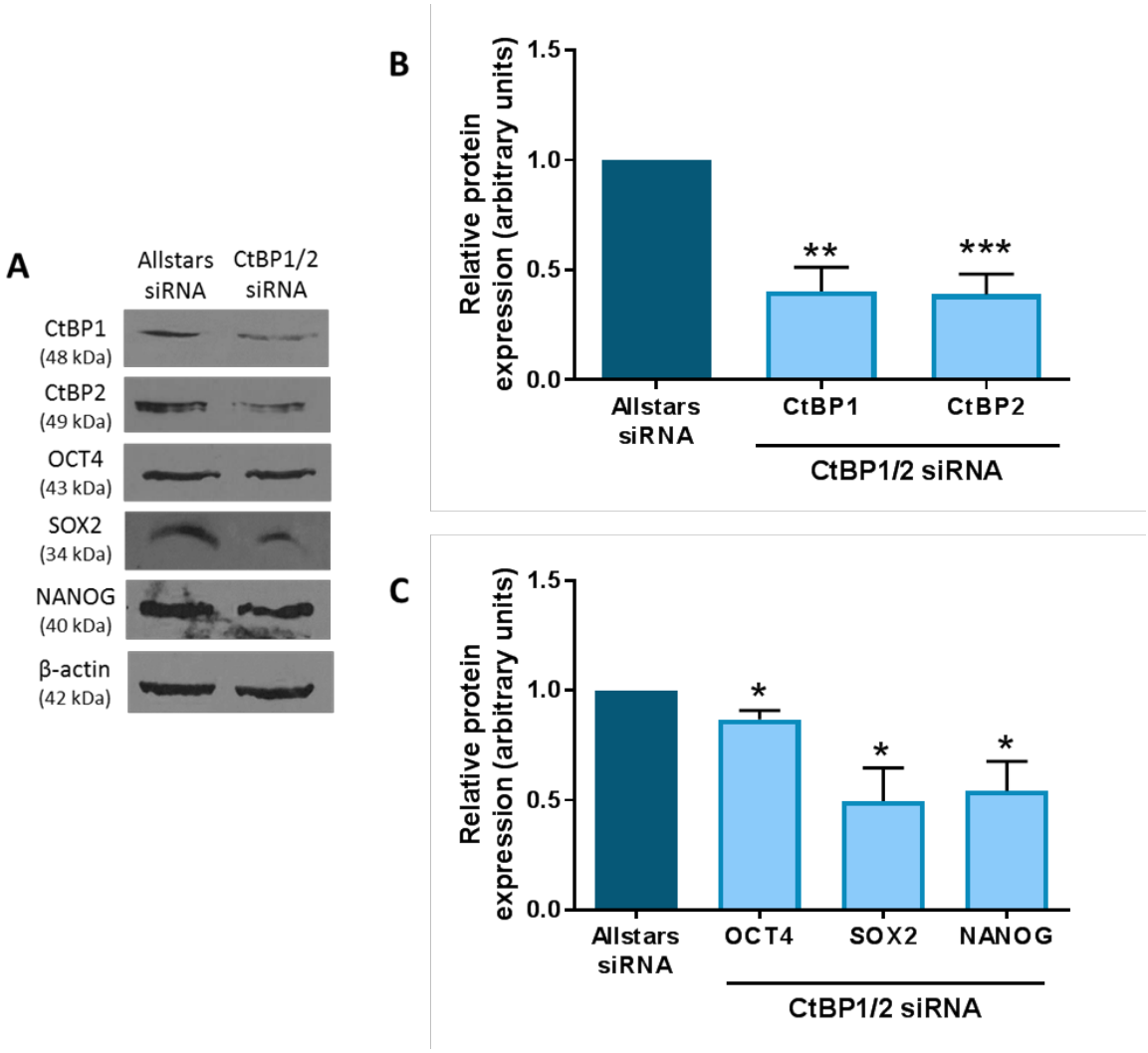

Figure 8.23. Silencing both CtBP isoforms decreases pluripotency marker expression in NT2 hECCs maintained at 5% oxygen using CtBP1/2 siRNA.

(A) Representative Western blots of CtBP1, CtBP2, OCT4, SOX2 and NANOG expression in NT2 hECCs cultured at 5% oxygen and transfected with either Allstars negative control siRNA or CtBP1/2 siRNA. (B) Quantification of CtBP1 and CtBP2 Western blots revealed the silencing of both CtBP isoforms in NT2 hECCs transfected with CtBP1/2 siRNA compared to the Allstars negative control. (C) Quantification of OCT4, SOX2 and NANOG Western blots in NT2 hECCs transfected with CtBP1/2 siRNA compared to the Allstars negative control siRNA. Data were normalised to β-actin, and then to 1 for Allstars control. Bars represent mean ± SEM. (n=5-7)

8.3 Discussion

A glycolytic phenotype is critical to the ability to self-renew in cell types that express pluripotency markers and can potentially open more avenues for the therapeutic use of hESCs and potential treatments against hECCs and other cancer stem cell types. However, the differences in the mechanisms behind the glycolytic phenotypes and the metabolic regulation of self-renewal between hESCs and hECCs may help to dissect the interface between stem cell biology and tumour progression.

The metabolic phenotype of a cell is strongly linked with self-renewal, and so this chapter aimed to investigate whether the rate of glycolysis regulated the ability to self-renew in hECCs maintained under hypoxia. Furthermore, the CtBP family of glycolytic sensors have been demonstrated in Chapter 4 and Chapter 6 to be regulated by glycolysis and have a role in the transcriptional activation of pluripotency marker expression in hESCs. Thus, deciphering whether these mechanisms of regulation were similar in hECCs would provide a valuable insight into the similarities between stem cell biology and tumour progression.

8.3.1. Increased rate of glycolysis supports self-renewal and CtBP expression in NT2 hECCs

It is well documented that hESCs use glycolysis to maintain a pluripotent state and the ability to self-renew, and previous studies have demonstrated that hESCs cultured in a less glycolytic environment expressed lower levels of the pluripotency markers OCT4, SOX2 and NANOG (Ezashi et al., 2005; Westfall et al., 2008; Forristal et al., 2010). hECCs also rely on a predominantly glycolytic metabolism (Abu Dawud et al., 2012; Jang et al., 2015). Previous studies have demonstrated that the expression of NANOG supports the maintenance of a glycolytic metabolic state by repressing the expression of genes associated with mitochondria and OXPHOS (Chen et al., 2016). However, it is not known whether metabolism, also, supports the maintenance of self-renewal in hECCs. Inhibiting glycolysis in NT2 cells maintained at 5% oxygen using the glycolytic inhibitor 2-DG demonstrated that pluripotency marker expression significantly decreased in the presence of 2-DG with no clear toxic effects to the cells compared to the control. These data demonstrated that an increased rate of glycolysis in hECCs enhances the expression of pluripotency genes; a mechanism that was also observed in hESCs (Chapter 4). This highlights the importance of the metabolic state in maintaining a pluripotent phenotype. This observation also reemphasised that a loss of pluripotency marker expression results

in a metabolic shift towards a more oxidative based metabolism as inhibiting glycolysis would result in a loss of NANOG expression, for example, and thus a loss of the repression of genes associated with OXPHOS.

Data from Chapter 7 has already demonstrated that CtBP expression is increased under hypoxia in hECCs, much like hESCs. However, whether CtBP expression was influenced by glycolytic rate in hECCs, as well as hESCs, remained to be characterised. Quantification of CtBP mRNA and protein expression in response to the addition of 2-DG, and therefore a reduced glycolytic rate, significantly decreased compared to the control. Both CtBP and pluripotency marker expression has been shown to be influenced by glycolytic rate in both hECCs and hESCs. These data suggest a role for glycolysis in maintaining self-renewal regardless of cell type.

Furthermore, HIF-2α expression significantly decreased in hECCs under hypoxia when glycolysis was inhibited. This trend was also observed in hESCs (Chapter 4) and suggests that glycolytic metabolism also regulates HIF-2α expression independent of cell type. This decrease in HIF-2α expression as a result of inhibiting glycolysis is one potential mechanism explaining the observed decreases in pluripotency marker and CtBP expression, as HIF-2α has been demonstrated to directly bind to HRE sites in the proximal promoters of these genes. Thus, decreasing HIF-2α protein expression would reduce the availability of the transcription factor to bind to the HREs, but any epigenetic effect induced by inhibiting glycolysis and resulting in a more heterochromatic state around the HRE sites cannot be overlooked as an alternative potential mechanism. In addition, it is also worth noting that HIF-2α is known to increase the expression of several glucose transporters and glycolytic enzymes that would form a feed-forward loop to maintain a high rate of flux through glycolysis in hECCs. Further work is required to determine if this metabolic regulation also applies to HIF-1α in hECCs, although it is hypothesised that HIF-1α expression would also be regulated by glycolysis due to its homogeny to HIF-2α.

The effect of inhibiting glycolysis in NT2 cells maintained under 20% oxygen was also investigated and results in this chapter revealed a significant reduction in OCT4, SOX2, NANOG, both CtBP isoforms and HIF-2α expression when glycolysis was inhibited. This suggests that the rate of flux through glycolysis is regulating the expression of pluripotency markers in hECCs via HIF-2α regardless of environmental oxygen tension;

the same observation as described previously in hESCs. It is also worth noting that 10mM 2-DG was added to NT2 cells maintained at 20% oxygen compared to the 30mM 2-DG concentration added to cells cultured at 5% oxygen. This likely reflects the higher rate of flux through glycolysis observed in NT2 cells maintained under hypoxia and required a higher concentration of 2-DG to inhibit glycolysis.

It has previously been reported that cancer stem cells display a unique metabolic plasticity switching between OXPHOS and glycolytic based metabolic phenotypes in the presence of oxygen to maintain homeostasis and promote tumour growth. There is contradicting evidence in the literature about which metabolic pathway cancer stem cells of certain tumours more strongly favour. For example, cancer stem cells from breast, lung and ovarian tumours and osteosarcomas all are reported to favour glycolysis. Whereas, the cancer stem cells derived from glioblastomas or ductal adenocarcinomas and even studies with breast cancer stem cells again favour OXPHOS as the preferred form of energy production. This may be due to the heterogeneity of cancer stem cells across different histological tumour types, or based on their location in the tumour microenvironment and as such the level of oxygen exposure (Snyder et al., 2018). Cancer stem cells maintained in normoxic conditions can engage in glycolysis and/or OXPHOS whereas, similar to embryonic stem cell maintenance, cancer stem cells maintained in a hypoxic environment results in the overexpression of HIF-1α and the activation of several glycolytic proteins, such as the glucose transporters GLUT1 and GLUT3, as well as various isoforms of glycolytic enzymes. In addition to this, a recent review highlights some potential differences in the transcriptional regulation of stem cell and cancer stem cell metabolism (Alptekin et al., 2017). Transcription factors promote either glycolysis or OXPHOS but not both. For example, HIF-1α and the pluripotency factors OCT4 and NANOG have been shown to induce a glycolytic phenotype, whereas the family of transcription coactivators, PGC1α and PGC1β, play a major role in the transcriptional activation of mitochondrial biogenesis and functional capacity. This suggests that normal stem cells and cancer stem cells might use distinct transcriptional programs for control of their metabolic states. Therefore, although the metabolic regulation of self-renewal remains the same between hECCs maintained at 5% oxygen and 20% oxygen, further work is required to determine if the exact mechanisms are different or not between oxygen tensions, including the measurement of the amount of OXPHOS occurring in hECCs maintained at either 5% or 20% oxygen and the measurement of ROS. These experiments

would provide further insight into whether HIF-1α, or HIF-2α, dynamically regulates glucose metabolism based on oxygen availability and defend against the risk of increased ROS production to maintain self-renewal similarly to a previous mechanism in breast cancer stem cells (Semenza, 2017), or whether there may also be a HIF-independent regulation of self-renewal.

Although the exact mechanisms of glycolytic regulation of HIF expression in hECCs remains to be fully characterised, data presented in this thesis reveal that the glycolytic phenotype is essential to maintaining the ability to self-renew in hECCs; akin to the data reported in hESCs. As there is this intrinsic requirement for a highly glycolytic metabolism in more than one pluripotent cell type, it reemphasises the importance of glycolysis in stem cell biology. However, it is worth noting that the acquisition of the ability to self-renew in both cell types may differ and may offer more insight into how a highly glycolytic phenotype is obtained in order to become pluripotent, however is beyond the scope of this work.

8.3.2. CtBPs in the transcriptional activation of pluripotency markers in NT2 hECCs cultured at 5% oxygen

Data in Chapter 6 has previously demonstrated that CtBPs had a role in the transcriptional activation of OCT4, SOX2 and NANOG in hESCs. Therefore, data in this chapter sought to investigate whether that regulation was maintained in hECCs, in order to provide further insight into how metabolism may influence the self-renewal of hECCs.

NT2 hECCs maintained at 5% oxygen were transfected with CtBP1/2 siRNA to silence both CtBP isoforms simultaneously and revealed a significant decrease in the mRNA and protein expression of OCT4, SOX2 and NANOG in hECCs. *Talin-1* (unpublished data) and *E-cadherin* are known CtBP-repressed genes (Grooteclaes and Frisch, 2000; Grooteclaes et al., 2003; Alpatov et al., 2004; Ichikawa et al., 2015) and hence the observed significant increase in their mRNA expression as a result of silencing CtBPs indicates that there is sufficient silencing to illicit a functional response in NT2 hECCs. This suggests that CtBPs have a potential role in the transcriptional activation of pluripotency genes in NT2 hECCs cultured at 5% oxygen.

These data demonstrate that CtBPs regulate pluripotency marker expression in hECCs, in addition to hESCs, and suggest that metabolic sensors may have a role in maintaining self-renewal independent of cell type. Unfortunately, there are still a lot of unknowns to

draw a conclusive mechanistic hypothesis for the role of CtBPs in maintaining self-renewal in hECCs. However, a higher rate of flux through glycolysis in theory results in an increase in the levels of free intracellular NADH. This increased NADH would increase the number of functional CtBP dimers available to translocate to the nucleus and aid in the activation of pluripotency markers in hECCs. This may be one potential mechanism of how hECCs gain a pluripotent state once a metabolic switch from OXPHOS to glycolysis has occurred in the malignant cell type.

Together, data in this chapter reemphasises that metabolism has a major role in the control of stem cell function and fate (Figure 8.24).

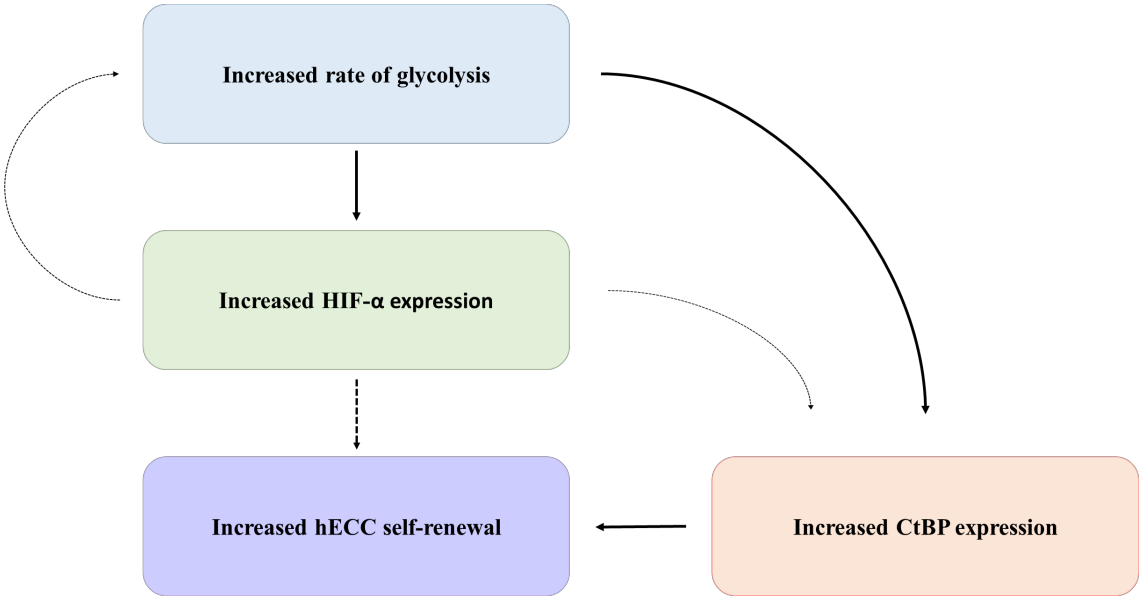

Figure 8.24. Schematic of the metabolic regulation of self-renewal in hECCs under hypoxia. hECCs maintained under hypoxia display a higher rate of flux through glycolysis leading to an increase in the expression of HIF-2α expression, but also CtBP and pluripotency marker expression. It is currently unclear as to whether the observed expression increases are a direct or indirect effect of an increased rate of glycolysis, but an increased glycolytic rate leads to increased hECC self-renewal, Furthermore, CtBPs were observed to drive pluripotency marker expression and thus self-renewal in hECCs under hypoxia, either by acting as a transcriptional coactivator and enhancing OCT4, SOX2 and NANOG expression or as a transcriptional corepressor and silencing the expression of early differentiation marker expression. Black arrows indicate data presented in this chapter, whereas dashed arrows represent data presented in other chapters in this thesis and previous literature.

8.4 Conclusions

Data presented in this chapter revealed that:

- Pluripotency marker, CtBP and HIF-2α expression is influenced by changes in glycolytic rate in NT2 hECCs maintained both 5% and 20% oxygen.
- Silencing both CtBP isoforms in NT2 hECCs cultured under hypoxic conditions decreases hECC self-renewal.

Chapter 9

Discussion

Chapter 9: Discussion

Understanding the mechanisms behind the acquisition of pluripotency and maintenance of self-renewal is critical for not only defining optimal hESC culture conditions, and therefore improve resources for hESC researchers, but also to better understand development and to ensure a highly pluripotent population of cells for use in regenerative medicine.

Much evidence now suggests that culturing hESCs under hypoxic conditions increases the rate of flux through glycolysis, and upregulates the expression of pluripotency markers (Ezashi et al., 2005; Westfall et al., 2008; Forristal et al., 2010; Forristal et al., 2013; Christensen et al., 2015). Yet, how alterations in hESC metabolism affect changes in gene expression has remained largely overlooked. The results presented in this thesis provide the foundations of evidence that glycolysis regulates the expression of pluripotency markers, CtBPs and JMJDs in hESCs by modulating HIF-2α expression and accumulating in increased hESC self-renewal. Furthermore, this study has revealed that the CtBP family of glycolytic sensors are involved in the transcriptional activation of pluripotency markers OCT4, SOX2 and NANOG in hESCs cultured under long-term hypoxia. These findings have an important impact on the maintenance of the pluripotent state in hESCs by re-emphasising the benefit of hypoxic culture of hESCs for maintaining a highly glycolytic and pluripotent population of cells whilst highlighting the link between cellular metabolism and gene expression patterns through CtBPs.

Data in this thesis has revealed a host of regulatory mechanisms and feedback loops involving glycolysis, hypoxia and epigenetics that ultimately collaborate to enhance hESC self-renewal (Figure 9.1). Although it is still not clear how pluripotency is acquired initially, it is clear that there are several feed forward loops at play that support the maintenance of a pluripotent state and the ability to self-renew, and to enhance that further.

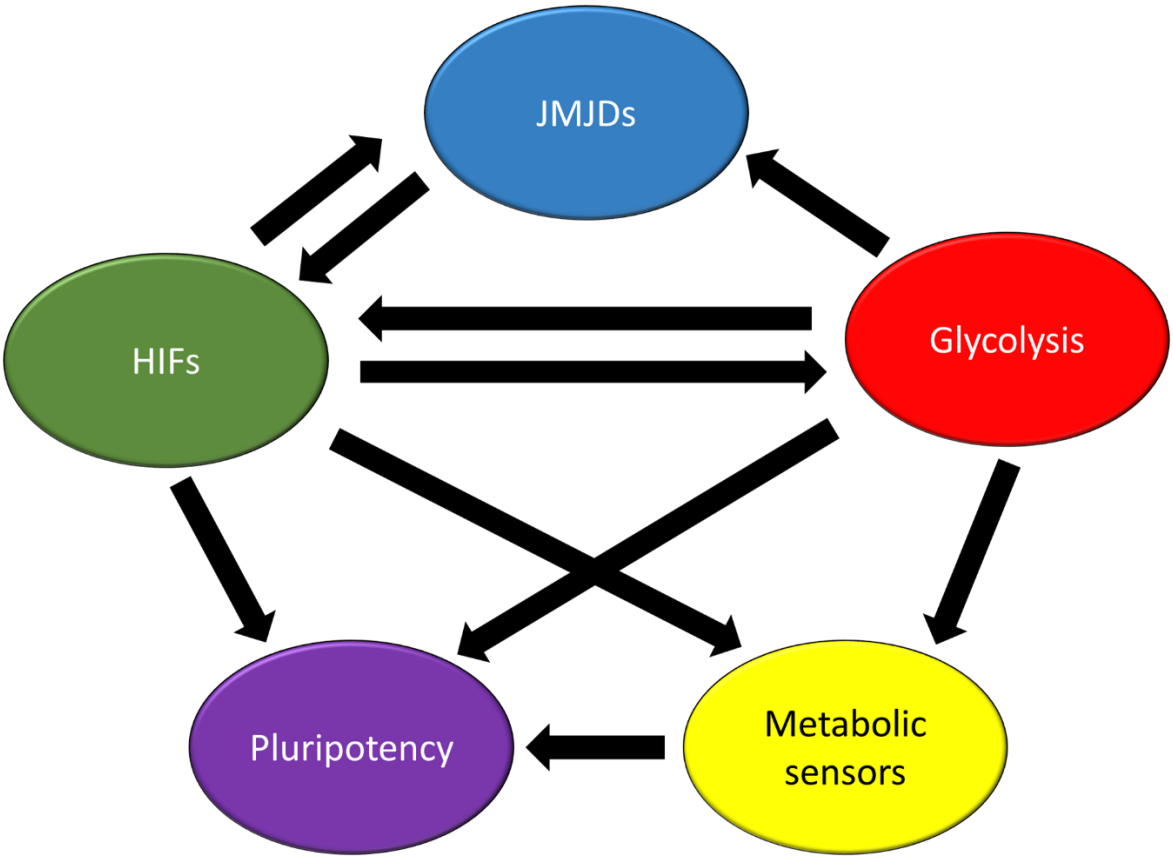

Figure 9.1 Overview of the relationships between epigenetics, glycolysis, hypoxia and pluripotency in hESCs.

hESCs maintained under atmospheric oxygen tensions already express the core pluripotency markers OCT4, SOX2 and NANOG and display a highly glycolytic metabolism. Several previous studies and data presented in this thesis have revealed that culturing hESCs under hypoxia is beneficial to hESC self-renewal as the low oxygen environment drives the expression of HIF-α subunits to further enhance the expression of genes associated with glycolysis to augment the rate of flux through glycolysis, but also increase the expression of pluripotency markers.

Adapting to the hypoxic environment within the first 48 hours of exposure is driven by HIF-1α expression. HIF-1α has been shown in a range of other cell types to directly bind and enhance the expression of genes associated with glycolysis such as LDHA, HK2 and GLUTs, which most likely accounts for the increased rate of flux through glycolysis observed in hESCs maintained under hypoxia. However, data from this thesis has revealed that HIF-1α regulates the expression of JMJD2c in order to open the chromatin

region around HREs in HIF-1α target genes to allow HIF-1α access to the relevant binding sites, although those molecular mechanisms still need to be investigated. This partnership between HIF-1α and JMJD2c plays a role in helping hESCs to prepare themselves for long-term hypoxic culture and also probably increase the expression of genes, potentially HIF-3α, that will reduce HIF-1α and JMJD2c expression so the long term response can take over whilst increasing the resistance to oxidative stress.

HIF-2α is the predominant regulator of the long term hypoxic response in hESCs (Forristal et al., 2010; Petruzzelli et al., 2014). HIF-2α is stabilised under hypoxic culture conditions and heterodimerises with HIF-1β to become active and bind to HRE binding sites in the promoter regions of HIF-2α target genes (Semenza and Wang, 1992; Wang and Semenza, 1993b; Semenza, 1996). Previous studies have shown that GLUT1, GLUT3, PKM2 and other glycolysis-associated genes are downstream targets of HIF-2α (Wang and Semenza, 1993b; Semenza et al., 1994; Semenza, 2000b; Forristal et al., 2013; Christensen et al., 2015) which leads to a further increased rate of flux through glycolysis when cells are cultured under hypoxic conditions. Data from this study has also demonstrated that HIF-2α regulates the expression of other JMJD family members which are responsible for removing the H3K9me3 marks from the proximal promoter genes of target genes and leaving them in a more euchromatic state to allow HIF-2α access to the HRE binding sites. JMJD2a, in particular, was demonstrated to play a role in hESC self-renewal. Although the exact mechanism remains to be fully characterised, it is likely that JMJD2a maintained a euchromatic site around the HREs in the OCT4, SOX2 and NANOG proximal promoters to allow HIF-2α binding and an increase in the expression of these pluripotency markers.

As a result of the data presented in this study, it is hypothesised that CtBP1 and CtBP2 expression is also upregulated as a result of HIF binding to the potential HRE binding sites in the proximal promoter regions of both CtBP genes in hESCs cultured under hypoxic conditions compared to atmospheric oxygen. Silencing HIF-2α led to a significant decrease in CtBP expression in hESCs maintained at 5% oxygen, which suggested that its expression is regulated by HIFs. Additionally, this would explain why a decrease in CtBP expression was seen in hESCs cultured at 20% oxygen compared to those cultured at 5% oxygen, as the HIFs expressed in hESCs maintained under atmospheric oxygen tensions would be ubiquitinated and therefore degraded, and so would not be able to enhance CtBP expression.

During glycolysis, NAD^+ is reduced to NADH. However, as previously described, hESCs cultured under hypoxic conditions have a higher glycolytic flux and as a result produce more NADH compared to those cultured under 20% oxygen tensions. The increased levels of free NADH and the increase expression of CtBPs observed in hESCs maintained under 5% oxygen tensions allows more CtBP dimerisation and therefore, more active CtBP dimers can translocate to the nucleus (Kumar et al., 2002; Balasubramanian et al., 2003), where data presented in this study revealed that CtBPs were located in hESCs at either oxygen tension. In the nucleus, CtBP dimers are recruited to DNA-binding TFs that contain a PXDLS binding motif, and in turn recruit chromatin modifying complexes to change the chromatin around CtBP target genes to a more euchromatic state, which we hypothesise could include proteins such as HDMs and HATs, and drive CtBP target gene expression, assuming CtBPs acting as coactivators uses the same basic mechanism as CtBP-mediated repression. Silencing CtBPs in this study has demonstrated a significant decrease in pluripotency markers as a consequence of the loss of CtBP. Therefore, the data suggests that OCT4, SOX2 and NANOG are downstream targets of CtBPs and consequently, CtBPs aid in the maintenance of hESC pluripotency under hypoxic conditions. However, it remains to be elucidated whether the significant reduction of pluripotency marker expression due to the silencing of CtBPs is a result of CtBPs directly binding to the promoter regions of OCT4, SOX2 and NANOG, or an indirect effect. Furthermore, the first histone lysine demethylase KDM1A, also known as LSD1, was identified as part of the CtBP1 corepressor complex (Shi et al., 2003). This suggests that perhaps other JMJD proteins are working in complexes to aid in the coactivation of target genes, notably OCT4, SOX2 and NANOG.

However, the overriding regulator of HIF, JMJD, CtBP and crucially pluripotency marker expression in hESCs is the metabolic state of the cell. While hypoxic culture supports a higher rate of flux through glycolysis in hESCs, data presented throughout this thesis has demonstrated that inhibiting glycolysis using multiple inhibitors has reduced the expression of all these aforementioned proteins and suggests that glycolysis is intrinsic to hESC self-renewal. Even though hypoxic culture enhances the rate of glycolysis, hESCs maintained under atmospheric oxygen tensions can also self-renew and display a reliance on glycolysis. While further work is required to decipher the mechanisms behind how a hESC acquires a highly glycolytic metabolism initially, more and more evidence supports the theory that that metabolic state of the cell, in combination with the plethora of feed

forward loops identified in this thesis, delay ESC differentiation and enhance self-renewal.

Further to this hypothesised mechanism, data in this study revealed that both pluripotency marker, JMJD and CtBP expression was significantly decreased after 2-DG or 3-BrP treatment and hence a lower rate of glycolysis in hESCs in hypoxic conditions. This trend had previously been documented for pluripotency markers (Folmes et al., 2011), but not for JMJD or CtBP expression. Interestingly, it appears that metabolism, as well as hypoxia, enhanced JMJD and CtBP expression and presents further insights into how glycolysis supports hESC self-renewal through the action of JMJDs and HIFs, and a potential additional mechanism of how increased CtBP expression and hence increased CtBP activity aid in the maintenance of the pluripotent state, although how this is regulated or directly affects pluripotency marker expression remains unknown. Previous studies have documented that several different metabolites, like acetyl-coenzyme A, S-adenosylmethionine and NAD^+, are required for histone acetylation, DNA methylation and histone deacetylation, respectively (Wellen et al., 2009; Moussaieff et al., 2015; Etchegaray and Mostoslavsky, 2016), so it is possible that certain metabolites are necessary to aid the action of JMJDs and other chromatin modifiers to change the chromatin around the CtBP and pluripotency marker genes to a more euchromatic state, and enhance the transcription of CtBPs, but crucially OCT4, SOX2 and NANOG. However, it is worth exploring further as to whether PKM2 plays a critical role in the glycolytic regulation of hESC self-renewal. Previous studies have linked the glycolytic enzyme with the activation of HIF-1α target genes, JMJD expression and also a correlation with the expression of the pluripotency marker OCT4. There is a possibility that PKM2 may be acting directly on these genes, or through signalling pathways such as NF-κB and STAT3 to support hESC self-renewal.

Overall, data presented in this thesis proposes a mechanism for the acquisition of a higher rate of flux through glycolysis in hESCs exposed to hypoxia for no more than 48 hours, and also how hESC self-renewal is regulated under long term hypoxic culture at the epigenetic and metabolic levels. Under normoxia, HIF-α subunits are degraded by PHDs and lead to a more heterochromatic state with increased expression of histone markers associated with gene silencing such as H3K9me3. Upon exposure to hypoxia, HIF-1α

expression increases to initiate adaptation to the hypoxic environment. This includes an increase in the expression of the histone demethylase JMJD2c, and is hypothesised to increase the rate of flux through glycolysis associated with hypoxic culture of hESCs, although further work is required to investigate this hypothesis. It is this hypothesised increase in glycolysis obtained in the first 48 hours of exposure to hypoxia that leads to the increased expression of HIF-2α potentially through PKM2, although this mechanism remains to be fully characterised also, to ultimately enhance the expression of JMJDs. The increased JMJD expression, particularly JMJD2a, generates a more euchromatic state within the HRE sites of the pluripotency markers OCT, SOX2 and NANOG where there is increased expression of the histone marker associated with gene activation H3K36me3. This euchromatic conformation facilitates HIF-2α binding to the HREs within the proximal promoter regions of OCT4, SOX2 and NANOG. Hypoxic culture and therefore increased glycolytic rate also leads to an increase in the expression of the glycolytic sensors CtBPs, which can dimerise and become active through the increased levels of free NADH produced during glycolysis, to again enhance the expression of pluripotency markers OCT4, SOX2, NANOG, LIN28b and SALL4 and increase hESC self-renewal (Figure 9.2).

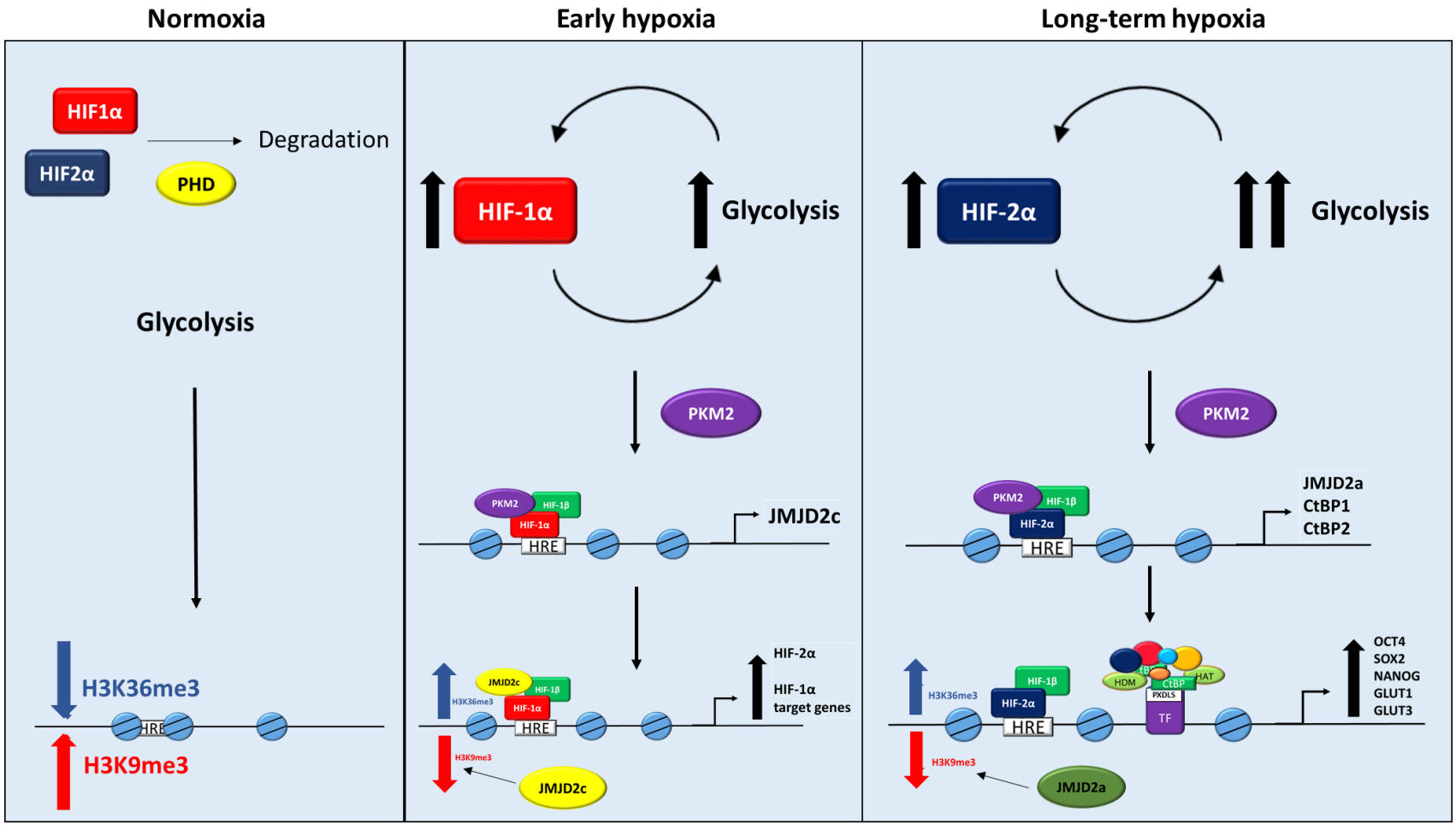

Figure 9.2. Schematic of the proposed mechanisms regulating hESC self-renewal under hypoxia.

Under hypoxia, HIF-α subunits are targeted for degradation by PHDs and VHL proteins. hESCs cultured under atmospheric oxygen display a highly glycolytic metabolism and express pluripotency markers. Upon exposure to hypoxia, HIF-1α expression is increased which helps hESCs to adapt to the hypoxic environment. Particularly, HIF-1α increases the expression of glycolytic enzymes and glucose transports, but also the chromatin modifier JMJD2c. Together, this results in a more euchromatic state in the proximal promoter regions of HIF-1α target genes, which potentially includes HIF-2α and also genes responsible for decreasing HIF-1α expression after 48 hours of hypoxic culture. HIF-2α becomes the predominant regulator of the hypoxic response and drives the expression of genes associated with glycolysis to further increase the rate of flux through glycolysis, but also other JMJD family members, notably JMJD2a, and the metabolic sensors CtBPs. The increased expression of JMJD2a creates a more euchromatic state around the HREs in the proximal promoter regions of OCT, SOX2, NANOG, GLUT1 and GLUT3, as well as the binding sites of transcription factors that contain a PXDLS-binding motif. Together, this DNA binding enhances the expression of pluripotency markers to maintain hESC self-renewal, but also maintain the expression of glycolytic genes to maintain the high rate of glycolytic flux and delay ESC differentiation. Further work is required to fully characterise these mechanisms.

Previous studies have addressed the similarities between hESCs and hECCs, primarily that both cell types express pluripotency markers. As a result, it was believed that hECCs could be a useful resource to understand the mechanisms behind pluripotency maintenance and therefore, provide a model system for hESC research, without the issues of spontaneous differentiation and difficulties maintaining hESCs in culture. Data presented in this thesis have highlighted some of those similarities and differences summarised in Table 9.1.

Table 9.1. Comparison of the mechanisms maintaining self-renewal in hESCs and hECCs maintained under hypoxia.

	hESC	hECC
Hypoxic regulation of pluripotency marker expression	Yes	No
Hypoxic regulation of CtBP expression	Yes	Yes
Glycolytic regulation of pluripotency marker expression	Yes	Yes
Glycolytic regulation of CtBP expression	Yes	Yes
Glycolytic regulation of HIF-2α	Yes	Yes
Regulation of pluripotency marker expression by CtBPs	Yes	Yes

Data currently presented in this study reveals that the mechanisms that maintain self-renewal are very similar between pluripotent cell types. While the glycolytic regulation, regulation of OCT4, SOX2 and NANOG expression by CtBPs and hypoxic regulation of CtBPs was maintained between hESCs and hECCs. Interestingly though, pluripotency marker expression was not regulated by oxygen tension in hECCs. Further investigations to attempt and understand these discrepancies revealed that in NT2 hECCs maintained under 20% oxygen both HIF-1α and HIF-2α protein was expressed and not degraded due to increased NO levels. While NO levels in hESCs maintained at either 5% or 20% oxygen have not currently been analysed, the fact that NO levels have been shown to prevent HIF degradation and ultimately lead to the accumulation of HIF-α subunits

provides an avenue of investigation that might provide insights into how hECCs acquire the ability to self-renew, but also how HIF-1α expression may be increased upon the initial exposure to hypoxia and start cellular adaptation to a low oxygen environment. Several studies in neurons, astrocytes and ovarian cancer cells have demonstrated that NO induces glycolysis in cells under both normoxia and hypoxia (Almeida et al., 2004; Benavides et al., 2013; Li et al., 2017), therefore may be a reason why even hESCs maintained under normoxia display a highly glycolytic metabolism. But further experiments are required in order to fully elucidate this potential role of NO in the acquisition of the ability to self-renew in all pluripotent cell types in order to understand how a cancer stem cell progresses but also to understand the earliest stages of development.

In summary, the data presented in this study suggest that, while hypoxic culture plays a role in enhancing pluripotency, the metabolic state of the cell is intrinsic to regulating all the mechanisms behind the regulation of stem cell self-renewal and maintaining that ability to prevent differentiation.

9.1 How an understanding of maintaining hESC self-renewal may benefit stem cell research

Given the potential of hESCs in regenerative medicine, the data presented in this study suggests that hESCs should be routinely cultured under hypoxic conditions in a high glucose medium, which as a result would increase the glycolytic rate of flux and the expression of HIF-2α, JMJDs and CtBPs and subsequently drive pluripotency marker expression, as previously described. Culture under hypoxia would allow increased HIF-2α driven expression of glycolytic genes to maintain a high rate of flux through glycolysis and form a feed forward loop to maintain a pluripotent cell identity. Culture under hypoxia would increase the expression of JMJDs leading to the continual removal of H3K9me3 repressive histone modifications and a more euchromatic state. This would give HIF-2α more access to HREs to driven target gene expression. Finally, culture under hypoxia would increase CtBP expression. This coupled with a high concentration of glucose in the culture medium would prevent the glycolytic rate from being limited by substrate availability and ensure CtBP dimerisation. With the increased CtBP expression,

there may not be enough NADH produced to create as many functional CtBP dimers as possible. It may be worth investigating whether supplementing a high glucose medium with proteins such as HIF-2α, JMJD2a and CtBPs may further increase the rate of flux through glycolysis in hESCs maintained under hypoxia in order to push hESCs further up the pluripotency scale and further away from the onset of early differentiation.

9.2 How an understanding of maintaining hESC self-renewal may benefit regenerative medicine

Understanding how a pluripotent state is supported by hypoxia and glycolytic metabolism in hESCs could also be beneficial for the generation of iPSCs for regenerative medicine applications. Many similarities have been drawn between hESCs and iPSCs including the expression of pluripotency markers and a dependence on a primarily glycolytic metabolism, which seems to be vital for maintaining self-renewal in both cell types (Prigione and Adjaye, 2010; Folmes et al., 2011; Varum et al., 2011). Current methods utilise a 'cocktail' of TFs; OCT4, SOX2, KLF4 and C-MYC, to drive reprogramming, but often requires viral transduction. Therefore, many studies have been performed to investigate whether small molecules could be used to replace the TF cocktail in the reprogramming of somatic cells (Hou et al., 2013; Kang et al., 2014; Lin and Wu, 2015), where these small molecules are required to induce changes that lead to a more glycolytic metabolism and increased expression of pluripotency genes. As the metabolic state of hESCs and iPSCs is very similar, it appears that a glycolytic metabolism is crucial to enhance the expression of pluripotency markers in both cell types. Linking these changes in metabolism to induce changes in gene expression may provide a new insight and direction in the production of iPSCs, where HIF-2α, JMJDs and/or CtBPs could be utilised as part of a small molecule cocktail, or as part of a series of small molecule additions, to enhance reprogramming.

Additionally, understanding that hypoxia and glycolytic rate are key influences on enhanced pluripotency marker expression in hESCs should be a primary focus for the design of small molecules for generating iPSCs. Small molecules could be designed to promote an increased rate of glycolysis in somatic cells undergoing reprogramming, whilst being maintained under hypoxic conditions. Then, the addition of other compounds, such as JMJDs or CtBPs, could link the activated glycolytic metabolism to increased pluripotency marker expression. However, the utilisation of JMJDs and CtBPs in reprogramming would rely on further investigation examining whether further

increasing JMJD and CtBP expression in hESCs maintained under hypoxic conditions increased pluripotency marker expression further.

Furthermore, monitoring the expression of these proteins may aid in the *in vitro* differentiation of pluripotent cell types into a desired cell type for regenerative medicine purposes and allow the derivation of much more efficient methodologies.

9.3 How an understanding of hECC self-renewal may benefit the development of cancer therapies

As the hypoxic regulation of pluripotency markers is lost in hECCs compared to hESCs, at least in part through NO, designing potential NO-based cancer therapeutics to reduce the expression of OCT4, SOX2 and NANOG specifically, and therefore tumourigenic capacity, would be a useful direction to explore, particularly for the treatment of testicular teratocarcinomas. Low levels of NO (<100nM) have been associated with increased proliferation and angiogenesis, medium levels of 100-500nM have been linked to increased invasiveness and repression of apoptosis, whereas high NO levels of >500nM are correlated with increased DNA damage, cytotoxicity and apoptosis (Vahora et al., 2016). Therefore, designing novel cancer treatments that could selectively target cancer stem cells and deliver compounds that could increase NO levels in those cells, or increase PHD expression, to ultimately reduce OCT4, SOX2 and NANOG expression and induce differentiation or apoptosis. Inhibiting the action of HIFs and reducing the rate of glycolysis through pharmacological means, in theory, would decrease CtBP expression and thus their role in supporting hECC self-renewal and additionally suppress the sensitivity of breast cancer cells to chemotherapy agents as demonstrated by previous studies (Grooteclaes et al., 2003; Wang et al., 2006b; Birts et al., 2010). Additionally, another previous study in breast cancer cells demonstrated that treating highly glycolytic cells with a CtBP inhibitor reduced the mitotic fidelity and proliferation of the breast cancer cells, whereas the mitotic fidelity of cells displaying a lower rate of glycolytic flux was not affected (Birts et al., 2013). This links the enhanced glycolytic metabolism with the tumour cell phenotype, but also identifies an alternative therapeutic strategy by disrupting the CtBP dimerisation and the formation of the CtBP chromatin-modifying complex.

Investigations highlighting the links between metabolism, hypoxia and pluripotency might be more beneficial to cancer research. It is widely acknowledged that cancer cells

display a similar metabolic state to hESCs, particularly a reliance on aerobic glycolysis known as the Warburg effect. It has also been documented that elevated HIF-1α expression is correlated with a poor clinical prognosis in various cancer types (Birner et al., 2000; Aebersold et al., 2001; Birner et al., 2001a; Birner et al., 2001b; Bos et al., 2001; Schindl et al., 2002) and OCT4 expression is associated with bladder, gastric and colorectal cancers and tumour recurrence (Atlasi et al., 2007; Saigusa et al., 2009; Asadi et al., 2011; Yasuda et al., 2011) and furthermore, HIF-2α expression is elevated in aggressive cancers such as renal cell carcinoma. Therefore, limiting the rate of glycolysis would reduce HIF-α expression and consequently pluripotency marker expression. In theory, this would mean that hECCs would no longer be pluripotent or classed as stem cells and should reduce the recurrence of the cancer.

Data from this thesis suggests that metabolism is influencing the pluripotent state of the cell, but the metabolic state of the cell itself is regulated in part by a hypoxic environment. Therefore, the potential pharmacological inhibition of HIFs offers a novel therapeutic strategy for cancer treatments, particularly HIF-2α as this subunit has been shown to directly bind to the proximal promoters of OCT4, SOX2, NANOG and CtBPs and all cells need glycolysis. In fact, a recent study has demonstrated that pharmacological HIF inhibition significantly limits tumour growth and progression in a colorectal cancer model (Shay et al., 2014). Specifically delivering microRNAs that target HIF-2α mRNA for degradation could be a feasible option to reduce HIF expression.

9.4 Future Work

The objective of any future work subsequent to this thesis would be to mechanistically determine how glycolysis, JMJDs, HIFs and CtBPs coordinate to maintain hESC self-renewal. Additionally, further characterisation of the differences between the mechanisms supporting self-renewal in hESC and hECCs may help to provide improved cancer treatments. In order to achieve this, the following investigations could be performed:

- To determine whether HIF-1α can also bind to the identified HRE sites in the OCT4, SOX2, NANOG and CtBP proximal promoters
- To determine whether HIF-2α can bind to other potential HRE sites in the proximal promoter regions of OCT4, SOX2 and NANOG genes
- To overexpress HIF-2α in hESCs maintained at either 5% and 20% oxygen and evaluate the effects on pluripotency marker, JMJD and CtBP expression
- To analyse the rate of glucose consumption in hESCs maintained under hypoxia and incubated in the presence or absence of glycolytic inhibitors
- To inhibit OXPHOS in hESCs maintained at either 5% or 20% oxygen to analyse whether pluripotency marker expression increases
- To further investigate how glycolysis is increasing JMJD expression
- To determine if PKM2 plays a role in the glycolytic regulation of self-renewal
- To evaluate the effect of inhibiting NF-κB signalling on hESC and hECC self-renewal, particularly HIF-2α expression
- To determine whether HIF-1α directly binds to the JMJD2c proximal promoter in hESCs exposed to hypoxia for less than 48 hours using ChIP assays
- To analyse the changes in metabolic rate and expression of glycolytic enzymes and glucose transporters within the first 48 hours of exposure to hypoxia
- To evaluate the chromatin modifications in the proximal promoter of JMJD2c between hESCs exposed to normoxia, early hypoxia and long term hypoxia
- To evaluate the changes in histone modifications within the proximal promoters of any HIF-1α target genes in early hypoxia when JMJD2c was silenced
- To silence the other JMJD family members individually and in combination with each other in hESCs maintained under hypoxia and evaluate the effects on pluripotency marker and HIF-2α expression

- To investigate whether HIF-2α directly binds to the proximal promoter regions of JMJD genes
- To investigate the expression and regulation of JMJDs in hECCs maintained at both 5% and 20% oxygen
- To investigate the DNA methylation status of chromatin isolated from hESCs incubated in the presence or absence of 2-DG, as well as investigating the changes in other histone modifications such as H3K4me3 and histone acetylation
- To determine the components of a potential CtBP coactivator complex in hESCs maintained under hypoxia
- To investigate the mechanism behind HIF stabilisation in hECCs cultured under normoxia
- To investigate whether NO levels are inhibiting PHD function in hECCs and hESCs
- To investigate whether the addition of L-NAME decreased HIF-1α expression, as well as HIF-2α, in hECCs maintained at either 5% or 20% oxygen
- To quantify NO levels using image analysis
- To repeat L-NAME experiments using another inhibitor; potentially PTIO, in hECCs maintained under either 5% or 20% oxygen
- To analyse the effects of the addition of DETA NONOate; a NO donor, on pluripotency marker, CtBP and HIF-2α expression in hECCs maintained at either 5% or 20% oxygen
- To investigate the expression of NO levels in hESCs maintained at either 5% or 20% oxygen
- To compare the rate of glycolysis between hESCs and hECCs maintained at either 5% or 20% oxygen
- To compare the levels of NO between hESCs and hECCs maintained at either 5% or 20% oxygen
- To compare these mechanisms identified to regulate stem cell self-renewal in iPSCs

Appendices

Appendix 1: QIAquick PCR Purification Kit

The QIAquick PCR purification kit (Qiagen) was used to clean up up to 10µg chromatin of ChIP samples before analysis by qPCR.

5 volumes of Buffer PB was added to 1 volume of ChIP sample and mixed thoroughly. If the colour of the mixture was orange or violet, then 10µl 3M sodium acetate pH5.0 was added to make the pH ≤ 7.5. To bind DNA, the sample was applied to the QIAquick column and centrifuged at 13,000 rpm for 60 seconds before discarding the flow-through. To wash, 750µl of Buffer PE was added to the QIAquick column before centrifuging the sample at 13,000 rpm for 60 seconds. The flow-through was discarded and centrifuged as described previously to remove any residual wash buffer before each QIAquick column was transferred to a clean 1.5ml microcentrifuge tube. To elute the DNA, 50µl Buffer EB (10mM Tris-Cl, pH8.5) was added to the centre of the QIAquick membrane and centrifuged as described previously.

Appendix 2: Melt curves of primers used in RT-qPCR

SOX17

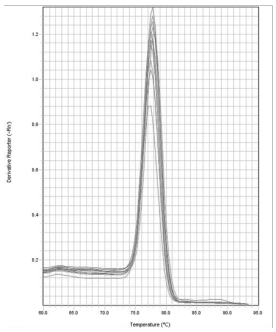

GATA4

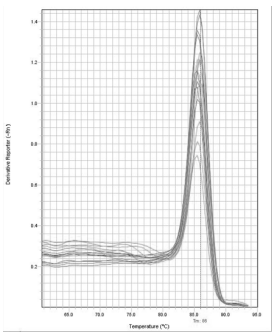

AFP

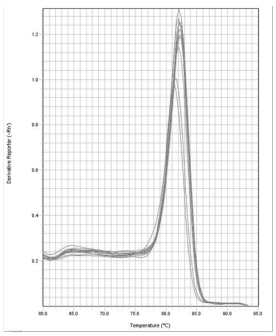

CLD6

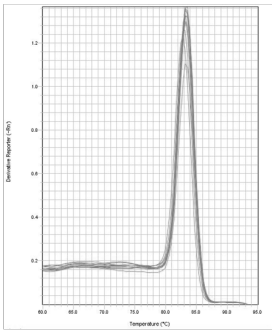

SOX1

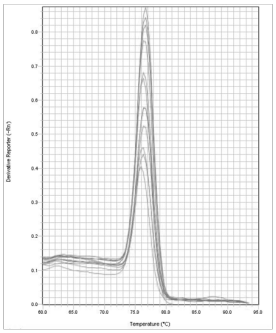

PAX6

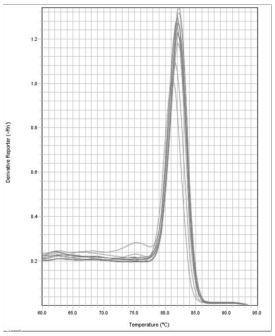

NODAL

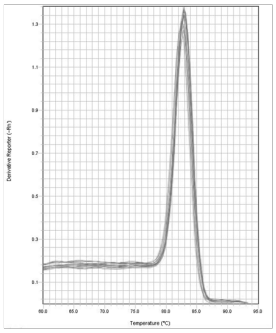

BMP4

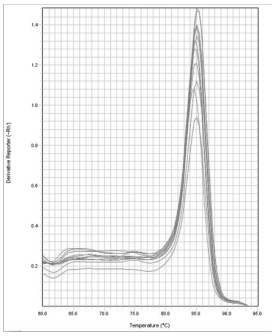

FOXC1

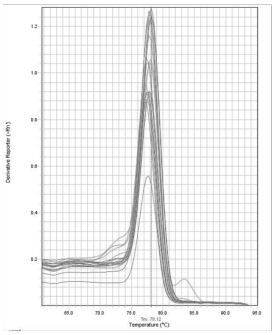

β-actin

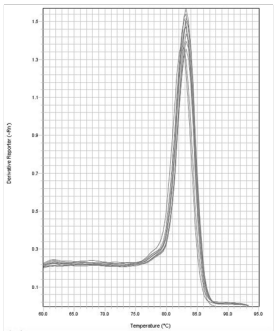

Appendix 3: Primer efficiency curves

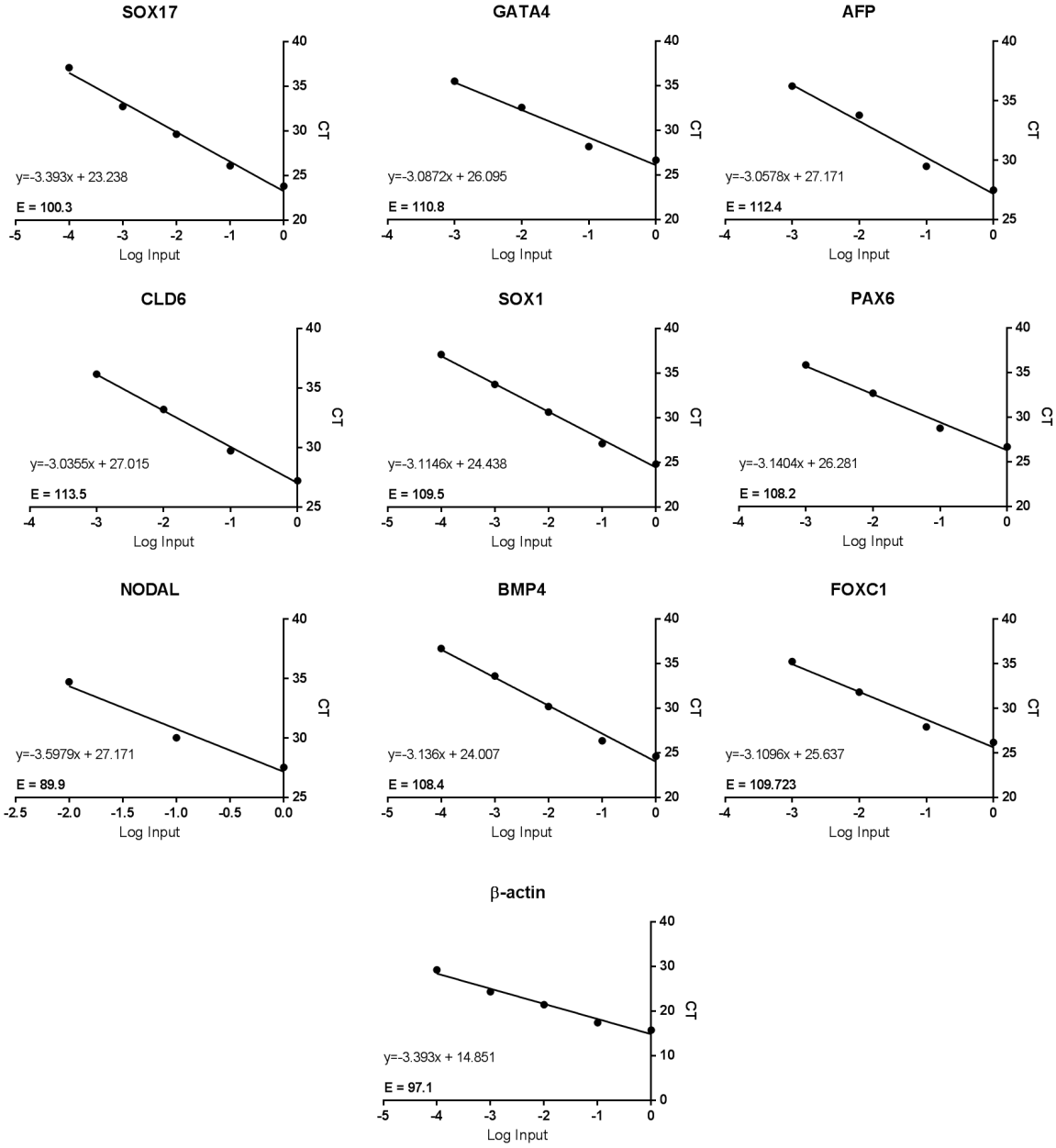

Appendix 4: Efficiency of primers versus endogenous control

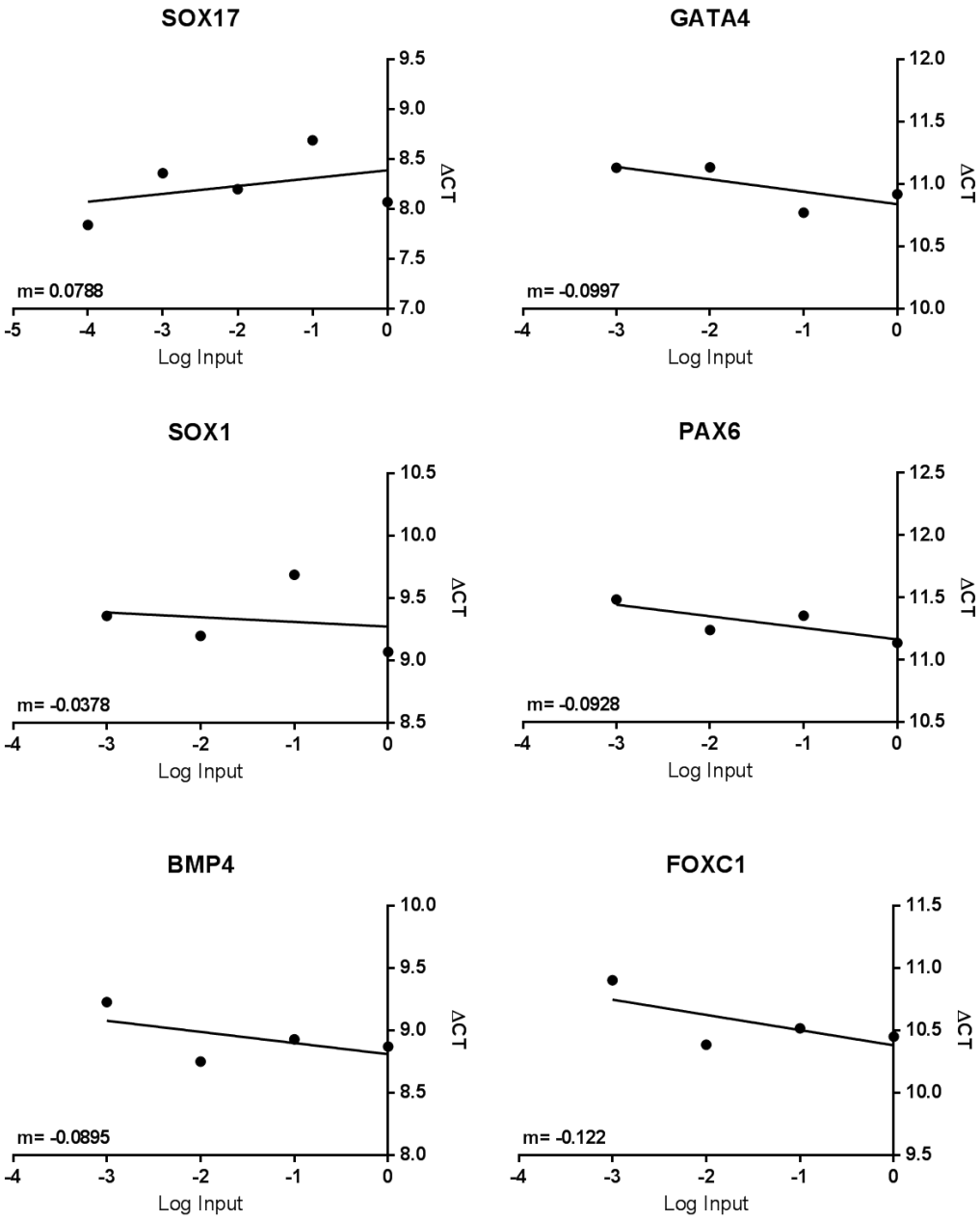

Appendix 5: Publication based on the work of this thesis

Stem Cell Reports
Article

ISSCR

OPEN ACCESS

Glycolysis Regulates Human Embryonic Stem Cell Self-Renewal under Hypoxia through HIF-2α and the Glycolytic Sensors CTBPs

Sophie A. Arthur,[1] Jeremy P. Blaydes,[2,*] and Franchesca D. Houghton[1,*]
[1]Centre for Human Development, Stem Cells and Regeneration, Faculty of Medicine, University of Southampton, Southampton SO16 6YD, UK
[2]Cancer Sciences Unit, Faculty of Medicine, University of Southampton, Southampton SO16 6YD, UK
*Correspondence: j.p.blaydes@soton.ac.uk (J.P.B.), f.d.houghton@soton.ac.uk (F.D.H.)
https://doi.org/10.1016/j.stemcr.2019.02.005

SUMMARY

Glycolysis and hypoxia are key regulators of human embryonic stem cell (hESC) self-renewal, but how changes in metabolism affect gene expression is poorly understood. C-terminal binding proteins (CTBPs) are glycolytic sensors that through NADH binding link the metabolic state of the cell to its gene expression, by acting as transcriptional corepressors, or coactivators. However, the role of CTBPs in hESCs has not previously been investigated. A direct interaction between hypoxia-inducible factor 2α (HIF-2α) and the *CTBP* proximal promoters in hESCs cultured only under hypoxia was demonstrated. Decreasing the rate of flux through glycolysis in hESCs maintained under hypoxia resulted in a reduction of CTBPs, OCT4, SOX2, and NANOG, but also in the expression of HIF-2α. Silencing CTBP expression resulted in the loss of pluripotency marker expression demonstrating that CTBPs are involved in hESC maintenance. These data suggest that under hypoxia, glycolysis regulates self-renewal through HIF-2α and the induction of the metabolic sensors CTBPs.

INTRODUCTION

Human embryonic stem cells (hESCs) are pluripotent cells derived from the inner cell mass of the blastocyst (Evans and Kaufman, 1981; Martin, 1981). They can proliferate indefinitely through self-renewal and differentiate into all somatic cell types (Thomson et al., 1998). Thus, hESCs may be used to investigate developmental mechanisms and have the potential to become an unlimited cell source for tissue replacement and regenerative medicine. However, for therapeutic use, hESCs need to be maintained in a highly pluripotent state before directing into a specific lineage.

hESCs are particularly difficult to maintain in culture, due to their tendency to spontaneously differentiate, suggesting that standard culture conditions at atmospheric, 20% oxygen tension are sub-optimal. It is now widely recognized that culturing hESCs at a lower oxygen tension is advantageous for their maintenance, in terms of reduced spontaneous differentiation, improved proliferation, and increased expression of key pluripotency markers (Chen et al., 2010; Ezashi et al., 2005; Forristal et al., 2010; Ludwig et al., 2006; Prasad et al., 2009; Westfall et al., 2008); an effect mediated by hypoxia-inducible factors (HIFs).

HIFs are responsible for the maintenance of oxygen homeostasis. HIFs function as heterodimers formed of the constitutively expressed HIF-1β (ARNT) subunit with one of the three different HIF-α subunits (HIF-1α, HIF-2α, and HIF-3α). Under normoxic conditions, HIF-α subunits are hydroxylated by prolyl hydroxylases. This allows them to be recognized by von Hippel Lindau tumor suppressor proteins to initiate their degradation via the ubiquitin/proteasome complex. However, under hypoxia, HIF-α subunits are stabilized, able to translocate to the nucleus, and bind HIF-1β to enhance the expression of HIF target genes (Kallio et al., 1998). HIF-α subunits bind a conserved consensus sequence (A/G)CGTG termed a hypoxic response element (HRE) in the proximal enhancer or promoter regions of HIF target genes (Semenza and Wang, 1992).

In hESCs, HIF-1α is only transiently expressed for ~48 h following exposure to hypoxia (Forristal et al., 2010). In contrast, HIF-2α is responsible for the long-term hypoxic response by directly regulating the expression of OCT4, SOX2, and NANOG; core transcription factors that are crucial for maintaining hESC self-renewal (Forristal et al., 2010; Petruzzelli et al., 2014).

Hypoxia has also been shown to alter the energy metabolism of hESCs, and in particular glycolysis. hESCs cultured at 5% oxygen tension consume more glucose and produce more lactate than those maintained at atmospheric oxygen tensions, and exhibit an increased expression of OCT4, SOX2, and NANOG in hESCs compared with those maintained at 20% oxygen (Forristal et al., 2013). Glucose enters hESCs via the facilitative glucose transporter GLUT3, which localizes to the cell membrane and is upregulated at 5% oxygen compared with 20% oxygen. Interestingly, there is a positive correlation between GLUT3 and OCT4 expression in hESCs (Christensen et al., 2015). Thus, hypoxia supports pluripotency by maintaining a high rate of flux through glycolysis, which sustains the increased bioenergetic requirements of the cell. Although HIF-2α has been shown to directly upregulate GLUT1 expression only in hESCs cultured under hypoxic conditions (Forristal et al., 2013), other potential

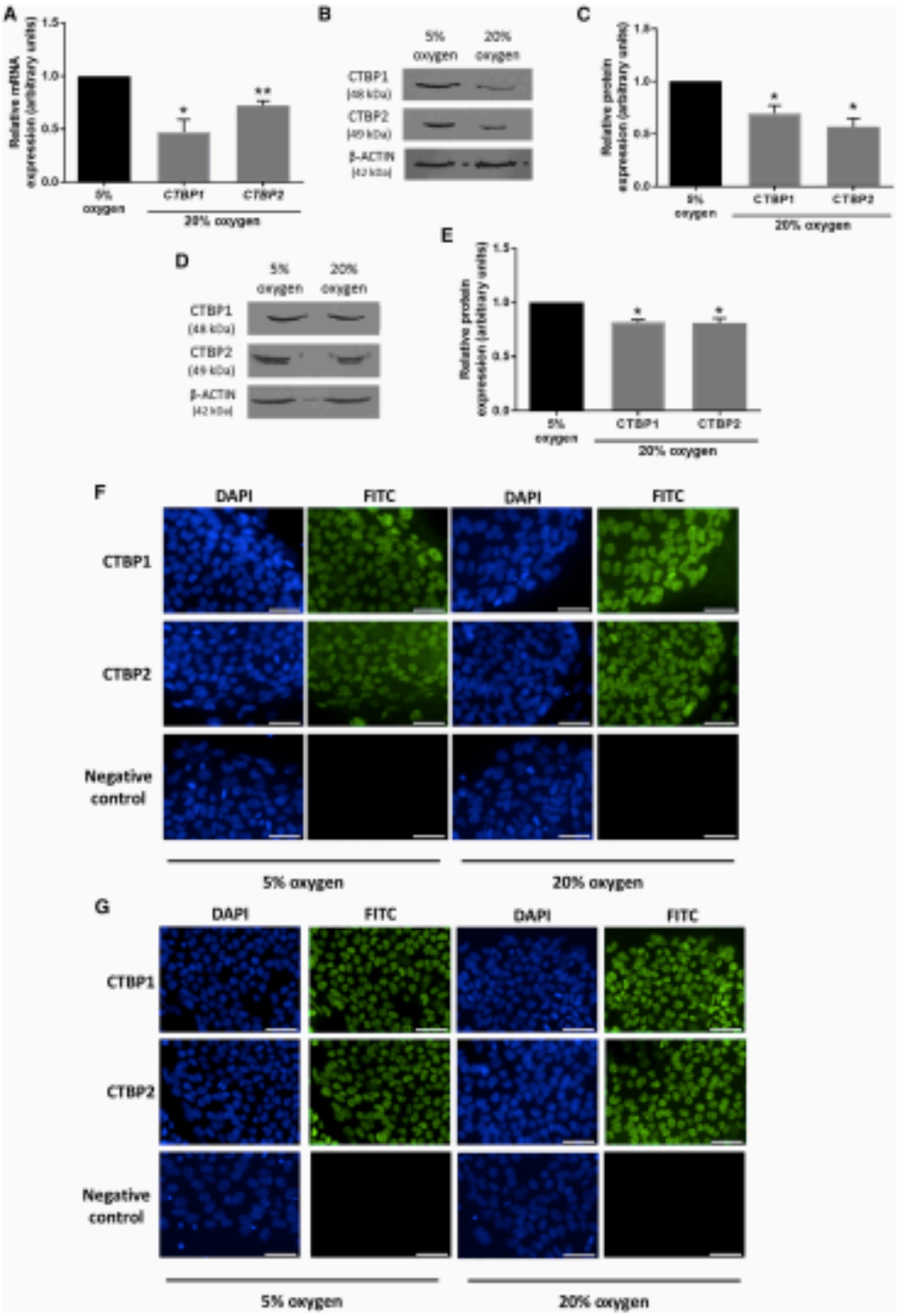

(legend on next page)

mechanisms that regulate hESC metabolism have yet to be investigated.

C-terminal binding proteins (CTBPs) are a family of glycolytic sensors that link changes in metabolism to gene expression, and were originally identified through their ability to interact with the C-terminal domain of the E1A adenovirus (Boyd et al., 1993; Schaeper et al., 1995). Humans have two CTBP genes, *CTBP1* and *CTBP2*, which generate different splice variants, CTBP1-L, CTBP1-S, CTBP2-L, and CTBP2-S, using alternative splicing and alternative promoter usage. CTBPs contain an NADH-binding domain which links the metabolic state of the cell to its gene transcription. The activity of CTBPs is predominantly regulated through binding NADH produced in glycolysis (Fjeld et al., 2003; Zhang et al., 2002). NADH binding induces a conformational change which allows CTBP monomers to either homo- or heterodimerize and assemble larger protein-protein interaction complexes (Kumar et al., 2002). The CTBP proteins are highly homologous and exhibit functionally redundant and unique roles throughout development (Hildebrand and Soriano, 2002). CTBPs are primarily known for their role as short-range transcriptional corepressors (Turner and Crossley, 2001; Chinnadurai, 2002, 2007) as they bind to DNA-binding transcription factors containing a PXDLS-binding motif and act as a scaffold to recruit chromatin-modifying enzymes such as histone deacetylases, histone methyltransferases, and Polycomb group proteins (Kuppuswamy et al., 2008; Shi et al., 2003), as well as various other cofactors to form a corepressor complex and repress expression of genes such as E-cadherin (Grooteclaes et al., 2003; Grooteclaes and Frisch, 2000), but both isoforms also possess cytosolic functions such as regulators of Golgi apparatus fission (Chinnadurai, 2007; Corda et al., 2006). Although CTBPs act mainly as transcriptional corepressors, there is increasing evidence of CTBPs acting as coactivators (Fang et al., 2006; Itoh et al., 2013). Even at the earliest stages of hESC differentiation, before any overt morphological changes, the rate of flux through glycolysis decreases as does the expression of key genes regulating hESC self-renewal (Forristal et al., 2013). Thus, this study aims to investigate how changes in hESC metabolism alters gene expression and regulates hESC self-renewal and whether CTBPs play a role.

We report that the increased rate of flux through glycolysis in hESCs cultured under hypoxia regulates CTBP expression via HIF-2α. Moreover, CTBP dimerization was found to enhance OCT4, SOX2, and NANOG expression to regulate the self-renewal of hESCs maintained under hypoxic conditions. These data demonstrate mechanisms by which metabolism regulates the self-renewal of hESCs.

RESULTS

CTBP Expression in hESCs Is Regulated by Environmental Oxygen Tension

hESCs rely on glycolysis for energy generation and the maintenance of pluripotency (Forristal et al., 2013). However, the mechanisms underlying how glycolysis might regulate hESC self-renewal has not been investigated. We hypothesized that the glycolytic sensors CTBP1 and CTBP2 may have a role.

In agreement with Forristal et al. (2013), hESCs cultured at 20% oxygen displayed a decreased expression of OCT4, SOX2, and NANOG protein compared with hESCs cultured at 20% oxygen (Figure S1). Both *CTBP1* and *CTBP2* mRNA expression levels were significantly decreased in Hues-7 cells cultured at 20% oxygen tension compared with those maintained under hypoxic conditions (Figure 1A). The expression of CTBP1 and CTBP2 proteins were also significantly reduced when cultured at 20% compared with 5% oxygen in both Hues-7 (Figures 1B and 1C) and Shef3 (Figures 1D and 1E) hESCs. Using the non-quantitative technique of immunocytochemistry, CTBP1 and CTBP2 were detected in the nucleus of two hESC lines; Hues-7 (Figure 1F) and Shef3 (Figure 1G).

These data reveal that CTBP1 and CTBP2 expression is regulated by environmental oxygen in hESCs.

HIF-2α Is an Upstream Regulator of CTBP1 and CTBP2 in hESCs Cultured under Hypoxia

As HIF-2α is an essential regulator of the long-term hypoxic response in hESCs (Forristal et al., 2010), small interfering RNA (siRNA) was used to determine whether HIF-2α was involved in the increased CTBP expression observed in Hues-7 hESCs maintained at 5% oxygen. Silencing HIF-2α

Figure 1. CTBP Expression Is Regulated by Environmental Oxygen Tension in hESCs

(A) qRT-PCR analysis of *CTBP1* and *CTBP2* expression in Hues-7 hESCs cultured at either 5% or 20% oxygen ($n = 3$ for *CTBP1*; $n = 4$ for *CTBP2*).

(B–E) Quantification of CTBP1 and CTBP2 expression using western blotting in Hues-7 (B and C) and Shef3 (D and E) cultured at 5% compared with 20% oxygen ($n = 3$ for Hues-7; $n = 4$ for Shef3). Bars represent mean ± SEM. $^{*}p < 0.05$, $^{**}p < 0.01$ significantly different to 5% oxygen.

(F and G) Representative immunocytochemistry images of CTBP1 and CTBP2 expression in Hues-7 (F) and Shef3 (G) hESCs cultured under either 5% or 20% oxygen. Nuclei were labeled using DAPI. Scale bars, 50 μm. FITC secondary antibodies alone were used as negative controls.

See also Figure S1.

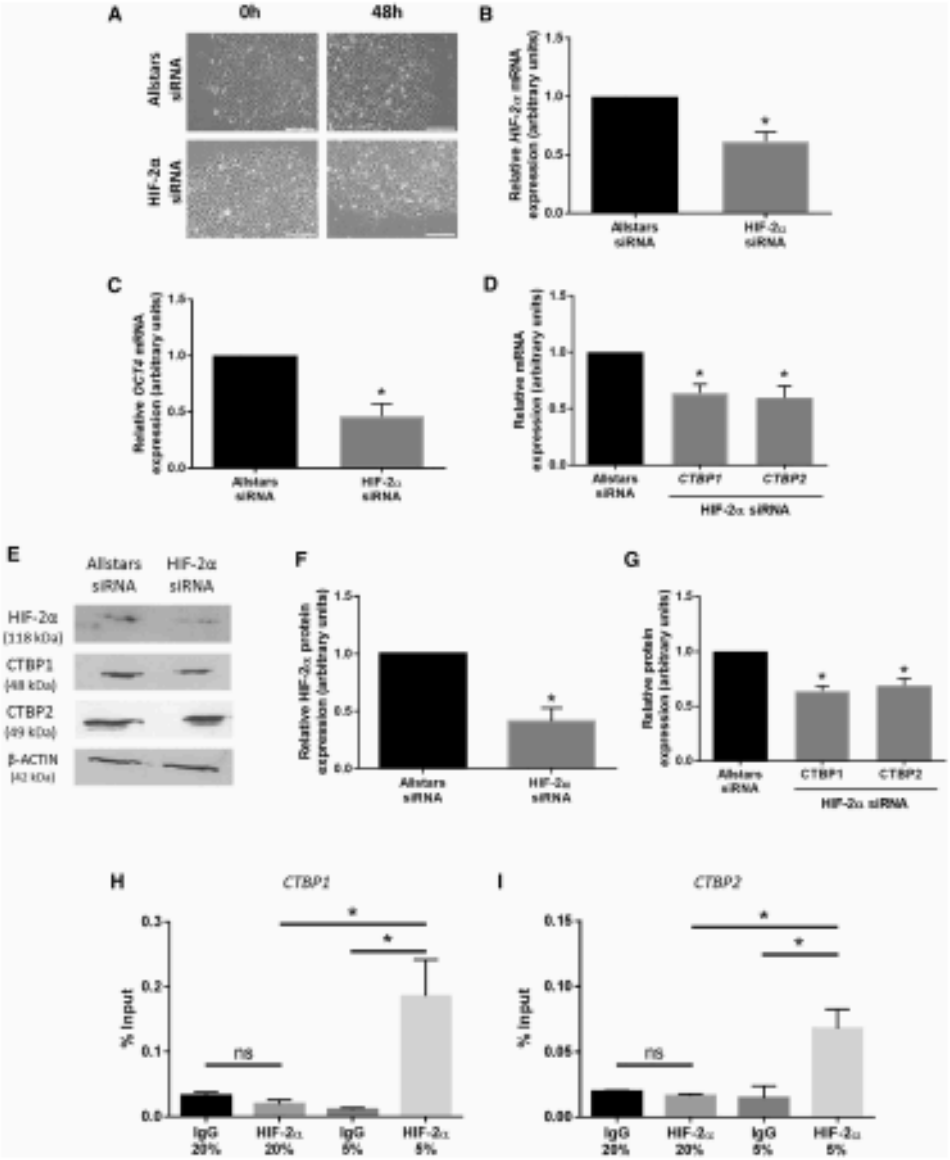

Figure 2. HIF-2α Directly Regulates CTBP Expression in hESCs Maintained under Hypoxic Conditions

(A) Phase contrast images demonstrating the morphology of Hues-7 hESCs cultured at 5% oxygen after transfection with either Allstars control or HIF-2α siRNA for 48 h. Scale bars, 200 μm.

(B–D) qRT-PCR analysis of *HIF-2α* (B), *OCT4* (C), *CTBP1*, and *CTBP2* (D) expression in Hues-7 hESCs transfected with either Allstars control or HIF-2α siRNA for 48 h (n = 4).

(E–G) Quantification of HIF-2α (F), and CTBP1 and CTBP2 (G) expression using western blotting (E) in Hues-7 hESCs transfected with either the Allstars control or HIF-2α siRNA for 48 h (n = 3). Bars represent mean ± SEM. *p < 0.05 significantly different to Allstars control siRNA.

(legend continued on next page)

had no overt effect on hESC morphology (Figure 2A), but resulted in a significant reduction in *HIF-2α* mRNA expression compared with cells transfected with Allstars control siRNA (Figure 2B). When *HIF-2α* was silenced, there was a significant reduction in *OCT4* ($p = 0.0165$; Figure 2C), *CTBP1* ($p = 0.0174$), and *CTBP2* ($p = 0.0297$; Figure 2D) mRNA expression compared with hESCs transfected with control siRNA. A similar effect was observed at the protein level. Silencing HIF-2α caused a 59% ($p = 0.0381$) reduction in HIF-2α protein (Figure 2F) and decreased both CTBP1 and CTBP2 protein expression by approximately 36% ($p = 0.0145$) and 32% ($p = 0.0418$), respectively, compared with hESCs transfected with control siRNA (Figure 2G). This suggests that HIF-2α is an upstream regulator of both CTBP1 and CTBP2 in hESCs cultured at 5% oxygen.

HIF-2α Binds *In Vivo* to the *CTBP1* and *CTBP2* Proximal Promoters under Hypoxic Conditions in hESCs

To determine whether HIF-2α binds directly to putative HRE sites in the proximal promoters of *CTBP1* and *CTBP2*, chromatin immunoprecipitation (ChIP) assays were performed on chromatin isolated from hESCs cultured at either 5% or 20% oxygen. Amplification of a potential HRE in both the *CTBP1* and *CTBP2* proximal promoter sequences revealed a 10-fold ($p = 0.0355$) and 4-fold ($p = 0.0389$) enrichment, respectively, in chromatin isolated from hESCs maintained under hypoxic conditions, when chromatin was precipitated with an anti-HIF2α antibody compared with the immunoglobulin G (IgG) control. In contrast, no significant enrichment of HIF-2α binding was observed in anti-HIF2α-precipitated chromatin isolated from hESCs maintained at 20% oxygen tension compared with the IgG control (Figures 2H and 2I). Amplification with a positive control probe designed to amplify a known HRE in the *SOX2* proximal promoter revealed a 10-fold enrichment in cells cultured at 5% oxygen when chromatin was precipitated with an anti-HIF2α antibody compared with the IgG control ($p = 0.0098$; Figure S2A), in agreement with Petruzzelli et al. (2014). To further verify the specificity of HIF-2α binding, a negative control probe specific to the *FOXP3* promoter was used. This probe did not amplify an HRE site but instead was designed to amplify a region in the proximal promoter situated between two predicted HREs at −670 and +104 bp from the transcription start site. In agreement with Petruzzelli et al. (2014), no significant enrichment by HIF-2α was observed in this *FOXP3* promoter region in hESCs cultured at either 5% or 20% oxygen (Figure S2B). Together, these data reveal a specific interaction between HIF-2α and an HRE in the proximal promoters of *CTBP1* and *CTBP2* only in hESCs maintained in hypoxic conditions.

Glycolytic Rate Regulates the Expression of CTBPs via HIF-2α in hESCs

It is well documented that hESCs use glycolysis to maintain pluripotency, and previous studies have demonstrated that hESCs with a reduced rate of flux through glycolysis also expressed lower levels of the core pluripotency factors OCT4, SOX2, and NANOG (Forristal et al., 2013). To investigate whether changing the rate of glycolysis in hESCs affected the expression of the glycolytic sensors CTBPs, in addition to pluripotency marker expression, hESCs maintained at 5% oxygen were cultured in the presence or absence of the glycolytic inhibitors 2-deoxyglucose (2-DG) or 3-bromopyruvate (3-BrP) for 48 h. 2-DG reduces the rate of flux through glycolysis by acting as a glucose analog and a competitive inhibitor of hexokinase, whereas 3-BrP inhibits hexokinase by alkylation.

There were no overt differences in hESC morphology between hESCs cultured in the presence or absence of 0, 0.2, 1, or 10 mM 2-DG, or 25 μM 3-BrP (Figure 3A). A dose-response curve of lactate production was produced in response to increasing 2-DG concentration (Figure 3B). A significant reduction in lactate production in Hues-7 hESCs maintained at 5% oxygen was only observed at the highest concentration (10 mM) of 2-DG, and thus was used for further investigation. The need for the 10 mM concentration of 2-DG in order to significantly reduce lactate production reflects the high concentration of glucose found in hESC culture medium. A dose of 25 μM 3-BrP also resulted in a significant decrease in lactate production in Hues-7 hESCs (Figure 3C). In agreement with the lactate production data, concentrations of 0.2 and 1 mM 2-DG had no effect on the expression of a range of pluripotency genes (Figure S3). However, Hues-7 hESCs treated with 10 mM 2-DG displayed a significant reduction in *OCT4* ($p = 0.0009$), *SOX2* ($p = 0.0121$), *NANOG* ($p = 0.0197$), *LIN28B* ($p = 0.0441$), and *SALL4* ($p = 0.0426$) mRNA expression compared with those maintained with 0 mM 2-DG (Figures 3D and S3). This loss of self-renewal was associated with a significantly increased mRNA expression of a panel of early differentiation markers representing the three germ layers when Hues-7 hESCs were treated with 10 mM 2-DG compared with 0 mM 2-DG (Figure 3E). Interestingly, expression of both *CTBP1* ($p = 0.0247$) and *CTBP2* ($p = 0.0325$) mRNA was also reduced in the presence of

(H and I) ChIP analysis of HIF-2α binding to predicted HRE sites in the proximal promoters of *CTBP1* (H) and *CTBP2* (I) on chromatin isolated from Hues-7 hESCs cultured at either 5% or 20% oxygen. DNA enrichment is expressed as a percentage of the Input ($n = 3$; ns, no significant difference, $^*p < 0.05$). Bars represent mean ± SEM.
See also Figure S2.

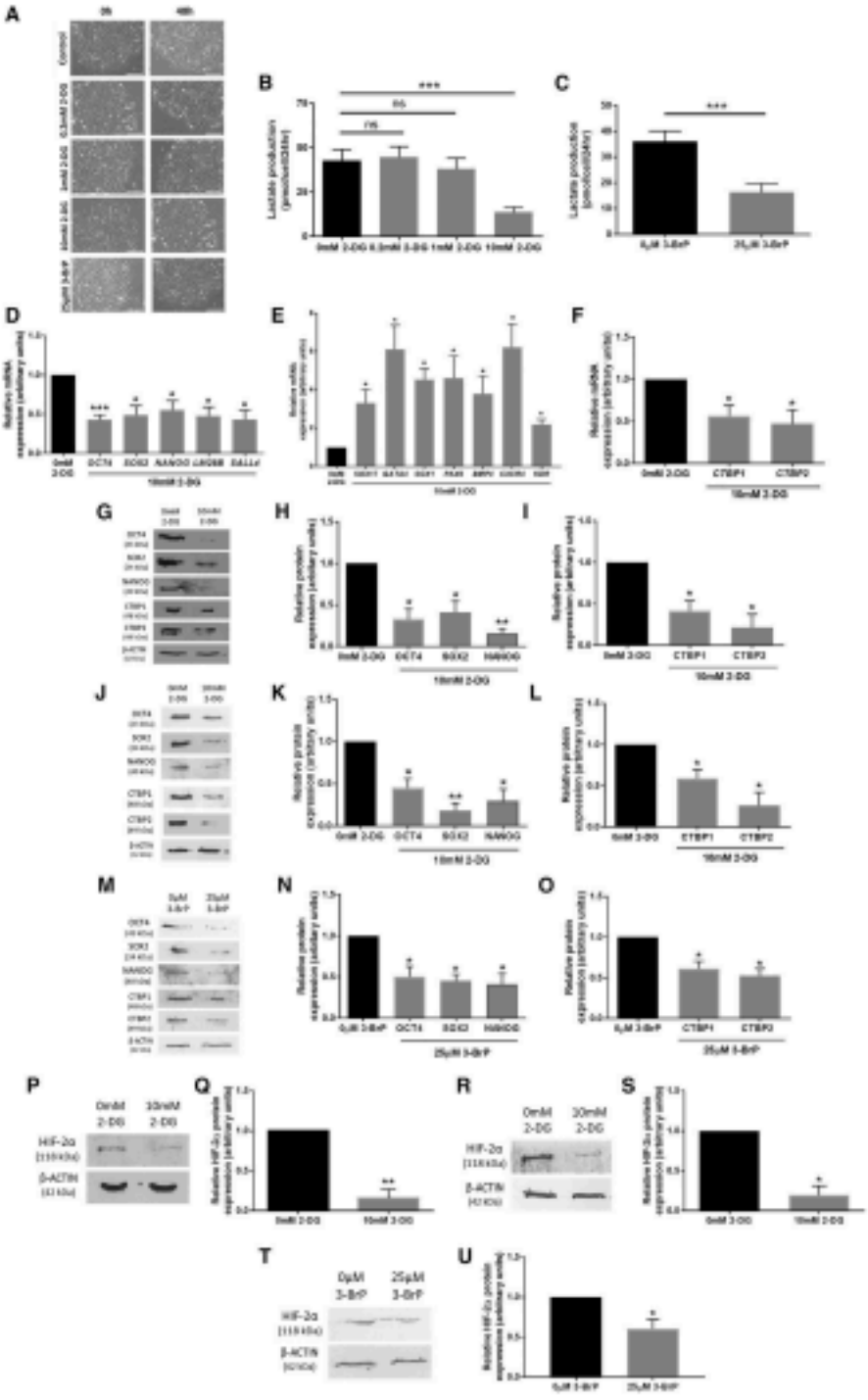

(legend on next page)

10 mM 2-DG compared with the control ($p < 0.05$; Figure 3F). Quantification at the protein level revealed a similar significant reduction in OCT4, SOX2, and NANOG expression in both Hues-7 hESCs (Figures 3G and 3H) and Shef3 hESCs (Figures 3J and 3K) cultured in the presence or absence of 10 mM 2-DG. Moreover, the addition of 10 mM 2-DG to Hues-7 and Shef3 hESCs caused a 59% ($p = 0.0410$) and 41% ($p = 0.0339$) reduction in CTBP1, and a 78% ($p = 0.0384$) and 74% ($p = 0.0197$) decrease in CTBP2 protein expression, respectively, compared with the control (Figures 3I and 3L). Similar results were obtained when Hues-7 hESCs were treated in the presence or absence of 25 μM 3-BrP (Figures 3M–3O).

As shown in Figure 2, HIF-2α directly binds to the proximal promoter region of both *CTBP1* and *CTBP2*. Therefore, to determine whether the reduction in expression of CTBPs and pluripotency markers in the presence of 2-DG and 3-BrP was HIF-2α regulated, quantification of HIF-2α protein levels in hESCs treated with 10 mM 2-DG or 25 μM 3-BrP was analyzed. The presence of 10 mM 2-DG caused a significant 84% and 81% reduction in HIF-2α protein expression compared with those maintained in the absence of 2-DG in Hues-7 (Figures 3P and 3Q) and Shef3 (Figures 3R–3S), respectively. HIF-2α expression was also significantly decreased in Hues-7 hESCs treated with 25 μM 3-BrP compared with the control (Figures 3T and 3U). Together, this suggests that glycolysis regulates HIF-2α expression in hESCs maintained at 5% oxygen. Moreover, these data reveal that glycolysis regulates CTBP1 and CTBP2 expression, as well as OCT4, SOX2, and NANOG, through the regulation of HIF-2α.

CTBPs Promote hESC Self-Renewal

To investigate whether the CTBP family of glycolytic sensors have a role in maintaining hESC self-renewal, siRNA was used to silence both CTBP isoforms in hESCs maintained at 5% oxygen using two alternative siRNA strategies; either with a single siRNA that targets both CTBP isoforms (CTBP1/2 siRNA) or using a combination of two individual siRNAs to silence each CTBP isoform independently (CTBP1+2 siRNA), and assessing any consequent effect on expression of the pluripotency markers OCT4, SOX2, and NANOG. Hues-7 hESCs transfected with CTBP1/2 siRNA displayed an 85% decrease in both *CTBP1* ($p = 0.0195$) and *CTBP2* ($p = 0.015$) mRNA expression (Figure 4A). Interestingly, *OCT4*, *SOX2*, and *NANOG* mRNA expression levels also decreased by 80% ($p = 0.0166$), 74% ($p = 0.0248$), and 84% ($p = 0.0079$), respectively (Figure 4B), and was coupled with a significant increase in the mRNA expression of a panel of differentiation markers (Figure 4C). Transfection with CTBP1/2 siRNA silenced CTBP1 and CTBP2 protein expression and caused a significant reduction in OCT4, SOX2, and NANOG expression compared with the Allstars control siRNA in both Hues-7 (Figures 4D–4F) and Shef3 hESCs (Figures 4G–4I). This observation was further supported using a different siRNA strategy where the expression of both CTBP isoforms were significantly decreased by approximately 50% in Hues-7 hESCs transfected with two single-targeting siRNAs (CTBP1+2 siRNA; Figures S4A and S4B). After silencing CTBP expression with CTBP1+2 siRNA, the expression of OCT4 ($p = 0.0371$), SOX2 ($p = 0.0120$), and NANOG ($p = 0.0294$) were, again, all decreased compared with the control siRNA transfected cells (Figures S4A and S4C).

To determine whether there was any functional redundancy between the CTBP isoforms, each CTBP isoform was silenced individually in Hues-7 hESCs maintained at 5% oxygen and the effect on OCT4, SOX2, and NANOG investigated. hESCs transfected with CTBP1 siRNA displayed a 75% reduction in CTBP1 expression

Figure 3. Glycolysis Regulates hESC Pluripotency and CTBP Expression by Regulating HIF-2α under Hypoxic Conditions

(A) Phase contrast images demonstrating the morphology of Hues-7 hESCs cultured at 5% oxygen in the presence or absence of 0.2, 1, or 10 mM 2-DG or 25 μM 3-BrP for 48 h. Scale bars, 200 μm.

(B and C) Enzyme-linked assays were used to measure lactate production. Hues-7 hESCs were cultured with either 0, 0.2, 1, or 10 mM 2-DG (B) or in the presence or absence 3-BrP (C) for 48 h prior to collecting media samples for use in the enzyme-linked assays ($n = 12–15$ wells from at least 3 independent experiments).

(D–F) qRT-PCR analysis of *OCT4*, *SOX2*, *NANOG*, *LIN28B*, and *SALL4* (D), a panel of differentiation markers from the three developmental germ layers (E), and *CTBP1* and *CTBP2* (F) in Hues-7 hESCs treated with 10 mM 2-DG for 48 h compared with control cells ($n = 3–5$). See also Figure S3.

(G–L) Quantification of OCT4, SOX2, NANOG, CTBP1, and CTBP2 expression using western blotting in Hues-7 (G–I) and Shef3 (J–L) hESCs treated with 10 mM 2-DG for 48 h compared with 0 mM 2-DG ($n = 3$ for Hues-7; $n = 4$ for Shef3).

(M–O) Quantification of OCT4, SOX2, NANOG (M and N), CTBP1, and CTBP2 (M and O) expression using western blotting in Hues-7 hESCs cultured in the presence or absence of 25 μM 3-BrP for 48 h ($n = 3–4$).

(P–S) Quantification of HIF-2α expression using western blotting in Hues-7 (P and Q) and Shef3 (R and S) hESCs treated with or without 10 mM 2-DG for 48 h ($n = 4$ for Hues-7; $n = 3$ for Shef3). (T and U) Quantification of HIF-2α expression using western blotting in Hues-7 hESCs cultured in the presence or absence of 25 μM 3-BrP for 48 h ($n = 4$).

Bars represent mean ± SEM. *$p < 0.05$, **$p < 0.01$, ***$p < 0.001$ significantly different to no treatment control; ns, no significant difference.

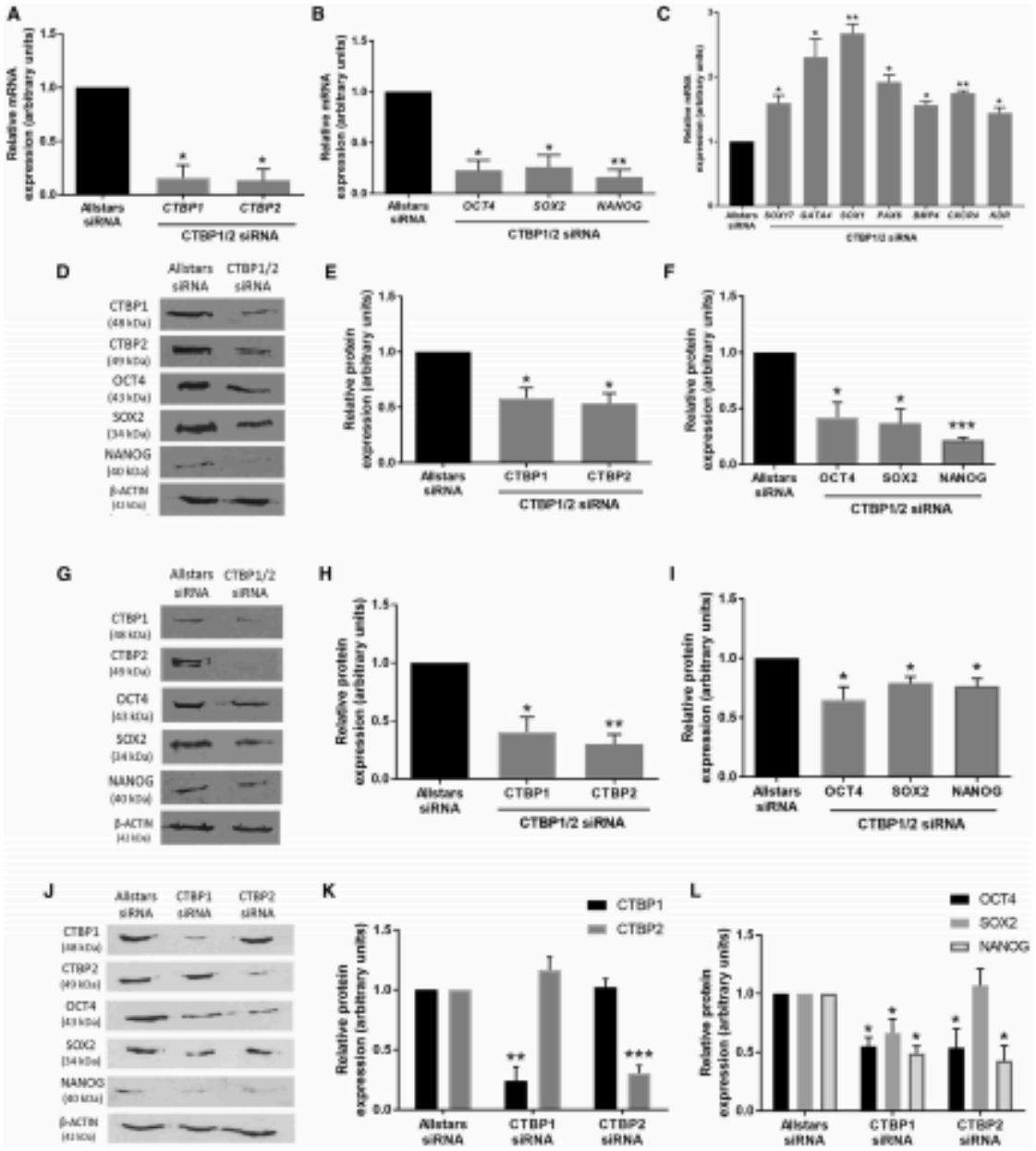

Figure 4. CTBPs Mediate the Activation of Pluripotency Markers in hESCs Maintained under Hypoxic Conditions

(A–C) mRNA expression of *CTBP1*, *CTBP2* (A), *OCT4*, *SOX2*, and *NANOG* (B) and a panel of differentiation markers (C) in Hues-7 hESCs cultured at 5% oxygen 48 h post-transfection with either Allstars control or CTBP1/2 siRNA (n = 3).

(D–I) Quantification of CTBP1, CTBP2, OCT4, SOX2, and NANOG expression using western blotting in Hues-7 (D–F) and Shef3 (G–I) hESCs maintained at 5% oxygen and transfected with either Allstars control or CTBP1/2 siRNA for 48 h (n = 3 for Hues-7; n = 4 for Shef3).

(J–L) Quantification of CTBP1, CTBP2 (J and K), OCT4, SOX2, and NANOG (J and L) expression in Hues-7 hESCs transfected with either CTBP1 siRNA or CTBP2 siRNA compared with those transfected with Allstars control siRNA for 48 h (n = 3–5).

Bars represent mean ± SEM. *p < 0.05, **p < 0.01, ***p < 0.001 significantly different to Allstars control siRNA. See also Figure S4.

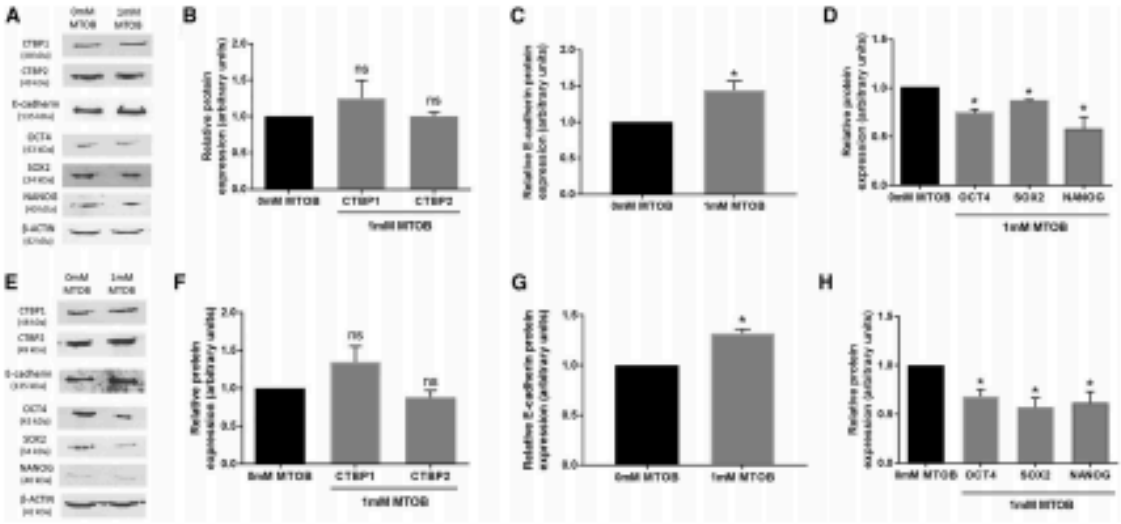

Figure 5. CTBP Dimerization Enhances the Self-Renewal of hESCs Cultured under Hypoxia

Quantification of CTBP1, CTBP2, E-cadherin, OCT4, SOX2, and NANOG expression using western blotting in Hues-7 (A–D) and Shef3 (E–H) hESCs cultured at 5% oxygen and treated with either 0 or 1 mM MTOB for 48 h (n = 3–4). Bars represent mean ± SEM. *p < 0.05 significantly different to no treatment control; ns, no significant difference.

(p = 0.0028), while importantly there was no effect on CTBP2 protein expression compared with Allstars negative control siRNA transfected cells. Likewise, hESCs transfected with CTBP2 siRNA displayed a 70% decrease in CTBP2 expression (p = 0.0004) with no consequent effect on CTBP1 expression compared with the control (Figures 4J and 4K). Silencing CTBP1 alone revealed a decrease in OCT4 (p = 0.0292), SOX2 (p = 0.0495), and NANOG (p = 0.0156) compared with the Allstars control siRNA (Figures 4J and 4L). Likewise, silencing CTBP2 alone revealed a 2-fold reduction in OCT4 (p = 0.0482) and NANOG (p = 0.0475) protein expression, but no difference in SOX2 protein expression was observed compared with control transfected cells (Figures 4J and 4L).

CTBP Dimerization Aids the Maintenance of hESC Self-Renewal

To investigate whether the reduction of self-renewal marker expression after silencing CTBPs was a result of CTBP activity and not differential CTBP expression alone, the effects of inhibiting CTBP activity on OCT4, SOX2, and NANOG expression were investigated by treating hESCs maintained at 5% oxygen with either 0 or 1 mM of the CTBP inhibitor, 4-methylthio-2-oxobutyric acid (MTOB). MTOB functions by preventing NADH-dependent dimerization of CTBPs and hence inhibiting their downstream activity (Straza et al., 2010). As expected, no significant difference was observed in CTBP1 or CTBP2 protein expression in Hues-7 (Figures 5A and 5B) or Shef3 (Figures 5E and 5F) hESCs treated with 0 or 1 mM MTOB. However, CTBP function had been inhibited as a significant increase in E-cadherin protein expression was observed in the presence of 1 mM MTOB in both Hues-7 (Figure 5C) and Shef3 (Figure 5G) hESCs. Inhibiting CTBP function with the addition of MTOB resulted in a significant decrease in OCT4, SOX2, and NANOG protein expression compared with the control in Hues-7 (Figure 5D) and Shef3 (Figure 5H) hESCs. Together, these data suggest a role for the active NADH-dependent dimeric form of the glycolytic sensors CTBPs in the activation of proteins regulating hESC self-renewal.

DISCUSSION

Understanding the mechanisms which regulate self-renewal is critical not only for defining optimal conditions to culture hESCs, but also to ensure a highly pluripotent population of cells for use in regenerative medicine. Much evidence now suggests that culturing hESCs under hypoxic conditions increases the rate of flux through glycolysis, and upregulates the expression of pluripotency markers (Christensen et al., 2015; Ezashi et al., 2005; Forristal et al., 2010, 2013; Westfall et al., 2008). How alterations in hESC metabolism affect changes in gene expression has remained largely overlooked. The results presented in this study provide evidence that glycolysis regulates CTBP1

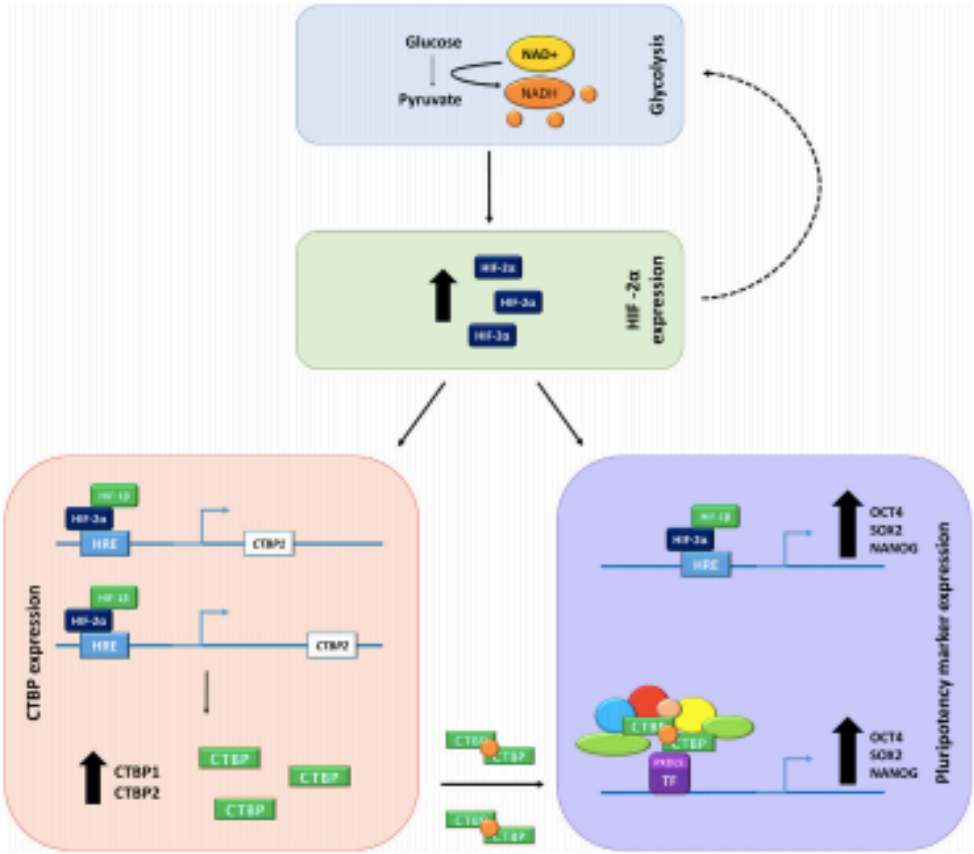

Figure 6. Proposed Mechanism of the Glycolytic Regulation of CTBP and Pluripotency Marker Expression via HIF-2α in hESCs Cultured under Hypoxia

Under hypoxic conditions, hESCs display an increase in the rate of flux through glycolysis which promotes HIF-2α protein expression, and thus the activity of HIF-2α-regulated genes, including OCT4, SOX2, NANOG, and the glycolytic sensors CTBPs. HIF-2α can also enhance glycolysis through the upregulation of glycolytic enzyme and glucose transporter expression. HIF-2α directly binds to putative HRE sites in the proximal promoters of pluripotency markers and *CTBPs*, resulting in their increased protein expression. An increased rate of flux through glycolysis results in higher levels of free NADH; which is required for CTBPs to form functional dimers. CTBP dimers bind to transcription factors containing a PXDLS-binding motif and form a scaffold for a CTBP coactivator complex containing chromatin modifiers and a series of unknown cofactors to enhance the expression of OCT4, SOX2, and NANOG.

and CTBP2 by modulating HIF-2α protein expression, and that the CTBP family of glycolytic sensors are involved in the activation of the pluripotency markers OCT4, SOX2, and NANOG in hESCs cultured under hypoxic conditions (Figure 6).

Both CTBP isoforms were expressed in the nucleus of hESCs, suggesting that they could be acting as either transcriptional coactivators or corepressors. Western blots displayed only one band for CTBP1 expression, while clearly showing a doublet for CTBP2 expression in hESCs. Previous studies indicate that the doublet band displayed both splice variants, which differ in size by 25 amino acids (Verger et al., 2006). The additional amino acids contained in the CTBP2-L isoform include a basic KVKRQR motif, which could contribute to the altered mobility of the two protein isoforms during SDS-PAGE (Bergman et al., 2006; Birts et al., 2010; Verger et al., 2006; Zhao et al., 2006). However, two distinct bands representing the CTBP1 isoforms were not observed; a trend which was previously seen in human breast cancer cell lines (Birts et al., 2010). The small difference in size between CTBP1-S and CTBP1-L may explain why two bands cannot be visualized as the additional amino acids present in the CTBP1-L isoform do not contain a motif that

changes the electrophoretic mobility of the isoforms (Birts et al., 2010).

Mechanisms that regulate CTBP expression in hESCs were also previously unknown. Our data show that CTBP1 and CTBP2 expression is hypoxia regulated. This was verified by demonstrating that HIF-2α directly interacts with a putative HRE site in the proximal promoters of both *CTBP1* and *CTBP2* in hESCs maintained under hypoxic conditions only. HIF-2α is the key regulator of the hypoxic response in hESCs, and has been shown to bind directly to the proximal promoters of *OCT4*, *SOX2*, and *NANOG* (Petruzzelli et al., 2014). Although HIFs directly regulate GLUTs and glycolytic enzymes (Christensen et al., 2015; Forristal et al., 2013; Semenza, 2000; Semenza et al., 1994), our data demonstrate that HIF-2α directly regulates the expression of the glycolytic sensors, CTBPs, and corresponds with the increased rate of flux through glycolysis observed in hESCs maintained under hypoxia compared with 20% oxygen (Forristal et al., 2013).

Pluripotent hESCs have immature mitochondria (Sathananthan et al., 2002) and hence rely on glycolysis for their energy requirements. A hypoxic environment supports a higher rate of flux through glycolysis by enhancing the expression of PKM2 and the glucose transporter GLUT3 (Christensen et al., 2015), and is associated with an increased expression of pluripotency markers compared with culture at atmospheric oxygen tensions (Forristal et al., 2013). Our data support this observation as inhibiting glycolysis in hESCs maintained at 5% oxygen using either the glycolytic inhibitor 2-DG or 3-BrP resulted in a significant decrease in *OCT4*, *SOX2*, *NANOG*, *LIN28B*, and *SALL4*, and a concomitant increase in the expression of a range of early differentiation markers representing all three germ lineages. This suggests that inhibition of glycolysis results in the loss of self-renewal and onset of early differentiation of hESCs agreeing with a previously published report (Gu et al., 2016).

Inhibiting glycolysis also significantly decreased the protein expression of CTBP1 and CTBP2 and, of particular interest, HIF-2α. Together, these data suggest the rate of flux through glycolysis regulates not only CTBP1 and CTBP2, but also OCT4, SOX2, and NANOG expression in hESCs via HIF-2α, since HIF-2α is known to directly bind to the proximal promoters of these genes (Petruzzelli et al., 2014). Much evidence suggests that HIFs support the glycolytic metabolism of hESCs, by enhancing the expression of glucose transporters and glycolytic enzymes (Semenza, 2000; Varum et al., 2011; Forristal et al., 2013; Christensen et al., 2015). Our data show glycolysis promoting HIF-2α protein expression in hESCs cultured under hypoxia. Although the mechanisms that regulate this effect are unclear, it is tempting to speculate that glycolytic metabolites may control HIF-2α stability by regulating the activity of HIF prolyl hydroxylases in a similar way to that observed for HIF-1α (Lu et al., 2002, 2005). Moreover, since HIF-2α itself promotes glycolytic metabolism (Forristal et al., 2013), enhancement of HIF-2α by glycolysis constitutes a potential feedforward mechanism that is critical for the acquisition and maintenance of hESC self-renewal (Figure 6). Furthermore, it is worth noting that these data provide evidence that CTBP expression, and not just their activity, is influenced by the metabolic state of the cell. It is hypothesized that the reduction in CTBP expression in the presence of 2-DG or 3-BrP is due to the observed decrease in HIF-2α expression. However, it cannot be ruled out that there could be an unknown direct mechanism where glycolysis is influencing CTBP expression in order to utilize the increased levels of NADH produced in hESCs cultured under hypoxic conditions (Fjeld et al., 2003; Zhang et al., 2002).

This study shows that CTBPs increase pluripotency marker expression. CTBP1 enhanced the expression of OCT4, SOX2, and NANOG, while CTBP2 increased only OCT4 and NANOG protein levels. No compensatory increase was reported in either CTBP isoform, which is contrasting to that observed in human breast cancer cell lines (Birts et al., 2010). These data suggest that only CTBP1 is required for the enhancement of SOX2 expression. A previous study indicated that CTBP1 can function as a monomer and interact with a bromodomain (Kim et al., 2005). However, data from this study shows that CTBP dimerization and activity is essential for the enhancement of OCT4, SOX2, and NANOG in hESCs, as inhibiting CTBP function using the CTBP inhibitor MTOB displayed no effect on CTBP expression, but demonstrated a significant decrease in pluripotency marker expression.

Although the exact mechanism(s) of regulation remains to be elucidated, it is possible that CTBPs are activating OCT4, SOX2, and NANOG expression directly by acting as a coactivator at the promoter regions of the three pluripotency factors. This theory is supported by a previous study, which identified both CTBP1 and CTBP2 as OCT4-associated proteins (Pardo et al., 2010), and *Ctbp2* was identified as a target of NANOG in mouse ESCs (Kim et al., 2015). Alternatively, CTBPs may still be functioning in a gene-specific manner, but indirectly affecting hESC self-renewal. For example, CTBPs could act as a corepressor by inhibiting the expression of a lineage-specific gene(s), which results in the observed increase in OCT4, SOX2, and NANOG expression when CTBPs are expressed in hESCs. However, a recent study described CTBPs interacting with a known component of the CTBP corepressor complex, LSD1, in human gastrointestinal endocrine cells. However, LSD1 was shown to activate the expression of the protein NeuroD1 (Ray et al., 2014), suggesting that components of the CTBP complex may have dual functions.

Although the mechanism behind CTBP-mediated transcriptional activation is not fully characterized, the study by Ray et al. (2014) demonstrated that a PXDLS motif-containing DNA-binding transcription factor recruited CTBPs and the associated chromatin-modifying complexes and cofactors, including LSD1, to a promoter region to drive target gene expression. This is one of the few examples describing CTBPs as transcriptional coactivators in human cell types, but may provide a basis for the mechanism behind CTBPs directly promoting hESC self-renewal cultured under hypoxic conditions.

In conclusion, we demonstrate that the oligomerization and activity of the CTBP family of metabolic sensors enhance the expression of OCT4, SOX2, and NANOG. Moreover, the rate of flux through glycolysis was found to regulate CTBP1 and CTBP2 as well as self-renewal of hESCs by modulating HIF-2α expression. These data demonstrate mechanisms by which metabolism regulates hESC self-renewal.

EXPERIMENTAL PROCEDURES

hESC Culture

Hues-7 hESCs (D. Melton, Howard Hughes Medical Institute/Harvard University) and Shef3 hESCs (UK Stem Cell Bank) were cultured at 20% oxygen in KnockOut DMEM (Invitrogen) supplemented with 15% knockout serum replacement (Invitrogen), 100 mg/mL penicillin streptomycin (Invitrogen), 1% L-GlutaMAX (Invitrogen), 1% non-essential amino acids (Invitrogen), 55 μM β-mercaptoethanol and 10 ng/μL basic fibroblast growth factor (PeproTech) on γ-irradiated mouse embryonic fibroblasts (MEFs) (a primary source derived in institutional facilities at University of Southampton following approval by the ethical review committee and according to UK Home Office regulations). hESCs were then transferred to Matrigel (BD Biosciences)-coated plates and cultured in MEF-conditioned medium (CM) at both 20% and 5% oxygen. They were maintained for a minimum of three passages on Matrigel at both oxygen tensions prior to use.

Immunocytochemistry

hESCs cultured on γ-irradiated MEFs on chamber slides were fixed in 4% paraformaldehyde for 15 min. Non-specific antibody binding was blocked with 10% fetal calf serum and, where necessary, cells were permeabilized with 0.2% Triton X-100 for 30 min. Cells were incubated with primary antibodies diluted in 0.6% BSA for 90 min. Primary antibodies used were CTBP1 (BD Biosciences; 612042) 1:200, CTBP2 (BD Biosciences; 612044) 1:250, OCT4 (Santa Cruz; sc-5279) 1:100, SOX2 (Cell Signaling Technology; D6D9) 1:200, NANOG (Abcam; ab109250) 1:100, and TRA-1-60 (Santa Cruz; sc-21705) 1:100. Cells were incubated with secondary antibody, goat anti-mouse IgG-fluorescein isothiocyanate (FITC) (Sigma; F2012) 1:100, Alexa Fluor 488 goat anti-rabbit IgG (Invitrogen; A-11008) 1:700, or goat anti-mouse IgM-FITC (Sigma; F9259) 1:200, for 60 min. Cells were mounted in VECTASHIELD with DAPI (Vector Laboratories) and visualized using a Zeiss fluorescence microscope and Axiovision imaging software.

qRT-PCR

mRNA was isolated from hESCs cultured on Matrigel on day 3 post-passage using TRIzol (Invitrogen) and RNA (1 μg) was reverse transcribed into cDNA using Moloney murine leukemia virus reverse transcriptase (Promega). Real-time -qPCR was performed using a 7500 Real-Time PCR system using Applied Biosystems reagents in 20-μL reactions containing either 1 μg cDNA, 14 μL 2× TaqMan Universal PCR Master Mix, 1 μL TaqMan probe (*POU5F1*: Hs01895061_u1; *SOX2*: Hs00602736_s1; *NANOG*: Hs02387400_g1; *LIN28B*: Hs01013729_m1; *SALL4*: Hs00360675_m1: *CTBP1*: Hs00972288_g1; *CTBP2*: Hs00949547_g1; *EPAS1*: Hs01026142_m1; *ubiquitin C* (*UBC*): Hs00824723_m1; *CXCR4*: Hs00607978_s1; *KDR*: Hs00911700_m1) and diethyl pyrocarbonate (DEPC) water, or containing 1 μg cDNA, 10 μL SYBR Green Master Mix, 2 μL forward primer (5 μM; Table S1), 2 μL reverse primer (5 μM; Table S1), and DEPC water. The following cycling parameters were used: 50°C for 2 min, 95°C for 10 min, followed by 45 cycles of 95°C for 15 s, and 60°C for 1 min. All target transcripts were analyzed in duplicate and normalized to *UBC* for TaqMan probes or *β-ACTIN* for SYBR Green. Relative gene expression was calculated as described previously using the comparative Ct method ($2^{-\Delta\Delta Ct}$) (Livak and Schmittgen, 2001).

Western Blotting

Protein was isolated from hESCs cultured on Matrigel on day 3 post-passage by incubating in ice-cold radio immuno-precipitation assay buffer for 20 min followed by sonication for 30 s. Protein concentration was quantified using the Bradford assay (Bradford, 1976) and lysates (50 μg) resolved on either 8% or 12% acrylamide gels, transferred to nitrocellulose membranes and blocked in either Tris-buffered saline (TBS) or PBS containing 0.1% Tween 20 and 5% non-fat powdered milk for 1 h at room temperature, with the exception of HIF-2α, which was blocked with TBS containing 0.1% Tween 20, 5% non-fat powdered milk and 1% BSA. Membranes were incubated in primary antibody (OCT4 [Santa Cruz; sc-5279] 1:1,000; SOX2 [Cell Signaling Technology; D6D9] 1:3,000; NANOG [Abcam; ab109250] 1:500; CTBP1 [BD Biosciences; 612042] 1:2,000; CTBP2 [BD Biosciences; 612044] 1:2000; HIF-2α [Novus Biologicals; NB100-122] 1:250; E-cadherin [Cell Signaling Technology; 24E10] 1:500) diluted in blocking buffer overnight at 4°C. Membranes were washed and incubated in horse radish peroxidase-conjugated secondary antibodies (anti-mouse [GE Healthcare; NXA931] 1:100,000; or anti-rabbit [GE Healthcare; NA934] 1:50,000) for 1 h at room temperature. Protein expression was quantified relative to β-ACTIN expression which was detected with mouse anti-β-ACTIN peroxidase-conjugated antibody (Sigma; A3854; 1:50,000). Membranes were developed using the ECL advanced Western Blotting Kit (Amersham).

siRNA Transfection

hESCs maintained on Matrigel at 5% oxygen were passaged and incubated overnight. For each transfection, 50 nM siRNA (CTBP1/2 [Ambion]; CTBP1 [Ambion]; CTBP2 [Ambion]; HIF-2α [QIAGEN]), along with 12 μL INTERFERin for CTBP siRNAs (Polyplus) or HiPerFect for HIF-2α siRNA (QIAGEN) transfection reagent were mixed in 200 μL of KnockOut DMEM (Invitrogen) and added

in a drop-wise manner to 1 well of a 6-well plate. Cells were harvested 48 h post-transfection and RNA or protein extracted. Allstars control siRNA (QIAGEN) that has no homology to any known mammalian gene was used as a negative control for each transfection.

For double knockdowns (CTBP1+2 siRNA), 50 nM of each siRNA and 12 μL InterferIN transfection reagent were added to 200 μL of KnockOut DMEM. Twice the volume of Allstars negative control siRNA was added to the controls.

Pharmacological Treatment of hESCs

hESCs cultured on Matrigel at 5% oxygen were passaged and incubated overnight. Cells were treated with either 0, 0.2, 1, or 10 mM 2-DG (Sigma), 0 or 25 μM 3-BrP (Sigma); or 0 or 1 mM MTOB (Sigma), supplemented CM for 48 h. Cells were harvested 48 h after treatment and RNA or protein extracted.

ChIP Assays

ChIP assays were performed on chromatin isolated from Hues-7 hESCs maintained on Matrigel at either 5% or 20% oxygen using the ChIP-IT Express Enzymatic Kit (Active Motif) and the following antibodies: HIF-2α (Novus Biologicals; NB100-122) and rabbit IgG (Santa Cruz; sc-2027). DNA samples were cleaned up before PCR analysis using the QIAquick PCR Purification Kit (QIAGEN). Recovered DNA was amplified using SYBR Green qPCR with custom primers (Sigma) spanning the potential HRE sites at −128 and −2,114 bp upstream of the transcription start site of the *CTBP1* and *CTBP2* proximal promoters, respectively (*CTBP1* forward: ACACGTGTTCCCTCCTTCATG; *CTBP1* reverse: CAGGTGTCACC AGAGCTTTGG; *CTBP2* forward: CCTATGAAGGTCACGCGAAAA; *CTBP2* reverse: TTGCCCGCTAGTCCACGTA).

Lactate Assay

hESCs were passaged onto 12-well Matrigel-coated plates and incubated overnight. Cells were cultured in 0, 0.2, 1, or 10 mM 2-DG, or 0 or 25 μM 3-BrP, supplemented CM for 48 h, where the CM was changed after 24 h. CM samples were collected prior to trypsinizing the cells to perform a cell count. Enzyme-linked biochemical assays were used to calculate lactate production in pmol/cell/24 h and adapted from methods described previously (Houghton et al., 1996). Fluorescence at 460 nm was measured for each sample after excitation of NADH at 340 nm using a FLUOstar Optima microplate reader (BMG Labtech) and Optima software. The same CM was used for all lactate assays.

Statistical Analysis

Using Minitab or Graphpad Prism, the Anderson-Darling normality test was used to determine whether data were normally distributed. Any differences in gene or protein expression with oxygen tension or siRNA transfection were analyzed using a one-sample t-test. Differences in gene expression were normalized to either *UBC* or *β-ACTIN* and then to 1. Protein expression was normalized to β-ACTIN and then to 1 for cells cultured at 5% oxygen, to Allstars transfection controls or untreated control cells. Percentage of Input (non-immunoprecipitated chromatin) was calculated as $100 \times 2^{[Ct(Input) - Ct(IP)]}$ for each sample. Differences in chromatin relative enrichment between cells cultured at 5% and 20% oxygen tension were analyzed using a one-sample t-test. Differences in lactate production between cells cultured in the presence or absence of either 2-DG, or 3-BrP were analyzed using unpaired Student's t tests.

Graphs represent means ± SEM of at least three individual experiments unless otherwise stated. A value of $p \leq 0.05$ was used to indicate significance. *$p < 0.05$, **$p < 0.01$, ***$p < 0.001$.

SUPPLEMENTAL INFORMATION

Supplemental Information can be found online at https://doi.org/10.1016/j.stemcr.2019.02.005.

AUTHOR CONTRIBUTIONS

S.A.A., J.P.B., and F.D.H. conceived and designed the experiments. S.A.A. performed the experiments. S.A.A. analyzed the data. S.A.A., J.P.B., and F.D.H. contributed to the writing of the manuscript.

ACKNOWLEDGMENTS

We thank Kate Parry for technical support. This work is funded by a Vice Chancellor's Scholarship, the Faculty of Medicine, University of Southampton and the UK Medical Research Council G0701153 awarded to F.D.H.

Received: September 12, 2017
Revised: February 13, 2019
Accepted: February 14, 2019
Published: March 14, 2019

REFERENCES

Bergman, L.M., Morris, L., Darley, M., Mirnezami, A.H., Gunatilake, S.C., and Blaydes, J.P. (2006). Role of the unique N-terminal domain of CtBP2 in determining the subcellular localisation of CtBP family proteins. BMC Cell Biol. *7*, 35.

Birts, C.N., Harding, R., Soosaipillai, G., Halder, T., Azim-Araghi, A., Darley, M., Cutress, R.I., Bateman, A.C., and Blaydes, J.P. (2010). Expression of CtBP family protein isoforms in breast cancer and their role in chemoresistance. Biol. Cell *103*, 1–19.

Boyd, J.M., Subramanian, T., Schaeper, U., La Regina, M., Bayley, S., and Chinnadurai, G. (1993). A region in the C-terminus of adenovirus 2/5 E1a protein is required for association with a cellular phosphoprotein and important for the negative modulation of T24-ras mediated transformation, tumorigenesis and metastasis. EMBO J. *12*, 469–478.

Bradford, M.M. (1976). A rapid and sensitive method for the quantitation of microgram quantities of protein utilizing the principle of protein-dye binding. Anal. Biochem. *72*, 248–254.

Chen, H.F., Kuo, H.C., Lin, S.P., Chien, C.L., Chiang, M.S., and Ho, H.N. (2010). Hypoxic culture maintains self-renewal and enhances embryoid body formation of human embryonic stem cells. Tissue Eng. Part A *16*, 2901–2913.

Chinnadurai, G. (2002). CtBP, an unconventional transcriptional corepressor in development and oncogenesis. Mol. Cell *9*, 213–224.

Chinnadurai, G. (2007). CtBP family proteins: unique transcriptional regulators in the nucleus with diverse cytosolic functions. In CtBP Family Proteins, G. Chinnadurai, ed. (Springer), pp. 1–17.

Christensen, D.R., Calder, P.C., and Houghton, F.D. (2015). GLUT3 and PKM2 regulate OCT4 expression and support hypoxic culture of human embryonic stem cells. Sci. Rep. *5*, 17500.

Corda, D., Colanzi, A., and Luini, A. (2006). The multiple activities of CtBP/BARS proteins: the Golgi view. Trends Cell Biol. *16*, 167–173.

Evans, M.J., and Kaufman, M.H. (1981). Establishment in culture of pluripotential cells from mouse embryos. Nature *292*, 154–156.

Ezashi, T., Das, P., and Roberts, R.M. (2005). Low O_2 tensions and the prevention of differentiation of hES cells. Proc. Natl. Acad. Sci. U S A *102*, 4783–4788.

Fang, M., Li, J., Blauwkamp, T., Bhambhani, C., Campbell, N., and Cadigan, K.M. (2006). C-terminal-binding protein directly activates and represses Wnt transcriptional targets in *Drosophila*. EMBO J. *25*, 2735–2745.

Fjeld, C.C., Birdsong, W.T., and Goodman, R.H. (2003). Differential binding of NAD+ and NADH allows the transcriptional corepressor carboxyl-terminal binding protein to serve as a metabolic sensor. Proc. Natl. Acad. Sci. U S A *100*, 9202–9207.

Forristal, C.E., Christensen, D.R., Chinnery, F.E., Petruzzelli, R., Parry, K.L., Sanchez-Elsner, T., and Houghton, F.D. (2013). Environmental oxygen tension regulates the energy metabolism and self-renewal of human embryonic stem cells. PLoS One *8*, e62507.

Forristal, C.E., Wright, K.L., Hanley, N.A., Oreffo, R.O.C., and Houghton, F.D. (2010). Hypoxia inducible factors regulate pluripotency and proliferation in human embryonic stem cells cultured at reduced oxygen tensions. Reproduction *139*, 85–97.

Grooteclaes, M., Deveraux, Q., Hildebrand, J., Zhang, Q., Goodman, R.H., and Frisch, S.M. (2003). C-terminal-binding protein corepresses epithelial and proapoptotic gene expression programs. Proc. Natl. Acad. Sci. U S A *100*, 4568–4573.

Grooteclaes, M.L., and Frisch, S.M. (2000). Evidence for a function of CtBP in epithelial gene regulation and anoikis. Oncogene *19*, 3823–3828.

Gu, W., Gaeta, X., Sahakyan, A., Chan, A.B., Hong, C.S., Kim, R., Braas, D., Plath, K., Lowry, W.E., and Christofk, H.R. (2016). Glycolytic metabolism plays a functional role in regulating human pluripotent stem cell State. Cell Stem Cell *19*, 476–490.

Hildebrand, J.D., and Soriano, P. (2002). Overlapping and unique roles for C-terminal binding protein 1 (CtBP1) and CtBP2 during mouse development. Mol. Cell. Biol. *22*, 5296–5307.

Houghton, F.D., Thompson, J.G., Kennedy, C.J., and Leese, H.J. (1996). Oxygen consumption and energy metabolism of the early mouse embryo. Mol. Reprod. Dev. *44*, 476–485.

Itoh, T.Q., Matsumoto, A., and Tanimura, T. (2013). C-terminal binding protein (CtBP) activates the expression of E-box clock genes with CLOCK/CYCLE in *Drosophila*. PLoS One *8*, e63113.

Kallio, P.J., Okamoto, K., O'Brien, S., Carrero, P., Makino, Y., Tanaka, H., and Poellinger, L. (1998). Signal transduction in hypoxic cells: inducible nuclear translocation and recruitment of the CBP/p300 coactivator by the hypoxia-inducible factor-1alpha. EMBO J. *17*, 6573–6586.

Kim, J.H., Cho, E.J., Kim, S.T., and Youn, H.D. (2005). CtBP represses p300-mediated transcriptional activation by direct association with its bromodomain. Nat. Struct. Mol. Biol. *12*, 423–428.

Kim, T.W., Kang, B.H., Jang, H., Kwak, S., Shin, J., Kim, H., Lee, S.-E., Lee, S.-M., Lee, J.-H., Kim, J.-H., et al. (2015). Ctbp2 modulates NuRD-medicated deacetylation of H3K27 and facilitates PRC2-mediated H3K27me3 in active embryonic stem cell genes during exit from pluripotency. Stem Cells *33*, 2442–2455.

Kumar, V., Carlson, J.E., Ohgi, K.A., Edwards, T.A., Rose, D.W., Escalante, C.R., Rosenfeld, M.G., and Aggarwal, A.K. (2002). Transcription corepressor CtBP is an NAD(+)-regulated dehydrogenase. Mol. Cell *10*, 857–869.

Kuppuswamy, M., Vijayalingam, S., Zhao, L.J., Zhou, Y., Subramanian, T., Ryerse, J., and Chinnadurai, G. (2008). Role of the PLDLS-binding cleft region of CtBP1 in recruitment of core and auxiliary components of the corepressor complex. Mol. Cell. Biol. *28*, 269–281.

Livak, K.J., and Schmittgen, T.D. (2001). Analysis of relative gene expression data using real-time quantitative PCR and the 2(-Delta Delta C(T)) method. Methods *25*, 402–408.

Lu, H., Dalgard, C.L., Mohyeldin, A., McFate, T., Tait, A.S., and Verma, A. (2005). Reversible inactivation of HIF-1 prolyl hydroxylases allows cell metabolism to control basal HIF-1. J. Biol. Chem. *280*, 41928–41939.

Lu, H., Forbes, R.A., and Verma, A. (2002). Hypoxia-inducible factor 1 activation by aerobic glycolysis implicates the Warburg effect in carcinogenesis. J. Biol. Chem. *277*, 23111–23115.

Ludwig, T.E., Levenstein, M.E., Jones, J.M., Berggren, W.T., Mitchen, E.R., Frane, J.L., Crandall, L.J., Daigh, C.A., Conard, K.R., Piekarczyk, M.S., et al. (2006). Derivation of human embryonic stem cells in defined conditions. Nat. Biotechnol. *24*, 185–187.

Martin, G.R. (1981). Isolation of a pluripotent cell line from early mouse embryos cultured in medium conditioned by teratocarcinoma stem cells. Proc. Natl. Acad. Sci. U S A *78*, 7634–7638.

Pardo, M., Lang, B., Yu, L., Prosser, H., Bradley, A., Babu, M.M., and Choudhary, J. (2010). An expanded Oct4 interaction network: implications for stem cell biology, development, and disease. Cell Stem Cell *6*, 382–395.

Petruzzelli, R., Christensen, D.R., Parry, K.L., Sanchez-Elsner, T., and Houghton, F.D. (2014). HIF-2alpha regulates NANOG expression in human embryonic stem cells following hypoxia and reoxygenation through the interaction with an Oct-Sox *cis* regulatory element. PLoS One *9*, e108309.

Prasad, S.M., Czepiel, M., Cetinkaya, C., Smigielska, K., Weli, S.C., Lysdahl, H., Gabrielsen, A., Petersen, K., Ehlers, N., Fink, T., et al. (2009). Continuous hypoxic culturing maintains activation of Notch and allows long-term propagation of human embryonic stem cells without spontaneous differentiation. Cell Prolif. *42*, 63–74.

Ray, S.K., Li, H.J., Metzger, E., Schule, R., and Leiter, A.B. (2014). CtBP and associated LSD1 are required for transcriptional activation by NeuroD1 in gastrointestinal endocrine cells. Mol. Cell. Biol. *34*, 2308–2317.

Sathananthan, H., Pera, M., and Trounson, A. (2002). The fine structure of human embryonic stem cells. Reprod. Biomed. Online *4*, 56–61.

Schaeper, U., Boyd, J.M., Verma, S., Uhlmann, E., Subramanian, T., and Chinnadurai, G. (1995). Molecular cloning and characterization of a cellular phosphoprotein that interacts with a conserved C-terminal domain of adenovirus E1A involved in negative modulation of oncogenic transformation. Proc. Natl. Acad. Sci. U S A *92*, 10467–10471.

Semenza, G.L. (2000). HIF-1: mediator of physiological and pathophysiological responses to hypoxia. J. Appl. Physiol. (1985) *88*, 1474–1480.

Semenza, G.L., and Wang, G.L. (1992). A nuclear factor induced by hypoxia via de novo protein synthesis binds to the human erythropoietin gene enhancer at a site required for transcriptional activation. Mol. Cell. Biol. *12*, 5447–5454.

Semenza, G.L., Roth, P.H., Fang, H.M., and Wang, G.L. (1994). Transcriptional regulation of genes encoding glycolytic enzymes by hypoxia-inducible factor 1. J. Biol. Chem. *269*, 23757–23763.

Shi, Y., Sawada, J., Sui, G., Affar el, B., Whetstine, J.R., Lan, F., Ogawa, H., Luke, M.P., Nakatani, Y., and Shi, Y. (2003). Coordinated histone modifications mediated by a CtBP co-repressor complex. Nature *422*, 735–738.

Straza, M.W., Paliwal, S., Kovi, R.C., Rajeshkumar, B., Trenh, P., Parker, D., Whalen, G.F., Lyle, S., Schiffer, C.A., and Grossman, S.R. (2010). Therapeutic targeting of C-terminal binding protein in human cancer. Cell Cycle *9*, 3740–3750.

Thomson, J.A., Itskovitz-Eldor, J., Shapiro, S.S., Waknitz, M.A., Swiergiel, J.J., Marshall, V.S., and Jones, J.M. (1998). Embryonic stem cell lines derived from human blastocysts. Science *282*, 1145–1147.

Turner, J., and Crossley, M. (2001). The CtBP family: enigmatic and enzymatic transcriptional co-repressors. BioEssays *23*, 683–690.

Varum, S., Rodrigues, A.S., Moura, M.B., Momcilovic, O., Easley, C.A.t., Ramalho-Santos, J., Van Houten, B., and Schatten, G. (2011). Energy metabolism in human pluripotent stem cells and their differentiated counterparts. PLoS One *6*, e20914.

Verger, A., Quinlan, K.G., Crofts, L.A., Spano, S., Corda, D., Kable, E.P., Braet, F., and Crossley, M. (2006). Mechanisms directing the nuclear localization of the CtBP family proteins. Mol. Cell. Biol. *26*, 4882–4894.

Westfall, S.D., Sachdev, S., Das, P., Hearne, L.B., Hannink, M., Roberts, R.M., and Ezashi, T. (2008). Identification of oxygen-sensitive transcriptional programs in human embryonic stem cells. Stem Cells Dev. *17*, 869–881.

Zhang, Q., Piston, D.W., and Goodman, R.H. (2002). Regulation of corepressor function by nuclear NADH. Science *295*, 1895–1897.

Zhao, L.J., Subramanian, T., Zhou, Y., and Chinnadurai, G. (2006). Acetylation by p300 regulates nuclear localization and function of the transcriptional corepressor CtBP2. J. Biol. Chem. *281*, 4183–4189.

References

Abu Dawud, R., Schreiber, K., Schomburg, D., and Adjaye, J. (2012). Human embryonic stem cells and embryonal carcinoma cells have overlapping and distinct metabolic signatures. PLoS One *7*, e39896.

Aebersold, D.M., Burri, P., Beer, K.T., Laissue, J., Djonov, V., Greiner, R.H., and Semenza, G.L. (2001). Expression of hypoxia-inducible factor-1alpha: a novel predictive and prognostic parameter in the radiotherapy of oropharyngeal cancer. Cancer research *61*, 2911-2916.

Aguilar-Gallardo, C., Poo, M., Gomez, E., Galan, A., Sanchez, E., Marques-Mari, A., Ruiz, V., Medrano, J., Riboldi, M., Valbuena, D*., et al.* (2010). Derivation, characterization, differentiation, and registration of seven human embryonic stem cell lines (VAL-3, -4, -5, -6M, -7, -8, and -9) on human feeder. In vitro cellular & developmental biology Animal *46*, 317-326.

Alderton, W.K., Cooper, C.E., and Knowles, R.G. (2001). Nitric oxide synthases: structure, function and inhibition. The Biochemical journal *357*, 593-615.

Almeida, A., Moncada, S., and Bolanos, J.P. (2004). Nitric oxide switches on glycolysis through the AMP protein kinase and 6-phosphofructo-2-kinase pathway. Nature cell biology *6*, 45-51.

Alpatov, R., Munguba, G.C., Caton, P., Joo, J.H., Shi, Y., Shi, Y., Hunt, M.E., and Sugrue, S.P. (2004). Nuclear speckle-associated protein Pnn/DRS binds to the transcriptional corepressor CtBP and relieves CtBP-mediated repression of the E-cadherin gene. Mol Cell Biol *24*, 10223-10235.

Alptekin, A., Ye, B., and Ding, H.F. (2017). Transcriptional Regulation of Stem Cell and Cancer Stem Cell Metabolism. Curr Stem Cell Rep *3*, 19-27.

Ambrosetti, D.C., Basilico, C., and Dailey, L. (1997). Synergistic activation of the fibroblast growth factor 4 enhancer by Sox2 and Oct-3 depends on protein-protein interactions facilitated by a specific spatial arrangement of factor binding sites. Mol Cell Biol *17*, 6321-6329.

Ambrosetti, D.C., Scholer, H.R., Dailey, L., and Basilico, C. (2000). Modulation of the activity of multiple transcriptional activation domains by the DNA binding domains mediates the synergistic action of Sox2 and Oct-3 on the fibroblast growth factor-4 enhancer. The Journal of biological chemistry *275*, 23387-23397.

Amit, M., Carpenter, M.K., Inokuma, M.S., Chiu, C.P., Harris, C.P., Waknitz, M.A., Itskovitz-Eldor, J., and Thomson, J.A. (2000). Clonally derived human embryonic stem cell lines maintain pluripotency and proliferative potential for prolonged periods of culture. Developmental biology *227*, 271-278.

Amit, M., Margulets, V., Segev, H., Shariki, K., Laevsky, I., Coleman, R., and Itskovitz-Eldor, J. (2003). Human feeder layers for human embryonic stem cells. Biology of reproduction *68*, 2150-2156.

Amit, M., Shariki, C., Margulets, V., and Itskovitz-Eldor, J. (2004). Feeder layer- and serum-free culture of human embryonic stem cells. Biology of reproduction *70*, 837-845.

Andrews, P.W. (1984). Retinoic acid induces neuronal differentiation of a cloned human embryonal carcinoma cell line in vitro. Developmental biology *103*, 285-293.

Andrews, P.W. (2002). From teratocarcinomas to embryonic stem cells. Philosophical transactions of the Royal Society of London Series B, Biological sciences *357*, 405-417.

Andrews, P.W., Banting, G., Damjanov, I., Arnaud, D., and Avner, P. (1984). Three monoclonal antibodies defining distinct differentiation antigens associated with different high molecular weight polypeptides on the surface of human embryonal carcinoma cells. Hybridoma *3*, 347-361.

Andrews, P.W., Matin, M.M., Bahrami, A.R., Damjanov, I., Gokhale, P., and Draper, J.S. (2005). Embryonic stem (ES) cells and embryonal carcinoma (EC) cells: opposite sides of the same coin. Biochem Soc Trans *33*, 1526-1530.

Asadi, M.H., Mowla, S.J., Fathi, F., Aleyasin, A., Asadzadeh, J., and Atlasi, Y. (2011). OCT4B1, a novel spliced variant of OCT4, is highly expressed in gastric cancer and acts as an antiapoptotic factor. Int J Cancer *128*, 2645-2652.

Atchison, L., Ghias, A., Wilkinson, F., Bonini, N., and Atchison, M.L. (2003). Transcription factor YY1 functions as a PcG protein in vivo. EMBO J *22*, 1347-1358.

Atlasi, Y., Mowla, S.J., Ziaee, S.A., and Bahrami, A.R. (2007). OCT-4, an embryonic stem cell marker, is highly expressed in bladder cancer. Int J Cancer *120*, 1598-1602.

Atlasi, Y., Mowla, S.J., Ziaee, S.A., Gokhale, P.J., and Andrews, P.W. (2008). OCT4 spliced variants are differentially expressed in human pluripotent and nonpluripotent cells. Stem Cells *26*, 3068-3074.

Avery, S., Inniss, K., and Moore, H. (2006). The regulation of self-renewal in human embryonic stem cells. Stem Cells Dev *15*, 729-740.

Avilion, A.A., Nicolis, S.K., Pevny, L.H., Perez, L., Vivian, N., and Lovell-Badge, R. (2003). Multipotent cell lineages in early mouse development depend on SOX2 function. Genes Dev *17*, 126-140.

Avvakumov, G.V., Walker, J.R., Xue, S., Li, Y., Duan, S., Bronner, C., Arrowsmith, C.H., and Dhe-Paganon, S. (2008). Structural basis for recognition of hemi-methylated DNA by the SRA domain of human UHRF1. Nature *455*, 822-825.

Babaie, Y., Herwig, R., Greber, B., Brink, T.C., Wruck, W., Groth, D., Lehrach, H., Burdon, T., and Adjaye, J. (2007). Analysis of Oct4-dependent transcriptional networks regulating self-renewal and pluripotency in human embryonic stem cells. Stem Cells *25*, 500-510.

Bajpe, P.K., Heynen, G.J., Mittempergher, L., Grernrum, W., de Rink, I.A., Nijkamp, W., Beijersbergen, R.L., Bernards, R., and Huang, S. (2013). The corepressor CTBP2 is a coactivator of retinoic acid receptor/retinoid X receptor in retinoic acid signaling. Mol Cell Biol *33*, 3343-3353.

Balasubramanian, P., Zhao, L.J., and Chinnadurai, G. (2003). Nicotinamide adenine dinucleotide stimulates oligomerization, interaction with adenovirus E1A and an intrinsic dehydrogenase activity of CtBP. FEBS letters *537*, 157-160.

Ball, K.A., Nelson, A.W., Foster, D.G., and Poyton, R.O. (2012). Nitric oxide produced by cytochrome c oxidase helps stabilize HIF-1alpha in hypoxic mammalian cells. Biochemical and biophysical research communications *420*, 727-732.

Ballas, N., Battaglioli, E., Atouf, F., Andres, M.E., Chenoweth, J., Anderson, M.E., Burger, C., Moniwa, M., Davie, J.R., Bowers, W.J.*, et al.* (2001). Regulation of neuronal traits by a novel transcriptional complex. Neuron *31*, 353-365.

Baltus, G.A., Kowalski, M.P., Zhai, H., Tutter, A.V., Quinn, D., Wall, D., and Kadam, S. (2009). Acetylation of sox2 induces its nuclear export in embryonic stem cells. Stem Cells *27*, 2175-2184.

Barker, R.A., Parmar, M., Studer, L., and Takahashi, J. (2017). Human Trials of Stem Cell-Derived Dopamine Neurons for Parkinson's Disease: Dawn of a New Era. Cell Stem Cell *21*, 569-573.

Barnes, C.J., Vadlamudi, R.K., Mishra, S.K., Jacobson, R.H., Li, F., and Kumar, R. (2003). Functional inactivation of a transcriptional corepressor by a signaling kinase. Nature structural biology *10*, 622-628.

Basu, A., and Atchison, M.L. (2010). CtBP levels control intergenic transcripts, PHO/YY1 DNA binding, and PcG recruitment to DNA. Journal of cellular biochemistry *110*, 62-69.

Baxter, M.A., Camarasa, M.V., Bates, N., Small, F., Murray, P., Edgar, D., and Kimber, S.J. (2009). Analysis of the distinct functions of growth factors and tissue culture substrates necessary for the long-term self-renewal of human embryonic stem cell lines. Stem Cell Res *3*, 28-38.

Becker, K.A., Ghule, P.N., Therrien, J.A., Lian, J.B., Stein, J.L., van Wijnen, A.J., and Stein, G.S. (2006). Self-renewal of human embryonic stem cells is supported by a shortened G1 cell cycle phase. Journal of cellular physiology *209*, 883-893.

Benavides, G.A., Liang, Q., Dodson, M., Darley-Usmar, V., and Zhang, J. (2013). Inhibition of autophagy and glycolysis by nitric oxide during hypoxia-reoxygenation impairs cellular bioenergetics and promotes cell death in primary neurons. Free Radic Biol Med *65*, 1215-1228.

Benham, F.J., Andrews, P.W., Knowles, B.B., Bronson, D.L., and Harris, H. (1981). Alkaline phosphatase isozymes as possible markers of differentiation in human testicular teratocarcinoma cell lines. Developmental biology *88*, 279-287.

Benhar, M., and Stamler, J.S. (2005). A central role for S-nitrosylation in apoptosis. Nature cell biology *7*, 645-646.

Bergman, L.M., Birts, C.N., Darley, M., Gabrielli, B., and Blaydes, J.P. (2009). CtBPs promote cell survival through the maintenance of mitotic fidelity. Mol Cell Biol *29*, 4539-4551.

Bergman, L.M., Morris, L., Darley, M., Mirnezami, A.H., Gunatilake, S.C., and Blaydes, J.P. (2006). Role of the unique N-terminal domain of CtBP2 in determining the subcellular localisation of CtBP family proteins. BMC cell biology *7*, 35.

Bernstein, B.E., Mikkelsen, T.S., Xie, X., Kamal, M., Huebert, D.J., Cuff, J., Fry, B., Meissner, A., Wernig, M., Plath, K.*, et al.* (2006). A bivalent chromatin structure marks key developmental genes in embryonic stem cells. Cell *125*, 315-326.

Berry, W.L., and Janknecht, R. (2013). KDM4/JMJD2 histone demethylases: epigenetic regulators in cancer cells. Cancer research *73*, 2936-2942.

Bertero, A., Madrigal, P., Galli, A., Hubner, N.C., Moreno, I., Burks, D., Brown, S., Pedersen, R.A., Gaffney, D., Mendjan, S.*, et al.* (2015). Activin/nodal signaling and NANOG orchestrate human embryonic stem cell fate decisions by controlling the H3K4me3 chromatin mark. Genes Dev *29*, 702-717.

Bertout, J.A., Patel, S.A., and Simon, M.C. (2008). The impact of O2 availability on human cancer. Nature reviews Cancer *8*, 967-975.

Beyer, S., Kristensen, M.M., Jensen, K.S., Johansen, J.V., and Staller, P. (2008). The histone demethylases JMJD1A and JMJD2B are transcriptional targets of hypoxia-inducible factor HIF. The Journal of biological chemistry *283*, 36542-36552.

Bibikova, M., Chudin, E., Wu, B., Zhou, L., Garcia, E.W., Liu, Y., Shin, S., Plaia, T.W., Auerbach, J.M., Arking, D.E.*, et al.* (2006). Human embryonic stem cells have a unique epigenetic signature. Genome research *16*, 1075-1083.

Billeter, M. (1996). Homeodomain-type DNA recognition. Progress in biophysics and molecular biology *66*, 211-225.

Bilodeau, S., Kagey, M.H., Frampton, G.M., Rahl, P.B., and Young, R.A. (2009). SetDB1 contributes to repression of genes encoding developmental regulators and maintenance of ES cell state. Genes Dev *23*, 2484-2489.

Bird, A. (2002). DNA methylation patterns and epigenetic memory. Genes Dev *16*, 6-21.

Birner, P., Gatterbauer, B., Oberhuber, G., Schindl, M., Rossler, K., Prodinger, A., Budka, H., and Hainfellner, J.A. (2001a). Expression of hypoxia-inducible factor-1 alpha in oligodendrogliomas: its impact on prognosis and on neoangiogenesis. Cancer *92*, 165-171.

Birner, P., Schindl, M., Obermair, A., Breitenecker, G., and Oberhuber, G. (2001b). Expression of hypoxia-inducible factor 1alpha in epithelial ovarian tumors: its impact on prognosis and on response to chemotherapy. Clin Cancer Res *7*, 1661-1668.

Birner, P., Schindl, M., Obermair, A., Plank, C., Breitenecker, G., and Oberhuber, G. (2000). Overexpression of hypoxia-inducible factor 1alpha is a marker for an unfavorable prognosis in early-stage invasive cervical cancer. Cancer research *60*, 4693-4696.

Birts, C.N., Harding, R., Soosaipillai, G., Halder, T., Azim-Araghi, A., Darley, M., Cutress, R.I., Bateman, A.C., and Blaydes, J.P. (2010). Expression of CtBP family protein isoforms in breast cancer and their role in chemoresistance. Biology of the cell / under the auspices of the European Cell Biology Organization *103*, 1-19.

Birts, C.N., Nijjar, S.K., Mardle, C.A., Hoakwie, F., Duriez, P.J., Blaydes, J.P., and Tavassoli, A. (2013). A cyclic peptide inhibitor of C-terminal binding protein dimerization links metabolism with mitotic fidelity in breast cancer cells. Chemical Science *4*, 3046-3057.

Bissell, D.M., Arenson, D.M., Maher, J.J., and Roll, F.J. (1987). Support of cultured hepatocytes by a laminin-rich gel. Evidence for a functionally significant subendothelial matrix in normal rat liver. The Journal of clinical investigation *79*, 801-812.

Boheler, K.R. (2009). Stem cell pluripotency: a cellular trait that depends on transcription factors, chromatin state and a checkpoint deficient cell cycle. Journal of cellular physiology *221*, 10-17.

Bonazzi, M., Spano, S., Turacchio, G., Cericola, C., Valente, C., Colanzi, A., Kweon, H.S., Hsu, V.W., Polishchuck, E.V., Polishchuck, R.S.*, et al.* (2005). CtBP3/BARS drives membrane fission in dynamin-independent transport pathways. Nature cell biology *7*, 570-580.

Bos, R., Zhong, H., Hanrahan, C.F., Mommers, E.C., Semenza, G.L., Pinedo, H.M., Abeloff, M.D., Simons, J.W., van Diest, P.J., and van der Wall, E. (2001). Levels of hypoxia-inducible factor-1 alpha during breast carcinogenesis. J Natl Cancer Inst *93*, 309-314.

Bowles, J., Schepers, G., and Koopman, P. (2000). Phylogeny of the SOX family of developmental transcription factors based on sequence and structural indicators. Developmental biology *227*, 239-255.

Boyd, J.M., Subramanian, T., Schaeper, U., La Regina, M., Bayley, S., and Chinnadurai, G. (1993). A region in the C-terminus of adenovirus 2/5 E1a protein is required for association with a cellular phosphoprotein and important for the negative modulation of T24-ras mediated transformation, tumorigenesis and metastasis. EMBO J *12*, 469-478.

Boyer, L.A., Lee, T.I., Cole, M.F., Johnstone, S.E., Levine, S.S., Zucker, J.P., Guenther, M.G., Kumar, R.M., Murray, H.L., Jenner, R.G.*, et al.* (2005). Core transcriptional regulatory circuitry in human embryonic stem cells. Cell *122*, 947-956.

Boyer, L.A., Plath, K., Zeitlinger, J., Brambrink, T., Medeiros, L.A., Lee, T.I., Levine, S.S., Wernig, M., Tajonar, A., Ray, M.K., *et al.* (2006). Polycomb complexes repress developmental regulators in murine embryonic stem cells. Nature *441*, 349-353.

Braam, S.R., Zeinstra, L., Litjens, S., Ward-van Oostwaard, D., van den Brink, S., van Laake, L., Lebrin, F., Kats, P., Hochstenbach, R., Passier, R., *et al.* (2008). Recombinant vitronectin is a functionally defined substrate that supports human embryonic stem cell self-renewal via alphavbeta5 integrin. Stem Cells *26*, 2257-2265.

Bradford, M.M. (1976). A rapid and sensitive method for the quantitation of microgram quantities of protein utilizing the principle of protein-dye binding. Analytical biochemistry *72*, 248-254.

Brons, I.G., Smithers, L.E., Trotter, M.W., Rugg-Gunn, P., Sun, B., Chuva de Sousa Lopes, S.M., Howlett, S.K., Clarkson, A., Ahrlund-Richter, L., Pedersen, R.A., *et al.* (2007). Derivation of pluripotent epiblast stem cells from mammalian embryos. Nature *448*, 191-195.

Brook, F.A., and Gardner, R.L. (1997). The origin and efficient derivation of embryonic stem cells in the mouse. Proceedings of the National Academy of Sciences of the United States of America *94*, 5709-5712.

Brown, G.C. (1992). Control of respiration and ATP synthesis in mammalian mitochondria and cells. The Biochemical journal *284 (Pt 1)*, 1-13.

Bruick, R.K., and McKnight, S.L. (2001). A conserved family of prolyl-4-hydroxylases that modify HIF. Science *294*, 1337-1340.

Buecker, C., Srinivasan, R., Wu, Z., Calo, E., Acampora, D., Faial, T., Simeone, A., Tan, M., Swigut, T., and Wysocka, J. (2014). Reorganization of enhancer patterns in transition from naive to primed pluripotency. Cell Stem Cell *14*, 838-853.

Bustamante, E., Morris, H.P., and Pedersen, P.L. (1981). Energy metabolism of tumor cells. Requirement for a form of hexokinase with a propensity for mitochondrial binding. The Journal of biological chemistry *256*, 8699-8704.

Bustamante, E., and Pedersen, P.L. (1977). High aerobic glycolysis of rat hepatoma cells in culture: role of mitochondrial hexokinase. Proceedings of the National Academy of Sciences of the United States of America *74*, 3735-3739.

Candelario, K.M., Shuttleworth, C.W., and Cunningham, L.A. (2013). Neural stem/progenitor cells display a low requirement for oxidative metabolism independent of hypoxia inducible factor-1alpha expression. J Neurochem *125*, 420-429.

Carter, A.C., Davis-Dusenbery, B.N., Koszka, K., Ichida, J.K., and Eggan, K. (2014). Nanog-independent reprogramming to iPSCs with canonical factors. Stem cell reports *2*, 119-126.

Castello, P.R., David, P.S., McClure, T., Crook, Z., and Poyton, R.O. (2006). Mitochondrial cytochrome oxidase produces nitric oxide under hypoxic conditions: implications for oxygen sensing and hypoxic signaling in eukaryotes. Cell metabolism *3*, 277-287.

Cauffman, G., Liebaers, I., Van Steirteghem, A., and Van de Velde, H. (2006). POU5F1 isoforms show different expression patterns in human embryonic stem cells and preimplantation embryos. Stem Cells *24*, 2685-2691.

Chachami, G., Paraskeva, E., Mingot, J.M., Braliou, G.G., Gorlich, D., and Simos, G. (2009). Transport of hypoxia-inducible factor HIF-1alpha into the nucleus involves importins 4 and 7. Biochemical and biophysical research communications *390*, 235-240.

Chambers, I., Colby, D., Robertson, M., Nichols, J., Lee, S., Tweedie, S., and Smith, A. (2003). Functional expression cloning of Nanog, a pluripotency sustaining factor in embryonic stem cells. Cell *113*, 643-655.

Chambers, I., Silva, J., Colby, D., Nichols, J., Nijmeijer, B., Robertson, M., Vrana, J., Jones, K., Grotewold, L., and Smith, A. (2007). Nanog safeguards pluripotency and mediates germline development. Nature *450*, 1230-1234.

Chambers, I., and Tomlinson, S.R. (2009). The transcriptional foundation of pluripotency. Development *136*, 2311-2322.

Chen, A.E., and Melton, D.A. (2007). Derivation of human embryonic stem cells by immunosurgery. Journal of visualized experiments : JoVE, 574.

Chen, C., Pore, N., Behrooz, A., Ismail-Beigi, F., and Maity, A. (2001). Regulation of glut1 mRNA by hypoxia-inducible factor-1. Interaction between H-ras and hypoxia. The Journal of biological chemistry *276*, 9519-9525.

Chen, C.L., Uthaya Kumar, D.B., Punj, V., Xu, J., Sher, L., Tahara, S.M., Hess, S., and Machida, K. (2016). NANOG Metabolically Reprograms Tumor-Initiating Stem-like Cells through Tumorigenic Changes in Oxidative Phosphorylation and Fatty Acid Metabolism. Cell metabolism *23*, 206-219.

Chen, H.F., Kuo, H.C., Lin, S.P., Chien, C.L., Chiang, M.S., and Ho, H.N. (2010). Hypoxic culture maintains self-renewal and enhances embryoid body formation of human embryonic stem cells. Tissue engineering Part A *16*, 2901-2913.

Chen, L., Shi, Y., Liu, S., Cao, Y., Wang, X., and Tao, Y. (2014). PKM2: the thread linking energy metabolism reprogramming with epigenetics in cancer. International journal of molecular sciences *15*, 11435-11445.

Chen, X., Vega, V.B., and Ng, H.H. (2008a). Transcriptional regulatory networks in embryonic stem cells. Cold Spring Harbor symposia on quantitative biology *73*, 203-209.

Chen, X., Xu, H., Yuan, P., Fang, F., Huss, M., Vega, V.B., Wong, E., Orlov, Y.L., Zhang, W., Jiang, J.*, et al.* (2008b). Integration of external signaling pathways with the core transcriptional network in embryonic stem cells. Cell *133*, 1106-1117.

Chia, N.Y., Chan, Y.S., Feng, B., Lu, X., Orlov, Y.L., Moreau, D., Kumar, P., Yang, L., Jiang, J., Lau, M.S., *et al.* (2010). A genome-wide RNAi screen reveals determinants of human embryonic stem cell identity. Nature *468*, 316-320.

Chinnadurai, G. (2002). CtBP, an unconventional transcriptional corepressor in development and oncogenesis. Mol Cell *9*, 213-224.

Chinnadurai, G. (2003). CtBP family proteins: more than transcriptional corepressors. BioEssays : news and reviews in molecular, cellular and developmental biology *25*, 9-12
.
Chinnadurai, G. (2007a). CtBP family proteins: unique transcriptional regulators in the nucleus with diverse cytosolic functions. In CtBP family proteins, G. Chinnadurai, ed. (New York, NY: Springer), pp. pg. 1-17.

Chinnadurai, G. (2007b). Transcriptional regulation by C-terminal binding proteins. Int J Biochem Cell Biol *39*, 1593-1607.

Chinnadurai, G. (2009). The transcriptional corepressor CtBP: a foe of multiple tumor suppressors. Cancer research *69*, 731-734.

Cho, M., Lee, E.J., Nam, H., Yang, J.H., Cho, J., Lim, J.M., and Lee, G. (2010). Human feeder layer system derived from umbilical cord stromal cells for human embryonic stem cells. Fertility and sterility *93*, 2525-2531.

Cho, Y.M., Kwon, S., Pak, Y.K., Seol, H.W., Choi, Y.M., Park do, J., Park, K.S., and Lee, H.K. (2006). Dynamic changes in mitochondrial biogenesis and antioxidant enzymes during the spontaneous differentiation of human embryonic stem cells. Biochemical and biophysical research communications *348*, 1472-1478.

Chowdhury, R., Flashman, E., Mecinovic, J., Kramer, H.B., Kessler, B.M., Frapart, Y.M., Boucher, J.L., Clifton, I.J., McDonough, M.A., and Schofield, C.J. (2011). Studies on the reaction of nitric oxide with the hypoxia-inducible factor prolyl hydroxylase domain 2 (EGLN1). Journal of molecular biology *410*, 268-279.

Chowdhury, R., Godoy, L.C., Thiantanawat, A., Trudel, L.J., Deen, W.M., and Wogan, G.N. (2012). Nitric oxide produced endogenously is responsible for hypoxia-induced HIF-1alpha stabilization in colon carcinoma cells. Chem Res Toxicol *25*, 2194-2202.

Christensen, D.R., Calder, P.C., and Houghton, F.D. (2014). Effect of Oxygen Tension on the Amino Acid Utilisation of Human Embryonic Stem Cells. Cellular Physiology and Biochemistry *33*, 237-246.

Christensen, D.R., Calder, P.C., and Houghton, F.D. (2015). GLUT3 and PKM2 regulate OCT4 expression and support hypoxic culture of human embryonic stem cells. Scientific Reports *5*.

Chung, S., Dzeja, P.P., Faustino, R.S., Perez-Terzic, C., Behfar, A., and Terzic, A. (2007). Mitochondrial oxidative metabolism is required for the cardiac differentiation of stem cells. Nature clinical practice Cardiovascular medicine *4 Suppl 1*, S60-67.

Cioffi, C.L., Liu, X.Q., Kosinski, P.A., Garay, M., and Bowen, B.R. (2003). Differential regulation of HIF-1 alpha prolyl-4-hydroxylase genes by hypoxia in human cardiovascular cells. Biochemical and biophysical research communications *303*, 947-953.

Clark, A.T. (2007). The stem cell identity of testicular cancer. Stem cell reviews *3*, 49-59.

Cockman, M.E., Masson, N., Mole, D.R., Jaakkola, P., Chang, G.W., Clifford, S.C., Maher, E.R., Pugh, C.W., Ratcliffe, P.J., and Maxwell, P.H. (2000). Hypoxia inducible factor-alpha binding and ubiquitylation by the von Hippel-Lindau tumor suppressor protein. The Journal of biological chemistry *275*, 25733-25741.

Cole, M.F., Johnstone, S.E., Newman, J.J., Kagey, M.H., and Young, R.A. (2008). Tcf3 is an integral component of the core regulatory circuitry of embryonic stem cells. Genes Dev *22*, 746-755.

Compernolle, V., Brusselmans, K., Acker, T., Hoet, P., Tjwa, M., Beck, H., Plaisance, S., Dor, Y., Keshet, E., Lupu, F.*, et al.* (2002). Loss of HIF-2alpha and inhibition of VEGF impair fetal lung maturation, whereas treatment with VEGF prevents fatal respiratory distress in premature mice. Nature medicine *8*, 702-710.

Corda, D., Colanzi, A., and Luini, A. (2006). The multiple activities of CtBP/BARS proteins: the Golgi view. Trends in cell biology *16*, 167-173.

Covello, K.L., Kehler, J., Yu, H., Gordan, J.D., Arsham, A.M., Hu, C.J., Labosky, P.A., Simon, M.C., and Keith, B. (2006). HIF-2alpha regulates Oct-4: effects of hypoxia on stem cell function, embryonic development, and tumor growth. Genes Dev *20*, 557-570.

Cowan, C.A., Klimanskaya, I., McMahon, J., Atienza, J., Witmyer, J., Zucker, J.P., Wang, S., Morton, C.C., McMahon, A.P., Powers, D.*, et al.* (2004). Derivation of embryonic stem-cell lines from human blastocysts. The New England journal of medicine *350*, 1353-1356.

Cowger, J.J., Zhao, Q., Isovic, M., and Torchia, J. (2007). Biochemical characterization of the zinc-finger protein 217 transcriptional repressor complex: identification of a ZNF217 consensus recognition sequence. Oncogene *26*, 3378-3386.

Criqui-Filipe, P., Ducret, C., Maira, S.M., and Wasylyk, B. (1999). Net, a negative Ras-switchable TCF, contains a second inhibition domain, the CID, that mediates repression through interactions with CtBP and de-acetylation. EMBO J *18*, 3392-3403.

Cui, X.G., Han, Z.T., He, S.H., Wu, X.D., Chen, T.R., Shao, C.H., Chen, D.L., Su, N., Chen, Y.M., Wang, T.*, et al.* (2017). HIF1/2alpha mediates hypoxia-induced LDHA expression in human pancreatic cancer cells. Oncotarget *8*, 24840-24852.

D'Angelo, G., Duplan, E., Boyer, N., Vigne, P., and Frelin, C. (2003). Hypoxia up-regulates prolyl hydroxylase activity: a feedback mechanism that limits HIF-1 responses during reoxygenation. The Journal of biological chemistry *278*, 38183-38187.

Dai, B., and Rasmussen, T.P. (2007). Global epiproteomic signatures distinguish embryonic stem cells from differentiated cells. Stem Cells *25*, 2567-2574.

Damjanov, I. (1990). Teratocarcinoma stem cells. Cancer Surv *9*, 303-319.

Damjanov, I. (1993). Pathobiology of germ cell tumors. Eur Urol *23 Suppl 2*, 5.

Darr, H., Mayshar, Y., and Benvenisty, N. (2006). Overexpression of NANOG in human ES cells enables feeder-free growth while inducing primitive ectoderm features. Development *133*, 1193-1201.

De Miguel, M.P., Alcaina, Y., de la Maza, D.S., and Lopez-Iglesias, P. (2015). Cell metabolism under microenvironmental low oxygen tension levels in stemness, proliferation and pluripotency. Current molecular medicine *15*, 343-359.

Denslow, S.A., and Wade, P.A. (2007). The human Mi-2/NuRD complex and gene regulation. Oncogene *26*, 5433-5438.

Depping, R., Steinhoff, A., Schindler, S.G., Friedrich, B., Fagerlund, R., Metzen, E., Hartmann, E., and Kohler, M. (2008). Nuclear translocation of hypoxia-inducible factors (HIFs): involvement of the classical importin alpha/beta pathway. Biochimica et biophysica acta *1783*, 394-404.

Desai, N., Rambhia, P., and Gishto, A. (2015). Human embryonic stem cell cultivation: historical perspective and evolution of xeno-free culture systems. Reproductive biology and endocrinology : RB&E *13*, 9.

Dhaliwal, N.K., Miri, K., Davidson, S., Tamim El Jarkass, H., and Mitchell, J.A. (2018). KLF4 Nuclear Export Requires ERK Activation and Initiates Exit from Naive Pluripotency. Stem cell reports *10*, 1308-1323.

Ding, J., Xu, H., Faiola, F., Ma'ayan, A., and Wang, J. (2012). Oct4 links multiple epigenetic pathways to the pluripotency network. Cell research *22*, 155-167.

Dioum, E.M., Chen, R., Alexander, M.S., Zhang, Q., Hogg, R.T., Gerard, R.D., and Garcia, J.A. (2009). Regulation of hypoxia-inducible factor 2alpha signaling by the stress-responsive deacetylase sirtuin 1. Science *324*, 1289-1293.

Dixon, F.J., and Moore, R.A. (1952). Tumors of the testicle. Acta - Unio Internationalis Contra Cancrum *8*, 310-315.

Dumoulin, J.C., Meijers, C.J., Bras, M., Coonen, E., Geraedts, J.P., and Evers, J.L. (1999). Effect of oxygen concentration on human in-vitro fertilization and embryo culture. Human reproduction *14*, 465-469.

Elvert, G., Kappel, A., Heidenreich, R., Englmeier, U., Lanz, S., Acker, T., Rauter, M., Plate, K., Sieweke, M., Breier, G.*, et al.* (2003). Cooperative interaction of hypoxia-inducible factor-2alpha (HIF-2alpha) and Ets-1 in the transcriptional activation of

vascular endothelial growth factor receptor-2 (Flk-1). The Journal of biological chemistry *278*, 7520-7530.

Etchegaray, J.P., and Mostoslavsky, R. (2016). Interplay between Metabolism and Epigenetics: A Nuclear Adaptation to Environmental Changes. Mol Cell *62*, 695-711.

Evans, M.J., and Kaufman, M.H. (1981). Establishment in culture of pluripotential cells from mouse embryos. Nature *292*, 154-156.

Ezashi, T., Das, P., and Roberts, R.M. (2005). Low O2 tensions and the prevention of differentiation of hES cells. Proceedings of the National Academy of Sciences of the United States of America *102*, 4783-4788.

Ezeh, U.I., Turek, P.J., Reijo, R.A., and Clark, A.T. (2005). Human embryonic stem cell genes OCT4, NANOG, STELLAR, and GDF3 are expressed in both seminoma and breast carcinoma. Cancer *104*, 2255-2265.

Fagnocchi, L., Mazzoleni, S., and Zippo, A. (2016). Integration of Signaling Pathways with the Epigenetic Machinery in the Maintenance of Stem Cells. Stem cells international *2016*, http://dx.doi.org/10.1155/2016/8652748.

Fang, L., Zhang, J., Zhang, H., Yang, X., Jin, X., Zhang, L., Skalnik, D.G., Jin, Y., Zhang, Y., Huang, X.*, et al.* (2016). H3K4 Methyltransferase Set1a Is A Key Oct4 Coactivactor Essential for Generation of Oct4 Positive Inner Cell Mass. Stem Cells *34*, 565-580.

Fang, L., Zhang, L., Wei, W., Jin, X., Wang, P., Tong, Y., Li, J., Du, J.X., and Wong, J. (2014). A methylation-phosphorylation switch determines Sox2 stability and function in ESC maintenance or differentiation. Mol Cell *55*, 537-551.

Fang, M., Li, J., Blauwkamp, T., Bhambhani, C., Campbell, N., and Cadigan, K.M. (2006). C-terminal-binding protein directly activates and represses Wnt transcriptional targets in Drosophila. EMBO J *25*, 2735-2745.

Farthing, C.R., Ficz, G., Ng, R.K., Chan, C.F., Andrews, S., Dean, W., Hemberger, M., and Reik, W. (2008). Global mapping of DNA methylation in mouse promoters reveals epigenetic reprogramming of pluripotency genes. PLoS genetics *4*, e1000116.

Fazzio, T.G., and Panning, B. (2010). Control of embryonic stem cell identity by nucleosome remodeling enzymes. Current opinion in genetics & development *20*, 500-504.

Feldman, N., Gerson, A., Fang, J., Li, E., Zhang, Y., Shinkai, Y., Cedar, H., and Bergman, Y. (2006). G9a-mediated irreversible epigenetic inactivation of Oct-3/4 during early embryogenesis. Nature cell biology *8*, 188-194.

Feldser, D., Agani, F., Iyer, N.V., Pak, B., Ferreira, G., and Semenza, G.L. (1999). Reciprocal positive regulation of hypoxia-inducible factor 1alpha and insulin-like growth factor 2. Cancer research *59*, 3915-3918.

Festuccia, N., Osorno, R., Halbritter, F., Karwacki-Neisius, V., Navarro, P., Colby, D., Wong, F., Yates, A., Tomlinson, S.R., and Chambers, I. (2012). Esrrb is a direct Nanog target gene that can substitute for Nanog function in pluripotent cells. Cell Stem Cell *11*, 477-490.

Fjeld, C.C., Birdsong, W.T., and Goodman, R.H. (2003). Differential binding of NAD+ and NADH allows the transcriptional corepressor carboxyl-terminal binding protein to serve as a metabolic sensor. Proceedings of the National Academy of Sciences of the United States of America *100*, 9202-9207.

Flamme, I., Frohlich, T., von Reutern, M., Kappel, A., Damert, A., and Risau, W. (1997). HRF, a putative basic helix-loop-helix-PAS-domain transcription factor is closely related to hypoxia-inducible factor-1 alpha and developmentally expressed in blood vessels. Mechanisms of development *63*, 51-60.

Fluckiger, A.C., Marcy, G., Marchand, M., Negre, D., Cosset, F.L., Mitalipov, S., Wolf, D., Savatier, P., and Dehay, C. (2006). Cell cycle features of primate embryonic stem cells. Stem Cells *24*, 547-556.

Fogh, J., and Trempe, G. (1975). New human tumor cell lines. In Human Tumor Cells *in Vitro* (Springer US), pp. 115-159.

Folmes, C.D., Nelson, T.J., Martinez-Fernandez, A., Arrell, D.K., Lindor, J.Z., Dzeja, P.P., Ikeda, Y., Perez-Terzic, C., and Terzic, A. (2011). Somatic oxidative bioenergetics transitions into pluripotency-dependent glycolysis to facilitate nuclear reprogramming. Cell metabolism *14*, 264-271.

Folmes, C.D., and Terzic, A. (2016). Energy metabolism in the acquisition and maintenance of stemness. Seminars in cell & developmental biology *52*, 68-75.

Forristal, C.E., Christensen, D.R., Chinnery, F.E., Petruzzelli, R., Parry, K.L., Sanchez-Elsner, T., and Houghton, F.D. (2013). Environmental Oxygen Tension Regulates the Energy Metabolism and Self-Renewal of Human Embryonic Stem Cells. PLoS ONE *8*.

Forristal, C.E., Wright, K.L., Hanley, N.A., Oreffo, R.O.C., and Houghton, F.D. (2010). Hypoxia inducible factors regulate pluripotency and proliferation in human embryonic stem cells cultured at reduced oxygen tensions. Reproduction (Cambridge, England) *139*.

Forsyth, N.R., Kay, A., Hampson, K., Downing, A., Talbot, R., and McWhir, J. (2008). Transcriptome alterations due to physiological normoxic (2% O2) culture of human embryonic stem cells. Regenerative medicine *3*, 817-833.

Forsyth, N.R., Musio, A., Vezzoni, P., Simpson, A.H., Noble, B.S., and McWhir, J. (2006). Physiologic oxygen enhances human embryonic stem cell clonal recovery and reduces chromosomal abnormalities. Cloning and stem cells *8*, 16-23.

Furusawa, T., Moribe, H., Kondoh, H., and Higashi, Y. (1999). Identification of CtBP1 and CtBP2 as corepressors of zinc finger-homeodomain factor deltaEF1. Mol Cell Biol *19*, 8581-8590.

Gafni, O., Weinberger, L., Mansour, A.A., Manor, Y.S., Chomsky, E., Ben-Yosef, D., Kalma, Y., Viukov, S., Maza, I., Zviran, A.*, et al.* (2013). Derivation of novel human ground state naive pluripotent stem cells. Nature *504*, 282-286.

Gao, X., Wang, H., Yang, J.J., Liu, X., and Liu, Z.R. (2012). Pyruvate kinase M2 regulates gene transcription by acting as a protein kinase. Mol Cell *45*, 598-609.

Gardner, R.L. (1998). Contributions of blastocyst micromanipulation to the study of mammalian development. BioEssays : news and reviews in molecular, cellular and developmental biology *20*, 168-180.

Gehring, W.J., Qian, Y.Q., Billeter, M., Furukubo-Tokunaga, K., Schier, A.F., Resendez-Perez, D., Affolter, M., Otting, G., and Wuthrich, K. (1994). Homeodomain-DNA recognition. Cell *78*, 211-223.

Genbacev, O., Krtolica, A., Zdravkovic, T., Brunette, E., Powell, S., Nath, A., Caceres, E., McMaster, M., McDonagh, S., Li, Y.*, et al.* (2005). Serum-free derivation of human embryonic stem cell lines on human placental fibroblast feeders. Fertility and sterility *83*, 1517-1529.

Gifford, C.A., Ziller, M.J., Gu, H., Trapnell, C., Donaghey, J., Tsankov, A., Shalek, A.K., Kelley, D.R., Shishkin, A.A., Issner, R.*, et al.* (2013). Transcriptional and epigenetic dynamics during specification of human embryonic stem cells. Cell *153*, 1149-1163.

Gomes Sobrinho, D.B., Oliveira, J.B., Petersen, C.G., Mauri, A.L., Silva, L.F., Massaro, F.C., Baruffi, R.L., Cavagna, M., and Franco, J.G., Jr. (2011). IVF/ICSI outcomes after culture of human embryos at low oxygen tension: a meta-analysis. Reproductive biology and endocrinology : RB&E *9*, doi: 10.1186/1477-7827-1189-1143.

Gorlach, A. (2004). Redox control of blood coagulation. Antioxidants & redox signaling *6*, 687-690.

Greber, B., Lehrach, H., and Adjaye, J. (2007a). Fibroblast growth factor 2 modulates transforming growth factor beta signaling in mouse embryonic fibroblasts and human ESCs (hESCs) to support hESC self-renewal. Stem Cells *25*, 455-464.

Greber, B., Lehrach, H., and Adjaye, J. (2007b). Silencing of core transcription factors in human EC cells highlights the importance of autocrine FGF signaling for self-renewal. BMC developmental biology *7*, 46.

Greber, B., Wu, G., Bernemann, C., Joo, J.Y., Han, D.W., Ko, K., Tapia, N., Sabour, D., Sterneckert, J., Tesar, P.*, et al.* (2010). Conserved and divergent roles of FGF signaling in mouse epiblast stem cells and human embryonic stem cells. Cell Stem Cell *6*, 215-226.

Grooteclaes, M., Deveraux, Q., Hildebrand, J., Zhang, Q., Goodman, R.H., and Frisch, S.M. (2003). C-terminal-binding protein corepresses epithelial and proapoptotic gene expression programs. Proceedings of the National Academy of Sciences of the United States of America *100*, 4568-4573.

Grooteclaes, M.L., and Frisch, S.M. (2000). Evidence for a function of CtBP in epithelial gene regulation and anoikis. Oncogene *19*, 3823-3828.

Gu, W., Gaeta, X., Sahakyan, A., Chan, A.B., Hong, C.S., Kim, R., Braas, D., Plath, K., Lowry, W.E., and Christofk, H.R. (2016). Glycolytic Metabolism Plays a Functional Role in Regulating Human Pluripotent Stem Cell State. Cell Stem Cell *19*, 476-490.

Gu, Y.Z., Moran, S.M., Hogenesch, J.B., Wartman, L., and Bradfield, C.A. (1998). Molecular characterization and chromosomal localization of a third alpha-class hypoxia inducible factor subunit, HIF3alpha. Gene expression *7*, 205-213.

Guo, X., Tian, Z., Wang, X., Pan, S., Huang, W., Shen, Y., Gui, Y., Duan, X., and Cai, Z. (2015). Regulation of histone demethylase KDM6B by hypoxia-inducible factor-2alpha. Acta Biochim Biophys Sin (Shanghai) *47*, 106-113.

Hall, J., Guo, G., Wray, J., Eyres, I., Nichols, J., Grotewold, L., Morfopoulou, S., Humphreys, P., Mansfield, W., Walker, R.*, et al.* (2009). Oct4 and LIF/Stat3 additively induce Kruppel factors to sustain embryonic stem cell self-renewal. Cell Stem Cell *5*, 597-609.

Hanna, J., Cheng, A.W., Saha, K., Kim, J., Lengner, C.J., Soldner, F., Cassady, J.P., Muffat, J., Carey, B.W., and Jaenisch, R. (2010a). Human embryonic stem cells with biological and epigenetic characteristics similar to those of mouse ESCs. Proceedings of the National Academy of Sciences of the United States of America *107*, 9222-9227.

Hanna, J., Markoulaki, S., Mitalipova, M., Cheng, A.W., Cassady, J.P., Staerk, J., Carey, B.W., Lengner, C.J., Foreman, R., Love, J.*, et al.* (2009). Metastable pluripotent states in NOD-mouse-derived ESCs. Cell Stem Cell *4*, 513-524.

Hanna, J.H., Saha, K., and Jaenisch, R. (2010b). Pluripotency and cellular reprogramming: facts, hypotheses, unresolved issues. Cell *143*, 508-525.

Harley, C.B. (1991). Telomere loss: mitotic clock or genetic time bomb? Mutation research *256*, 271-282.

Harley, C.B., Vaziri, H., Counter, C.M., and Allsopp, R.C. (1992). The telomere hypothesis of cellular aging. Experimental gerontology *27*, 375-382.

Harris, A.L. (2002). Hypoxia--a key regulatory factor in tumour growth. Nature reviews Cancer *2*, 38-47.

Harvey, A.J., Rathjen, J., Yu, L.J., and Gardner, D.K. (2014). Oxygen modulates human embryonic stem cell metabolism in the absence of changes in self-renewal. Reproduction, fertility, and development *28*, 446-458.

Heidbreder, M., Frohlich, F., Johren, O., Dendorfer, A., Qadri, F., and Dominiak, P. (2003). Hypoxia rapidly activates HIF-3alpha mRNA expression. FASEB journal : official publication of the Federation of American Societies for Experimental Biology *17*, 1541-1543.

Heikkila, M., Pasanen, A., Kivirikko, K.I., and Myllyharju, J. (2011). Roles of the human hypoxia-inducible factor (HIF)-3alpha variants in the hypoxia response. Cellular and molecular life sciences : CMLS *68*, 3885-3901.

Henderson, J.K., Draper, J.S., Baillie, H.S., Fishel, S., Thomson, J.A., Moore, H., and Andrews, P.W. (2002). Preimplantation human embryos and embryonic stem cells show comparable expression of stage-specific embryonic antigens. Stem Cells *20*, 329-337.

Herr, W., and Cleary, M.A. (1995). The POU domain: versatility in transcriptional regulation by a flexible two-in-one DNA-binding domain. Genes Dev *9*, 1679-1693.

Hewitson, L.C., and Leese, H.J. (1993). Energy metabolism of the trophectoderm and inner cell mass of the mouse blastocyst. The Journal of experimental zoology *267*, 337-343.

Hilbert, B.J., Grossman, S.R., Schiffer, C.A., and Royer, W.E., Jr. (2014). Crystal structures of human CtBP in complex with substrate MTOB reveal active site features useful for inhibitor design. FEBS Lett *588*, 1743-1748.

Hildebrand, J.D., and Soriano, P. (2002). Overlapping and unique roles for C-terminal binding protein 1 (CtBP1) and CtBP2 during mouse development. Mol Cell Biol *22*, 5296-5307.

Ho, L., Jothi, R., Ronan, J.L., Cui, K., Zhao, K., and Crabtree, G.R. (2009). An embryonic stem cell chromatin remodeling complex, esBAF, is an essential component of the core pluripotency transcriptional network. Proceedings of the National Academy of Sciences of the United States of America *106*, 5187-5191.

Holden, S., Bernard, O., Artzt, K., Whitmore, W.F., Jr., and Bennett, D. (1977). Human and mouse embryonal carcinoma cells in culture share an embryonic antigen (F9). Nature *270*, 518-520.

Holness, M.J., and Sugden, M.C. (2003). Regulation of pyruvate dehydrogenase complex activity by reversible phosphorylation. Biochem Soc Trans *31*, 1143-1151.

Hou, P., Li, Y., Zhang, X., Liu, C., Guan, J., Li, H., Zhao, T., Ye, J., Yang, W., Liu, K., *et al.* (2013). Pluripotent stem cells induced from mouse somatic cells by small-molecule compounds. Science *341*, 651-654.

Houghton, F.D. (2006). Energy metabolism of the inner cell mass and trophectoderm of the mouse blastocyst. Differentiation; research in biological diversity *74*, 11-18.

Hu, C.J., Iyer, S., Sataur, A., Covello, K.L., Chodosh, L.A., and Simon, M.C. (2006). Differential regulation of the transcriptional activities of hypoxia-inducible factor 1 alpha (HIF-1alpha) and HIF-2alpha in stem cells. Mol Cell Biol *26*, 3514-3526.

Hu, C.J., Wang, L.Y., Chodosh, L.A., Keith, B., and Simon, M.C. (2003). Differential roles of hypoxia-inducible factor 1alpha (HIF-1alpha) and HIF-2alpha in hypoxic gene regulation. Mol Cell Biol *23*, 9361-9374.

Hu, G., Kim, J., Xu, Q., Leng, Y., Orkin, S.H., and Elledge, S.J. (2009). A genome-wide RNAi screen identifies a new transcriptional module required for self-renewal. Genes Dev *23*, 837-848.

Huang, G., Ye, S., Zhou, X., Liu, D., and Ying, Q.L. (2015). Molecular basis of embryonic stem cell self-renewal: from signaling pathways to pluripotency network. Cellular and molecular life sciences : CMLS *72*, 1741-1757.

Ichikawa, K., Kubota, Y., Nakamura, T., Weng, J.S., Tomida, T., Saito, H., and Takekawa, M. (2015). MCRIP1, an ERK substrate, mediates ERK-induced gene silencing during epithelial-mesenchymal transition by regulating the co-repressor CtBP. Mol Cell *58*, 35-46.

Ignarro, L.J. (1990). Nitric oxide. A novel signal transduction mechanism for transcellular communication. Hypertension *16*, 477-483.

Ishimura, A., Minehata, K., Terashima, M., Kondoh, G., Hara, T., and Suzuki, T. (2012). Jmjd5, an H3K36me2 histone demethylase, modulates embryonic cell proliferation through the regulation of Cdkn1a expression. Development *139*, 749-759.

Itoh, T.Q., Matsumoto, A., and Tanimura, T. (2013). C-terminal binding protein (CtBP) activates the expression of E-box clock genes with CLOCK/CYCLE in Drosophila. PLoS One *8*, e63113.

Ivanova, N., Dobrin, R., Lu, R., Kotenko, I., Levorse, J., DeCoste, C., Schafer, X., Lun, Y., and Lemischka, I.R. (2006). Dissecting self-renewal in stem cells with RNA interference. Nature *442*, 533-538.

Jackson, M., Krassowska, A., Gilbert, N., Chevassut, T., Forrester, L., Ansell, J., and Ramsahoye, B. (2004). Severe global DNA hypomethylation blocks differentiation and induces histone hyperacetylation in embryonic stem cells. Mol Cell Biol *24*, 8862-8871.

Jaenisch, R., and Young, R. (2008). Stem cells, the molecular circuitry of pluripotency and nuclear reprogramming. Cell *132*, 567-582.

Jang, H., Yang, J., Lee, E., and Cheong, J.H. (2015). Metabolism in embryonic and cancer stemness. Archives of pharmacal research *38*, 381-388.

Jauch, R., Ng, C.K., Saikatendu, K.S., Stevens, R.C., and Kolatkar, P.R. (2008). Crystal structure and DNA binding of the homeodomain of the stem cell transcription factor Nanog. Journal of molecular biology *376*, 758-770.

Jia, D., Jurkowska, R.Z., Zhang, X., Jeltsch, A., and Cheng, X. (2007). Structure of Dnmt3a bound to Dnmt3L suggests a model for de novo DNA methylation. Nature *449*, 248-251.

Joo, J.Y., Choi, H.W., Kim, M.J., Zaehres, H., Tapia, N., Stehling, M., Jung, K.S., Do, J.T., and Scholer, H.R. (2014). Establishment of a primed pluripotent epiblast stem cell in FGF4-based conditions. Sci Rep *4*, 7477.

Jung, G.W., Kwak, J.Y., Yoon, S., Yoon, J.H., and Lue, T.F. (1999). IGF-I and TGF-beta2 have a key role on regeneration of nitric oxide synthase (NOS)-containing nerves after cavernous neurotomy in rats. Int J Impot Res *11*, 247-259.

Kaelin, W.G., Jr. (2005). ROS: really involved in oxygen sensing. Cell metabolism *1*, 357-358.

Kagey, M.H., Melhuish, T.A., and Wotton, D. (2003). The polycomb protein Pc2 is a SUMO E3. Cell *113*, 127-137.

Kagey, M.H., Newman, J.J., Bilodeau, S., Zhan, Y., Orlando, D.A., van Berkum, N.L., Ebmeier, C.C., Goossens, J., Rahl, P.B., Levine, S.S.*, et al.* (2010). Mediator and cohesin connect gene expression and chromatin architecture. Nature *467*, 430-435.

Kaji, K., Caballero, I.M., MacLeod, R., Nichols, J., Wilson, V.A., and Hendrich, B. (2006). The NuRD component Mbd3 is required for pluripotency of embryonic stem cells. Nature cell biology *8*, 285-292.

Kaji, K., Nichols, J., and Hendrich, B. (2007). Mbd3, a component of the NuRD co-repressor complex, is required for development of pluripotent cells. Development *134*, 1123-1132.

Kallio, P.J., Okamoto, K., O'Brien, S., Carrero, P., Makino, Y., Tanaka, H., and Poellinger, L. (1998). Signal transduction in hypoxic cells: inducible nuclear translocation and recruitment of the CBP/p300 coactivator by the hypoxia-inducible factor-1alpha. EMBO J *17*, 6573-6586.

Kaluz, S., Kaluzova, M., and Stanbridge, E.J. (2008). Regulation of gene expression by hypoxia: integration of the HIF-transduced hypoxic signal at the hypoxia-responsive element. Clinica chimica acta; international journal of clinical chemistry *395*, 6-13.

Kamura, T., Sato, S., Iwai, K., Czyzyk-Krzeska, M., Conaway, R.C., and Conaway, J.W. (2000). Activation of HIF1alpha ubiquitination by a reconstituted von Hippel-Lindau (VHL) tumor suppressor complex. Proceedings of the National Academy of Sciences of the United States of America *97*, 10430-10435.

Kang, P.J., Moon, J.H., Yoon, B.S., Hyeon, S., Jun, E.K., Park, G., Yun, W., Park, J., Park, M., Kim, A.*, et al.* (2014). Reprogramming of mouse somatic cells into pluripotent stem-like cells using a combination of small molecules. Biomaterials *35*, 7336-7345.

Kapinas, K., Grandy, R., Ghule, P., Medina, R., Becker, K., Pardee, A., Zaidi, S.K., Lian, J., Stein, J., van Wijnen, A.*, et al.* (2013). The abbreviated pluripotent cell cycle. Journal of cellular physiology *228*, 9-20.

Katsanis, N., and Fisher, E.M. (1998). A novel C-terminal binding protein (CTBP2) is closely related to CTBP1, an adenovirus E1A-binding protein, and maps to human chromosome 21q21.3. Genomics *47*, 294-299.

Keirstead, H.S., Nistor, G., Bernal, G., Totoiu, M., Cloutier, F., Sharp, K., and Steward, O. (2005). Human embryonic stem cell-derived oligodendrocyte progenitor cell

transplants remyelinate and restore locomotion after spinal cord injury. The Journal of neuroscience : the official journal of the Society for Neuroscience *25*, 4694-4705.

Keith, B., Adelman, D.M., and Simon, M.C. (2001). Targeted mutation of the murine arylhydrocarbon receptor nuclear translocator 2 (Arnt2) gene reveals partial redundancy with Arnt. Proceedings of the National Academy of Sciences of the United States of America *98*, 6692-6697.

Kidder, B.L., Hu, G., Yu, Z.X., Liu, C., and Zhao, K. (2013). Extended self-renewal and accelerated reprogramming in the absence of Kdm5b. Mol Cell Biol *33*, 4793-4810.

Kidder, B.L., Hu, G., and Zhao, K. (2014). KDM5B focuses H3K4 methylation near promoters and enhancers during embryonic stem cell self-renewal and differentiation. Genome biology *15*, R32.

Kim, H., Jang, H., Kim, T.W., Kang, B.H., Lee, S.E., Kyung Jeon, Y., Hyun Chung, D., Choi, J., Shin, J., Cho, E.J.*, et al.* (2015). Core Pluripotency Factors Directly Regulate Metabolism in Embryonic Stem Cell to Maintain Pluripotency. Stem Cells *33*, 2699-2711.

Kim, J., Chu, J., Shen, X., Wang, J., and Orkin, S.H. (2008). An extended transcriptional network for pluripotency of embryonic stem cells. Cell *132*, 1049-1061.

Kim, J.H., Cho, E.J., Kim, S.T., and Youn, H.D. (2005a). CtBP represses p300-mediated transcriptional activation by direct association with its bromodomain. Nature structural & molecular biology *12*, 423-428.

Kim, J.S., Kim, J., Kim, B.S., Chung, H.Y., Lee, Y.Y., Park, C.S., Lee, Y.S., Lee, Y.H., and Chung, I.Y. (2005b). Identification and functional characterization of an alternative splice variant within the fourth exon of human nanog. Experimental & molecular medicine *37*, 601-607.

Kirkegaard, K., Hindkjaer, J.J., and Ingerslev, H.J. (2013). Effect of oxygen concentration on human embryo development evaluated by time-lapse monitoring. Fertility and sterility *99*, 738-744 e734.

Kleinman, H.K., McGarvey, M.L., Liotta, L.A., Robey, P.G., Tryggvason, K., and Martin, G.R. (1982). Isolation and characterization of type IV procollagen, laminin, and heparan sulfate proteoglycan from the EHS sarcoma. Biochemistry *21*, 6188-6193.

Kleinsmith, L.J., and Pierce, G.B., Jr. (1964). Multipotentiality of Single Embryonal Carcinoma Cells. Cancer research *24*, 1544-1551.

Klemm, J.D., and Pabo, C.O. (1996). Oct-1 POU domain DNA interactions: Cooperative binding of isolated subdomains and effects of covalent linkage. Genes & Development *10*, 27-36.

Kondoh, H., Lleonart, M.E., Nakashima, Y., Yokode, M., Tanaka, M., Bernard, D., Gil, J., and Beach, D. (2007). A high glycolytic flux supports the proliferative potential of murine embryonic stem cells. Antioxidants & redox signaling *9*, 293-299.

Kooistra, S.M., and Helin, K. (2012). Molecular mechanisms and potential functions of histone demethylases. Nature reviews Molecular cell biology *13*, 297-311.

Kornberg, R.D. (1974). Chromatin structure: a repeating unit of histones and DNA. Science *184*, 868-871.

Kouzarides, T. (2007). Chromatin modifications and their function. Cell *128*, 693-705.

Kress, S., Stein, A., Maurer, P., Weber, B., Reichert, J., Buchmann, A., Huppert, P., and Schwarz, M. (1998). Expression of hypoxia-inducible genes in tumor cells. J Cancer Res Clin Oncol *124*, 315-320.

Krieg, A.J., Rankin, E.B., Chan, D., Razorenova, O., Fernandez, S., and Giaccia, A.J. (2010). Regulation of the histone demethylase JMJD1A by hypoxia-inducible factor 1 alpha enhances hypoxic gene expression and tumor growth. Mol Cell Biol *30*, 344-353.

Kumar, V., Carlson, J.E., Ohgi, K.A., Edwards, T.A., Rose, D.W., Escalante, C.R., Rosenfeld, M.G., and Aggarwal, A.K. (2002). Transcription corepressor CtBP is an NAD(+)-regulated dehydrogenase. Mol Cell *10*, 857-869.

Kuppuswamy, M., Vijayalingam, S., Zhao, L.J., Zhou, Y., Subramanian, T., Ryerse, J., and Chinnadurai, G. (2008). Role of the PLDLS-binding cleft region of CtBP1 in recruitment of core and auxiliary components of the corepressor complex. Mol Cell Biol *28*, 269-281.

Kurimoto, K., Yabuta, Y., Ohinata, Y., Ono, Y., Uno, K.D., Yamada, R.G., Ueda, H.R., and Saitou, M. (2006). An improved single-cell cDNA amplification method for efficient high-density oligonucleotide microarray analysis. Nucleic Acids Res *34*, e42.

Kuroda, T., Tada, M., Kubota, H., Kimura, H., Hatano, S.Y., Suemori, H., Nakatsuji, N., and Tada, T. (2005). Octamer and Sox elements are required for transcriptional cis regulation of Nanog gene expression. Mol Cell Biol *25*, 2475-2485.

Landeira, D., Sauer, S., Poot, R., Dvorkina, M., Mazzarella, L., Jorgensen, H.F., Pereira, C.F., Leleu, M., Piccolo, F.M., Spivakov, M*., et al.* (2010). Jarid2 is a PRC2 component in embryonic stem cells required for multi-lineage differentiation and recruitment of PRC1 and RNA Polymerase II to developmental regulators. Nature cell biology *12*, 618-624.

Lando, D., Peet, D.J., Whelan, D.A., Gorman, J.J., and Whitelaw, M.L. (2002). Asparagine hydroxylation of the HIF transactivation domain a hypoxic switch. Science *295*, 858-861.

Lanner, F., and Rossant, J. (2010). The role of FGF/Erk signaling in pluripotent cells. Development *137*, 3351-3360.

Lee, H.Y., Choi, K., Oh, H., Park, Y.K., and Park, H. (2014). HIF-1-dependent induction of Jumonji domain-containing protein (JMJD) 3 under hypoxic conditions. Mol Cells *37*, 43-50.

Lee, J., Kim, H.K., Han, Y.M., and Kim, J. (2008). Pyruvate kinase isozyme type M2 (PKM2) interacts and cooperates with Oct-4 in regulating transcription. Int J Biochem Cell Biol *40*, 1043-1054.

Lee, J., Kim, H.K., Rho, J.Y., Han, Y.M., and Kim, J. (2006a). The human OCT-4 isoforms differ in their ability to confer self-renewal. The Journal of biological chemistry *281*, 33554-33565.

Lee, T.I., Jenner, R.G., Boyer, L.A., Guenther, M.G., Levine, S.S., Kumar, R.M., Chevalier, B., Johnstone, S.E., Cole, M.F., Isono, K.*, et al.* (2006b). Control of developmental regulators by Polycomb in human embryonic stem cells. Cell *125*, 301-313.

Leese, H.J., and Barton, A.M. (1984). Pyruvate and glucose uptake by mouse ova and preimplantation embryos. Journal of reproduction and fertility *72*, 9-13.

Lehninger, A.L., Nelson, D.L., and Cox, M.M. (1993). Principles of Biochemistry (New York, NY: Worth Publishers).

Lengner, C.J., Gimelbrant, A.A., Erwin, J.A., Cheng, A.W., Guenther, M.G., Welstead, G.G., Alagappan, R., Frampton, G.M., Xu, P., Muffat, J.*, et al.* (2010). Derivation of pre-X inactivation human embryonic stem cells under physiological oxygen concentrations. Cell *141*, 872-883.

Lessard, J.A., and Crabtree, G.R. (2010). Chromatin regulatory mechanisms in pluripotency. Annual review of cell and developmental biology *26*, 503-532.

Levings, P.P., Zhou, Z., Vieira, K.F., Crusselle-Davis, V.J., and Bungert, J. (2006). Recruitment of transcription complexes to the beta-globin locus control region and transcription of hypersensitive site 3 prior to erythroid differentiation of murine embryonic stem cells. FEBS J *273*, 746-755.

Li, E., Bestor, T.H., and Jaenisch, R. (1992). Targeted mutation of the DNA methyltransferase gene results in embryonic lethality. Cell *69*, 915-926.

Li, J., Wang, G., Wang, C., Zhao, Y., Zhang, H., Tan, Z., Song, Z., Ding, M., and Deng, H. (2007). MEK/ERK signaling contributes to the maintenance of human embryonic stem cell self-renewal. Differentiation; research in biological diversity *75*, 299-307.

Li, L., Bennett, S.A., and Wang, L. (2012). Role of E-cadherin and other cell adhesion molecules in survival and differentiation of human pluripotent stem cells. Cell adhesion & migration *6*, 59-70.

Li, L., Wang, B.H., Wang, S., Moalim-Nour, L., Mohib, K., Lohnes, D., and Wang, L. (2010a). Individual cell movement, asymmetric colony expansion, rho-associated kinase, and E-cadherin impact the clonogenicity of human embryonic stem cells. Biophysical journal *98*, 2442-2451.

Li, L., Wang, S., Jezierski, A., Moalim-Nour, L., Mohib, K., Parks, R.J., Retta, S.F., and Wang, L. (2010b). A unique interplay between Rap1 and E-cadherin in the endocytic pathway regulates self-renewal of human embryonic stem cells. Stem Cells *28*, 247-257.

Li, L., Zhu, L., Hao, B., Gao, W., Wang, Q., Li, K., Wang, M., Huang, M., Liu, Z., Yang, Q.*, et al.* (2017). iNOS-derived nitric oxide promotes glycolysis by inducing pyruvate kinase M2 nuclear translocation in ovarian cancer. Oncotarget *8*, 33047-33063.

Li, X., Egervari, G., Wang, Y., Berger, S.L., and Lu, Z. (2018). Regulation of chromatin and gene expression by metabolic enzymes and metabolites. Nature reviews Molecular cell biology *19*, 563-578.

Liang, J., Wan, M., Zhang, Y., Gu, P., Xin, H., Jung, S.Y., Qin, J., Wong, J., Cooney, A.J., Liu, D.*, et al.* (2008). Nanog and Oct4 associate with unique transcriptional repression complexes in embryonic stem cells. Nature cell biology *10*, 731-739.

Lim, J.H., Lee, Y.M., Chun, Y.S., Chen, J., Kim, J.E., and Park, J.W. (2010). Sirtuin 1 modulates cellular responses to hypoxia by deacetylating hypoxia-inducible factor 1alpha. Mol Cell *38*, 864-878.

Lin, T., and Wu, S. (2015). Reprogramming with Small Molecules instead of Exogenous Transcription Factors. Stem cells international *2015*, doi: 10.1155/2015/794632.

Lin, X., Sun, B., Liang, M., Liang, Y.Y., Gast, A., Hildebrand, J., Brunicardi, F.C., Melchior, F., and Feng, X.H. (2003). Opposed regulation of corepressor CtBP by SUMOylation and PDZ binding. Mol Cell *11*, 1389-1396.

Livak, K.J., and Schmittgen, T.D. (2001). Analysis of relative gene expression data using real-time quantitative PCR and the 2(-Delta Delta C(T)) Method. Methods *25*, 402-408.

Loh, Y.H., Wu, Q., Chew, J.L., Vega, V.B., Zhang, W., Chen, X., Bourque, G., George, J., Leong, B., Liu, J.*, et al.* (2006). The Oct4 and Nanog transcription network regulates pluripotency in mouse embryonic stem cells. Nature genetics *38*, 431-440.

Loh, Y.H., Zhang, W., Chen, X., George, J., and Ng, H.H. (2007). Jmjd1a and Jmjd2c histone H3 Lys 9 demethylases regulate self-renewal in embryonic stem cells. Genes Dev *21*, 2545-2557.

Lonergan, T., Bavister, B., and Brenner, C. (2007). Mitochondria in stem cells. Mitochondrion *7*, 289-296.

Lu, H., Dalgard, C.L., Mohyeldin, A., McFate, T., Tait, A.S., and Verma, A. (2005). Reversible inactivation of HIF-1 prolyl hydroxylases allows cell metabolism to control basal HIF-1. The Journal of biological chemistry *280*, 41928-41939.

Lu, H., Forbes, R.A., and Verma, A. (2002). Hypoxia-inducible factor 1 activation by aerobic glycolysis implicates the Warburg effect in carcinogenesis. The Journal of biological chemistry *277*, 23111-23115.

Lum, J.J., Bui, T., Gruber, M., Gordan, J.D., DeBerardinis, R.J., Covello, K.L., Simon, M.C., and Thompson, C.B. (2007). The transcription factor HIF-1alpha plays a critical role in the growth factor-dependent regulation of both aerobic and anaerobic glycolysis. Genes Dev *21*, 1037-1049.

Lund, A.H., and van Lohuizen, M. (2004). Polycomb complexes and silencing mechanisms. Current opinion in cell biology *16*, 239-246.

Lundholm, L., Mohme-Lundholm, E., and Vamos, N. (1963). Lactic acid assay with L(plus)lactic acid dehydrogenase from rabbit muscle. Acta Physiol Scand *58*, 243-249.

Luo, J.C., and Shibuya, M. (2001). A variant of nuclear localization signal of bipartite-type is required for the nuclear translocation of hypoxia inducible factors (1alpha, 2alpha and 3alpha). Oncogene *20*, 1435-1444.

Luo, W., Chang, R., Zhong, J., Pandey, A., and Semenza, G.L. (2012). Histone demethylase JMJD2C is a coactivator for hypoxia-inducible factor 1 that is required for breast cancer progression. Proceedings of the National Academy of Sciences of the United States of America *109*, E3367-3376.

Luo, W., Hu, H., Chang, R., Zhong, J., Knabel, M., O'Meally, R., Cole, R.N., Pandey, A., and Semenza, G.L. (2011). Pyruvate kinase M2 is a PHD3-stimulated coactivator for hypoxia-inducible factor 1. Cell *145*, 732-744.

Luo, W., and Semenza, G.L. (2012). Emerging roles of PKM2 in cell metabolism and cancer progression. Trends Endocrinol Metab *23*, 560-566.

Mahon, P.C., Hirota, K., and Semenza, G.L. (2001). FIH-1: a novel protein that interacts with HIF-1alpha and VHL to mediate repression of HIF-1 transcriptional activity. Genes Dev *15*, 2675-2686.

Majmundar, A.J., Wong, W.J., and Simon, M.C. (2010). Hypoxia-inducible factors and the response to hypoxic stress. Mol Cell *40*, 294-309.

Makino, Y., Cao, R., Svensson, K., Bertilsson, G., Asman, M., Tanaka, H., Cao, Y., Berkenstam, A., and Poellinger, L. (2001). Inhibitory PAS domain protein is a negative regulator of hypoxia-inducible gene expression. Nature *414*, 550-554.

Makino, Y., Kanopka, A., Wilson, W.J., Tanaka, H., and Poellinger, L. (2002). Inhibitory PAS domain protein (IPAS) is a hypoxia-inducible splicing variant of the hypoxia-inducible factor-3alpha locus. The Journal of biological chemistry *277*, 32405-32408.

Mandal, S., Lindgren, A.G., Srivastava, A.S., Clark, A.T., and Banerjee, U. (2011). Mitochondrial function controls proliferation and early differentiation potential of embryonic stem cells. Stem Cells *29*, 486-495.

Manor, Y.S., Massarwa, R., and Hanna, J.H. (2015). Establishing the human naive pluripotent state. Current opinion in genetics & development *34*, 35-45.

Martello, G., Sugimoto, T., Diamanti, E., Joshi, A., Hannah, R., Ohtsuka, S., Gottgens, B., Niwa, H., and Smith, A. (2012). Esrrb is a pivotal target of the Gsk3/Tcf3 axis regulating embryonic stem cell self-renewal. Cell Stem Cell *11*, 491-504.

Martin, G.R. (1981). Isolation of a pluripotent cell line from early mouse embryos cultured in medium conditioned by teratocarcinoma stem cells. Proceedings of the National Academy of Sciences of the United States of America *78*, 7634-7638.

Masui, S. (2009). Transcriptional network controlling pluripotency in embryonic stem cells. Seikagaku The Journal of Japanese Biochemical Society *81*, 597-601.

Masui, S., Nakatake, Y., Toyooka, Y., Shimosato, D., Yagi, R., Takahashi, K., Okochi, H., Okuda, A., Matoba, R., Sharov, A.A.*, et al.* (2007). Pluripotency governed by Sox2 via regulation of Oct3/4 expression in mouse embryonic stem cells. Nature cell biology *9*, 625-635.

Mateo, J., Garcia-Lecea, M., Cadenas, S., Hernandez, C., and Moncada, S. (2003). Regulation of hypoxia-inducible factor-1alpha by nitric oxide through mitochondria-dependent and -independent pathways. The Biochemical journal *376*, 537-544.

Mathieu, J., Zhang, Z., Nelson, A., Lamba, D.A., Reh, T.A., Ware, C., and Ruohola-Baker, H. (2013). Hypoxia induces re-entry of committed cells into pluripotency. Stem Cells *31*, 1737-1748.

Mathieu, J., Zhang, Z., Zhou, W., Wang, A.J., Heddleston, J.M., Pinna, C.M., Hubaud, A., Stadler, B., Choi, M., Bar, M.*, et al.* (2011). HIF induces human embryonic stem cell markers in cancer cells. Cancer research *71*, 4640-4652.

Matin, M.M., Walsh, J.R., Gokhale, P.J., Draper, J.S., Bahrami, A.R., Morton, I., Moore, H.D., and Andrews, P.W. (2004). Specific knockdown of Oct4 and beta2-microglobulin expression by RNA interference in human embryonic stem cells and embryonic carcinoma cells. Stem Cells *22*, 659-668.

Maxwell, P.H., Wiesener, M.S., Chang, G.W., Clifford, S.C., Vaux, E.C., Cockman, M.E., Wykoff, C.C., Pugh, C.W., Maher, E.R., and Ratcliffe, P.J. (1999). The tumour suppressor protein VHL targets hypoxia-inducible factors for oxygen-dependent proteolysis. Nature *399*, 271-275.

Maynard, M.A., Evans, A.J., Hosomi, T., Hara, S., Jewett, M.A., and Ohh, M. (2005). Human HIF-3alpha4 is a dominant-negative regulator of HIF-1 and is down-regulated in renal cell carcinoma. FASEB journal : official publication of the Federation of American Societies for Experimental Biology *19*, 1396-1406.

Meissner, A., Mikkelsen, T.S., Gu, H., Wernig, M., Hanna, J., Sivachenko, A., Zhang, X., Bernstein, B.E., Nusbaum, C., Jaffe, D.B.*, et al.* (2008). Genome-scale DNA methylation maps of pluripotent and differentiated cells. Nature *454*, 766-770.

Menasche, P., Vanneaux, V., Hagege, A., Bel, A., Cholley, B., Cacciapuoti, I., Parouchev, A., Benhamouda, N., Tachdjian, G., Tosca, L.*, et al.* (2015). Human

embryonic stem cell-derived cardiac progenitors for severe heart failure treatment: first clinical case report. European heart journal *36*, 2011-2017.

Menasche, P., Vanneaux, V., Hagege, A., Bel, A., Cholley, B., Parouchev, A., Cacciapuoti, I., Al-Daccak, R., Benhamouda, N., Blons, H.*, et al.* (2018). Transplantation of Human Embryonic Stem Cell-Derived Cardiovascular Progenitors for Severe Ischemic Left Ventricular Dysfunction. J Am Coll Cardiol *71*, 429-438.

Meng, G., Liu, S., Li, X., Krawetz, R., and Rancourt, D.E. (2010a). Derivation of human embryonic stem cell lines after blastocyst microsurgery. Biochemistry and cell biology = Biochimie et biologie cellulaire *88*, 479-490.

Meng, G., Liu, S., Li, X., Krawetz, R., and Rancourt, D.E. (2010b). Extracellular matrix isolated from foreskin fibroblasts supports long-term xeno-free human embryonic stem cell culture. Stem Cells Dev *19*, 547-556.

Meshorer, E., and Misteli, T. (2006). Chromatin in pluripotent embryonic stem cells and differentiation. Nature reviews Molecular cell biology *7*, 540-546.

Meshorer, E., Yellajoshula, D., George, E., Scambler, P.J., Brown, D.T., and Misteli, T. (2006). Hyperdynamic plasticity of chromatin proteins in pluripotent embryonic stem cells. Developmental cell *10*, 105-116.

Metzen, E., Zhou, J., Jelkmann, W., Fandrey, J., and Brune, B. (2003). Nitric oxide impairs normoxic degradation of HIF-1alpha by inhibition of prolyl hydroxylases. Molecular biology of the cell *14*, 3470-3481.

Mikkelsen, T.S., Ku, M., Jaffe, D.B., Issac, B., Lieberman, E., Giannoukos, G., Alvarez, P., Brockman, W., Kim, T.K., Koche, R.P.*, et al.* (2007). Genome-wide maps of chromatin state in pluripotent and lineage-committed cells. Nature *448*, 553-560.

Mirnezami, A.H., Campbell, S.J., Darley, M., Primrose, J.N., Johnson, P.W., and Blaydes, J.P. (2003). Hdm2 recruits a hypoxia-sensitive corepressor to negatively regulate p53-dependent transcription. Current biology : CB *13*, 1234-1239.

Mitalipov, S., and Wolf, D. (2009). Totipotency, pluripotency and nuclear reprogramming. Advances in biochemical engineering/biotechnology *114*, 185-199.

Mitsui, K., Tokuzawa, Y., Itoh, H., Segawa, K., Murakami, M., Takahashi, K., Maruyama, M., Maeda, M., and Yamanaka, S. (2003). The homeoprotein Nanog is required for maintenance of pluripotency in mouse epiblast and ES cells. Cell *113*, 631-642.

Mohn, F., Weber, M., Rebhan, M., Roloff, T.C., Richter, J., Stadler, M.B., Bibel, M., and Schubeler, D. (2008). Lineage-specific polycomb targets and de novo DNA methylation define restriction and potential of neuronal progenitors. Mol Cell *30*, 755-766.

Moncada, S., Palmer, R.M., and Higgs, E.A. (1991). Nitric oxide: physiology, pathophysiology, and pharmacology. Pharmacol Rev *43*, 109-142.

Mora-Castilla, S., Tejedo, J.R., Hmadcha, A., Cahuana, G.M., Martin, F., Soria, B., and Bedoya, F.J. (2010). Nitric oxide repression of Nanog promotes mouse embryonic stem cell differentiation. Cell death and differentiation *17*, 1025-1033.

Moussaieff, A., Rouleau, M., Kitsberg, D., Cohen, M., Levy, G., Barasch, D., Nemirovski, A., Shen-Orr, S., Laevsky, I., Amit, M.*, et al.* (2015). Glycolysis-mediated changes in acetyl-CoA and histone acetylation control the early differentiation of embryonic stem cells. Cell metabolism *21*, 392-402.

Nardini, M., Spano, S., Cericola, C., Pesce, A., Massaro, A., Millo, E., Luini, A., Corda, D., and Bolognesi, M. (2003). CtBP/BARS: a dual-function protein involved in transcription co-repression and Golgi membrane fission. EMBO J *22*, 3122-3130.

Nibu, Y., Zhang, H., Bajor, E., Barolo, S., Small, S., and Levine, M. (1998a). dCtBP mediates transcriptional repression by Knirps, Kruppel and Snail in the Drosophila embryo. EMBO J *17*, 7009-7020.

Nibu, Y., Zhang, H., and Levine, M. (1998b). Interaction of short-range repressors with Drosophila CtBP in the embryo. Science *280*, 101-104.

Nichols, J., and Smith, A. (2009). Naive and primed pluripotent states. Cell Stem Cell *4*, 487-492.

Nichols, J., Zevnik, B., Anastassiadis, K., Niwa, H., Klewe-Nebenius, D., Chambers, I., Scholer, H., and Smith, A. (1998). Formation of pluripotent stem cells in the mammalian embryo depends on the POU transcription factor Oct4. Cell *95*, 379-391.

Niwa, H., Burdon, T., Chambers, I., and Smith, A. (1998). Self-renewal of pluripotent embryonic stem cells is mediated via activation of STAT3. Genes Dev *12*, 2048-2060.

Niwa, H., Miyazaki, J., and Smith, A.G. (2000). Quantitative expression of Oct-3/4 defines differentiation, dedifferentiation or self-renewal of ES cells. Nature genetics *24*, 372-376.

Niwa, H., Ogawa, K., Shimosato, D., and Adachi, K. (2009). A parallel circuit of LIF signalling pathways maintains pluripotency of mouse ES cells. Nature *460*, 118-122.

Oda, H., and Takeichi, M. (2011). Evolution: structural and functional diversity of cadherin at the adherens junction. The Journal of cell biology *193*, 1137-1146.

Oh, S.K., Kim, H.S., Ahn, H.J., Seol, H.W., Kim, Y.Y., Park, Y.B., Yoon, C.J., Kim, D.W., Kim, S.H., and Moon, S.Y. (2005). Derivation and characterization of new human embryonic stem cell lines: SNUhES1, SNUhES2, and SNUhES3. Stem Cells *23*, 211-219.

Okumura-Nakanishi, S., Saito, M., Niwa, H., and Ishikawa, F. (2005). Oct-3/4 and Sox2 regulate Oct-3/4 gene in embryonic stem cells. The Journal of biological chemistry *280*, 5307-5317.

Palsson-McDermott, E.M., Curtis, A.M., Goel, G., Lauterbach, M.A., Sheedy, F.J., Gleeson, L.E., van den Bosch, M.W., Quinn, S.R., Domingo-Fernandez, R., Johnston, D.G., *et al.* (2015). Pyruvate kinase M2 regulates Hif-1alpha activity and IL-1beta induction and is a critical determinant of the warburg effect in LPS-activated macrophages. Cell metabolism *21*, 65-80.

Pan, G., Tian, S., Nie, J., Yang, C., Ruotti, V., Wei, H., Jonsdottir, G.A., Stewart, R., and Thomson, J.A. (2007). Whole-genome analysis of histone H3 lysine 4 and lysine 27 methylation in human embryonic stem cells. Cell Stem Cell *1*, 299-312.

Panning, B., and Jaenisch, R. (1996). DNA hypomethylation can activate Xist expression and silence X-linked genes. Genes Dev *10*, 1991-2002.

Panopoulos, A.D., Yanes, O., Ruiz, S., Kida, Y.S., Diep, D., Tautenhahn, R., Herrerias, A., Batchelder, E.M., Plongthongkum, N., Lutz, M., *et al.* (2012). The metabolome of induced pluripotent stem cells reveals metabolic changes occurring in somatic cell reprogramming. Cell research *22*, 168-177.

Papamichos, S.I., Kotoula, V., Tarlatzis, B.C., Agorastos, T., Papazisis, K., and Lambropoulos, A.F. (2009). OCT4B1 isoform: the novel OCT4 alternative spliced variant as a putative marker of stemness. Molecular human reproduction *15*, 269-270.

Pardo, M., Lang, B., Yu, L., Prosser, H., Bradley, A., Babu, M.M., and Choudhary, J. (2010). An expanded Oct4 interaction network: implications for stem cell biology, development, and disease. Cell Stem Cell *6*, 382-395.

Park, Y.K., Ahn, D.R., Oh, M., Lee, T., Yang, E.G., Son, M., and Park, H. (2008). Nitric oxide donor, (+/-)-S-nitroso-N-acetylpenicillamine, stabilizes transactive hypoxia-inducible factor-1alpha by inhibiting von Hippel-Lindau recruitment and asparagine hydroxylation. Mol Pharmacol *74*, 236-245.

Parslow, T.G., Blair, D.L., Murphy, W.J., and Granner, D.K. (1984). Structure of the 5' ends of immunoglobulin genes: a novel conserved sequence. Proceedings of the National Academy of Sciences of the United States of America *81*, 2650-2654.

Pasini, D., Bracken, A.P., Agger, K., Christensen, J., Hansen, K., Cloos, P.A., and Helin, K. (2008). Regulation of stem cell differentiation by histone methyltransferases and demethylases. Cold Spring Harbor symposia on quantitative biology *73*, 253-263.

Pasini, D., Cloos, P.A., Walfridsson, J., Olsson, L., Bukowski, J.P., Johansen, J.V., Bak, M., Tommerup, N., Rappsilber, J., and Helin, K. (2010). JARID2 regulates binding of the Polycomb repressive complex 2 to target genes in ES cells. Nature *464*, 306-310.

Pedersen, M.T., Kooistra, S.M., Radzisheuskaya, A., Laugesen, A., Johansen, J.V., Hayward, D.G., Nilsson, J., Agger, K., and Helin, K. (2016). Continual removal of H3K9 promoter methylation by Jmjd2 demethylases is vital for ESC self-renewal and early development. EMBO J *35*, 1550-1564.

Peng, J., Zhang, L., Drysdale, L., and Fong, G.H. (2000). The transcription factor EPAS-1/hypoxia-inducible factor 2alpha plays an important role in vascular remodeling.

Proceedings of the National Academy of Sciences of the United States of America *97*, 8386-8391.

Peng, J.C., Valouev, A., Swigut, T., Zhang, J., Zhao, Y., Sidow, A., and Wysocka, J. (2009). Jarid2/Jumonji coordinates control of PRC2 enzymatic activity and target gene occupancy in pluripotent cells. Cell *139*, 1290-1302.

Pera, M.F., Cooper, S., Mills, J., and Parrington, J.M. (1989). Isolation and characterization of a multipotent clone of human embryonal carcinoma cells. Differentiation; research in biological diversity *42*, 10-23.

Pera, M.F., Reubinoff, B., and Trounson, A. (2000). Human embryonic stem cells. Journal of cell science *113 (Pt 1)*, 5-10.

Pera, M.F., and Tam, P.P. (2010). Extrinsic regulation of pluripotent stem cells. Nature *465*, 713-720.

Petersen, A., Mikkelsen, A.L., and Lindenberg, S. (2005). The impact of oxygen tension on developmental competence of post-thaw human embryos. Acta obstetricia et gynecologica Scandinavica *84*, 1181-1184.

Petruzzelli, R., Christensen, D.R., Parry, K.L., Sanchez-Elsner, T., and Houghton, F.D. (2014). HIF-2alpha regulates NANOG expression in human embryonic stem cells following hypoxia and reoxygenation through the interaction with an Oct-Sox cis regulatory element. PLoS One *9*, e108309.

Petryniak, B., Staudt, L.M., Postema, C.E., McCormack, W.T., and Thompson, C.B. (1990). Characterization of chicken octamer-binding proteins demonstrates that POU domain-containing homeobox transcription factors have been highly conserved during vertebrate evolution. Proceedings of the National Academy of Sciences of the United States of America *87*, 1099-1103.

Phillips, K., and Luisi, B. (2000). The virtuoso of versatility: POU proteins that flex to fit. Journal of molecular biology *302*, 1023-1039.

Pierce, B., Verney, E.L., and Dixon, F.J. (1957). The biology of testicular cancer. I. Behavior after transplantation. Cancer research *17*, 134-138.

Pollard, P.J., Loenarz, C., Mole, D.R., McDonough, M.A., Gleadle, J.M., Schofield, C.J., and Ratcliffe, P.J. (2008). Regulation of Jumonji-domain-containing histone demethylases by hypoxia-inducible factor (HIF)-1alpha. The Biochemical journal *416*, 387-394.

Poortinga, G., Watanabe, M., and Parkhurst, S.M. (1998). Drosophila CtBP: a Hairy-interacting protein required for embryonic segmentation and hairy-mediated transcriptional repression. EMBO J *17*, 2067-2078.

Postigo, A.A., and Dean, D.C. (1999). ZEB represses transcription through interaction with the corepressor CtBP. Proceedings of the National Academy of Sciences of the United States of America *96*, 6683-6688.

Poyton, R.O., Ball, K.A., and Castello, P.R. (2009). Mitochondrial generation of free radicals and hypoxic signaling. Trends Endocrinol Metab *20*, 332-340.

Prasad, S.M., Czepiel, M., Cetinkaya, C., Smigielska, K., Weli, S.C., Lysdahl, H., Gabrielsen, A., Petersen, K., Ehlers, N., Fink, T.*, et al.* (2009). Continuous hypoxic culturing maintains activation of Notch and allows long-term propagation of human embryonic stem cells without spontaneous differentiation. Cell proliferation *42*, 63-74.

Prigione, A., and Adjaye, J. (2010). Modulation of mitochondrial biogenesis and bioenergetic metabolism upon in vitro and in vivo differentiation of human ES and iPS cells. The International journal of developmental biology *54*, 1729-1741.

Prigione, A., Lichtner, B., Kuhl, H., Struys, E.A., Wamelink, M., Lehrach, H., Ralser, M., Timmermann, B., and Adjaye, J. (2011). Human induced pluripotent stem cells harbor homoplasmic and heteroplasmic mitochondrial DNA mutations while maintaining human embryonic stem cell-like metabolic reprogramming. Stem Cells *29*, 1338-1348.

Prigione, A., Rohwer, N., Hoffmann, S., Mlody, B., Drews, K., Bukowiecki, R., Blumlein, K., Wanker, E.E., Ralser, M., Cramer, T.*, et al.* (2014). HIF1alpha modulates cell fate reprogramming through early glycolytic shift and upregulation of PDK1-3 and PKM2. Stem Cells *32*, 364-376.

Przanowski, P., Dabrowski, M., Ellert-Miklaszewska, A., Kloss, M., Mieczkowski, J., Kaza, B., Ronowicz, A., Hu, F., Piotrowski, A., Kettenmann, H.*, et al.* (2014). The signal transducers Stat1 and Stat3 and their novel target Jmjd3 drive the expression of inflammatory genes in microglia. Journal of molecular medicine *92*, 239-254.

Quinlan, K.G., Nardini, M., Verger, A., Francescato, P., Yaswen, P., Corda, D., Bolognesi, M., and Crossley, M. (2006a). Specific recognition of ZNF217 and other zinc finger proteins at a surface groove of C-terminal binding proteins. Mol Cell Biol *26*, 8159-8172.

Quinlan, K.G., Verger, A., Kwok, A., Lee, S.H., Perdomo, J., Nardini, M., Bolognesi, M., and Crossley, M. (2006b). Role of the C-terminal binding protein PXDLS motif binding cleft in protein interactions and transcriptional repression. Mol Cell Biol *26*, 8202-8213.

Rafalski, V.A., Mancini, E., and Brunet, A. (2012). Energy metabolism and energy-sensing pathways in mammalian embryonic and adult stem cell fate. Journal of cell science *125*, 5597-5608.

Rajala, K., Lindroos, B., Hussein, S.M., Lappalainen, R.S., Pekkanen-Mattila, M., Inzunza, J., Rozell, B., Miettinen, S., Narkilahti, S., Kerkela, E.*, et al.* (2010). A defined and xeno-free culture method enabling the establishment of clinical-grade human embryonic, induced pluripotent and adipose stem cells. PLoS One *5*, e10246.

Ramalho-Santos, J., Varum, S., Amaral, S., Mota, P.C., Sousa, A.P., and Amaral, A. (2009). Mitochondrial functionality in reproduction: from gonads and gametes to embryos and embryonic stem cells. Human reproduction update *15*, 553-572.

Ray, S.K., Li, H.J., Metzger, E., Schule, R., and Leiter, A.B. (2014). CtBP and associated LSD1 are required for transcriptional activation by NeuroD1 in gastrointestinal endocrine cells. Mol Cell Biol *34*, 2308-2317.

Reik, W., and Dean, W. (2001). DNA methylation and mammalian epigenetics. Electrophoresis *22*, 2838-2843.

Reubinoff, B.E., Pera, M.F., Fong, C.Y., Trounson, A., and Bongso, A. (2000). Embryonic stem cell lines from human blastocysts: somatic differentiation in vitro. Nature biotechnology *18*, 399-404.

Richards, M., Fong, C.Y., Chan, W.K., Wong, P.C., and Bongso, A. (2002). Human feeders support prolonged undifferentiated growth of human inner cell masses and embryonic stem cells. Nature biotechnology *20*, 933-936.

Riefler, G.M., and Firestein, B.L. (2001). Binding of neuronal nitric-oxide synthase (nNOS) to carboxyl-terminal-binding protein (CtBP) changes the localization of CtBP from the nucleus to the cytosol: a novel function for targeting by the PDZ domain of nNOS. The Journal of biological chemistry *276*, 48262-48268.

Rinaudo, P.F., Giritharan, G., Talbi, S., Dobson, A.T., and Schultz, R.M. (2006). Effects of oxygen tension on gene expression in preimplantation mouse embryos. Fertility and sterility *86*, 1252-1265.

Roche, T.E., and Hiromasa, Y. (2007). Pyruvate dehydrogenase kinase regulatory mechanisms and inhibition in treating diabetes, heart ischemia, and cancer. Cellular and molecular life sciences : CMLS *64*, 830-849.

Rodda, D.J., Chew, J.L., Lim, L.H., Loh, Y.H., Wang, B., Ng, H.H., and Robson, P. (2005). Transcriptional regulation of nanog by OCT4 and SOX2. The Journal of biological chemistry *280*, 24731-24737.

Rolfs, A., Kvietikova, I., Gassmann, M., and Wenger, R.H. (1997). Oxygen-regulated transferrin expression is mediated by hypoxia-inducible factor-1. The Journal of biological chemistry *272*, 20055-20062.

Rossant, J. (2008). Stem cells and early lineage development. Cell *132*, 527-531.

Saigusa, S., Tanaka, K., Toiyama, Y., Yokoe, T., Okugawa, Y., Ioue, Y., Miki, C., and Kusunoki, M. (2009). Correlation of CD133, OCT4, and SOX2 in rectal cancer and their association with distant recurrence after chemoradiotherapy. Ann Surg Oncol *16*, 3488-3498.

Sandau, K.B., Fandrey, J., and Brune, B. (2001). Accumulation of HIF-1alpha under the influence of nitric oxide. Blood *97*, 1009-1015.

Sathananthan, H., Pera, M., and Trounson, A. (2002). The fine structure of human embryonic stem cells. Reproductive biomedicine online *4*, 56-61.

Sato, N., Meijer, L., Skaltsounis, L., Greengard, P., and Brivanlou, A.H. (2004). Maintenance of pluripotency in human and mouse embryonic stem cells through activation of Wnt signaling by a pharmacological GSK-3-specific inhibitor. Nature medicine *10*, 55-63.

Savatier, P., Huang, S., Szekely, L., Wiman, K.G., and Samarut, J. (1994). Contrasting patterns of retinoblastoma protein expression in mouse embryonic stem cells and embryonic fibroblasts. Oncogene *9*, 809-818.

Schaeper, U., Boyd, J.M., Verma, S., Uhlmann, E., Subramanian, T., and Chinnadurai, G. (1995). Molecular cloning and characterization of a cellular phosphoprotein that interacts with a conserved C-terminal domain of adenovirus E1A involved in negative modulation of oncogenic transformation. Proceedings of the National Academy of Sciences of the United States of America *92*, 10467-10471.

Schaeper, U., Subramanian, T., Lim, L., Boyd, J.M., and Chinnadurai, G. (1998). Interaction between a cellular protein that binds to the C-terminal region of adenovirus E1A (CtBP) and a novel cellular protein is disrupted by E1A through a conserved PLDLS motif. The Journal of biological chemistry *273*, 8549-8552.

Schindl, M., Schoppmann, S.F., Samonigg, H., Hausmaninger, H., Kwasny, W., Gnant, M., Jakesz, R., Kubista, E., Birner, P., Oberhuber, G.*, et al.* (2002). Overexpression of hypoxia-inducible factor 1alpha is associated with an unfavorable prognosis in lymph node-positive breast cancer. Clin Cancer Res *8*, 1831-1837.

Schmitz, F., Konigstorfer, A., and Sudhof, T.C. (2000). RIBEYE, a component of synaptic ribbons: a protein's journey through evolution provides insight into synaptic ribbon function. Neuron *28*, 857-872.

Schulz, T.C. (2015). Concise Review: Manufacturing of Pancreatic Endoderm Cells for Clinical Trials in Type 1 Diabetes. Stem cells translational medicine *4*, 927-931.

Schwartz, S.D., Hubschman, J.P., Heilwell, G., Franco-Cardenas, V., Pan, C.K., Ostrick, R.M., Mickunas, E., Gay, R., Klimanskaya, I., and Lanza, R. (2012). Embryonic stem cell trials for macular degeneration: a preliminary report. Lancet *379*, 713-720.

Schwartz, S.D., Regillo, C.D., Lam, B.L., Eliott, D., Rosenfeld, P.J., Gregori, N.Z., Hubschman, J.P., Davis, J.L., Heilwell, G., Spirn, M.*, et al.* (2015). Human embryonic stem cell-derived retinal pigment epithelium in patients with age-related macular degeneration and Stargardt's macular dystrophy: follow-up of two open-label phase 1/2 studies. Lancet *385*, 509-516.

Schwarz, B.A., Bar-Nur, O., Silva, J.C., and Hochedlinger, K. (2014). Nanog is dispensable for the generation of induced pluripotent stem cells. Current biology : CB *24*, 347-350.

Scortegagna, M., Ding, K., Oktay, Y., Gaur, A., Thurmond, F., Yan, L.J., Marck, B.T., Matsumoto, A.M., Shelton, J.M., Richardson, J.A.*, et al.* (2003a). Multiple organ pathology, metabolic abnormalities and impaired homeostasis of reactive oxygen species in Epas1-/- mice. Nature genetics *35*, 331-340.

Scortegagna, M., Ding, K., Zhang, Q., Oktay, Y., Bennett, M.J., Bennett, M., Shelton, J.M., Richardson, J.A., Moe, O., and Garcia, J.A. (2005). HIF-2alpha regulates murine hematopoietic development in an erythropoietin-dependent manner. Blood *105*, 3133-3140.

Scortegagna, M., Morris, M.A., Oktay, Y., Bennett, M., and Garcia, J.A. (2003b). The HIF family member EPAS1/HIF-2alpha is required for normal hematopoiesis in mice. Blood *102*, 1634-1640.

Semenza, G.L. (1996). Transcriptional regulation by hypoxia-inducible factor 1 molecular mechanisms of oxygen homeostasis. Trends in cardiovascular medicine *6*, 151-157.

Semenza, G.L. (2000a). HIF-1 and human disease: one highly involved factor. Genes Dev *14*, 1983-1991.

Semenza, G.L. (2000b). HIF-1: mediator of physiological and pathophysiological responses to hypoxia. Journal of applied physiology *88*, 1474-1480.

Semenza, G.L. (2017). Hypoxia-inducible factors: coupling glucose metabolism and redox regulation with induction of the breast cancer stem cell phenotype. EMBO J *36*, 252-259.

Semenza, G.L., Roth, P.H., Fang, H.M., and Wang, G.L. (1994). Transcriptional regulation of genes encoding glycolytic enzymes by hypoxia-inducible factor 1. The Journal of biological chemistry *269*, 23757-23763.

Semenza, G.L., and Wang, G.L. (1992). A nuclear factor induced by hypoxia via de novo protein synthesis binds to the human erythropoietin gene enhancer at a site required for transcriptional activation. Mol Cell Biol *12*, 5447-5454.

Senyuk, V., Sinha, K.K., and Nucifora, G. (2005). Corepressor CtBP1 interacts with and specifically inhibits CBP activity. Arch Biochem Biophys *441*, 168-173.

Sewalt, R.G., Gunster, M.J., van der Vlag, J., Satijn, D.P., and Otte, A.P. (1999). C-Terminal binding protein is a transcriptional repressor that interacts with a specific class of vertebrate Polycomb proteins. Mol Cell Biol *19*, 777-787.

Shakya, A., Callister, C., Goren, A., Yosef, N., Garg, N., Khoddami, V., Nix, D., Regev, A., and Tantin, D. (2015). Pluripotency transcription factor Oct4 mediates stepwise nucleosome demethylation and depletion. Mol Cell Biol *35*, 1014-1025.

Shay, J.E., Imtiyaz, H.Z., Sivanand, S., Durham, A.C., Skuli, N., Hsu, S., Mucaj, V., Eisinger-Mathason, T.S., Krock, B.L., Giannoukos, D.N., *et al.* (2014). Inhibition of hypoxia-inducible factors limits tumor progression in a mouse model of colorectal cancer. Carcinogenesis *35*, 1067-1077.

Shi, Y., Lan, F., Matson, C., Mulligan, P., Whetstine, J.R., Cole, P.A., Casero, R.A., and Shi, Y. (2004). Histone demethylation mediated by the nuclear amine oxidase homolog LSD1. Cell *119*, 941-953.

Shi, Y., Sawada, J., Sui, G., Affar el, B., Whetstine, J.R., Lan, F., Ogawa, H., Luke, M.P., Nakatani, Y., and Shi, Y. (2003). Coordinated histone modifications mediated by a CtBP co-repressor complex. Nature *422*, 735-738.

Shi, Y.J., Matson, C., Lan, F., Iwase, S., Baba, T., and Shi, Y. (2005). Regulation of LSD1 histone demethylase activity by its associated factors. Mol Cell *19*, 857-864.

Silva, J., and Smith, A. (2008). Capturing pluripotency. Cell *132*, 532-536.

Smith, T.G., Robbins, P.A., and Ratcliffe, P.J. (2008). The human side of hypoxia-inducible factor. British journal of haematology *141*, 325-334.

Snyder, V., Reed-Newman, T.C., Arnold, L., Thomas, S.M., and Anant, S. (2018). Cancer Stem Cell Metabolism and Potential Therapeutic Targets. Front Oncol *8*, doi: 10.3389/fonc.2018.00203.

Srinivasan, L., and Atchison, M.L. (2004). YY1 DNA binding and PcG recruitment requires CtBP. Genes Dev *18*, 2596-2601.

St John, J.C., Amaral, A., Bowles, E., Oliveira, J.F., Lloyd, R., Freitas, M., Gray, H.L., Navara, C.S., Oliveira, G., Schatten, G.P*., et al.* (2006). The analysis of mitochondria and mitochondrial DNA in human embryonic stem cells. Methods in molecular biology *331*, 347-374.

Stead, E., White, J., Faast, R., Conn, S., Goldstone, S., Rathjen, J., Dhingra, U., Rathjen, P., Walker, D., and Dalton, S. (2002). Pluripotent cell division cycles are driven by ectopic Cdk2, cyclin A/E and E2F activities. Oncogene *21*, 8320-8333.

Stevanovic, M., Zuffardi, O., Collignon, J., Lovell-Badge, R., and Goodfellow, P. (1994). The cDNA sequence and chromosomal location of the human SOX2 gene. Mammalian genome : official journal of the International Mammalian Genome Society *5*, 640-642.

Stiehl, D.P., Jelkmann, W., Wenger, R.H., and Hellwig-Burgel, T. (2002). Normoxic induction of the hypoxia-inducible factor 1alpha by insulin and interleukin-1beta involves the phosphatidylinositol 3-kinase pathway. FEBS Lett *512*, 157-162.

Strom, S., Inzunza, J., Grinnemo, K.H., Holmberg, K., Matilainen, E., Stromberg, A.M., Blennow, E., and Hovatta, O. (2007). Mechanical isolation of the inner cell mass is effective in derivation of new human embryonic stem cell lines. Human reproduction *22*, 3051-3058.

Sturm, R.A., and Herr, W. (1988). The POU domain is a bipartite DNA-binding structure. Nature *336*, 601-604.

Subramanian, T., La Regina, M., and Chinnadurai, G. (1989). Enhanced ras oncogene mediated cell transformation and tumorigenesis by adenovirus 2 mutants lacking the C-terminal region of E1a protein. Oncogene *4*, 415-420.

Subramanian, T., Malstrom, S.E., and Chinnadurai, G. (1991). Requirement of the C-terminal region of adenovirus E1a for cell transformation in cooperation with E1b. Oncogene *6*, 1171-1173.

Sun, C., Nakatake, Y., Akagi, T., Ura, H., Matsuda, T., Nishiyama, A., Koide, H., Ko, M.S., Niwa, H., and Yokota, T. (2009). Dax1 binds to Oct3/4 and inhibits its transcriptional activity in embryonic stem cells. Mol Cell Biol *29*, 4574-4583.

Sutrias-Grau, M., and Arnosti, D.N. (2004). CtBP contributes quantitatively to Knirps repression activity in an NAD binding-dependent manner. Mol Cell Biol *24*, 5953-5966.

Swaney, D.L., Wenger, C.D., Thomson, J.A., and Coon, J.J. (2009). Human embryonic stem cell phosphoproteome revealed by electron transfer dissociation tandem mass spectrometry. Proceedings of the National Academy of Sciences of the United States of America *106*, 995-1000.

Tae Wan, K., Byung-Hee, K., Hyonchol, J., Sojung, K., Jihoon, S., Hyunsoo, K., Sang-Eun, L., Soon-Min, L., Jong-Hyuk, L., Jae-Hwan, K.*, et al.* (2015). Ctbp2 Modulates NuRD-Mediated Deacetylation of H3K27 and Facilitates PRC2-Mediated H3K27me3 in Active Embryonic Stem Cell Genes During Exit from Pluripotency. STEM CELLS *33*, 2442-2455.

Takahashi, K., Tanabe, K., Ohnuki, M., Narita, M., Ichisaka, T., Tomoda, K., and Yamanaka, S. (2007). Induction of pluripotent stem cells from adult human fibroblasts by defined factors. Cell *131*, 861-872.

Takahashi, K., and Yamanaka, S. (2006). Induction of pluripotent stem cells from mouse embryonic and adult fibroblast cultures by defined factors. Cell *126*, 663-676.

Takeda, J., Seino, S., and Bell, G.I. (1992). Human Oct3 gene family: cDNA sequences, alternative splicing, gene organization, chromosomal location, and expression at low levels in adult tissues. Nucleic Acids Res *20*, 4613-4620.

Tam, W.L., Lim, C.Y., Han, J., Zhang, J., Ang, Y.S., Ng, H.H., Yang, H., and Lim, B. (2008). T-cell factor 3 regulates embryonic stem cell pluripotency and self-renewal by the transcriptional control of multiple lineage pathways. Stem Cells *26*, 2019-2031.

Tanaka, N., Takeuchi, T., Neri, Q.V., Sills, E.S., and Palermo, G.D. (2006). Laser-assisted blastocyst dissection and subsequent cultivation of embryonic stem cells in a serum/cell free culture system: applications and preliminary results in a murine model. Journal of translational medicine *4*, 20.

Tapia-Limonchi, R., Cahuana, G.M., Caballano-Infantes, E., Salguero-Aranda, C., Beltran-Povea, A., Hitos, A.B., Hmadcha, A., Martin, F., Soria, B., Bedoya, F.J.*, et al.* (2016). Nitric Oxide Prevents Mouse Embryonic Stem Cell Differentiation Through

Regulation of Gene Expression, Cell Signaling, and Control of Cell Proliferation. Journal of cellular biochemistry *117*, 2078-2088.

Tejedo, J.R., Tapia-Limonchi, R., Mora-Castilla, S., Cahuana, G.M., Hmadcha, A., Martin, F., Bedoya, F.J., and Soria, B. (2010). Low concentrations of nitric oxide delay the differentiation of embryonic stem cells and promote their survival. Cell death & disease *7*, doi: 10.1038/cddis.2010.1057.

ten Berge, D., Kurek, D., Blauwkamp, T., Koole, W., Maas, A., Eroglu, E., Siu, R.K., and Nusse, R. (2011). Embryonic stem cells require Wnt proteins to prevent differentiation to epiblast stem cells. Nature cell biology *13*, 1070-1075.

Tesar, P.J., Chenoweth, J.G., Brook, F.A., Davies, T.J., Evans, E.P., Mack, D.L., Gardner, R.L., and McKay, R.D. (2007). New cell lines from mouse epiblast share defining features with human embryonic stem cells. Nature *448*, 196-199.

Theunissen, T.W., Powell, B.E., Wang, H., Mitalipova, M., Faddah, D.A., Reddy, J., Fan, Z.P., Maetzel, D., Ganz, K., Shi, L.*, et al.* (2014). Systematic identification of culture conditions for induction and maintenance of naive human pluripotency. Cell Stem Cell *15*, 471-487.

Thio, S.S., Bonventre, J.V., and Hsu, S.I. (2004). The CtBP2 co-repressor is regulated by NADH-dependent dimerization and possesses a novel N-terminal repression domain. Nucleic Acids Res *32*, 1836-1847.

Thomson, J.A., Itskovitz-Eldor, J., Shapiro, S.S., Waknitz, M.A., Swiergiel, J.J., Marshall, V.S., and Jones, J.M. (1998). Embryonic stem cell lines derived from human blastocysts. Science *282*, 1145-1147.

Tian, H., McKnight, S.L., and Russell, D.W. (1997). Endothelial PAS domain protein 1 (EPAS1), a transcription factor selectively expressed in endothelial cells. Genes Dev *11*, 72-82.

Tomioka, M., Nishimoto, M., Miyagi, S., Katayanagi, T., Fukui, N., Niwa, H., Muramatsu, M., and Okuda, A. (2002). Identification of Sox-2 regulatory region which is under the control of Oct-3/4-Sox-2 complex. Nucleic Acids Res *30*, 3202-3213.

Tripathi, M.K., Misra, S., Khedkar, S.V., Hamilton, N., Irvin-Wilson, C., Sharan, C., Sealy, L., and Chaudhuri, G. (2005). Regulation of BRCA2 gene expression by the SLUG repressor protein in human breast cells. The Journal of biological chemistry *280*, 17163-17171.

Tsuruzoe, S., Ishihara, K., Uchimura, Y., Watanabe, S., Sekita, Y., Aoto, T., Saitoh, H., Yuasa, Y., Niwa, H., Kawasuji, M.*, et al.* (2006). Inhibition of DNA binding of Sox2 by the SUMO conjugation. Biochemical and biophysical research communications *351*, 920-926.

Turetsky, T., Aizenman, E., Gil, Y., Weinberg, N., Shufaro, Y., Revel, A., Laufer, N., Simon, A., Abeliovich, D., and Reubinoff, B.E. (2008). Laser-assisted derivation of

human embryonic stem cell lines from IVF embryos after preimplantation genetic diagnosis. Human reproduction *23*, 46-53.

Turner, J., and Crossley, M. (2001). The CtBP family: enigmatic and enzymatic transcriptional co-repressors. BioEssays : news and reviews in molecular, cellular and developmental biology *23*, 683-690.

Vahora, H., Khan, M.A., Alalami, U., and Hussain, A. (2016). The Potential Role of Nitric Oxide in Halting Cancer Progression Through Chemoprevention. J Cancer Prev *21*, 1-12.

Valk-Lingbeek, M.E., Bruggeman, S.W., and van Lohuizen, M. (2004). Stem cells and cancer; the polycomb connection. Cell *118*, 409-418.

Vallier, L., Alexander, M., and Pedersen, R.A. (2005). Activin/Nodal and FGF pathways cooperate to maintain pluripotency of human embryonic stem cells. Journal of cell science *118*, 4495-4509.

Vallier, L., Mendjan, S., Brown, S., Chng, Z., Teo, A., Smithers, L.E., Trotter, M.W., Cho, C.H., Martinez, A., Rugg-Gunn, P.*, et al.* (2009). Activin/Nodal signalling maintains pluripotency by controlling Nanog expression. Development *136*, 1339-1349.

van den Berg, D.L., Snoek, T., Mullin, N.P., Yates, A., Bezstarosti, K., Demmers, J., Chambers, I., and Poot, R.A. (2010). An Oct4-centered protein interaction network in embryonic stem cells. Cell Stem Cell *6*, 369-381.

Varum, S., Rodrigues, A.S., Moura, M.B., Momcilovic, O., Easley, C.A.t., Ramalho-Santos, J., Van Houten, B., and Schatten, G. (2011). Energy metabolism in human pluripotent stem cells and their differentiated counterparts. PLoS One *6*, e20914.

Vega-Naredo, I., Loureiro, R., Mesquita, K.A., Barbosa, I.A., Tavares, L.C., Branco, A.F., Erickson, J.R., Holy, J., Perkins, E.L., Carvalho, R.A.*, et al.* (2014). Mitochondrial metabolism directs stemness and differentiation in P19 embryonal carcinoma stem cells. Cell death and differentiation *21*, 1560-1574.

Verger, A., Quinlan, K.G., Crofts, L.A., Spano, S., Corda, D., Kable, E.P., Braet, F., and Crossley, M. (2006). Mechanisms directing the nuclear localization of the CtBP family proteins. Mol Cell Biol *26*, 4882-4894.

Vermeulen, M., Eberl, H.C., Matarese, F., Marks, H., Denissov, S., Butter, F., Lee, K.K., Olsen, J.V., Hyman, A.A., Stunnenberg, H.G.*, et al.* (2010). Quantitative interaction proteomics and genome-wide profiling of epigenetic histone marks and their readers. Cell *142*, 967-980.

Wade, P.A., Gegonne, A., Jones, P.L., Ballestar, E., Aubry, F., and Wolffe, A.P. (1999). Mi-2 complex couples DNA methylation to chromatin remodelling and histone deacetylation. Nature genetics *23*, 62-66.

Walker, E., Chang, W.Y., Hunkapiller, J., Cagney, G., Garcha, K., Torchia, J., Krogan, N.J., Reiter, J.F., and Stanford, W.L. (2010). Polycomb-like 2 associates with PRC2 and

regulates transcriptional networks during mouse embryonic stem cell self-renewal and differentiation. Cell Stem Cell *6*, 153-166.

Wan, W., Peng, K., Li, M., Qin, L., Tong, Z., Yan, J., Shen, B., and Yu, C. (2017). Histone demethylase JMJD1A promotes urinary bladder cancer progression by enhancing glycolysis through coactivation of hypoxia inducible factor 1alpha. Oncogene *36*, 3868-3877.

Wang, G.L., Jiang, B.H., Rue, E.A., and Semenza, G.L. (1995). Hypoxia-inducible factor 1 is a basic-helix-loop-helix-PAS heterodimer regulated by cellular O2 tension. Proceedings of the National Academy of Sciences of the United States of America *92*, 5510-5514.

Wang, G.L., and Semenza, G.L. (1993a). Characterization of hypoxia-inducible factor 1 and regulation of DNA binding activity by hypoxia. The Journal of biological chemistry *268*, 21513-21518.

Wang, G.L., and Semenza, G.L. (1993b). General involvement of hypoxia-inducible factor 1 in transcriptional response to hypoxia. Proceedings of the National Academy of Sciences of the United States of America *90*, 4304-4308.

Wang, G.L., and Semenza, G.L. (1995). Purification and characterization of hypoxia-inducible factor 1. The Journal of biological chemistry *270*, 1230-1237.

Wang, H.J., Hsieh, Y.J., Cheng, W.C., Lin, C.P., Lin, Y.S., Yang, S.F., Chen, C.C., Izumiya, Y., Yu, J.S., Kung, H.J.*, et al.* (2014). JMJD5 regulates PKM2 nuclear translocation and reprograms HIF-1alpha-mediated glucose metabolism. Proceedings of the National Academy of Sciences of the United States of America *111*, 279-284.

Wang, J., Rao, S., Chu, J., Shen, X., Levasseur, D.N., Theunissen, T.W., and Orkin, S.H. (2006a). A protein interaction network for pluripotency of embryonic stem cells. Nature *444*, 364-368.

Wang, J., Scully, K., Zhu, X., Cai, L., Zhang, J., Prefontaine, G.G., Krones, A., Ohgi, K.A., Zhu, P., Garcia-Bassets, I.*, et al.* (2007). Opposing LSD1 complexes function in developmental gene activation and repression programmes. Nature *446*, 882-887.

Wang, S.Y., Iordanov, M., and Zhang, Q. (2006b). c-Jun NH2-terminal kinase promotes apoptosis by down-regulating the transcriptional co-repressor CtBP. The Journal of biological chemistry *281*, 34810-34815.

Wang, V., Davis, D.A., Haque, M., Huang, L.E., and Yarchoan, R. (2005). Differential gene up-regulation by hypoxia-inducible factor-1alpha and hypoxia-inducible factor-2alpha in HEK293T cells. Cancer research *65*, 3299-3306.

Warburg, O. (1956). On respiratory impairment in cancer cells. Science *124*, 269-270.

Ware, C.B., Nelson, A.M., Mecham, B., Hesson, J., Zhou, W., Jonlin, E.C., Jimenez-Caliani, A.J., Deng, X., Cavanaugh, C., Cook, S.*, et al.* (2014). Derivation of naive human

embryonic stem cells. Proceedings of the National Academy of Sciences of the United States of America *111*, 4484-4489.

Warrier, S., Popovic, M., Van der Jeught, M., and Heindryckx, B. (2016). Establishment and Characterization of Naive Pluripotency in Human Embryonic Stem Cells. Methods in molecular biology *1516*, 13-46.

Webb, J.D., Coleman, M.L., and Pugh, C.W. (2009). Hypoxia, hypoxia-inducible factors (HIF), HIF hydroxylases and oxygen sensing. Cellular and molecular life sciences : CMLS *66*, 3539-3554.

Wegner, M. (2010). All purpose Sox: The many roles of Sox proteins in gene expression. Int J Biochem Cell Biol *42*, 381-390.

Wei, F., Scholer, H.R., and Atchison, M.L. (2007). Sumoylation of Oct4 enhances its stability, DNA binding, and transactivation. The Journal of biological chemistry *282*, 21551-21560.

Wellen, K.E., Hatzivassiliou, G., Sachdeva, U.M., Bui, T.V., Cross, J.R., and Thompson, C.B. (2009). ATP-citrate lyase links cellular metabolism to histone acetylation. Science *324*, 1076-1080.

Wenger, R.H. (2000). Mammalian oxygen sensing, signalling and gene regulation. The Journal of experimental biology *203*, 1253-1263.

Wenger, R.H. (2002). Cellular adaptation to hypoxia: O2-sensing protein hydroxylases, hypoxia-inducible transcription factors, and O2-regulated gene expression. FASEB journal : official publication of the Federation of American Societies for Experimental Biology *16*, 1151-1162.

Westfall, S.D., Sachdev, S., Das, P., Hearne, L.B., Hannink, M., Roberts, R.M., and Ezashi, T. (2008). Identification of oxygen-sensitive transcriptional programs in human embryonic stem cells. Stem Cells Dev *17*, 869-881.

Whyte, W.A., Bilodeau, S., Orlando, D.A., Hoke, H.A., Frampton, G.M., Foster, C.T., Cowley, S.M., and Young, R.A. (2012). Enhancer decommissioning by LSD1 during embryonic stem cell differentiation. Nature *482*, 221-225.

Wiesener, M.S., Jurgensen, J.S., Rosenberger, C., Scholze, C.K., Horstrup, J.H., Warnecke, C., Mandriota, S., Bechmann, I., Frei, U.A., Pugh, C.W.*, et al.* (2003). Widespread hypoxia-inducible expression of HIF-2alpha in distinct cell populations of different organs. FASEB journal : official publication of the Federation of American Societies for Experimental Biology *17*, 271-273.

Wissmuller, S., Kosian, T., Wolf, M., Finzsch, M., and Wegner, M. (2006). The high-mobility-group domain of Sox proteins interacts with DNA-binding domains of many transcription factors. Nucleic Acids Res *34*, 1735-1744.

Wood, H.B., and Episkopou, V. (1999). Comparative expression of the mouse Sox1, Sox2 and Sox3 genes from pre-gastrulation to early somite stages. Mechanisms of development *86*, 197-201.

Xu, C., Inokuma, M.S., Denham, J., Golds, K., Kundu, P., Gold, J.D., and Carpenter, M.K. (2001). Feeder-free growth of undifferentiated human embryonic stem cells. Nature biotechnology *19*, 971-974.

Xu, Y., Zhu, X., Hahm, H.S., Wei, W., Hao, E., Hayek, A., and Ding, S. (2010). Revealing a core signaling regulatory mechanism for pluripotent stem cell survival and self-renewal by small molecules. Proceedings of the National Academy of Sciences of the United States of America *107*, 8129-8134.

Yang, S.H., Kalkan, T., Morrisroe, C., Smith, A., and Sharrocks, A.D. (2012a). A genome-wide RNAi screen reveals MAP kinase phosphatases as key ERK pathway regulators during embryonic stem cell differentiation. PLoS genetics *8*, e1003112.

Yang, W., Xia, Y., Hawke, D., Li, X., Liang, J., Xing, D., Aldape, K., Hunter, T., Alfred Yung, W.K., and Lu, Z. (2012b). PKM2 phosphorylates histone H3 and promotes gene transcription and tumorigenesis. Cell *150*, 685-696.

Yang, W., Xia, Y., Ji, H., Zheng, Y., Liang, J., Huang, W., Gao, X., Aldape, K., and Lu, Z. (2011). Nuclear PKM2 regulates beta-catenin transactivation upon EGFR activation. Nature *480*, 118-122.

Yasuda, H., Tanaka, K., Okita, Y., Araki, T., Saigusa, S., Toiyama, Y., Yokoe, T., Yoshiyama, S., Kawamoto, A., Inoue, Y.*, et al.* (2011). CD133, OCT4, and NANOG in ulcerative colitis-associated colorectal cancer. Oncology letters *2*, 1065-1071.

Yates, A., and Chambers, I. (2005). The homeodomain protein Nanog and pluripotency in mouse embryonic stem cells. Biochem Soc Trans *33*, 1518-1521.

Yeo, J.C., and Ng, H.H. (2013). The transcriptional regulation of pluripotency. Cell research *23*, 20-32.

Ying, Q.L., Wray, J., Nichols, J., Batlle-Morera, L., Doble, B., Woodgett, J., Cohen, P., and Smith, A. (2008). The ground state of embryonic stem cell self-renewal. Nature *453*, 519-523.

Yoshida, T., Hazan, I., Zhang, J., Ng, S.Y., Naito, T., Snippert, H.J., Heller, E.J., Qi, X., Lawton, L.N., Williams, C.J.*, et al.* (2008). The role of the chromatin remodeler Mi-2beta in hematopoietic stem cell self-renewal and multilineage differentiation. Genes Dev *22*, 1174-1189.

Young, R.A. (2011). Control of the embryonic stem cell state. Cell *144*, 940-954.

Yu, S., Chen, X., Xiu, M., He, F., Xing, J., Min, D., and Guo, F. (2017). The regulation of Jmjd3 upon the expression of NF-kappaB downstream inflammatory genes in LPS activated vascular endothelial cells. Biochemical and biophysical research communications *485*, 62-68.

Yuan, H.B., Corbi, N., Basilico, C., and Dailey, L. (1995). Developmental-Specific Activity of the Fgf-4 Enhancer Requires the Synergistic Action of Sox2 and Oct-3. Genes & Development *9*, 2635-2645.

Zelzer, E., Levy, Y., Kahana, C., Shilo, B.Z., Rubinstein, M., and Cohen, B. (1998). Insulin induces transcription of target genes through the hypoxia-inducible factor HIF-1alpha/ARNT. EMBO J *17*, 5085-5094.

Zhang, C.L., McKinsey, T.A., Lu, J.R., and Olson, E.N. (2001). Association of COOH-terminal-binding protein (CtBP) and MEF2-interacting transcription repressor (MITR) contributes to transcriptional repression of the MEF2 transcription factor. The Journal of biological chemistry *276*, 35-39.

Zhang, H., Badur, M.G., Divakaruni, A.S., Parker, S.J., Jager, C., Hiller, K., Murphy, A.N., and Metallo, C.M. (2016). Distinct Metabolic States Can Support Self-Renewal and Lipogenesis in Human Pluripotent Stem Cells under Different Culture Conditions. Cell reports *16*, 1536-1547.

Zhang, Q., Piston, D.W., and Goodman, R.H. (2002). Regulation of corepressor function by nuclear NADH. Science *295*, 1895-1897.

Zhao, L.J., Subramanian, T., Zhou, Y., and Chinnadurai, G. (2006). Acetylation by p300 regulates nuclear localization and function of the transcriptional corepressor CtBP2. The Journal of biological chemistry *281*, 4183-4189.

Zhao, X.D., Han, X., Chew, J.L., Liu, J., Chiu, K.P., Choo, A., Orlov, Y.L., Sung, W.K., Shahab, A., Kuznetsov, V.A.*, et al.* (2007). Whole-genome mapping of histone H3 Lys4 and 27 trimethylations reveals distinct genomic compartments in human embryonic stem cells. Cell Stem Cell *1*, 286-298.

Zhong, D., Liu, X., Schafer-Hales, K., Marcus, A.I., Khuri, F.R., Sun, S.Y., and Zhou, W. (2008). 2-Deoxyglucose induces Akt phosphorylation via a mechanism independent of LKB1/AMP-activated protein kinase signaling activation or glycolysis inhibition. Mol Cancer Ther *7*, 809-817.

Zhong, L., D'Urso, A., Toiber, D., Sebastian, C., Henry, R.E., Vadysirisack, D.D., Guimaraes, A., Marinelli, B., Wikstrom, J.D., Nir, T.*, et al.* (2010). The histone deacetylase Sirt6 regulates glucose homeostasis via Hif1alpha. Cell *140*, 280-293.

Zhou, J., Schmid, T., Frank, R., and Brune, B. (2004). PI3K/Akt is required for heat shock proteins to protect hypoxia-inducible factor 1alpha from pVHL-independent degradation. The Journal of biological chemistry *279*, 13506-13513.

Zhou, W., Choi, M., Margineantu, D., Margaretha, L., Hesson, J., Cavanaugh, C., Blau, C.A., Horwitz, M.S., Hockenbery, D., Ware, C.*, et al.* (2012). HIF1alpha induced switch from bivalent to exclusively glycolytic metabolism during ESC-to-EpiSC/hESC transition. EMBO J *31*, 2103-2116.

Zhu, H., Hu, S., and Baker, J. (2014). JMJD5 regulates cell cycle and pluripotency in human embryonic stem cells. Stem Cells *32*, 2098-2110.